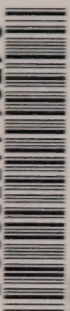


3 1761 11552832 5





Digitized by the Internet Archive
in 2022 with funding from
University of Toronto

<https://archive.org/details/31761115528325>

CAI (3)
EP 321
- 80R09

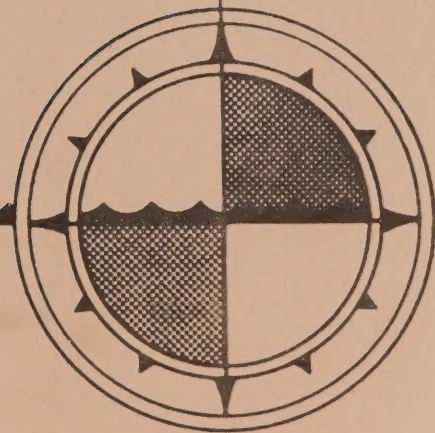


**BUTTERWORTH AND LANCZOS-WINDOW
COSINE DIGITAL FILTERS:
WITH APPLICATION TO DATA PROCESSING ON THE
UNIVAC 1106 COMPUTER**

by

R.E. Thomson and K.Y. Chow

**INSTITUTE OF OCEAN SCIENCES
Sidney, B.C.**



For additional copies or further information please write to:

Department of Fisheries and Oceans

Institute of Ocean Sciences

P.O. Box 6000

Sidney, B.C. CANADA

V8L 4B2

CAI
EP 321
-80R09

BUTTERWORTH AND LANCZOS-WINDOW COSINE DIGITAL FILTERS:

WITH APPLICATION TO DATA PROCESSING ON THE

UNIVAC 1106 COMPUTER

by

R.E. Thomson and K.Y. Chow

Institute of Ocean Sciences
Sidney, B.C.

1980

TABLE OF CONTENTS

	Page
Abstract	<i>i</i>
1. Introduction	1
2. Basic Filter Theory	2
2.1 Filter coefficients	2
2.2 Transfer functions	4
2.3 Aliasing	6
2.4 Truncation effects	9
3. Butterworth Filters	12
3.1 Characteristics	12
3.2 Mathematical formulation	12
3.3 Design	13
3.4 Filter coefficients (time domain)	15
3.5 Truncation effects	17
4. Lanczos-Window Cosine Filters	18
4.1 Characteristics	18
4.2 Mathematical formulation	18
4.3 Design	20
4.4 Impulse response functions	21
5. Filter Application	
5.1 High pass filters	22
5.2 Low pass filters	25
5.3 Butterworth versus Lanczos-window cosine filters	26
6. Acknowledgements	43
7. References	44
8. List of Figure Captions	45
Appendix A	47
Appendix B	54

Abstract

This manuscript describes the characteristics and design of Butterworth and Lanczos-window cosine digital filters for the analysis of uniformly sampled geophysical data using the Univac 1100 series computer. A digitally recorded tidal record is used to illustrate application of the two filter methods. Listings of the well documented programmes are provided in the Appendices.

1. Introduction

When analyzing digitally recorded time series data, we are usually interested in extracting from the background of random noise and unwanted signal statistical information related to a limited spectrum of the Fourier components assumed to make up the signal. Prior to the application of any analytical procedure, however, it is often advantageous to apply digital filters to the recorded sequence in order to pass Fourier components whose frequencies lie within specified bands and to attenuate those components whose frequencies lie outside these bands. Ideally, we would like to apply a rectangular "window" to the data by multiplying by zero (0) the amplitudes of all undesired frequency components and by one (1) the amplitudes of components whose frequencies fall within the frequency bands of interest. In reality, we deal with truncated Fourier series approximations to ideal step-like filter amplitudes and with finite length data sets having finite bit precisions for the word length of all variables (quantized values). This leads to inaccuracies due to round-off errors (truncation effects) in the data as well as in the coefficients of the filters and in the machine calculations. As a consequence, the ability of a filter to enhance the data by isolating specific frequency bands is dependent upon the frequency separation of the bands and the characteristics of the filter. In determining the optimal type of filter, consideration must be given also to the computing time, computational errors and the amount of data that is inadvertently lost from the ends of the record.

The primary purpose of this manuscript is to illustrate the design and characteristics of Butterworth and Lanczos-window cosine digital filters for application to equally-spaced, stationary, linear and deterministic digital input sequences. The filter programmes listed in Appendices A and B have been written specifically for the Univac 1100 series computer presently in use at the Institute of Ocean Sciences; although designed with oceanographic data in mind, they should be directly applicable to most types of chronologically ordered data sets. The text is intended to serve as an introduction to digital filters and as a guide in the use of the computer programmes. In no sense have we attempted to provide a definitive study of filter theory and application. Moreover, in our elementary treatment of the subject of digital filtering we have assumed that the user is familiar with Fourier transform theory and no attempt has been made to present a comprehensive treatment of such fundamental concepts as convolution, sampling or aliasing. Nor do we address problems associated with record gaps and spikes; data sequence are assumed to be "piecewise continuous" and well-edited. The examples presented in § 5 are meant to illustrate certain differences in the two filters using the special case of digitally recorded tide heights known to contain high frequency seiche activity. For specific digital records, filters other than the Butterworth or Lanczos-cosine filter may be more suitable. The user is directed to the references for additional types of filters and for a more thorough treatment of the subject of digital filter theory.

2. Basic Filter Theory

2.1 Filter coefficients

We deal with linear time invariant (LTI) filters which provide an algorithm for converting an input sequence $x(n) \equiv x_n$ into an output sequence $y(n) \equiv y_n$ for quantized values at $n = 0, 1, \dots$ (or $n = 1, 2, \dots$ in the usual computer notation). This provides a functional relationship

$$y_n = F(x_n)$$

where $F(\cdot)$ is determined by the specific filter. The filter is linear in that if $x_n^{(1)}$ and $x_n^{(2)}$ are inputs having respective outputs $y_n^{(1)}$ and $y_n^{(2)}$, then the input $ax_n^{(1)} + bx_n^{(2)}$ has output $ay_n^{(1)} + by_n^{(2)}$ for arbitrary constants a and b . The filter is time-invariant in that, if an input x_n produces an output y_n , then the input x_{n-m} produces the output y_{n-m} for all m . For such LTI systems a convolutional relation exists between the input and output sequences given by

$$y_n = \sum_{m=-N}^N x_m h_{n-m}, \quad (1a)$$

or equivalently,

$$y_n = \sum_{m=-N}^N h_m x_{n-m} \quad (1b)$$

where h_n completely characterizes the system or filter (Figure 1).

The function $h_n \equiv h(n)$ is called the impulse response or unit sample response and is the response of the filter to a digital impulse.

An important subset of (1a) and (1b) are filters for which the input-output sequences are related via constant coefficient linear equations of the form

$$y_n = \sum_{m=-N}^N c_m x_{n-m} + \sum_{m=1}^N b_m y_{n-m}. \quad (2)$$

Note that in the second summation m is positive so that only past values of y are included whereas in the first summation past, present and future values of x are used. Filters for which

$$-N \leq m \leq N, c_m \neq 0,$$

are sometimes called physically nonrealizable filters because they react to future events; physically realizable (casual) filters are those for which $0 \leq m \leq N$. This becomes somewhat meaningless, however, when we work with pre-recorded data since future values are available prior to the computation. On the other hand, when predicting future values from a given set, a physically

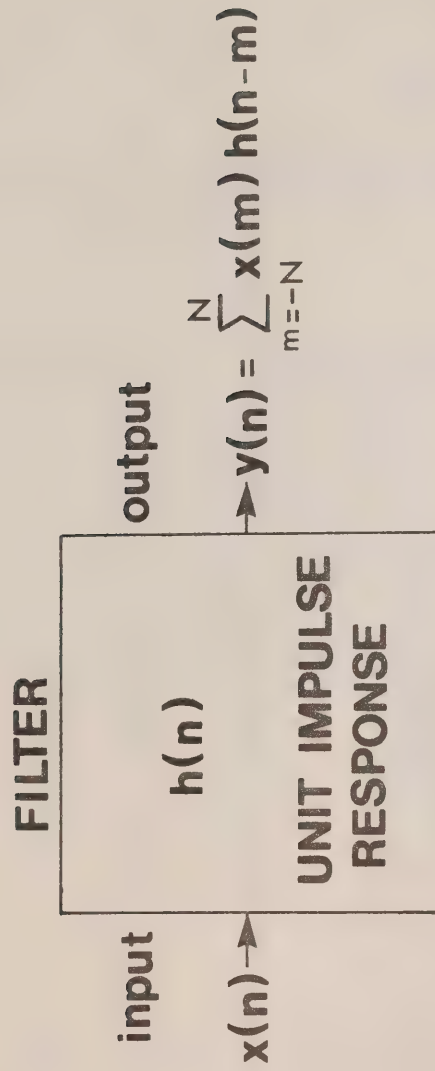


Figure 1. Linear time-invariant filtering viewed as a convolution in the time domain. Data are at times $n \cdot \Delta t$ where Δt is the sampling interval.

realizable filter is required. We may further categorize the filter (2) as recursive ($b_m \neq 0$) or nonrecursive ($b_m = 0$). Butterworth filters* are physically realizable, recursive filters having the time-domain relationship

$$y_n = \sum_{m=0}^N c_m x_{n-m} + \sum_{m=1}^N b_m y_{n-m}, \quad (3)$$

while Lanczos-window cosine filters are physically nonrealizable nonrecursive filters,

$$y_n = \sum_{m=-N}^N c_m x_{n-m}. \quad (4)$$

The index N determines the order of the Butterworth filter. For the Lanczos-cosine filter, N determines the number of weights to be applied to the input on either side of $m=0$.

2.2 Transfer functions

To this point we have viewed filtering as a convolution problem in the time domain where, as schematized in Figure 1, an input is operated on by an impulse response to generate an output. The convolution integral prescribes a linear time-invariant transformation from an input to an output. However analysis of a data sequence can also be prescribed in the frequency domain. In fact, it is usually much simpler to envision the filtering process in the frequency, rather than the time, domain. As illustrated in Figure 2, linear time-invariant filtering in the frequency domains involves multiplication of the Fourier transformed input $X(f)$ by the transfer function, $H(f)$, to derive the output $Y(f)$. The time and frequency domains in this case are related through Fourier integral transform pairs (denoted by \leftrightarrow):

$$x_n \equiv x(t) \leftrightarrow X(f)$$

$$y_n \equiv y(t) \leftrightarrow Y(f)$$

$$h_n \equiv h(t) \leftrightarrow H(f)$$

where t is time and

$$f = 2\pi/\omega$$

is the rotational frequency (e.g. cycles per second) and ω is the angular frequency (e.g. radians per second). The transfer function is a complex quantity describable in terms of an amplitude, or gain $|H(f)|$ and phase angle $\phi(f)$, or equivalently terms of its real and imaginary parts, $R(f)$ and $I(f)$, respectively. Since the input is made up of various Fourier constituents, $X(f)$, filtering involves the modification of the amplitude and phase of each

*There is some confusion in the literature regarding what constitutes a Butterworth filter. Hamming (1977), for example, calls both (3) and its square "Butterworth filters" although the formal definition is confined to the former. In the present case, the linear system (3) defines the time-domain convolution for design of a Butterworth filter. However it is the square of the response of this filter which is described in the Appendix and which is used to process the input data.

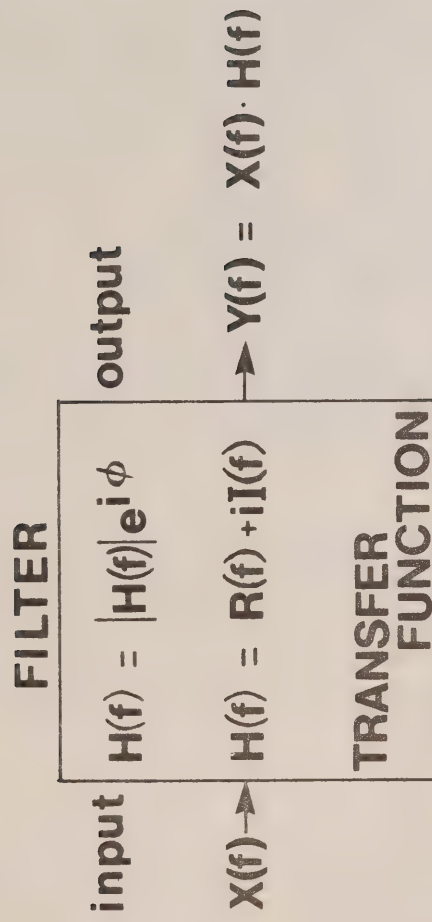


Figure 2. Linear time-invariant filtering viewed as a multiplication in the frequency domain. In general the phase lag $\phi = \phi(f)$. Capitalized functions are the Fourier transforms of the lower case variable in Figure 1.

of these constituents through multiplication by the filter's transfer function. An ideal filter is one which has a gain of unity ($|H(f)| = 1$) for frequency components within the pass-bands and zero for this within the stop-bands (Figure 3a). Moreover, it is advantageous that the filter produce zero phase shift, so that $\phi(f) = 0$ for all frequencies.

For any practical filter, the transfer function has a finite-slope transition between the stop and pass bands. Therefore, unless the spectral peaks of the various Fourier components are well separated relative to the width of the transition zone, there will be a degree of leakage of unwanted signal into the filtered data. Furthermore, the need to approximate ideal rectangular filters with truncated Fourier series's leads to severe truncation effects, known as Gibbs phenomenon, at points of large curvature (Figs. 3b and 4). The oscillatory lobes associated with this phenomenon mean that signal "noise" at certain frequencies in the stop band is not completely removed and that information at certain frequencies in the pass band is modified. This effect can be important for example when attempting to filter tidal records having sharp, pronounced peaks at the semi-diurnal and diurnal periods. To attenuate the Gibbs phenomenon we could increase the number of operations to produce a steeper filter response. However, increasing the number of operations decreases the computational efficiency and magnifies the truncation errors. A better procedure is to taper the original "rectangular" filter using a window which linearly weights the low-frequency components to average-out the side-lobe oscillations. Although the advantage gained by this procedure is somewhat offset by a broadening of the transition zone between the pass and stop bands, it does give improved control of the filter design. In the end, finding the optimal filter becomes a trial and error procedure where advantages and disadvantages must be weighed by the user for the particular task at hand.

As is customary in filter design, we first determine the desired transfer function $H(f)$ based on the filter requirements in the frequency domain. We then calculate the associated impulse (time domain) response whose coefficients appear in the output calculations of (3) and (4). The programmes presented in the Appendices allow us to generate low or high pass Butterworth and Lanczos cosine zero-phase filters. Band pass filters can be generated using combinations of low and high pass filters.

2.3 Aliasing

Although not strictly related to filter design, the problem of data sampling restricts the capability of a digital filter to accurately isolate information in selected frequency bands. Two of the more important sampling problems are now outlined.

For data that has been digitized every Δt units of time, there is no way to distinguish between the contribution of a Fourier component of frequency $f < f_N$ in the digital signal and a component of higher frequency $f > f_N$ where

$$f_N = 1/(2\Delta t) \quad (5)$$

is the Nyquist (or folding) frequency. In other words, there must be two or more sample points per cycle for every frequency component present in a continuous signal if that component is to be properly retained in the digital

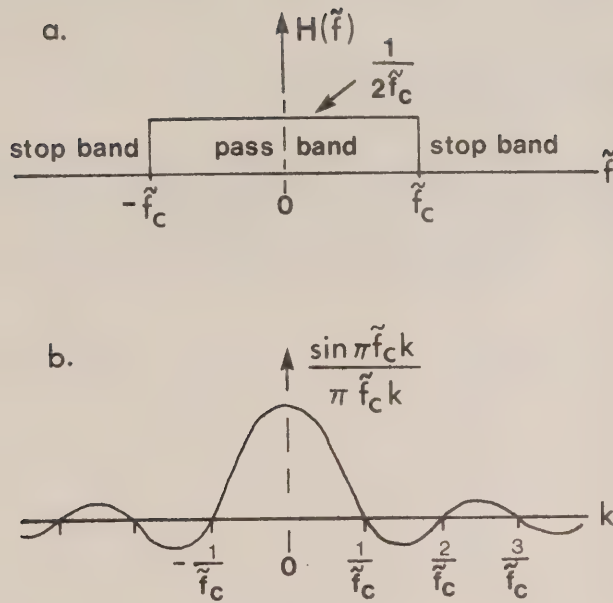


Figure 3. An ideal rectangular transfer function (a) and its Fourier transform (b) in the time domain. The upper curve represents a band-limited function of amplitude unity in the range $\pm \tilde{f}_c = f_c/f_N$ and zero elsewhere. The lower curve is its normalized transform $a_k/(2f_c)$ where $k=0, \dots, N-1$, (see §4.1).

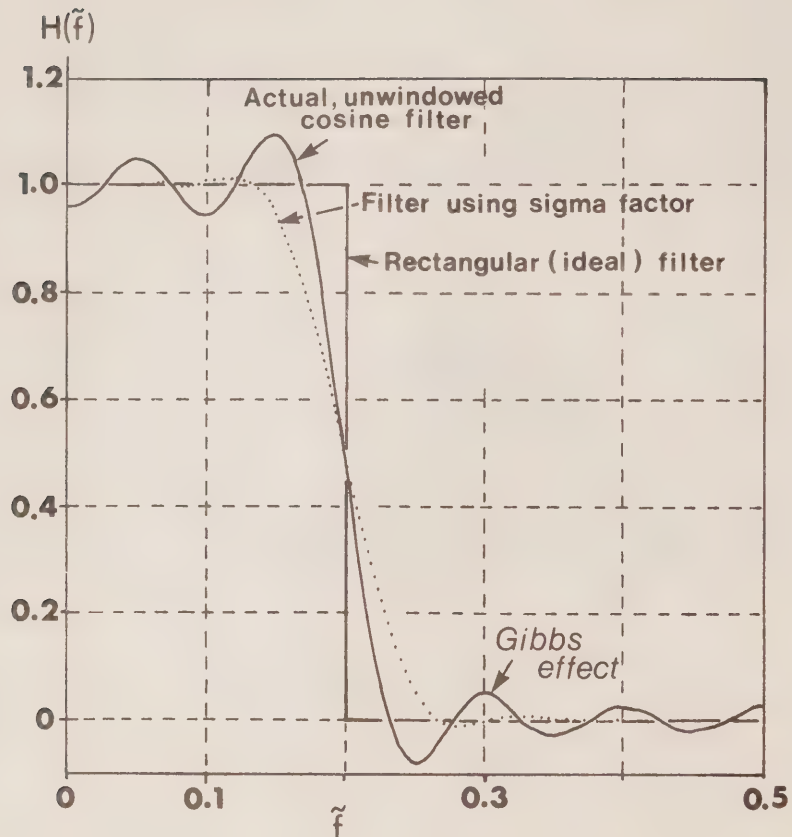


Figure 4. Three forms of the transfer function for a low pass filter having a normalized cutoff frequency $\tilde{f}_c = f_c/f_s = 0.2$. The cosine Fourier expansion of the ideal rectangular filter has been truncated at $N = 10$ terms resulting in the overshoot ripples of Gibbs phenomenon in the unwindowed filter. The dotted curve represents the transfer function following application of the sigma factors of the Lanczos window. (Adapted from Hamming, 1977.)

signal. If there are fewer than two sample points per cycle for a particular frequency, the sampling process is unable to retain this component accurately. This leads to the problem of aliasing whereby power at frequencies higher than f_N in the continuous signal is folded back to lower frequencies to the range $0 \leq f \leq f_N$ in the digital signal. Only if the rate of sampling is twice as great as the highest frequency contained in the signal is all information (power) preserved in the sampling process, (e.g. Shannon and Weaver, 1964).

The filters described in the present manuscript operate on digitized data. Consequently, the frequencies over which the transfer functions can be realistically applied lie in the principal interval $0 \leq f \leq f_N$ or, $0 \leq f \leq \frac{1}{2}f_s$ where

$$f_s = 1/\Delta t$$

is the sampling frequency. Moreover the filtered data will be subject to aliasing problems of the input digital record. If we let $P(f)$ be the true power spectrum of the continuous signal, then the aliased power spectrum $P_a(f)$ of the digitized data record is (Kanasewich, 1973),

$$\begin{aligned} P_a(f) &= P(f) + \sum_{n=1}^{\infty} [P(2nf_N - f) + P(2nf_N + f)] \\ &= P(f) + P(2f_N - f) + P(2f_N + f) + P(4f_N - f) + P(4f_N + f) + \dots \end{aligned}$$

Thus for the data in §5, where $\Delta t = 5 \text{ min} = 0.083 \text{ hours}$, the Nyquist frequency is 6 cph. The calculated power at 1 cph, for example, would then be aliased by power at frequencies $(2f_N - f)$, $(2f_N + f)$, $(4f_N - f)$, $4f_N + f$, etc., or at 11, 13, 23, 25, etc. cph such that

$$P_a(1) = P(1) + P(11) + P(13) + P(23) + P(25) + \dots$$

2.4 Truncation effects

As noted in §2.2, the need to approximate an ideal rectangular transfer function by a truncated Fourier summation leads to Gibbs phenomenon. The role of the Lanczos window described in §4 is to attenuate the overshoot ripples of the transfer function through application of the so-called sigma factors. Butterworth filters do not possess this problem since they are monotonic functions throughout their frequency range. On the other hand, when we apply these filters to the data we can expect similar effects to originate with the discontinuities at the ends of the input. The overshoot ripples in this case are linked with the fact that the finite length of the digitized record can be viewed as resulting from multiplication of an infinitely long record by a finite rectangular window, which in turn introduces terms of the form $\sin x/x$ in the frequency domain. Discontinuities at the ends of the input sequences generate the ringing effect in Butterworth filters and give rise to erroneous end-values in the output. The time for such filters to settle down after an initial transient is an important factor to be considered when deciding on the optimum filter for a given task. In §5 we discuss a number of ways that the ringing effect of Butterworth filters can be reduced. However, regardless of what technique is used the problem of shortened output cannot be totally alleviated.

Quantization of numerical values in the data and in the computer programmes is another form of truncation. Use of double precision partly eliminates errors associated with the programme calculations at the expense of computation speed.

Ultimately, the user will want to process the filtered data to understand certain aspects of the environment in which the observations were taken. Power spectral analysis is typically one of the first post-filtering techniques to be applied to the data and is usually based on Fast Fourier Transform (FFT) calculations requiring 2^n points. Rarely are the number of data points "satisfactorily" close to an exact factor of 2, thus leaving the user with the choice of analyzing considerably fewer data than desired or padding the record with zeroes to artificially create the needed extra values. The latter procedure is not recommended, however, since it does not eliminate the effects of discontinuities. Even if one has exactly 2^n samples problems remain since the Fourier expansion assumes that the data are periodic whereas in reality the two ends of a record have different values. The vogue today is to first remove the mean and trend and then use the weights

$$w(k) = \frac{1 + \cos(\pi k / N')}{2}$$

to taper the ends of the input (Figure 5). Hamming (1977) recommends that N' be about 10% of the existing data with 80% in the flat part of the window. The data can then be padded with zeroes. In this way, there are no discontinuities to initiate transients during the Fourier transform.

It might also be tempting to taper the input sequence to a Butterworth filter in an attempt to reduce ringing effects. Our experience argues against this step especially for low pass filters. At times it may be better to input the unaltered record than to apply modifications which work to the detriment of the resultant output.

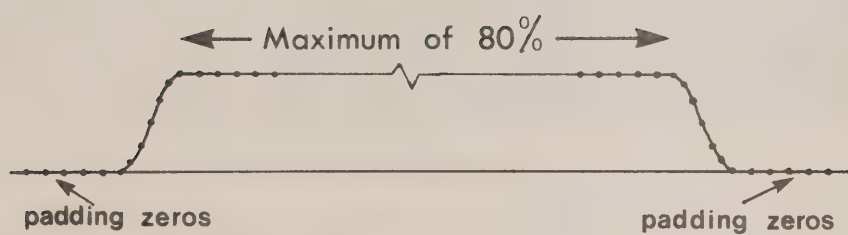


Figure 5. A tapered data set. The data may be padded at one end only or at both ends.

3. Butterworth filters

3.1 Characteristics

Butterworth filters fall into the class of physically realizable recursive filters, constructed by constant coefficient relationships of the form (3). These may also be classified as infinite impulse response (IIR) filters since the effects of a single impulse input can be predicted to an arbitrary time into the future.

Butterworth filters have a number of advantages. Their transfer functions are smooth and maximally flat both inside and outside the pass band with high tangency at the origin ($f=0$) and the Nyquist frequency. The squared filter produces zero phase shift and its amplitude is down by 3 db (factor of $\frac{1}{2}$) at the cutoff frequency. (The cutoff frequency determines the half-power point of the filter.) Gibbs phenomena caused by truncation of an ideal rectangular pass filter does not enter into the design of the transfer function although it is a factor that affects the beginning of the filtered data set (see previous section).

3.2 Mathematical formulation

We define the square of a low pass Butterworth filter by the rotational functional (Hamming, 1977).

$$|\bar{H}(f)|^2 = \bar{H}(f) \cdot \bar{H}(-f) = \frac{1}{1 + (w/w_c)^{2N}}, \quad (6)$$

and the square of a high pass Butterworth filter by the function

$$|\hat{H}(f)|^2 = \hat{H}(f) \cdot \hat{H}(-f) = \frac{(w/w_c)^{2N}}{1 + (w/w_c)^{2N}}, \quad (7)$$

where f is the rotational frequency and N is an integer specifying the order of the filter. The bilinear z -transform variable, w , is defined as

$$w = i \left(\frac{1-z}{1+z} \right) = \tan(\pi f/f_s) \quad (8)$$

in which $z = \exp(2\pi i f \Delta t)$ is the standard z -transform and w_c is the value of w at the cutoff frequency, f_c , (e.g. Kanasewich, 1973; Rabiner and Gold, 1975). Use of the bilinear transform eliminates aliasing errors which arise when the standard z -transform is used to derive the transfer function, such errors being large if the digitizing interval is large. Mathematically, the bilinear z -transform variable maps the inside of the unit circle ($|z| < 1$, for stability) into the upper half plane (imaginary part of w greater than zero). (For a more thorough discussion of filter design on the basis of the poles and zeroes of the rational function, $H(f)$, the reader is referred to Rabiner and Gold (1975) pages 30 to 50.)

We note that the above relationships define the square of the response of the filter $H(f)$ formed by multiplying the transfer function by its complex

conjugate $H^*(f) = H(-f)$. The product $H(f) \cdot H(-f)$ eliminates any frequency dependent phase shift associated with the individual filters (eg. Figure 6) and produces a squared, and therefore sharper, frequency response. When designating the characteristics of a Butterworth filter in the frequency domain, we work with eqns. 6 or 7; in the time domain, however, we first determine the filter coefficients c_m and b_m in (2) corresponding to the low pass filter $\bar{H}(f)$ only, and then manipulate the data output from $\bar{H}(f)$ to generate the output produced by $|\bar{H}(f)|^2$. To obtain the output for a high pass Butterworth filter, the output from the corresponding low pass filter is first obtained and the resulting data values subtracted from the original input values on a point for point basis.

3.3 Design

We now illustrate the design procedure for a Butterworth filter based on a modified version of Hamming (1977), pages 189 to 195. There are also numerous errors in the book that are corrected in the present manuscript. (Hamming has corrected some of the errors in a more recent edition; surprisingly, neither the author nor the publishers acknowledge the fact that the book has been altered during reprinting!)

The first programme requirement is to specify the sampling period or time interval, Δt , between the values of the input. In our case, Δt is given in minutes. From this the programme calculates the sampling frequency, $f_s = 1/\Delta t$, and the range of acceptable normalized input frequencies,

$$0 \leq f/f_s \leq 0.5, \quad (9)$$

where $0.5 = f_N/f_s$ and f_N is the Nyquist frequency (5). The next input parameter is the desired cutoff frequency f_c (in cycles per minute) which automatically determines the half-power point (or -3db level) of the filter. At the cutoff frequency, the amplitude of all frequency components near f_c will be attenuated by a factor of $\sqrt{2}$; power associated with these components will be down by a factor of 2. For the best results, the normalized cutoff frequency, f_c/f_s , should be removed from the ends of the domain (9); otherwise the transfer function may not be steep enough to meet the requisite values $\bar{H}(0) = 1$ in the case of a low pass filter or $\hat{H}(\frac{1}{2}) = 1$ in the case of a high pass filter. After the user has specified whether a high or low pass is required, the final input parameter required is the order N of the filter. Despite the use of double precision throughout the programmes, round-off errors are unavoidable and in our case require that $1 \leq N \leq 9$.* The programme offers two options: N can be specified, so that the attenuation levels in the stop and pass bands are automatically determined; or N can be calculated based on the required attenuation in decibels. Suppose we want an attenuation of $-D$ (decibels) at frequency f_q in the stop band of a low pass filter having a cutoff frequency $f_c < f_q$. From (5) and (8), and the definition

$$-D = 10 \log_{10} [\text{Amplitude/Reference amplitude}], \quad (10)$$

we find, using a reference amplitude = 1 for the pass band,

$$-D = 10 \log_{10} [1/(1 + (w_q/w_c)^{2N})]$$

*For higher order Butterworth filters see Digital Signal Processing Committee, 1969.

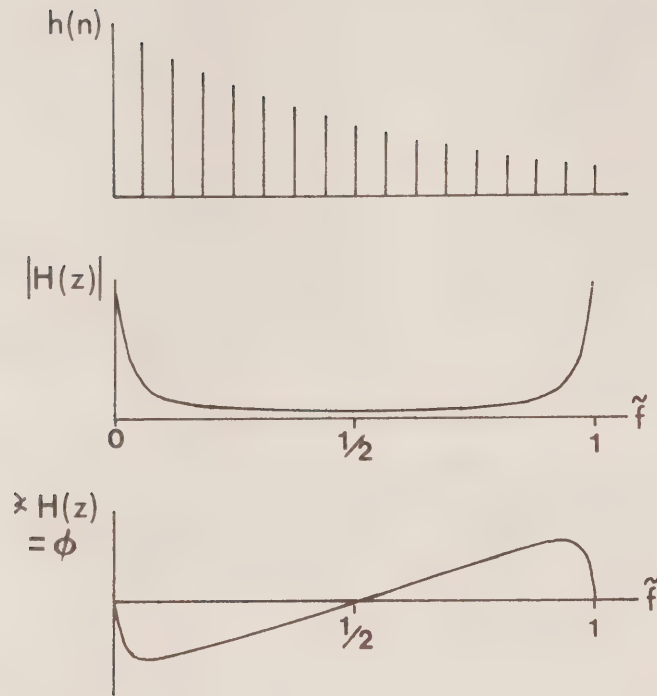


Figure 6. An example of the time and frequency responses of a simple Linear Time Invariant system having a complex-valued transfer function, $H(z)$. The impulse response $h(n) = a^n \cdot u^*(n)$ ($|a| < 1$, and $u^* = 1$ for $n > 0$, $u^* = 0$ for $n < 0$). The function $H(z) = \sum_{n=0}^{\infty} (a/z)^n = 1/(1-a/z)$ where $z = \exp(i2\pi f)$. (After Rabiner and Gold, 1975.)

whereby

$$N = 0.5 \log_{10} (10^{D/10} - 1) / \log_{10} (w_q/w_c) \quad (11)$$

$$\sim (D/20) / \log_{10} (w_q/w_c), D > 10.$$

(D is a positive number; -D is the db level decrease.) The programme will take the nearest integer value of the above equation as the filter order, N, provided of course that f_q (w_q) and D have been properly specified to ensure that $N \leq 9$. Otherwise the imposed constraints are too severe and new parameters must be specified. The above calculation applies equally to an attenuation -D at frequency $f_q < f_c$ in the stop band of a high pass filter except that $\log_{10}(w_q/w_c)$ in (11) is replaced by $\log_{10}(w_c/w_q)$. Since $\log(x) = -\log(1/x)$ this presents no difficulty; by simply ignoring the minus sign we retain expression (11) which now applies to the high pass filter.

With all parameters specified, the programmes will upon request plot the transfer function $|H(f)|^2$ or $\log_{10}(|H(f)|^2)$ versus the normalized sampling frequency, f/f_s .

3.4 Filter coefficients (time domain)

Having determined the characteristics of our filter in the frequency domain, we now want to derive the filter coefficients to be applied to the data in the time domain. To this end we first assume that the transfer function $\bar{H}(f)$ of the low pass filter can be constructed as a product (or cascade) of second order ($N=2$) Butterworth filters $\bar{H}_2(f)$ and, if necessary, one first order ($N=1$) Butterworth filter $\bar{H}_1(f)$. Thus if $N = 5$,

$$\bar{H}(f;5) = \bar{H}_1(f) \times \bar{H}_2(f) \times \bar{H}_2(f).$$

Use of cascade filtering simplifies the algebra in the filter design and reduces the round-off error relative to a brute force calculation of $\bar{H}(f)$ for each order.

It can be shown (e.g. Hamming, 1977) that the second-order transfer functions whose product generates an Nth order low pass Butterworth filter have the form*

$$\bar{H}_2(f;N) = \frac{w_c^2(z^2 + 2z + 1)/a_k}{z^2 + 2z(w_c^2 - 1)/a_k + \{1 - 2w_c \sin[\pi(2k+1)/2N] + w_c^2\}/a_k}, \quad (12)$$

$$\text{where } a_k = 1 + 2w_c \sin[\pi(2k+1)/2N] + w_c^2, \quad (13)$$

*Hamming has a number of incorrect minus signs in his specification of

$$\hat{H}_c(f) \equiv \bar{H}_2(f;N).$$

and integer k is such that

$$0 \leq k \leq (N-1)/2 \quad (14)$$

If N is odd, there is one additional factor which gives rise to the first order transfer function,

$$\bar{H}_1(f) = \frac{[w_c/(1+w_c)](z+1)}{z - (1-w_c)/(1+w_c)} \quad (15)$$

Suppose that $N = 5$, as before. Then we clearly need (15) as our leading term in the transfer function cascade. From (14) k takes the values 0 and 1 so that the first second-order transfer function in the cascade is found by setting $k=0$ in (12) and (13); the second second-order transfer function is found by setting $k=1$ in these equations. Had we chosen $N=7$ we would add $k=2$ to our calculations to obtain a third second-order filter, and so on.

The next state in the process is to recognize that the second-order function (12) has the general form

$$\bar{H}_2(f) = \frac{c_0 z^2 + c_1 z + c_2}{z^2 - b_1 z - b_2} \quad (16)$$

while the first-order function (15) has the general form

$$\bar{H}_1(f) = \frac{d_0 z + d_1}{z - e_1} \quad (17)$$

where only the sine contributions in the coefficients of (12) change with filter order N . The recursive digital filters whose time-domain algorithms have the above transfer functions are, respectively,

$$y_n = c_0 x_n + c_1 x_{n-1} + c_2 x_{n-2} + b_1 y_{n-1} + b_2 y_{n-2} \quad (18)$$

and

$$y_n = d_0 x_n + d_1 x_{n-1} + e_1 y_{n-1} \quad (19)$$

Direct comparisons of (16) with (18) and (17) with (19) yield the needed filter coefficients. The latter comparisons, for instance, give $d_0 = d_1 = w_c/(1+w_c)$ and $e_1 = (1-w_c)/(1+w_c)$. Hence to apply our $N=5$ filter, we process the input data x_n ($n=0,1, \dots$) by the first-order filter (19), take the output and process it by the first second-order filter (18) with $k=0$, then take the output from these calculations and process it by the next second-order filter (18) with $k=1$. The resultant y_n ($n=0,1, \dots$) from the three

manipulations is the low-pass output for a 5th order filter, $\bar{H}(f;5)$.

But the task is only half completed. According to (6), the smoothing procedure for a squared Butterworth filter requires that we further process the output from $\bar{H}(f)$ with the filter $\bar{H}(-f)$. We could do this by separately designing $\bar{H}(-f)$. Or we invert the order of calculations such that the output y_n from $H(f)$ is run through the inverted version of this filter, the last second-order filter being used first and the first order filter (if N is odd) being used last. Alternatively, we can simply invert the chronological order of the data y_n and pass this new data set through the same filter. Since all the data are recorded beforehand we take the latter tack, remembering that in the end we must re-invert the output sequence so that it is again in proper chronological order. Clearly, if there is a phase shift at a given frequency in the first pass through the filter, there will be an equal phase shift of opposite sign at that frequency in the second pass. (Figure 5c can be used to visualize this effect.) By processing the data in reversed chronological order through the filter the two phase shifts cancel exactly.

The computer program described in Appendix A performs the operations (18) and (19), each time reassigning the output y_n as a "new" input x_n until the filter $\bar{H}(f)$ is achieved. The last set of output is then inverted and re-run through the same filter. Following the final set of calculations, the output sequence is inverted to ensure correct ordering in time. If a high pass Butterworth filter was specified there is one additional operation; the final output sequence y_n ($n=0,1, \dots$) is subtracted point for point from the original input sequence x_n ($n=0,1, \dots$) to create the high pass filtered data $\hat{y}_n = x_n - y_n$.

3.5 Truncation effects

Owing to the finite length and often step-like beginning of digital data sets, the output from a Butterworth filter will have non-useable values at its two ends. That is, there will be fewer output than input values. This "ringing" effect of the filter derives from the absence of data prior to the start of the record and only dies away after the effects of the initial amplitude discontinuity have been smoothed by the integrations. Both ends of the final output are affected since the data are passed forward and backward through the filter. Padding the beginning of the record with zeroes appears to serve no useful purpose. However, if in the case of the tidal record (§5) we begin the high pass filter at a zero-crossing of the signal (tide height zero) the ringing effect is attenuated with comparatively little loss of data.

4. Lanczos-window cosine filters

4.1 Characteristics

In this section we describe a type of nonrecursive filter of the form (4). These filters are simpler to understand, design, and apply than the recursive type filter of the previous section. They present neither the stability problems which limited the Butterworth filter to $N \leq 9$ nor the ambiguity in deciding where at the ends of the filtered record the effects of the finite length input are unimportant. Moreover, it is straightforward to design a high pass filter directly rather than indirectly using the output of a low pass filter. As before, the amplitude of the Lanczos-window cosine filter is down by 3 db (factor of $\frac{1}{2}$) at the cut-off frequency. The main drawback with these filters is that increased steepness within the transition zone can only be achieved by increasing N , resulting in further shortening of the output sequence relative to the input.

4.2 Mathematical formulation

The formulation is based on an ideal rectangular filter having a response of unity in the pass band and zero elsewhere. The effect of the Lanczos window is to reduce the ripples of Gibbs phenomenon associated with the discontinuities in the rectangular filter (cf Figure 4).

We may formally write the transfer function $H(f)$ of a rectangular high or low pass filter as the Fourier expansion

$$H(f) = a_0/2 + \sum_{k=1}^{\infty} [a_k \cos(\pi k f) + b_k \sin(\pi k f)] \quad (20)$$

where \tilde{f} is the rotational frequency f normalized by f_N , $\tilde{f} = f \cdot (2\Delta t)$, and the a_k and b_k are constant coefficients obtainable from the Fourier transform of (20). Since a_0 is the "dc level" between 0 and 1 of the filter, we need to take $a_0/2$ as the first term. To eliminate any frequency dependent phase shift we insist that the transfer function have even symmetry, $H(f) = H(-f)$, whereby $b_k = 0$. To be realistic we must also truncate (20) after a reasonable number of terms (N) so that

$$H(f) = a_0/2 + \sum_{k=1}^{N-1} a_k \cos(\pi k f) \quad (21)$$

which in turn gives rise to significant overshoot ripples in both the stop and pass bands of the filter (Figure 4). The period, T , of the ripples for sampling interval Δt is

$$T = N \cdot \Delta t \quad (22)$$

As we shall see, the effect of the Lanczos-window is to smooth out the ripples by averaging over oscillations in $H(f)$ at this period.

Suppose we begin with the ideal filter such that the Fourier transform of (21) yields

$$\begin{aligned}
 a_k &= \int_{-1}^1 H(\tilde{f}) \cos(\pi k \tilde{f}) d\tilde{f} \\
 &= 2 \int_0^1 H(\tilde{f}) \cos(\pi k \tilde{f}) d\tilde{f} .
 \end{aligned}$$

For a low pass rectangular filter with normalized cutoff frequency $\tilde{f}_c = f_c/f_N$, the lower bound of the integral becomes \tilde{f}_c whereby

$$a_0 = 2\tilde{f}_c/f_N = 2\tilde{f}_c, \quad k=0, \quad (23a)$$

$$a_k = 2\tilde{f}_c \sin(\pi k \tilde{f}_c)/(\pi k \tilde{f}_c), \quad k=1, \dots, N-1, \quad (23b)$$

while for a high pass rectangular filter having the same cutoff frequency the upper bound becomes \tilde{f}_c so that,

$$a_0 = 2(1-\tilde{f}_c), \quad k=0, \quad (24a)$$

$$a_k = -2\tilde{f}_c \sin(\pi k \tilde{f}_c)/(\pi k \tilde{f}_c), \quad k=1, \dots, N-1. \quad (24b)$$

In other words, a_0 (high pass) = $1 - a_0$ (low pass) and for $k \neq 0$ the coefficients a_k of the two filters are of opposite sign but identical amplitude. An example of the Fourier transform pairs $a_k \leftrightarrow H(\tilde{f})$ for the low pass case is plotted in Figures 3a and 3b. This illustrates the effect in the time domain of the finite width of the window in the frequency domain. The main lobe extends from $\pm 1/\tilde{f}_c$; for larger k the function oscillates at constant period and the amplitude decays as $1/k$. The larger the \tilde{f}_c (i.e. the more closely the function $H(\tilde{f})$ approaches a spike or Dirac delta function) the narrower the central peak and the shorter the period of the oscillations.

To obtain the coefficients a_k for the Lanczos-window modification to the rectangular filter, we simply multiply (23b) or (24b) by the sigma factors,

$$\sigma(N,k) = \sin(\pi k/N)/(\pi k/N), \quad (25)$$

where as before N is the number of filter coefficients.

Thus, for example, the transfer function for a cosine (rectangular) low pass filter (21),

$$\bar{H}(\tilde{f}) = \tilde{f}_c + 2\tilde{f}_c \sum_{k=1}^{N-1} \left\{ \sin(\pi k \tilde{f}_c)/(\pi k \tilde{f}_c) \cdot \cos(\pi k \tilde{f}) \right\} \quad (26)$$

becomes for a low pass Lanczos-window cosine filter,

$$\bar{H}(\tilde{f}) = \tilde{f}_c + 2\tilde{f}_c \sum_{k=1}^{N-1} \left\{ \sigma(N,k) \cdot \sin(\pi k \tilde{f}_c)/(\pi k \tilde{f}_c) \cdot \cos(\pi k \tilde{f}) \right\}. \quad (27)$$

The sigma terms represent a long period modulation of the weighting terms a_k and have the effect of smoothing out the oscillations of (23b) while at the same time broadening the width of the main lobe (see Figure 4). These effects can be readily seen by taking a value of $N=20$ and calculating $\tilde{H}(\tilde{f})$ with and without the sigma factors. The exercise is instructive in other ways also: it emphasizes the presence of truncation errors during the calculations and indicates what happens if \tilde{f}_c is too close to the ends of the principal interval $0 \leq \tilde{f}_c \leq 1$.

As an example, using $\tilde{f}_c = 0.022$, $N = 25$ and truncating values at the 4th decimal place, we find that for a high pass filter,

$$\begin{aligned} H(0) &= 0.0740 && \text{no Lanczos window} \\ &= 0.4015 && \text{with Lanczos window.} \end{aligned}$$

Increasing N to 50 for the same \tilde{f}_c improves matters considerably; $H(0) = 0.0527$ and $H(1) \approx 0.9997$ using the sigma factors.

4.3 Design

The design of low or high pass Lanczos-window cosine filters follows the general procedure of §3.3 for the Butterworth filter. First, the sampling interval Δt in minutes is entered into the programme which then determines the Nyquist frequency $f_N = 1/(2\Delta t)$ in cycles per minute. The desired cutoff frequency (cpm) is read in and normalized by f_N . (In the previous section we normalized via the sampling frequency.) As with the Butterworth filter, it is advantageous to keep the normalized cutoff frequency away from the ends of the principal interval which in this case is,

$$0 \leq f/f_N \leq 1.$$

The user then specifies the number of weighting terms, N , to be applied and whether a high or low pass filter is required. Band pass filters can be constructed using combinations of the high and low pass filters. As before, the programme will, if requested, plot the transfer function $H(\tilde{f})$ or $10 \log_{10} |H(\tilde{f})|$ versus normalized frequency $\tilde{f} = f/f_N$ in units of 0.01 from zero to one. The weights a_k may also be listed together with their sum, S ,

$$S = \frac{1}{2} \sum_{k=0}^N a_k, \quad (28)$$

where $S = 1$ for a low pass filter and $S = 0$ for a high pass filter. The proximity of the calculated sum to these values is a measure of the filter's quality. (The factor $\frac{1}{2}$ enters because the impulse response function coefficients are $a_k/2$.)

The value N depends upon a compromise between the desired filter roll-off and the acceptable number of data points (N) that are lost from the two ends of the record. The greater the N , the sharper the filter and the greater the information loss. Repeated processing of a given record by the same filter m times generates a response for a cascade filter $[H(f)]^m$ with a loss of $m \cdot N$

data points from the ends of the records. For a high pass filter, N should be large enough that in the time domain the $2N$ weights span roughly one period of the higher frequency end of the oscillations that are to be smoothed out. Typically the user could start with $25 \leq N \leq 50$ and then modify this number until a satisfactory result is attained.

4.4 Impulse response functions

As we saw in § 2.1 the output from a rectangular non-recursive filter, $y_n = y(n)$ can be written as

$$y_n = \sum_{k=-N}^N c_k x_{n-k}, \quad (29)$$

where for a symmetric (cosine) filter,

$$c_k = c_{-k}. \quad (30)$$

Since the system is assumed linear, a sum of inputs of different frequencies f_k having the form

$$x_n = \sum_{k=1}^M A_k e^{2\pi i \tilde{f}_k n}, \quad \tilde{f}_k = k \cdot \Delta t,$$

will give the output as

$$y_n = \sum_{k=1}^M A_k H(\tilde{f}_k) e^{2\pi i \tilde{f}_k n},$$

where using (29) together with $2\tilde{f}_k \rightarrow \tilde{f}$,

$$\begin{aligned} H(\tilde{f}) &= \sum_{k=-N}^N c_k e^{\pi i \tilde{f} k} \\ &= c_0 + 2 \sum_{k=1}^M c_k \cos(\pi \tilde{f} k). \end{aligned} \quad (31)$$

Comparing (31) with (21) we obtain the impulse response functions

$$c_k = a_k/2, \quad k=0,1, \dots, N, \quad (32)$$

as defined by (23a,b) and (24a,b) for low and high pass filters, respectively. The c_k are then used in (29) to convert the input x_n into the output y_n . In the process we make use of (30) to reduce the number of steps in the calculation.

5. Filter Application

To demonstrate the use of the filters and compare their outputs, we have chosen a digital $14\frac{1}{2}$ day ambient pressure record obtained from a chart depth of about 10 m in Pedder Bay near Victoria (Figure 7). The pressure gauge record was one of a pair obtained between 9 December 1977 and 13 January 1978 as part of a study of high frequency seiche activity in the embayment.

Pedder Bay is a shallow wedge-shaped inlet approximately 3 km long and 1 km wide at its mouth which adjoins water of 100 m depth in Juan de Fuca Strait. In addition to the short (< 2 hour) period intermittent seiche activity, the basin is near the nodal point for the M_2 (semidiurnal) tide in the inside coastal waters. As a consequence, tides are mixed, predominantly diurnal with a mean range of 1.83 m.

The pressure gauge was anchored by divers in a specially designed concrete block and set to record once every five minutes using an integration (averaging) time of 28 seconds; during the observation period there was no significant drift in the timing mechanism (clock). According to the manufacturer (Aanderaa Instruments Ltd.), the gauges are accurate to 1 part in 10^6 , or 10^{-2} mm in 10 m of water, making it possible to discern any significant seiche activity within the basin. Data from the gauge has been edited to remove spikes as well as values recorded during deployment and recovery.

Four separate filters have been applied to the data: a high pass, 100 weights Lanczos-cosine filter; a high pass, 7th order Butterworth filter; a low pass, 400 weights, Lanczos-cosine filter; and a low pass 7th order Butterworth filter. We have further tested the filters by comparing the results using the unabridged tidal record and the tidal record with the major tidal constituents removed. In the latter case, the full record is subject to a standard harmonic analysis (e.g. Foreman, 1977) to determine the main constituents (Table 1). These specific Fourier components are then subtracted from the original record leaving a residual "non-tidal" record of considerably reduced magnitude. For each analysis we present plots of: the filter's transfer function; the input data sequence; the filtered output sequence; and the envelope curve for the filtered data. The envelope plots, obtained by squaring the filtered output and low-pass filtering the result using the cutoff frequency of the high pass filter, readily allow a visual comparison of the output from different filters, especially those of the high pass filters.

5.1 High pass filters

For both the Lanczos-cosine and Butterworth high pass filters, we have set the high frequency cutoff, f_c , at $0.50 \text{ cph} (2 \text{ hours})^{-1}$ or $8.33 \times 10^{-3} \text{ cpm}$. The sampling frequency in all cases is $f_s = (5 \text{ min})^{-1} = 0.2 \text{ cpm}$ and the Nyquist frequency $f_N = 0.1 \text{ cpm}$. In order to have a sharp frequency cutoff, we have specified a 7th order Butterworth filter and, by trial and error, found that an $N = 100$ Lanczos-window cosine filter gave an almost identical transfer function (Figures 8a,b).

The resultant output for the two filters, with the tides in and tides removed, are plotted in Figures 9a-d. The filters, it seems, produce identical filtered data and have sharp enough responses to effectively remove the tidal

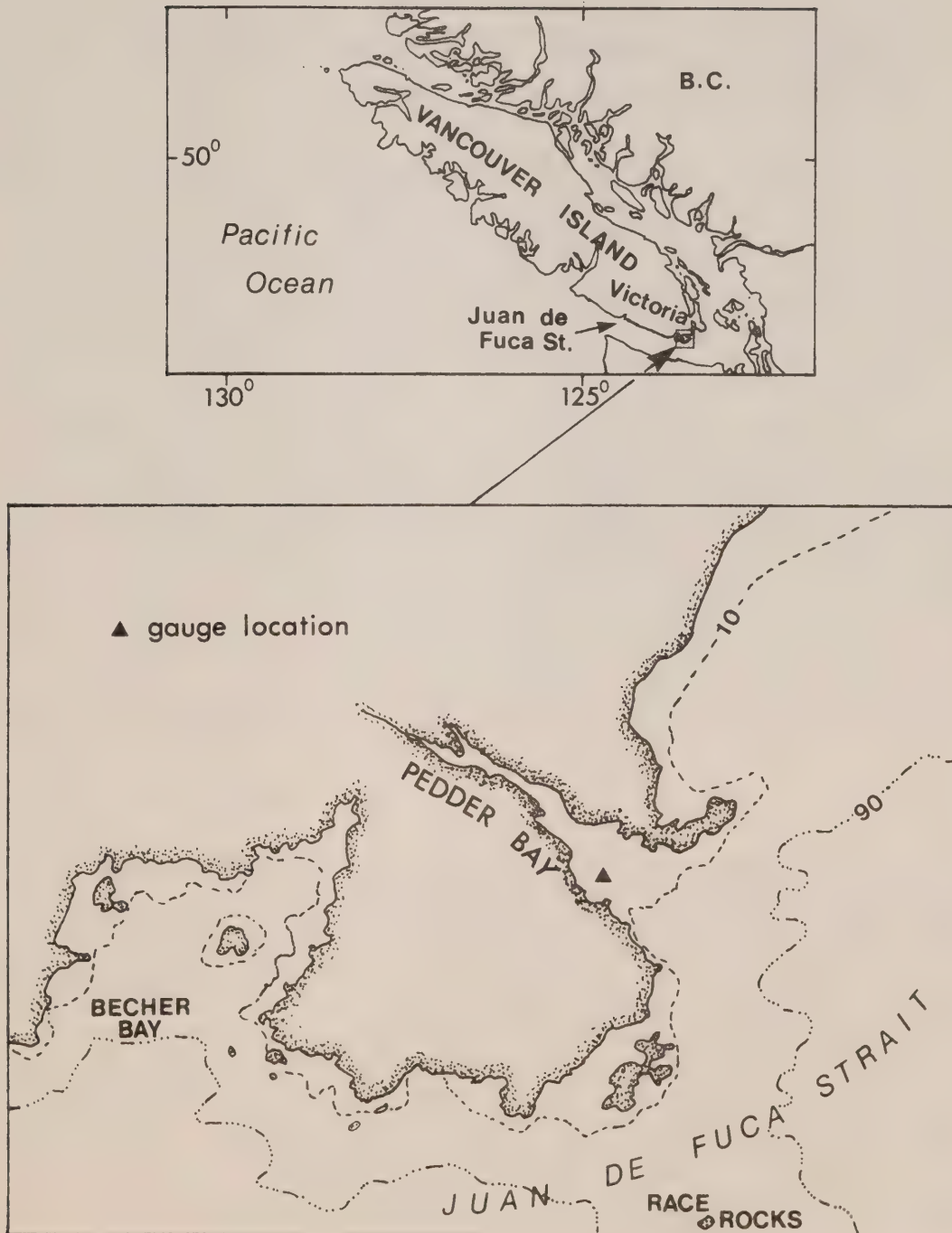


Figure 7. Location map for Pedder Bay. Depths in metres.

Table 1. Listing of major tidal constituents for Pedder Bay from 01:00 hr on December 9 to 19:00 hr on December 23, 1977. Amplitude (A) is in metres and phase (G), relative to 120° W longitude, is in degrees. P_1 and K_2 have been inferred from K_1 and S_2 , respectively, using ratios determined by previous measurements by the Canadian Hydrographic Service.

CONSTITUENT		FREQUENCY	AMPLITUDE	PHASE
No.	Name	cycles/hour	(metres)	(°)
1	Z_0	0.0000	20.097	0.00
2	O_1	0.0387	3.834	310.69
3	P_1	0.0416	2.059	300.42
4	K_1	0.0418	6.581	301.72
5	M_2	0.0805	3.438	45.54
6	S_2	0.0833	1.259	28.03
7	K_2	0.0836	0.250	36.03

oscillations. Therefore in this case it would have been expedient to work directly with the original tidal record rather than make the effort of first removing the tidal harmonics.

For the Lanczos-cosine filter, the tidal records were analyzed in unabridged form so that the output sequence was shorter by 200 values ($2N \cdot \Delta t = 1000$ min) than the input sequence. Analysis of the tidal record using the high pass Butterworth filter was less straightforward. Direct application of the filter to the unaltered input resulted in abnormally large amplitude, low frequency oscillations at the beginning and ends of the output, such oscillations being associated with the step-like terminations of the record. We first attempted to eliminate this problem by applying cosine tapers (see § 2.4) to the ends of the record but only succeeded in aggravating the situation. The difficulty of course is that the high pass Butterworth filter derives from the low pass version of the same filter. By tapering the input we introduce Fourier components that are confined to the end points of the input but whose effect is propagated into the filtered sequence. When, on the other hand, we removed those records prior to the first zero crossing at the beginning of the tidal record and those after the last zero crossing at the end of the record, the problem was essentially avoided (see Figures 9a and 9b). The suggestion, therefore, is that for signals possessing a constant mean (dc) level, the user should first remove the mean and analyze the resultant data set between the first and last zero values. In this manner, large amplitude erroneous output at the ends of the filtered data may be reduced.

A comparison of the results from the two high pass filters shows that for the parameters specified there is typically less information loss using the Butterworth filter. In general, however, the validity of this result will depend on the characteristics of the designed filters and, for the Butterworth filter on the degree of initial ringing or alternatively on the number of points to the first and last zero crossing. If the raw data record starts near its constant (or zero) level then the Butterworth is decidedly superior; if a large number of records must be dropped before a zero crossing is attained, either filter may suffice. For the present programmes, the Butterworth filter is roughly 10% faster in computation time than the Lanczos-cosine filter, although it may be possible to change this by improving the efficiency of the programmes.

5.2 Low pass filters

The cutoff frequency for the low pass filters was fixed at 2.083×10^{-2} cph (48 hours) $^{-1}$ or 3.4722×10^{-4} cpm; the sampling frequency, as before is 0.2 cpm. We again specified a 7th order Butterworth filter but this time required $N = 400$ in order to generate a Lanczos-cosine filter with the same frequency response (Figures 10a,b). The proximity of the cutoff frequency to the origin, $f=0$ necessitates use of such a narrow transition band for the filter. A lower order filter would not rise rapidly enough from the stop band $f > f_c$ to meet the requirement that $H(0) = 1$. This difficulty could have been lessened somewhat had we used a cascade of lower order filters with cutoff frequencies farther removed from the origin or had we first decreased the sampling frequency. Provided there were no serious aliasing effects, the latter could be accomplished by selecting every j 'th point from the original digitized record or by linearizing averaging over a number of adjacent points

to create new more highly smoothed input data (in essence a simple form of low pass filtering).

Results for the two low pass filters with the tides in and with the tides removed are plotted in Figures 11a-d. Unlike the examples in the previous section, the low pass filters operate best on the tide-removed data, as one might expect. Moreover, we could have used a shorter Lanczos-window cosine filter on these data thereby reducing the amount of information loss after filtering. The same is true of the Butterworth filter. In particular, the ringing effect associated with tidal record was so severe that to permit a direct amplitude comparison of the low pass results we had to omit the first part of the output of Figure 11c. Nevertheless, comparing the analyses based on the full tidal records we see that the Butterworth filter produces a longer better smoothed curve than the Lanczos-cosine filter; with the tides removed, the analyses are essentially the same.

5.3 Butterworth versus Lanczos-window cosine filters

The major advantage of the Butterworth filter would appear to be its sharp transition band for the comparatively shorter computational time and loss of output. Where it is possible to subject the input to a pre-filter preparation, such as removing the tidal harmonics in the case of tide height records, this advantage may be minimal. The one minor feature favouring the Lanczos-cosine filter is that the entire output is free of transient effects associated with the finite length of the input whereas with the Butterworth filtered data it is often necessary to decide where the transients have been effectively dampened. Thus, for a particular situation, it may turn out that one filter has an obvious advantage over the other, though in most instances the differences may not be pronounced. The fact that each of the filters has two adjustable parameters (the cutoff frequency and the "order" of the filter) makes them equally flexible and therefore equally capable of meeting the conditions set out for most filtering requirements.

Figure 8. Frequency response curves for the high pass filters; cutoff frequency = 8.33×10^{-3} cpm and sampling frequency = 0.2 cpm.
a) Seventh order Butterworth filter. b) 100 term Lanczos-window cosine filter.

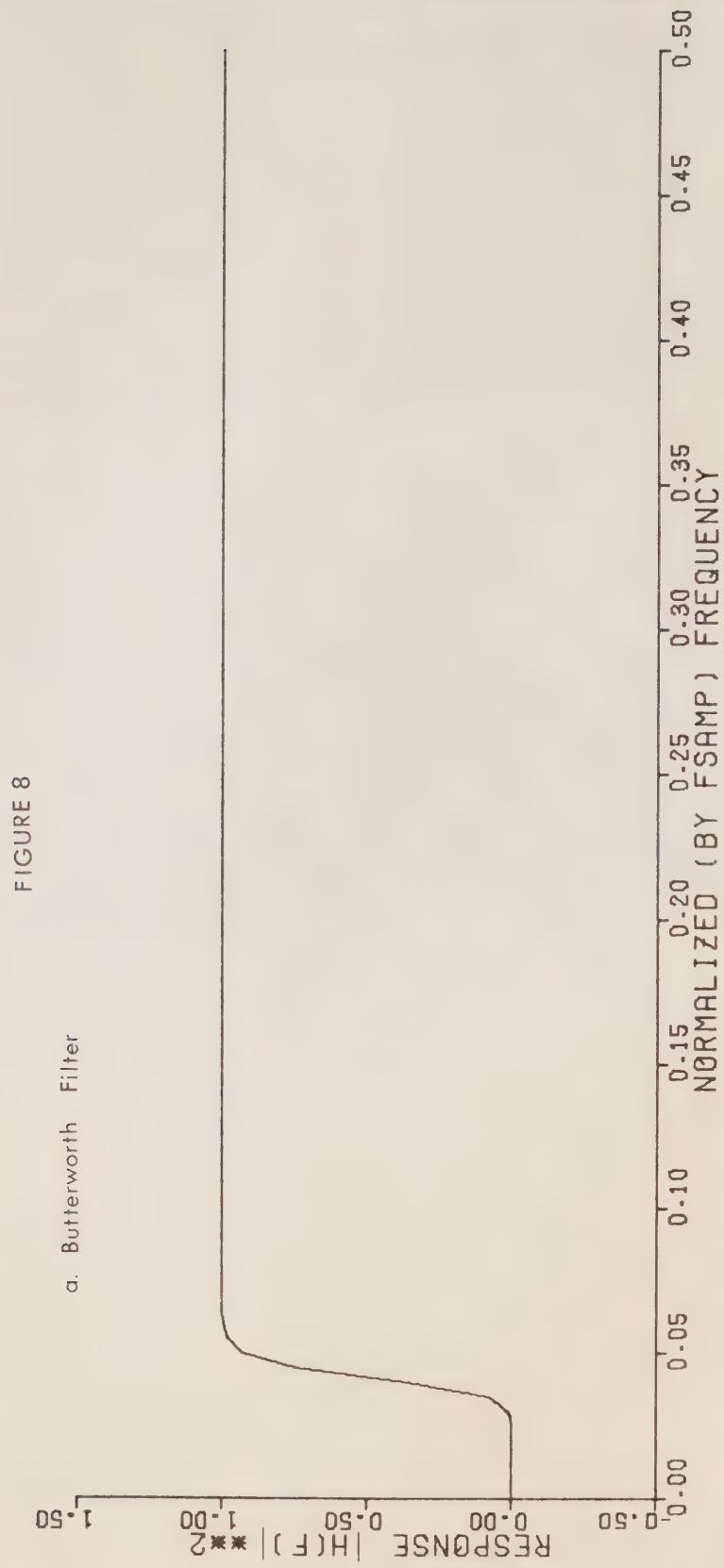


FIGURE 8

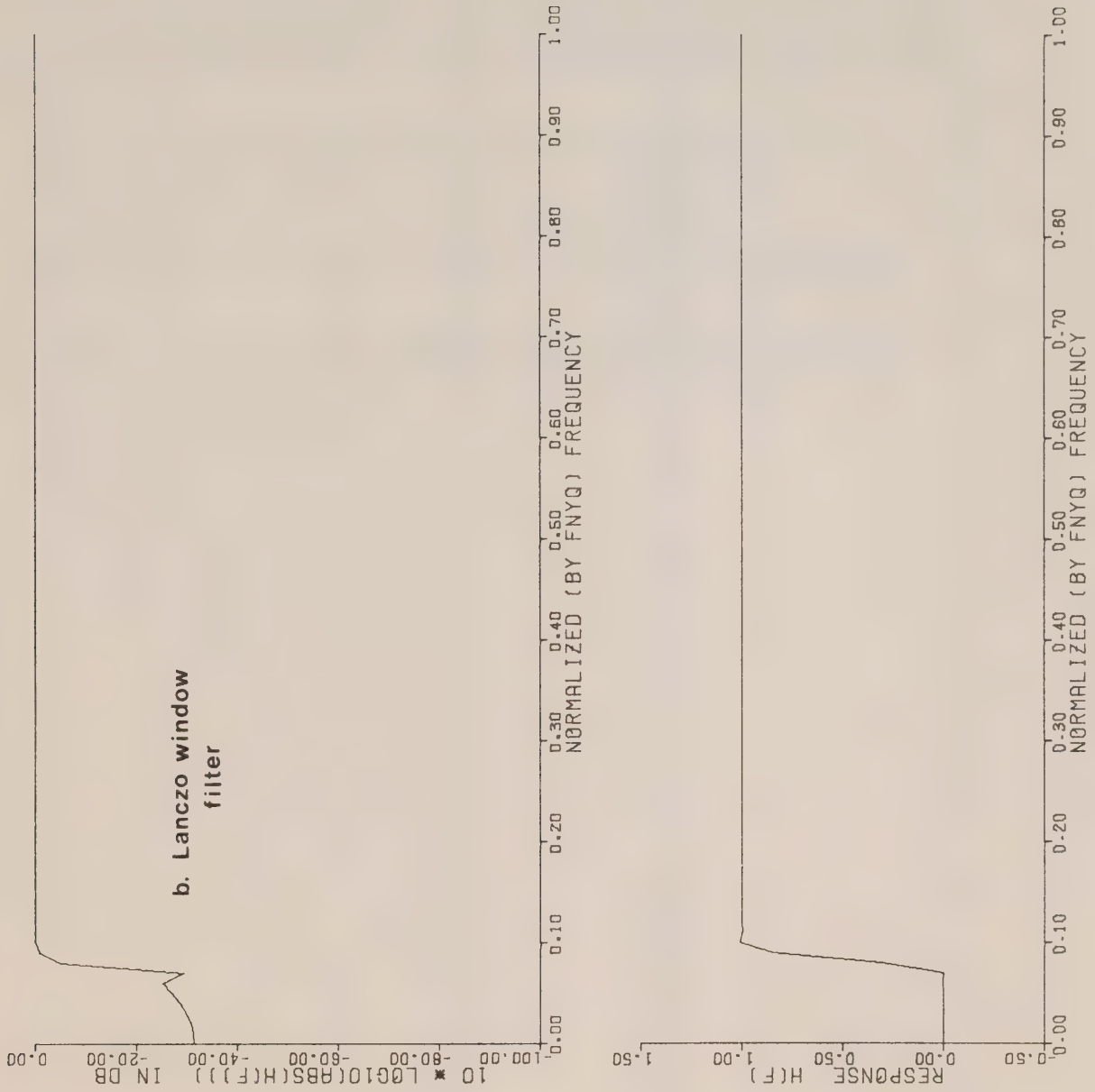


Figure 9. Input and output tidal height data for the high pass filters of Figure 8. Lower plot is the input; middle plot for the high pass filtered output, and the upper plot the output envelope. Heights are in millimetres and time is Pacific Standard Time. The top header gives the filter characteristics while each of the individual headers gives the start time of the record (minutes: hours: day: month: year), station identification, whether tidal constituents were removed, sampling period in minutes, gauge number and type of filter applied.

- a. Butterworth filter of the full tide-height record;
- b. Lanczos-window cosine filter of the full tide-height record;
- c. Butterworth filter of the tide-height record with major tidal harmonics subtracted out;
- d. Lanczos-window cosine filter of the tide-height record with major tidal harmonics subtracted out.

FIGURE 9

a. FILTER: BUTTERWORTH ORDER: 7 FCUT: .833300-002 CYC/MIN

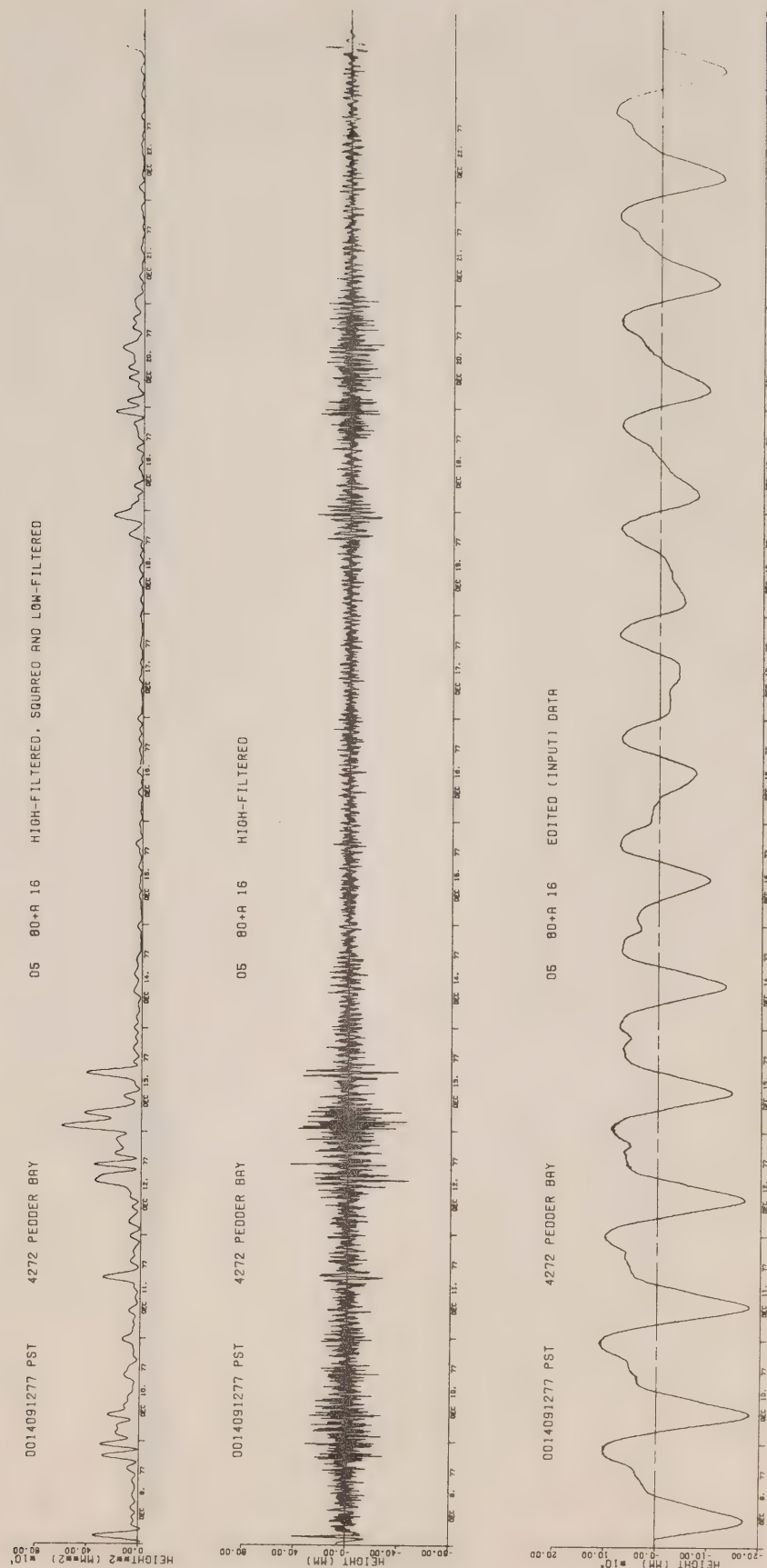


FIGURE 9

b. FILTER: IANCZ0 NUTS:100 FCUT: .83300-002 CYC/MIN

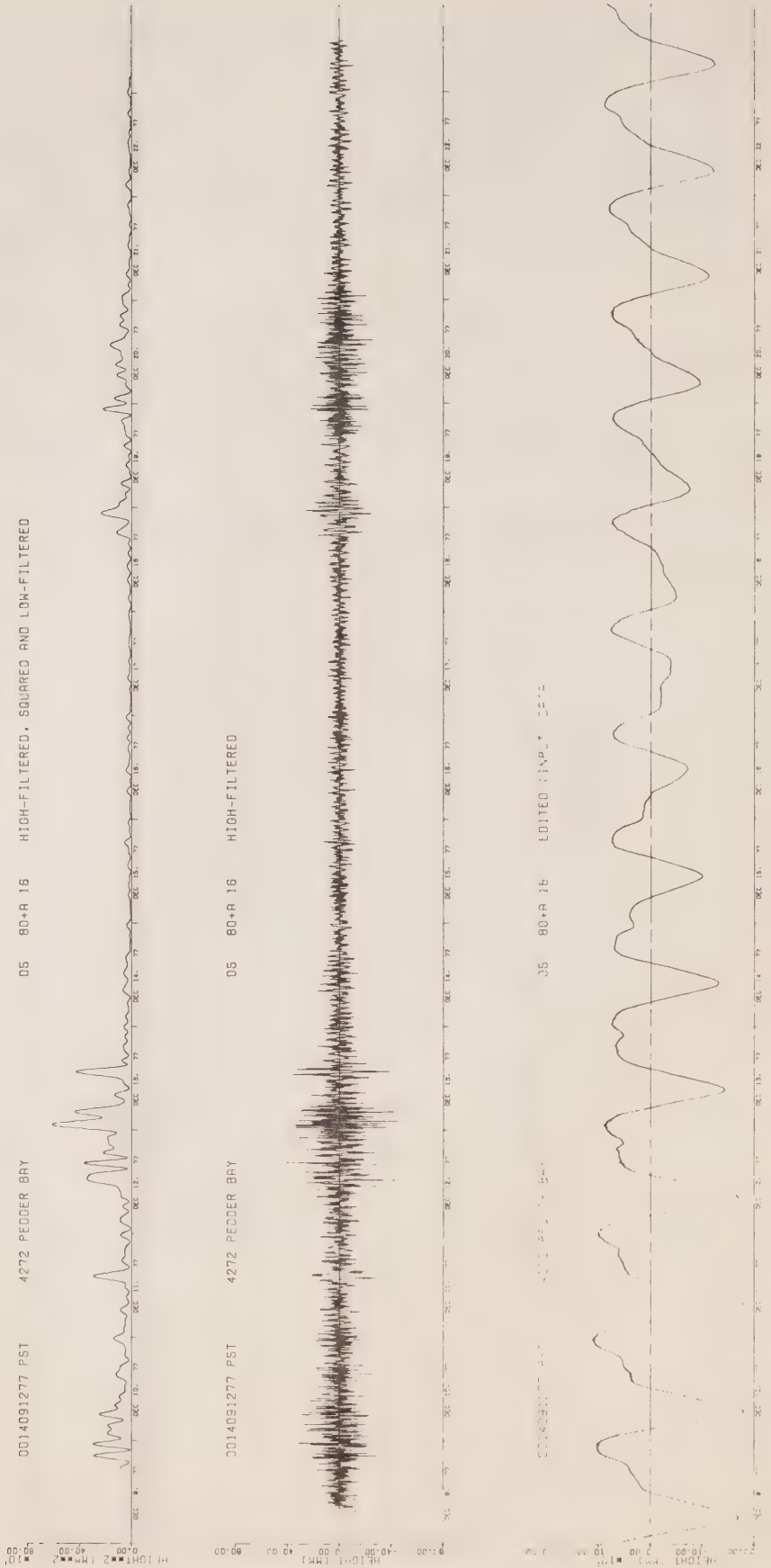


FIGURE 9

C. FILTER: BUTTERWORTH ORDER: 7 FCUT: .833300-002 CYC/MIN

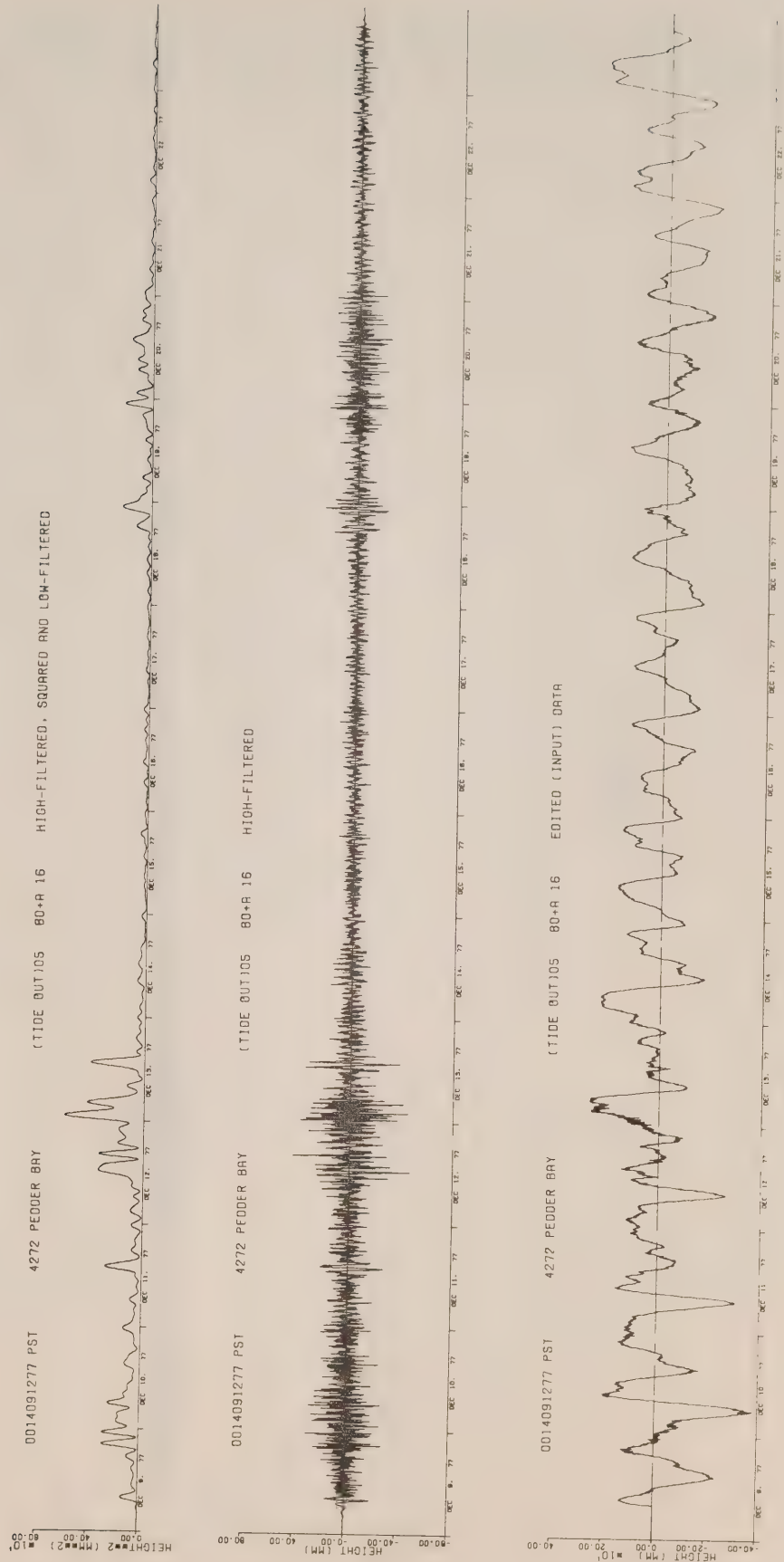


FIGURE 9

d. FILTER: LANCZ0 NWTS:100 FCUT: .833300-002 CYC/MIN

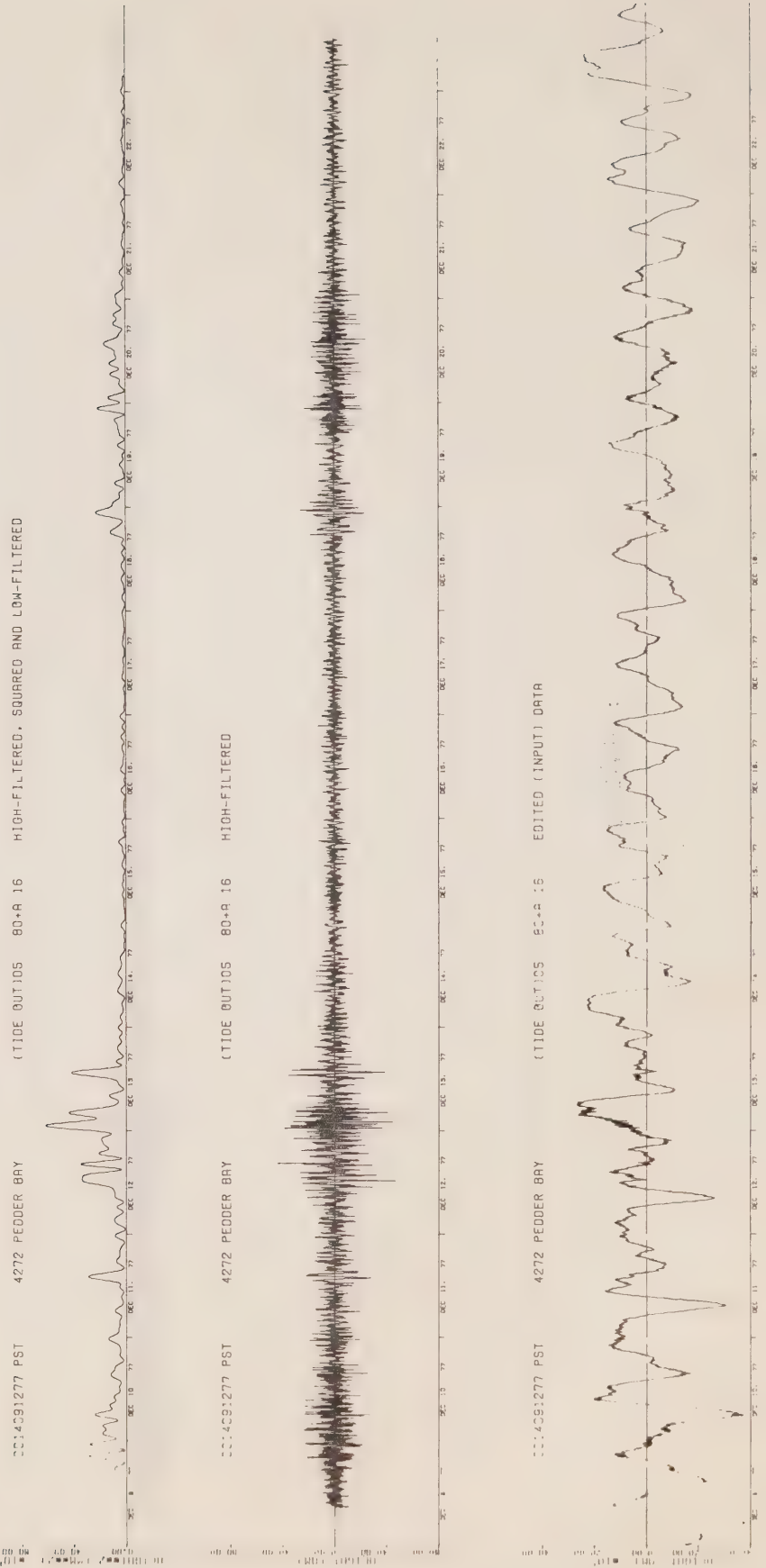


Figure 10. Frequency response curves for the low pass filters; cutoff frequency = 3.457×10^{-4} cpm and sampling frequency = 0.2 cpm.
a) Seventh order Butterworth filter. b) 400 term Lanczos-window cosine filter.

FIGURE 10

a. Butterworth Filter

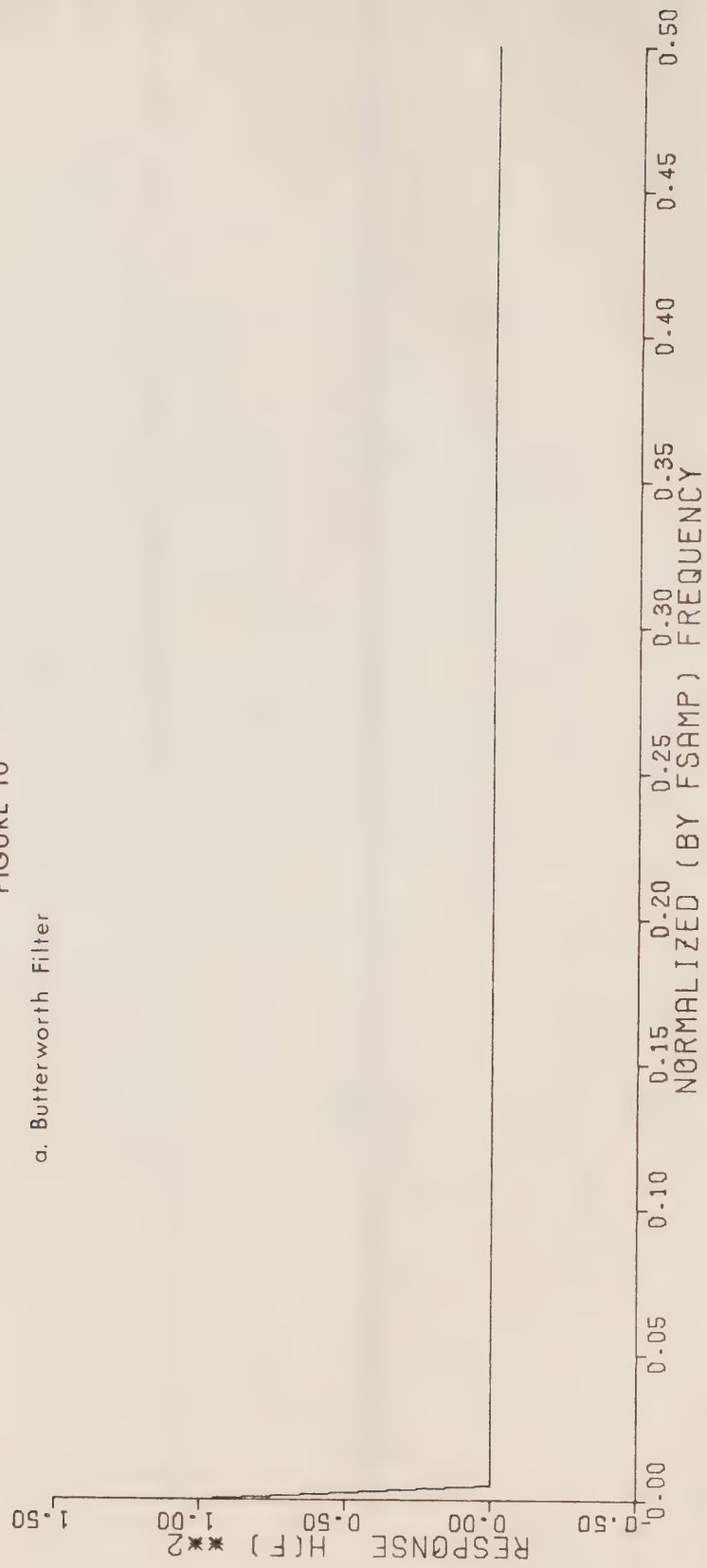


FIGURE 10

b. Lanczo window
filter

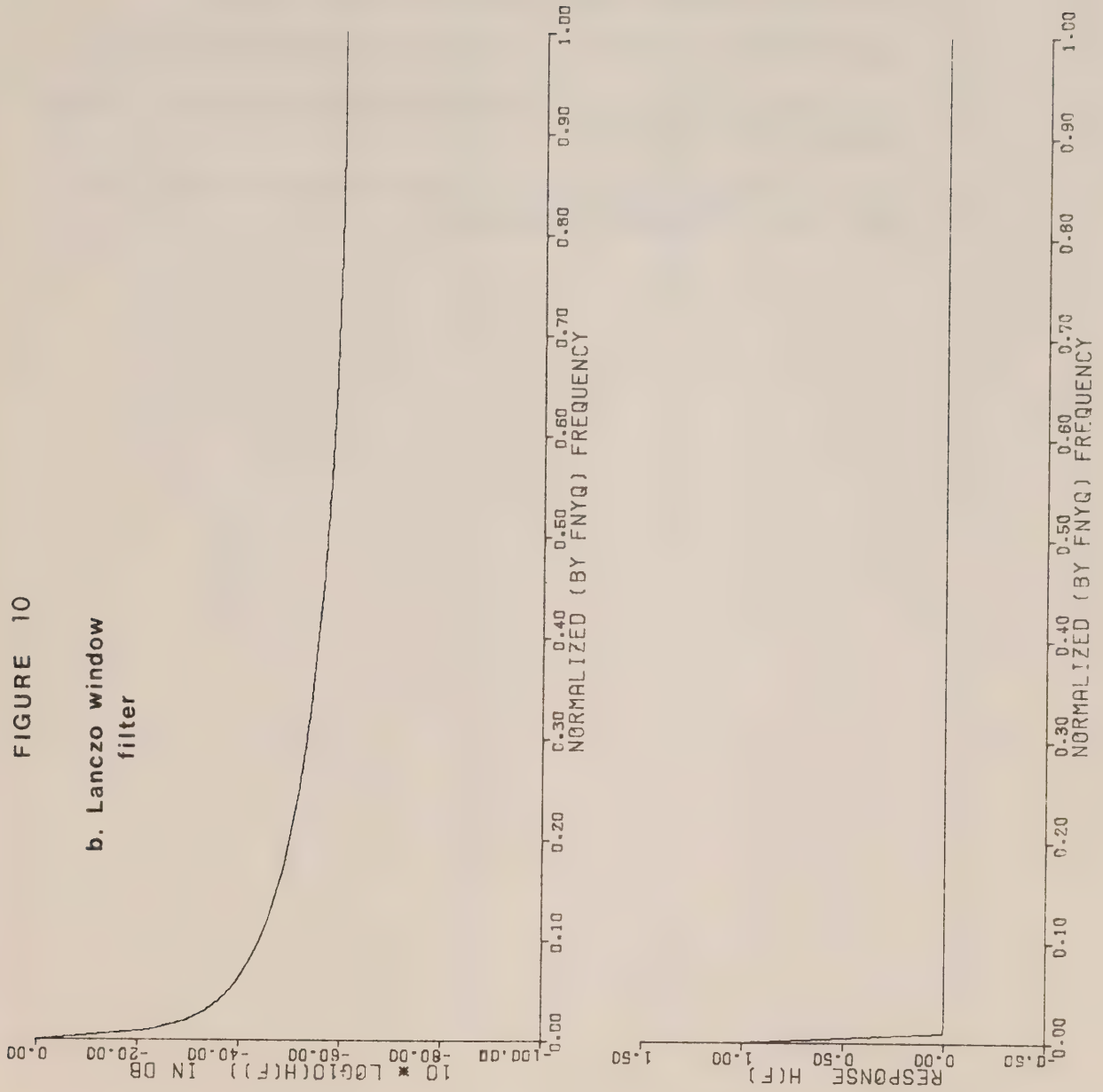


Figure 11. Input and output tidal height data for the low pass filters of Figure 10. Lower plot is the input, middle plot the low pass filtered output, and the upper plot the output envelope. Heights are in millimetres and time is Pacific Standard Time. Headers are the same as those described in Figure 9.

- a. Butterworth filter of the full tide-height record;
- b. Lanczos-window cosine filter of the full tide-height record;
- c. Butterworth filter of the tide-height record with major tidal harmonics subtracted out;
- d. Lanczos-window cosine filter of the tide-height record with major tidal harmonics subtracted out.

FIGURE 11

a. FILTER: BUTTERWORTH ORDER: 7 FCUT: .347222-003 CYC/MIN

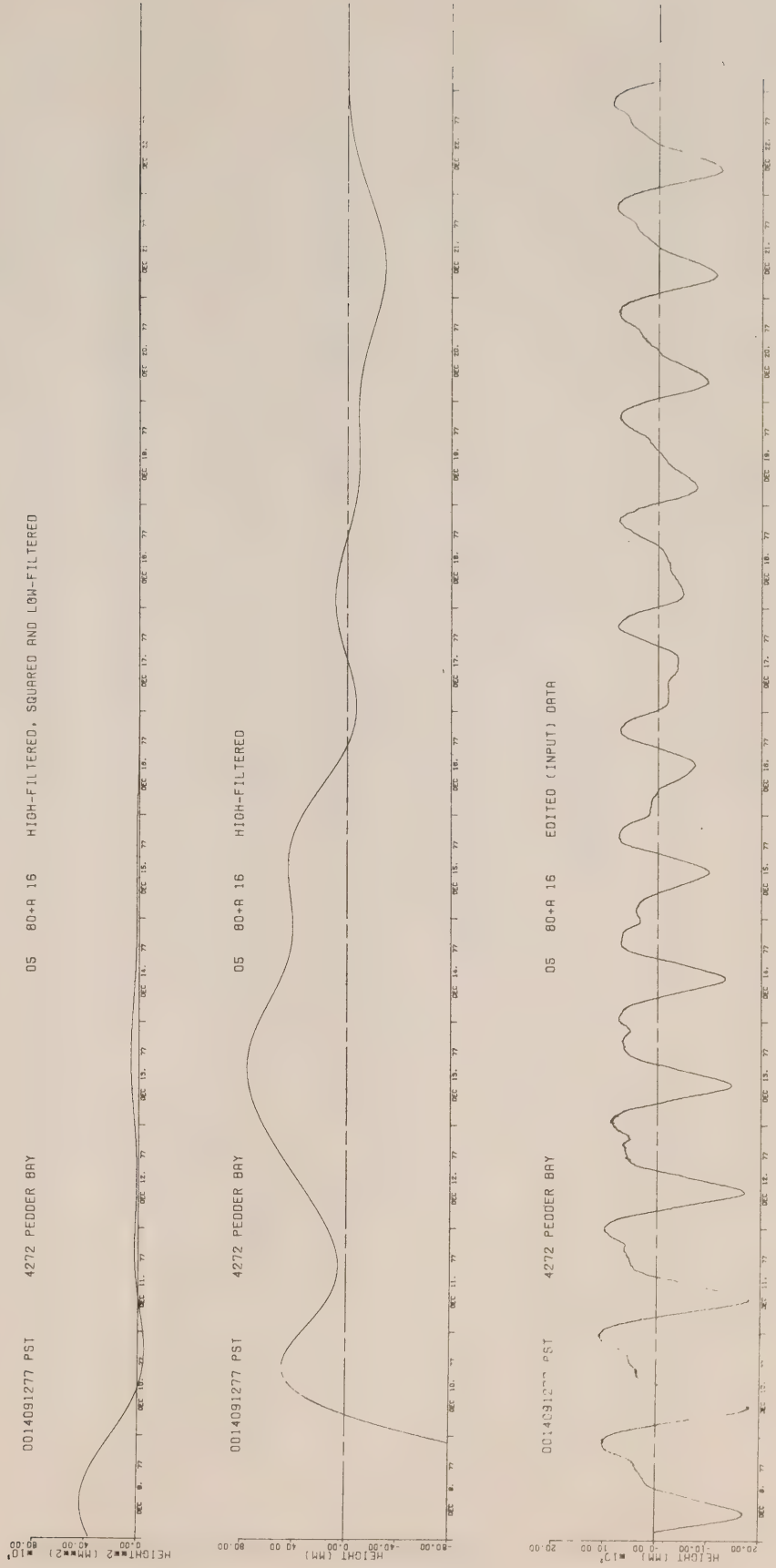


FIGURE 11

b. FILTER: LANCZOS NPTS:400 FCUT: .34722-003 CYC/MIN

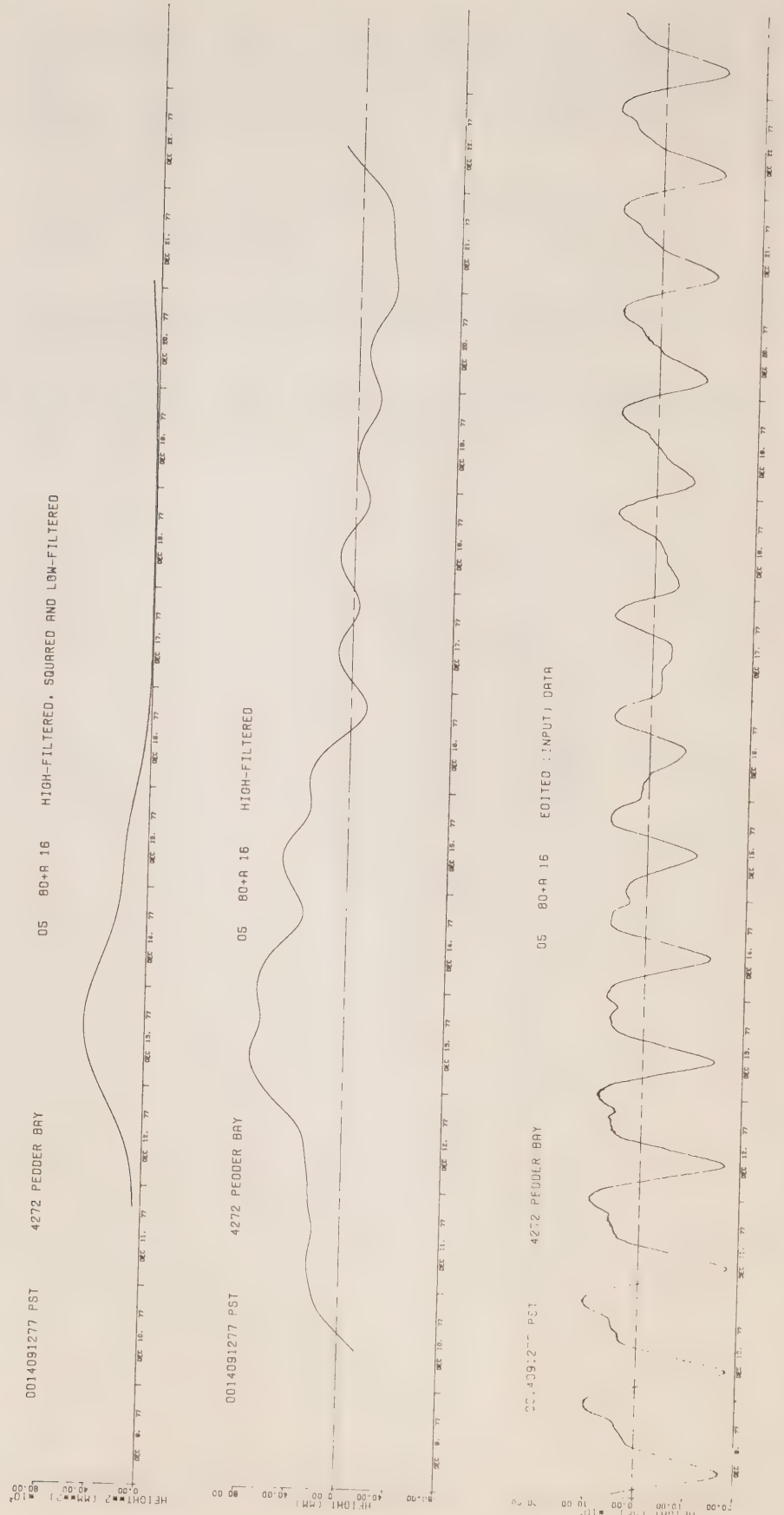


FIGURE 11

C. FILTER: BUTTERWORTH ORDER: 7 FCJT: .347222-003 CYC/MIN

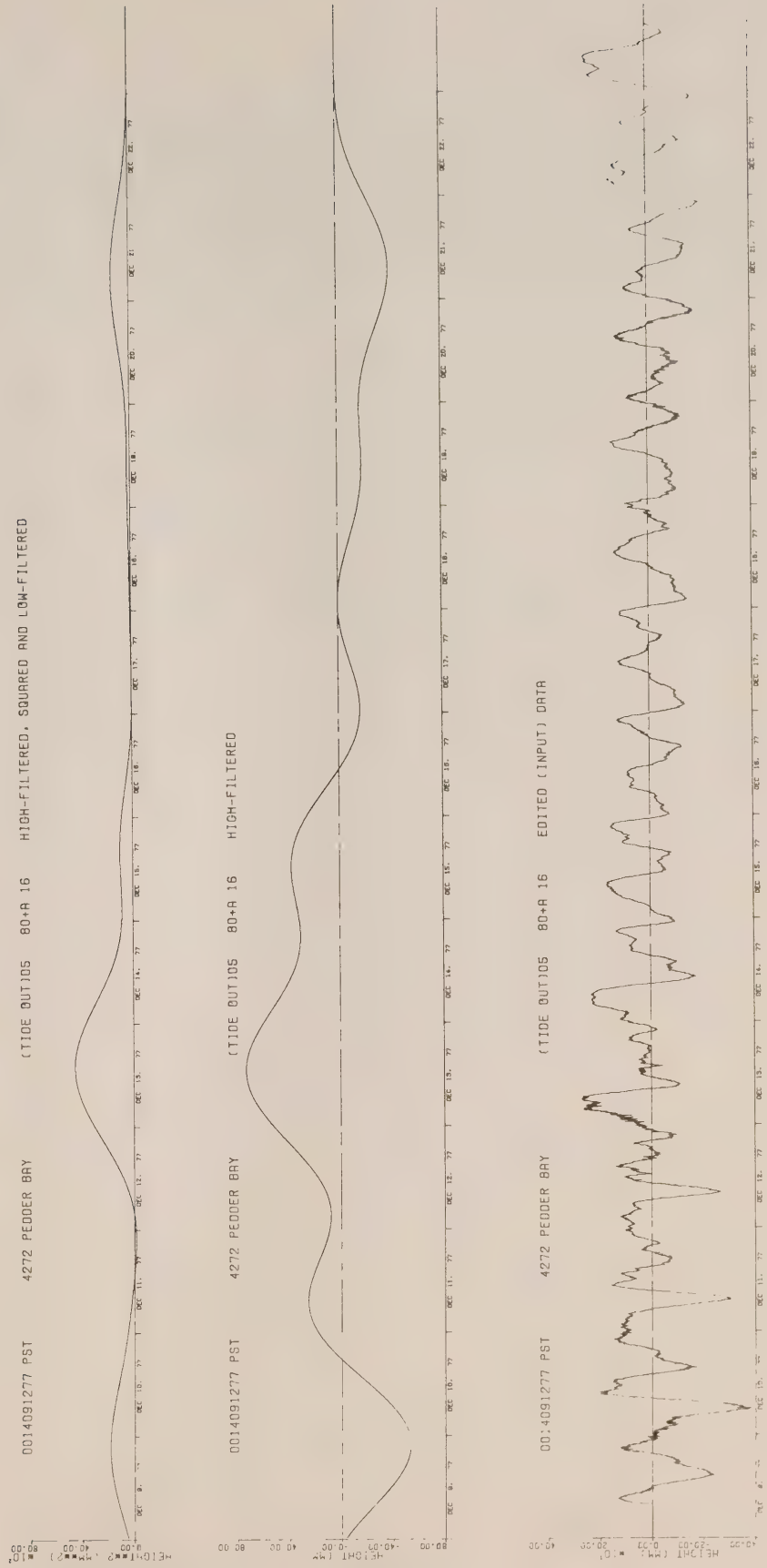
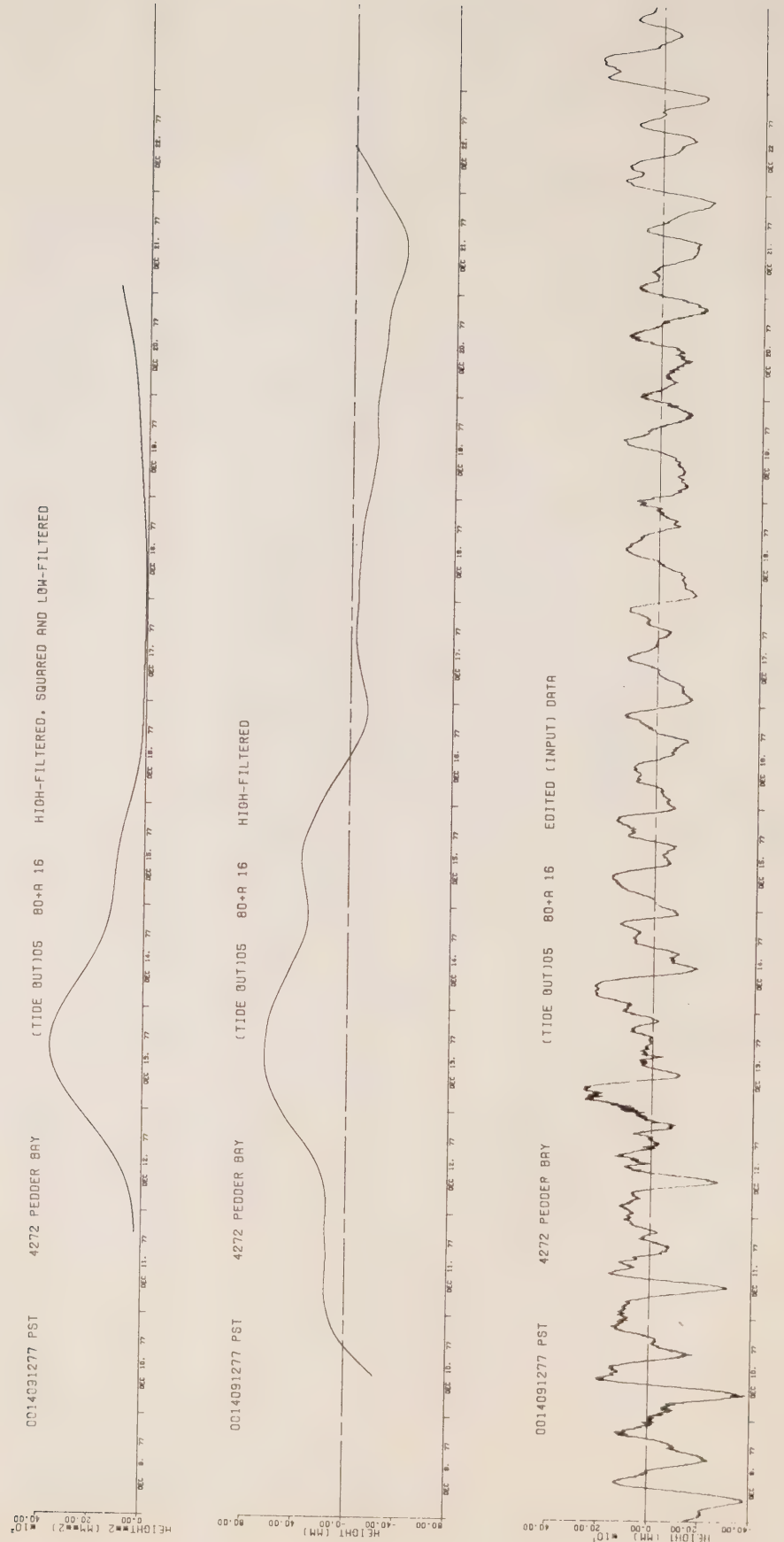


FIGURE 11

d. FILTER: LANCZ0 NMTS:400 FCUT: .347222-003 CYC/MIN



6. Acknowledgements

We thank J. Papadakis and T. Curran for constructive reviews of the manuscript, W. Butcher and D. Ramsden for helpful suggestions during the programme development and M. Foreman for assistance with the harmonic analysis of the tidal data. We also gratefully acknowledge F. Stephenson and M. Woodward for their effort in collecting the tidal data, A. Douglas and L. Kuwahara for helping analyse the recovered records, and A. Mathias for so carefully typing the manuscript.

References

- Digital Signal Processing Committee, 1979. Programs for Digital Signal Processing, the Institute of Electrical and Electronics Engineering Press, New York.
- Foreman, M., 1977. Manual for Tidal Heights Analysis and Prediction, Pacific Marine Science Report 77-10, Institute of Ocean Sciences, Sidney, B.C., 97 p.
- Hamming, R.W., 1977. Digital Filters, Prentice-Hall, Inc., Englewood Cliffs, New Jersey, 226 p.
- Kanasewich, E.R., 1973. Time Sequence Analysis in Geophysics, The University of Alberta Press, Edmonton, Alberta, 352 p.
- Rabiner, L.R., and B. Gold, 1975. Theory and Applications of Digital Signal Processing, Prentice-Hall, Inc., Englewood Cliffs, New Jersey. 762 p.
- Shannon, C.E. and W. Weaver, 1964. The Mathematical Theory of Communication, The University of Illinois Press, Urbana.

List of Figure Captions

- Figure 1. Linear time-invariant filtering viewed as a convolution in the time domain. Data are at times $n \cdot \Delta t$ where Δt is the sampling interval.
- Figure 2. Linear time-invariant filtering viewed as a multiplication in the frequency domain. In general the phase lag $\phi = \phi(f)$. Capitalized functions are the Fourier transforms of the lower case variable in Figure 1.
- Figure 3. An ideal rectangular transfer function (a) and its Fourier transform (b) in the time domain. The upper curve represents a band-limited function of amplitude unity in the range $\pm f_c = f / f_N$ and zero elsewhere. The lower curve is its normalized transform $a_k / (2f_c)$ where $k = 0, \dots, N-1$ (see § 4.1).
- Figure 4. Three forms of the transfer function for a low pass filter having a normalized cutoff frequency $f_c = f / f_N = 0.2$. The cosine Fourier expansion of the ideal rectangular filter has been truncated at $N = 10$ terms resulting in the overshoot ripples of Gibbs phenomenon in the unwindowed filter. The dotted curve represents the transfer function following application of the sigma factors of the Lanczos window. (Adapted from Hamming, 1977).
- Figure 5. A tapered data set. The data may be padded at one end only or at both ends.
- Figure 6. An example of the time and frequency responses of a simple Linear Time Invariant system having a complex-valued transfer function, $H(z)$. The impulse response $h(n) = a^n u^*(n)$ ($|a| < 1$) $u^* = 1$ for $n \geq 0$, $u^* = 0$ for $n < 0$). The function $H(z) = \sum_{n=0}^{\infty} (a/z)^n = 1/(1-a/z)$ where $z = \exp(i2\pi f)$.
- Figure 7. Location map for Pedder Bay. Depths in metres.
- Figure 8. Frequency response curves for the high pass filters; cutoff frequency = 8.33×10^{-3} cpm and sampling frequency = 0.2 cpm. a) seventh order Butterworth filter. b) 100 term Lanczos-window cosine filter.
- Figure 9. Input and output tidal height data for the high pass filters of Figure 8. Lower plot is the input; middle plot the high pass filtered output, and the upper plot the output envelope. Heights are in millimetres and time is Pacific Standard Time. The top header gives the filter characteristics while each of the individual headers gives the start time of the record (minutes: hours: day: month: year), station identification, whether tidal constituents were removed, sampling period in minutes, gauge number and type of filter applied.

- a. Butterworth filter of the full tide-height record;
- b. Lanczos-window cosine filter of the full tide-height record;
- c. Butterworth filter of the tide-height record with major tidal harmonics subtracted out;
- d. Lanczos-window cosine filter of the tide-height record with major tidal harmonics subtracted out.

Figure 10. Frequency response curves for the low pass filters; cutoff frequency = 3.47×10^{-4} cpm and sampling frequency = 0.2 cpm. a) Seventh order Butterworth filter. b) 400 term Lanczos-window cosine filter.

Figure 11. Input and output tidal height data for the low pass filters of Figure 10. Lower part is the input, middle plot the low pass filtered output, and the upper plot the output envelope. Heights are in millimetres and time is Pacific Standard Time. Headers are the same as those described in Figure 9.

- a. Butterworth filter of the full tide-height record;
- b. Lanczos-window cosine filter of the full tide-height record;
- c. Butterworth filter of the tide-height record with major tidal harmonics subtracted out;
- d. Lanczos-window cosine filter of the tide-height record with major tidal harmonics subtracted out.

Appendix A

Listing of Butterworth filter programme.

```

C *****
C *
C *      SUBROUTINES FOR:  BUTTERWORTH HIGH OR LOW PASS FILTER      *
C *
C *      BY : R.E.THOMSON AND K.Y.CHOW - MAY 1980                    *
C *
C *****
C
C THIS PROGRAM DESIGNS A BUTTERWORTH FILTER OF ORDER N (=1 TO 9) FOR
C A SPECIFIED CUTOFF FREQUENCY, FCUT, AND A GIVEN SAMPLING FREQUENCY,
C FSAMP, WHERE FSAMP=1/T FOR DIGITIZED SAMPLES (THE INPUT DATA)
C TAKEN T UNITS APART IN TIME OR SPACE.
C   THE BASIC DESIGN IS FOR A LOW-PASS FILTER, HOWEVER, PROVISION
C IS MADE FOR A HIGH-PASS FILTER IN WHICH THE HIGH-PASS DATA SET
C PH(M) IS OBTAINED BY SUBTRACTING THE LOW-PASS DATA SET PL(M) FROM
C THE ORIGINAL DATA SET X(M):  PH(M) = X(M)-PL(M)  WHERE DATA ARE
C AT M*T UNITS.
C   BUTTERWORTH FILTERS HAVE THE FOLLOWING CHARACTERISTICS:  THEY
C HAVE HIGH TANGENCY AT BOTH THE LOW AND HIGH FREQUENCY ENDS OF THE
C FREQUENCY SCALE (IE. AT F=0 AND F=FNYQ, THE NYQUIST FREQUENCY); THEY
C ARE MAXIMALLY FLAT IN BOTH THE PASSBAND AND STOPBAND, AND THEREFORE
C MONOTONIC IN THESE BANDS; THE AMPLITUDE OF THE FILTER FALLS BY 3 DB
C ( = 1/2 ) AT THE CUTOFF FREQUENCY AND THE NATURE OF THE FILTER IS
C SOLELY DETERMINED BY THE NORMALIZED CUTOFF FREQUENCY AND THE DESIRED
C AMOUNT OF ATTENUATION BETWEEN THE PASS AND STOPBANDS WHICH DETER-
C MINES N.
C   APPLICATION OF THE FILTER:  ALL INPUT FREQUENCIES, FIN, ARE NORM-
C ALIZED BY THE SAMPLING FREQUENCY, FSAMP=2*FNYQ, SO THAT F=FIN/FSAMP
C WITH  0 <= F <= 0.5 (NORMALIZED) AND FCO=FCUT/FSAMP (=FNYQ).  TO EN-
C SURE THAT THE FILTER RESPONSE DOESN'T INTRODUCE A FREQUENCY DEPENDENT
C PHASE SHIFT (IE. WE REQUIRE A ZERO PHASE FILTER), THE INPUT DATA IS
C FIRST RUN FORWARDS THEN BACKWARDS THROUGH THE FILTER.  HENCE THE
C TRANSFER FUNCTION OF FILTER, H(FIN), IS ACTUALLY THE SQUARED RES-
C PONSE: H(FIN)**2 = H(FIN)*H(-FIN).  THE RESPONSE FOR A LOW-PASS FIL-
C TER IS GIVEN BY H(FIN)**2 = 1/(1+(W/WCO)**(2*N)), AND FOR A HIGH
C PASS FILTER IS  H(FIN)**2 = (W/WCO)**(2*N)/(1+(W/WCO)**(2*N)),
C WHERE W=TAN(PI*F) AND WCO=TAN(PI*FCO).  TO AVOID ALIASING ERRORS
C ASSOCIATED WITH TAKING THE STANDARD Z-TRANSFORM FROM THE CONTIN-
C UOUS S-PLANE, WE USE THE BILINEAR Z-TRANSFORM GIVEN BY
C      Z = (1+I*W)/(1-I*W)  WHERE I=SQRT(-1).
C THIS TRANSFORM WARPS THE FREQUENCY SUCH THAT FOR 0 <= F <= 0.5
C WE GET 0 <= w <= INFINITY.  FINALLY, THE FILTER IS DESIGNED AS A
C CASCADE OF N/2 SECOND-ORDER BUTTERWORTH FILTERS AND ONE FIRST
C ORDER BUTTERWORTH FILTER (IF N IS AN ODD NUMBER).  THAT IS, THE
C OUTPUT FROM THE FIRST FILTER (OF ORDER 1 OR 2) IS PASSED THROUGH
C THE SECOND FILTER (OF ORDER 2), THEN THAT OUTPUT IS PASSED THRU
C THE THIRD FILTER (OF ORDER 2), AND SO ON UNTIL THE SUM OF THE
C FILTER ORDERS =N.  THE ORDER OF THE OUTPUT IS THEN REVERSED
C (Y(M) BECOMES Y(-M)) AND THE PROCESS IS REPEATED. (THE FILTER
C IS A RECURSIVE TYPE.)  WHEN THE TWO PASSES THRU THE FILTER IS COM-
C PLETE, THE DATA SET IS AGAIN REVERSED TO RESTORE THE ORIGINAL ORDER.
C   TO DETERMINE THE ORDER N OF THE FILTER WE SPECIFY THE DECREASE
C (IN DECIBARS) IN AMPLITUDE OF FILTER RESPONSE AT SOME FREQUENCY
C FD RELATIVE TO A REFERENCE LEVEL.  FOR A LOW PASS FILTER THE AM-
C PLITUDE IS 1 AT FIN=0 AND FOR A HIGH PASS FILTER THE AMPLITUDE IS
C 1 AT THE NYQUIST FREQUENCY, FNYQ=0.5*FSAMP.  THUS THE REFERENCE

```


C LEVEL IS 1 AND $N = 0.5 * (\log_{10}(10^{**}(D/10)) / \log_{10}(WFD/WCO))$, OR N CAN
 C BE APPROXIMATED BY $N = (D/20) / (\log_{10}(WFD/WCO))$ WHEN $10^{**}(D/10) \gg 1$.
 C D IS DECIBAR DECREASE . FOR A LOW PASS FILTER $FD > FCUT$; FOR A HIGH PASS
 C FILTER $FD < FCUT$. N SHOULD BE AS SMALL AS POSSIBLE TO AVOID
 C RINGING AND ROUND-OFF ERRORS.

C NOTE: WE WORK IN ROTATIONAL INPUT FREQUENCIES, FIN, IN UNITS OF
 C CYCLES PER (SECOND, MINUTE, METER,...). TO OBTAIN ANGULAR FREQUENCIES
 C $FRAD = 2*PI*FIN$.

C SUBROUTINES INCLUDED HERE ARE:

C BWDSGN(H,WCO,N,ANS) - DESIGN THE FILTER
 C BWTRAN(H) - PLOT THE TRANSFER FUNCTION
 C BWFILT(X,NDATA,N,WCO,Y,NLOST) - FILTER DATA IN ARRAY X

C ARRAYS USED ARE:

C X(8000) - INPUT DATA (EDITED)
 C H(101) - TRANSFER FCN SQUARED RESPONSE VALUES
 C P(8000) - FILTERED DATA

C - MAIN PROGRAM.

C REAL*8 WCO
 C REAL H(101), X(8000), P(8000)
 C CHARACTER*1 ANS
 C CALL PLOTS
 C CALL BWDSGN(H,WCO,N,ANS,FCUT)
 C CALL INPUT(X,NDATA,HEADER,DATE,INTERV)
 C CALL BWTRAN(H)
 C CALL BWFILT(X,NDATA,N,WCO,P,ANS,NLOST)
 C CALL PLOTND
 C STOP
 C END

C SUBROUTINE BWDSGN(H,WCO,N,ANS,FCUT)

C *****
 C *
 C * DESIGN THE APPROPRIATE FILTER BASED ON THE SAMPLING INTERVAL, *
 C * AND CUTOFF FREQUENCY. THE ORDER OF THE FILTER WILL BE DETERMINED *
 C * ALONG WITH THE TRANSFER FUNCTION (FREQUENCY RESPONSE) OF THE FIL-*
 C * TER. RETURNS: ARRAY H (SQUARED RESPONSE VALUES OF TRANS FCN) *
 C *
 C *****

C IMPLICIT REAL*8 (A-H,O-Z)
 C CHARACTER*1 ANS, SIGN/'<'/, NSPEC
 C REAL*8 PI/3.1415926535897932D0/
 C REAL H(101)

C - INPUT PARAMETERS FOR FILTER DESIGN.

C WRITE(6,10)
 C 10 FORMAT('0B U T T E R W O R T H HIGH OR LOW PASS FILTER ***'/
 C &'OWHAT IS YOUR SAMPLING PERIOD? (MINUTES)')

```

      READ(5,*) T
      FSAMP = 1.0D0/T
      FNYQ = 1.0D0/(2.0D0*T)

```

```

C
13  WRITE(6,15) FSAMP*0.5D0
15  FORMAT('0 DIMENSIONAL CUTOFF FREQ (CYC/MIN)? (FCUT <'F4.2,')')
      READ(5,*) FCUT
      FCO = FCUT*T
      IF(FCO.LT.0.5D0) GO TO 25

```

```

C
      WRITE(6,20)
20  FORMAT('0YOUR CUTOFF FREQUENCY EXCEEDS THE ALLOWABLE VALUE')
      GOTO 13

```

```

C
25  WCO = DTAN(PI*FCO)
      WRITE(6,30)
30  FORMAT('0DO YOU WANT A HIGH OR LOW PASS FILTER? (H/L)')
      READ(5,32) ANS
32  FORMAT(A1)
      WRITE(6,33)
33  FORMAT('0DO YOU WANT TO SPECIFY N? (Y/N)')
      READ(5,34) NSPEC
34  FORMAT(A1)
      IF (NSPEC.EQ.'Y') THEN
          WRITE(6,35)
35  FORMAT('0ENTER ORDER N OF FILTER:')
          READ(5,*) N
          GOTO 65
      END IF

```

```

C
36  WRITE(6,37)
37  FORMAT('///' WHAT IS THE AMPLITUDE DROP IN DECIBARS?')
      READ(5,*) D
      IF(ANS.EQ.'L') SIGN = '>'
      WRITE(6,40) SIGN
40  FORMAT('0AT WHICH FREQ. IS THIS DROP VALID? ( FD'A2,' FCUT )')
      READ(5,*) FD
      IF((ANS.EQ.'L').AND.(FD.GT.FCUT).OR.
      * (ANS.EQ.'H').AND.(FD.LT.FCUT)) GO TO 50
      WRITE(6,45)
45  FORMAT('0INVALID FD VALUE. MUST CHANGE')
      GO TO 36

```

```

C
C - CALCULATE ORDER OF THE FILTER.
C

```

```

50  WFD = DTAN(PI*FD/FSAMP)
      BN = 0.5 * LOG10(10.0**(D/10)-1.0) / DLOG10(DABS(WFD/WCO))
      N = DABS( DINT(BN) + DINT(BN-DINT(BN)+0.5D0) )
      WRITE(6,55) N
55  FORMAT('0THE ORDER OF THE FILTER IS',I5)
      IF(N.GE.1.AND.N.LE.9) GO TO 65
      WRITE(6,60)
60  FORMAT('0YOUR VALUE OF N IS OUTSIDE THE POSSIBLE LIMITS OF 1 AND'
      &' 9. INCREASE FD OR DECREASE DROP D IF N > 9')
      GOTO 36
65  IF(ANS.EQ.'H') GO TO 75

```

C

C - CALCULATE SET OF LOW PASS FILTERED DATA.

```

C
  DO 70 I=1,101
    W = DTAN(PI*(I-1)*0.005)
    TEMP = 1.000 + (W/WCO)**(2*N)
    H(I) = 1.000/TEMP
70  CONTINUE
    GO TO 85

```

C - CALCULATE SET OF HIGH PASS FILTERED DATA.

```

C
75  DO 80 I=1,101
    W = DTAN(PI*(I-1)*0.005)
    TEMP = (W/WCO)**(2*N)
    H(I) = TEMP/(TEMP+1.000)
80  CONTINUE
C
85  WRITE(6,90)
90  FORMAT('0','*** BUTTERWORTH FILTER NOW DESIGNED ***')
    RETURN
    END

```

C SUBROUTINE BWTRAN(YVAL)

```

C
C *****
C *
C * ROUTINE TO PLOT A GRAPH OF THE BUTTERWORTH TRANSFER FUNCTION.
C * YVAL IS AN ARRAY OF SQUARED RESPONSE VALUES. X-VALUES, THE NOR-
C * MALIZED FREQUENCIES RANGING FROM 0.0 TO 0.5,
C *
C *****

```

C REAL YVAL(101)

C - OUTPUT TABLE OF SQUARED RESPONSE VALUES AND PLOT AXES.

```

C
  WRITE(6,70)
70  FORMAT('1*** TABLE OF RESPONSE VALUES ***'///
    *'-NORM.FREQ.      AMPLITUDE')
85  DO 90 I=1,101
    WRITE(6,95) (I-1)*0.01,YVAL(I)
95  FORMAT(' ',F5.2,' ',F10.5)
90  CONTINUE
C
  CALL AXIS(1.0,1.0,'NORMALIZED (BY FSAMP) FREQUENCY',-31,
    *10.0,0.0,0.0,0.05)
  CALL AXIS(1.0,1.0,'RESPONSE H(F) **2',18,4.0,90.0,-0.5,0.5)

```

C - PLOT ACTUAL GRAPH.

```

C
  CALL PLOT(1.0,1.0,-3)
  CALL PLOT(0.0,YVAL(1)*2.0+1.0,3)
  DO 20 I = 2,101
    CALL PLOT((I-1)*0.1,YVAL(I)*2.0+1.0,2)
20  CONTINUE
  CALL FRAME
  WRITE(6,30)

```

```

30  FORMAT('0*** BW TRANSFER FUNCTION NOW PLOTTED ***')
    RETURN
    END

C
    SUBROUTINE BWFILT(X,NDATA,N,WCO,Y,ANS,NLOST)
C
C *****
C *
C * SUBROUTINE TO APPLY A CASCADE OF SECOND ORDER FILTERS TO DATA IN
C * ARRAY X TO OBTAIN THE FILTERED DATA IN ARRAY Y AS EXPLAINED ABOVE
C * A FIRST ORDER FILTER IS ALSO APPLIED IF THE ORDER N IS AN ODD
C * INTEGER.  CONSTANTS USED THE FIRST TIME THRU ARE NOT CALCULATED
C * AGAIN.
C *
C *****
C
    IMPLICIT REAL*8 (A-H,O-Z)
    REAL*8 PI/3.1415926535897932D0/,WCO
    REAL ORIG(8000),TEMP(8000),X(NDATA),Y(NDATA)
    INTEGER TEST
    CHARACTER*1 ANS

C
C - THE VARIABLE TEST HAS VALUE '1' IF N IS ODD, OR '0' IF N IS EVEN
C
    TEST = MOD(N,2)

C
C - SAVE ORIGINAL DATA ARRAY X
C
    DO 3 I=1,NDATA
        ORIG(I) = X(I)
    3  CONTINUE

C
C - LOOP TO HANDLE TWO PASSES THRU DATA (FORWARD AND BACKWARD).
C
    DO 70 L=1,2
        IF(TEST.EQ.0) GO TO 15

C
C - FIRST ORDER FILTER (USED IF N IS ODD).
C
        CO = WCO/(1.0D0+WCO)
        C1 = CO
        B1 = (1-WCO)/(1+WCO)
        Y(1) = CO*X(1)
        DO 10 I=2,NDATA
            Y(I) = CO*X(I)+C1*X(I-1)+B1*Y(I-1)
        10  CONTINUE
        IF(N.EQ.1.AND.L.EQ.1) GO TO 55
        IF(N.EQ.1.AND.L.EQ.2) GO TO 71
        IF(TEST.EQ.1) GO TO 25

C
C - SET INPUT ARRAY X TO Y IF N IS EVEN
C
        15  DO 20 I=1,NDATA
            Y(I) = X(I)
        20  CONTINUE

C
C - CASCADE OF SECOND ORDER FILTERS.

```



```

C
25  AA = 1.0D0+WCO**2
    DO 50 J=1,(N-TEST)/2
      A = AA + 2.0D0*WCO*DSIN(PI*(J*2-1)/FLOAT(2*N))
      CO = (WCO**2)/A
      C1 = 2.0D0*CO
      C2 = CO
      B1 = -C1+2.0D0/A
      B2 = (A-2.0D0*AA)/A
      DO 30 I=1,NDATA
        TEMP(I) = Y(I)
30  CONTINUE
    Y(1) = CO*TEMP(1)
    Y(2) = CO*TEMP(2)+C1*TEMP(1)+B1*Y(1)
    DO 40 I=3,NDATA
      Y(I) = CO*TEMP(I)+C1*TEMP(I-1)+C2*TEMP(I-2)+B1*Y(I-1)
      *      +B2*Y(I-2)
40  CONTINUE
50  CONTINUE
    IF(L.EQ.2) GO TO 71
C
C - REVERSE DATA IF ONLY FIRST PASS THRU CASCADE.
C
55  DO 60 I=1,NDATA
      X(I) = Y(NDATA+1-I)
60  CONTINUE
70  CONTINUE
C
C - INVERT OUTPUT AND DETERMINE IF H/L PASS DATA SET IS TO OUTPUT.
C
71  DO 78 I=1,NDATA/2
      TEMP(I) = Y(NDATA+1-I)
      Y(NDATA+1-I) = Y(I)
      Y(I) = TEMP(I)
78  CONTINUE
    IF(ANS.EQ.'L') GOTO 90
C
C - EXECUTE ONLY IF HIGH-PASS FILTER WANTED.
C
    DO 80 I=1,NDATA
      Y(I)=ORIG(I)-Y(I)
80  CONTINUE
C
C - PRINT OUT FIRST 50 VALUES OF FILTERED DATA FOR CHECKING.
C
90  NLOST = 0
    DO 100 I=1,50
      WRITE(6,110) Y(I)
110  FORMAT(' ',F14.5)
100  CONTINUE
    WRITE(6,130)
130  FORMAT('0*** DATA NOW FILTERED ***')
    RETURN
    END

```


Appendix B

Listing of Lanczos-window cosine filter programme.

```

C *****
C *
C *   SUBROUTINES FOR : LANCZO-WINDOW, LOW OR HIGH PASS FILTER
C *
C *   BY : R.E.THOMSON AND K.Y.CHOW - MAY 1980
C *
C *****
C
C THIS PROGRAM CREATES A LOW OR HIGH PASS STEP-TYPE FILTER WITH A
C LANCZO-WINDOW TO ELIMINATE RIPPLES IN THE PASS AND STOP BANDS THAT
C RESULT FROM GIBBS PHENOMENON. THE TRANSFER FUNCTION H OF THE FILTER
C IS REAL SO THAT IT PRODUCES ZERO PHASE SHIFT. DOUBLE PRECISION HAS
C BEEN USED TO REDUCE ROUND OFF ERRORS.
C
C APPLICATION OF THE FILTER :
C ALL INPUT FREQUENCIES, FIN, ARE NORMALIZED BY THE NYQUIST FREQUENCY.
C THE CUTOFF FREQUENCY, FCUT, MUST LIE IN THE INTERVAL 0 < FCUT < FNYQ
C AND FOR BEST RESULTS, BE SIGNIFICANTLY REMOVED FROM THE ENDS OF
C THIS INTERVAL. SINCE THE FILTER IS BASED ON A NONRECURSIVE RELATION
C FOR WEIGHTING THE INPUT DATA, THE NUMBER N OF DESIRED WEIGHTS MUST
C BE SPECIFIED.
C FOR EACH FILTER DESIGN, THERE IS A BEST N: INCREASING N INCREASES
C THE SMOOTHNESS OF THE FILTER AND THE SHARPNESS OF THE CUTOFF BUT ALSO
C INCREASES THE AMOUNT OF DATA LOST FROM EITHER END OF THE DATA SET.
C (=N DATA VALUES FROM EACH END). AN INITIAL CHOICE N=50 APPEARS SUIT-
C ABLE FOR MOST APPLICATIONS. (DEPENDENT ON INITIAL PARAMETERS.)
C
C THE TRANSFER FUNCTION H(F) OF THE FILTER HAS THE FOLLOWING FORM:
C
C   
$$H(F) = A(0)/2 + \text{SUM}( A(K)*\text{COS}(PI*K*F) )$$

C
C WHERE THE A'S ARE CONSTANT FOR K=1 TO N-1, N IS THE NUMBER OF WEIGHTING
C TERMS OF THE FILTER IMPULSE RESPONSE, AND F IS THE NORMALIZED FRE-
C QUENCY. FOR A LOW PASS FILTER,
C
C   
$$A(0) = 2*FCUT/FNYQ = 2*F$$

C   
$$A(K) = A(0)*\text{SIGMA}*\text{SIN}(K*F*PI)/(K*F*PI)$$

C
C WHILE FOR A HIGH PASS FILTER
C
C   
$$A(0) = 2*(1-F)$$

C   
$$A(K) = -2*F*\text{SIGMA}*\text{SIN}(K*F*PI)/(K*F*PI)$$

C
C WHERE THE FACTOR  $\text{SIGMA} = \text{SIN}(PI*K/N)/(PI*K/N)$  IS THE LANCZO-
C WINDOW WHICH AVERAGES OUT THE RIPPLES IN THE FREQUENCY DOMAIN OF
C THE STEP-LIKE TRANSFER FUNCTION.
C
C THE DIGITAL WEIGHTS (IMPULSE RESPONSES) ARE GIVEN BY THE  $A(K)/2$  WHERE
C  $A(K) = A(-K)$ .
C
C SUBROUTINES USED ARE:
C
C LZDSGN(H,FCO,N,A,A0,ANS,FCUT)      - DESIGN THE FILTER
C LZTRAN(H)                          - PLOT THE TRANSFER FUNCTION
C LZWTS(A,A0,N)                      - PLOT THE WEIGHTING TERMS
C LZFILT(N,FCO,X,NDATA,P,ANS,NLOST) - FILTER DATA IN ARRAY X

```

```

C
C   ARRAYS USED ARE:
C
C   X(8000)           - INPUT DATA (EDITED)
C   A(400)            - WEIGHTING TERMS
C   H(101)            - TRANSFER FCN RESPONSE VALUES
C   P(NDATA-2*N)      - FILTERED DATA
C
C
C   SUBROUTINE LZDSGN(H,FCO,NWTS,A,A0,ANS,FCUT)
C
C *****
C *
C *   DESIGN THE APPROPRIATE FILTER BASED ON THE SAMPLING INTERVAL,
C *   DESIRED CUTOFF FREQUENCY AND THE NUMBER OF WEIGHTING TERMS. THIS
C *   SUBROUTINE ALSO DETERMINES THE TRANSFER FUNCTION (FREQ. RESPONSE)
C *   OF THE FILTER
C *
C *   RETURNS:  ARRAY H (RESPONSE VALUES OF TRANSFER FUNCTION)
C *
C *****
C
C   IMPLICIT REAL*8 (A-H,O-Z)
C   REAL*8 PI/3.1415926535897932D0/, A(400)
C   REAL H(101)
C   CHARACTER*1 ANS
C
C - DETERMINE THE NYQUIST FREQUENCY FOR THE INPUT DATA USING T, THE
C - SAMPLING PERIOD.
C
C   WRITE(6,4)
C   4  FORMAT('1L A N C Z O - W I N D O W  HIGH OR LOW PASS FILTER ***'/)
C   5  WRITE(6,10)
C   10 FORMAT('0WHAT IS THE SAMPLING PERIOD? (MINUTES)')
C   READ(5,*) T
C   FNYQ = 1.0D0/(2.0D0*T)
C
C - SPECIFY DIMENSIONAL CUTOFF FREQUENCY, FCUT, USING SAME UNITS AS
C - FNYQ AND THEN NONDIMENSIONALIZE.
C
C   WRITE(6,20) FNYQ
C   20  FORMAT('0DIMENSIONAL CUTOFF FREQ (CYC/MIN)? (FCUT <'F7.4,')')
C   READ(5,*) FCUT
C   FCO = FCUT/FNYQ
C
C - TEST IF CUTOFF FREQUENCY, FCO, IS ACCEPTABLE OR NOT
C
C   IF(FCO.LT.1.0D0) GO TO 40
C   WRITE(6,35)
C   35  FORMAT('0YOUR CUTOFF FREQUENCY EXCEEDS THE ALLOWABLE VALUE'/
C   *'0CHECK YOUR SPECIFICATIONS AGAIN')
C   GO TO 5
C
C - SPECIFY THE NUMBER OF WEIGHTING TERMS REQUIRED, 10<= N<= 500.
C
C   40  WRITE(6,45)
C   45  FORMAT('0WHAT IS THE NUMBER OF WEIGHTING TERMS REQUIRED?')

```

```
      READ(5,*) NWTS
```

```
C
C - DO YOU WANT A HIGH OR LOW PASS FILTER?
C
```

```
      WRITE(6,70)
```

```
70  FORMAT('DO YOU WANT A HIGH OR LOW PASS FILTER? (H/L)')
```

```
      READ(5,75) ANS
```

```
75  FORMAT(A1)
```

```
C
C - CALCULATE WEIGHTING TERMS FOR HIGH/LOW PASS TRANSFER FUNCTION.
C
```

```
      IF (ANS.EQ.'L') THEN
```

```
        A0 = 2*FC0
```

```
        DO 80 K=1,NWTS
```

```
          SIGMA = DSIN(K*PI/NWTS)/(K*PI/NWTS)
```

```
          A(K) = SIGMA*2*DSIN(K*PI*FC0)/(K*PI)
```

```
80    CONTINUE
```

```
1000  FORMAT(F15.5)
```

```
      ELSE
```

```
        A0 = 2*(1-FC0)
```

```
        DO 90 K=1,NWTS
```

```
          SIGMA = DSIN(K*PI/NWTS)/(K*PI/NWTS)
```

```
          A(K) = -SIGMA*2*DSIN(K*PI*FC0)/(K*PI)
```

```
90    CONTINUE
```

```
      END IF
```

```
C
C - CALCULATE TRANSFER FUNCTION.
C
```

```
      DO 110 J=1,101
```

```
        SUM = 0.000
```

```
        DO 100 K=1,NWTS
```

```
          SUM = SUM + A(K)*DCOS(K*PI*(J-1)/100)
```

```
100    CONTINUE
```

```
        H(J) = A0/2 + SUM
```

```
110  CONTINUE
```

```
C
C - THIS IS THE TRANSFER FUNCTION FOR NORMALIZED FREQUENCIES  $0 \leq F \leq 1$ ,
C - OR  $0 \leq F_{IN} \leq F_{NYQ}$ . FOR THE LOW PASS FILTER,  $H(1)=1$ ,  $H(101)=0$ .
C - FOR THE HIGH PASS FILTER,  $H(1)=0$ ,  $H(101)=1$ .
C
```

```
      WRITE(6,120)
```

```
120  FORMAT('0*** FILTER IS NOW DESIGNED ***')
```

```
      RETURN
```

```
      END
```

```
C
C SUBROUTINE LZTRAN(H)
```

```
C *****
C *
C * ROUTINE TO PLOT 2 GRAPHS OF THE TRANSFER FUNCTION: (1) H(F) VS
C * NORMALIZED FREQUENCIES AND (2)  $10 \cdot \log_{10}(\text{ABS}(H(F)))$  VS NORMALIZED
C * FREQUENCIES. H(F) RANGES FROM 0 TO 1 IN STEPS OF 0.01.
C *
C *****
```

```
      REAL H(101), H1(101)
```


C - CALCULATE LOG RESPONSE , ARRAY H1.

```

C
  DO 5 I=1,101
  IF(H(I) .NE. 0.)GO TO 2
  H1(I)=-100.
  GO TO 5
2 H1(I)=10*LOG10(ABS(H(I)))
5 CONTINUE

```

C
C - OUTPUT TABLE OF RESPONSE VALUES AND PLOT X,Y AXES.

```

C
  WRITE(6,70)
70  FORMAT('1*** TABLE OF RESPONSE VALUES ***'///
*' NORM. FREQ.      AMPLITUDE      AMPLITUDE (IN DB)'/)
  DO 999 I=1,101
    WRITE(6,888) (I-1)*0.01, H(I), H1(I)
888  FORMAT(' ',F5.2,' ',F10.5,' ',F10.5)
999  CONTINUE

```

```

C
  CALL AXIS(1.0,1.0,'NORMALIZED (BY FNYQ) FREQUENCY',-30,
*10.0,0.0,0.0,0.1)
  CALL AXIS(1.0,1.0,'RESPONSE H(F)',14,4.0,90.0,-0.5,0.5)

```

C
C - PLOT GRAPH OF H(F) VS NORM. FREQ..

```

C
  CALL PLOT(1.0,1.0,-3)
  CALL PLOT(0.0,H(1)*2.0+1.0,3)
  DO 20 I = 2,101
    CALL PLOT((I-1)*0.1,H(I)*2.0+1.0,2)
20  CONTINUE

```

```

C
  CALL AXIS(0.0,5.0,'NORMALIZED (BY FNYQ) FREQUENCY',-30,
*10.0,0.0,0.0,0.1)
  CALL AXIS(0.0,5.0,'10 * LOG10(ABS(H(F))) IN DB',28,5.0,
*90.0,-100.0,20.0)

```

C
C - PLOT GRAPH OF 10*LOG10(ABS(H(F))) VS NORM.FREQ.

```

C
  CALL PLOT(0.0,5.0,-3)
  IF (H1(1).LT.-100.0) H1(1)= -100.0
  CALL PLOT(0.0,H1(1)*0.05+5.0,3)
  DO 25 I = 2,101
    IF (H1(I).LT.-100.0) H1(I)= -100.0
    CALL PLOT((I-1)*0.1,H1(I)*0.05+5.0,2)
25  CONTINUE

```

```

C
  CALL FRAME
  WRITE(6,30)
30  FORMAT('0*** TRANSFER FUNCTION IS NOW PLOTTED ***')
  RETURN
  END

```

```

C
  SUBROUTINE LZWTS(A,A0,NWTS)

```

```

C *****
C *
C * ROUTINE TO PLOT THE WEIGHTING TERMS FOR THE FILTER DESIGNED IN *

```



```

C * 'LZDSGN' IN A GRAPH OF WEIGHT VS NORMALIZED FREQUENCY.
C *
C *****
C
    REAL*8 A(400), A0
C
C
    CALL AXIS(1.0,1.0,'NORMALIZED FREQUENCY',-20,10.,
*0.0,0.0,.1)
    CALL AXIS(1.0,1.0,'WEIGHTING VALUE',15,6.0,90.0,-1.0,0.5)
    CALL PLOT(1.0,1.0,-3)
    TEMP = A0
    CALL PLOT(0.0,TEMP*2.0+2.0,3)
    DO 20 I=1,NWTS-1
        TEMP = A(I)
        CALL PLOT(I*(10./NWTS),TEMP*2.0+2.0,2)
20  CONTINUE
    WRITE(6,22) A0
22  FORMAT('0*** WEIGHTING TERMS ***'/'0 0',F10.4)
    DO 26 I=1,NWTS-1
        WRITE(6,24) I,A(I)
24  FORMAT(' ',I3,F10.4)
        SUMWTS = SUMWTS + 2*A(I)/2
26  CONTINUE
    WRITE(6,28) A0/2+SUMWTS
28  FORMAT('0*** SUM OF WEIGHTING TERMS (BOTH SIDES): ',F7.4,' ***')
    CALL FRAME
    WRITE(6,30)
30  FORMAT('0*** WEIGHTING VALUES ARE NOW PLOTTED ***')
    RETURN
    END
C
    SUBROUTINE LZFILTER(NWTS,FCO,X,NDATA,P,ANS,NLOST)
C
C *****
C *
C * ROUTINE TO GENERATE DIGITAL DATA USING THE LANCOZ-WINDOW FILTER *
C * (HIGH OR LOW PASS). THE IMPULSE RESPONSE (IE.WEIGHTS) OF THE FIL- *
C * TER IS GIVEN BY THE COEFFICIENTS  $A(K)/2 = A(-K)/2$ . FOR A GIVEN N *
C * TERMS OF THE FILTER, THERE ARE N-1 VALUES LOST FROM EITHER END OF *
C * THE DATA SET, THE FIRST FILTERED VALUE OCCURRING AT  $P(N+1) = P(1)$ . *
C * RETURNS: ARRAY P (FILTERED DATA SET - HIGH OR LOW) *
C *
C *****
C
    IMPLICIT REAL*8 (A-H,O-Z)
    CHARACTER*1 ANS
    REAL*8 PI/3.1415926535897932D0/, A(400)
    REAL P(NDATA-2*NWTS), X(NDATA)
C
C - CALCULATE WEIGHTING TERMS FOR HIGH/LOW PASS FILTER.
C
    IF (ANS.EQ.'L') THEN
        A0 = 2*FCO
        DO 10 K=1,NWTS
            SIGMA = DSIN(K*PI/NWTS)/(K*PI/NWTS)
            A(K) = SIGMA*2*DSIN(K*PI*FCO)/(K*PI)

```

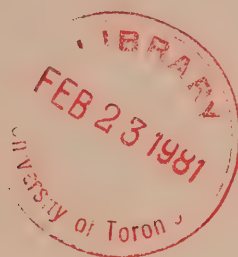
```

10      CONTINUE
      ELSE
        A0 = 2*(1-FC0)
        DO 20 K=1,NWTS
          SIGMA = DSIN(K*PI/NWTS)/(K*PI/NWTS)
          A(K) = -SIGMA*2*DSIN(K*PI*FC0)/(K*PI)
20      CONTINUE
      END IF
C
C - DETERMINE SET OF FILTERED DIGITAL DATA P(M) FOR M=1 TO NDATA-2*NLOST
C
      DO 35 M=1,NDATA-2*(NWTS-1)
        SUM = 0.0D0
        DO 30 K=1,NWTS
          SUM = SUM+A(K)/2*(X(NWTS+M-K)+X(NWTS+M+K))
30      CONTINUE
        P(M) = A0/2*X(M+NWTS)+SUM
35      CONTINUE
C
C - P(M), M=1 TO NDATA-2*NLOST, IS THE NEW, HIGH/LOW PASS FILTERED DATA
C - SET WHICH IS TRUNCATED BY THE N VALUES AT EACH END OF THE ORIGINAL
C - DATA SET X(M), M=1 TO NDATA.
C
      DO 999 I=1,50
        WRITE(6,888) P(I)
888      FORMAT(' ',F10.3)
999      CONTINUE
C
60      WRITE(6,70)
70      FORMAT('0*** DATA IS NOW FILTERED ***')
      NLOST = NWTS-1
      RETURN
      END

```

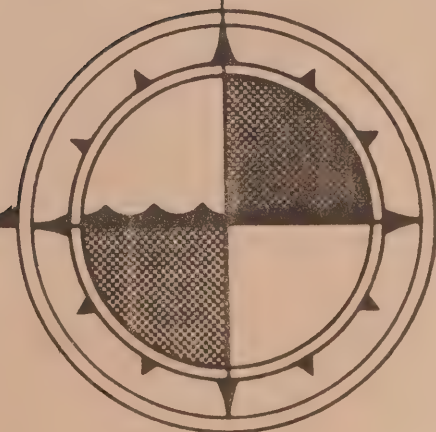

CAI
EP 321
-80R10

**OBSERVATIONS OF SEAWATER TEMPERATURE AND
SALINITY AT BRITISH COLUMBIA SHORE STATIONS
1978**



by
L.F. Giovando

**INSTITUTE OF OCEAN SCIENCES
Sidney, B.C.**



For additional copies or further information please write to:

Department of Fisheries and Oceans

Institute of Ocean Sciences

P.O. Box 6000

Sidney, B.C. CANADA

V8L 4B2

CAI
EP 371
-R0215

Pacific Marine Science Report 80-10

OBSERVATIONS OF SEAWATER TEMPERATURE AND SALINITY AT
BRITISH COLUMBIA SHORE STATIONS
1978

by

L.F. Giovando

Institute of Ocean Sciences
Sidney, B.C.

1980

Abstract

Surface (approximately 1-metre-depth) oceanic salinities and temperatures have been recorded once a day at several locations on the coast of British Columbia for varying lengths of time - from a few months to a few decades. This publication presents the data obtained in 1978 from eighteen such shore stations. Fifteen of the sites are Ministry of Transport (MOT) lightstations. The remaining three are: the Pacific Biological Station at Departure Bay, the Bamfield Marine Station at Bamfield, and the meteorological station at Cape St. James.

Temperatures are determined at all eighteen sites by means of mercury-in-glass thermometers. Salinities are obtained at only sixteen locations; they are determined at thirteen by hydrometer and at the remaining three by laboratory-model inductive (electrodeless) salinometer.

The data obtained are presented in two forms. Firstly, tables provide, for each site, the monthly means and the associated standard deviations, as well as the maximum and minimum values recorded during each month; the annual means are also listed. Secondly, graphs indicate the behaviour, throughout the year, of the data after the higher-frequency oscillations (e.g., those associated with lunar tides) have been removed ("smoothed") by the use of a seven-day normally-weighted running mean.

Introduction

A program involving once-daily observations of sea-surface salinities and/or temperatures at numerous locations on the coast of British Columbia has been in effect since the early 1930's. Most of these sampling sites have been at lightstations maintained by the Ministry of Transport (MOT) or its organizational predecessors. The number of sites reporting at any given time has varied throughout the course of the program; sampling has been discontinued (and in a few cases later resumed) at some places and commenced (not necessarily simultaneously) at others.

Sixteen such shore stations have provided sea-surface data for several years prior to 1978. Fourteen of these are MOT lightstations. The remaining two are the Pacific Biological Station (of the Department of Fisheries and Environment (DFE)) at Departure Bay, and the meteorological station (of the Atmospheric Environment Service (AES) of (DFE)) at Cape St. James. These data have received initial processing and have been published (see e.g. Giovando, 1980).

In 1978, such data became available not only from these sixteen stations again but also, for the first time, from two additional sites - the MOT lightstation at Cape Beale, and the Marine Biological Station at Bamfield (hereafter termed "Bamfield"). This report presents the information obtained from all eighteen sites throughout 1978.

The stations in question are shown (underlined) in Figure 1. Table 1 lists them in northwest-to-southeast order, along the "outside coast" (Langara Island to Race Rocks) and along the Strait of Georgia (Cape Mudge to Active Pass); the general location of each station, as well as the observers that obtained the data during 1978, are also given.

It may also be noted that sea-surface sampling commenced at Bamfield on 12 July 1969, and at Cape Beale on 9 January 1971. All the data (available) obtained at these two locations prior to 1978 will be published in a separate report (Giovando, 1980; in preparation).

Observational Equipment and Procedures

Except at Bamfield, Cape Beale and Active Pass, each daily observation is made at daytime high tide. At Bamfield and Cape Beale, sampling is carried out one hour before the daytime high tide. At Active Pass, observations are done at daylight high-water slack as obtained from the Canadian Tide and Current Tables (Fisheries and Environment Canada, 1978). On occasion this schedule will not be strictly adhered to, because of weather conditions or the press of the observers' primary duties; however, results obtained within \pm one hour of the desired time are recorded. Sampling is never attempted in darkness at any station.

At each location, the water temperature is measured by means of a mercury-in-glass thermometer. At fifteen stations (all except Departure Bay, Bamfield and Cape Beale) the thermometers used in 1978 recorded in degrees Fahrenheit ($^{\circ}\text{F}$) as has been the case since the inception of sampling. The instruments cover the range -10° to 145°F , and are graduated in 1° intervals.

At the remaining three stations Celsius thermometers, of range -10° to 60° and of interval 0.5°C , are employed. Before use in the field, each instrument is checked against a calibrated thermometer; the maximum error allowed is $\pm 0.4^{\circ}\text{F}$ or $\pm 0.02^{\circ}\text{C}$. The seawater temperature is estimated to within $\pm 0.1^{\circ}\text{F}$ or $\pm 0.1^{\circ}\text{C}$.

Because of the near-total predominance of the Celsius scale that now prevails in marine affairs, the temperatures for 1978 (this publication) as well as those to be obtained in subsequent years, will be reported in $^{\circ}\text{C}$. For the fifteen stations, the 1978 Fahrenheit readings have therefore been converted to the corresponding Celsius values - rounded off to the first decimal place. The $^{\circ}\text{F}$ thermometers presently in use will be replaced by $^{\circ}\text{C}$ ones (-25 to $+55^{\circ}$, interval 1°) as attrition demands.

At all the stations except Bamfield and Cape Beale, the thermometer is (partially) enclosed in a protective case of 2.5-cm (1-in.) aluminum pipe: this case also provides a "well" around the bulb of the thermometer. The case is attached to the end of a pole (also of aluminum pipe) which can be as long as about 6 m (20 ft.); the greater pole lengths are necessary at sites where observations are carried out from steep bluffs. The thermometer is lowered to a depth of 1 m, and left for about two minutes. It is then raised and the water temperature recorded. At a few of these stations, seawater is obtained by bucket (during inclement weather). At Cape Beale, a bucket is used for all oceanographic observations; at Bamfield a Van Dorn sampling bottle is used at all times. When bucket or bottle is used, the temperature recorded is that obtained by immersion of the thermometer in the water thus collected.

At all sites at which the pole assembly is usually utilized (except Sheringham Point¹ and Cape St. James¹), a plastic or glass bottle - usually of about 710-cc (25-oz.) capacity - is also attached to the assembly. The uncapped bottle will fill during immersion. At the same time that the temperature of the water is recorded, a sample is drawn from the bottle for use in the measurements of salinity. (When a bucket or a Van Dorn bottle is used, the sample is drawn from the bucket or bottle.)

At all but three of these (sixteen) stations, the density of each sample is determined by hydrometer. (The salinity is then obtained from this value of density.) The hydrometers employed are similar to those used by the U.S. Coast and Geodetic Survey (USC&GS) at its tidal stations²; they actually measure the *specific gravity*³ of a seawater sample. Specific gravity

¹ Measurements of salinity were terminated at Sheringham Point on 31 March 1970 and at Cape St. James on 31 May 1971.

² Since 1970, the USC&GS has been a component of the National Ocean Surveys of the National Oceanic and Atmospheric Administration (NOAA).

³ It should be noted that the term "specific gravity" has recently been replaced, in scientific usage at least, by the term "relative density."

is a ratio of two densities and is therefore a dimensionless quantity. If however, by definition, distilled water at a temperature 4°C (39.2°F) has a density $\rho_m = 1$, then the specific gravity of a substance having a density ρ is ρ/ρ_m and will be numerically equal to the value of ρ .

The density (or specific gravity) of a seawater sample depends upon both the salinity (the quantity of dissolved material in the sample) and the temperature of the sample at the time the measurement is made. Densities determined by hydrometer without temperature control must therefore be reduced to some "standard" temperature for conversion to the corresponding salinities. The standard adopted for this program is 15°C (59°F), the same as that presently used by the USC&GS.

An expression of the general form *Sp. Gr. Tp. (or Temp.)* 15.4°C is provided on every hydrometer utilized in this program. It incorporates both the basis of specific gravity (distilled water at 4°C (39.2°F)) and the standard temperature (15°C , or 59°F) employed.

Hydrometers are supplied to the stations in one or more of three ranges of specific gravity: 0.9960 - 1.0110, 1.0100 - 1.0210, and 1.0200 - 1.0310. The scales are divided into intervals of 0.0002, and the instruments are claimed to be accurate to ± 0.001 . The hydrometers are read employing techniques described by the USC&GS (Adams, 1942). Each instrument has its calibration checked immediately before being sent to a station.

Salinities at the remaining three stations (Departure Bay, Bamfield and Cape Beale) are determined by laboratory inductive (electrodeless) salinometer; an Auto-Lab Model 601 Mark III is employed at Departure Bay, and a Kahlsico Model RSB-7 is utilized for Bamfield and Cape Beale samples. The accuracy of these instruments, with duplicate determinations, is claimed to be ± 0.003 parts per thousand ($^{\circ}/\text{oo}$). Because of the greater accuracy of the salinometer-determined values, salinities at these three sites are reported to two decimal places, rather than to only one as is the case for values obtained by hydrometer.

It may be noted that comparison determinations involving several dozen samples collected at British Columbia shore stations have indicated that about 85% of the "hydrometer" salinity values obtained were within $\pm 0.03^{\circ}/\text{oo}$ of the corresponding ones obtained by salinometer (Hollister, unpublished).

The time of each daily observation (usually), as well as the associated seawater temperature and hydrometer or salinometer readings, are recorded on monthly field sheets. These sheets are forwarded to the Pacific Environment Institute, West Vancouver, where they undergo preliminary processing.

Preliminary Processing of the Data

The temperature data are scanned, and values are rejected if it is discovered that a faulty thermometer has been used, or if the value is obviously the result of a misreading or of any other error in technique. Observed hydrometer readings are reduced to densities at the standard

temperature, 15°C (59°F), by means of tables prepared by the USC&GS (Zerbe and Taylor, 1953). The appropriate calibration correction is then applied to each such density value. These corrected values are in turn converted to salinities. A salinity value is rejected, again, only if it obviously results from a misreading of hydrometer or salinometer, or from other procedural errors.

If observations are missing for *one* day or for *two consecutive* days, the resulting gap is filled by value(s) obtained by linear interpolation utilizing the two observations bounding the gap. No interpolated values are provided when readings have been missed for *three or more* consecutive days (whether by accident or by design).

Machine Processing of the Data

For each calendar year, the daily temperature and salinity data remaining after the preliminary procedures noted above are processed into final form by the Marine Environmental Data Services Branch (MEDS) of Ocean and Aquatic Sciences (OAS), DFE, in Ottawa. For each station, this computer processing involves the determination of the twelve monthly means for temperature and for salinity, as well as of the corresponding standard deviations. The annual means are also computed (Somers, 1965). Means - except those for salinity at the three stations where a salinometer is employed - are rounded off to the first decimal place; at the three stations, salinities are rounded to two places. All standard deviations are truncated at the second decimal place. Data obtained by interpolation are not utilized in the computation of the means.

A form of smoothing has been performed on the data to minimize the effect of any variability associated with frequencies large compared to the annual frequency (those associated with lunar tides, for example). For simplicity, the daily values of salinity and/or temperature at each sampling station are here considered to be equally spaced in time - with a sampling interval, therefore, of 24 hours. A seven-day, normally-weighted running mean (Holloway, 1958) has been utilized to smooth the resulting series; this form of filtering is considered to result in an output free of such defects as "polarity reversals" or phase shifts. The running mean is computed, for the entire year, for both temperature and salinity. In order that these means for each station be as continuous as possible consistent with the data involved, interpolated daily values *have* been utilized in the associated computations. However when a period of greater than *two* consecutive days of missed data is encountered the computations will be interrupted.

Presentation of Data

The data from each station are presented in two forms:

(1) Tabulations, in monthly format, of the daily values of temperature in $^{\circ}\text{C}$ and of salinity in parts per thousand ($^{\circ}/\text{oo}$) - pages 16 to 87. The results are listed in the same station order as that given in Table 1. Three months' data are listed on each page. Also recorded for each month are the mean, the standard deviation (STD. DEV.), the number of observations (OBSVNS.) involved in the computations of these two quantities, and the MAXIMUM and

MINIMUM values. The *annual* means (YRLY. MEANS) for temperature and salinity are included with the December output for each station. Each interpolated daily value is identified by an asterisk (*). "Missed" values with which no interpolation is associated are denoted by a "*0.0(0)" entry. Invalid days, such as April 31, are indicated by a "0.0(0)" entry. Both the latitude and longitude of each station (in degrees, minutes and seconds) are noted on every page, immediately after the station designation. For ease in reference, the monthly- and annual-mean temperatures and salinities have been summarized. Temperatures in °C are given in Table 2. In addition, the °F equivalents of the values in Table 2 are provided in Table 3 - primarily for the convenience of those who, because of either choice or necessity, still employ the Fahrenheit scale. It may be noted that no equivalent given here differs by more than $\pm 0.1^{\circ}\text{F}$ from the corresponding value obtained from the "original" Fahrenheit data. Salinities are given in Table 4.

(2) "Annual" graphs of the seven-day, normally-weighted running means for temperature and salinity - pages 90 to 125. The graphs are copies of the computer-generated plots of the means. Any interruption - due to missing data - in the associated computations will result in a gap in the plotted output as well. Each graph for temperature is provided with scales in both °C and °F.

Several features associated with the data presented should be noted:

- (a) At Bamfield, no data were available from January through April. Because of these omissions, the annual means calculated for temperature and salinity at this station are considered to be unrepresentative of actual values, and have therefore not been given on pages 12, 13 or 14. Observer's illness and equipment failures markedly reduced the number of observations carried out at this station during the remainder of the year.

At Cape Mudge and Cape Beale, several factors - primarily heavy seas - reduced the available daily values to the mid- or low twenties in several months (e.g. March, May, September and November).

At Departure Bay, circumstances beyond the control of the program have rendered it impossible - from May 1974 onward - to carry out observations on weekends (Saturdays and Sundays) and on statutory holidays. The maximum number of (non-interpolated) values available for determination of each monthly mean has therefore been permanently reduced from, approximately, thirty to twenty at this station.

- (b) At Active Pass, the daily salinity values (and the associated running means) during June through August of each year are in general relatively low - quite often $< 20^{\circ}/\text{oo}$. The salinity range utilized for the running-mean graph at Active Pass (page 125) has therefore been chosen to be 16 to $30^{\circ}/\text{oo}$, rather than the 20-to- $34^{\circ}/\text{oo}$ range employed elsewhere. It is felt that the *variability* in the mean during the three-month period can thus be better displayed.

- (c) At Kains Island, salinities of 33 ‰ or more were recorded during July and August of 1978. Such values have also been obtained in some previous years at B. C. shorestations (see e.g. Giovando, 1980). All physical-oceanographic studies so far conducted indicate that salinities of this magnitude are extremely unlikely in the nearshore surface waters of B. C. The observer at the station had previously been apprised of this fact, and therefore checked both equipment and procedures thoroughly during the "high-value" periods. No obvious faults or errors were revealed; however, with due regard to the uncertainties associated with salinities determined by hydrometer, such values should be regarded with extreme caution pending a satisfactory explanation of their occurrences.

The salinities in question have been retained in the tabular output but have been "flagged" by an asterisk (*); they have been utilized in the computations of the running means but not in those of the monthly means.

Brief mention may be made of some recent efforts at analysis (as opposed to "annual" tabulations) of the B. C. shorestation data obtained up to the end of 1976. A preliminary study (Webster and Farmer, 1976) examined data from three of the stations on the outer coast - Langara Island, Kains Island and Amphitrite Point. The primary purpose was the development of techniques for the presentation of important features of the data - such as long- and short-term variations at each station, and the possible relationships between the data from different stations. The techniques applied were simple annual and monthly averaging, and the relatively modern technique of spectral analysis. The same authors later extended these analytical techniques to a further fourteen stations (Webster and Farmer, 1977).

A third publication (Associated Engineering Services Ltd., 1977) dealt with the general efficiency of the present shorestation sampling program, especially in the light of financial constraints involved. Sampling errors, especially those inherent in salinity determination by hydrometry, are exhaustively discussed. Central to the study was a questionnaire - forwarded to all present and potential users of the data - seeking to clarify such information as the time scales of interest and the required accuracy of the data. Responses to this questionnaire, and the sampling accuracies determined, were utilized to prepare several options (further versions of the sampling program). These options, each of different sampling intensities and/or instrumentation mixes, and cost, are presented for consideration by the users.

Acknowledgements

The sea-sampling program at British Columbia shore stations owes its success primarily to the dedication of the many observers who are taking, or have taken, part in the obtaining of data. These observers have maintained a remarkable continuity of effort, often in the face of extremely hazardous sea and weather conditions. The several vital contributions of MOT to the program are gratefully acknowledged: the provision of the voluntarily services

of the lightkeepers as observers, as well as the excellent assistance received from the District Managers and staffs of the Marine Transportation Division in Victoria and Prince Rupert, and from its Radio Branch, which transmits the numerous messages involved in the program. The services of the meteorological staff at Cape St. James have been made available to the program through the kind permission of the Regional Director of the Pacific Region of AES. The observers at all stations except Bamfield, Cape Beale and Departure Bay receive payment from Ocean and Aquatic Sciences, DFE, for their work on behalf of the program. Observations at Bamfield are carried out by members of the support staff; the observer at Cape Beale is paid by Bamfield. Thanks are due to the Director at Bamfield, Dr. J. E. McInerney, for permission to publish the Bamfield and Cape Beale data included in this report, and to Miss Miriam Preker for her efforts in making these data available. The computations were carried out by the Data Processing and Analysis Section of MEDS, under the direction of Mr. J. Nasr.

References

- Adams, K.T. 1942. Hydrographic manual. Rev. ed. U.S. Coast and Geodetic Survey. Special Publication No. 143.
- Associated Engineering Services Ltd. 1977. Analysis of Lighthouse Oceanographic Data - Phase III. Contract Report Series 77-5. For: Institute of Ocean Sciences, Patricia Bay - Sidney, B.C.
- Fisheries and Environment Canada. 1978. Canadian Tide and Current Tables, Volume 5. Juan de Fuca and Georgia Straits. Fisheries and Marine Service, Ottawa.
- Giovando, L.F. 1980. Observations of Seawater Temperature and Salinity at British Columbia Shore Stations - 1977. Pacific Marine Science Report 80-1. Institute of Ocean Sciences, Sidney, B.C.
- Giovando, L.F. 1980. Observations of Seawater Temperature and Salinity at Cape Beale Lightstation and Bamfield Marine Station, 1969-1977. In preparation.
- Hollister, H.J. and A.M. Sandnes. 1972. Sea surface temperature and salinities at shore stations on the British Columbia coast, 1914-1970. Pacific Marine Science Report 72-13. Environment Canada, Marine Sciences Directorate, Pacific Region, Victoria, B.C.
- Holloway, J.L., Jr. 1958. Smoothing and filtering of time series and space fields. In: Advances in Geophysics, Vol. 4. pp. 351-389. Academic Press Inc., New York.
- Somers, H. 1965. Program G20106, daily seawater observations. Memorandum 1220-2-4/April 30, 1965. Canadian Oceanographic Data Centre, Special Administrative Services Division, Ottawa.
- Webster, Ian and David M. Farmer. 1976. Analysis of Salinity and Temperature Records Taken at Three Lighthouses on the B.C. Coast. Pacific Marine Science Report 76-11. Institute of Ocean Sciences, Patricia Bay - Victoria, B.C.
- Webster, I. and D.M. Farmer. Analysis of Lighthouse Station Temperature and Salinity Data - Phase II. Pacific Marine Science Report 77-21. Institute of Ocean Sciences, Patricia Bay - Sidney, B.C.
- Zerbe, W.B. and C.B. Taylor. 1953. Sea water temperature and density reduction tables. U.S. Coast and Geodetic Survey. Special Publication No. 298.



Figure 1. Location of B.C. shore stations making daily oceanographic observations (1978) reported in this publication.

Table 1. B.C. shore stations providing the oceanographic data reported in this publication: general locations, and names of observers.

STATION	LOCATION	OBSERVER(S)
<u>Outside Coast</u>		
Langara Island	Dixon Entrance, south side	J.E. Redhead (Mrs.)
Bonilla Island	Hecate Strait, north	M. Slater D. Graham
McInnes Island	Milbanke Sound entrance, north side	K. Coldwell (Mrs.)
Cape St. James	Queen Charlotte Islands, south end	C. Hilliar D. A. Veale C. Anderson
Egg Island	Smith Sound, southern entrance	K. Ashe (Mrs.)
Pine Island	Queen Charlotte Strait, western entrance	K.E. Watson (Mrs.) S.E. Plumptre (Mrs.)
Kains Island	Quatsino Sound entrance, north side	L.C. Collins (Mrs.)
Amphitrite Point	Barkley Sound, western entrance	M.V. Stewart (Mrs.)
Cape Beale	Barkley Sound, eastern entrance	A.D. Thomson
Bamfield	Barkley Sound, near eastern entrance	R. Miller (Miss)
Sheringham Point	Juan de Fuca Strait, northern shore	E. Bruton (Mrs.)
Race Rocks	Juan de Fuca Strait eastern end	F.B. Anderson (Mrs.)

Table 1 continued

STATION	LOCATION	OBSERVER(S)
<u>Strait of Georgia</u>		
Cape Mudge	Strait of Georgia, northern entrance	R. Wilkie
Sisters Island	Strait of Georgia, central	W. Milne D.J. McNeil T.G. Smith R.J. Grunert
Chrome Island	Strait of Georgia, off central western shore	F. McWilliams F.M. Collette (Mrs.)
Departure Bay	Strait of Georgia, central western shore	A. Ballantyne (Mrs.)
Entrance Island	Strait of Georgia, off central western shore	E. Cihak (Mrs.)
Active Pass	Strait of Georgia, southwestern shore	J.E. Ruck

Table 2. Monthly- and annual-mean temperatures ($^{\circ}\text{C}$) - 1978

Station	Jan	Feb	Mar	Apr	May	Jun	Jul	Aug	Sep	Oct	Nov	Dec	Annual
Langara I.	5.9	6.5	6.6	7.5	8.9	9.9	10.2	11.5	12.6	11.3	9.0	6.9	8.9
Bonilla I.	5.9	6.6	7.2	8.3	9.8	10.7	10.9	12.7	12.7	11.3	9.0	7.2	9.4
McInnes I.	6.6	7.0	7.0	8.3	9.8	10.9	11.2	13.5	13.0	11.3	8.8	7.1	9.6
Cape St. James	7.7	8.1	7.9	8.6	9.4	11.1	12.9	12.8	11.3	10.7	9.6	8.0	9.9
Egg I.	7.2	7.4	7.6	8.8	10.0	12.0	13.3	13.2	11.7	11.3	8.4	6.8	9.8
Pine I.	7.4	7.4	7.7	8.5	9.2	10.2	10.2	10.1	11.1	10.8	8.9	7.7	9.1
Kains I.	7.8	8.4	8.9	10.0	10.7	12.7	12.6	14.1	14.2	12.8	9.7	8.2	10.8
Amphitrite Pt.	8.2	8.8	9.1	10.1	11.1	13.7	13.3	13.1	14.2	12.9	8.3	6.9	10.8
Cape Beale	8.2	8.8	9.2	10.6	11.2	13.2	12.3	12.2	13.3	11.9	8.5	7.3	10.5
Bamfield	-	-	-	-	13.0	16.6	16.8	14.7	14.8	13.5	9.1	7.6	- +
Sheringham Pt.	7.7	8.2	8.6	9.0	9.3	10.8	11.6	10.5	11.2	9.8	7.8	7.3	9.3
Race Rocks	7.7	8.0	8.3	9.0	9.4	10.4	10.5	10.9	10.6	9.8	8.2	7.4	9.2
Cape Mudge	7.1	7.2	8.2	9.4	11.1	13.0	14.2	15.5	13.0	11.3	8.5	7.4	10.6
Sisters I.	6.1	6.8	7.9	9.2	11.6	15.9	18.6	18.0	14.1	12.1	8.7	7.6	11.4
Chrome I.	6.4	7.0	7.9	9.3	11.9	15.8	19.1	17.2	13.2	11.8	9.0	8.1	11.4
Departure Bay	6.0	6.8	8.1	9.5	12.4	15.9	18.4	17.8	13.9	12.3	9.0	7.7	11.5
Entrance I.	6.3	7.0	7.9	9.3	11.7	15.2	18.5	17.3	13.5	12.3	8.7	7.9	11.4
Active Pass	6.4	7.2	8.1	9.4	11.7	14.1	16.3	15.0	13.0	11.9	8.4	7.0	10.8

+ Computed value not listed, being considered unrepresentative because of lack of data from Jan. through Apr.

Table 3. Monthly- and annual-mean temperatures ($^{\circ}\text{F}$) - 1978

Station	Jan	Feb	Mar	Apr	May	Jun	Jul	Aug	Sep	Oct	Nov	Dec	Annual
Langara I.	42.6	43.7	43.9	45.5	48.0	49.8	50.4	52.7	54.7	52.3	48.2	44.4	48.0
Bonilla I.	42.6	43.9	45.0	46.9	49.6	51.3	51.6	54.9	54.9	52.3	48.2	45.0	
McInnes I.	43.9	44.6	44.6	46.9	49.6	51.6	52.2	56.3	55.4	52.3	47.8	44.8	49.1
Cape St. James	45.9	46.6	46.2	47.5	48.9	52.0	55.2	55.0	52.3	51.3	49.3	46.4	49.8
Egg I.	45.0	45.3	45.7	47.8	50.0	53.6	55.9	55.8	45.5	52.3	47.1	44.2	49.6
Pine I.	45.3	45.3	45.9	47.3	48.6	50.4	50.4	50.2	52.0	51.4	48.0	45.9	48.4
Kains I.	46.0	47.1	48.0	50.0	51.3	54.9	54.7	57.4	57.6	55.0	49.5	46.8	51.4
Amphitrite Pt.	46.8	47.8	48.4	50.2	52.0	56.7	55.9	55.6	57.6	55.2	46.9	44.4	51.4
Cape Beale	46.8	47.8	48.6	51.1	52.2	55.8	54.1	54.0	55.9	53.4	47.3	45.1	50.9
Bamfield	-	-	-	-	55.4	61.9	62.2	58.5	58.6	56.3	48.4	45.7	- +
Sheringham Pt.	45.9	46.8	47.5	48.2	48.7	51.4	52.9	50.9	52.2	49.6	46.0	45.1	48.7
Race Rocks	45.9	46.4	46.9	48.2	48.9	50.7	50.9	51.6	51.1	49.6	46.8	45.3	48.6
Cape Mudge	44.8	45.0	46.8	48.9	52.0	55.4	57.6	59.9	55.4	52.3	47.3	45.3	51.1
Sisters I.	43.0	44.2	46.2	48.6	52.9	60.6	65.5	64.4	57.4	53.8	47.7	45.7	52.5
Chrome I.	43.5	44.6	46.2	48.7	53.4	60.4	66.4	63.0	55.8	53.2	48.2	46.6	52.5
Departure Bay	42.8	44.2	46.6	49.1	54.3	60.6	65.1	64.0	57.0	54.1	48.2	45.9	52.7
Entrance I.	43.3	44.6	46.2	48.7	53.1	59.4	65.3	63.1	56.3	54.1	47.7	46.2	52.5
Active Pass	43.5	45.0	46.6	48.9	53.1	57.4	61.3	59.0	55.4	53.4	47.1	44.6	51.4

+ Computed value not listed, being considered unrepresentative because of lack of data from Jan. through Apr.

Table 4. Monthly- and annual-mean salinities ($^{\circ}/\text{oo}$) - 1978.

Station	Jan	Feb	Mar	Apr	May	Jun	Jul	Aug	Sep	Oct	Nov	Dec	Annual
Langara I.	32.0	31.5	31.2	31.4	31.0	31.2	31.6	31.5	31.5	31.3	31.1	31.3	31.4
Bonilla I.	31.3	31.3	31.2	31.3	31.4	31.8	32.0	32.0	31.8	31.5	30.6	30.6	31.4
McInnes I.	31.3	31.3	31.0	30.7	31.4	31.3	31.8	30.1	30.1	30.3	29.9	30.7	30.8
Egg I.	30.5	30.4	31.0	30.8	30.5	29.9	30.0	30.4	31.0	30.1	30.4	31.2	30.5
Pine I.	30.7	30.6	30.6	31.0	31.3	31.3	31.4	31.5	31.5	31.3	31.2	31.3	31.1
Kains I.	29.7	29.8	29.6	30.4	31.4	31.8	32.6	32.1	31.3	30.0	29.4	30.7	30.7
Amphitrite Pt.	28.2	28.7	29.5	29.6	30.2	30.0	31.7	30.9	28.9	30.0	29.3	30.3	29.8
*Cape Beale	29.39	29.57	30.44	30.49	30.60	31.66	31.80	31.59	31.06	30.99	31.19	31.54	30.94
*Bamfield	-	-	-	-	27.64	26.70	29.67	30.02	27.37	28.85	30.67	30.77	-
Race Rocks	30.8	30.7	30.7	30.9	31.3	31.3	31.1	31.5	31.2	31.2	31.3	31.7	31.1
Cape Mudge	28.5	28.8	28.9	28.7	28.8	28.4	27.7	26.9	27.4	28.1	28.6	28.9	28.3
Sisters I.	27.9	28.2	28.6	28.7	28.4	27.5	25.8	26.0	26.3	27.8	28.5	29.3	27.8
Chrome I.	28.4	28.8	29.2	29.2	28.7	27.5	27.2	27.0	27.7	28.2	28.7	29.2	28.3
*Departure Bay	26.42	26.87	27.46	27.45	26.74	25.17	24.13	24.20	25.15	26.41	28.20	28.63	26.40
Entrance I.	27.2	27.5	27.6	27.9	27.5	25.5	23.8	24.6	25.8	26.0	27.5	28.5	26.6
Active Pass	27.3	28.0	28.1	28.4	25.6	24.5	23.8	25.4	26.2	25.5	26.9	28.4	26.5

*Values were obtained by salinometer at these stations during 1978.

+Computed value not listed, being considered unrepresentative because of lack of data from Jan. through Apr.

Tabulations of Daily Sea-surface
Temperature and Salinity

1978

TEMP: Temperature ($^{\circ}\text{C}$)

SAL: Salinity ($^{\circ}/\text{oo}$)

LANGARA ISLAND

54 15 19 N

133 03 30 W

JANUARY

FEBRUARY

MARCH

1978

DATE	TEMP	SAL	TEMP	SAL	TEMP	SAL
1	5.6	31.9	5.6	31.4	5.8	31.5
2	5.6	32.0	5.4	31.0	5.8	31.6
3	5.7	31.9	5.5	31.2	5.2	31.2
4	4.9	32.0	6.2	31.8	5.1	30.8
5	4.7	32.0	6.6	31.6	5.2	31.0
6	4.4	31.9	6.6	31.4	6.1	31.6
7	4.8	31.6	6.7	31.6	6.9	31.4
8	6.0	32.0	6.6	31.6	6.7	30.6
9	5.7	32.0	6.6	31.9	* 6.6	* 31.1
10	6.1	32.0	6.4	31.6	6.6	31.6
11	6.5	31.9	6.7	32.0	6.5	31.6
12	6.0	31.6	6.6	31.5	6.4	31.6
13	6.1	31.9	6.7	31.9	6.6	31.5
14	6.2	32.0	7.0	31.4	6.8	31.2
15	6.0	31.8	6.7	31.4	6.5	31.2
16	6.1	32.1	6.8	31.6	6.7	30.2
17	6.1	31.5	6.6	31.6	6.4	30.8
18	6.2	32.0	6.8	31.4	6.3	30.7
19	6.2	32.5	7.1	31.2	6.9	31.0
20	6.5	32.5	7.7	30.4	7.2	31.4
21	6.7	31.8	* 7.1	* 30.7	7.1	31.2
22	6.1	32.1	6.4	31.1	7.2	31.9
23	6.8	31.8	6.6	31.8	6.7	31.5
24	6.8	31.6	6.7	32.1	7.1	31.6
25	6.1	32.1	6.5	31.1	6.9	31.1
26	6.1	31.9	6.4	30.8	7.3	31.2
27	6.1	32.3	6.3	31.9	6.7	31.5
28	6.3	32.1	6.0	31.9	7.1	31.1
29	6.2	32.1	0.0	0.0	7.6	31.1
30	6.0	32.3	0.0	0.0	7.2	30.8
31	5.7	32.3	0.0	0.0	7.1	31.6

MEANS	5.9	32.0	6.5	31.5	6.6	31.2
OBSVNS.	31	31	27	27	30	30

MAXIMUM	6.8	32.5	7.7	32.1	7.6	31.9
MINIMUM	4.4	31.5	5.4	30.4	5.1	30.2

STD.DEV.	.58	.24	.48	.39	.64	.38
----------	-----	-----	-----	-----	-----	-----

LANGARA ISLAND

54 15 19 N

133 03 30 W

APRIL

MAY

JUNE

1978

DATE	TEMP	SAL	TEMP	SAL	TEMP	SAL
1	7.3	31.8	8.4	31.0	9.4	31.0
2	6.8	32.0	8.4	30.8	9.6	31.2
3	7.1	31.5	8.4	31.2	9.9	30.6
4	7.4	31.8	8.7	31.2	10.0	30.0
5	7.6	31.4	8.5	31.4	9.9	31.1
6	7.5	31.9	8.2	31.5	10.9	31.0
7	7.2	31.8	8.9	31.4	10.6	31.6
8	6.8	31.5	8.6	31.2	10.0	31.4
9	7.4	32.0	8.7	31.2	11.4	31.5
10	7.3	31.5	8.8	30.8	11.9	31.4
11	7.3	31.2	* 9.0	* 30.9	11.1	31.4
12	7.7	30.6	9.2	31.1	12.6	31.6
13	7.4	31.4	9.8	31.2	10.3	31.5
14	7.2	30.8	9.7	31.2	10.1	31.2
15	6.8	31.4	9.1	31.1	10.3	31.5
16	7.2	31.4	8.9	30.6	9.9	31.1
17	6.8	* 31.3	9.5	31.4	9.6	31.6
18	7.2	31.2	9.1	31.1	10.0	31.4
19	6.8	31.1	9.1	31.0	8.7	31.2
20	7.6	31.5	9.4	31.5	9.4	31.5
21	8.2	32.1	8.9	31.1	9.9	31.1
22	7.9	30.7	9.3	31.2	9.2	31.2
23	7.8	31.4	8.4	31.2	8.7	31.0
24	8.6	32.0	8.6	30.7	8.9	30.7
25	8.0	31.4	8.8	30.2	8.9	31.6
26	8.5	31.5	8.7	30.7	9.1	30.8
27	8.3	31.4	8.3	30.7	9.5	31.2
28	8.0	31.1	8.7	30.6	9.3	31.1
29	7.7	31.4	9.1	30.6	9.4	31.1
30	8.3	31.0	8.9	30.8	10.0	31.0
31	0.0	0.0	9.1	30.8	0.0	0.0
MEANS	7.5	31.4	8.9	31.0	9.9	31.2
OBSVNS.	30	29	30	30	30	30
MAXIMUM	8.6	32.1	9.8	31.5	12.6	31.6
MINIMUM	6.8	30.6	8.2	30.2	8.7	30.0
STD.DEV.	.52	.39	.41	.32	.91	.35

LANGARA ISLAND

54 15 19 N

133 03 30 W

JULY

AUGUST

SEPTEMBER 1978

DATE	TEMP	SAL	TEMP	SAL	TEMP	SAL
1	10.1	31.4	10.8	30.7	12.4	31.6
2	10.1	31.5	11.0	31.8	12.5	31.9
3	10.0	31.5	10.8	31.9	12.7	31.6
4	10.6	31.1	10.9	31.9	12.8	32.0
5	10.7	31.1	10.5	31.9	13.0	31.5
6	10.6	31.1	10.6	31.8	13.6	31.6
7	10.7	31.6	11.1	31.2	12.9	31.5
8	* 10.2	* 31.7	12.4	31.9	12.8	31.5
9	9.7	31.9	* 12.6	* 31.6	12.8	31.5
10	9.3	31.6	12.8	31.2	13.4	31.4
11	10.0	31.6	13.0	31.1	12.7	31.6
12	9.9	31.4	12.9	31.8	12.8	31.6
13	10.3	31.1	13.0	31.4	13.8	32.0
14	10.7	31.1	12.8	31.2	13.4	31.5
15	10.3	30.8	12.9	31.2	13.2	31.8
16	10.6	31.0	12.7	31.4	12.6	32.0
17	10.7	31.8	11.3	31.1	11.8	31.9
18	* 10.5	* 31.9	11.3	31.0	12.7	31.6
19	10.3	32.0	10.6	31.5	12.2	31.4
20	10.6	31.9	10.2	31.9	11.7	31.5
21	9.4	31.5	10.2	31.6	12.0	31.0
22	9.4	32.1	9.6	31.9	11.9	31.1
23	9.3	32.0	10.1	32.4	11.9	31.0
24	9.5	32.1	11.1	32.1	12.2	30.6
25	10.3	32.1	10.8	32.0	12.8	30.6
26	9.8	31.9	11.4	31.6	12.3	31.6
27	9.7	31.8	11.8	31.0	12.3	31.9
28	10.0	31.5	11.6	31.4	12.5	31.6
29	10.6	31.9	12.3	31.2	12.5	31.0
30	10.6	32.0	12.4	30.6	12.4	31.0
31	11.1	31.6	12.3	30.3	0.0	0.0
MEANS	10.2	31.6	11.5	31.5	12.6	31.5
OBSVNS.	29	29	30	30	30	30
MAXIMUM	11.1	32.1	13.0	32.4	13.8	32.0
MINIMUM	9.3	30.8	9.6	30.3	11.7	30.6
STD.DEV.	.50	.38	1.02	.49	.52	.38

LANGARA ISLAND

54 15 19 N

133 03 30 W

OCTOBER

NOVEMBER

DECEMBER 1978

DATE	TEMP	SAL	TEMP	SAL	TEMP	SAL
1	11.3	30.7	10.7	31.2	8.2	31.4
2	11.2	31.4	10.5	31.1	8.8	31.8
3	12.1	31.5	10.2	31.5	8.5	31.2
4	11.2	31.2	10.3	31.1	7.9	31.2
5	11.3	31.2	10.1	31.2	7.8	31.5
6	11.8	31.8	9.9	31.5	7.8	31.4
7	11.6	30.8	9.4	31.4	7.8	31.1
8	11.7	30.8	9.3	31.4	7.8	31.1
9	11.9	31.2	9.7	31.0	7.8	30.8
10	11.3	31.5	9.1	31.0	7.1	31.1
11	11.7	31.5	9.3	30.8	7.1	31.1
12	11.2	30.8	9.4	31.1	7.2	31.4
13	11.4	31.0	8.8	31.0	7.9	31.2
14	11.3	31.4	9.0	31.0	7.6	31.2
15	11.3	31.8	8.9	31.0	7.0	31.6
16	11.2	31.0	8.8	31.4	6.2	31.6
17	11.4	31.8	8.4	31.1	5.9	32.0
18	11.7	31.8	7.2	31.0	5.9	30.8
19	11.6	31.6	7.1	30.8	6.9	31.1
20	11.2	31.4	7.4	30.7	6.8	31.2
21	11.1	31.2	* 8.1	* 30.7	7.3	31.5
22	11.5	31.5	8.8	30.8	6.3	31.2
23	11.1	31.1	* 8.8	* 30.6	6.7	31.0
24	11.3	31.5	8.7	30.4	5.8	30.8
25	11.7	31.2	8.6	30.8	5.8	31.2
26	10.8	31.5	8.6	30.8	5.9	31.6
27	10.5	31.0	9.1	31.1	5.8	31.4
28	10.4	31.4	8.8	31.2	5.7	31.8
29	10.3	31.6	8.4	31.4	* 5.4	* 31.5
30	10.1	31.2	8.3	31.9	5.1	31.2
31	10.6	31.5	0.0	0.0	4.9	31.8
MEANS	11.3	31.3	9.0	31.1	6.9	31.3
OBSVNS.	31	31	28	28	30	30
YRLY. MEANS.....					8.9	31.4
MAXIMUM	12.1	31.8	10.7	31.9	8.8	32.0
MINIMUM	10.1	30.7	7.1	30.4	4.9	30.8
STD. DEV.	.48	.31	.91	.30	1.03	.31

BONILLA ISLAND

53 29 39 N

130 38 04 W

JANUARY

FEBRUARY

MARCH

1978

DATE	TEMP	SAL	TEMP	SAL	TEMP	SAL
1	6.1	31.4	5.5	31.5	7.2	31.5
2	5.6	31.2	5.3	31.2	6.6	31.6
3	5.1	31.1	5.4	31.4	6.3	31.2
4	5.1	31.4	* 6.0	* 31.3	5.9	31.2
5	* 4.9	* 31.3	6.6	31.1	6.0	31.5
6	4.6	31.2	6.8	31.2	6.7	31.1
7	4.6	31.2	7.1	31.1	7.3	31.1
8	4.8	31.2	6.5	31.5	7.6	31.6
9	5.7	31.0	6.6	31.2	7.2	31.4
10	6.1	31.1	5.7	30.8	7.3	31.1
11	5.8	31.1	6.0	31.2	7.2	31.5
12	6.2	31.2	6.0	31.5	6.5	31.2
13	6.2	31.4	5.6	31.1	7.2	31.1
14	6.2	31.8	5.7	31.4	7.7	31.1
15	6.3	31.4	6.1	30.8	6.7	30.8
16	6.2	31.2	6.0	31.1	7.3	30.8
17	6.1	31.2	6.4	31.4	6.7	31.1
18	6.1	31.5	7.1	31.2	6.9	31.2
19	6.2	31.5	7.7	31.4	7.1	31.1
20	6.3	31.1	7.5	31.5	7.3	31.1
21	6.2	31.4	7.3	31.4	7.5	31.2
22	6.0	31.2	7.3	31.1	7.6	31.2
23	6.1	30.8	7.3	31.4	7.7	31.2
24	6.6	30.8	7.3	31.5	7.8	31.4
25	6.4	31.1	7.4	31.4	6.9	31.1
26	6.2	31.4	7.2	31.5	6.8	31.0
27	5.8	31.4	7.3	31.4	8.2	31.1
28	6.1	31.6	7.1	31.4	7.6	31.1
29	6.2	31.5	0.0	0.0	* 8.1	* 31.1
30	6.0	31.2	0.0	0.0	8.6	31.2
31	5.7	31.2	0.0	0.0	7.8	31.4
MEANS	5.9	31.3	6.6	31.3	7.2	31.2
OBSVNS.	30	30	27	27	30	30
MAXIMUM	6.6	31.8	7.7	31.5	8.6	31.6
MINIMUM	4.6	30.8	5.3	30.8	5.9	30.8
STD.DEV.	.53	.22	.75	.20	.61	.20

BONILLA ISLAND

53 29 39 N

130 38 04 W

APRIL

MAY

JUNE

1978

DATE	TEMP	SAL	TEMP	SAL	TEMP	SAL
1	7.2	31.2	8.4	31.4	10.4	31.8
2	7.0	30.8	8.3	31.5	11.1	31.9
3	7.2	31.1	8.3	31.4	11.6	31.8
4	7.7	31.1	9.8	31.0	11.1	31.9
5	7.8	31.2	10.0	31.2	10.6	31.6
6	7.9	31.1	9.8	31.0	11.1	31.9
7	7.7	31.1	9.4	31.1	11.7	31.8
8	7.8	31.1	10.6	31.4	11.4	32.0
9	7.3	30.7	9.5	31.5	10.3	32.0
10	7.9	31.0	10.1	31.1	11.4	31.8
11	8.3	31.1	9.9	31.5	* 11.8	* 31.7
12	* 8.3	* 31.1	9.9	31.4	12.3	31.6
13	8.4	31.0	9.9	31.4	11.2	31.4
14	8.7	31.2	9.9	31.6	11.1	31.9
15	8.3	31.5	10.0	31.5	11.1	31.9
16	7.7	31.4	9.8	31.5	11.0	31.6
17	7.8	31.2	9.8	31.4	11.1	31.8
18	8.2	31.2	10.1	31.5	10.5	31.9
19	8.6	31.6	9.9	31.2	10.0	31.9
20	8.4	31.6	9.8	31.6	10.5	31.9
21	8.9	31.6	9.9	31.5	9.7	31.4
22	8.8	31.5	9.4	31.6	9.8	31.8
23	9.4	31.5	9.6	31.6	9.8	32.0
24	9.6	31.5	10.4	31.5	10.6	31.9
25	9.0	31.5	9.7	31.2	10.6	32.0
26	9.0	31.6	10.1	31.4	10.7	31.9
27	9.1	31.9	10.4	31.6	9.9	31.5
28	9.3	31.5	10.1	31.6	9.5	31.8
29	8.4	31.5	11.0	31.5	9.7	32.0
30	8.6	31.2	9.8	31.6	10.8	31.8
31	0.0	0.0	10.6	31.6	0.0	0.0
MEANS	8.3	31.3	9.8	31.4	10.7	31.8
OBSVNS.	29	29	31	31	29	29
MAXIMUM	9.6	31.9	11.0	31.6	12.3	32.0
MINIMUM	7.0	30.7	8.3	31.0	9.5	31.4
STD.DEV.	.70	.27	.60	.18	.69	.17

BONILLA ISLAND

53 29 39 N

130 38 04 W

JULY

AUGUST

SEPTEMBER 1978

DATE	TEMP	SAL	TEMP	SAL	TEMP	SAL
1	11.1	31.9	11.6	31.9	13.6	31.6
2	11.2	32.0	11.9	31.9	* 13.6	*31.6
3	10.6	31.8	13.2	32.0	13.6	31.6
4	11.3	31.6	13.3	31.8	* 13.2	*31.7
5	11.2	31.5	12.1	31.4	12.7	31.9
6	11.7	31.8	12.2	31.8	13.4	32.1
7	12.4	31.6	13.5	32.1	15.0	32.4
8	10.8	31.2	14.7	32.0	* 13.9	*32.2
9	10.9	31.8	* 14.6	*32.0	12.7	32.0
10	9.9	31.9	14.5	32.0	13.2	32.0
11	9.7	31.9	13.4	32.0	13.1	32.1
12	10.0	32.0	12.2	31.9	12.9	32.1
13	10.7	31.8	12.2	32.3	12.8	32.1
14	11.2	31.9	12.8	31.9	13.2	31.5
15	12.2	31.5	12.2	32.0	13.1	31.9
16	12.1	31.6	12.6	32.0	13.3	32.0
17	12.2	31.9	11.6	31.9	12.2	31.9
18	12.2	31.6	12.3	32.1	12.0	32.0
19	10.9	32.1	12.2	32.0	12.1	31.2
20	10.4	32.4	12.1	32.1	12.2	31.8
21	9.6	32.4	10.1	32.9	12.3	31.9
22	9.9	32.5	12.2	32.1	12.3	31.6
23	11.2	32.8	13.3	32.1	12.2	31.5
24	11.1	32.5	12.8	32.1	12.1	31.9
25	11.7	32.4	13.8	32.7	11.6	31.8
26	9.8	32.7	12.2	32.1	12.1	31.9
27	9.5	32.3	12.8	31.4	* 12.0	*31.8
28	9.7	32.0	12.8	31.4	11.9	31.6
29	9.8	32.4	12.8	31.4	* 12.0	*31.6
30	12.1	31.8	13.9	31.8	12.1	31.6
31	11.6	32.1	13.6	31.6	0.0	0.0
MEANS	10.9	32.0	12.7	32.0	12.7	31.8
OBSVNS.	31	31	30	30	25	25
MAXIMUM	12.4	32.8	14.7	32.9	15.0	32.4
MINIMUM	9.5	31.2	10.1	31.4	11.6	31.2
STD.DEV.	.91	.38	.93	.33	.75	.26

BONILLA ISLAND

53 29 39 N

130 38 04 W

OCTOBER

NOVEMBER

DECEMBER 1978

DATE	TEMP	SAL	TEMP	SAL	TEMP	SAL
1	12.3	31.6	10.4	31.4	8.1	29.9
2	11.7	31.1	10.3	31.0	* 8.2	*30.0
3	12.2	31.6	10.1	30.8	8.3	30.0
4	11.8	31.8	9.7	30.8	8.3	30.2
5	12.1	31.9	10.1	31.2	8.2	30.3
6	12.3	31.9	10.4	31.2	8.1	30.3
7	* 12.1	*31.7	10.1	31.2	* 8.1	*30.4
8	11.9	31.4	9.7	31.4	8.1	30.6
9	11.6	31.6	9.7	31.4	8.1	30.6
10	11.4	31.4	9.4	31.4	7.8	30.6
11	11.4	31.4	* 9.4	*31.3	8.0	30.6
12	11.1	31.2	9.4	31.2	7.8	30.8
13	11.6	31.5	8.9	30.3	8.3	31.2
14	11.2	31.6	8.8	29.9	7.8	30.8
15	11.7	31.5	8.9	29.1	7.3	30.6
16	11.7	31.6	8.8	29.5	7.2	30.7
17	11.6	31.8	8.7	29.9	7.2	31.0
18	11.5	31.6	8.6	30.2	* 7.2	*30.6
19	11.6	31.6	8.3	31.1	7.2	30.2
20	11.6	31.8	8.4	30.8	7.3	30.4
21	11.0	31.6	8.3	30.8	7.2	30.4
22	11.1	31.4	8.3	31.0	7.2	30.7
23	10.8	31.6	8.3	30.8	6.7	30.7
24	10.7	31.8	8.4	30.8	6.9	30.7
25	10.6	31.6	8.3	30.3	6.6	30.8
26	10.6	31.2	8.3	30.3	6.6	30.7
27	* 10.5	*31.2	8.5	29.8	6.4	30.8
28	10.3	31.1	8.2	30.3	5.9	30.7
29	10.3	31.5	7.9	29.9	5.8	30.7
30	10.5	31.5	8.3	29.8	5.6	31.0
31	10.7	31.1	0.0	0.0	4.4	30.7

MEANS	11.3	31.5	9.0	30.6	7.2	30.6
OBSVNS.	29	29	29	29	28	28
YRLY. MEANS.....					9.4	31.4
MAXIMUM	12.3	31.9	10.4	31.4	8.3	31.2
MINIMUM	10.3	31.1	7.9	29.1	4.4	29.9
STO.DEV.	.59	.23	.79	.64	.97	.29

MCINNES ISLAND

52 15 48 N

128 43 10 W

JANUARY

FEBRUARY

MARCH

1978

DATE	TEMP	SAL	TEMP	SAL	TEMP	SAL
1	5.8	30.6	6.1	31.2	7.0	30.8
2	6.0	31.1	6.0	31.1	6.3	31.0
3	5.9	30.8	6.0	31.2	6.3	31.0
4	5.5	30.8	6.6	31.1	6.1	31.0
5	5.1	31.2	6.4	31.1	5.8	30.7
6	5.3	31.1	6.4	31.1	6.4	31.1
7	6.0	31.1	6.5	31.4	6.3	31.1
8	6.2	31.2	7.1	31.5	7.4	31.2
9	6.3	31.2	6.7	31.4	6.9	31.4
10	6.3	31.0	7.4	31.4	7.2	31.4
11	6.2	31.4	7.3	31.4	7.0	31.5
12	6.2	31.4	7.5	31.5	6.6	31.5
13	6.1	31.4	7.3	31.4	7.3	31.8
14	6.1	31.4	7.4	31.4	7.4	31.4
15	6.8	31.4	7.7	31.4	7.3	31.5
16	6.8	31.4	7.4	31.4	7.2	31.5
17	6.8	31.4	7.3	31.2	7.1	31.2
18	6.8	31.4	7.4	31.2	7.2	31.1
19	6.8	31.4	7.3	31.2	6.9	31.1
20	7.6	31.8	7.4	31.5	7.2	30.3
21	7.2	31.4	7.8	31.5	7.2	30.4
22	7.3	31.4	7.8	31.5	7.3	30.4
23	7.6	31.4	7.1	31.4	7.3	30.3
24	7.5	31.4	7.1	31.4	7.2	30.2
25	7.3	31.5	7.0	31.4	7.6	31.5
26	7.2	31.4	7.0	31.4	7.5	31.0
27	7.3	31.4	7.0	30.8	7.4	31.0
28	6.9	31.1	6.9	30.6	6.9	30.7
29	7.0	31.4	0.0	0.0	7.2	30.6
30	6.9	31.0	0.0	0.0	7.2	30.6
31	6.8	31.2	0.0	0.0	7.2	31.8
MEANS	6.6	31.3	7.0	31.3	7.0	31.0
OBSVNS.	31	31	28	28	31	31
MAXIMUM	7.6	31.8	7.8	31.5	7.6	31.8
MINIMUM	5.1	30.6	6.0	30.6	5.8	30.2
STD. DEV.	.68	.24	.52	.22	.45	.45

MCINNES ISLAND

52 15 48 N

128 43 10 W

APRIL

MAY

JUNE

1978

DATE	TEMP	SAL	TEMP	SAL	TEMP	SAL
1	7.4	30.4	9.5	31.1	10.5	31.5
2	7.7	30.4	9.5	31.4	10.5	31.4
3	7.8	30.7	9.2	31.6	11.0	31.1
4	7.7	30.6	9.4	31.1	10.8	31.1
5	7.7	30.4	9.4	31.1	11.2	31.0
6	7.6	30.6	9.7	31.6	11.4	31.1
7	7.6	30.6	9.6	31.2	11.2	30.7
8	7.7	30.7	9.5	31.2	11.4	31.0
9	7.6	31.0	9.6	31.4	11.1	31.2
10	7.7	31.0	9.9	31.6	10.9	31.5
11	7.8	31.0	9.3	31.6	10.8	31.5
12	7.7	30.7	9.3	31.6	10.9	31.1
13	7.7	31.0	9.4	31.4	11.9	31.0
14	7.7	31.0	9.4	31.8	11.5	31.0
15	7.7	31.0	9.7	31.9	11.4	31.0
16	7.8	30.7	9.6	31.5	11.6	31.2
17	7.7	30.4	10.0	31.5	11.5	31.1
18	7.7	30.3	9.8	31.2	11.0	31.0
19	9.1	30.0	10.4	31.4	11.2	31.1
20	8.9	30.0	10.2	31.2	11.0	31.2
21	8.6	30.4	9.8	31.1	10.4	31.5
22	8.3	30.8	10.0	31.4	10.6	31.5
23	9.2	30.8	9.8	31.4	10.2	31.8
24	9.2	30.8	9.9	31.4	10.4	31.8
25	9.6	30.8	9.8	31.4	10.2	31.8
26	9.3	30.8	10.3	31.5	10.2	31.5
27	9.0	30.8	10.0	31.5	10.6	31.6
28	9.7	30.8	10.1	31.5	10.5	31.5
29	9.2	30.7	10.0	31.5	10.6	31.8
30	9.7	31.4	10.3	31.5	10.4	31.8
31	0.0	0.0	10.3	31.6	0.0	0.0
MEANS	8.3	30.7	9.8	31.4	10.9	31.3
OBSVNS.	30	30	31	31	30	30
MAXIMUM	9.7	31.4	10.4	31.9	11.9	31.8
MINIMUM	7.4	30.0	9.2	31.1	10.2	30.7
STD.DEV.	.78	.31	.34	.20	.47	.31

MCINNES ISLAND

52 15 48 N

128 43 10 W

JULY

AUGUST

SEPTEMBER 1978

DATE	TEMP	SAL	TEMP	SAL	TEMP	SAL
1	10.4	31.8	12.2	32.0	14.0	30.3
2	10.4	31.6	12.1	31.8	13.7	29.9
3	10.5	31.8	12.7	31.6	13.9	29.8
4	11.0	31.8	12.3	31.9	13.4	29.4
5	11.1	31.8	13.7	32.4	13.5	29.7
6	11.6	31.8	12.7	32.1	13.6	30.2
7	11.4	31.5	12.2	32.1	13.9	30.6
8	11.5	31.9	13.9	31.4	13.8	30.0
9	11.0	31.9	14.0	30.3	13.6	29.9
10	10.8	31.8	13.7	30.8	14.0	29.8
11	11.0	31.9	13.7	29.9	14.4	29.4
12	10.9	32.0	14.3	27.7	14.5	29.7
13	11.0	32.0	14.1	28.4	13.2	30.0
14	11.0	31.8	14.3	29.0	13.5	30.4
15	10.9	31.8	13.3	30.0	13.0	31.1
16	11.2	31.8	14.3	29.4	12.3	31.2
17	11.6	31.5	13.5	30.4	12.2	31.1
18	11.5	31.4	13.4	30.4	12.7	29.5
19	11.7	31.6	12.9	30.6	12.5	30.2
20	11.5	31.6	14.3	29.1	12.5	31.1
21	11.3	32.0	14.1	29.4	12.3	31.8
22	11.5	32.0	13.2	29.7	11.9	31.5
23	11.5	32.1	13.5	29.1	12.1	31.4
24	11.5	32.3	13.7	27.4	12.3	29.9
25	10.7	32.3	13.5	28.4	12.3	28.2
26	11.0	31.8	13.2	29.4	12.5	29.0
27	* 11.4	* 31.8	13.9	30.0	11.9	29.4
28	11.8	31.8	14.2	28.8	11.8	29.1
29	11.8	31.8	14.4	29.5	11.9	29.1
30	11.2	31.9	14.2	29.7	12.1	29.9
31	11.7	32.0	14.1	30.4	0.0	0.0
MEANS	11.2	31.8	13.5	30.1	13.0	30.1
OBSVNS.	30	30	31	31	30	30
MAXIMUM	11.8	32.3	14.4	32.4	14.5	31.8
MINIMUM	10.4	31.4	12.1	27.4	11.8	28.2
STD.DEV.	.40	.21	.70	1.34	.84	.84

MCINNES ISLAND

52 15 48 N

128 43 10 W

OCTOBER

NOVEMBER

DECEMBER 1978

DATE	TEMP	SAL	TEMP	SAL	TEMP	SAL
1	12.1	29.7	11.4	32.1	7.4	30.0
2	12.0	30.4	11.2	31.5	7.6	30.2
3	12.1	31.2	11.0	30.8	7.6	30.2
4	12.4	29.9	9.3	29.7	7.8	30.3
5	12.6	29.7	9.5	30.7	7.2	30.0
6	12.4	29.9	10.9	31.6	7.2	29.9
7	12.3	30.2	10.3	30.6	7.1	29.8
8	12.3	31.5	10.0	30.0	7.3	29.8
9	11.6	30.8	9.5	28.8	7.3	30.0
10	11.9	31.2	8.2	27.2	7.4	30.3
11	11.7	31.4	8.5	27.6	7.2	30.4
12	11.4	30.6	8.3	27.4	7.2	30.6
13	11.3	30.8	8.3	28.8	* 7.5	* 31.0
14	11.7	29.3	8.5	29.5	7.8	31.5
15	11.3	29.3	9.0	29.9	7.8	31.5
16	11.4	29.3	8.9	29.7	7.5	31.5
17	11.0	29.3	8.8	29.4	7.3	31.2
18	11.2	29.5	7.8	29.3	7.2	31.2
19	10.8	29.8	7.6	29.5	7.4	31.2
20	11.3	30.2	8.1	30.0	7.7	31.5
21	11.2	30.2	7.9	29.8	7.1	31.4
22	11.2	30.7	7.3	29.8	7.2	31.4
23	10.6	31.5	7.5	29.9	7.4	31.4
24	10.7	30.8	8.1	30.4	7.3	31.5
25	10.6	31.0	8.1	30.3	7.2	31.1
26	10.6	30.7	7.9	30.0	6.9	31.1
27	10.3	29.0	8.2	30.0	6.0	30.4
28	9.3	28.9	8.2	30.3	6.0	30.4
29	9.2	29.3	8.0	30.6	5.6	30.4
30	10.7	30.8	8.0	30.6	5.8	30.4
31	10.6	31.2	0.0	0.0	6.0	30.7
MEANS	11.3	30.3	8.8	29.9	7.1	30.7
OBSVNS.	31	31	30	30	30	30
YRLY. MEANS.....					9.6	30.8
MAXIMUM	12.6	31.5	11.4	32.1	7.8	31.5
MINIMUM	9.2	28.9	7.3	27.2	5.6	29.8
STD. DEV.	.84	.80	1.16	1.11	.61	.61

CAPE ST JAMES

51 56 18 N

131 00 50 W

JANUARY

FEBRUARY

MARCH

1978

DATE	TEMP	SAL	TEMP	SAL	TEMP	SAL
1	7.1	* 0.0	7.9	* 0.0	7.7	* 0.0
2	7.1	* 0.0	7.4	* 0.0	7.7	* 0.0
3	7.1	* 0.0	7.7	* 0.0	7.6	* 0.0
4	6.6	* 0.0	8.2	* 0.0	7.6	* 0.0
5	6.7	* 0.0	8.6	* 0.0	7.5	* 0.0
6	6.9	* 0.0	8.7	* 0.0	8.1	* 0.0
7	* 7.2	* 0.0	* 8.5	* 0.0	8.0	* 0.0
8	7.5	* 0.0	8.3	* 0.0	7.5	* 0.0
9	7.5	* 0.0	8.1	* 0.0	7.3	* 0.0
10	7.7	* 0.0	7.9	* 0.0	8.0	* 0.0
11	7.3	* 0.0	8.1	* 0.0	7.7	* 0.0
12	7.5	* 0.0	7.9	* 0.0	7.9	* 0.0
13	7.4	* 0.0	8.3	* 0.0	7.9	* 0.0
14	7.6	* 0.0	8.2	* 0.0	8.2	* 0.0
15	7.6	* 0.0	8.1	* 0.0	8.1	* 0.0
16	7.4	* 0.0	8.0	* 0.0	7.9	* 0.0
17	7.6	* 0.0	8.1	* 0.0	7.6	* 0.0
18	7.9	* 0.0	8.2	* 0.0	7.8	* 0.0
19	7.8	* 0.0	8.3	* 0.0	7.9	* 0.0
20	7.8	* 0.0	8.1	* 0.0	8.0	* 0.0
21	7.9	* 0.0	8.2	* 0.0	8.1	* 0.0
22	7.9	* 0.0	8.1	* 0.0	7.9	* 0.0
23	8.3	* 0.0	8.0	* 0.0	8.3	* 0.0
24	8.5	* 0.0	8.1	* 0.0	8.2	* 0.0
25	8.4	* 0.0	8.1	* 0.0	8.1	* 0.0
26	8.3	* 0.0	8.0	* 0.0	8.1	* 0.0
27	8.2	* 0.0	7.8	* 0.0	8.2	* 0.0
28	8.5	* 0.0	7.7	* 0.0	8.2	* 0.0
29	8.3	* 0.0	0.0	0.0	8.0	* 0.0
30	8.2	* 0.0	0.0	0.0	8.5	* 0.0
31	8.0	* 0.0	0.0	0.0	8.3	* 0.0
MEANS	7.7	0.0	8.1	0.0	7.9	0.0
OBSVNS.	30	0	27	0	31	0
MAXIMUM	8.5	0.0	8.7	0.0	8.5	0.0
MINIMUM	6.6	0.0	7.4	0.0	7.3	0.0
STD.DEV.	.53	0.00	.26	0.00	.28	0.00

CAPE ST JAMES

51 56 18 N

131 00 50 W

APRIL

MAY

JUNE

1978

DATE	TEMP	SAL	TEMP	SAL	TEMP	SAL
1	8.2	* 0.0	8.7	* 0.0	10.0	* 0.0
2	8.0	* 0.0	8.6	* 0.0	10.4	* 0.0
3	8.1	* 0.0	8.8	* 0.0	10.3	* 0.0
4	8.1	* 0.0	9.1	* 0.0	10.1	* 0.0
5	8.3	* 0.0	9.4	* 0.0	11.2	* 0.0
6	8.4	* 0.0	9.4	* 0.0	11.1	* 0.0
7	8.3	* 0.0	9.2	* 0.0	11.2	* 0.0
8	8.5	* 0.0	9.1	* 0.0	10.8	* 0.0
9	8.4	* 0.0	9.4	* 0.0	11.2	* 0.0
10	8.5	* 0.0	9.4	* 0.0	10.7	* 0.0
11	8.6	* 0.0	9.4	* 0.0	10.7	* 0.0
12	8.4	* 0.0	9.4	* 0.0	10.8	* 0.0
13	8.7	* 0.0	9.4	* 0.0	10.7	* 0.0
14	8.6	* 0.0	9.8	* 0.0	10.2	* 0.0
15	8.4	* 0.0	9.2	* 0.0	10.3	* 0.0
16	8.3	* 0.0	9.2	* 0.0	10.4	* 0.0
17	8.4	* 0.0	9.3	* 0.0	10.8	* 0.0
18	8.5	* 0.0	9.6	* 0.0	11.3	* 0.0
19	8.7	* 0.0	9.4	* 0.0	11.3	* 0.0
20	8.8	* 0.0	9.8	* 0.0	11.6	* 0.0
21	8.7	* 0.0	9.7	* 0.0	11.1	* 0.0
22	8.8	* 0.0	9.6	* 0.0	11.8	* 0.0
23	9.1	* 0.0	9.7	* 0.0	11.5	* 0.0
24	9.2	* 0.0	9.6	* 0.0	11.5	* 0.0
25	9.1	* 0.0	9.6	* 0.0	11.8	* 0.0
26	8.7	* 0.0	9.9	* 0.0	12.1	* 0.0
27	8.8	* 0.0	9.3	* 0.0	11.3	* 0.0
28	9.1	* 0.0	9.2	* 0.0	11.8	* 0.0
29	8.8	* 0.0	9.3	* 0.0	11.9	* 0.0
30	8.5	* 0.0	9.2	* 0.0	12.2	* 0.0
31	0.0	0.0	9.6	* 0.0	0.0	0.0
MEANS	8.6	0.0	9.4	0.0	11.1	0.0
OBSVNS.	30	0	31	0	30	0
MAXIMUM	9.2	0.0	9.9	0.0	12.2	0.0
MINIMUM	8.0	0.0	8.6	0.0	10.0	0.0
STD.DEV.	.31	0.00	.31	0.00	.62	0.00

CAPE ST JAMES

51 56 18 N

131 00 50 W

JULY

AUGUST

SEPTEMBER 1978

DATE	TEMP	SAL	TEMP	SAL	TEMP	SAL
1	13.1	* 0.0	13.6	* 0.0	12.4	* 0.0
2	12.8	* 0.0	14.7	* 0.0	11.4	* 0.0
3	12.7	* 0.0	15.2	* 0.0	12.4	* 0.0
4	12.7	* 0.0	14.9	* 0.0	12.6	* 0.0
5	12.5	* 0.0	13.4	* 0.0	12.3	* 0.0
6	12.7	* 0.0	12.3	* 0.0	11.2	* 0.0
7	12.4	* 0.0	12.8	* 0.0	11.9	* 0.0
8	12.8	* 0.0	12.6	* 0.0	11.3	* 0.0
9	12.8	* 0.0	12.6	* 0.0	11.4	* 0.0
10	13.2	* 0.0	12.1	* 0.0	12.2	* 0.0
11	13.0	* 0.0	12.2	* 0.0	12.5	* 0.0
12	12.9	* 0.0	12.6	* 0.0	12.0	* 0.0
13	12.8	* 0.0	11.4	* 0.0	12.1	* 0.0
14	12.7	* 0.0	11.3	* 0.0	11.1	* 0.0
15	12.2	* 0.0	12.6	* 0.0	10.3	* 0.0
16	12.6	* 0.0	13.0	* 0.0	10.6	* 0.0
17	12.6	* 0.0	11.9	* 0.0	10.7	* 0.0
18	12.7	* 0.0	12.3	* 0.0	11.3	* 0.0
19	13.3	* 0.0	13.2	* 0.0	10.4	* 0.0
20	13.3	* 0.0	12.9	* 0.0	10.3	* 0.0
21	12.2	* 0.0	12.2	* 0.0	10.4	* 0.0
22	13.2	* 0.0	12.4	* 0.0	10.2	* 0.0
23	12.8	* 0.0	13.1	* 0.0	10.8	* 0.0
24	12.4	* 0.0	12.5	* 0.0	11.4	* 0.0
25	12.7	* 0.0	12.2	* 0.0	11.5	* 0.0
26	12.8	* 0.0	13.3	* 0.0	11.5	* 0.0
27	13.0	* 0.0	12.8	* 0.0	11.2	* 0.0
28	13.6	* 0.0	12.6	* 0.0	10.5	* 0.0
29	13.7	* 0.0	12.7	* 0.0	11.1	* 0.0
30	13.6	* 0.0	12.8	* 0.0	10.4	* 0.0
31	12.8	* 0.0	11.9	* 0.0	0.0	0.0
MEANS	12.9	0.0	12.8	0.0	11.3	0.0
OBSVNS.	31	0	31	0	30	0
MAXIMUM	13.7	0.0	15.2	0.0	12.6	0.0
MINIMUM	12.2	0.0	11.3	0.0	10.2	0.0
STD.DEV.	.38	0.00	.89	0.00	.75	0.00

CAPE ST JAMES

51 56 18 N

131 00 50 W

OCTOBER

NOVEMBER

DECEMBER 1978

DATE	TEMP	SAL	TEMP	SAL	TEMP	SAL
1	10.9	* 0.0	10.1	* 0.0	9.1	* 0.0
2	10.7	* 0.0	9.5	* 0.0	9.1	* 0.0
3	10.5	* 0.0	9.9	* 0.0	8.8	* 0.0
4	11.9	* 0.0	10.2	* 0.0	8.6	* 0.0
5	11.2	* 0.0	10.2	* 0.0	9.2	* 0.0
6	10.9	* 0.0	10.4	* 0.0	8.9	* 0.0
7	10.4	* 0.0	10.0	* 0.0	8.6	* 0.0
8	10.1	* 0.0	9.9	* 0.0	8.9	* 0.0
9	10.0	* 0.0	9.9	* 0.0	8.4	* 0.0
10	9.8	* 0.0	9.6	* 0.0	8.6	* 0.0
11	10.1	* 0.0	9.8	* 0.0	8.2	* 0.0
12	10.2	* 0.0	9.8	* 0.0	8.4	* 0.0
13	10.4	* 0.0	9.7	* 0.0	8.5	* 0.0
14	10.7	* 0.0	9.6	* 0.0	8.1	* 0.0
15	10.9	* 0.0	9.9	* 0.0	8.1	* 0.0
16	11.1	* 0.0	9.4	* 0.0	7.9	* 0.0
17	10.9	* 0.0	9.5	* 0.0	7.8	* 0.0
18	10.9	* 0.0	8.8	* 0.0	7.8	* 0.0
19	10.5	* 0.0	8.9	* 0.0	8.0	* 0.0
20	11.1	* 0.0	9.1	* 0.0	7.7	* 0.0
21	11.1	* 0.0	9.3	* 0.0	7.8	* 0.0
22	10.9	* 0.0	9.4	* 0.0	7.6	* 0.0
23	10.6	* 0.0	9.4	* 0.0	7.8	* 0.0
24	11.0	* 0.0	9.6	* 0.0	7.5	* 0.0
25	10.7	* 0.0	9.4	* 0.0	7.6	* 0.0
26	10.8	* 0.0	9.4	* 0.0	7.7	* 0.0
27	10.9	* 0.0	9.6	* 0.0	7.0	* 0.0
28	10.8	* 0.0	9.1	* 0.0	7.1	* 0.0
29	10.7	* 0.0	9.0	* 0.0	6.9	* 0.0
30	10.7	* 0.0	9.1	* 0.0	6.6	* 0.0
31	10.1	* 0.0	0.0	0.0	6.9	* 0.0
MEANS	10.7	0.0	9.6	0.0	8.0	0.0
OBSVNS.	31	0	30	0	31	0
YRLY. MEANS.....					9.9	0.0
MAXIMUM	11.9	0.0	10.4	0.0	9.2	0.0
MINIMUM	9.8	0.0	8.8	0.0	6.6	0.0
STD.DEV.	.43	0.00	.41	0.00	.70	0.00

EGG ISLAND

51 15 06 N

127 49 53 W

JANUARY

FEBRUARY

MARCH

1978

DATE	TEMP	SAL	TEMP	SAL	TEMP	SAL
1	6.2	30.7	6.7	30.3	7.2	30.7
2	6.1	30.6	6.7	30.3	6.7	30.8
3	6.4	30.7	7.0	30.4	6.6	30.8
4	6.3	30.3	7.5	30.3	6.9	31.0
5	6.3	30.7	7.6	30.4	7.2	31.2
6	6.5	30.8	7.7	30.4	7.5	30.8
7	6.8	30.6	7.7	30.4	7.5	30.8
8	7.1	30.7	* 7.8	* 30.5	7.8	31.1
9	7.5	30.4	7.9	30.6	7.7	31.1
10	7.5	30.4	7.8	30.8	7.2	31.2
11	7.6	30.4	7.5	30.6	7.6	31.0
12	7.5	30.4	7.5	30.6	7.6	31.0
13	7.3	30.4	7.5	30.4	7.6	31.2
14	7.6	30.3	7.2	30.7	7.8	31.4
15	7.5	30.4	7.3	30.4	8.1	31.2
16	* 7.5	* 30.4	7.1	30.2	7.6	30.8
17	7.5	30.3	7.1	30.2	7.7	31.0
18	7.4	30.6	7.4	30.4	7.4	31.2
19	7.6	30.4	7.9	30.3	7.6	30.8
20	7.6	30.4	7.7	30.6	7.7	30.7
21	7.7	30.6	7.8	30.6	7.7	30.6
22	7.4	30.8	7.7	30.7	8.1	30.4
23	7.3	30.4	7.4	30.3	8.3	31.0
24	7.7	30.3	7.3	30.3	8.1	30.8
25	7.7	30.3	7.4	30.4	7.8	31.1
26	7.3	30.3	7.2	30.3	7.8	31.1
27	7.1	30.4	7.3	30.3	7.9	31.1
28	7.3	30.4	7.2	30.3	8.1	31.6
29	7.1	30.4	0.0	0.0	8.2	31.4
30	7.2	31.0	0.0	0.0	8.3	31.2
31	6.7	30.4	0.0	0.0	7.8	31.2
MEANS	7.2	30.5	7.4	30.4	7.6	31.0
OBSVNS.	30	30	27	27	31	31
MAXIMUM	7.7	31.0	7.9	30.8	8.3	31.6
MINIMUM	6.1	30.3	6.7	30.2	6.6	30.4
STD.DEV.	.50	.19	.32	.16	.43	.26

EGG ISLAND

51 15 06 N

127 49 53 W

APRIL

MAY

JUNE

1978

DATE	TEMP	SAL	TEMP	SAL	TEMP	SAL
1	8.1	30.7	8.9	31.2	10.4	30.8
2	7.8	30.7	8.9	31.5	12.7	28.4
3	8.2	30.8	8.9	31.2	12.6	28.2
4	8.4	31.2	8.9	31.5	11.7	29.7
5	8.3	31.5	9.4	31.5	10.7	29.8
6	8.6	31.2	* 9.6	*30.9	12.2	29.3
7	8.6	31.5	9.9	30.2	* 12.8	*29.1
8	8.9	31.2	9.6	30.0	13.5	28.9
9	8.3	31.0	9.7	30.0	14.4	29.1
10	8.4	31.5	9.9	30.4	13.7	29.3
11	8.8	30.6	9.4	30.4	11.6	30.8
12	8.2	31.0	10.1	30.3	12.1	31.2
13	8.3	30.7	10.0	30.3	13.7	27.7
14	9.0	30.2	11.1	30.2	12.2	26.5
15	8.4	30.0	11.5	29.3	11.9	27.4
16	8.3	30.0	10.1	30.0	11.1	29.4
17	8.4	30.0	10.7	29.4	11.7	28.5
18	8.2	31.0	10.0	30.2	11.1	30.8
19	8.9	30.6	10.3	30.4	10.2	31.2
20	9.2	30.7	9.5	30.6	11.7	30.4
21	9.3	30.2	9.9	30.0	11.1	31.1
22	9.3	30.7	10.2	30.6	12.2	31.1
23	9.0	30.4	10.7	30.0	11.9	31.0
24	9.7	30.8	11.8	29.7	11.7	30.7
25	9.4	31.2	9.9	30.4	13.9	30.7
26	10.6	30.3	10.6	30.3	12.2	30.7
27	9.4	31.2	10.6	30.7	11.2	30.8
28	9.9	31.2	10.1	31.4	11.2	31.4
29	9.4	31.2	10.1	31.1	12.8	31.4
30	9.1	31.5	10.1	30.7	11.4	31.0
31	0.0	0.0	* 10.2	*30.7	0.0	0.0
MEANS	8.0	30.8	10.0	30.5	12.0	29.9
OBSVNS.	30	30	29	29	29	29
MAXIMUM	10.6	31.5	11.8	31.5	14.4	31.4
MINIMUM	7.8	30.0	8.9	29.3	10.2	26.5
STD.DEV.	.63	.47	.72	.60	1.05	1.35

EGG ISLAND

51 15 06 N

127 49 53 W

JULY

AUGUST

SEPTEMBER 1978

DATE	TEMP	SAL	TEMP	SAL	TEMP	SAL
1	11.1	31.0	14.9	29.7	12.7	30.8
2	11.6	30.8	15.0	29.7	12.2	31.2
3	12.1	30.7	15.8	29.9	12.2	30.7
4	13.1	30.0	15.0	29.7	11.7	30.6
5	13.8	30.6	15.3	29.0	12.3	30.4
6	14.9	29.9	13.3	29.9	12.2	30.4
7	13.2	30.2	15.1	29.8	12.5	30.8
8	12.2	30.0	13.4	30.8	11.8	30.8
9	13.9	28.6	13.8	30.7	11.2	31.6
10	12.2	29.5	14.9	30.0	11.6	31.6
11	14.4	28.0	* 14.9	* 30.0	11.2	31.6
12	17.2	29.5	14.9	30.0	* 10.9	* 31.5
13	13.7	28.6	13.8	30.6	10.6	31.4
14	13.8	29.0	13.4	30.7	10.4	31.0
15	13.8	28.8	13.3	30.7	11.3	31.6
16	13.6	29.3	12.8	30.6	10.8	31.4
17	14.0	28.2	13.4	29.7	11.2	31.6
18	13.0	29.9	13.4	30.4	13.1	31.2
19	12.8	30.4	13.8	29.8	11.2	31.6
20	12.9	29.8	15.1	29.7	11.4	31.6
21	12.2	31.0	13.3	30.0	12.3	31.8
22	12.2	31.0	12.8	28.6	12.2	31.9
23	13.8	30.7	12.7	29.1	11.8	31.4
24	12.1	32.0	11.1	31.9	11.3	29.3
25	12.4	31.2	10.8	31.8	12.2	29.4
26	13.3	30.7	10.1	31.9	11.6	30.3
27	15.1	31.0	10.5	31.8	11.7	30.4
28	13.4	30.6	10.6	31.5	11.1	30.8
29	14.7	30.3	11.2	31.6	11.1	30.6
30	13.4	29.5	11.4	31.1	11.1	30.6
31	13.4	29.4	11.4	30.7	0.0	0.0
MEANS	13.3	30.0	13.2	30.4	11.7	31.0
OBSVNS.	31	31	30	30	29	29
MAXIMUM	17.2	32.0	15.8	31.9	13.1	31.9
MINIMUM	11.1	28.0	10.1	28.6	10.4	29.3
STD.DEV.	1.20	.96	1.66	.89	.65	.66

EGG ISLAND

51 15 06 N

127 49 53 W

OCTOBER

NOVEMBER

DECEMBER 1978

DATE	TEMP	SAL	TEMP	SAL	TEMP	SAL
1	11.3	30.8	9.9	30.8	7.7	30.7
2	11.2	30.6	9.7	31.4	7.8	31.0
3	12.1	31.0	9.6	31.2	8.1	31.4
4	* 11.9	*30.9	9.5	31.2	7.7	30.6
5	11.7	30.7	10.2	31.4	7.3	30.8
6	12.1	30.8	10.6	31.4	7.2	30.8
7	12.3	31.8	9.9	31.2	6.9	30.8
8	12.3	31.8	* 9.4	*30.6	7.6	30.3
9	12.6	31.8	8.9	30.0	7.6	30.6
10	12.1	31.6	8.1	29.8	7.5	30.3
11	11.3	31.6	8.4	30.0	7.7	30.4
12	11.1	31.6	8.6	28.0	7.7	30.3
13	11.3	30.6	8.1	28.5	7.2	31.4
14	11.6	29.8	8.0	28.5	7.5	31.8
15	11.7	28.5	7.9	26.1	7.4	31.4
16	11.8	26.7	* 8.2	*28.0	7.0	31.4
17	12.3	26.8	8.5	29.9	6.9	31.2
18	11.7	28.1	7.7	30.8	7.0	31.4
19	11.6	29.3	7.3	31.0	6.8	31.4
20	11.2	30.3	8.4	31.4	7.2	31.6
21	11.0	31.4	8.5	31.0	6.7	31.6
22	10.7	30.3	7.0	31.1	6.8	31.6
23	11.1	31.0	7.1	30.8	* 6.8	*31.5
24	10.8	30.4	7.4	31.5	6.7	31.4
25	10.5	31.5	7.8	31.2	6.2	31.5
26	10.4	30.2	7.8	30.7	6.2	31.5
27	10.2	27.6	7.7	31.1	6.0	31.8
28	10.1	29.3	8.0	31.1	5.0	31.6
29	9.8	28.1	7.9	30.7	4.2	32.0
30	10.1	30.0	7.8	30.7	4.2	31.9
31	* 10.0	*30.4	0.0	0.0	5.0	32.0
MEANS	11.3	30.1	8.4	30.4	6.8	31.2
OBSVNS.	29	29	28	28	30	30
YRLY. MEANS.....					9.8	30.5
MAXIMUM	12.6	31.8	10.6	31.5	8.1	32.0
MINIMUM	9.8	26.7	7.0	26.1	4.2	30.3
STD.DEV.	.76	1.50	.98	1.26	1.03	.53

PINE ISLAND

50 58 33 N

127 43 35 W

JANUARY

FEBRUARY

MARCH

1978

DATE	TEMP	SAL	TEMP	SAL	TEMP	SAL
1	7.5	31.1	7.1	30.6	7.8	31.0
2	7.5	31.5	7.0	30.7	7.6	30.8
3	7.7	30.8	7.0	31.0	7.2	31.0
4	7.2	30.6	7.4	30.6	7.1	31.0
5	7.3	29.9	7.3	30.4	7.0	30.7
6	7.3	30.7	7.2	30.4	7.1	30.8
7	7.0	30.7	7.5	30.4	7.4	30.6
8	7.3	31.1	7.5	30.8	7.8	30.3
9	7.8	30.8	7.6	30.8	7.7	30.3
10	7.7	30.8	7.5	30.8	8.1	30.6
11	7.5	30.6	7.5	30.8	8.0	30.4
12	7.5	30.6	7.5	30.8	7.8	30.3
13	7.3	30.3	7.2	30.6	8.2	30.3
14	7.2	31.0	7.2	30.7	8.0	30.4
15	7.2	31.0	7.2	30.8	8.2	31.0
16	7.2	30.7	7.2	30.3	7.7	30.6
17	7.4	30.4	7.0	30.3	7.6	30.6
18	7.3	31.1	7.0	30.2	7.2	30.6
19	7.5	30.8	7.3	30.3	7.4	30.4
20	7.8	30.7	7.2	30.4	7.4	30.8
21	7.3	30.4	7.2	30.6	7.4	30.7
22	7.5	30.4	7.5	30.4	7.7	30.4
23	7.2	30.4	7.4	30.8	8.0	30.3
24	7.1	30.7	7.5	30.8	7.8	30.4
25	7.4	31.0	7.7	30.8	7.8	30.6
26	7.2	30.8	7.7	30.8	7.9	30.6
27	7.4	30.8	7.8	30.6	8.2	30.7
28	7.2	30.4	7.9	30.7	8.2	30.6
29	7.3	30.3	0.0	0.0	8.4	30.6
30	7.2	30.7	0.0	0.0	8.4	31.0
31	7.1	30.7	0.0	0.0	7.8	30.8
MEANS	7.4	30.7	7.4	30.6	7.7	30.6
OBSVNS.	31	31	28	28	31	31
MAXIMUM	7.8	31.5	7.9	31.0	8.4	31.0
MINIMUM	7.0	29.9	7.0	30.2	7.0	30.3
STD.DEV.	.20	.31	.25	.21	.39	.23

PINE ISLAND

50 58 33 N

127 43 35 W

APRIL

MAY

JUNE

1978

DATE	TEMP	SAL	TEMP	SAL	TEMP	SAL
1	8.0	30.6	8.5	31.1	9.4	31.1
2	8.2	31.1	8.7	31.2	9.8	30.8
3	8.4	30.7	8.6	30.7	10.2	31.0
4	8.2	30.4	8.8	31.4	10.3	31.1
5	8.2	30.6	9.0	31.5	10.0	31.8
6	8.5	30.4	9.4	31.5	10.4	31.5
7	8.5	31.0	9.3	30.8	10.7	31.2
8	8.8	31.4	9.3	31.1	10.0	31.5
9	8.4	31.2	9.5	31.2	10.2	31.4
10	8.6	31.0	9.2	31.8	9.9	31.1
11	8.7	30.8	9.2	31.2	10.5	31.2
12	8.4	30.7	8.8	31.2	10.0	31.1
13	8.8	30.7	9.2	31.2	10.7	31.4
14	8.6	31.0	9.2	31.1	10.2	31.5
15	8.3	31.1	9.2	31.1	10.2	31.4
16	8.0	31.4	9.2	31.2	10.5	31.0
17	8.1	30.8	9.2	31.4	10.5	31.5
18	8.2	31.1	9.0	31.4	10.3	31.2
19	8.3	30.8	9.2	31.6	10.0	31.2
20	8.3	30.8	9.3	31.2	9.8	31.4
21	8.8	30.8	9.4	31.2	9.8	31.5
22	8.9	31.0	9.6	31.5	10.1	31.4
23	9.0	31.5	9.4	31.2	10.2	31.2
24	8.9	31.2	9.7	31.5	10.2	31.1
25	9.0	31.4	9.3	31.4	10.5	31.2
26	9.0	31.2	9.2	31.2	10.0	31.6
27	8.9	31.0	9.2	31.5	10.3	31.4
28	9.0	31.4	9.1	31.5	10.2	31.8
29	8.8	31.2	9.1	31.5	9.8	31.9
30	8.6	31.1	9.0	31.9	10.2	31.5
31	0.0	0.0	9.0	31.9	0.0	0.0
MEANS	8.5	31.0	9.2	31.3	10.2	31.3
ORSVNS.	30	30	31	31	30	30
MAXIMUM	9.0	31.5	9.7	31.9	10.7	31.9
MINIMUM	8.0	30.4	8.5	30.7	9.4	30.8
STD.DEV.	.32	.30	.27	.27	.29	.26

PINE ISLAND

50 58 33 N

127 43 35 W

JULY

AUGUST

SEPTEMBER 1978

DATE	TEMP	SAL	TEMP	SAL	TEMP	SAL
1	10.5	31.2	10.0	31.5	10.2	30.8
2	10.0	31.2	10.4	31.0	10.1	30.7
3	10.3	31.4	11.2	31.5	10.1	31.2
4	10.4	31.5	10.9	31.2	10.1	31.5
5	11.0	31.6	10.7	31.0	10.6	31.2
6	10.8	31.4	10.0	31.5	10.2	31.6
7	10.3	31.5	10.8	31.5	10.6	31.4
8	10.9	31.4	10.1	31.9	10.2	31.5
9	10.6	31.2	10.5	31.5	10.1	31.0
10	10.0	31.5	10.1	31.5	10.3	30.8
11	9.8	31.6	10.2	31.1	11.5	31.6
12	10.5	31.2	10.4	31.2	11.5	32.3
13	10.8	31.2	9.8	31.5	12.5	32.0
14	10.2	31.2	10.4	31.5	12.8	31.6
15	9.8	31.2	9.9	31.1	12.2	31.8
16	10.9	31.2	10.0	31.4	11.2	31.9
17	11.2	30.8	10.2	31.6	11.0	31.2
18	10.6	31.1	10.1	31.5	10.8	31.2
19	10.0	31.4	9.9	31.5	10.5	31.2
20	9.8	31.5	10.0	31.6	10.3	31.5
21	10.0	31.4	9.8	31.9	10.3	32.0
22	9.5	31.5	9.4	31.6	10.0	31.8
23	10.3	31.8	9.4	31.9	10.7	31.8
24	10.0	31.9	9.8	32.0	11.0	31.4
25	10.0	31.6	9.5	31.6	11.2	31.8
26	9.8	31.6	9.8	32.1	13.0	31.6
27	10.0	31.5	9.8	31.6	12.4	31.6
28	9.6	31.8	10.0	31.0	13.0	31.5
29	9.7	31.5	9.8	31.5	11.8	31.2
30	9.6	31.6	10.2	31.2	12.3	31.1
31	9.5	31.6	10.2	31.1	0.0	0.0
MEANS	10.2	31.4	10.1	31.5	11.1	31.5
OBSVNS.	31	31	31	31	30	30
MAXIMUM	11.2	31.9	11.2	32.1	13.0	32.3
MINIMUM	9.5	30.8	9.4	31.0	10.0	30.7
STD.DEV.	.48	.23	.42	.30	.98	.38

PINE ISLAND

50 58 33 N

127 43 35 W

OCTOBER

NOVEMBER

DECEMBER 1978

DATE	TEMP	SAL	TEMP	SAL	TEMP	SAL
1	12.6	31.2	9.6	31.2	8.2	31.1
2	11.8	31.1	9.6	31.2	8.0	30.8
3	12.0	31.4	9.8	31.0	8.3	30.8
4	11.4	31.1	9.4	30.8	8.0	31.1
5	10.8	31.4	9.0	31.1	8.0	31.6
6	10.7	31.1	9.2	30.3	8.0	31.6
7	10.7	31.4	9.8	30.8	8.0	31.4
8	10.7	31.2	9.4	30.8	7.8	31.4
9	11.5	31.2	9.0	31.1	7.7	31.8
10	12.8	31.9	9.2	30.8	7.7	31.4
11	12.6	31.8	9.0	31.2	7.8	31.9
12	12.0	31.5	9.0	31.2	7.8	31.8
13	11.2	31.4	8.8	31.1	* 7.8	* 31.7
14	10.9	31.1	8.5	31.2	7.9	31.6
15	10.7	31.4	8.2	31.6	7.5	30.8
16	10.4	31.2	8.7	31.2	7.7	31.2
17	10.2	31.4	9.0	31.4	7.5	31.0
18	10.5	31.1	9.2	31.6	7.8	31.9
19	10.5	31.2	9.3	31.6	7.8	31.6
20	10.2	31.8	9.0	31.4	7.8	31.4
21	10.4	31.5	8.8	31.1	7.5	31.2
22	10.0	31.1	8.8	31.4	7.8	31.5
23	10.4	30.8	8.5	31.0	7.2	30.7
24	10.8	31.5	8.1	31.1	7.5	31.2
25	10.2	31.2	8.0	31.4	7.8	31.6
26	10.0	31.4	8.2	31.4	7.5	31.1
27	10.2	31.5	8.1	31.4	7.5	31.2
28	10.0	31.2	8.2	31.5	7.2	31.1
29	9.7	31.0	8.0	31.4	7.2	31.0
30	9.6	31.5	8.3	31.1	7.1	31.5
31	9.5	31.0	0.0	0.0	7.0	31.6
MEANS	10.8	31.3	8.9	31.2	7.7	31.3
OBSVNS.	31	31	30	30	30	30
YRLY. MEANS.....					9.1	31.1
MAXIMUM	12.8	31.9	9.8	31.6	8.3	31.9
MINIMUM	9.5	30.8	8.0	30.3	7.0	30.7
STD. DEV.	.89	.25	.55	.29	.32	.34

KAINS ISLAND

50 26 39 N

128 01 47 W

JANUARY

FEBRUARY

MARCH

1978

DATE	TEMP	SAL	TEMP	SAL	TEMP	SAL
1	7.2	29.0	7.6	30.2	8.4	30.2
2	6.8	29.0	7.7	29.9	8.3	30.6
3	6.6	29.5	8.2	29.5	8.3	30.4
4	6.7	29.4	8.6	30.6	8.7	30.0
5	6.8	29.8	8.8	30.6	8.6	30.3
6	6.7	29.3	8.5	29.7	8.9	30.4
7	7.3	29.3	8.7	30.6	9.2	30.6
8	7.1	29.1	8.4	29.5	9.1	30.2
9	7.9	29.5	8.2	30.0	8.8	29.7
10	7.6	29.7	8.1	28.9	8.8	29.5
11	7.8	30.2	8.6	30.0	8.7	29.9
12	7.3	29.4	7.8	29.4	8.7	29.7
13	7.8	30.6	8.1	30.0	8.7	29.5
14	8.2	29.9	8.4	30.2	8.8	29.9
15	8.2	30.0	8.3	29.5	8.8	30.0
16	8.2	30.4	8.4	29.8	8.9	29.7
17	8.2	30.0	8.5	29.7	8.8	29.4
18	8.3	30.3	8.4	30.0	8.7	29.3
19	8.4	29.5	8.6	29.8	8.8	29.5
20	8.7	30.4	8.7	29.7	8.9	29.3
21	8.2	29.7	8.8	30.0	9.3	28.6
22	7.9	29.3	8.8	29.5	9.6	28.8
23	8.4	29.3	8.4	29.3	9.5	29.5
24	8.5	29.4	8.4	29.7	9.3	30.4
25	8.1	29.3	8.5	30.4	9.3	30.0
26	8.2	29.3	8.4	29.5	9.0	28.9
27	7.7	29.5	8.4	29.5	9.2	28.8
28	7.9	29.5	8.2	29.5	9.4	28.4
29	8.1	29.4	0.0	0.0	9.3	28.1
30	8.1	30.4	0.0	0.0	9.3	29.7
31	8.2	30.6	0.0	0.0	8.9	28.5
MEANS	7.8	29.7	8.4	29.8	8.9	29.6
OBSVNS.	31	31	28	28	31	31
MAXIMUM	8.7	30.6	8.8	30.6	9.6	30.6
MINIMUM	6.6	29.0	7.6	28.9	8.3	28.1
STD.DEV.	.60	.48	.31	.42	.34	.68

KAINS ISLAND

50 26 39 N

128 01 47 W

APRIL

MAY

JUNE

1978

DATE	TEMP	SAL	TEMP	SAL	TEMP	SAL
1	9.4	29.1	10.1	31.1	12.3	31.6
2	9.6	29.1	10.4	30.7	12.5	31.6
3	9.3	29.7	10.1	31.1	12.6	31.5
4	9.3	29.7	10.4	31.1	13.7	32.1
5	9.6	29.7	10.4	31.2	13.2	31.8
6	9.7	30.2	11.2	31.0	12.9	32.0
7	9.7	29.9	10.2	31.4	11.6	32.3
8	10.0	30.3	10.7	31.6	11.9	32.4
9	9.8	30.7	10.8	31.5	12.4	31.5
10	9.8	30.4	10.1	31.5	12.4	31.5
11	9.9	30.6	9.9	31.5	12.8	31.5
12	9.7	30.7	10.1	31.5	12.5	31.6
13	9.9	30.4	10.5	31.1	13.5	31.8
14	9.7	30.3	11.0	31.4	13.1	31.2
15	9.5	30.6	11.0	31.1	13.1	31.6
16	9.8	30.8	10.9	31.2	13.6	31.8
17	9.6	30.8	11.3	31.2	13.1	31.8
18	10.1	29.8	11.5	31.4	12.9	31.9
19	10.2	30.7	11.6	31.4	12.8	31.8
20	10.3	30.6	11.2	31.4	12.8	31.9
21	10.3	30.0	10.4	31.4	12.3	31.8
22	10.3	30.7	10.5	31.1	12.3	32.1
23	10.4	30.8	9.9	31.5	11.8	31.6
24	10.0	30.8	10.1	31.1	11.6	32.1
25	10.4	31.0	10.4	31.9	11.8	32.5
26	11.2	30.8	10.6	31.6	12.6	31.2
27	10.4	30.8	10.8	32.1	13.8	32.7
28	10.9	31.1	11.0	32.3	13.4	32.7
29	10.0	31.1	11.3	31.5	13.2	31.6
30	10.4	31.2	11.3	31.8	12.4	31.9
31	0.0	0.0	12.1	31.9	0.0	0.0
MEANS	10.0	30.4	10.7	31.4	12.7	31.8
OBSVNS.	30	30	31	31	30	30
MAXIMUM	11.2	31.2	12.1	32.3	13.8	32.7
MINIMUM	9.3	29.1	9.9	30.7	11.6	31.2
STD.DEV.	.45	.56	.55	.34	.61	.39

KAINS ISLAND

50 26 39 N

128 01 47 W

JULY

AUGUST

SEPTEMBER 1978

DATE	TEMP	SAL	TEMP	SAL	TEMP	SAL
1	13.3	32.5	15.6	*33.0	15.2	31.0
2	12.3	32.1	14.1	*33.4	14.3	32.0
3	12.1	32.1	14.3	*33.4	14.5	32.0
4	12.1	32.7	13.5	*33.4	15.4	31.1
5	13.2	32.3	13.2	*33.4	15.1	32.1
6	13.7	32.8	13.4	*33.4	14.7	32.0
7	14.1	32.8	14.6	32.8	14.9	32.5
8	12.6	32.7	15.4	32.4	14.6	32.3
9	12.7	32.4	14.3	32.7	14.3	30.7
10	12.0	32.3	13.6	31.9	14.8	31.5
11	12.4	32.5	13.8	31.9	14.7	31.2
12	12.3	32.3	14.3	32.0	14.5	31.6
13	12.8	32.8	14.6	31.9	14.8	30.8
14	12.4	32.8	14.1	31.9	14.3	32.0
15	13.1	32.9	14.6	32.1	14.1	31.6
16	13.0	32.4	15.4	32.0	14.1	31.8
17	12.6	32.5	14.4	31.9	13.8	31.9
18	13.1	32.9	13.8	32.0	13.7	31.9
19	12.4	32.8	14.3	32.5	13.5	31.9
20	12.1	32.8	14.1	31.9	13.8	31.9
21	12.3	32.9	14.1	32.4	13.4	31.4
22	12.7	*33.0	13.4	31.9	13.5	31.2
23	12.4	*33.2	13.2	31.9	13.6	31.0
24	12.1	*33.0	13.9	32.5	13.2	29.0
25	12.3	*33.2	13.6	32.4	13.5	28.5
26	12.9	32.9	14.1	32.1	13.9	30.3
27	11.9	32.8	14.0	32.2	13.8	31.5
28	11.8	32.9	13.8	31.8	14.1	31.4
29	11.2	32.8	14.2	31.9	13.8	30.6
30	12.3	32.4	14.2	32.0	13.5	31.5
31	14.5	32.8	14.1	32.3	0.0	0.0
MEANS	12.6	32.6	14.1	32.1	14.2	31.3
OBSVNS.	31	27	31	25	30	30
MAXIMUM	14.5	32.9	15.6	32.8	15.4	32.5
MINIMUM	11.2	32.1	13.2	31.8	13.2	28.5
STD.DEV.	.68	.26	.59	.29	.60	.88

KAINS ISLAND

50 26 39 N

128 01 47 W

OCTOBER

NOVEMBER

DECEMBER 1978

DATE	TEMP	SAL	TEMP	SAL	TEMP	SAL
1	13.2	29.5	11.7	29.7	9.3	31.1
2	13.4	28.5	11.6	29.0	9.3	30.0
3	13.5	28.9	10.9	28.6	9.3	31.2
4	13.2	29.1	10.9	29.9	8.9	31.0
5	13.4	30.2	11.2	30.4	9.0	31.2
6	13.2	29.9	11.4	30.4	8.8	31.5
7	13.4	30.4	11.4	27.8	8.7	31.8
8	13.5	30.6	9.9	22.9	9.1	31.2
9	13.7	30.7	9.9	24.7	9.0	31.4
10	13.8	30.7	9.3	25.9	9.1	30.7
11	13.4	30.7	9.1	27.8	8.6	31.6
12	12.7	30.2	9.2	28.0	8.8	30.8
13	13.0	30.2	9.1	28.6	8.4	30.8
14	13.2	30.2	10.1	30.0	8.2	31.4
15	12.7	30.4	10.0	30.3	8.5	31.6
16	13.4	29.3	9.4	29.9	8.2	31.0
17	13.6	29.5	9.3	30.2	8.2	30.2
18	13.6	30.6	8.9	30.6	8.3	30.2
19	13.1	30.3	8.7	30.8	8.1	30.7
20	13.1	30.6	8.5	30.8	8.2	29.7
21	12.4	30.7	8.7	31.0	7.9	30.2
22	12.4	30.7	8.7	31.1	8.1	31.0
23	12.4	30.6	9.0	30.7	8.3	30.2
24	11.4	29.9	9.3	31.2	7.9	29.8
25	11.4	28.1	8.7	29.8	7.6	29.5
26	11.5	28.1	8.4	30.4	8.0	29.5
27	11.6	30.0	9.3	30.6	7.1	29.1
28	11.6	30.0	9.0	30.2	6.6	29.5
29	11.2	29.9	9.4	31.0	6.9	31.1
30	11.6	30.4	9.3	31.2	6.6	31.6
31	11.9	30.8	0.0	0.0	5.9	31.1
MEANS	12.8	30.0	9.7	29.4	8.2	30.7
OBSVNS.	31	31	30	30	31	31
YRLY. MEANS.....					10.8	30.7
MAXIMUM	13.8	30.8	11.7	31.2	9.3	31.8
MINIMUM	11.2	28.1	8.4	22.9	5.9	29.1
STD.DEV.	.83	.77	1.01	1.98	.86	.75

AMPHITRITE POINT

48 55 16 N

125 32 17 W

JANUARY

FEBRUARY

MARCH

1978

DATE	TEMP	SAL	TEMP	SAL	TEMP	SAL
1	6.9	26.8	8.0	28.4	8.7	28.5
2	6.7	26.9	7.9	28.5	8.7	29.1
3	6.6	26.8	8.3	28.8	7.9	28.5
4	7.4	25.8	8.3	28.4	7.9	28.6
5	* 7.5	*27.1	8.7	29.1	8.1	28.8
6	7.7	28.4	8.6	29.1	8.6	28.5
7	7.2	26.3	8.3	28.9	8.8	29.5
8	* 7.8	*27.3	8.5	29.4	9.1	30.0
9	8.4	28.4	8.8	30.2	9.1	29.8
10	8.6	28.4	9.8	28.5	8.9	29.5
11	8.7	28.6	9.1	28.8	9.1	29.9
12	8.5	28.2	8.6	28.1	9.0	29.5
13	8.3	28.2	8.7	29.1	8.9	29.9
14	8.7	28.9	8.7	29.0	9.3	30.0
15	8.4	28.6	8.7	28.9	9.0	29.5
16	8.2	28.1	7.9	29.0	8.8	28.5
17	8.1	28.4	8.3	29.0	8.8	28.9
18	8.6	29.3	8.6	28.1	8.9	28.8
19	8.6	29.7	8.8	28.1	8.9	29.5
20	8.8	29.9	8.9	28.5	9.1	30.0
21	8.9	29.7	9.1	28.0	9.3	30.4
22	9.0	29.4	9.1	27.4	9.6	29.9
23	8.4	27.8	9.7	29.5	9.7	28.0
24	8.2	27.3	9.2	28.5	9.4	29.8
25	8.7	28.6	9.3	28.2	9.8	30.2
26	9.1	28.9	9.2	28.8	9.7	29.7
27	8.7	27.6	9.1	28.0	9.7	28.5
28	8.5	27.8	9.1	28.8	9.8	30.4
29	8.6	28.1	0.0	0.0	10.3	30.2
30	8.1	27.7	0.0	0.0	9.8	31.8
31	8.2	28.1	0.0	0.0	9.7	29.9
MEANS	8.2	28.2	8.8	28.7	9.1	29.5
OBSVNS.	29	29	28	28	31	31
MAXIMUM	9.1	29.9	9.8	30.2	10.3	31.8
MINIMUM	6.6	25.8	7.9	27.4	7.9	28.0
STD.DEV.	.67	1.01	.48	.56	.57	.80

AMPHITRITE POINT 48 55 16 N 125 32 17 W

APRIL

MAY

JUNE

1978

DATE	TEMP	SAL	TEMP	SAL	TEMP	SAL
1	9.7	29.7	10.6	29.7	12.6	30.0
2	8.6	29.4	10.5	29.5	13.0	30.3
3	8.9	28.4	10.0	30.7	14.0	29.7
4	9.5	29.5	9.8	30.7	13.7	30.4
5	9.4	29.3	10.8	30.6	14.3	30.3
6	9.7	28.5	11.0	31.0	14.7	29.8
7	10.0	29.9	10.8	31.2	13.9	30.8
8	10.1	30.7	* 11.1	* 31.2	12.4	31.0
9	10.8	30.6	11.4	31.2	12.6	30.2
10	9.7	30.7	10.4	31.0	12.7	30.2
11	10.0	31.0	10.7	30.7	12.4	28.1
12	10.6	30.2	10.6	30.4	14.3	28.4
13	10.7	30.6	10.8	29.4	13.4	25.1
14	10.0	29.7	10.9	29.5	13.4	30.4
15	9.7	29.0	11.1	30.8	13.1	30.2
16	10.0	30.4	10.9	30.4	13.4	29.9
17	9.7	29.4	10.7	30.3	14.1	29.9
18	9.7	29.3	11.1	30.4	14.0	30.2
19	9.7	28.4	11.9	30.0	14.6	30.2
20	10.0	28.6	12.0	30.6	14.9	30.2
21	10.3	28.9	10.9	30.8	14.2	29.7
22	10.0	27.8	11.1	30.7	13.8	29.5
23	10.3	29.3	12.1	30.3	14.3	30.6
24	10.3	29.5	12.4	30.0	13.4	29.5
25	11.1	29.5	11.7	29.9	13.2	31.1
26	10.8	29.5	11.3	27.4	14.3	30.8
27	11.4	29.8	11.3	28.4	13.6	31.2
28	10.8	30.0	11.5	31.0	13.7	31.1
29	10.8	29.8	11.7	30.6	13.9	31.1
30	10.3	29.7	11.1	30.0	14.1	30.8
31	0.0	0.0	11.5	29.9	0.0	0.0
MEANS	10.1	29.6	11.1	30.2	13.7	30.0
OBSVNS.	30	30	30	30	30	30
MAXIMUM	11.4	31.0	12.4	31.2	14.9	31.2
MINIMUM	8.6	27.8	9.8	27.4	12.4	25.1
STD.DEV.	.62	.77	.60	.82	.69	1.17

AMPHITRITE POINT 48 55 16 N 125 32 17 W

JULY

AUGUST

SEPTEMBER 1978

DATE	TEMP	SAL	TEMP	SAL	TEMP	SAL
1	14.4	30.8	12.4	32.0	13.6	29.8
2	14.2	31.2	12.5	32.1	14.3	28.5
3	13.0	31.2	12.5	32.0	14.3	29.7
4	12.1	31.6	12.8	32.0	14.6	31.2
5	12.9	31.2	13.1	32.4	15.3	29.0
6	13.3	31.1	12.8	32.1	15.2	28.8
7	13.6	31.1	14.7	32.7	15.6	28.8
8	12.4	31.1	13.9	31.8	15.2	28.9
9	11.8	31.6	12.2	32.7	14.6	29.1
10	11.9	31.6	12.8	32.0	15.3	27.6
11	12.6	31.6	12.8	28.8	14.4	26.4
12	13.1	32.0	12.9	29.8	14.1	28.6
13	12.9	31.9	13.2	31.4	14.2	28.6
14	12.8	31.5	12.9	29.4	14.0	28.9
15	11.4	31.9	12.5	29.7	13.6	30.2
16	11.1	31.9	13.9	31.1	13.6	29.8
17	12.3	31.9	13.6	32.1	12.9	29.7
18	12.2	32.1	13.2	30.2	14.1	29.8
19	12.7	32.3	13.8	31.0	14.1	29.7
20	13.8	32.7	14.1	31.5	13.9	29.4
21	15.3	31.6	14.2	31.5	13.9	28.6
22	16.4	32.0	* 13.7	* 29.5	13.8	28.5
23	15.7	31.8	13.1	27.4	13.8	27.2
24	15.4	31.4	11.9	30.3	13.9	29.7
25	* 15.1	* 31.5	12.2	28.6	13.6	29.7
26	14.7	31.6	12.5	29.1	14.0	28.6
27	14.9	31.9	12.6	29.9	13.8	28.2
28	13.6	32.4	12.7	30.2	13.7	23.4
29	12.7	32.0	13.2	31.0	14.1	29.9
30	12.1	31.9	13.1	31.1	14.0	30.2
31	12.2	31.8	13.6	29.9	0.0	0.0
MEANS	13.3	31.7	13.1	30.9	14.2	28.9
OBSVNS.	30	30	30	30	30	30
MAXIMUM	16.4	32.7	14.7	32.7	15.6	31.2
MINIMUM	11.1	30.8	11.9	27.4	12.9	23.4
STD.DEV.	1.34	.43	.67	1.35	.62	1.41

AMPHITRITE POINT 48 55 16 N 125 32 17 W

OCTOBER

NOVEMBER

DECEMBER 1978

DATE	TEMP	SAL	TEMP	SAL	TEMP	SAL
1	14.1	30.0	10.8	30.8	8.3	30.4
2	14.1	29.7	10.4	30.7	8.2	30.8
3	14.3	29.5	10.0	30.8	8.4	28.4
4	14.6	28.5	9.8	31.2	8.2	31.1
5	14.5	29.9	* 9.8	*22.1	* 7.7	*30.8
6	14.7	29.7	9.7	12.9	7.2	30.4
7	14.6	29.8	9.9	23.4	6.9	30.3
8	14.4	29.1	9.2	30.3	6.9	30.7
9	14.4	29.8	8.3	30.4	7.2	30.7
10	14.1	30.2	6.9	29.4	6.9	30.2
11	13.3	30.6	8.1	29.4	7.8	30.6
12	13.1	30.8	8.1	29.8	7.2	31.0
13	12.8	29.8	7.8	29.0	6.2	30.2
14	13.3	30.0	7.5	29.0	7.5	30.4
15	13.7	29.9	7.5	29.4	7.7	31.8
16	13.9	29.9	8.6	30.6	* 7.6	*31.3
17	14.0	29.4	8.6	30.4	7.5	30.7
18	13.9	29.9	7.8	29.9	7.4	30.7
19	13.1	30.2	7.9	29.9	6.7	29.0
20	11.9	31.6	7.5	30.0	6.8	29.7
21	12.8	30.7	7.6	30.3	7.5	30.3
22	12.3	30.4	7.7	30.4	7.9	31.0
23	12.1	28.0	7.3	30.4	7.8	30.4
24	10.8	30.0	7.3	30.2	7.8	30.2
25	10.8	30.2	7.7	28.9	6.8	30.6
26	10.8	30.7	7.8	30.6	6.1	30.2
27	11.1	31.2	7.5	30.6	6.1	30.3
28	11.0	30.6	8.2	30.8	4.4	28.4
29	10.7	29.7	8.3	30.8	4.7	29.1
30	10.4	30.2	8.4	29.9	4.7	29.8
31	10.6	30.6	0.0	0.0	4.6	30.2

MEANS	12.9	30.0	8.3	29.3	6.9	30.3
OBSVNS.	31	31	29	29	29	29
YRLY. MEANS.....					10.8	29.8
MAXIMUM	14.7	31.6	10.8	31.2	8.4	31.8
MINIMUM	10.4	28.0	6.9	12.9	4.4	28.4
STD. DEV.	1.47	.71	1.04	3.45	1.14	.75

CAPE BEALE

48 47 12 N

125 12 53 W

JANUARY

FEBRUARY

MARCH

1978

DATE	TEMP	SAL	TEMP	SAL	TEMP	SAL
1	6.0	28.42	7.6	29.05	9.6	30.35
2	5.8	28.34	7.9	29.37	7.8	29.43
3	7.0	28.38	8.2	29.36	* 7.8	*30.05
4	8.0	28.86	8.4	29.36	7.7	30.68
5	8.0	29.10	8.8	29.63	7.6	31.04
6	7.1	29.71	9.1	29.33	8.5	30.71
7	7.6	29.33	* 9.1	*29.13	8.6	30.15
8	8.6	29.57	9.2	28.93	8.6	30.13
9	8.5	29.29	9.2	29.32	8.6	30.54
10	8.8	29.79	8.9	29.16	8.6	30.75
11	8.6	29.66	8.6	29.51	9.4	30.50
12	8.6	29.55	8.6	29.23	9.3	30.61
13	8.5	30.05	9.1	29.66	9.6	29.96
14	8.6	29.06	8.3	28.59	9.6	30.73
15	8.6	29.44	9.3	28.93	* 9.7	*30.79
16	8.0	29.53	8.6	29.59	* 9.9	*30.85
17	8.3	29.38	8.6	29.36	10.1	30.92
18	8.6	29.47	8.8	29.78	9.6	30.98
19	8.8	29.77	8.8	30.09	9.2	30.71
20	9.1	29.73	8.6	30.16	9.4	30.50
21	9.4	28.73	9.1	29.31	9.4	30.34
22	8.6	29.64	10.2	29.91	9.4	30.18
23	* 8.6	*29.58	* 9.4	*30.02	9.6	30.92
24	* 8.7	*29.52	8.6	30.12	9.6	30.89
25	8.8	29.45	8.9	30.12	9.8	30.43
26	8.7	29.41	8.7	30.21	9.6	30.81
27	8.7	30.00	8.9	30.36	9.6	29.42
28	8.6	30.02	8.9	30.33	9.6	30.29
29	8.6	30.09	0.0	0.00	9.7	29.99
30	* 8.3	*29.75	0.0	0.00	* 10.1	*30.05
31	* 8.0	*29.40	0.0	0.00	10.5	30.11
MEANS	8.2	29.39	8.8	29.53	9.2	30.44
OBSVNS.	27	27	26	26	27	27
MAXIMUM	9.4	30.09	10.2	30.36	10.5	30.98
MINIMUM	5.8	28.34	7.6	28.59	7.6	29.43
STD.DEV.	.86	.50	.49	.48	.72	.43

CAPE REALE

48 47 12 N

125 12 53 W

APRIL

MAY

JUNE

1978

DATE	TEMP	SAL	TEMP	SAL	TEMP	SAL
1	10.6	30.91	10.6	29.91	12.8	30.98
2	9.6	30.95	10.4	29.91	13.7	31.16
3	9.6	31.13	10.0	29.27	13.2	31.37
4	9.6	30.90	9.7	31.00	13.9	31.66
5	9.6	30.73	10.5	31.88	* 13.9	*31.81
6	9.8	30.39	11.1	31.28	13.9	31.96
7	10.2	30.78	12.3	25.04	13.6	32.07
8	10.6	30.60	11.6	31.37	13.5	31.55
9	10.6	31.06	* 11.3	*31.08	12.2	31.53
10	11.0	30.87	10.9	30.78	13.4	31.82
11	11.6	31.25	11.6	30.67	12.9	31.66
12	* 11.5	*31.14	10.6	30.20	* 12.6	*31.30
13	* 11.4	*31.03	10.6	30.52	12.2	30.93
14	11.3	30.91	10.6	30.37	* 12.9	*31.24
15	* 11.4	*30.56	10.4	30.63	13.7	31.56
16	11.6	30.21	* 10.6	*30.78	12.6	31.70
17	9.8	30.61	10.8	30.94	13.6	32.50
18	9.7	29.03	* 10.9	*31.00	13.6	31.56
19	9.7	30.46	11.0	31.06	* 13.7	*31.59
20	9.6	30.70	11.6	31.19	13.8	31.63
21	10.0	30.72	11.6	31.18	13.2	31.72
22	* 0.0	* 0.00	11.2	31.10	* 13.0	*31.71
23	11.1	30.07	11.9	31.86	12.8	31.70
24	10.8	29.66	11.7	31.21	13.2	31.15
25	11.4	29.32	11.3	31.22	13.5	31.19
26	11.5	29.37	11.6	31.03	* 13.6	*31.41
27	* 11.4	*29.81	12.6	30.23	13.7	31.63
28	* 11.2	*30.24	* 12.1	*31.06	* 13.0	*31.99
29	11.0	30.67	11.5	31.89	12.3	32.35
30	12.9	30.37	13.4	29.73	11.6	32.77
31	0.0	0.00	12.1	30.82	0.0	0.00
MEANS	10.6	30.49	11.2	30.42	13.2	31.66
OBSVNS.	24	24	27	27	23	23
MAXIMUM	12.9	31.25	13.4	31.88	13.9	32.77
MINIMUM	9.6	29.03	9.7	25.04	11.6	30.93
STD.DEV.	.89	.60	.82	1.29	.64	.46

CAPE BEALE

48 47 12 N

125 12 53 W

JULY

AUGUST

SEPTEMBER 1978

DATE	TEMP	SAL	TEMP	SAL	TEMP	SAL
1	13.1	32.20	11.5	32.32	* 14.0	*31.69
2	13.0	32.31	11.6	31.95	13.9	31.65
3	13.6	32.07	12.6	31.88	13.4	31.19
4	12.1	32.17	11.6	32.08	* 13.7	*31.18
5	13.0	31.61	11.6	32.22	14.0	31.18
6	13.5	31.29	12.0	31.08	14.5	31.20
7	12.5	31.82	11.1	32.39	* 14.4	*31.03
8	12.5	31.85	11.0	32.61	14.3	30.86
9	12.0	31.86	11.1	32.49	13.9	29.86
10	11.5	31.87	12.6	32.26	* 0.0	* 0.00
11	13.5	31.30	12.0	30.44	* 0.0	* 0.00
12	13.5	31.24	12.6	31.92	* 0.0	* 0.00
13	12.8	31.08	12.0	31.93	* 0.0	* 0.00
14	12.6	31.85	11.8	31.42	* 0.0	* 0.00
15	11.6	32.04	12.0	31.70	* 0.0	* 0.00
16	11.0	31.12	11.6	31.95	* 0.0	* 0.00
17	11.0	32.16	12.5	31.63	* 0.0	* 0.00
18	11.0	32.24	12.5	31.51	12.8	31.33
19	11.6	32.17	* 12.6	*31.52	12.6	31.65
20	11.5	32.19	12.8	31.53	12.6	31.84
21	12.5	31.98	* 12.4	*31.75	12.6	31.43
22	13.0	31.75	11.9	31.98	12.4	31.42
23	11.0	32.24	11.7	31.80	* 12.4	*31.35
24	11.6	32.06	12.6	29.96	12.5	31.27
25	13.0	31.77	12.3	28.47	12.8	31.01
26	12.0	31.95	13.0	30.76	12.6	30.49
27	12.9	31.83	* 13.3	*30.95	12.9	31.10
28	14.0	30.95	* 13.6	*31.14	13.1	30.79
29	14.0	31.17	14.0	31.33	13.7	30.86
30	10.6	31.25	* 14.0	*31.52	14.0	30.76
31	10.6	32.28	14.1	31.72	0.0	0.00
MEANS	12.3	31.80	12.2	31.59	13.3	31.06
OBSVNS.	31	31	26	26	18	18
MAXIMUM	14.0	32.31	14.1	32.61	14.5	31.84
MINIMUM	10.6	30.95	11.0	28.47	12.4	29.06
STD.DEV.	1.01	.41	.78	.89	.70	.61

CAPE BEALE

48 47 12 N 125 12 53 W

OCTOBER

NOVEMBER

DECEMBER 1978

DATE	TEMP	SAL	TEMP	SAL	TEMP	SAL
1	14.2	31.06	9.5	30.84	7.9	31.70
2	* 14.5	*30.36	9.6	30.87	7.9	31.78
3	14.8	29.66	* 9.4	*31.00	7.9	31.05
4	13.7	30.09	9.1	31.13	7.6	31.33
5	13.6	30.01	8.8	31.01	* 7.6	*31.57
6	* 13.6	*30.19	9.1	29.18	7.6	31.80
7	13.6	30.37	9.5	27.82	7.0	31.79
8	13.6	30.51	* 8.9	*29.64	7.4	31.80
9	13.5	30.36	8.3	31.46	7.4	31.58
10	13.1	30.38	* 8.2	31.83	7.6	31.58
11	12.4	30.63	8.0	31.95	7.5	31.26
12	11.7	30.09	8.6	31.89	7.3	31.86
13	11.9	31.38	8.5	31.69	6.9	31.90
14	12.1	31.44	8.4	30.38	7.4	32.13
15	12.5	31.56	8.4	30.89	* 7.4	*31.81
16	12.5	31.26	8.5	31.54	7.4	31.49
17	12.5	30.47	8.4	31.75	7.6	31.50
18	* 12.0	*30.96	8.0	31.79	7.5	32.48
19	11.4	31.45	7.4	32.00	7.5	31.93
20	* 10.9	*31.58	* 7.9	*32.01	7.5	31.12
21	10.4	31.72	8.4	32.02	7.5	30.88
22	9.9	31.86	* 0.0	* 0.00	7.6	31.21
23	9.8	31.39	* 0.0	* 0.00	7.5	31.10
24	* 9.8	*31.52	* 0.0	* 0.00	7.5	30.76
25	* 9.7	*31.65	* 0.0	* 0.00	7.4	31.37
26	9.6	31.78	* 0.0	* 0.00	7.6	31.69
27	9.6	31.59	8.1	31.88	7.0	31.26
28	9.4	31.54	8.1	31.56	6.6	31.67
29	9.4	31.50	* 8.1	*31.50	6.6	31.68
30	9.4	31.74	8.2	31.43	6.0	31.45
31	* 9.4	*31.29	0.0	0.00	6.0	31.51

MEANS	11.9	30.99	8.5	31.19	7.3	31.54
OBSVNS.	24	24	20	21	29	29
YRLY. MEANS.....					10.5	30.94
MAXIMUM	14.8	31.86	9.6	32.02	7.9	32.48
MINIMUM	9.4	29.66	7.4	27.82	6.0	30.76
STD. DEV.	1.76	.68	.57	1.03	.49	.38

BANFIELD

48 50 05 N

125 08 07 W

JANUARY

FEBRUARY

MARCH

1978

DATE	TEMP	SAL	TEMP	SAL	TEMP	SAL
1	* 0.0	* 0.0	* 0.0	* 0.0	* 0.0	* 0.0
2	* 0.0	* 0.0	* 0.0	* 0.0	* 0.0	* 0.0
3	* 0.0	* 0.0	* 0.0	* 0.0	* 0.0	* 0.0
4	* 0.0	* 0.0	* 0.0	* 0.0	* 0.0	* 0.0
5	* 0.0	* 0.0	* 0.0	* 0.0	* 0.0	* 0.0
6	* 0.0	* 0.0	* 0.0	* 0.0	* 0.0	* 0.0
7	* 0.0	* 0.0	* 0.0	* 0.0	* 0.0	* 0.0
8	* 0.0	* 0.0	* 0.0	* 0.0	* 0.0	* 0.0
9	* 0.0	* 0.0	* 0.0	* 0.0	* 0.0	* 0.0
10	* 0.0	* 0.0	* 0.0	* 0.0	* 0.0	* 0.0
11	* 0.0	* 0.0	* 0.0	* 0.0	* 0.0	* 0.0
12	* 0.0	* 0.0	* 0.0	* 0.0	* 0.0	* 0.0
13	* 0.0	* 0.0	* 0.0	* 0.0	* 0.0	* 0.0
14	* 0.0	* 0.0	* 0.0	* 0.0	* 0.0	* 0.0
15	* 0.0	* 0.0	* 0.0	* 0.0	* 0.0	* 0.0
16	* 0.0	* 0.0	* 0.0	* 0.0	* 0.0	* 0.0
17	* 0.0	* 0.0	* 0.0	* 0.0	* 0.0	* 0.0
18	* 0.0	* 0.0	* 0.0	* 0.0	* 0.0	* 0.0
19	* 0.0	* 0.0	* 0.0	* 0.0	* 0.0	* 0.0
20	* 0.0	* 0.0	* 0.0	* 0.0	* 0.0	* 0.0
21	* 0.0	* 0.0	* 0.0	* 0.0	* 0.0	* 0.0
22	* 0.0	* 0.0	* 0.0	* 0.0	* 0.0	* 0.0
23	* 0.0	* 0.0	* 0.0	* 0.0	* 0.0	* 0.0
24	* 0.0	* 0.0	* 0.0	* 0.0	* 0.0	* 0.0
25	* 0.0	* 0.0	* 0.0	* 0.0	* 0.0	* 0.0
26	* 0.0	* 0.0	* 0.0	* 0.0	* 0.0	* 0.0
27	* 0.0	* 0.0	* 0.0	* 0.0	* 0.0	* 0.0
28	* 0.0	* 0.0	* 0.0	* 0.0	* 0.0	* 0.0
29	* 0.0	* 0.0	0.0	0.0	* 0.0	* 0.0
30	* 0.0	* 0.0	0.0	0.0	* 0.0	* 0.0
31	* 0.0	* 0.0	0.0	0.0	* 0.0	* 0.0
MEANS	0.0	0.0	0.0	0.0	0.0	0.0
OBSVNS.	0	0	0	0	0	0
MAXIMUM	0.0	0.0	0.0	0.0	0.0	0.0
MINIMUM	0.0	0.0	0.0	0.0	0.0	0.0
STD.DEV.	0.00	0.00	0.00	0.00	0.00	0.00

BAMFIELD

48 50 05 N

125 08 07 W

APRIL

MAY

JUNE

1978

DATE	TEMP	SAL	TEMP	SAL	TEMP	SAL
1	* 0.0	* 0.0	* 0.0	* 0.00	16.0	22.75
2	* 0.0	* 0.0	* 0.0	* 0.00	15.8	24.71
3	* 0.0	* 0.0	* 0.0	* 0.00	15.9	27.86
4	* 0.0	* 0.0	11.0	28.80	17.0	26.56
5	* 0.0	* 0.0	11.5	29.03	16.0	27.37
6	* 0.0	* 0.0	12.0	28.09	17.5	26.83
7	* 0.0	* 0.0	13.0	27.34	18.5	26.97
8	* 0.0	* 0.0	13.0	28.31	17.0	28.06
9	* 0.0	* 0.0	13.0	28.89	11.2	28.43
10	* 0.0	* 0.0	12.5	29.62	* 0.0	* 0.00
11	* 0.0	* 0.0	13.5	27.53	* 0.0	* 0.00
12	* 0.0	* 0.0	11.5	30.18	* 0.0	* 0.00
13	* 0.0	* 0.0	12.0	27.02	15.0	28.25
14	* 0.0	* 0.0	13.0	25.73	16.5	24.91
15	* 0.0	* 0.0	* 13.0	* 26.40	16.0	25.57
16	* 0.0	* 0.0	* 13.1	27.06	* 16.5	* 26.02
17	* 0.0	* 0.0	13.2	28.52	17.0	26.47
18	* 0.0	* 0.0	13.3	28.32	17.0	26.46
19	* 0.0	* 0.0	13.5	23.92	* 17.2	* 27.20
20	* 0.0	* 0.0	15.5	23.06	17.5	27.94
21	* 0.0	* 0.0	13.0	29.56	18.0	25.69
22	* 0.0	* 0.0	12.5	29.79	14.5	* 26.18
23	* 0.0	* 0.0	14.0	29.40	* 15.7	* 26.67
24	* 0.0	* 0.0	14.2	28.64	17.0	27.16
25	* 0.0	* 0.0	13.0	29.40	16.5	27.91
26	* 0.0	* 0.0	13.1	29.42	* 17.7	* 27.04
27	* 0.0	* 0.0	* 13.7	* 28.42	* 18.9	* 26.16
28	* 0.0	* 0.0	* 14.3	* 27.42	20.2	25.28
29	* 0.0	* 0.0	15.0	26.42	16.0	28.80
30	* 0.0	* 0.0	15.8	23.92	18.0	26.62
31	0.0	0.0	11.0	23.08	0.0	0.00
MEANS	0.0	0.0	13.0	27.64	16.6	26.70
OBSVNS.	0	0	24	25	22	21
MAXIMUM	0.0	0.0	15.8	30.18	20.2	28.80
MINIMUM	0.0	0.0	11.0	23.08	11.2	22.71
STD.DEV.	0.00	0.00	1.25	2.15	1.71	1.48

BANFIELD

48 50 05 N

125 08 07 W

JULY

AUGUST

SEPTEMBER 1978

DATE	TEMP	SAL	TEMP	SAL	TEMP	SAL
1	17.8	27.01	15.4	30.72	* 15.1	*27.44
2	18.0	28.20	13.8	31.43	* 15.0	*27.86
3	12.0	28.36	12.3	31.74	14.8	28.29
4	* 14.8	*28.83	14.0	31.69	15.3	*27.61
5	17.7	29.31	14.0	31.66	16.0	26.92
6	17.8	28.71	16.1	31.44	15.9	26.01
7	17.3	28.45	* 0.0	* 0.00	16.8	27.34
8	15.7	30.97	* 0.0	* 0.00	15.5	28.63
9	15.5	29.95	* 0.0	* 0.00	* 0.0	* 0.00
10	14.2	29.92	14.2	31.70	* 0.0	* 0.00
11	* 16.0	*28.98	14.0	31.58	* 0.0	* 0.00
12	17.8	28.05	14.5	31.37	15.0	25.94
13	17.6	28.98	16.9	29.18	15.0	25.65
14	17.3	29.72	* 15.3	*30.21	15.5	21.32
15	15.0	31.96	13.7	31.24	14.6	26.37
16	14.7	31.74	14.3	31.12	* 14.8	*27.43
17	14.3	31.80	14.9	30.67	15.1	28.50
18	* 15.6	*31.34	* 14.9	*30.33	* 14.8	*28.39
19	16.9	30.88	14.9	29.99	* 14.5	*28.27
20	* 18.3	*30.53	* 0.0	* 0.00	14.2	28.15
21	19.8	30.18	* 0.0	* 0.00	14.2	28.56
22	19.5	*30.15	* 0.0	* 0.00	* 0.0	* 0.00
23	* 18.8	*30.12	* 0.0	* 0.00	* 0.0	* 0.00
24	18.0	30.08	15.2	29.53	* 0.0	* 0.00
25	* 8.0	* 0.00	* 15.0	*29.02	* 0.0	* 0.00
26	* 0.0	* 0.00	14.8	28.51	13.0	28.51
27	* 0.0	* 0.00	15.2	29.90	13.0	30.06
28	18.0	29.09	* 15.1	*29.10	13.5	30.18
29	17.7	*29.55	15.0	28.30	14.0	27.45
30	16.8	30.02	16.5	21.61	* 14.1	*27.91
31	* 16.1	*30.37	15.2	27.02	0.0	0.00
MEANS	16.8	29.67	14.7	30.02	14.8	27.37
OBSVNS.	22	20	20	20	17	16
MAXIMUM	19.8	31.96	16.9	31.74	16.8	30.18
MINIMUM	12.0	27.01	12.3	21.61	13.0	21.32
STD.DEV.	1.85	1.35	1.05	2.40	1.05	2.11

BAMFIELD

48 50 05 N

125 08 07 W

OCTOBER

NOVEMBER

DECEMBER 1978

DATE	TEMP	SAL	TEMP	SAL	TEMP	SAL
1	* 14.3	*28.37	10.5	29.75	8.0	31.51
2	14.5	28.83	* 10.2	*29.85	* 8.0	*31.42
3	15.5	28.31	9.8	29.94	* 8.1	*31.32
4	15.4	27.85	* 9.8	*30.36	8.1	31.22
5	15.2	27.84	9.7	30.78	7.8	31.89
6	* 0.0	* 0.00	* 0.0	* 0.00	7.0	* 0.00
7	* 0.0	* 0.00	* 0.0	* 0.00	* 0.0	* 0.00
8	* 0.0	* 0.00	* 0.0	* 0.00	* 0.0	* 0.00
9	* 0.0	* 0.00	* 0.0	* 0.00	* 0.0	* 0.00
10	* 0.0	* 0.00	* 0.0	* 0.00	7.6	31.02
11	14.0	28.93	9.0	29.07	7.8	31.46
12	13.9	28.50	9.0	30.51	* 7.6	*31.47
13	13.6	28.25	* 9.0	*30.62	7.3	31.48
14	13.5	28.55	* 9.0	*30.74	* 0.0	* 0.00
15	13.3	27.35	9.0	30.86	* 0.0	* 0.00
16	* 13.4	*28.00	9.4	30.91	* 0.0	* 0.00
17	* 13.5	*28.66	9.1	30.16	* 0.0	* 0.00
18	13.6	29.32	8.8	31.23	* 0.0	* 0.00
19	* 13.4	*28.97	* 8.6	*31.33	7.5	28.33
20	13.2	28.62	* 8.4	*31.43	7.5	29.27
21	13.4	29.74	8.2	31.53	* 0.0	* 0.00
22	* 0.0	* 0.00	* 0.0	* 0.00	* 0.0	* 0.00
23	* 0.0	* 0.00	* 0.0	* 0.00	* 0.0	* 0.00
24	* 0.0	* 0.00	* 0.0	* 0.00	* 0.0	* 0.00
25	* 0.0	* 0.00	* 0.0	* 0.00	* 0.0	* 0.00
26	* 0.0	* 0.00	8.0	31.85	* 0.0	* 0.00
27	11.0	30.02	* 0.0	* 0.00	* 0.0	* 0.00
28	11.5	30.29	* 0.0	* 0.00	* 0.0	* 0.00
29	10.8	30.40	* 0.0	* 0.00	* 0.0	* 0.00
30	* 10.7	*30.19	8.5	31.44	* 0.0	* 0.00
31	* 10.6	*29.97	0.0	0.00	* 0.0	* 0.00
MEANS	13.5	28.85	9.1	30.67	7.6	30.77
OBSVNS.	15	15	12	12	9	8
YRLY. MEANS.....						
MAXIMUM	15.5	30.40	10.5	31.85	8.1	31.89
MINIMUM	10.8	27.35	8.0	29.07	7.0	28.33
STD. DEV.	1.45	.93	.70	.82	.35	1.27

SHERINGHAM POINT

48 22 40 N

123 55 10 W

JANUARY

FEBRUARY

MARCH

1978

DATE	TEMP	SAL	TEMP	SAL	TEMP	SAL
1	7.4	* 0.0	7.9	* 0.0	8.2	* 0.0
2	7.1	* 0.0	7.9	* 0.0	8.4	* 0.0
3	7.2	* 0.0	7.8	* 0.0	8.3	* 0.0
4	7.2	* 0.0	8.1	* 0.0	8.4	* 0.0
5	7.2	* 0.0	8.0	* 0.0	8.4	* 0.0
6	7.4	* 0.0	8.2	* 0.0	8.4	* 0.0
7	7.3	* 0.0	8.1	* 0.0	8.4	* 0.0
8	7.8	* 0.0	8.4	* 0.0	8.6	* 0.0
9	7.7	* 0.0	8.3	* 0.0	8.6	* 0.0
10	7.4	* 0.0	8.4	* 0.0	8.7	* 0.0
11	8.2	* 0.0	8.3	* 0.0	8.6	* 0.0
12	7.7	* 0.0	8.2	* 0.0	8.5	* 0.0
13	7.9	* 0.0	8.1	* 0.0	8.5	* 0.0
14	7.7	* 0.0	8.3	* 0.0	8.8	* 0.0
15	8.2	* 0.0	8.2	* 0.0	8.6	* 0.0
16	7.6	* 0.0	8.2	* 0.0	8.8	* 0.0
17	7.7	* 0.0	8.2	* 0.0	8.5	* 0.0
18	7.7	* 0.0	8.2	* 0.0	8.8	* 0.0
19	7.7	* 0.0	8.1	* 0.0	8.9	* 0.0
20	7.6	* 0.0	8.3	* 0.0	8.8	* 0.0
21	7.9	* 0.0	8.4	* 0.0	8.6	* 0.0
22	7.9	* 0.0	8.4	* 0.0	8.9	* 0.0
23	7.9	* 0.0	8.3	* 0.0	8.6	* 0.0
24	7.7	* 0.0	8.3	* 0.0	8.9	* 0.0
25	8.2	* 0.0	8.3	* 0.0	8.7	* 0.0
26	7.8	* 0.0	8.2	* 0.0	8.8	* 0.0
27	8.3	* 0.0	8.3	* 0.0	8.8	* 0.0
28	8.2	* 0.0	8.5	* 0.0	8.8	* 0.0
29	7.9	* 0.0	0.0	0.0	8.9	* 0.0
30	8.0	* 0.0	0.0	0.0	8.8	* 0.0
31	8.1	* 0.0	0.0	0.0	9.0	* 0.0
MEANS	7.7	0.0	8.2	0.0	8.6	0.0
OBSVNS.	31	0	28	0	31	0
MAXIMUM	8.3	0.0	8.5	0.0	9.0	0.0
MINIMUM	7.1	0.0	7.8	0.0	8.2	0.0
STD.DEV.	.33	0.00	.17	0.00	.21	0.00

SHERINGHAM POINT

48 22 40 N

123 55 10 W

APRIL

MAY

JUNE

1978

DATE	TEMP	SAL	TEMP	SAL	TEMP	SAL
1	8.9	* 0.0	9.3	* 0.0	9.6	* 0.0
2	8.8	* 0.0	8.9	* 0.0	11.4	* 0.0
3	8.8	* 0.0	9.3	* 0.0	10.4	* 0.0
4	8.8	* 0.0	9.0	* 0.0	10.8	* 0.0
5	8.8	* 0.0	9.4	* 0.0	11.3	* 0.0
6	8.9	* 0.0	8.9	* 0.0	10.9	* 0.0
7	8.9	* 0.0	9.0	* 0.0	10.8	* 0.0
8	8.9	* 0.0	8.9	* 0.0	10.8	* 0.0
9	9.1	* 0.0	9.8	* 0.0	10.8	* 0.0
10	9.0	* 0.0	9.0	* 0.0	10.7	* 0.0
11	8.9	* 0.0	9.4	* 0.0	10.9	* 0.0
12	9.1	* 0.0	8.9	* 0.0	10.4	* 0.0
13	8.9	* 0.0	9.4	* 0.0	10.8	* 0.0
14	8.9	* 0.0	9.3	* 0.0	11.0	* 0.0
15	8.9	* 0.0	9.4	* 0.0	10.7	* 0.0
16	8.9	* 0.0	8.9	* 0.0	10.7	* 0.0
17	8.9	* 0.0	9.3	* 0.0	10.2	* 0.0
18	9.0	* 0.0	9.0	* 0.0	10.1	* 0.0
19	8.9	* 0.0	9.9	* 0.0	10.2	* 0.0
20	9.1	* 0.0	9.1	* 0.0	10.8	* 0.0
21	8.9	* 0.0	9.9	* 0.0	10.9	* 0.0
22	9.2	* 0.0	9.1	* 0.0	10.7	* 0.0
23	9.2	* 0.0	9.1	* 0.0	10.7	* 0.0
24	9.1	* 0.0	9.0	* 0.0	10.8	* 0.0
25	9.4	* 0.0	9.6	* 0.0	10.7	* 0.0
26	8.9	* 0.0	9.1	* 0.0	10.9	* 0.0
27	9.8	* 0.0	9.8	* 0.0	11.3	* 0.0
28	* 9.8	* 0.0	9.8	* 0.0	11.0	* 0.0
29	9.9	* 0.0	9.2	* 0.0	11.7	* 0.0
30	9.1	* 0.0	9.4	* 0.0	11.4	* 0.0
31	0.0	0.0	9.8	* 0.0	0.0	0.0
MEANS	9.0	0.0	9.3	0.0	10.8	0.0
OBSVNS.	29	0	31	0	30	0
MAXIMUM	9.9	0.0	9.9	0.0	11.7	0.0
MINIMUM	8.8	0.0	8.9	0.0	9.6	0.0
STD.DEV.	.27	0.00	.33	0.00	.42	0.00

SHERINGHAM POINT 48 22 40 N 123 55 10 W

JULY

AUGUST

SEPTEMBER 1978

DATE	TEMP	SAL	TEMP	SAL	TEMP	SAL
1	11.7	* 0.0	11.2	* 0.0	11.2	* 0.0
2	11.3	* 0.0	10.3	* 0.0	11.2	* 0.0
3	10.9	* 0.0	10.7	* 0.0	11.2	* 0.0
4	11.6	* 0.0	10.2	* 0.0	11.2	* 0.0
5	11.7	* 0.0	10.6	* 0.0	11.2	* 0.0
6	11.8	* 0.0	10.6	* 0.0	11.1	* 0.0
7	11.3	* 0.0	10.4	* 0.0	11.4	* 0.0
8	11.8	* 0.0	10.4	* 0.0	11.6	* 0.0
9	11.2	* 0.0	10.8	* 0.0	11.1	* 0.0
10	10.1	* 0.0	10.2	* 0.0	11.7	* 0.0
11	10.7	* 0.0	10.6	* 0.0	11.7	* 0.0
12	11.1	* 0.0	10.3	* 0.0	11.3	* 0.0
13	10.7	* 0.0	10.3	* 0.0	11.7	* 0.0
14	11.0	* 0.0	10.1	* 0.0	11.4	* 0.0
15	11.7	* 0.0	10.2	* 0.0	11.7	* 0.0
16	12.3	* 0.0	10.1	* 0.0	11.3	* 0.0
17	12.9	* 0.0	10.7	* 0.0	11.4	* 0.0
18	11.9	* 0.0	10.2	* 0.0	11.3	* 0.0
19	12.3	* 0.0	10.9	* 0.0	10.5	* 0.0
20	11.6	* 0.0	10.4	* 0.0	11.0	* 0.0
21	12.9	* 0.0	10.3	* 0.0	10.6	* 0.0
22	11.9	* 0.0	9.4	* 0.0	11.1	* 0.0
23	12.1	* 0.0	10.1	* 0.0	10.7	* 0.0
24	12.3	* 0.0	10.0	* 0.0	11.0	* 0.0
25	11.6	* 0.0	10.1	* 0.0	11.1	* 0.0
26	12.2	* 0.0	10.1	* 0.0	11.0	* 0.0
27	11.6	* 0.0	10.1	* 0.0	10.6	* 0.0
28	12.4	* 0.0	10.3	* 0.0	11.4	* 0.0
29	10.4	* 0.0	12.2	* 0.0	11.1	* 0.0
30	10.5	* 0.0	12.2	* 0.0	11.2	* 0.0
31	11.2	* 0.0	11.1	* 0.0	0.0	0.0
MEANS	11.6	0.0	10.5	0.0	11.2	0.0
OBSVNS.	31	0	31	0	30	0
MAXIMUM	12.9	0.0	12.2	0.0	11.7	0.0
MINIMUM	10.1	0.0	9.4	0.0	10.5	0.0
STD.DEV.	.69	0.00	.58	0.00	.32	0.00

SHERINGHAM POINT

48 22 40 N

123 55 10 W

OCTOBER

NOVEMBER

DECEMBER 1978

DATE	TEMP	SAL	TEMP	SAL	TEMP	SAL
1	10.6	* 0.0	8.9	* 0.0	6.5	* 0.0
2	10.6	* 0.0	9.4	* 0.0	7.8	* 0.0
3	10.1	* 0.0	9.1	* 0.0	7.8	* 0.0
4	11.0	* 0.0	8.9	* 0.0	7.8	* 0.0
5	10.1	* 0.0	8.6	* 0.0	7.6	* 0.0
6	10.6	* 0.0	8.3	* 0.0	7.8	* 0.0
7	10.0	* 0.0	8.8	* 0.0	7.7	* 0.0
8	10.6	* 0.0	8.3	* 0.0	7.8	* 0.0
9	10.0	* 0.0	8.4	* 0.0	7.7	* 0.0
10	10.2	* 0.0	7.8	* 0.0	7.6	* 0.0
11	9.5	* 0.0	8.3	* 0.0	7.6	* 0.0
12	10.3	* 0.0	8.2	* 0.0	7.3	* 0.0
13	10.0	* 0.0	8.1	* 0.0	7.2	* 0.0
14	10.2	* 0.0	7.8	* 0.0	7.3	* 0.0
15	9.6	* 0.0	8.2	* 0.0	7.3	* 0.0
16	9.8	* 0.0	7.7	* 0.0	7.2	* 0.0
17	9.7	* 0.0	7.5	* 0.0	7.4	* 0.0
18	9.5	* 0.0	7.4	* 0.0	7.3	* 0.0
19	9.4	* 0.0	6.1	* 0.0	7.3	* 0.0
20	9.6	* 0.0	6.1	* 0.0	7.2	* 0.0
21	10.0	* 0.0	6.9	* 0.0	7.3	* 0.0
22	9.4	* 0.0	6.7	* 0.0	7.2	* 0.0
23	9.5	* 0.0	7.1	* 0.0	7.2	* 0.0
24	9.4	* 0.0	7.3	* 0.0	5.0	* 0.0
25	8.9	* 0.0	7.0	* 0.0	6.7	* 0.0
26	9.2	* 0.0	6.8	* 0.0	7.2	* 0.0
27	9.4	* 0.0	6.9	* 0.0	7.1	* 0.0
28	9.4	* 0.0	7.8	* 0.0	7.2	* 0.0
29	9.3	* 0.0	6.8	* 0.0	7.1	* 0.0
30	9.2	* 0.0	7.8	* 0.0	7.3	* 0.0
31	9.1	* 0.0	0.0	0.0	7.2	* 0.0
MEANS	9.8	0.0	7.8	0.0	7.3	0.0
OBSVNS.	31	0	30	0	31	0
YRLY. MEANS.....					9.3	0.0
MAXIMUM	11.0	0.0	9.4	0.0	7.8	0.0
MINIMUM	8.9	0.0	6.1	0.0	5.0	0.0
STD. DEV.	.53	0.00	.87	0.00	.53	0.00

RACE ROCKS

48 17 57 N

123 31 48 W

JANUARY

FEBRUARY

MARCH

1978

DATE	TEMP	SAL	TEMP	SAL	TEMP	SAL
1	7.2	30.3	7.5	30.6	8.0	30.6
2	7.2	30.2	7.4	30.4	8.0	31.0
3	7.3	30.4	7.7	30.6	7.8	30.4
4	7.2	30.4	7.8	30.6	7.8	30.3
5	7.4	30.3	8.0	30.7	8.1	30.6
6	7.6	30.6	8.1	30.8	8.2	30.8
7	7.6	30.4	8.1	30.8	8.2	30.7
8	7.7	30.8	8.2	31.0	8.2	31.0
9	7.8	31.1	8.2	31.0	8.3	30.8
10	7.9	31.1	8.2	30.7	8.4	31.0
11	7.9	31.2	8.2	30.6	8.3	31.2
12	7.9	31.1	8.1	30.8	8.4	31.1
13	7.9	31.2	8.0	30.8	8.4	31.4
14	8.0	31.0	7.8	31.0	8.4	31.5
15	7.9	31.0	7.9	30.7	8.3	30.8
16	7.8	30.8	7.8	31.0	8.3	30.7
17	7.8	30.8	7.9	30.6	8.4	30.4
18	7.8	30.7	8.0	30.3	8.5	30.6
19	7.7	30.6	8.1	30.2	8.6	30.6
20	7.7	30.7	8.0	30.4	8.6	30.7
21	7.8	30.8	8.1	30.4	8.6	30.8
22	7.7	30.7	7.9	30.7	8.6	30.7
23	7.7	30.8	7.8	30.4	8.5	30.7
24	7.6	30.7	7.9	30.6	8.4	30.4
25	7.7	30.8	8.1	30.7	8.5	30.7
26	7.6	30.8	8.1	30.8	8.5	30.8
27	7.6	31.0	8.0	30.6	8.4	30.7
28	7.7	30.7	7.9	31.0	8.4	30.4
29	7.6	30.7	0.0	0.0	8.6	30.3
30	7.6	31.0	0.0	0.0	8.5	30.6
31	7.5	30.6	0.0	0.0	8.3	30.3
MEANS	7.7	30.8	8.0	30.7	8.3	30.7
OBSVNS.	31	31	28	28	31	31
MAXIMUM	8.0	31.2	8.2	31.0	8.6	31.5
MINIMUM	7.2	30.2	7.4	30.2	7.8	30.3
STD.DEV.	.22	.27	.20	.22	.22	.30

RACE ROCKS

48 17 57 N

123 31 48 W

APRIL

MAY

JUNE

1978

DATE	TEMP	SAL	TEMP	SAL	TEMP	SAL
1	8.6	30.8	9.1	31.4	9.9	31.1
2	8.5	31.0	9.1	31.4	10.3	31.1
3	8.6	31.0	9.2	31.5	10.4	31.0
4	8.6	31.1	9.1	31.5	10.6	31.1
5	8.7	31.1	9.1	31.2	10.4	31.1
6	8.7	31.0	9.0	31.2	10.1	31.1
7	8.7	31.0	8.9	31.4	10.2	31.1
8	8.8	31.1	8.9	31.5	10.2	31.0
9	8.8	30.8	8.9	31.5	10.3	30.8
10	8.9	30.8	9.0	31.6	10.3	31.1
11	9.0	30.8	9.2	31.4	10.4	31.0
12	9.1	30.6	9.4	31.0	10.5	30.7
13	9.0	30.8	9.6	31.1	10.4	30.4
14	9.0	30.7	9.6	31.1	10.5	30.7
15	9.1	30.8	9.7	30.8	10.5	30.7
16	9.1	30.7	9.8	31.1	10.6	30.7
17	9.2	30.7	9.9	31.0	10.6	30.8
18	9.2	30.6	9.8	31.0	10.6	31.1
19	9.1	30.6	9.8	31.1	10.5	31.2
20	9.1	30.6	9.7	31.2	10.4	31.5
21	9.2	30.8	9.7	31.2	10.2	31.6
22	9.1	31.0	9.6	31.2	10.1	31.5
23	9.1	30.8	9.7	31.5	10.1	31.8
24	9.2	31.1	9.8	31.5	10.2	31.8
25	9.2	31.0	9.7	31.4	10.2	31.9
26	9.2	31.1	9.7	31.5	10.4	32.0
27	9.3	31.1	9.6	31.5	10.5	32.0
28	9.2	31.2	9.6	31.2	10.6	32.3
29	9.2	31.2	9.5	31.4	10.7	32.3
30	9.2	31.5	9.5	31.4	10.6	32.1
31	0.0	0.0	9.6	31.2	0.0	0.0
MEANS	9.0	30.9	9.4	31.3	10.4	31.3
OBSVNS.	30	30	31	31	30	30
MAXIMUM	9.3	31.5	9.9	31.6	10.7	32.3
MINIMUM	8.5	30.6	8.9	30.8	9.9	30.4
STD.DEV.	.24	.22	.32	.20	.20	.53

RACE ROCKS

48 17 57 N

123 31 48 W

JULY

AUGUST

SEPTEMBER 1978

DATE	TEMP	SAL	TEMP	SAL	TEMP	SAL
1	10.6	31.4	11.1	30.7	10.8	31.4
2	10.4	31.1	10.9	31.1	10.9	31.5
3	10.3	31.2	10.8	31.4	10.7	31.1
4	10.2	31.1	10.8	31.0	10.8	30.8
5	10.1	31.1	10.7	31.4	10.8	31.0
6	10.0	31.2	10.8	31.5	10.7	31.0
7	10.1	31.1	10.9	31.4	10.7	31.2
8	10.1	31.4	11.1	31.1	10.4	31.1
9	10.2	31.2	10.9	31.1	10.5	31.1
10	10.3	31.1	11.2	31.4	10.3	31.2
11	10.4	31.2	11.4	31.1	10.2	31.4
12	10.6	31.0	11.2	30.7	10.2	31.2
13	10.6	31.1	11.7	30.3	10.1	31.6
14	10.0	31.5	10.7	31.4	9.9	31.5
15	10.4	31.4	10.1	31.8	9.8	31.6
16	10.5	31.2	10.9	31.6	10.1	31.5
17	10.4	31.1	10.6	31.8	10.3	31.5
18	10.5	31.2	10.9	31.9	10.4	31.2
19	10.4	31.4	10.8	32.1	10.6	31.1
20	10.4	31.2	11.1	31.6	10.7	31.2
21	10.3	31.9	11.2	32.0	10.8	31.0
22	10.4	31.4	10.9	32.3	10.9	31.0
23	10.6	31.2	10.7	32.1	10.9	31.2
24	10.7	31.1	10.8	32.0	11.1	31.1
25	10.7	30.8	11.1	31.8	11.2	31.0
26	10.8	30.8	10.8	32.0	11.0	31.0
27	10.9	30.7	10.7	31.9	10.9	31.1
28	11.1	31.0	10.8	32.1	10.8	31.0
29	11.2	30.7	10.9	31.6	10.7	31.1
30	11.1	31.0	10.9	31.8	10.5	31.2
31	11.0	30.8	10.8	31.4	0.0	0.0
MEANS	10.5	31.1	10.9	31.5	10.6	31.2
OBSVNS.	31	31	31	31	30	30
MAXIMUM	11.2	31.9	11.7	32.3	11.2	31.6
MINIMUM	10.0	30.7	10.1	30.3	9.8	30.8
STD.DEV.	.33	.25	.28	.48	.35	.21

RACE ROCKS

48 17 57 N 123 31 48 W

OCTOBER

NOVEMBER

DECEMBER 1978

DATE	TEMP	SAL	TEMP	SAL	TEMP	SAL
1	10.4	31.2	9.2	31.2	7.9	31.6
2	10.4	31.1	9.1	31.2	7.9	31.8
3	10.3	31.1	8.9	31.2	7.8	31.5
4	10.2	31.2	8.9	31.0	7.6	31.8
5	10.2	31.1	8.8	31.2	7.5	31.8
6	10.3	30.8	8.8	31.4	7.4	31.8
7	10.2	30.8	8.7	31.2	7.2	32.0
8	10.1	31.0	8.6	31.4	7.3	31.5
9	10.0	31.1	8.4	31.2	7.4	31.8
10	10.0	31.1	8.4	31.4	7.5	31.5
11	10.1	31.0	8.3	31.2	7.6	31.6
12	10.2	31.1	8.4	31.1	7.6	31.6
13	10.2	31.4	8.3	31.2	7.6	31.8
14	10.2	31.1	8.3	31.6	7.5	31.8
15	10.2	31.2	8.1	31.5	7.6	32.0
16	10.1	31.2	8.1	31.4	7.4	31.9
17	9.9	31.2	8.0	31.4	7.5	32.0
18	9.7	31.4	7.8	31.5	7.4	32.1
19	9.6	31.4	7.9	31.1	7.4	31.9
20	9.6	31.5	7.7	31.0	7.3	32.1
21	9.4	31.2	7.6	31.1	7.3	31.9
22	9.5	31.1	7.5	31.1	7.2	31.9
23	9.4	31.0	7.6	31.2	7.3	31.6
24	9.3	31.2	7.8	31.2	7.2	31.6
25	9.3	31.4	7.9	31.1	7.2	31.6
26	9.3	31.4	7.9	31.2	7.2	31.5
27	9.3	31.1	8.0	31.2	7.1	31.5
28	9.2	31.5	7.9	31.4	7.0	31.4
29	9.2	31.4	7.9	31.2	6.9	31.2
30	9.2	31.2	7.9	31.5	6.9	31.1
31	* 9.2	* 31.2	0.0	0.0	6.8	31.2
MEANS	9.8	31.2	8.2	31.3	7.4	31.7
OBSVNS.	30	30	30	30	31	31
YRLY. MEANS					9.2	31.1
MAXIMUM	10.4	31.5	9.2	31.6	7.9	32.1
MINIMUM	9.2	30.8	7.5	31.0	6.8	31.1
STD. DEV.	.43	.18	.47	.16	.27	.26

CAPE MUDGE

49 59 56 N

125 11 38 W

JANUARY

FEBRUARY

MARCH

1978

DATE	TEMP	SAL	TEMP	SAL	TEMP	SAL
1	6.8	28.8	6.9	28.6	6.4	28.8
2	7.1	28.5	7.4	29.0	7.7	29.1
3	6.1	28.2	7.7	29.0	8.1	28.8
4	6.2	28.4	7.5	29.0	8.3	28.9
5	5.6	28.1	7.9	29.0	8.4	29.0
6	7.4	28.6	* 7.8	*29.0	* 8.5	*28.9
7	* 7.5	*28.7	7.7	28.9	* 8.6	*28.8
8	7.6	28.9	* 7.5	*28.8	8.7	28.6
9	7.5	28.8	* 7.3	*28.7	8.5	28.5
10	7.6	28.8	7.1	28.5	8.4	29.0
11	* 6.9	*28.1	6.7	28.4	7.2	28.8
12	6.1	27.3	7.1	28.6	7.6	29.1
13	6.3	28.1	6.3	28.6	7.8	29.0
14	6.7	28.1	* 6.9	*28.7	7.9	29.0
15	7.1	28.1	7.6	28.9	8.1	29.3
16	7.4	28.5	7.2	28.6	* 8.0	*28.9
17	7.5	28.0	7.2	28.5	7.8	28.5
18	7.2	28.2	* 7.4	*28.5	8.5	28.6
19	7.9	28.6	7.7	28.5	8.6	28.8
20	* 8.0	*28.6	7.6	28.9	8.4	29.0
21	* 8.1	*28.5	8.1	28.8	8.9	28.8
22	8.2	28.5	8.0	29.0	9.1	29.0
23	7.9	28.8	* 7.4	*28.9	* 9.3	*29.0
24	7.8	28.9	* 6.8	*28.8	* 9.5	*29.0
25	7.7	28.5	6.2	28.6	9.7	29.0
26	* 7.6	*28.5	6.3	28.8	8.4	29.0
27	* 7.4	*28.4	6.9	28.8	8.2	28.8
28	7.2	28.4	6.8	28.8	8.3	29.1
29	7.2	29.0	0.0	0.0	8.4	28.6
30	7.3	28.9	0.0	0.0	7.9	28.6
31	6.6	28.5	0.0	0.0	8.4	28.6
MEANS	7.1	28.5	7.2	28.8	8.2	28.9
OBSVNS.	25	25	21	21	26	26
MAXIMUM	8.2	29.0	8.1	29.0	9.7	29.3
MINIMUM	5.6	27.3	6.2	28.4	6.4	28.5
STD.DEV.	.66	.39	.56	.20	.62	.21

CAPE MUDGE

49 59 56 N

125 11 38 W

APRIL

MAY

JUNE

1978

DATE	TEMP	SAL	TEMP	SAL	TEMP	SAL
1	9.0	29.0	* 10.3	*28.9	14.8	28.9
2	8.8	28.8	* 10.7	*29.0	11.9	28.6
3	* 0.0	* 0.0	11.1	29.0	14.2	28.5
4	* 0.0	* 0.0	11.8	29.0	13.8	28.6
5	* 0.0	* 0.0	11.0	28.8	12.8	28.5
6	9.4	28.8	10.9	28.8	* 12.5	*28.5
7	11.2	28.8	11.2	29.0	12.1	28.6
8	10.0	28.9	10.7	29.1	11.4	28.5
9	9.6	28.8	10.7	28.4	11.8	28.6
10	8.4	28.9	9.1	29.0	* 11.2	*28.7
11	* 8.2	*28.9	* 9.1	*29.0	10.6	28.8
12	7.9	28.8	9.0	29.1	13.2	27.7
13	8.5	28.9	9.7	28.6	14.8	27.6
14	8.4	28.1	* 10.4	*28.7	* 14.3	*27.4
15	8.2	28.5	11.1	28.8	13.8	27.2
16	9.2	28.5	11.2	28.9	16.9	27.7
17	* 9.0	*28.7	11.1	28.9	17.1	27.4
18	8.8	28.9	11.6	28.8	14.2	28.6
19	8.8	28.6	13.1	28.4	15.0	28.0
20	10.7	28.8	13.1	28.6	12.4	28.6
21	11.4	29.0	12.1	28.6	12.2	28.6
22	9.6	28.5	11.7	28.6	10.1	28.8
23	10.9	28.5	12.0	28.9	9.5	29.1
24	9.3	28.5	10.6	28.8	9.8	29.1
25	10.2	28.5	* 0.0	* 0.0	10.4	28.9
26	9.0	28.6	* 0.0	* 0.0	12.3	28.6
27	9.1	29.0	* 0.0	* 0.0	12.6	28.6
28	9.1	28.6	10.6	28.9	13.4	28.8
29	9.1	28.8	10.9	28.8	16.3	28.1
30	10.0	28.9	11.8	28.9	14.7	27.3
31	0.0	0.0	* 13.3	*28.9	0.0	0.0
MEANS	9.4	28.7	11.1	28.8	13.0	28.4
OBSVNS.	25	25	23	23	27	27
MAXIMUM	11.4	29.0	13.1	29.1	17.1	29.1
MINIMUM	7.9	28.1	9.0	28.4	9.5	27.2
STD.DEV.	.93	.22	1.02	.20	2.07	.55

CAPE MUDGE

49 59 56 N

125 11 38 W

JULY

AUGUST

SEPTEMBER 1978

DATE	TEMP	SAL	TEMP	SAL	TEMP	SAL
1	15.0	28.1	15.3	27.3	* 0.0	* 0.0
2	15.7	28.2	17.2	27.3	* 0.0	* 0.0
3	* 15.9	* 28.1	16.8	26.9	14.6	26.9
4	16.2	28.0	* 17.5	* 26.7	13.2	27.2
5	11.4	28.2	18.3	26.5	12.4	27.4
6	11.6	28.2	14.6	28.2	11.9	27.6
7	12.9	27.6	13.1	28.0	12.6	27.3
8	13.3	28.0	15.7	25.9	13.6	26.7
9	11.8	28.5	14.0	26.3	* 13.9	* 26.7
10	13.9	27.3	13.5	25.9	14.3	26.8
11	15.7	27.2	* 14.0	* 26.8	14.6	27.6
12	15.7	27.2	14.6	27.8	15.1	27.4
13	17.3	27.3	18.8	26.1	15.1	26.9
14	18.4	26.0	* 18.0	* 26.7	* 14.3	* 27.1
15	17.2	26.4	17.2	27.4	13.5	27.4
16	18.2	26.7	15.3	27.8	12.3	27.6
17	15.6	27.4	18.4	26.0	14.2	27.7
18	14.6	28.2	* 16.6	* 26.6	12.7	28.0
19	13.6	27.8	14.8	27.2	11.1	28.2
20	14.4	28.2	15.7	27.2	10.8	28.0
21	10.8	27.8	13.2	27.3	* 10.8	* 27.9
22	10.8	28.4	13.4	26.9	10.8	27.7
23	11.1	28.1	* 0.0	* 0.0	12.1	27.4
24	11.3	28.4	* 0.0	* 0.0	12.4	27.3
25	11.2	28.1	* 0.0	* 0.0	13.2	27.1
26	11.4	28.5	14.4	27.2	14.0	26.8
27	12.1	27.6	15.2	27.1	12.4	28.0
28	14.6	27.7	15.2	26.5	* 12.9	* 27.9
29	15.2	27.7	15.6	26.9	13.5	27.8
30	17.9	27.2	16.6	25.6	12.3	27.8
31	16.6	26.9	* 0.0	* 0.0	0.0	0.0
MEANS	14.2	27.7	15.5	26.9	13.0	27.4
OBSVNS.	30	30	23	23	24	24
MAXIMUM	18.4	28.5	18.8	28.2	15.1	28.2
MINIMUM	10.8	26.0	13.1	25.6	10.8	26.7
STO.DEV.	2.44	.63	1.67	.72	1.26	.43

CAPE MUDGE

49 59 56 N 125 11 38 W

OCTOBER

NOVEMBER

DECEMBER 1978

DATE	TEMP	SAL	TEMP	SAL	TEMP	SAL
1	13.2	26.5	9.9	28.2	8.8	29.1
2	12.4	27.2	9.9	28.9	7.3	28.5
3	13.2	27.8	9.2	28.4	* 7.2	*28.6
4	12.3	27.8	8.5	28.6	7.1	28.8
5	10.7	27.3	* 0.0	* 0.0	7.2	28.5
6	11.1	26.9	* 0.0	* 0.0	6.9	28.8
7	* 11.5	*27.3	* 0.0	* 0.0	7.1	28.6
8	* 11.9	*27.7	8.9	28.2	* 7.6	*28.8
9	12.3	28.2	9.1	28.4	8.2	29.0
10	* 12.5	*28.0	9.2	28.5	* 8.2	*29.0
11	12.7	27.8	9.2	28.4	8.1	29.1
12	12.6	27.8	9.4	28.8	8.3	29.1
13	12.4	28.0	9.2	28.0	* 8.4	*29.2
14	12.5	28.1	8.7	28.9	8.5	29.3
15	11.9	28.0	* 8.8	*28.9	* 0.0	* 0.0
16	11.3	28.4	9.0	28.9	* 0.0	* 0.0
17	11.3	28.1	7.2	28.2	* 0.0	* 0.0
18	11.4	28.2	7.8	28.5	6.8	28.8
19	10.4	28.9	7.1	28.1	6.9	28.8
20	9.4	28.8	7.4	28.4	* 7.0	*28.8
21	9.3	28.6	7.4	28.5	7.2	28.8
22	10.1	28.1	7.3	28.4	7.2	28.9
23	* 10.2	*28.3	7.9	28.4	* 7.4	*28.9
24	10.3	28.6	8.0	28.8	7.6	28.8
25	10.6	28.5	8.5	28.9	7.7	29.1
26	* 0.0	* 0.0	8.8	29.0	7.8	28.9
27	* 0.0	* 0.0	* 8.7	*29.0	6.4	29.0
28	* 0.0	* 0.0	8.5	29.1	6.6	28.9
29	11.1	29.3	8.5	28.9	7.1	28.9
30	10.0	28.8	8.5	28.9	* 6.5	*28.9
31	9.6	28.8	0.0	0.0	5.8	28.8
MEANS	11.3	28.1	8.5	28.6	7.4	28.9
OBSVNS.	24	24	25	25	21	21
YRLY. MEANS.....					10.6	28.3
MAXIMUM	13.2	29.3	9.9	29.1	8.8	29.3
MINIMUM	9.3	26.5	7.1	28.0	5.8	28.5
STO. DEV.	1.21	.66	.82	.31	.74	.20

SISTERS ISLAND

49 29 13 N

124 26 00 W

JANUARY

FEBRUARY

MARCH

1978

DATE	TEMP	SAL	TEMP	SAL	TEMP	SAL
1	6.1	28.1	5.6	27.7	6.6	29.0
2	5.6	28.0	5.7	27.6	6.7	29.4
3	4.8	27.8	6.4	27.7	6.8	29.5
4	5.6	28.0	6.7	27.8	6.9	28.5
5	6.1	28.1	6.7	27.6	7.1	28.4
6	5.0	27.6	7.1	28.2	7.2	28.5
7	6.1	28.1	7.2	28.5	7.6	28.6
8	6.3	28.2	7.2	28.5	8.1	28.2
9	6.1	27.6	7.2	28.5	8.1	28.4
10	6.1	27.6	6.7	28.2	7.4	28.8
11	5.9	27.3	6.7	28.6	7.5	28.5
12	6.1	27.6	5.7	27.7	8.3	28.5
13	5.9	27.6	6.1	27.3	7.2	28.5
14	6.2	27.6	6.7	27.8	7.3	28.2
15	6.1	27.7	6.7	27.4	7.5	28.6
16	5.9	27.6	6.8	27.6	7.5	28.6
17	6.4	27.6	6.8	28.9	7.8	28.2
18	6.3	27.7	6.9	28.6	7.8	28.4
19	6.3	28.0	7.0	28.5	8.4	28.4
20	6.4	27.8	7.0	28.2	8.7	28.8
21	6.7	28.1	7.3	28.5	8.4	28.8
22	6.4	28.1	7.3	28.6	9.2	28.9
23	6.4	28.1	7.4	28.2	8.8	28.4
24	6.5	28.1	7.2	28.9	8.5	28.4
25	6.6	28.2	7.2	28.5	8.3	28.4
26	6.4	28.1	6.6	29.0	8.4	28.8
27	6.4	28.4	6.7	29.5	8.2	28.2
28	6.1	28.0	6.7	28.9	8.2	29.0
29	6.2	27.6	0.0	0.0	8.3	29.0
30	6.2	27.6	0.0	0.0	8.4	28.8
31	5.8	27.8	0.0	0.0	8.2	28.5
MEANS	6.1	27.9	6.8	28.2	7.9	28.6
OBSVNS.	31	31	28	28	31	31
MAXIMUM	6.7	28.4	7.4	29.5	9.2	29.5
MINIMUM	4.8	27.3	5.6	27.3	6.6	28.2
STD.DEV.	.41	.27	.49	.56	.67	.33

SISTERS ISLAND

49 29 13 N

124 26 00 W

APRIL

MAY

JUNE

1978

DATE	TEMP	SAL	TEMP	SAL	TEMP	SAL
1	8.6	29.1	11.1	28.2	14.7	26.9
2	9.1	28.8	10.8	28.2	16.4	28.6
3	9.2	28.8	10.8	28.5	15.7	28.5
4	8.7	28.6	10.6	28.2	15.4	28.8
5	8.5	28.6	11.7	28.5	18.2	28.0
6	9.7	28.6	10.6	28.4	15.7	28.5
7	10.0	28.8	10.8	28.4	15.9	28.2
8	9.2	28.8	11.4	28.6	15.2	28.4
9	9.1	28.9	11.1	28.4	14.9	28.2
10	9.7	28.0	11.4	28.4	15.2	28.1
11	8.9	28.5	10.8	28.6	15.3	27.3
12	8.6	28.4	11.1	28.6	15.1	27.6
13	8.6	28.6	10.4	28.5	14.6	26.5
14	8.6	29.0	10.4	28.4	15.2	25.2
15	8.6	28.5	11.0	28.5	15.7	25.0
16	9.1	28.8	11.1	28.8	15.9	25.4
17	8.8	28.9	12.9	28.5	17.1	24.7
18	8.9	28.6	11.9	27.7	16.1	26.8
19	9.2	28.6	14.7	26.7	16.8	26.5
20	9.0	28.5	14.3	28.5	16.2	27.8
21	9.6	28.4	11.5	28.2	15.9	28.2
22	8.3	28.5	11.7	28.5	15.9	28.6
23	10.0	28.5	12.1	27.8	14.3	28.4
24	9.0	29.4	11.8	28.4	16.1	26.9
25	10.4	28.5	12.1	28.9	14.9	28.4
26	9.6	29.0	12.2	28.5	15.4	27.7
27	9.8	29.3	11.5	29.3	16.5	27.7
28	9.9	29.3	11.0	28.6	16.4	28.1
29	10.1	29.0	11.5	28.6	17.0	28.0
30	10.4	29.0	12.9	28.9	18.1	27.4
31	0.0	0.0	12.8	28.8	0.0	0.0
MEANS	9.2	28.7	11.6	28.4	15.9	27.5
OBSVNS.	30	30	31	31	30	30
MAXIMUM	10.4	29.4	14.7	29.3	18.2	28.8
MINIMUM	8.3	28.0	10.4	26.7	14.3	24.7
STD.DEV.	.60	.31	1.03	.44	.93	1.15

SISTERS ISLAND

49 29 13 N

124 26 00 W

JULY

AUGUST

SEPTEMBER 1978

DATE	TEMP	SAL	TEMP	SAL	TEMP	SAL
1	17.0	27.2	20.2	26.9	15.5	26.0
2	17.9	26.3	23.2	26.5	15.2	26.9
3	18.1	26.7	21.7	26.4	14.8	27.1
4	18.0	27.1	20.3	26.9	14.9	25.1
5	18.3	27.3	21.0	26.5	14.7	25.4
6	18.7	27.2	19.5	26.7	14.6	26.5
7	18.4	26.8	19.9	26.8	14.6	27.1
8	17.9	26.5	21.1	26.5	14.4	27.7
9	16.9	26.1	20.7	26.0	14.8	27.3
10	16.9	28.1	20.0	27.2	14.0	27.7
11	17.5	24.8	18.3	26.5	15.0	24.2
12	17.8	23.7	18.7	26.4	15.0	24.2
13	18.4	20.4	18.7	26.9	15.0	24.4
14	19.4	20.8	18.1	26.1	14.7	25.2
15	20.3	25.0	18.2	26.3	15.0	25.1
16	19.6	24.6	17.8	24.0	14.2	26.4
17	20.2	24.7	17.8	26.0	13.9	26.4
18	20.0	24.7	17.1	25.4	13.9	27.4
19	19.2	25.2	17.1	25.9	13.3	27.2
20	20.2	25.0	16.4	26.0	13.3	26.9
21	20.2	25.8	16.4	26.8	13.1	26.8
22	18.6	26.4	16.6	26.8	12.5	27.1
23	17.8	27.1	16.1	26.7	12.7	27.6
24	17.5	27.2	15.4	27.2	13.3	25.6
25	17.0	28.1	14.4	26.5	13.3	25.2
26	19.1	26.5	14.8	25.1	14.2	24.8
27	18.4	26.5	15.7	24.4	13.9	25.5
28	18.7	26.3	15.9	22.2	12.8	27.3
29	19.6	26.4	16.0	22.9	12.8	27.3
30	19.4	26.4	15.1	26.7	12.8	27.8
31	19.6	26.4	15.9	25.0	0.0	0.0
MEANS	18.6	25.8	18.0	26.0	14.1	26.3
OBSVNS.	31	31	31	31	30	30
MAXIMUM	20.3	28.1	23.2	27.2	15.5	27.8
MINIMUM	16.9	20.4	14.4	22.2	12.5	24.2
STD.DEV.	1.06	1.75	2.28	1.20	.88	1.14

SISTERS ISLAND

49 29 13 N

124 26 00 W

OCTOBER

NOVEMBER

DECEMBER 1978

DATE	TEMP	SAL	TEMP	SAL	TEMP	SAL
1	12.8	28.5	10.6	28.2	8.0	29.0
2	14.0	27.1	10.3	28.6	7.7	29.1
3	13.1	28.0	10.1	28.8	8.0	29.1
4	12.8	28.4	10.1	28.6	7.9	29.5
5	13.1	28.0	9.8	28.0	8.1	29.9
6	12.9	27.8	9.8	28.1	7.6	29.1
7	12.5	29.1	9.7	28.2	7.3	29.1
8	13.1	27.8	9.6	28.8	7.6	29.7
9	12.5	28.4	9.3	28.9	7.8	29.5
10	12.2	28.4	8.8	28.5	8.2	29.5
11	13.1	28.0	8.6	28.4	8.0	29.7
12	12.6	27.6	9.0	28.8	7.7	29.5
13	12.8	27.3	8.3	28.6	7.8	29.3
14	12.8	27.4	8.3	28.4	7.8	29.1
15	12.8	27.7	7.8	28.5	7.8	29.3
16	12.6	27.7	8.4	28.8	8.1	29.1
17	12.2	27.7	8.4	28.5	8.1	29.3
18	11.9	27.4	8.6	28.5	7.8	29.3
19	11.7	27.6	8.2	28.5	7.4	29.0
20	11.9	27.4	8.1	28.4	7.6	29.1
21	11.7	27.4	7.9	28.4	7.8	29.1
22	11.8	27.2	7.9	28.4	7.8	29.0
23	11.6	27.8	7.6	28.1	7.9	29.1
24	11.1	27.7	7.7	28.1	7.6	29.1
25	11.1	27.7	7.5	27.8	7.6	29.0
26	11.1	27.8	7.5	28.5	7.6	29.1
27	11.1	27.7	7.8	28.6	7.4	29.3
28	10.8	27.6	8.1	29.0	6.9	29.5
29	10.7	27.8	7.9	29.0	* 6.5	* 29.5
30	10.7	28.0	7.9	29.0	6.0	29.4
31	10.6	28.1	0.0	0.0	5.4	29.5
MEANS	12.1	27.8	8.7	28.5	7.6	29.3
ORSVNS.	31	31	30	30	30	30
YRLY. MEANS.....					11.4	27.8
MAXIMUM	14.0	29.1	10.6	29.0	8.2	29.9
MINIMUM	10.6	27.1	7.5	27.8	5.4	29.0
STD. DEV.	.90	.43	.94	.31	.59	.24

CHROME ISLAND

49 28 20 N

124 40 57 N

JANUARY

FEBRUARY

MARCH

1978

DATE	TEMP	SAL	TEMP	SAL	TEMP	SAL
1	6.2	28.4	5.6	27.2	6.7	29.7
2	5.8	28.5	5.1	26.7	6.6	29.0
3	5.0	28.6	5.9	27.3	6.6	29.0
4	* 5.3	* 28.7	6.7	28.4	6.4	28.4
5	5.6	28.9	6.8	29.0	7.1	28.8
6	5.4	28.6	6.9	28.6	7.2	28.8
7	6.1	28.5	7.2	29.5	7.8	29.3
8	6.7	28.5	7.6	29.4	8.3	29.3
9	6.4	28.4	7.7	29.4	8.2	28.6
10	6.7	28.5	7.3	29.8	8.1	29.4
11	6.9	28.9	6.9	28.5	7.7	29.9
12	7.0	29.1	6.8	28.9	7.9	29.0
13	7.1	28.5	6.9	28.6	7.5	28.8
14	6.8	28.4	7.1	29.5	7.6	29.0
15	6.6	28.6	6.9	29.4	7.7	29.8
16	6.1	27.7	7.2	28.8	7.8	29.5
17	6.2	28.5	7.2	28.8	7.9	29.7
18	6.1	27.7	7.2	29.1	8.3	28.8
19	6.2	28.0	7.5	29.4	8.4	28.2
20	6.4	27.4	7.5	28.4	8.9	29.1
21	6.7	28.5	7.7	29.1	9.1	28.8
22	6.6	27.7	7.7	28.9	9.6	28.9
23	6.7	28.1	7.3	28.9	8.4	29.3
24	7.1	28.4	7.2	28.8	8.3	29.8
25	7.1	28.6	7.2	28.4	8.2	29.0
26	6.9	28.4	7.1	29.1	8.2	29.5
27	6.7	28.8	6.7	28.8	8.3	30.0
28	6.7	28.6	6.9	29.1	8.3	29.9
29	6.2	28.5	0.0	0.0	8.2	29.7
30	6.4	28.9	0.0	0.0	8.3	29.9
31	6.6	28.2	0.0	0.0	8.2	27.2
MEANS	6.4	28.4	7.0	28.8	7.9	29.2
OBSVNS.	30	30	28	28	31	31
MAXIMUM	7.1	29.1	7.7	29.8	9.6	30.0
MINIMUM	5.0	27.4	5.1	26.7	6.4	27.2
STD.DEV.	.51	.39	.60	.71	.73	.60

CHROME ISLAND

49 28 20 N

124 40 57 N

APRIL

MAY

JUNE

1978

DATE	TEMP	SAL	TEMP	SAL	TEMP	SAL
1	8.8	28.5	10.9	29.7	14.3	28.4
2	8.9	29.0	10.2	29.7	15.4	27.6
3	8.8	29.0	10.6	29.1	18.6	27.8
4	8.7	29.0	11.2	28.5	16.6	27.7
5	8.6	29.5	11.9	28.8	18.8	27.6
6	9.4	30.0	12.2	28.6	16.3	28.2
7	9.4	29.1	12.2	28.9	16.3	28.2
8	9.2	29.3	12.3	28.8	14.4	28.4
9	8.9	29.0	11.8	29.4	13.7	28.5
10	9.1	30.2	12.1	28.8	10.6	29.7
11	8.6	29.7	10.9	29.5	13.4	28.4
12	8.6	27.7	9.8	29.8	12.9	28.6
13	9.0	29.3	10.2	29.7	13.1	28.9
14	9.0	29.1	10.0	29.7	13.8	28.6
15	8.7	28.9	10.9	29.4	15.5	25.6
16	9.1	28.6	12.4	28.6	14.2	28.4
17	9.0	29.0	12.9	28.8	17.4	26.0
18	8.9	29.7	14.2	28.0	16.2	25.9
19	9.2	28.6	14.6	28.0	16.8	26.4
20	9.9	30.4	13.8	28.1	16.8	26.1
21	9.1	29.0	13.2	28.0	16.7	26.0
22	8.9	29.1	12.4	28.2	17.0	26.1
23	9.9	29.1	12.2	28.1	16.4	26.9
24	9.4	30.3	13.0	27.8	16.1	27.1
25	9.8	29.0	12.7	28.2	15.0	28.1
26	9.9	29.7	11.8	28.5	15.0	28.4
27	10.2	29.7	10.5	28.8	15.9	28.4
28	10.4	29.1	11.2	28.8	17.1	27.4
29	11.0	27.3	11.4	28.0	19.8	26.3
30	10.3	29.4	12.4	28.4	18.6	26.7
31	0.0	0.0	13.6	28.5	0.0	0.0
MEANS	9.3	29.2	11.9	28.7	15.8	27.5
OBSVNS.	30	30	31	31	30	30
MAXIMUM	11.0	30.4	14.6	29.8	19.8	29.7
MINIMUM	8.6	27.3	9.8	27.8	10.6	25.6
STD.DEV.	.62	.67	1.25	.61	2.00	1.10

CHROME ISLAND

49 28 20 N

124 40 57 N

JULY

AUGUST

SEPTEMBER 1978

DATE	TEMP	SAL	TEMP	SAL	TEMP	SAL
1	18.6	26.8	21.1	26.4	13.8	27.4
2	19.2	26.7	21.0	26.5	14.2	27.6
3	19.2	27.1	21.1	26.7	14.2	27.4
4	18.2	27.2	19.8	26.8	14.3	27.1
5	17.1	27.2	19.8	26.5	13.9	27.3
6	16.9	28.2	19.9	26.3	14.3	27.3
7	18.1	27.7	20.4	26.5	14.2	27.3
8	17.9	27.6	19.9	26.7	14.4	27.6
9	17.9	27.7	21.1	26.5	12.9	28.2
10	17.5	27.4	20.7	26.1	12.1	28.8
11	16.0	28.4	19.3	27.1	13.1	28.4
12	17.7	27.6	15.7	27.8	13.7	27.7
13	18.1	27.6	18.6	27.1	14.4	26.3
14	19.8	27.6	14.7	28.0	14.1	26.8
15	20.4	27.3	16.4	27.7	13.3	27.2
16	20.8	27.7	16.4	27.6	12.9	27.2
17	20.7	27.1	17.2	27.1	12.7	27.2
18	21.1	26.9	16.8	27.2	12.8	27.2
19	20.8	27.4	15.2	27.6	13.2	27.2
20	21.1	27.7	15.2	27.6	13.2	27.3
21	20.4	28.1	14.8	27.7	12.4	28.0
22	19.6	25.9	15.5	27.6	11.7	28.6
23	19.7	25.9	14.4	27.8	11.6	28.1
24	20.1	25.9	13.1	28.2	12.9	27.7
25	19.4	26.4	12.7	28.4	13.0	28.1
26	19.1	26.8	12.5	28.6	12.8	28.1
27	17.5	27.3	14.3	27.2	12.6	28.2
28	19.3	27.2	15.9	25.6	12.8	27.8
29	19.2	27.1	16.7	26.3	12.8	28.0
30	20.7	26.9	17.6	23.5	12.1	28.8
31	21.3	27.7	15.1	26.8	0.0	0.0
MEANS	19.1	27.2	17.2	27.0	13.2	27.7
OBSVNS.	31	31	31	31	30	30
MAXIMUM	21.3	28.4	21.1	28.6	14.4	28.8
MINIMUM	16.0	25.9	12.5	23.5	11.6	26.3
STD.DEV.	1.42	.62	2.74	.97	.82	.59

CHROME ISLAND

49 28 20 N

124 40 57 N

OCTOBER

NOVEMBER

DECEMBER 1978

DATE	TEMP	SAL	TEMP	SAL	TEMP	SAL
1	11.9	28.8	10.7	28.6	8.9	28.8
2	11.8	28.8	10.7	28.6	8.7	28.9
3	12.8	27.7	10.2	28.6	8.8	29.1
4	12.5	27.6	9.9	28.9	8.7	29.1
5	12.2	27.7	10.1	28.8	8.6	29.0
6	12.4	27.7	10.0	28.9	8.3	28.8
7	12.4	28.0	10.3	29.1	8.2	28.9
8	12.4	28.1	9.9	29.1	8.3	29.0
9	12.1	28.5	9.9	28.9	8.4	29.0
10	11.9	28.5	8.8	27.6	8.2	29.1
11	11.9	28.8	9.2	28.4	8.4	29.5
12	12.1	28.5	9.2	28.6	8.3	29.4
13	12.2	28.5	9.2	28.6	8.2	29.1
14	12.2	28.5	9.1	28.5	8.5	29.3
15	12.4	28.2	8.7	28.4	7.8	29.4
16	12.8	27.7	8.7	28.8	8.3	29.3
17	12.2	28.2	8.9	28.5	8.0	29.5
18	11.7	28.0	8.7	28.6	8.4	29.5
19	11.9	28.2	8.4	28.6	8.3	29.7
20	11.7	28.1	8.2	28.5	8.0	29.5
21	11.1	27.6	8.1	28.9	8.4	29.5
22	11.8	27.8	7.5	28.9	8.3	29.4
23	11.3	28.4	8.2	29.0	7.9	29.4
24	11.3	28.4	8.2	28.8	8.1	29.5
25	11.1	28.2	8.1	28.5	7.9	29.3
26	11.3	28.2	8.1	28.5	8.0	29.3
27	11.3	28.1	8.1	28.5	7.8	29.3
28	11.1	28.2	8.2	28.8	7.6	29.0
29	11.0	28.6	8.2	28.6	7.3	29.0
30	10.8	28.8	8.8	29.0	7.0	29.0
31	10.6	28.6	0.0	0.0	6.9	29.1

MEANS	11.8	28.2	9.0	28.7	8.1	29.2
OBSVNS.	31	31	30	30	31	31
YRLY. MEANS.....					11.4	28.3
MAXIMUM	12.8	28.8	10.7	29.1	8.9	29.7
MINIMUM	10.6	27.6	7.5	27.6	6.9	28.8
STD. DEV.	.59	.38	.89	.29	.47	.24

DEPARTURE BAY

49 12 38 N

123 57 17 W

JANUARY

FEBRUARY

MARCH

1978

DATE	TEMP	SAL	TEMP	SAL	TEMP	SAL
1	* 0.0	* 0.00	4.9	26.25	7.0	28.14
2	* 0.0	* 0.00	5.4	27.14	7.0	27.92
3	3.0	26.91	6.6	27.44	7.1	28.09
4	* 4.0	*27.01	* 6.8	*26.91	* 7.1	*28.01
5	5.1	27.11	* 7.0	*26.38	7.2	*27.93
6	5.7	28.00	7.2	25.85	7.3	27.85
7	* 5.9	*27.29	7.5	24.34	8.4	26.97
8	* 6.1	*26.57	7.4	25.96	8.4	27.87
9	6.4	25.85	7.0	25.64	8.5	29.01
10	6.7	27.45	8.0	29.30	7.2	28.80
11	5.9	24.35	* 7.4	*28.56	* 7.2	*28.39
12	6.1	26.82	* 6.8	*27.82	* 7.1	*27.97
13	6.0	26.22	6.2	27.07	7.0	27.55
14	* 5.8	*25.95	6.0	26.50	7.6	28.04
15	* 5.5	*25.68	6.5	27.43	7.4	27.02
16	5.2	25.41	6.2	27.06	7.3	24.81
17	6.4	26.00	6.5	26.83	7.9	26.99
18	6.1	24.08	* 6.6	*26.72	* 8.4	*25.96
19	6.6	24.96	* 6.8	*26.61	* 8.9	*24.92
20	6.2	21.80	7.0	26.50	9.5	23.88
21	* 6.2	*23.64	7.8	25.34	9.9	28.17
22	* 6.3	*25.48	7.7	27.31	9.7	28.09
23	6.3	27.32	7.7	28.17	9.6	26.52
24	6.4	27.27	6.9	27.94	* 0.0	* 0.00
25	6.5	27.27	* 6.9	*27.90	* 0.0	* 0.00
26	7.0	27.90	* 6.9	*27.85	* 0.0	* 0.00
27	6.5	27.92	6.9	27.80	* 0.0	* 0.00
28	* 6.4	*27.92	6.2	27.62	8.3	26.10
29	* 6.3	*27.91	0.0	0.00	8.6	28.06
30	6.2	27.90	0.0	0.00	8.2	28.43
31	6.1	27.81	0.0	0.00	8.8	28.45
MEANS	6.0	26.42	6.8	26.87	8.1	27.46
ORSVNS.	20	20	20	20	22	21
MAXIMUM	7.0	28.00	8.0	29.30	9.9	29.01
MINIMUM	3.0	21.80	4.9	24.34	7.0	23.88
STD.DEV.	.85	1.62	.82	1.12	.96	1.27

DEPARTURE BAY

49 12 38 N

123 57 17 W

APRIL

MAY

JUNE

1978

DATE	TEMP	SAL	TEMP	SAL	TEMP	SAL
1	* 9.0	*27.76	10.7	27.95	15.2	26.05
2	* 9.2	*27.07	10.8	28.45	16.4	26.17
3	9.4	26.37	11.7	27.91	* 16.3	*26.27
4	8.7	28.48	12.2	26.99	* 16.1	*26.38
5	9.0	27.36	12.9	27.14	16.0	26.49
6	9.5	29.20	* 12.7	*27.20	16.4	26.51
7	9.6	28.25	* 12.4	*27.26	16.9	26.48
8	* 9.6	*28.12	12.1	27.32	15.6	27.34
9	* 9.5	*27.99	11.6	27.64	15.3	27.54
10	9.5	27.86	11.6	27.68	* 14.4	*27.85
11	8.9	27.79	11.3	27.87	* 13.5	*28.16
12	8.9	27.91	10.1	28.38	12.5	28.48
13	9.0	27.52	* 10.5	*28.39	12.4	28.59
14	9.0	28.04	* 10.9	*28.41	12.5	28.43
15	* 9.0	*27.72	11.4	28.42	14.7	19.89
16	* 8.9	*27.40	11.2	28.69	15.6	16.51
17	8.8	27.08	13.3	23.20	* 16.2	*17.84
18	9.0	27.25	14.9	22.91	* 16.8	*19.17
19	9.4	28.15	15.3	23.11	17.5	20.51
20	10.1	27.32	* 0.0	* 0.00	16.5	24.28
21	10.1	27.98	* 0.0	* 0.00	15.5	25.33
22	* 9.8	*28.09	* 0.0	* 0.00	15.5	25.69
23	* 9.5	*28.20	12.0	26.22	15.7	25.96
24	9.2	28.32	12.5	26.90	* 16.0	*26.39
25	9.8	25.91	13.1	27.00	* 16.3	*26.83
26	10.5	25.20	12.2	27.10	16.6	27.27
27	11.0	25.28	* 12.4	*26.66	17.8	25.11
28	10.0	27.79	* 12.6	*26.22	18.5	22.83
29	* 10.2	*27.84	12.8	25.77	18.8	22.88
30	* 10.4	*27.89	13.8	25.79	16.8	25.33
31	0.0	0.00	14.5	25.88	0.0	0.00
MEANS	9.5	27.45	12.4	26.74	15.9	25.17
OBSVNS.	20	20	22	22	22	22
MAXIMUM	11.0	29.20	15.3	28.69	18.8	28.89
MINIMUM	8.7	25.20	10.1	22.91	12.4	16.51
STD.DEV.	.62	1.05	1.37	1.72	1.73	3.02

DEPARTURE BAY

49 12 38 N

123 57 17 W

JULY

AUGUST

SEPTEMBER 1978

DATE	TEMP	SAL	TEMP	SAL	TEMP	SAL
1	* 0.0	* 0.00	21.4	*23.84	15.7	23.21
2	* 0.0	* 0.00	21.2	24.32	* 0.0	* 0.00
3	* 0.0	* 0.00	19.4	25.05	* 0.0	* 0.00
4	17.5	26.14	19.6	25.44	* 0.0	* 0.00
5	17.0	26.61	* 0.0	25.48	14.0	26.20
6	14.8	27.81	* 0.0	*25.38	15.0	24.18
7	15.5	27.87	* 0.0	*25.27	15.3	24.83
8	* 15.9	*26.24	20.1	25.16	14.3	26.28
9	* 16.3	*24.61	21.0	22.21	* 13.9	*26.67
10	16.7	22.98	21.3	22.59	* 13.5	*27.06
11	16.5	25.08	18.7	25.74	13.0	27.45
12	16.9	25.81	* 18.3	*25.78	14.1	27.02
13	18.8	20.88	* 17.9	*25.83	14.5	24.66
14	20.5	17.20	17.5	25.88	14.9	22.25
15	* 20.2	*19.44	13.4	26.64	14.6	24.93
16	* 19.8	*21.69	17.5	23.30	* 14.3	*24.71
17	19.4	23.94	18.0	23.10	* 13.9	*24.48
18	19.4	24.70	16.6	23.71	13.5	24.25
19	20.0	22.91	* 16.3	*23.92	13.5	24.69
20	19.0	22.54	* 16.0	*24.13	13.4	24.28
21	19.7	22.46	15.6	24.34	12.3	26.57
22	* 19.6	*22.65	16.4	24.31	11.3	27.20
23	* 19.4	*22.84	16.3	24.90	* 12.0	*26.68
24	19.3	23.03	14.9	26.37	* 12.7	*26.16
25	19.1	24.06	13.9	27.92	13.5	25.63
26	19.5	23.55	* 14.7	*25.50	14.2	23.50
27	18.0	25.68	* 15.5	*23.08	14.0	24.60
28	18.1	25.94	16.4	20.66	* 13.9	*25.35
29	* 19.1	*25.08	17.5	20.62	13.8	26.10
30	* 20.2	*24.22	17.6	22.00	* 13.7	*25.54
31	21.3	23.36	17.4	22.56	0.0	0.00
MEANS	18.4	24.13	17.8	24.20	13.9	25.15
ORSVNS.	20	20	22	22	19	19
MAXIMUM	21.3	27.87	21.4	27.92	15.7	27.45
MINIMUM	14.8	17.20	13.4	20.62	11.3	22.25
STD.DEV.	1.70	2.47	2.34	1.91	1.04	1.43

DEPARTURE BAY

49 12 38 N

123 57 17 W

OCTOBER

NOVEMBER

DECEMBER 1978

DATE	TEMP	SAL	TEMP	SAL	TEMP	SAL
1	* 13.5	*24.97	10.6	28.09	8.7	28.92
2	13.4	24.40	10.3	28.19	* 8.7	*29.00
3	13.7	24.88	10.0	28.63	* 8.8	*29.09
4	13.4	25.11	* 9.9	*28.12	8.8	29.17
5	13.4	24.91	* 9.7	*27.60	8.5	29.17
6	13.5	25.45	9.5	27.08	8.0	28.58
7	* 0.0	* 0.00	9.7	27.54	7.0	28.38
8	* 0.0	* 0.00	10.1	29.57	6.9	28.22
9	* 0.0	* 0.00	9.6	27.89	* 7.3	*28.26
10	12.9	27.15	8.4	26.48	* 7.7	*28.30
11	13.3	27.02	* 0.0	* 0.00	8.2	28.34
12	13.1	25.86	* 0.0	* 0.00	7.9	29.01
13	13.4	25.51	* 0.0	* 0.00	6.6	28.52
14	* 13.1	*25.63	8.5	27.86	8.1	29.18
15	* 12.8	*25.76	8.3	28.01	8.1	29.53
16	12.4	25.89	9.0	28.24	* 8.3	* 0.00
17	12.4	26.20	9.3	27.83	* 8.6	* 0.00
18	12.4	25.99	* 8.9	*27.91	8.9	* 0.00
19	12.4	26.12	* 8.5	*27.99	7.1	* 0.00
20	12.3	26.55	8.1	28.08	7.0	26.53
21	* 12.2	*26.72	8.5	28.67	8.2	* 0.00
22	* 12.1	*26.90	8.6	28.84	7.9	* 0.00
23	12.0	27.08	8.3	28.63	* 0.0	* 0.00
24	10.9	28.33	7.8	28.31	* 0.0	* 0.00
25	11.4	27.57	* 7.8	*28.30	* 0.0	* 0.00
26	11.0	27.53	* 7.9	*28.29	* 0.0	* 0.00
27	11.0	27.22	8.0	28.28	7.0	* 0.00
28	* 10.9	*27.52	8.4	28.70	6.6	* 0.00
29	* 10.8	*27.83	8.7	28.76	6.0	* 0.00
30	10.7	28.14	8.5	28.51	* 0.0	* 0.00
31	10.2	27.78	0.0	0.00	* 0.0	* 0.00
MEANS	12.3	26.41	9.0	28.20	7.7	28.63
OBSVNS.	21	21	21	21	19	12
YRLY. MEANS.....					11.5	26.40
MAXIMUM	13.7	28.33	10.6	29.57	8.9	29.53
MINIMUM	10.2	24.40	7.8	26.48	6.0	26.53
STD.DEV.	1.08	1.14	.82	.66	.85	.78

ENTRANCE ISLAND

49 12 34 W

123 48 27 W

JANUARY

FEBRUARY

MARCH

1978

DATE	TEMP	SAL	TEMP	SAL	TEMP	SAL
1	4.4	26.1	5.9	27.3	6.6	27.2
2	4.5	26.1	6.0	27.2	6.7	27.3
3	4.1	26.4	7.3	28.2	7.0	27.3
4	6.7	28.0	7.2	27.8	7.3	27.4
5	7.6	28.5	6.8	27.6	7.2	27.4
6	7.2	28.6	7.4	28.1	7.4	28.0
7	7.2	28.4	7.8	28.5	7.9	28.4
8	5.9	27.3	7.8	28.8	8.3	28.8
9	6.4	27.6	7.9	28.9	8.2	28.0
10	7.2	28.1	7.9	28.9	8.1	28.1
11	6.7	27.2	7.1	27.8	7.7	27.4
12	5.9	26.1	6.4	26.9	7.8	27.3
13	5.9	23.9	6.6	27.4	7.8	27.4
14	6.1	26.9	6.3	26.9	7.4	27.2
15	6.0	27.4	6.0	26.8	7.4	27.3
16	5.9	26.5	6.7	27.4	7.7	27.8
17	5.7	26.3	6.9	27.7	7.8	27.8
18	5.9	26.1	7.6	28.1	7.9	28.0
19	6.0	27.3	7.6	28.0	8.4	27.2
20	6.0	27.2	7.0	26.9	9.0	25.5
21	7.1	28.4	7.2	27.2	8.6	27.1
22	7.2	28.2	7.1	27.1	9.0	27.1
23	6.9	27.7	7.2	26.8	8.3	27.3
24	7.2	28.1	7.0	26.8	8.2	28.0
25	7.3	28.2	7.2	26.7	8.3	27.3
26	7.2	28.1	6.9	26.9	8.4	28.2
27	7.2	28.1	6.8	27.1	8.2	28.4
28	6.6	27.6	6.6	26.9	* 8.2	* 28.4
29	6.3	26.9	0.0	0.0	8.2	28.4
30	6.0	26.8	0.0	0.0	8.5	28.0
31	5.8	26.3	0.0	0.0	8.5	28.0
MEANS	6.3	27.2	7.0	27.5	7.9	27.6
OBSVNS.	31	31	28	28	30	30
MAXIMUM	7.6	28.6	7.9	28.9	9.0	28.8
MINIMUM	4.1	23.9	5.9	26.7	6.6	25.5
STD.DEV.	.88	1.03	.56	.69	.61	.62

ENTRANCE ISLAND

49 12 34 W

123 48 27 W

APRIL

MAY

JUNE

1978

DATE	TEMP	SAL	TEMP	SAL	TEMP	SAL
1	8.9	27.4	10.6	27.7	14.6	26.8
2	9.1	28.0	10.1	28.1	15.0	26.7
3	8.6	28.8	10.8	28.0	16.4	26.5
4	8.3	28.4	11.3	27.8	16.6	26.5
5	8.2	29.7	11.7	27.4	16.2	26.4
6	9.2	27.3	11.3	28.0	16.5	26.5
7	9.7	25.8	12.3	28.0	15.3	26.8
8	8.6	28.1	12.1	28.4	14.2	28.5
9	9.8	28.0	11.8	28.4	12.5	28.6
10	9.3	27.8	11.2	28.1	12.4	28.6
11	9.2	28.0	10.6	28.2	12.1	29.1
12	9.4	28.0	10.2	28.8	11.4	29.0
13	9.2	28.1	9.4	29.4	11.4	28.8
14	8.9	29.1	9.1	29.3	12.1	29.1
15	8.9	28.0	9.3	29.3	15.0	19.7
16	9.0	28.4	10.6	28.9	16.2	16.6
17	9.0	28.6	12.4	25.9	16.7	18.2
18	8.9	29.1	13.1	23.1	15.6	20.4
19	9.2	28.8	13.8	23.9	16.8	21.6
20	9.3	28.2	13.3	25.8	16.1	25.4
21	9.6	28.9	14.4	25.9	16.6	25.1
22	8.3	29.9	13.9	25.9	16.4	26.1
23	9.8	28.8	13.8	26.5	15.7	26.1
24	8.7	29.3	13.1	26.4	14.8	27.3
25	10.4	24.7	13.0	26.9	14.6	28.1
26	11.1	24.7	11.1	28.4	14.6	28.0
27	10.3	26.0	9.8	29.3	16.3	25.6
28	9.7	27.6	10.3	28.8	17.9	23.1
29	10.0	27.4	11.3	28.2	17.8	23.1
30	10.2	27.6	13.2	26.9	17.9	23.9
31	0.0	0.0	13.5	27.1	0.0	0.0
MEANS	9.3	27.9	11.7	27.5	15.2	25.5
OBSVNS.	30	30	31	31	30	30
MAXIMUM	11.1	29.9	14.4	29.4	17.9	29.1
MINIMUM	8.2	24.7	9.1	23.1	11.4	16.6
STD.DEV.	.67	1.26	1.52	1.52	1.90	3.34

ENTRANCE ISLAND

49 12 34 W

123 48 27 W

JULY

AUGUST

SEPTEMBER 1978

DATE	TEMP	SAL	TEMP	SAL	TEMP	SAL
1	16.7	25.4	21.0	23.7	13.4	26.8
2	17.1	25.2	21.5	24.3	12.8	27.7
3	17.9	25.8	19.2	25.6	15.1	23.5
4	16.8	26.4	21.4	24.6	15.6	22.0
5	16.0	27.1	20.9	25.1	15.1	25.1
6	17.5	27.1	20.7	25.9	14.9	24.4
7	17.9	26.4	21.2	20.3	14.8	23.9
8	17.1	26.8	21.4	20.4	14.1	25.1
9	16.3	26.1	20.6	21.8	12.1	28.0
10	17.5	24.0	18.9	24.6	12.3	28.4
11	15.4	27.2	18.7	25.1	12.7	28.2
12	16.7	24.2	16.2	27.1	13.6	28.0
13	18.1	21.7	15.0	28.1	14.1	25.2
14	19.7	20.0	16.8	26.4	14.3	23.4
15	20.8	18.4	14.3	28.8	14.7	24.4
16	19.2	20.8	18.2	20.3	14.6	21.2
17	19.8	22.6	17.9	22.7	13.8	23.7
18	19.2	23.0	15.3	27.1	14.2	24.0
19	19.6	20.6	16.4	24.4	13.6	26.1
20	20.1	21.2	16.7	22.9	12.2	27.4
21	20.1	21.6	17.4	19.0	11.4	28.0
22	20.3	22.7	15.7	25.2	11.5	28.0
23	19.8	21.7	13.9	28.1	11.4	28.1
24	19.1	23.4	11.8	29.0	11.7	28.0
25	18.9	23.7	12.5	28.5	13.3	26.7
26	18.9	24.0	12.4	29.0	14.7	22.9
27	17.6	25.2	14.3	26.7	14.0	22.9
28	17.7	25.5	14.6	25.2	12.8	26.1
29	19.1	24.7	17.5	17.4	13.0	28.2
30	20.4	23.9	16.9	22.9	11.8	27.8
31	21.4	22.7	16.2	23.5	0.0	0.0
MEANS	18.5	23.8	17.3	24.6	13.5	25.8
OBSVNS.	31	31	31	31	30	30
MAXIMUM	21.4	27.2	21.5	29.0	15.6	28.4
MINIMUM	15.4	18.4	11.8	17.4	11.4	21.2
STD.DEV.	1.55	2.33	2.91	3.04	1.25	2.20

ENTRANCE ISLAND

49 12 34 W 123 48 27 W

OCTOBER

NOVEMBER

DECEMBER 1978

DATE	TEMP	SAL	TEMP	SAL	TEMP	SAL
1	13.1	26.3	10.3	28.0	8.2	28.1
2	14.6	23.4	10.2	28.2	8.2	28.0
3	14.1	23.7	10.0	28.1	9.3	28.8
4	13.9	24.2	9.8	26.7	7.8	27.7
5	13.7	24.8	9.7	26.3	8.3	28.6
6	13.3	24.0	9.9	28.6	7.9	28.4
7	13.6	25.0	9.9	29.3	7.7	28.1
8	12.9	26.1	9.7	28.4	7.9	28.1
9	11.6	27.8	9.4	27.4	8.6	28.6
10	12.1	27.3	9.1	27.3	* 8.6	*28.7
11	13.0	26.3	8.6	26.8	8.6	28.9
12	13.1	24.8	8.7	27.1	7.7	28.5
13	12.9	24.8	8.4	26.8	7.8	28.5
14	12.8	25.0	8.3	27.1	* 8.1	*28.6
15	12.9	25.4	8.3	27.4	* 8.4	*28.8
16	12.8	25.2	9.6	28.6	8.7	28.9
17	12.9	25.8	7.9	26.0	9.3	29.5
18	12.8	25.6	7.9	26.8	8.8	29.3
19	12.5	24.2	7.4	25.9	7.6	28.5
20	12.2	26.1	7.8	27.1	8.4	29.1
21	11.9	28.0	7.2	26.5	8.0	28.9
22	11.9	26.4	7.2	26.8	8.3	28.9
23	10.9	28.0	8.1	27.6	7.8	28.6
24	11.0	27.6	8.8	28.6	7.8	28.8
25	11.1	27.2	8.6	28.0	7.1	28.0
26	10.7	26.8	7.7	27.3	6.6	27.7
27	11.0	26.8	8.5	28.2	7.2	28.2
28	10.7	27.3	8.4	28.0	6.8	28.2
29	10.7	27.8	8.2	27.8	6.3	28.0
30	10.6	27.6	8.9	28.4	6.9	28.8
31	10.3	27.8	0.0	0.0	7.4	28.9
MEANS	12.3	26.0	8.7	27.5	7.9	28.5
OBSVNS.	31	31	30	30	28	28
YRLY. MEANS.....					11.4	26.6
MAXIMUM	14.6	28.0	10.3	29.3	9.3	29.5
MINIMUM	10.3	23.4	7.2	25.9	6.3	27.7
STD. DEV.	1.18	1.41	.92	.85	.75	.46

ACTIVE PASS

48 52 26 N

123 17 23 W

JANUARY

FEBRUARY

MARCH

1978

DATE	TEMP	SAL	TEMP	SAL	TEMP	SAL
1	5.3	28.0	5.9	27.7	6.3	27.2
2	4.6	26.9	6.0	28.0	6.3	27.2
3	4.2	26.7	7.6	28.8	7.1	27.7
4	6.3	29.1	7.3	27.8	7.1	26.8
5	7.1	29.5	6.2	26.4	7.8	28.8
6	7.2	29.3	7.1	27.7	7.6	28.8
7	7.3	29.1	7.7	29.0	8.3	29.5
8	7.3	29.0	7.9	28.6	8.3	28.9
9	* 6.9	*27.7	7.8	29.1	7.9	28.6
10	6.4	26.3	7.6	29.1	8.2	28.8
11	6.6	27.7	7.2	28.2	7.9	29.0
12	6.6	28.2	6.7	28.4	7.3	27.4
13	6.0	24.8	7.1	29.1	7.0	27.8
14	5.4	25.2	6.8	28.6	7.8	28.1
15	5.9	24.0	6.9	28.2	8.3	27.8
16	6.4	26.0	7.5	28.6	7.8	27.6
17	6.6	26.7	7.4	28.5	8.3	28.2
18	6.7	27.4	7.8	28.8	8.8	26.7
19	6.8	27.1	7.9	28.9	8.5	25.9
20	6.7	26.1	7.4	24.6	8.9	27.3
21	7.3	28.9	8.3	28.5	9.0	27.8
22	6.8	28.8	8.3	28.0	9.2	27.4
23	6.7	26.7	7.7	24.7	8.7	28.9
24	6.8	27.8	7.6	27.3	8.9	29.1
25	6.9	28.1	6.8	28.0	9.1	29.5
26	6.9	27.7	6.4	26.7	8.5	29.4
27	7.1	28.6	7.4	28.4	8.5	29.0
28	6.2	24.4	6.4	27.2	9.2	29.0
29	6.2	25.0	0.0	0.0	8.3	29.5
30	6.6	28.4	0.0	0.0	8.4	29.0
31	5.9	26.7	0.0	0.0	8.3	23.5
MEANS	6.4	27.3	7.2	28.0	8.1	28.1
OBSVNS.	30	30	28	28	31	31
MAXIMUM	7.3	29.5	8.3	29.1	9.2	29.5
MINIMUM	4.2	24.0	5.9	24.6	6.3	23.5
STD.DEV.	.75	1.55	.65	1.17	.78	1.27

ACTIVE PASS

48 52 26 N

123 17 23 W

APRIL

MAY

JUNE

1978

DATE	TEMP	SAL	TEMP	SAL	TEMP	SAL
1	9.0	25.2	10.7	29.0	14.4	26.4
2	9.3	28.1	11.0	28.4	18.2	16.9
3	9.4	29.1	11.4	21.7	13.3	28.4
4	8.8	29.1	11.6	25.4	15.4	25.8
5	9.0	29.7	11.8	25.6	14.6	25.6
6	9.0	29.1	12.3	20.5	14.3	26.3
7	9.4	28.5	11.2	28.1	12.7	28.5
8	9.6	27.7	11.0	28.5	11.6	28.6
9	9.7	28.5	11.0	27.8	11.2	28.8
10	9.0	27.4	10.6	28.9	11.4	28.8
11	8.9	27.8	10.6	29.1	13.9	28.2
12	8.9	27.8	10.6	29.7	12.1	28.6
13	8.6	28.2	9.7	30.0	11.5	28.9
14	8.6	29.0	9.6	29.8	11.9	29.1
15	9.6	28.2	10.0	28.9	13.9	24.8
16	9.3	23.4	10.7	28.6	15.6	2.5
17	9.9	29.0	13.4	13.3	14.3	23.9
18	9.8	29.3	13.9	15.0	14.6	21.4
19	* 9.7	* 29.3	16.1	18.0	17.3	20.5
20	9.6	29.3	14.9	23.5	17.0	18.3
21	9.3	29.5	12.9	26.7	15.4	23.3
22	8.8	30.0	12.5	28.4	15.3	25.4
23	10.9	29.3	12.1	28.2	13.3	27.6
24	9.9	28.8	10.1	29.3	12.1	28.0
25	10.1	27.6	10.4	29.0	11.8	28.2
26	11.0	29.1	10.7	29.1	12.8	28.1
27	9.4	28.8	10.6	29.7	15.4	22.2
28	9.3	28.4	10.6	29.7	17.9	12.2
29	9.3	28.5	12.4	21.3	15.3	25.4
30	9.4	28.2	14.8	12.9	14.9	25.6
31	8.0	0.0	14.1	18.3	0.0	0.0
MEANS	9.4	28.4	11.7	25.6	14.1	24.5
OBSVNS.	29	29	31	31	30	30
MAXIMUM	11.0	30.0	16.1	30.0	18.2	29.1
MINIMUM	8.6	23.4	9.6	12.9	11.2	2.5
STD.DEV.	.58	1.33	1.66	5.24	1.98	5.82

ACTIVE PASS

48 52 26 N

123 17 23 W

JULY

AUGUST

SEPTEMBER 1978

DATE	TEMP	SAL	TEMP	SAL	TEMP	SAL
1	15.5	24.7	15.6	26.7	12.9	27.7
2	17.6	16.5	17.9	25.9	12.9	27.3
3	15.7	25.6	17.0	27.2	13.2	26.0
4	12.6	28.8	17.9	25.4	12.9	27.6
5	12.1	29.4	17.0	26.0	13.9	24.0
6	13.2	28.9	16.2	25.2	13.9	26.3
7	13.0	27.8	20.9	12.9	14.0	25.8
8	12.7	27.2	21.5	16.1	13.8	27.3
9	12.5	27.6	17.1	26.0	12.3	29.1
10	12.1	28.9	14.8	26.9	12.1	29.4
11	12.7	27.3	13.7	27.4	11.9	31.9
12	13.2	28.4	13.4	28.0	15.2	25.1
13	14.3	22.6	15.1	25.6	12.4	28.8
14	13.1	27.1	12.7	27.8	13.5	24.2
15	19.4	17.1	11.3	29.1	15.0	14.9
16	17.4	24.0	12.3	28.5	12.6	28.4
17	19.3	24.2	14.2	28.0	13.9	19.9
18	19.9	17.6	11.6	28.9	13.7	22.5
19	19.3	13.1	12.1	28.6	12.3	27.1
20	19.7	19.5	16.0	22.9	12.3	27.7
21	20.3	19.6	15.3	22.5	11.8	28.5
22	19.7	19.5	12.5	27.8	11.4	28.5
23	19.0	21.6	11.8	28.1	11.3	28.6
24	17.4	25.1	12.7	28.4	12.4	28.0
25	18.0	20.3	12.6	28.4	13.7	15.8
26	16.4	24.6	13.4	28.2	14.4	23.9
27	16.3	25.6	14.2	25.6	14.1	27.7
28	20.1	27.3	14.8	24.7	12.0	28.1
29	18.3	23.5	17.9	13.5	* 12.0	* 28.2
30	17.0	27.4	18.1	20.5	12.1	28.4
31	16.4	16.0	14.8	25.1	0.0	0.0
MEANS	16.3	23.8	15.0	25.4	13.0	26.2
OBSVNS.	31	31	31	31	29	29
MAXIMUM	20.3	29.4	21.5	29.1	15.2	31.9
MINIMUM	12.1	13.1	11.3	12.9	11.3	14.9
STO.DEV.	2.87	4.53	2.64	4.24	1.04	3.81

ACTIVE PASS

48 52 26 N

123 17 23 W

OCTOBER

NOVEMBER

DECEMBER 1978

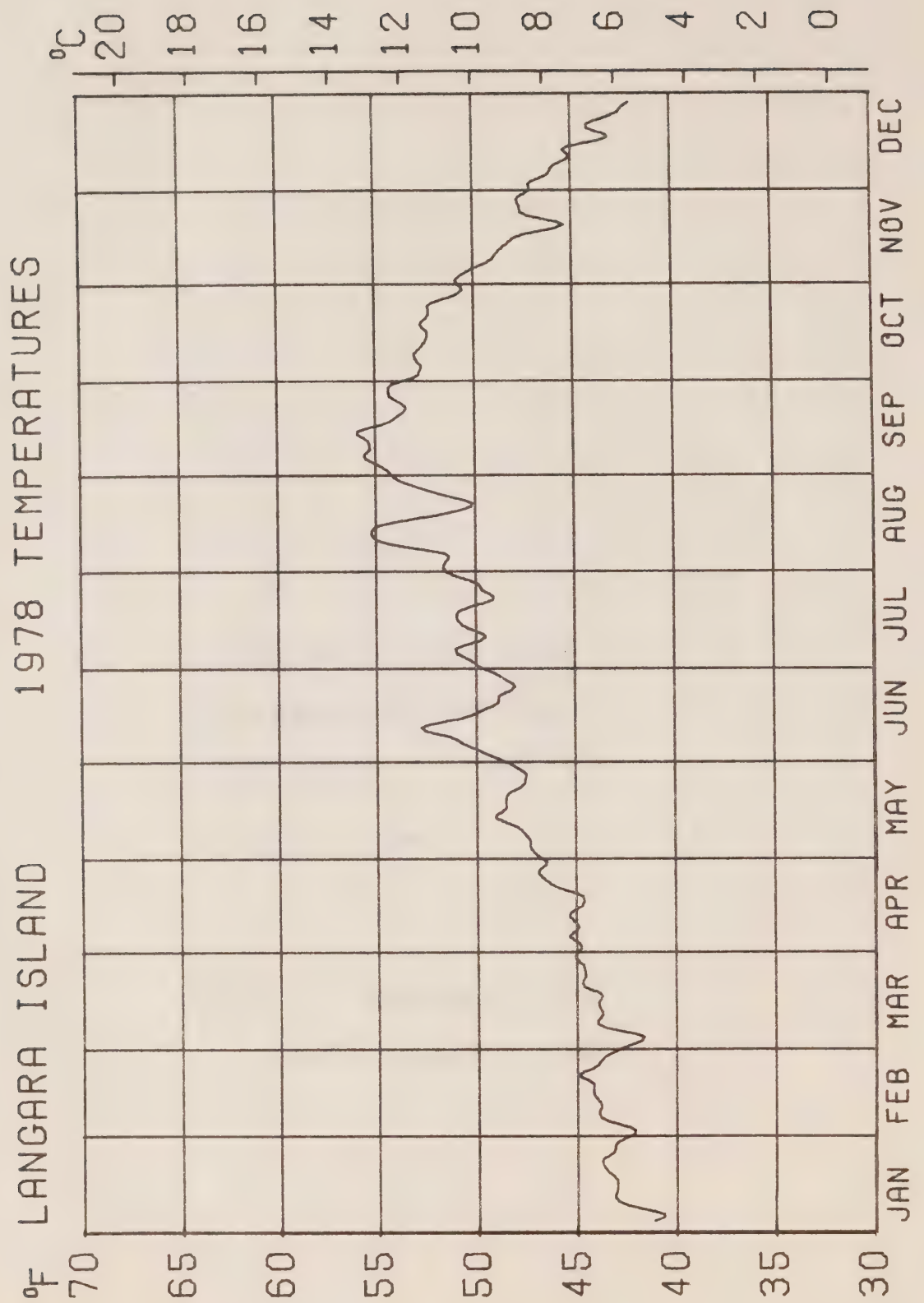
DATE	TEMP	SAL	TEMP	SAL	TEMP	SAL
1	12.7	23.7	10.7	27.8	7.8	28.0
2	12.3	27.1	10.5	28.0	8.1	28.5
3	12.4	24.4	10.3	26.9	8.3	28.9
4	14.0	20.8	9.5	28.4	7.3	28.9
5	13.5	24.2	9.2	28.0	7.1	27.2
6	12.4	20.9	9.8	29.1	7.1	28.1
7	12.3	27.1	9.7	28.9	6.9	28.1
8	12.2	27.4	9.6	28.2	7.6	28.8
9	11.6	28.1	7.9	13.9	8.3	28.5
10	11.6	28.1	* 7.9	*20.8	8.3	28.6
11	11.7	28.6	7.9	27.7	8.2	28.2
12	12.5	21.7	8.2	26.7	6.8	27.6
13	12.8	21.8	8.2	27.8	6.9	27.7
14	12.5	24.8	8.3	27.8	8.3	28.9
15	12.4	24.8	8.3	27.8	7.2	28.1
16	12.1	24.8	8.4	28.4	8.2	30.4
17	12.2	24.0	7.6	25.1	7.9	30.0
18	12.1	23.1	* 7.7	*26.4	7.3	29.7
19	11.4	25.9	* 7.9	*27.7	7.1	30.0
20	11.6	24.7	8.1	29.0	7.1	29.0
21	11.4	24.3	7.4	28.2	7.2	29.3
22	11.4	26.8	6.5	24.8	7.1	29.5
23	11.1	28.0	7.5	26.4	7.3	28.1
24	11.1	25.2	8.2	28.1	6.3	24.4
25	11.0	24.4	8.5	28.1	6.4	27.7
26	11.3	25.8	6.9	24.4	6.2	27.7
27	11.2	26.8	7.4	26.8	6.1	27.6
28	11.0	28.1	6.9	26.3	5.3	27.8
29	10.9	28.4	7.6	26.1	5.0	28.5
30	10.8	28.4	8.1	28.1	4.9	28.5
31	10.6	28.0	0.0	0.0	4.8	28.9
MEANS	11.9	25.5	8.4	26.9	7.0	28.4
OBSVNS.	31	31	27	27	31	31
YRLY.MEANS.....					10.8	26.5
MAXIMUM	14.0	28.6	10.7	29.1	8.3	30.4
MINIMUM	10.6	20.8	6.5	13.9	4.8	24.4
STD.DEV.	.80	2.32	1.13	2.88	1.02	1.09

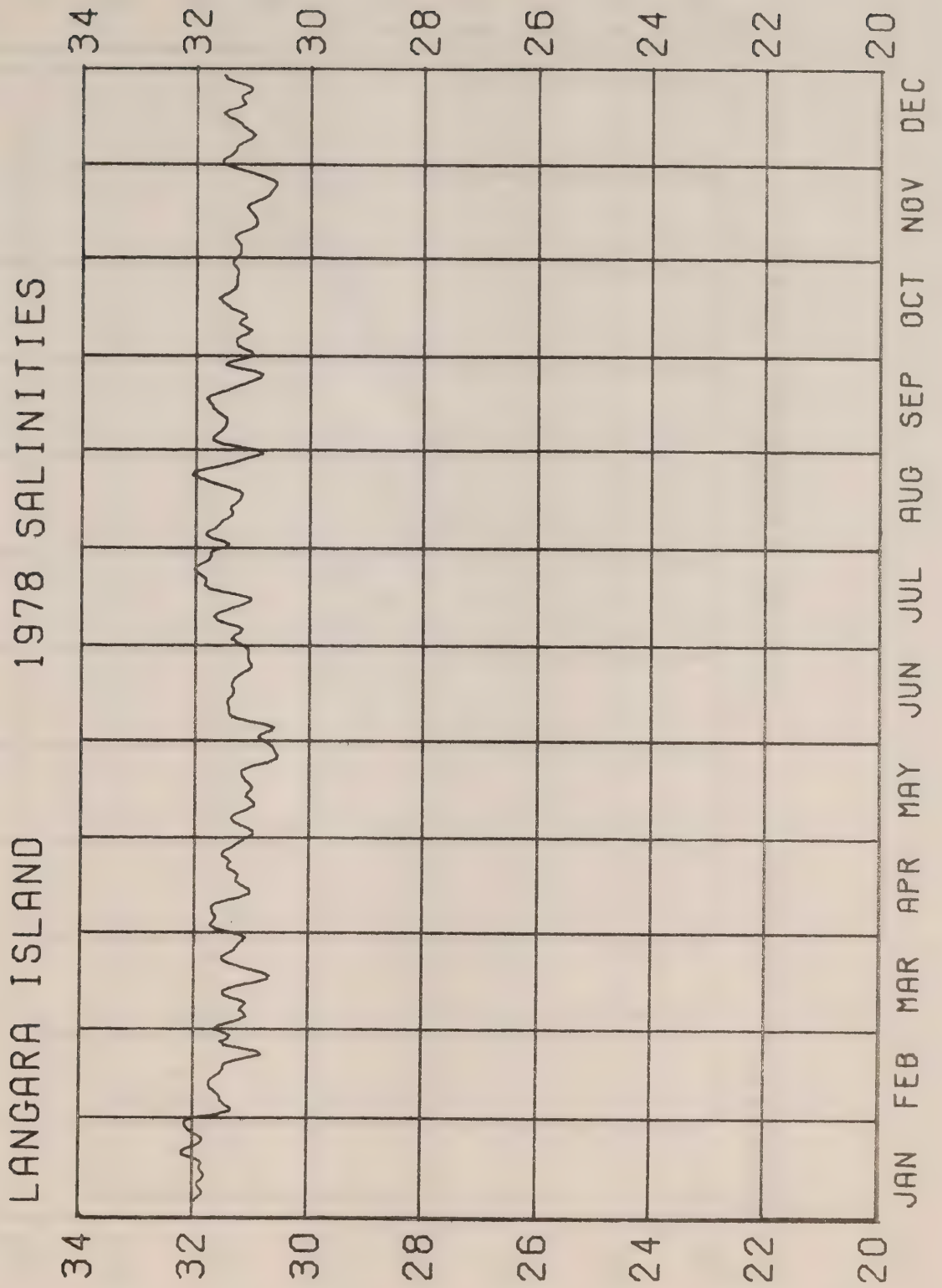
Annual Graphs of the 7-day
Normally-Weighted Running Means
for Temperature and Salinity

1978

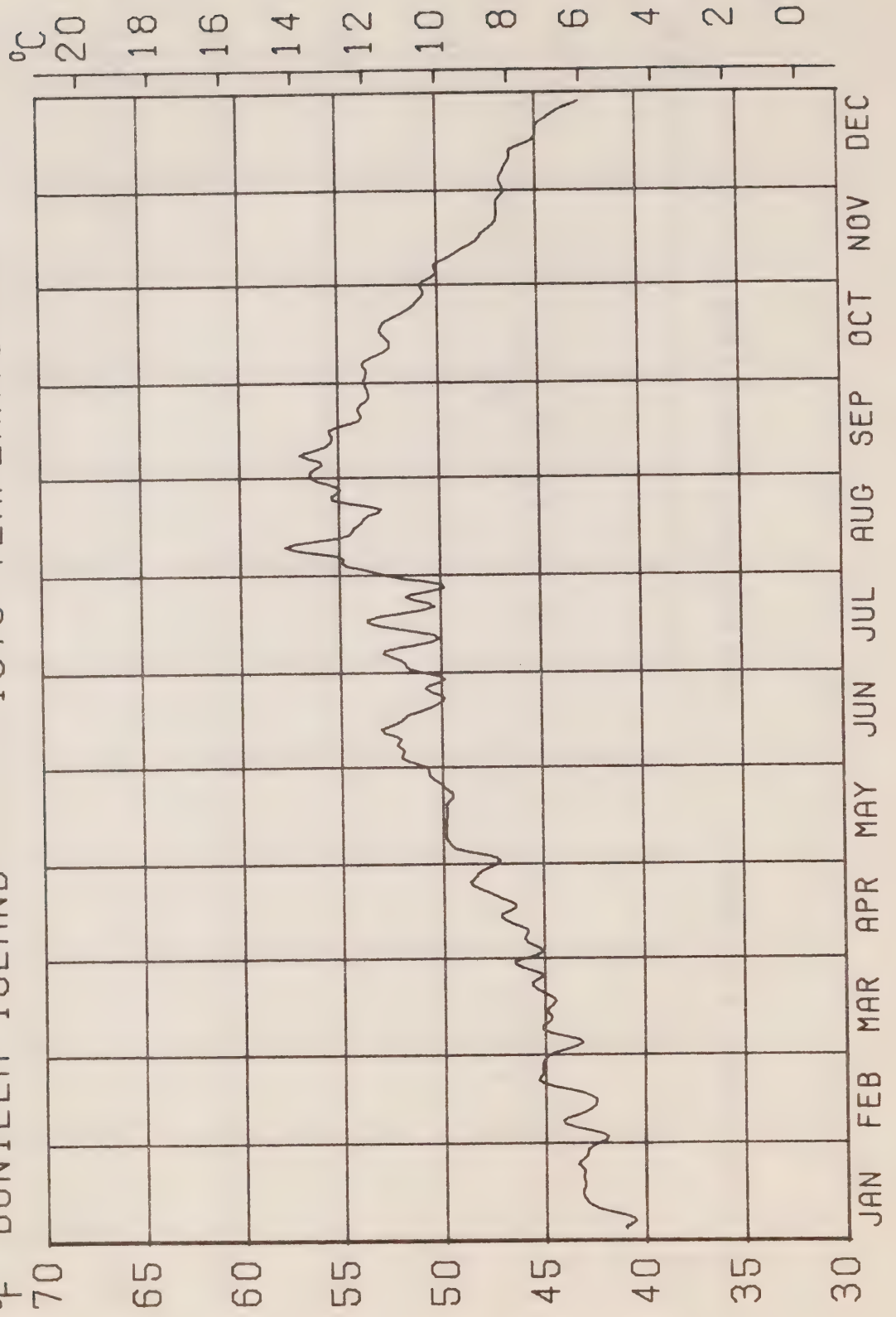
TEMP: Temperature ($^{\circ}\text{C}$ and $^{\circ}\text{F}$)

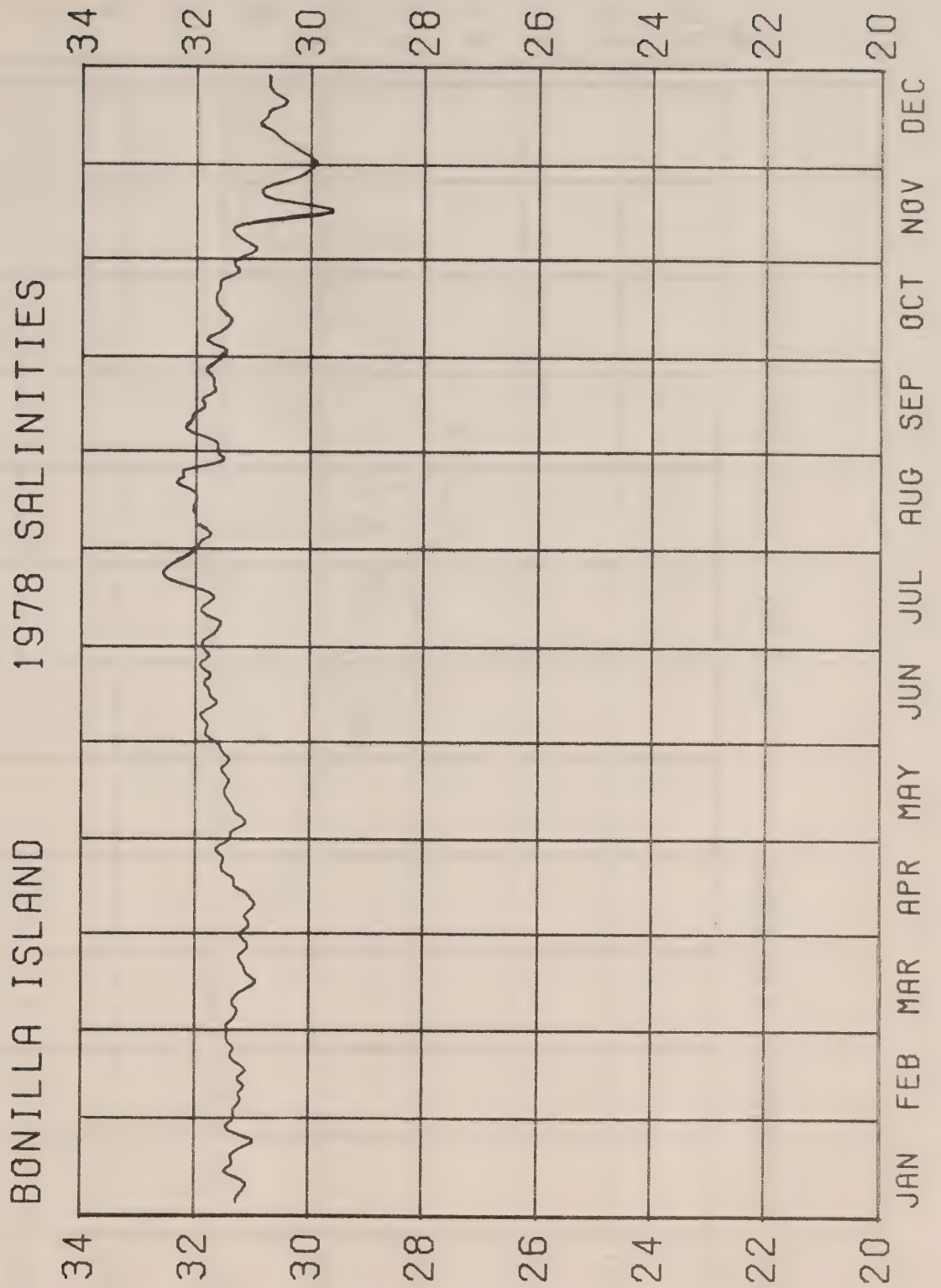
SAL: Salinity ($^{\circ}/\text{oo}$)



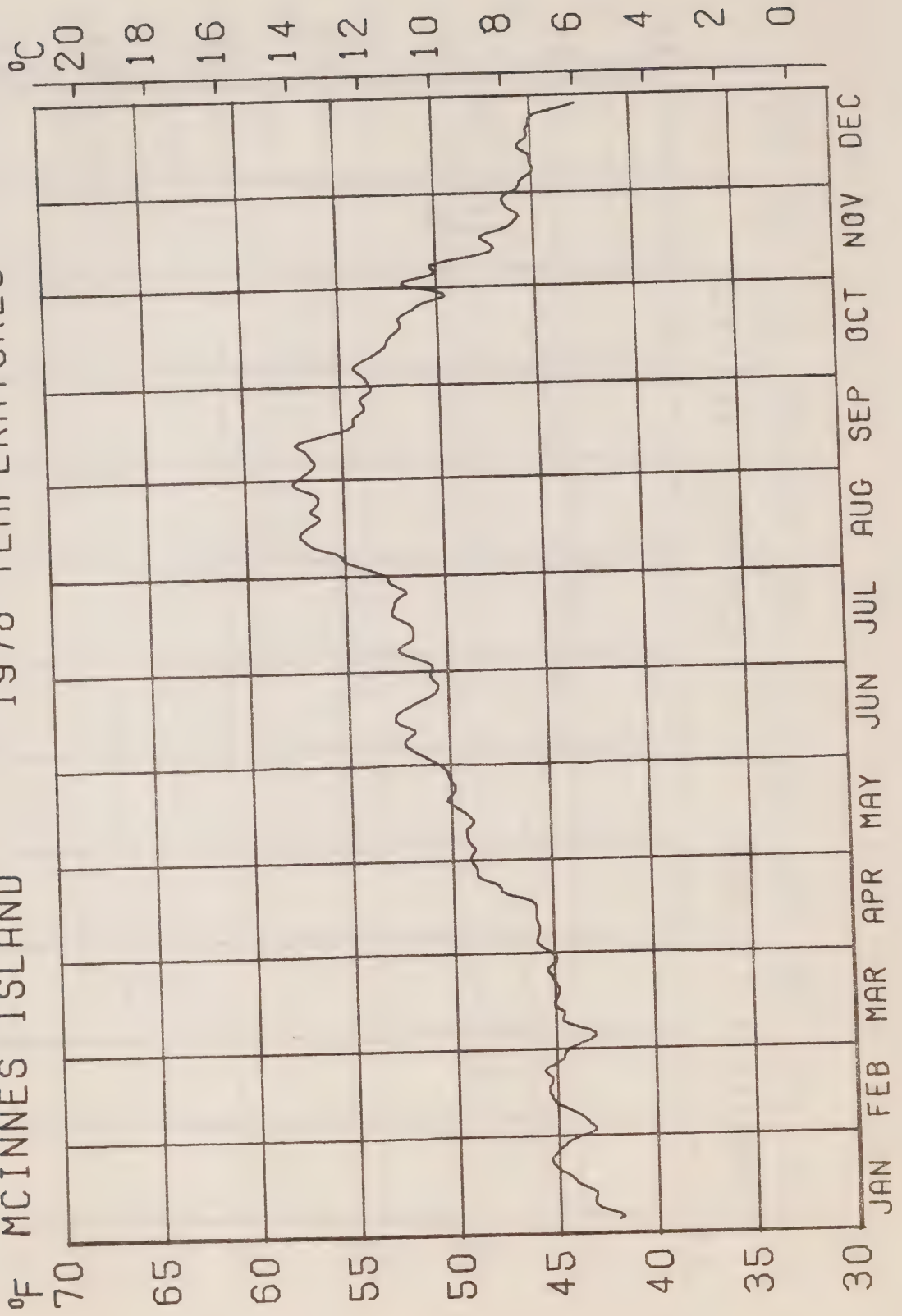


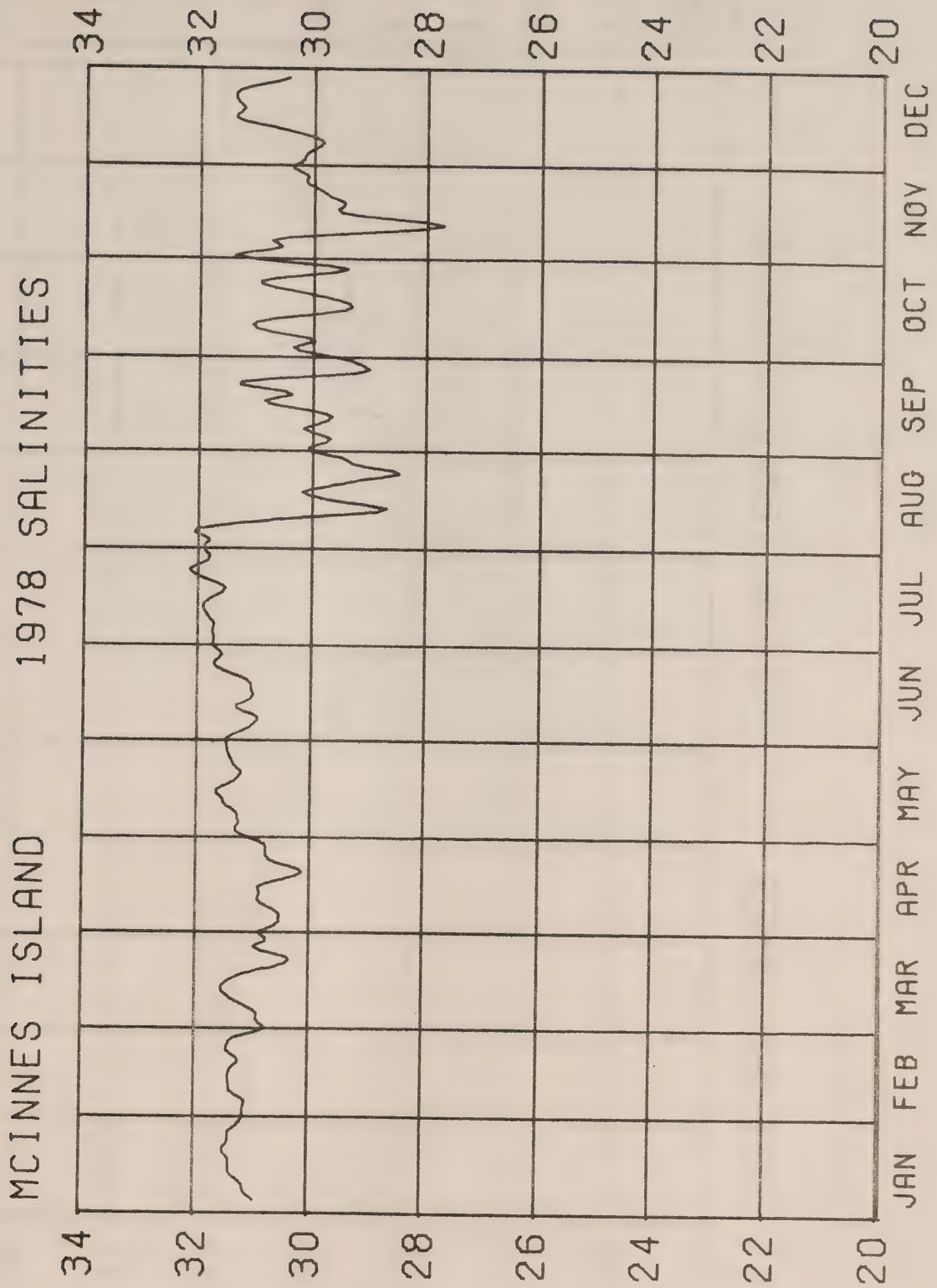
BONILLA ISLAND 1978 TEMPERATURES

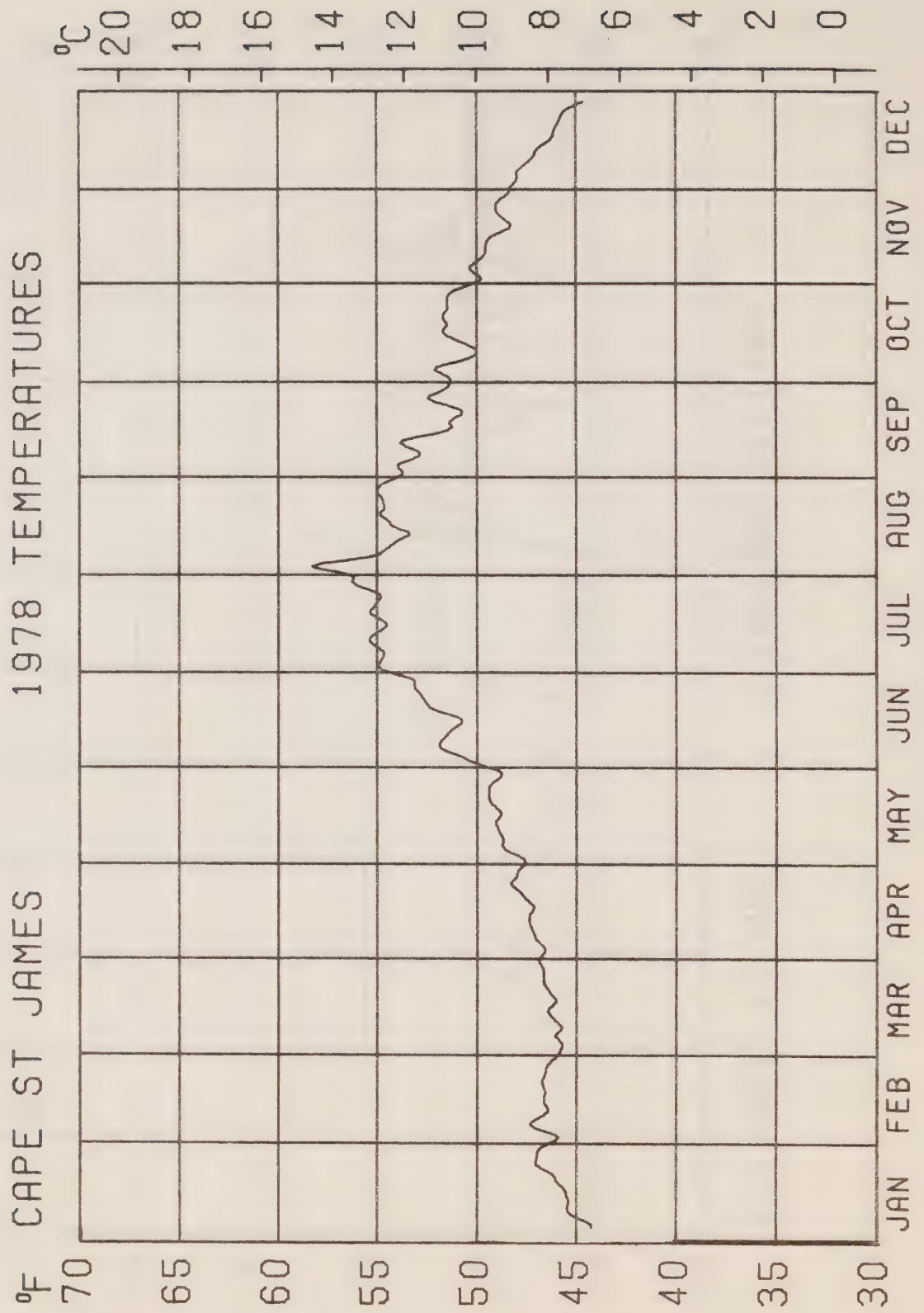


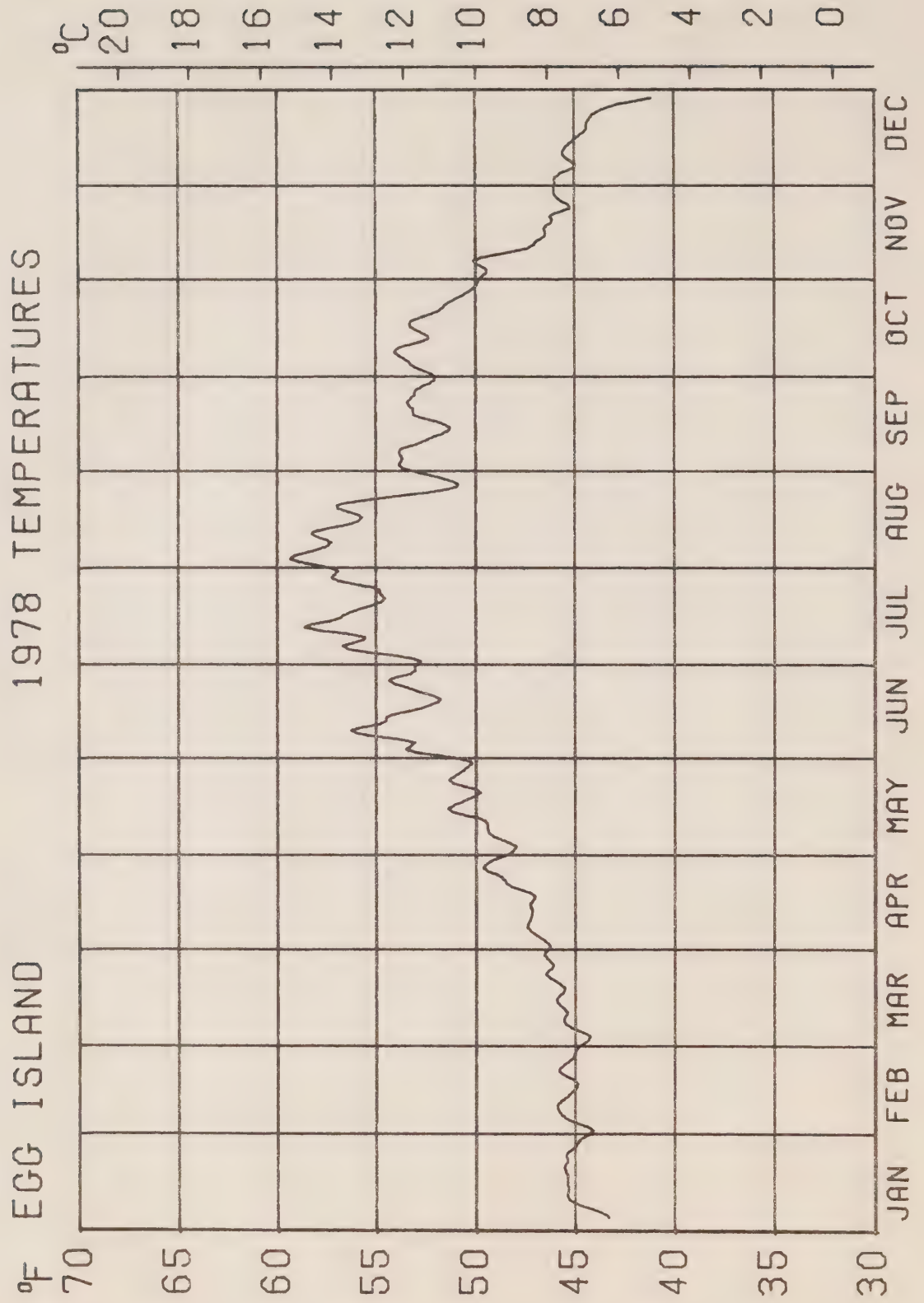


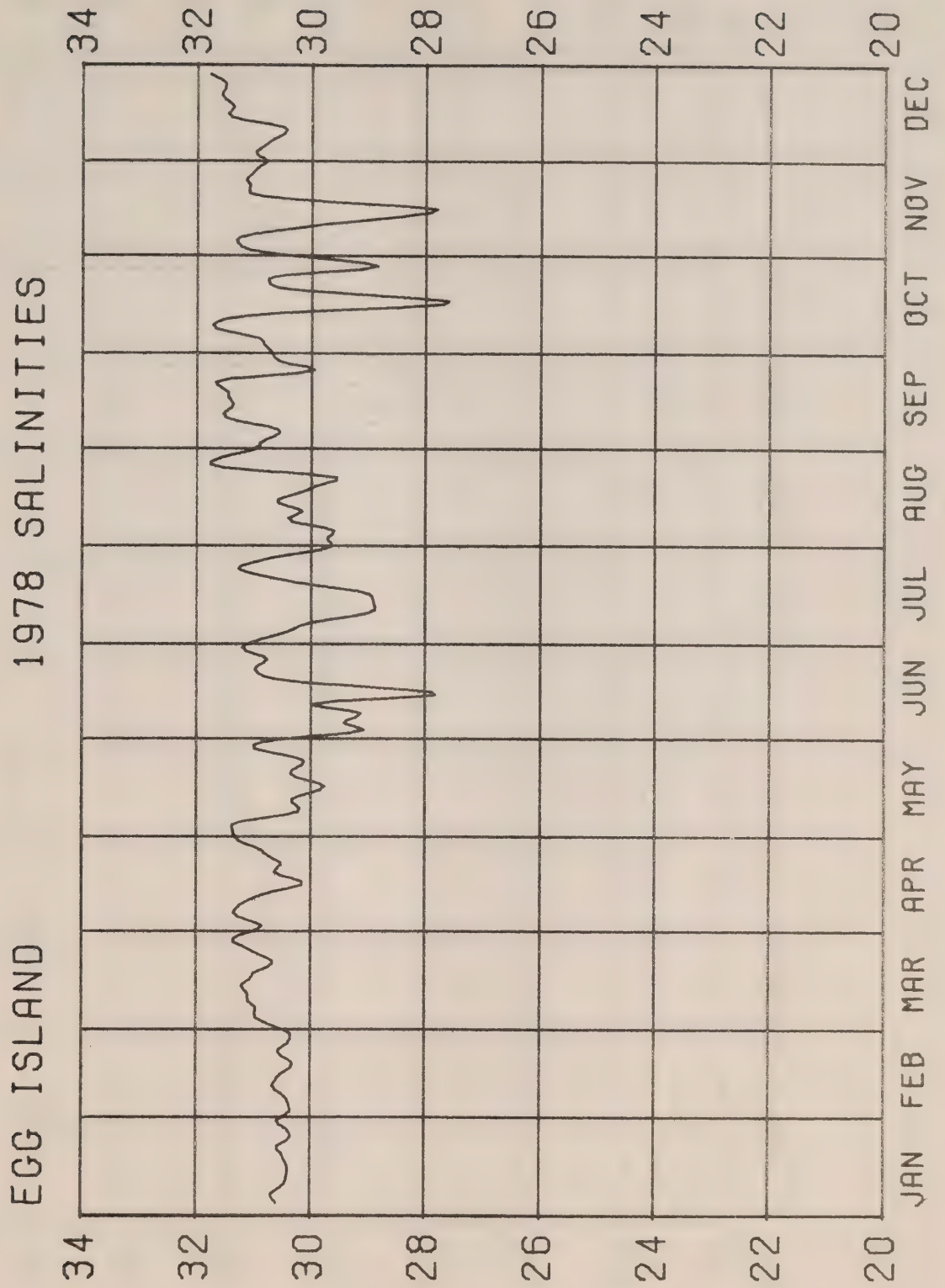
MCINNES ISLAND 1978 TEMPERATURES

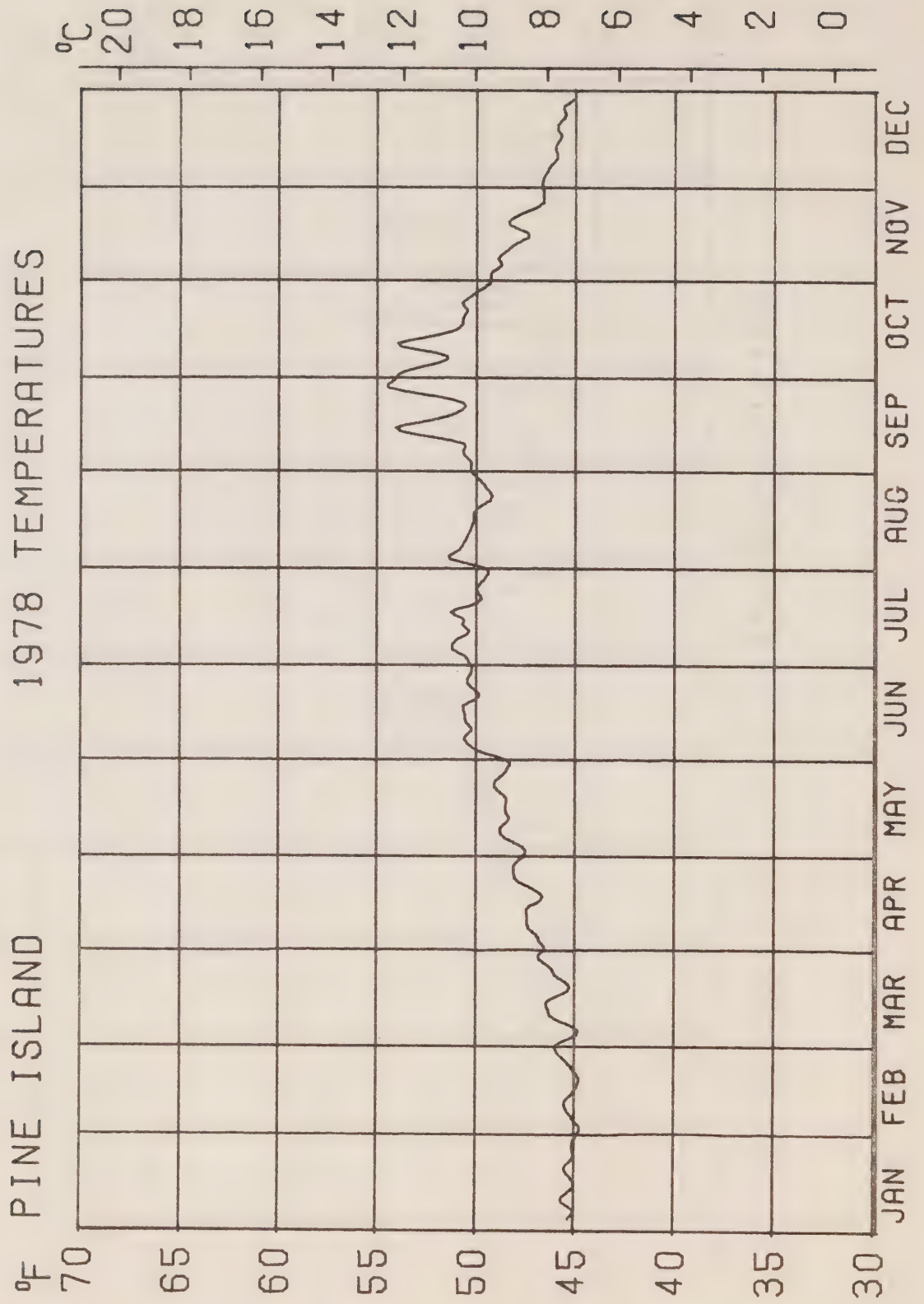


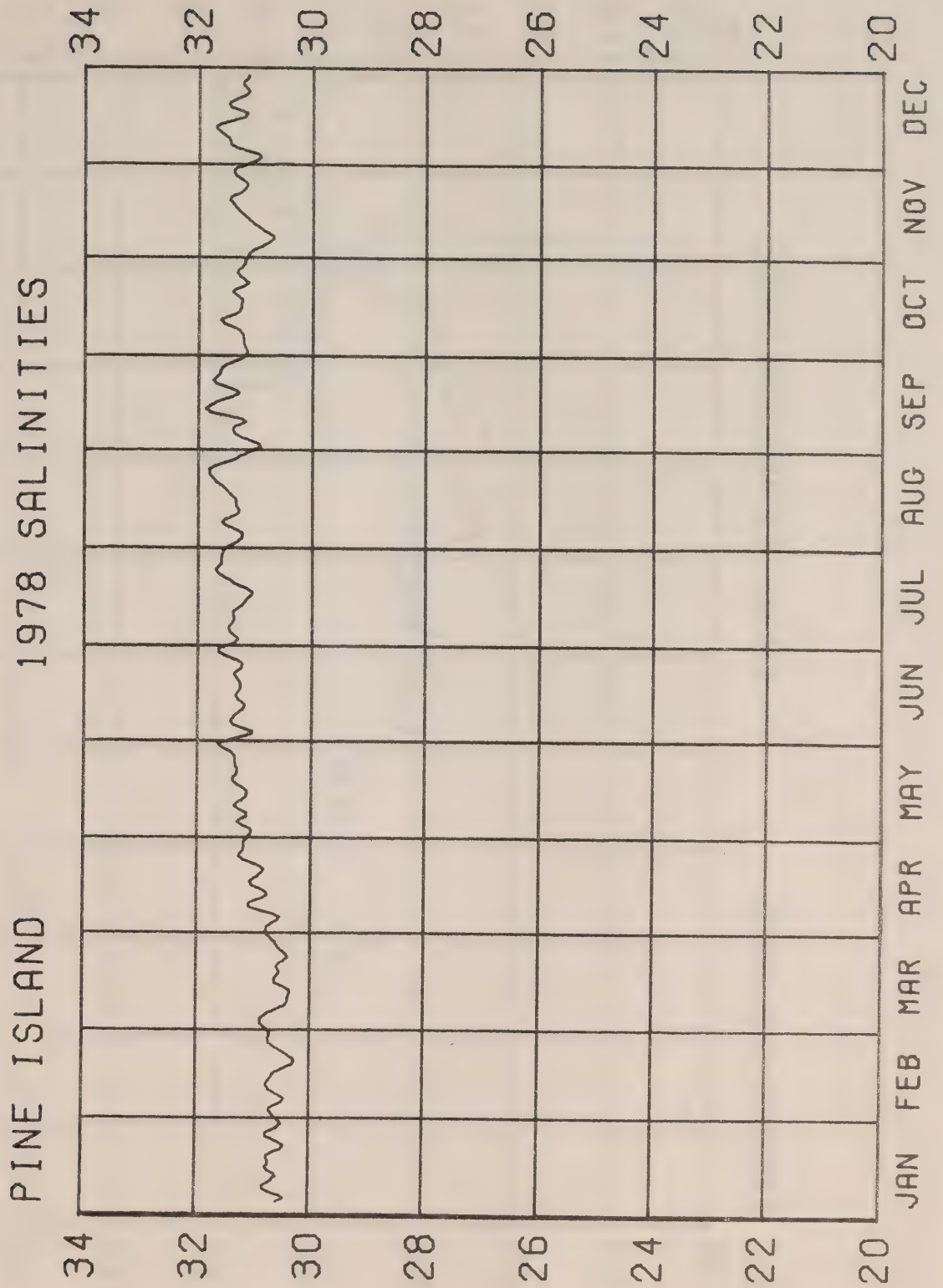


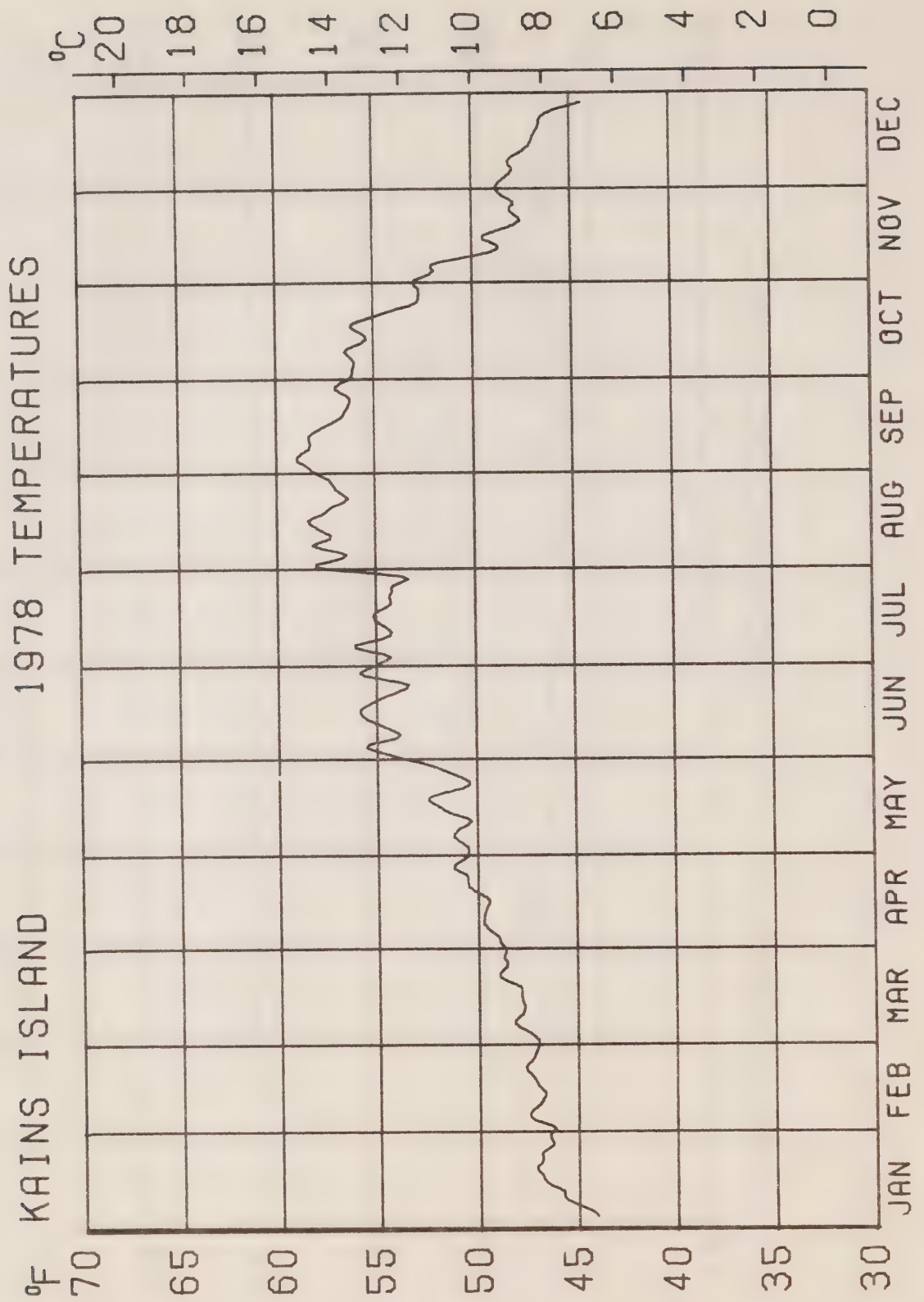


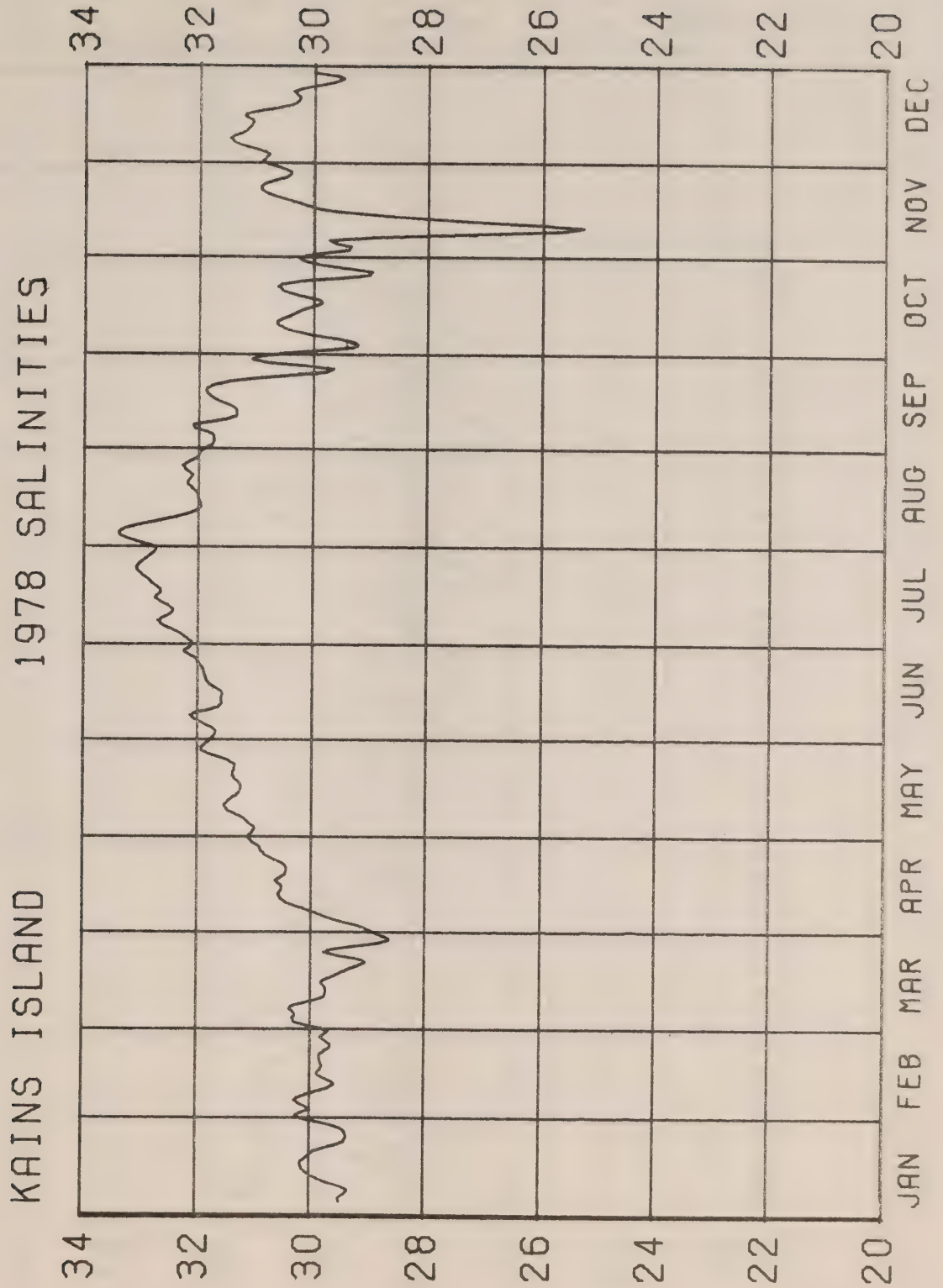




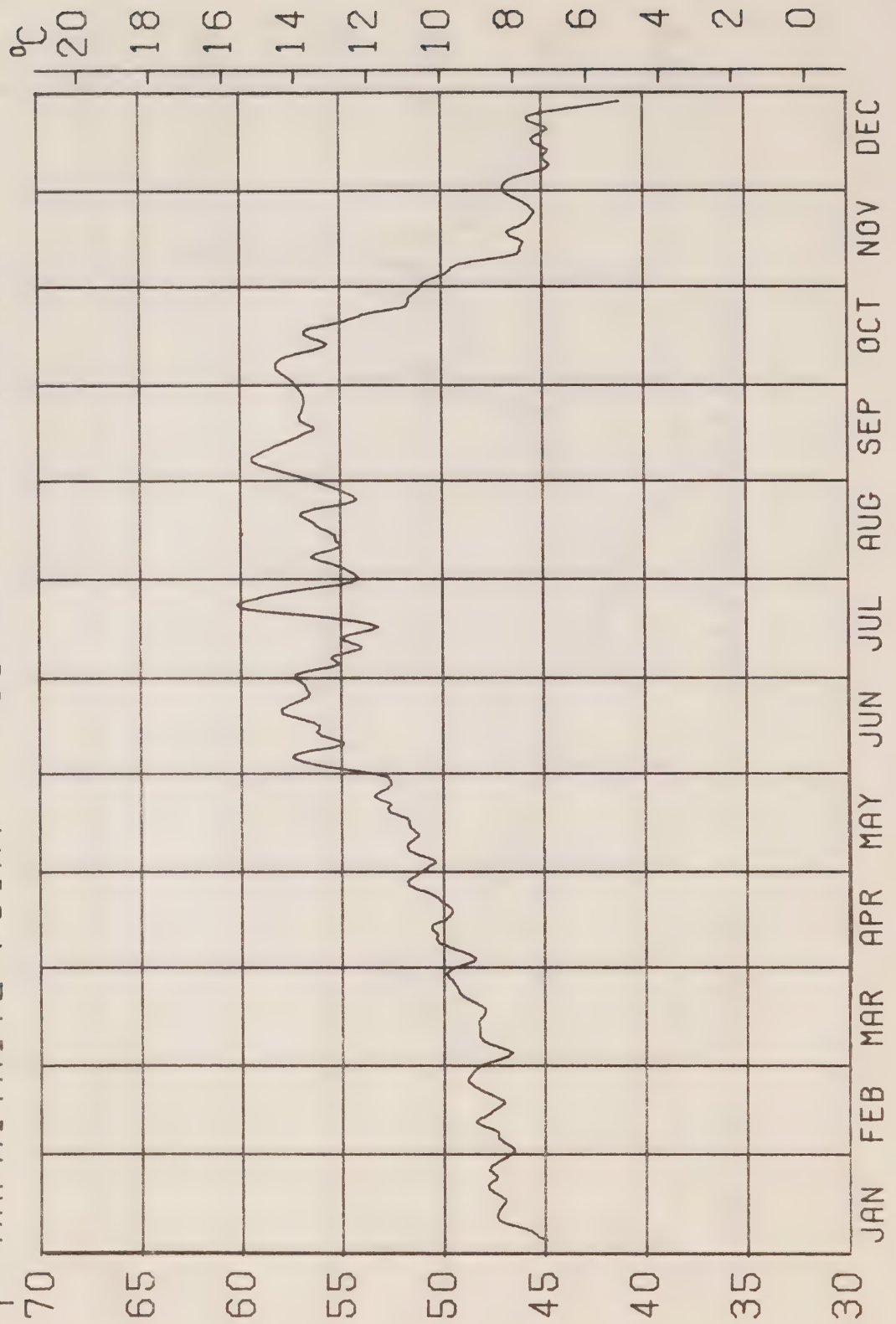




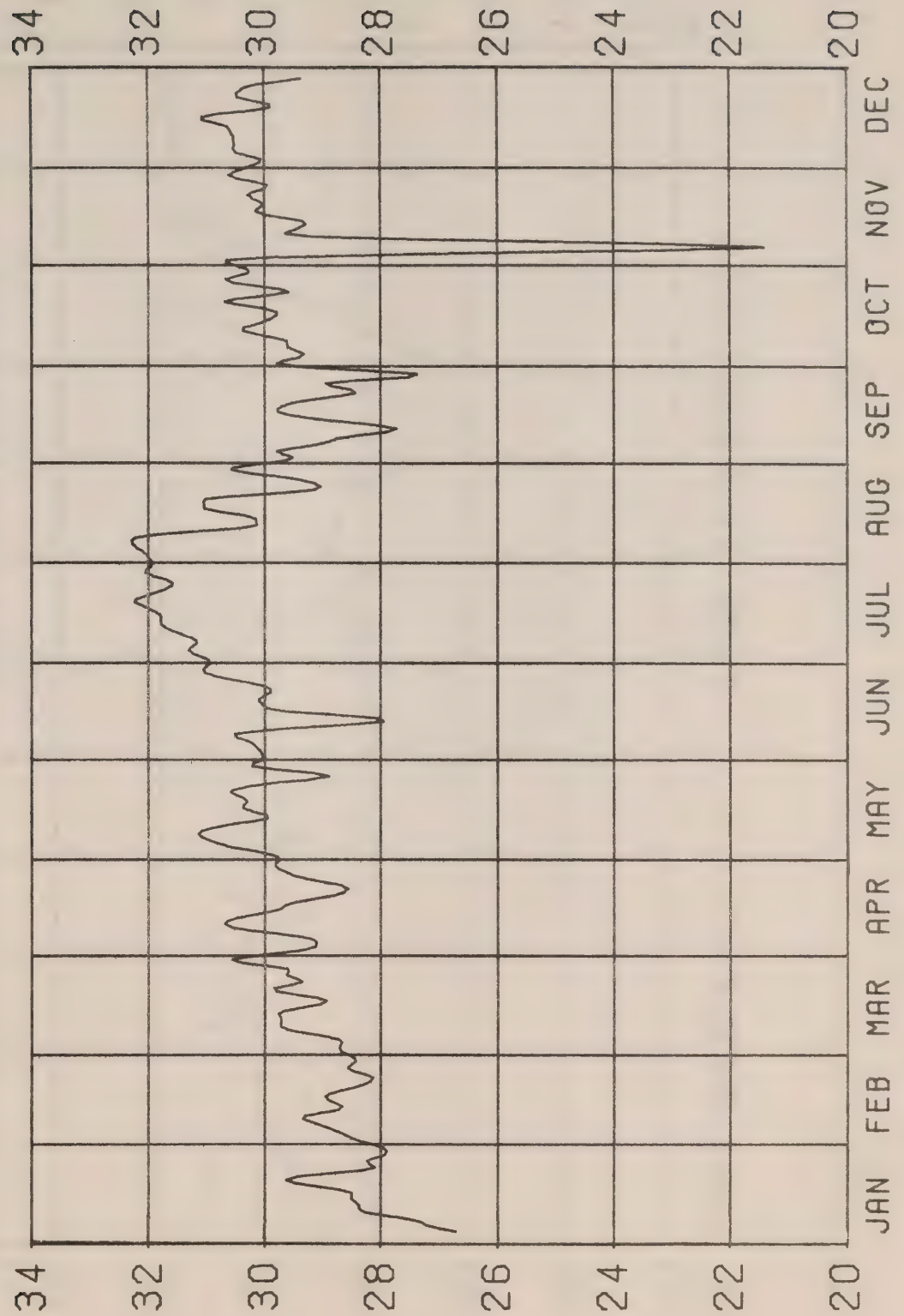


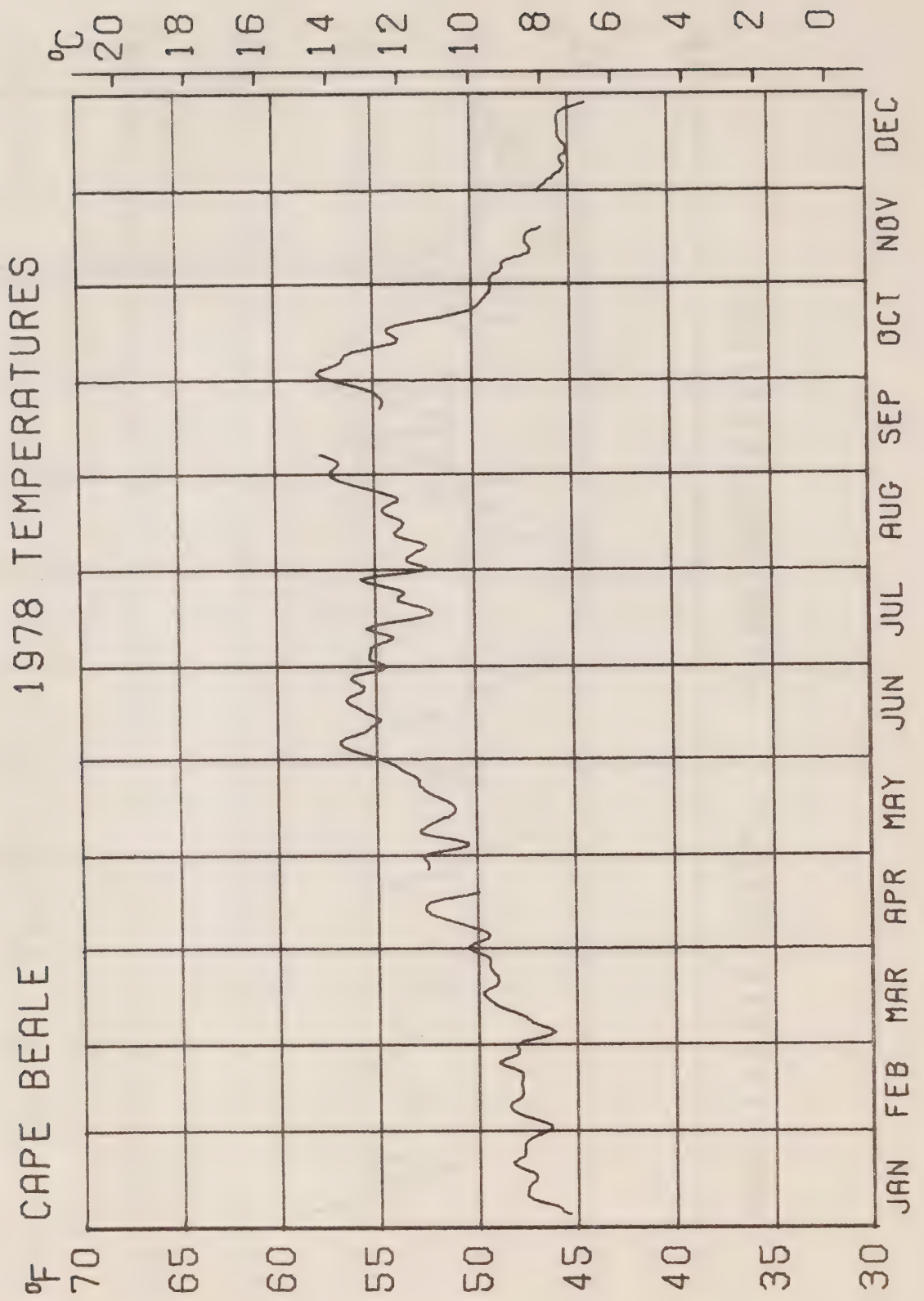


AMPHITRITE POINT 1978 TEMPERATURES

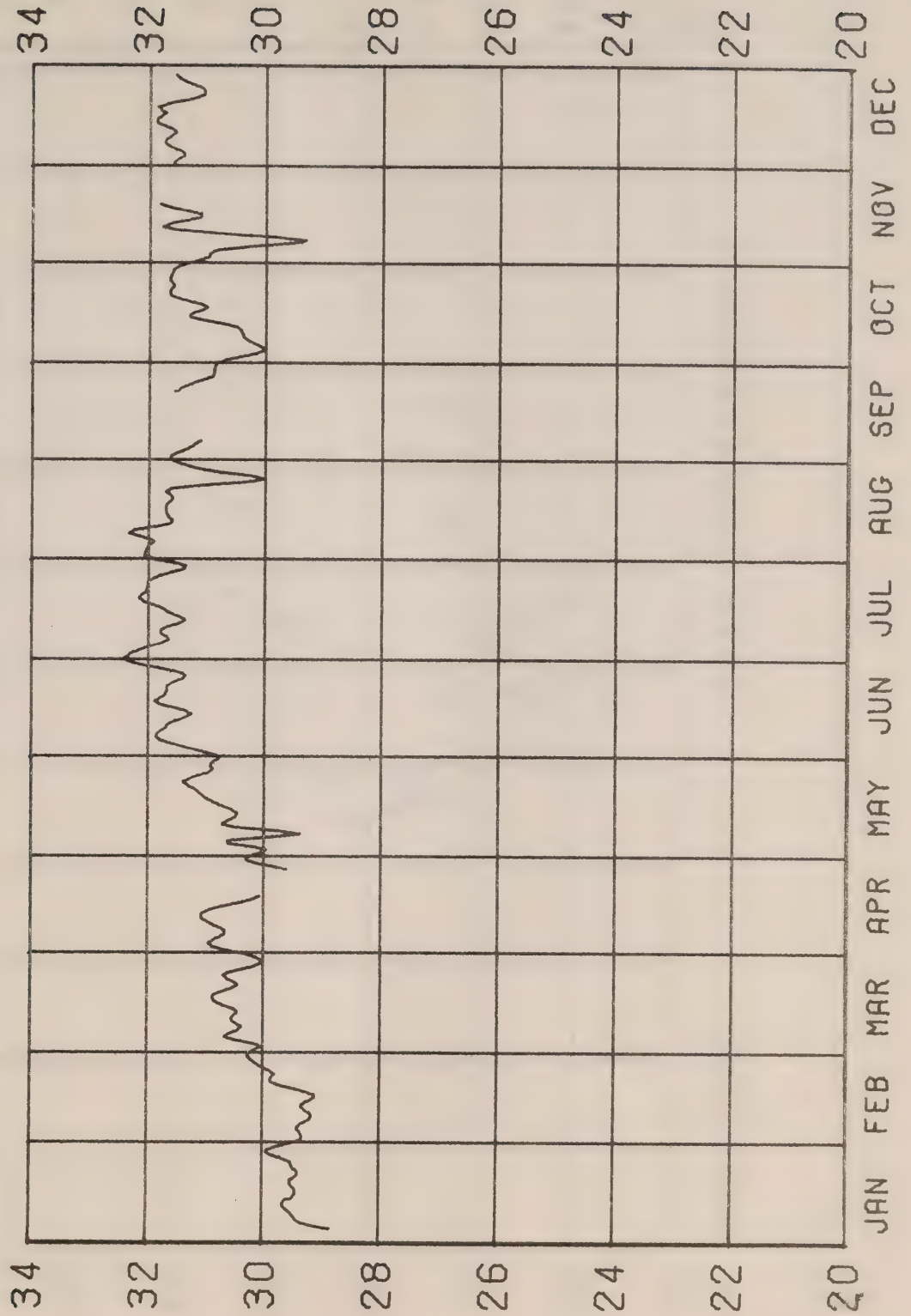


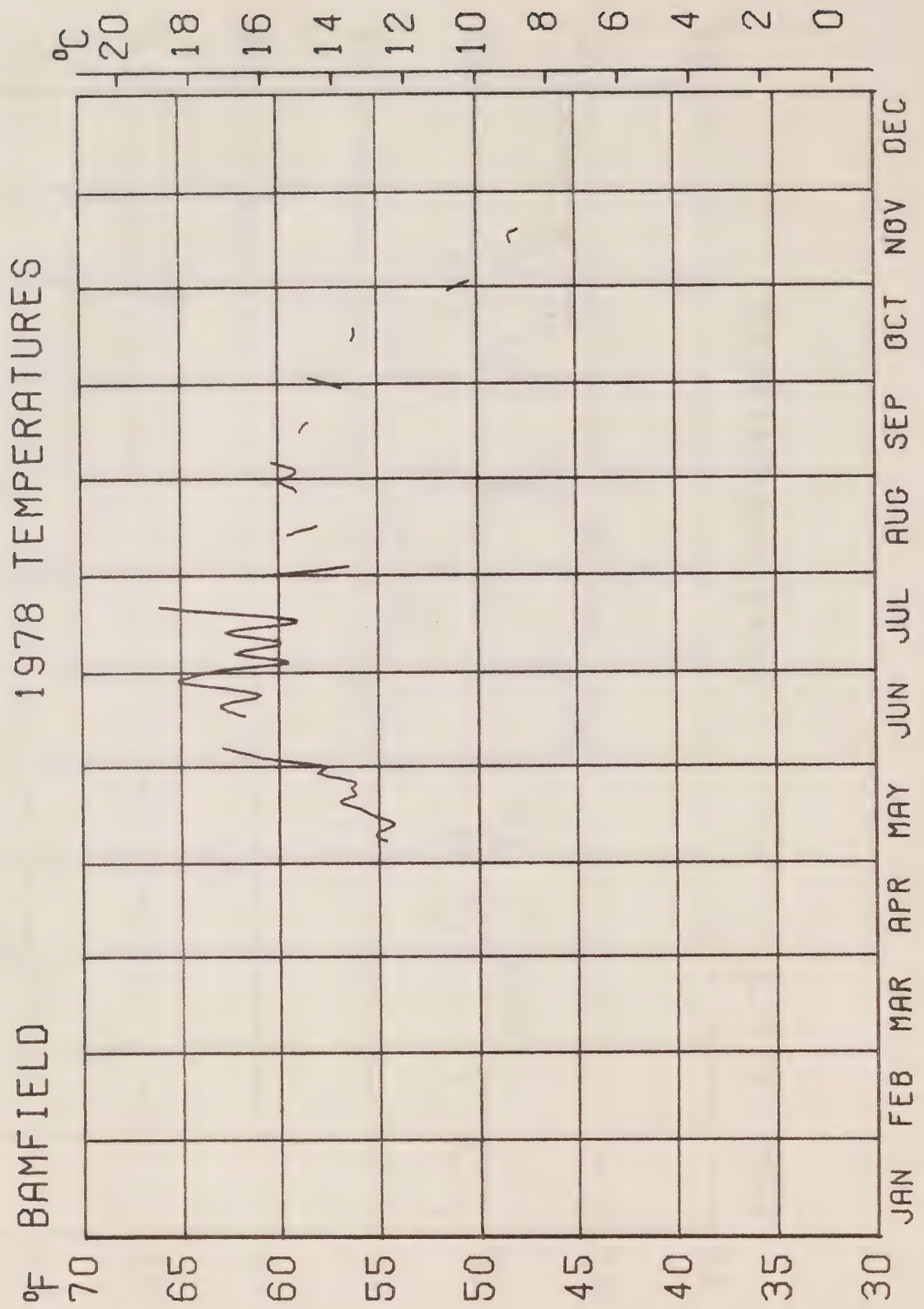
AMPHITRITE POINT 1978 SALINITIES

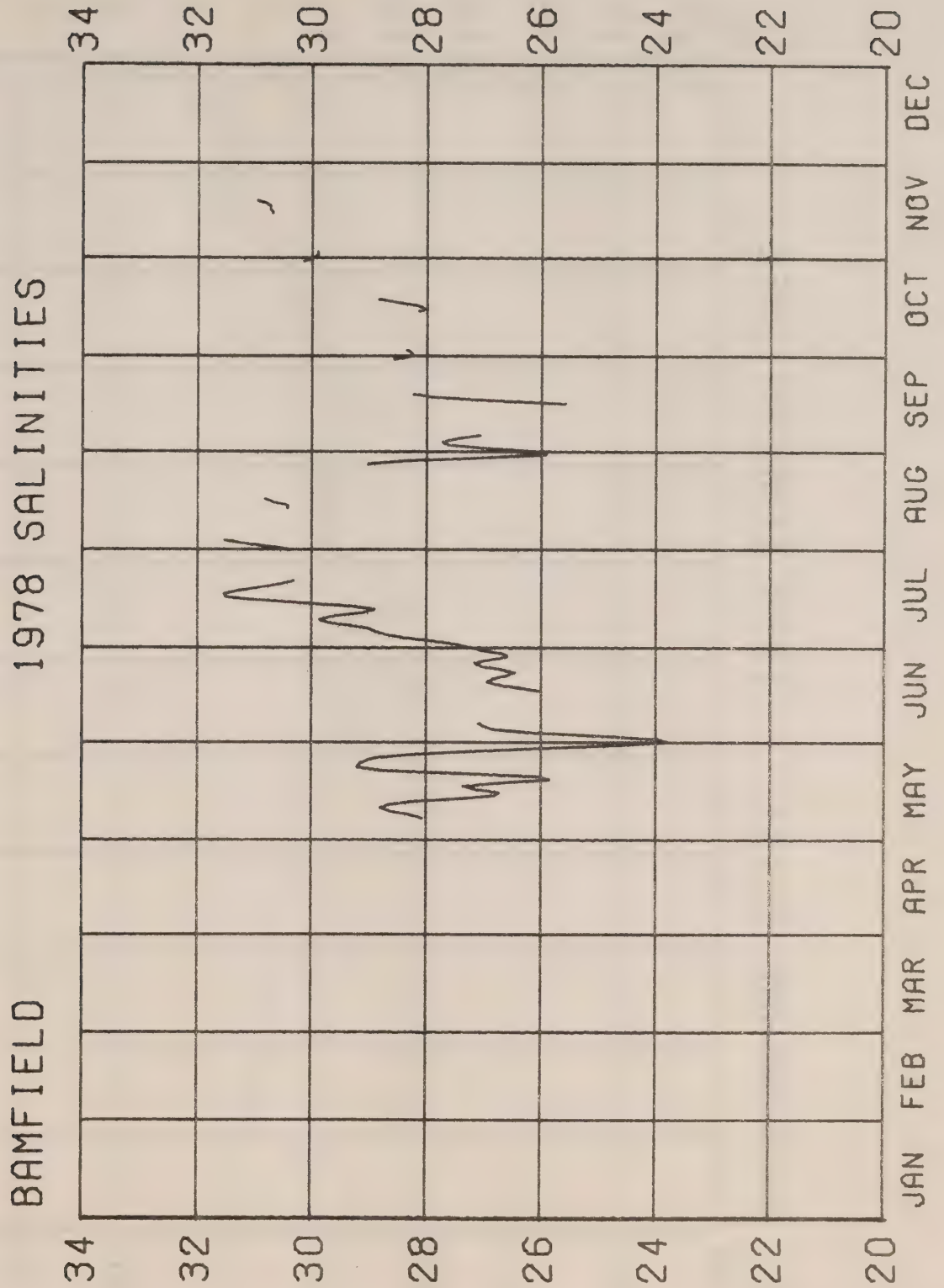




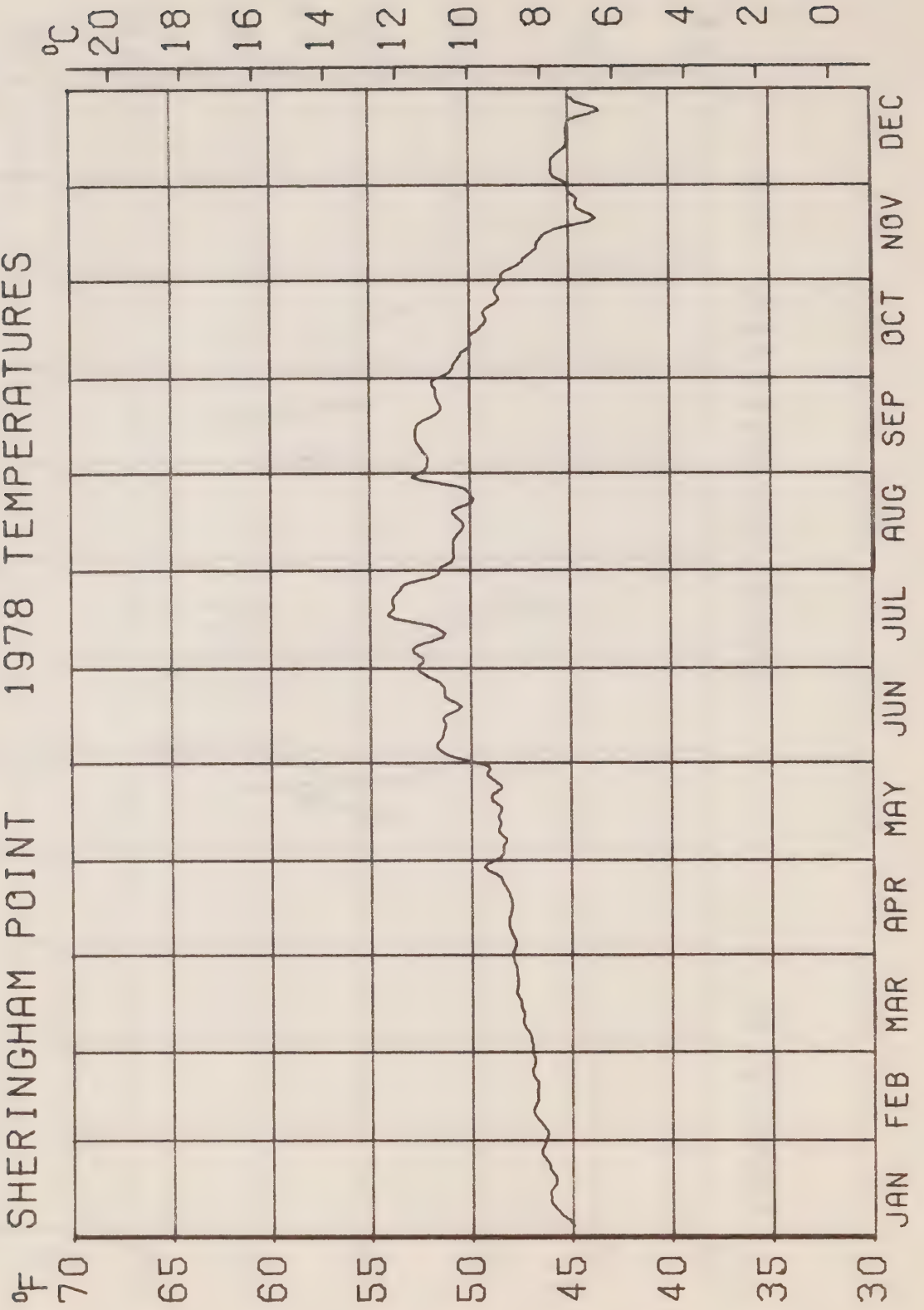
CAPE BEALE 1978 SALINITIES

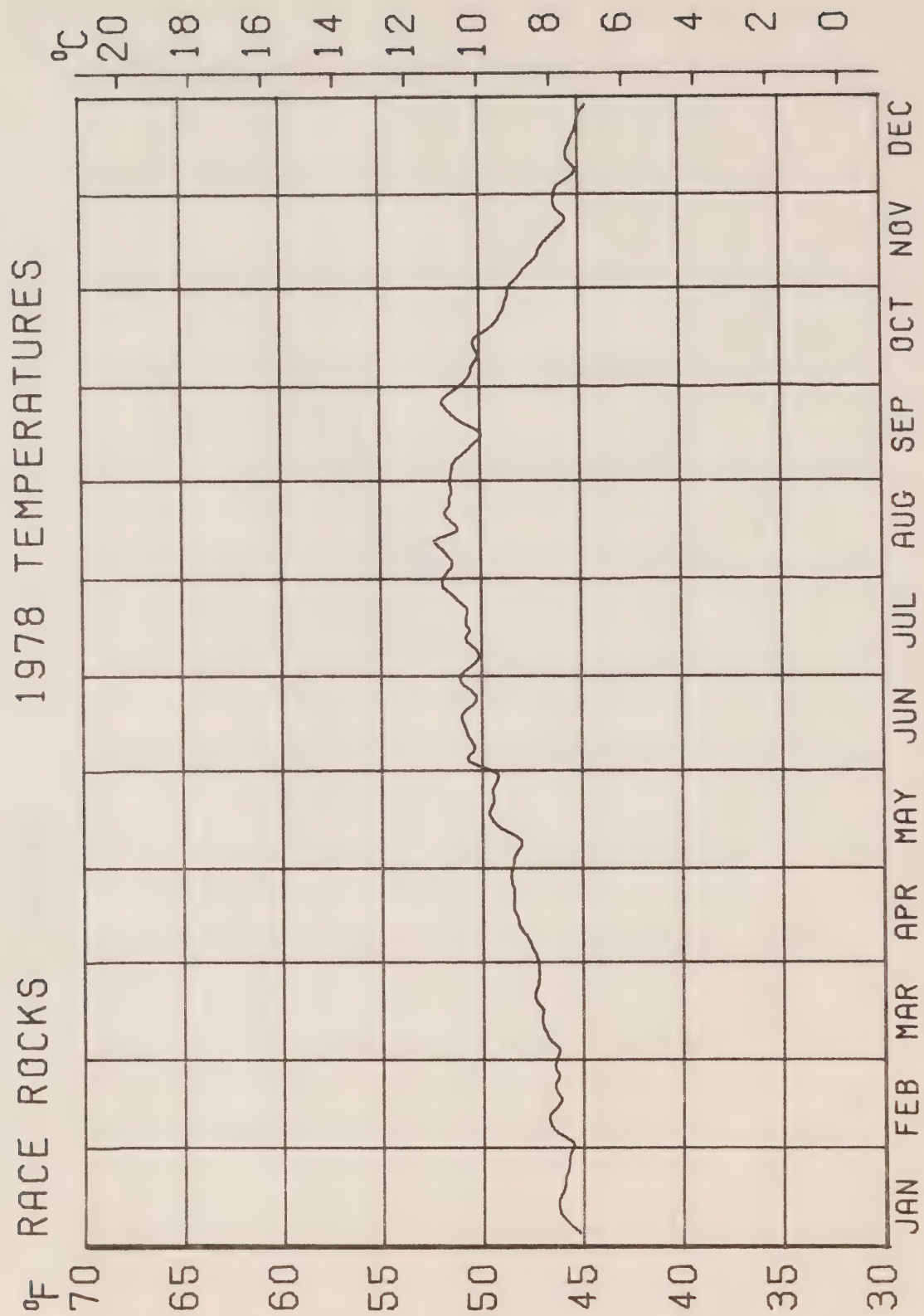


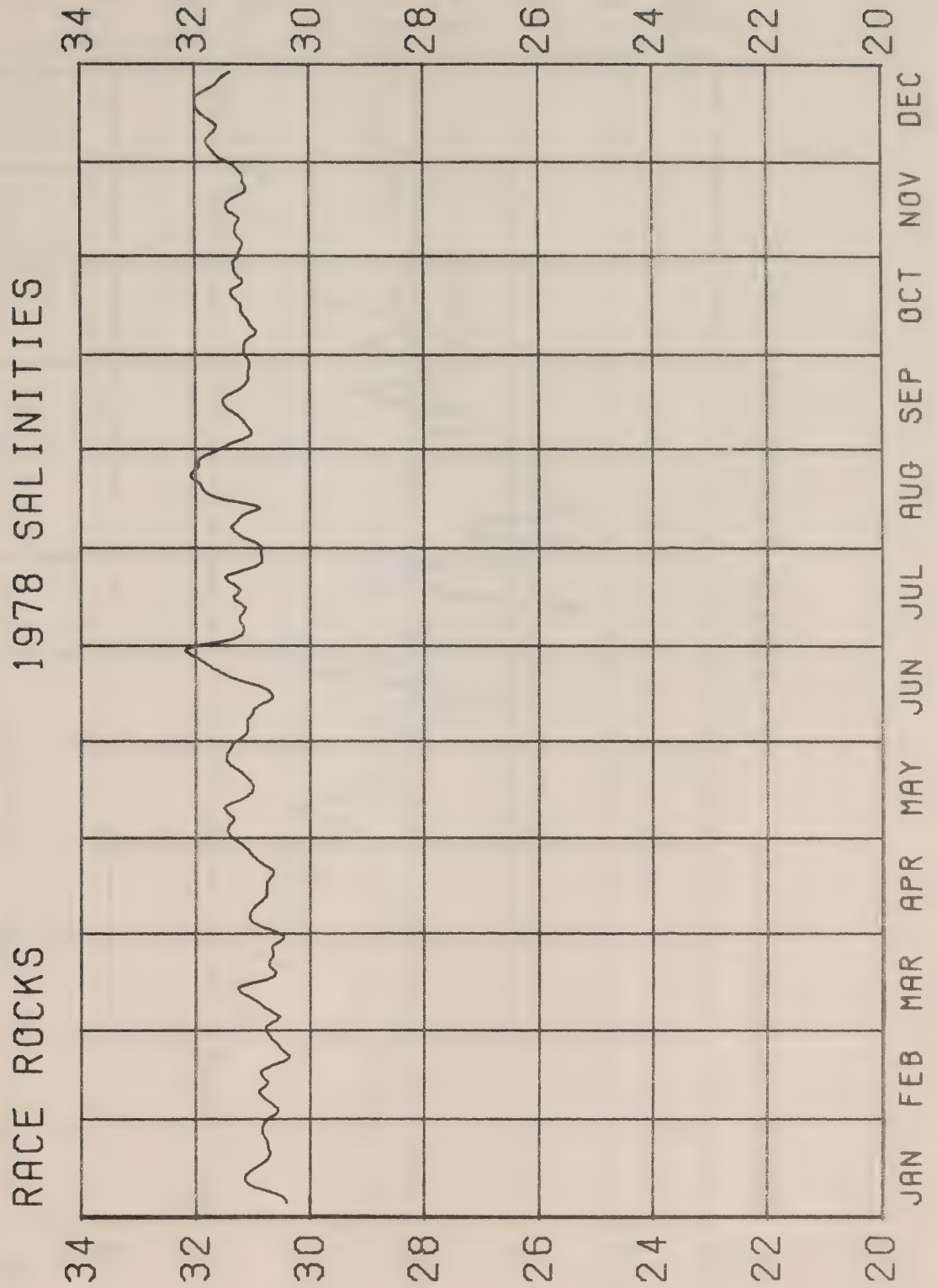




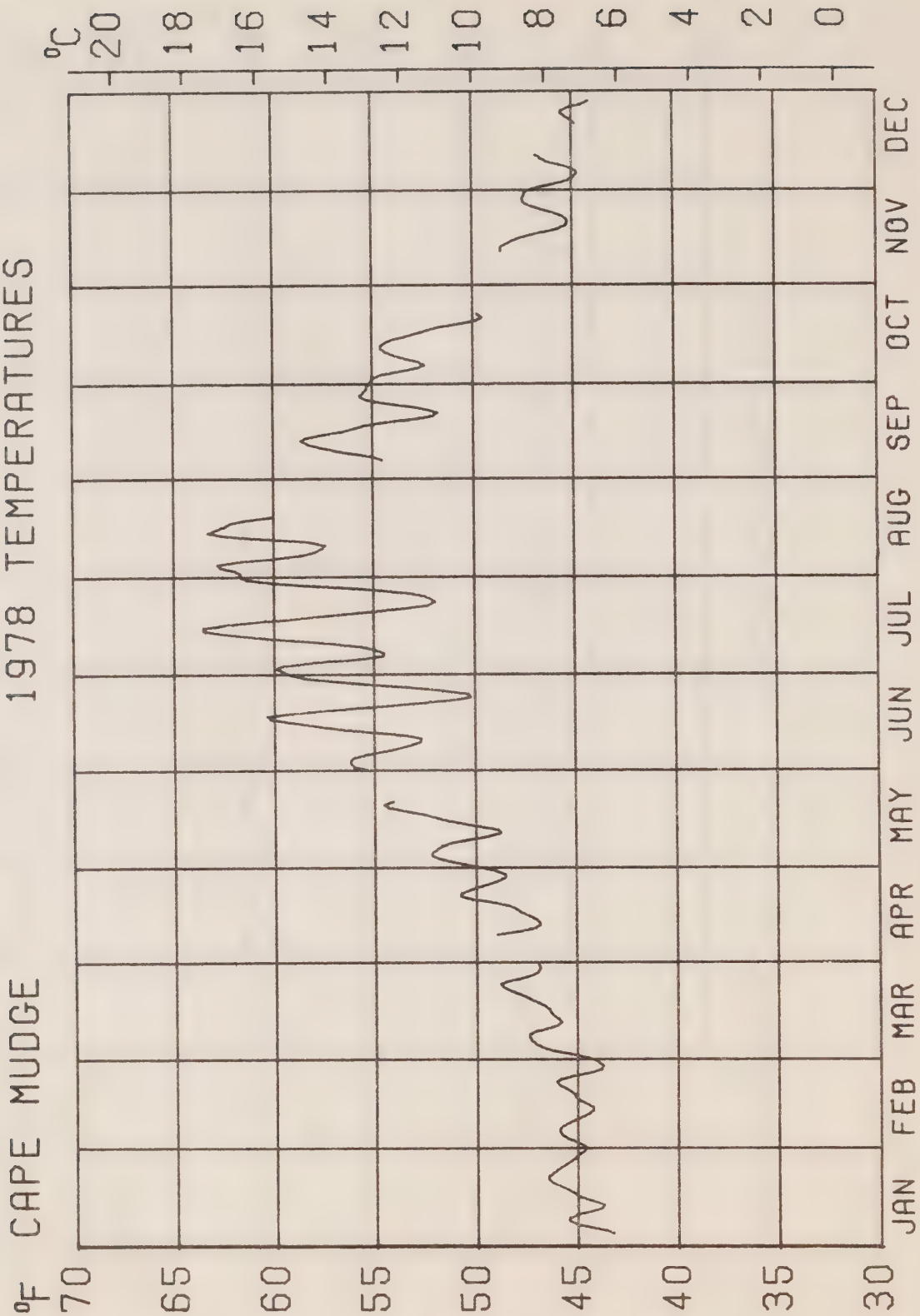
SHERINGHAM POINT 1978 TEMPERATURES

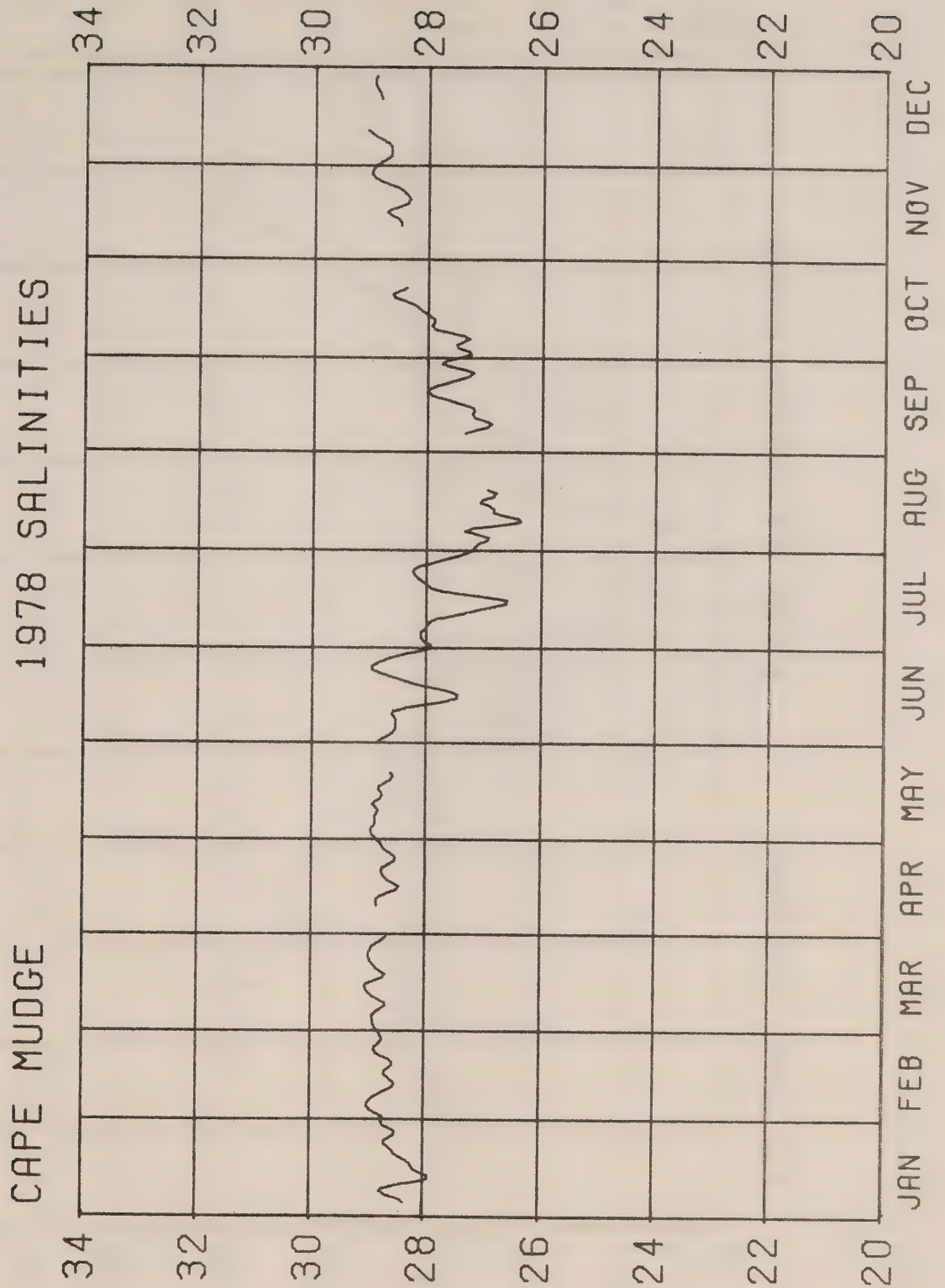


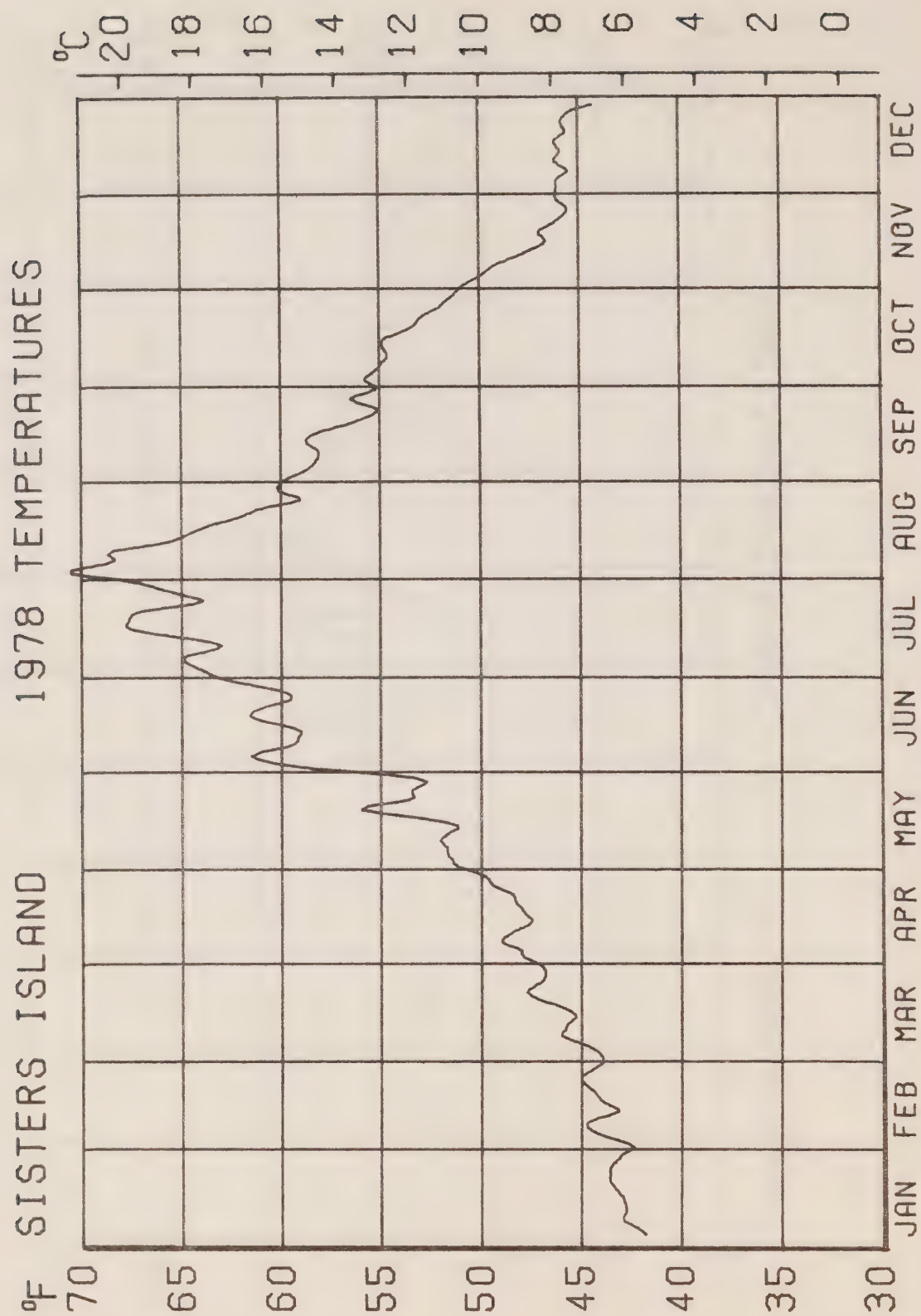




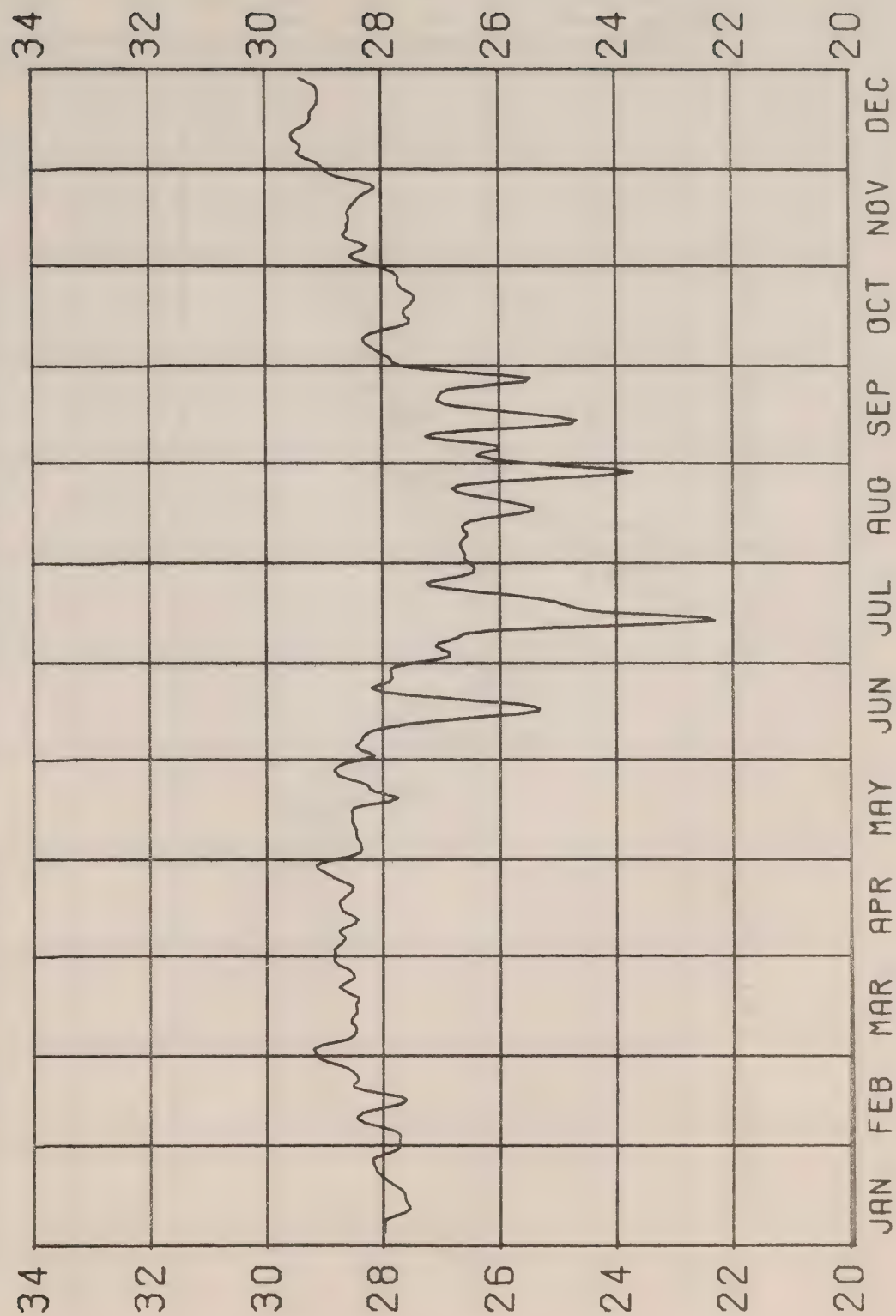
CAPE MUDGE 1978 TEMPERATURES

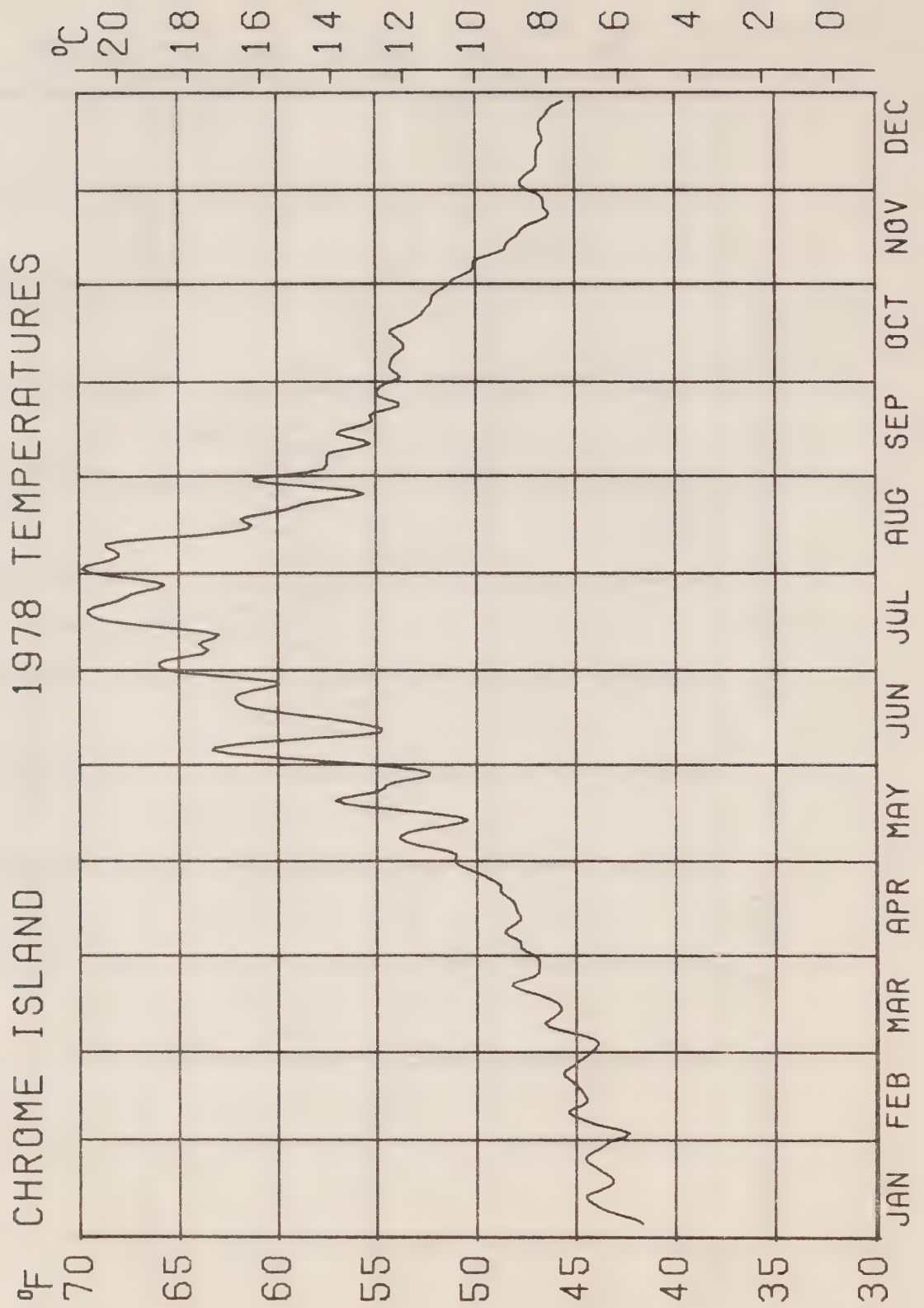




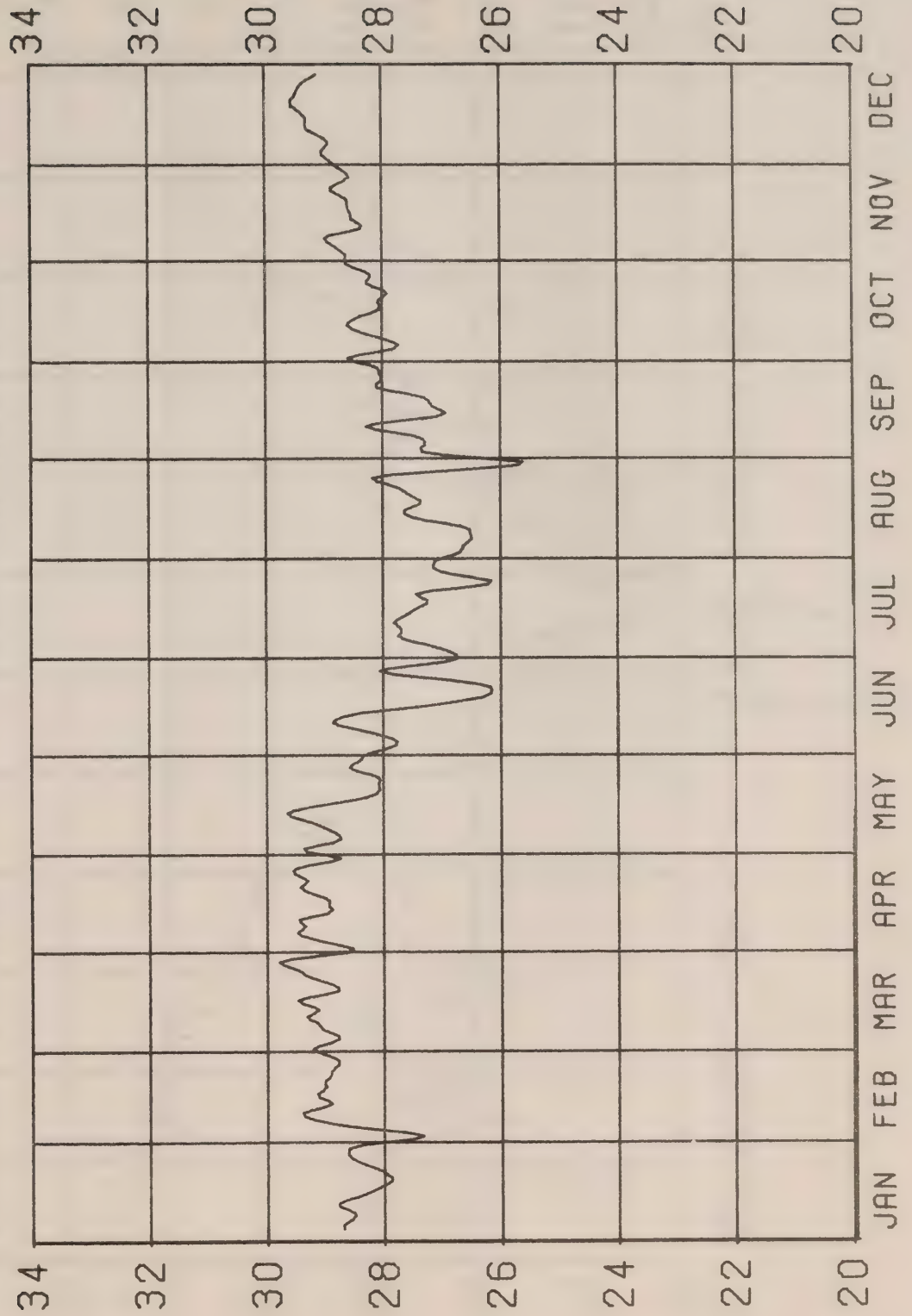


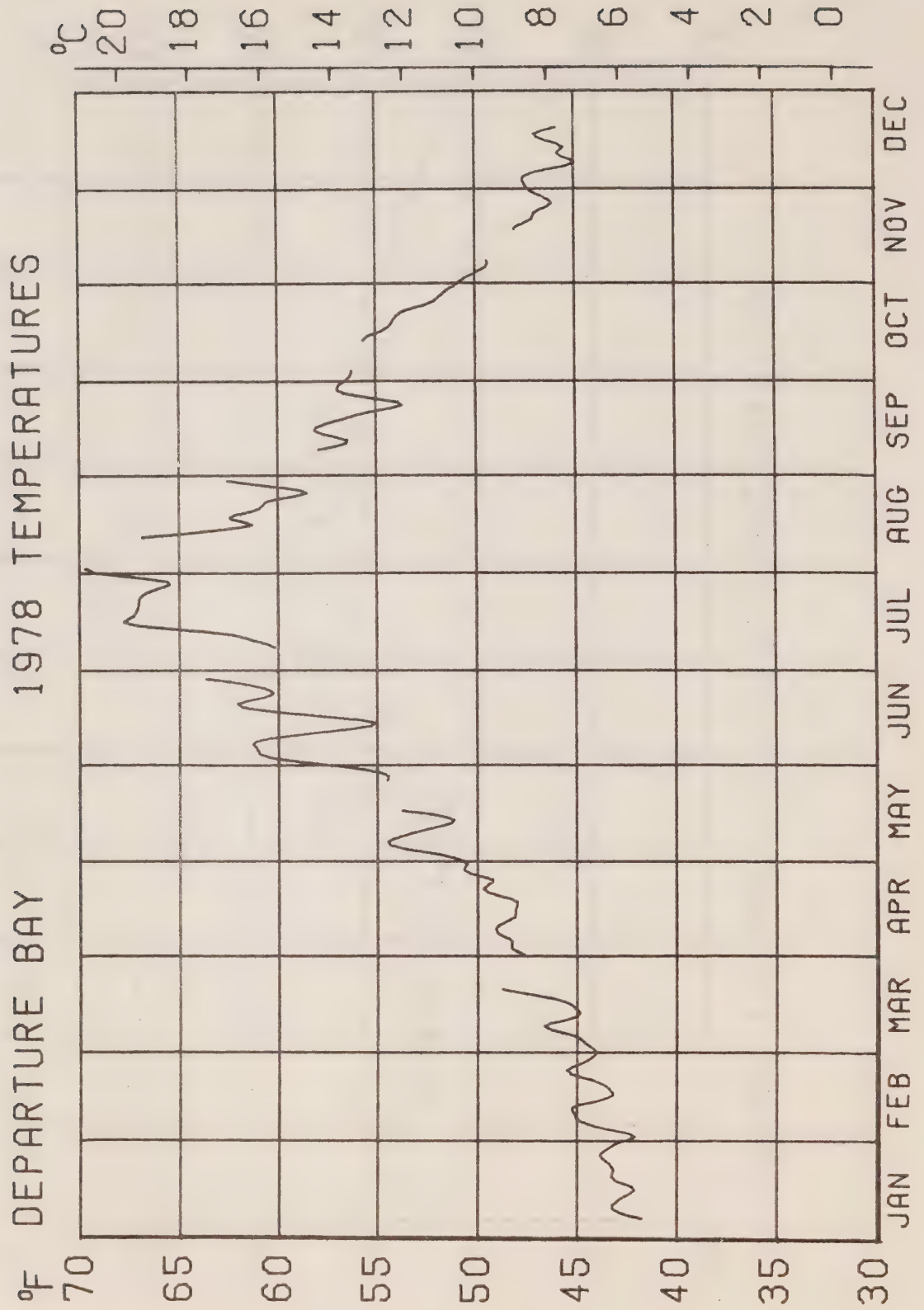
SISTERS ISLAND 1978 SALINITIES



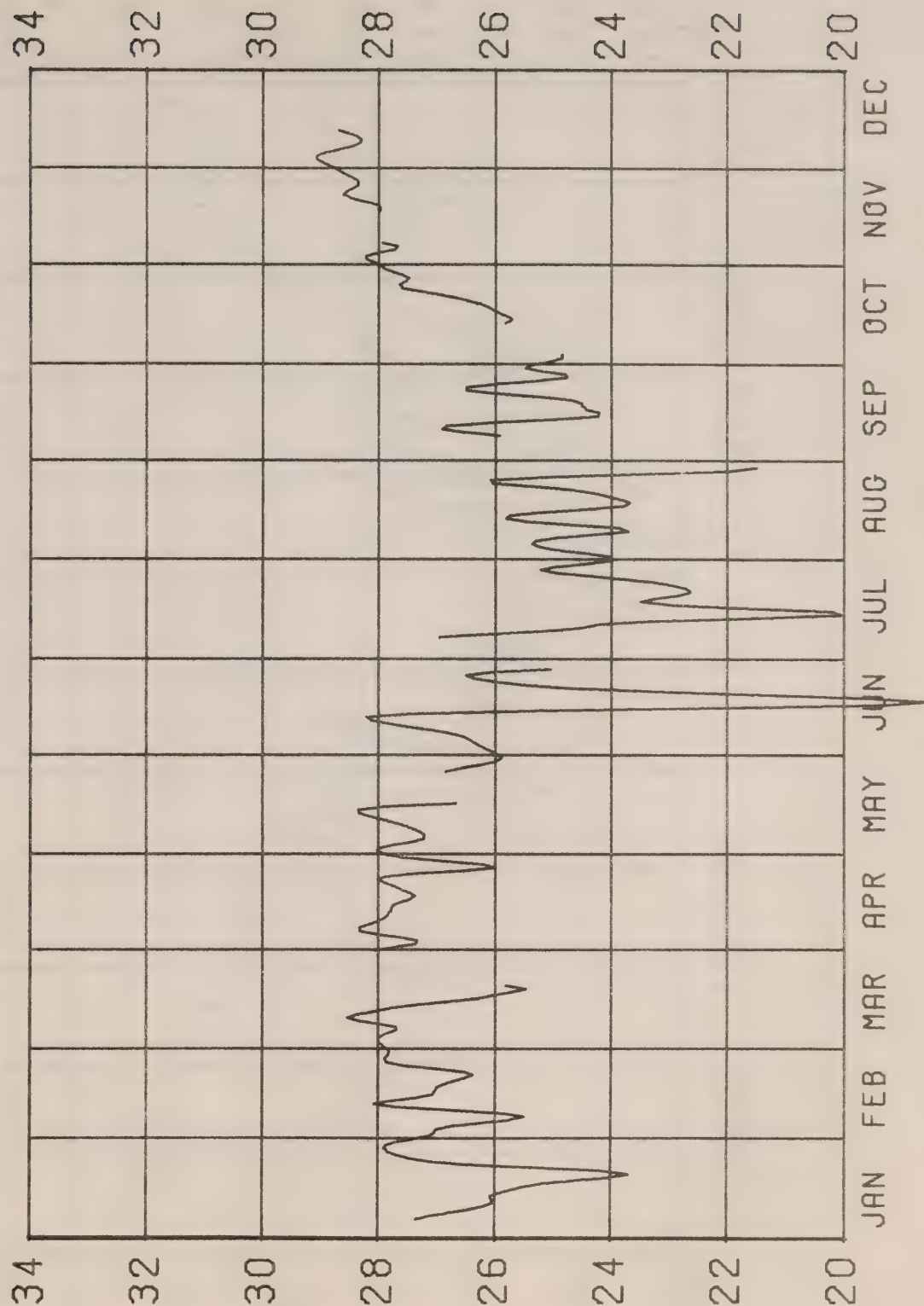


CHROME ISLAND 1978 SALINITIES

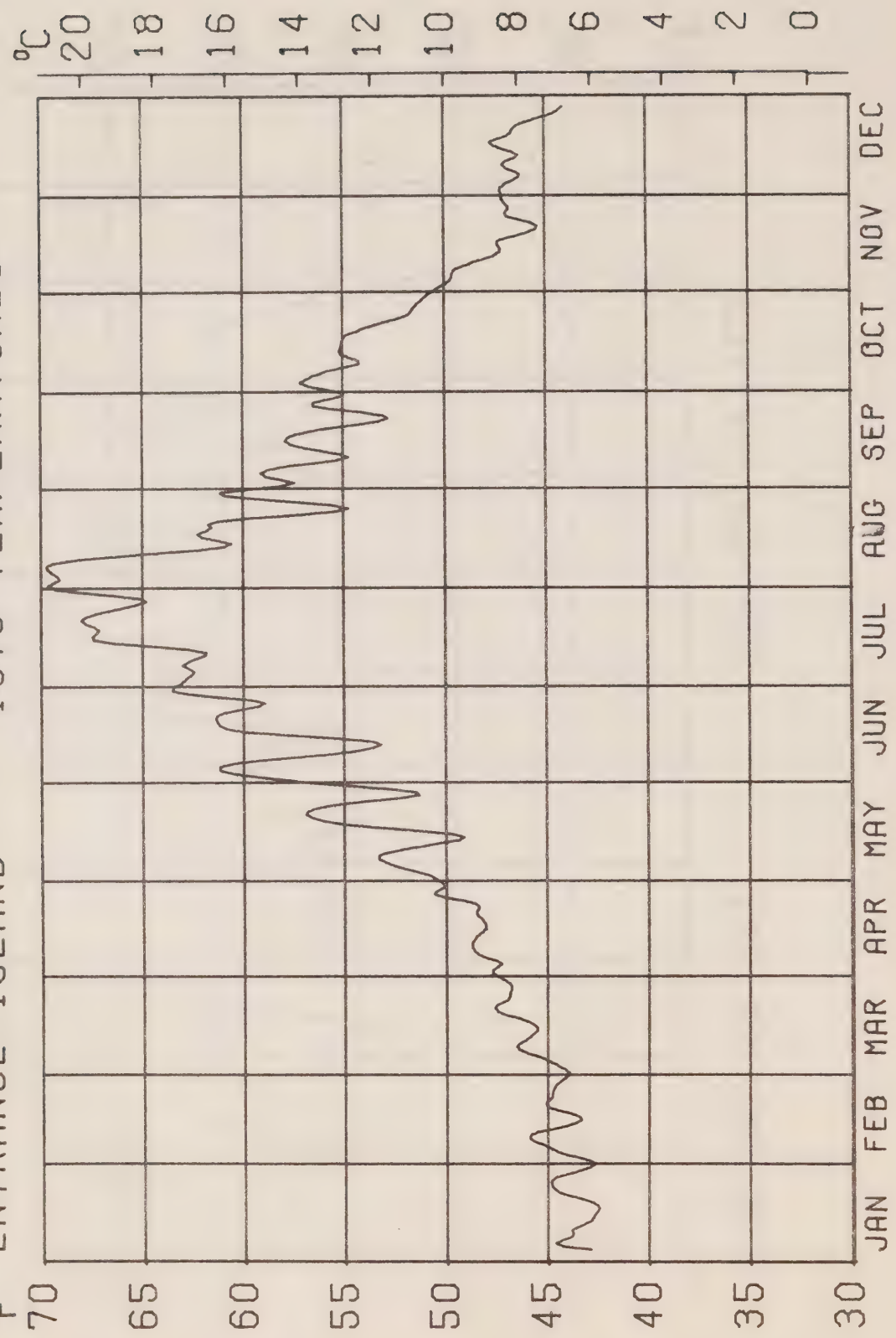




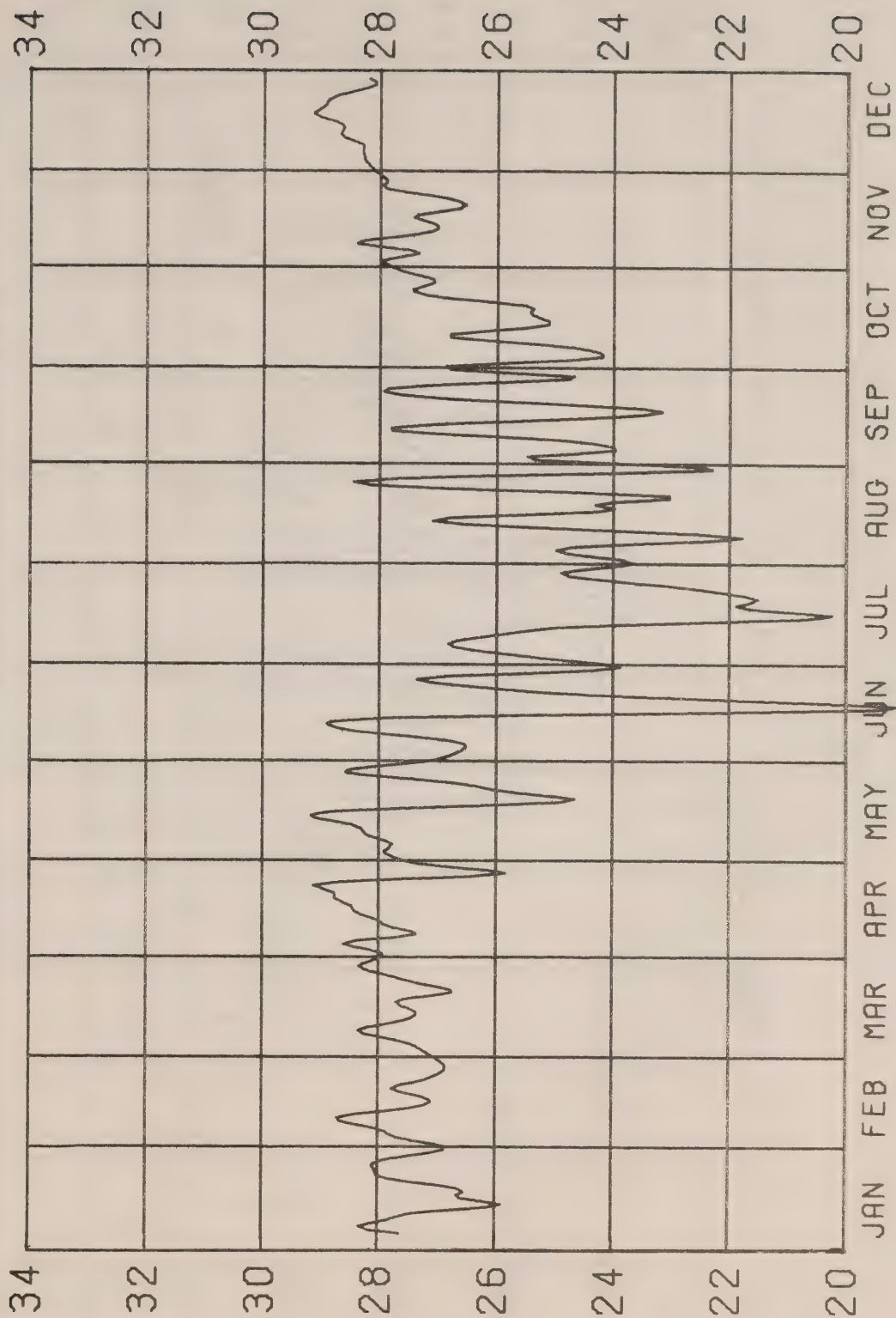
DEPARTURE BAY 1978 SALINITIES

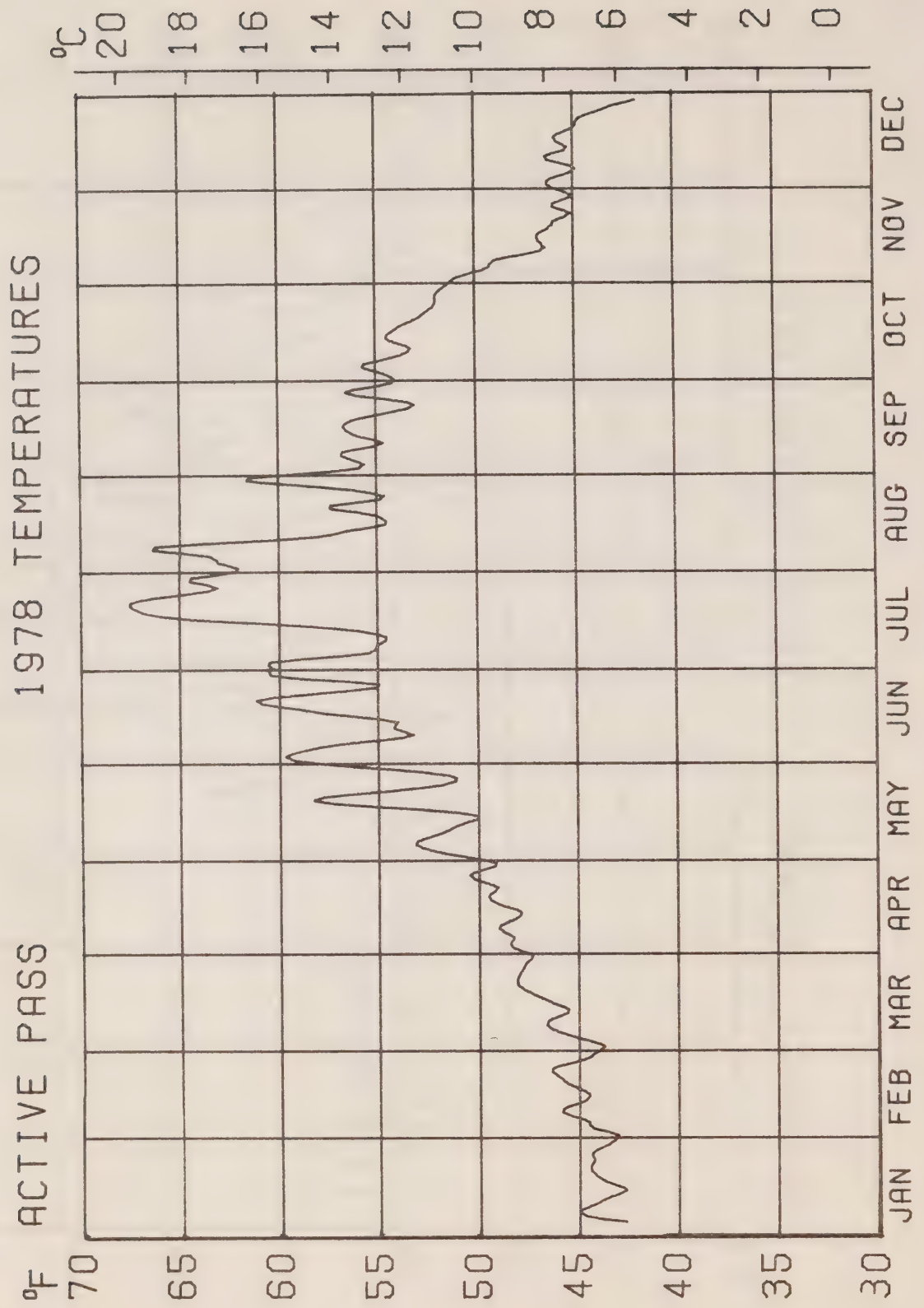


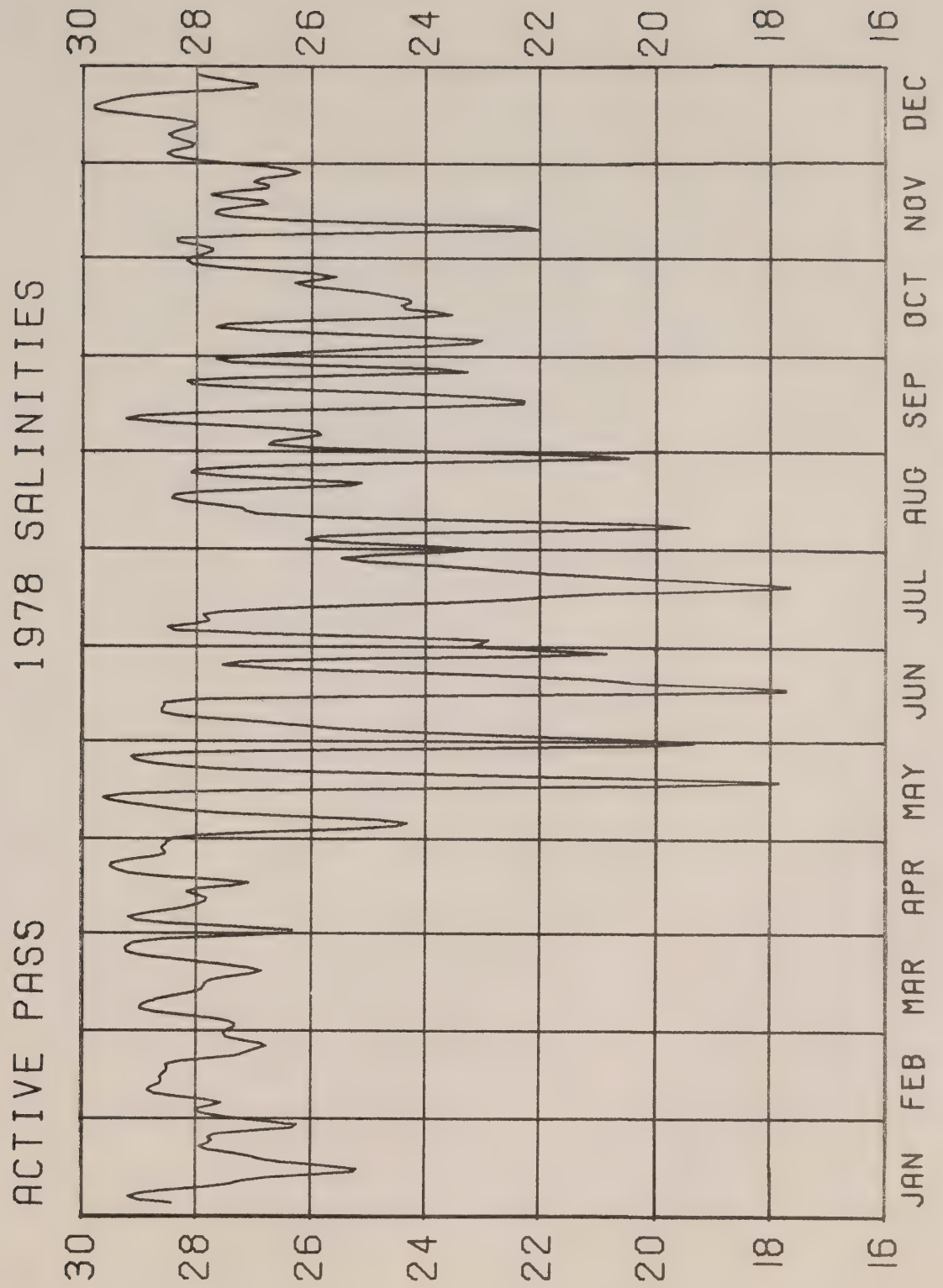
ENTRANCE ISLAND 1978 TEMPERATURES



ENTRANCE ISLAND 1978 SALINITIES







CAI
EP 321
- 80R11

FEB 11 1981

**A COMPOSITE SPECTRUM OF VERTICAL SHEAR
IN THE UPPER OCEAN FROM
THE PROFILERS EMVP, SCIMP AND CAMEL**

by

A.E. Gargett,

P.J. Hendricks, T.B. Sanford,

T.R. Osborn and A.J. Williams, III

**INSTITUTE OF OCEAN SCIENCES
Sidney, B.C.**



For additional copies or further information please write to:

Department of Fisheries and Oceans

Institute of Ocean Sciences

P.O. Box 6000

Sidney, B.C. CANADA

V8L 4B2

CAI
EP 151
- 80R11

A COMPOSITE SPECTRUM OF VERTICAL SHEAR IN THE UPPER OCEAN
FROM THE PROFILERS EMVP, SCIMP AND CAMEL

by

A.E. Gargett,
P.J. Hendricks, T.B. Sanford,
T.R. Osborn and A.J. Williams, III

Institute of Ocean Sciences
Sidney, B.C.

1980

The authors are associated with the following institutions:

A.E. Gargett	Institute of Ocean Sciences P.O. Box 6000 Sidney, B.C. V8L 4B2 Canada
P.J. Hendricks	Science Applications, Inc. NW Ste.36 - 13400B Northrup Way Bellevue, WA 98005 U.S.A.
T.B. Sanford	Applied Physics Laboratory University of Washington 1013 NE 40th St. Seattle, WA 98105 U.S.A.
T.R. Osborn	Department of Oceanography University of British Columbia 2075 Wesbrook Ave. Vancouver, B.C. V6T 1W5 Canada
A.J. Williams, III	Woods Hole Oceanographic Institution Woods Hole, MA 02543 U.S.A.

Table of Contents

	<u>Page No.</u>
1. Introduction	1
2. EMVP: Low Wavenumber Range	2
3. SCIMP: Intermediate Wavenumber Range	7
4. CAMEL: High Wavenumber Range	13
5. The Composite Spectrum	16
6. Conclusions	19
7. References	20
8. Figures 1 - 14	25-38

1. Introduction

This data report describes three shear profilers operated in close proximity to one another during FAME, the Fine and Microstructure Experiment (Sanford and Hogg, 1977). None of the profilers is individually able to measure the entire spectrum of vertical shear of horizontal velocity. Taken together, however, the three profilers cover almost the whole range of vertical scales from hundreds of metres down to centimetres. Our aim is to produce a composite shear spectrum, from energy-containing through dissipation scales; such a comprehensive measurement had not been made before FAME and has not been duplicated since. In addition, the process of matching portions of the spectrum of a geophysical variable, as measured by three completely different instrument/vehicle systems, offers a challenging cross-check on all three measurement techniques as well as subsequent data processing.

The three profilers involved, with the approximate range of vertical length scales spanned by each are EMVP (200 m - 10 m), SCIMP (25 m - 25 cm), and CAMEL (25 cm - 2 cm). Details of instruments, vehicles and calibration procedures (if necessary) have to a large extent already been documented in the published literature or readily available data reports (see references in following sections for each instrument). The main purpose of this data report is to archive detailed descriptions of the data analysis procedures used by each investigator to produce power spectral density of shear for contribution to the composite spectrum.

2. EMVP: LOW WAVENUMBER RANGE

Data Acquisition

The Electro-Magnetic Velocity Profiler senses the electric currents in the sea arising from the motion of sea water through the earth's magnetic field. The physics of motionally induced electric fields is discussed by Sanford (1971) and the EMVP has been extensively described by Sanford, Drever and Dunlap (1974, 1978). As configured for the FAME work, the instrument is shown in Fig. 1.

Motionally induced electric currents produce EMFs across the polyethylene cylinder which are sensed by electrodes beneath the insulating skin. Besides the induced voltages, the orientation, depth and fall speed of the instrument must be determined in order to compute velocity. A 12-bit digitizer is used to measure the analog signals at a rate of two scans of all signals per second with a resolution of 0.1 μ V for the electrode potential.

The potential between the two electrodes, spaced a horizontal distance L apart, and mounted at the center of the vehicle ($z = 0$) is given by Sanford, Drever and Dunlap (1978, Eq. A12) as:

$$\begin{aligned}\phi_m = & LF_z \cos\phi [(v-\bar{v})(1+C_1) + V(1+C_3)] \\ & - LF_z \sin\phi [(u-\bar{u})(1+C_1) + U(1+C_3)] \\ & + LF_H W(1+C_2) \cos\phi\end{aligned}$$

where ϕ is the angle of the electrode line measured anti-clockwise from magnetic east, F_H and F_z are the horizontal (north) and vertical components of the earth's magnetic field, u and v are the magnetic east and north water velocity components, \bar{u} and \bar{v} are depth-independent constants, U , V , and W are the velocity components of EMVP relative to the local water, and C_1 , C_2 , and C_3 are constants determined by the shape of the EMVP. The following values were generally assumed for the parameters appropriate to the open ocean site:

$$L = 36.5 \text{ cm} \pm 1\%$$

$$F_H, F_z = 0.212\Gamma, -0.48\Gamma \text{ (both } \pm 1\%)$$

$$U, V = 0, 0 \text{ (i.e. no relative velocity)}$$

$$W = \left[-\frac{1}{\rho g} \frac{dp}{dt} \right] \text{ where } p = \text{pressure and } [] \text{ denotes a linear least-square fit}$$

$$C_1, C_2, C_3 = 0.97 \pm 2\%, 0.02 \pm 100\%, -0.8 \pm 5\%$$

The terms $u-\bar{u}$ and $v-\bar{v}$ are the quantities determined from the measurements as follows:

$$u-\bar{u}_1 = \frac{A_1 \cos \psi_1}{F_z L(1+C_1)}$$

$$v-\bar{v}_1 = -\frac{A_1 \sin \psi_1}{F_z L(1+C_1)} + \frac{F_H}{F_z} W_c \frac{(1+C_2)}{c(1+C_1)}$$

where ψ_1 is the compass direction of the electric field, A_1 is the amplitude of the potential difference measured between electrode pair #1 and W_c is computed from the rate of change of pressure.

The assumption of nil relative horizontal velocity is not too severe since U and V are multiplied by 0(0.1) coefficients. It should be noted that the term involving W contributes to the $v-\bar{v}$ term. Hence errors in the determination of W influence the computed north velocity component. Since W_c is not well determined from the coarse pressure measurements, it could produce equivalent fluctuations in $v-\bar{v}$. This threat is avoided by assuming that the real fall speed is uniform ($\frac{dW}{dz} = 0$) and, hence, fluctuations to the computed W_c do not influence shear calculations. In effect let $C_2 = -1.00$, compute $u-\bar{u}$ and $v-\bar{v}$ and then compute shear.

The principal aspects of the measurements which determine method performance are:

1. The measurements of electrode potential ϕ_m
2. The values of F_H and F_z
3. The values of L , C_1 , C_2 , and C_3
4. Fluctuations of F_H and F_z at periods of order 10s.

The measurement of the electrode potential depends mostly on the gain of the amplifiers and the calibration of the digitizer. The combined uncertainties are less than 2% of full scale.

The magnetic field values are taken from a world chart which at the open ocean site, away from magnetic anomalies, are subject to less than 1% error, exclusive of temporal fluctuations.

The uncertainties of the important vehicle parameters result principally from distortions to the shape of the polyethylene skin due to temperature and pressure changes and from the approximation of the response of the vehicle to electric currents. The previously stated uncertainties for L , C_1 , C_2 , and C_3 are our best estimate of the variations to these parameters.

Temporal variations to F_H and F_z are not serious in terms of how they change the magnetic field values used in processing, but are significant sources for inducing extra, non-motionally induced electric currents. To influence shear measurement the magnetic fluctuation must be of high frequency

having periods of order 1-10 seconds. Except in certain types of magnetic storms the magnetic fluctuations have little energy at these frequencies. However, this matter should be studied more and error estimates determined.

Data Processing

The velocity values were determined from a least-square fit to 15 electric field measurements (7.5s). The resulting values were first differenced in the vertical and divided by the first difference of pressure in decibars:

$$U_{z1i} = \frac{U_{1i} - U_{1i-1}}{\Delta Z_i}$$

where $\Delta Z_i = P_{i-1} - P_i$ and similarly for U_{z2i} , V_{z1i} , and V_{z2i} .

The shear values from the two electrode pairs were averaged and the north component corrected to remove effects of fluctuations of W_c as follows:

$$U_{zi} = \frac{U_{1zi} + U_{2zi}}{2}$$

$$V_{zi} = \frac{V_{1zi} + V_{2zi}}{2} - .24 \frac{\Delta W_i}{\Delta Z_i}$$

where $\Delta W_i = W_i - W_{i-1}$ and

$$- .24 \approx \frac{F_H (1+C_2)}{F_Z (1+C_1)}$$

No correction has been made for the discrepancy between depth in metres and pressure in decibars. The error for the use of decibars rather than metres is about 1%.

For purposes of overall statistical summary, shear values between 200 and 1000 dbars were used. The vertical spacing was approximately uniform, with fluctuations of the order of $\pm 2\%$. The spectra were computed over the center 80 shear vectors (an interval of about 750 m) yielding east, north, clockwise and anti-clockwise spectral variance estimates at 40 vertical wave numbers.

Singleton's (1968) mixed radix FFT was used to provide the complex discrete Fourier transform of the complex shear as follows:

$$x_k + iy_k = \sum_{j=0}^{n-1} (u_{zj} + iv_{zj}) e^{+i2\pi jk/n} \text{ for } k = 0, \dots, n-1$$

The spectral variance estimates are computed as follows:

$$\hat{U}_k = \frac{[(x_k + x_j)^2 + (y_k - y_j)^2]}{2n^2} \text{ for } k = 1, \dots, n/2-1$$

where $j = n-k$

$$\hat{V}_k = \frac{[(y_k + y_j)^2 + (-x_k + x_j)^2]}{2n^2}$$

$$\hat{C}_k = \frac{(x_j^2 + y_j^2)}{n^2}$$

$$\hat{A}_k = \frac{(x_k^2 + y_k^2)}{n^2}$$

and the total spectral variance is defined as follows:

$$\hat{T}_k = \hat{U}_k + \hat{V}_k = \hat{C}_k + \hat{A}_k$$

Summations of these estimates were comparable in magnitude to the total variance of the original records, but slightly different since slightly different data intervals were used.

Three band averages of \hat{T}_k were printed. For $n = 80$ they are as follows:

$$\hat{B}_1 = \sum_{k=1}^{13} \hat{T}_k$$

$$\hat{B}_2 = \sum_{k=14}^{26} \hat{T}_k$$

$$\hat{B}_3 = \sum_{k=27}^{39} \hat{T}_k$$

The spectral estimates were computed by a program called QSHEAR05 and printed as variance estimates, not normalized by the frequency resolution and hence, were not of spectral density. Conversion to spectral density was done only when data was plotted for comparison with other shear measurements for publication. For the 200-1000 dbar intervals the record length was 750 m or $\Delta k = 1.33$ c/km. To normalize the band averages of the variance estimates to spectral density for plotting, we divide by $N\Delta k$ where N is the number of wave numbers in each band.

The first difference shear spectra from QSHEAR05 were not compensated for the response function of the first difference operator. An accurate estimate of shear spectra requires that the first difference spectra be corrected by the factor R , which in the present case is

$$R_k = \frac{2 \left[1 - \cos\left(\frac{\pi k}{80}\right) \right]}{\left(\frac{\pi k}{80}\right)^2} \quad k = 1, 2, \dots, 80.$$

Thus the shear spectra would be $\hat{S}_k = \hat{T}_k \cdot R_k$. For the FAME data, corrections were not made at each k , but rather were done for each band. In general, the two compensation methods are not equivalent. However, since the observed \hat{T}_k are nearly white, in this case the difference is not significant (<3%). $R^{(1)}$, $R^{(2)}$ and $R^{(3)}$ with the values of 1.02, 1.23 and 1.80 are the band averaged values of R_k for the three wave number bands: thus the corrected shear spectral estimates are

$$\hat{F}_i = R^{(i)} \hat{B}_i \quad \text{for } i = 1, 2, 3.$$

Shear spectral density estimates for the open ocean profiles are plotted in Fig. 2 for the interval 200-1000 dbar (81 velocities). There is considerable scatter among these 15 values for the earlier occupation and among the four more for the later occupation of this site. There is, however, a general trend toward slightly lower shear density at higher vertical wave numbers. The mean standard deviations for the total shear variances are 7.8 ± 1.1 and $5.2 \pm 0.9 \times 10^{-6} \text{s}^{-2}$, respectively for the two occupations.

Discussion of error

Estimates of the errors in the measurement of shear can be made based on the differences between shear measured by electrode systems 1 and 2 and on the shears found in deep water, say around a depth of 4 km. If we assume that the errors in the two shear measurements from the separate electrode systems are random and uncorrelated then the mean square value of shear difference should be twice the individual mean square error. On this basis the mean square error (error variance) for the open ocean data is $0.6 \times 10^{-6} \text{s}^{-2}$.

There is generally little dependence of the level of difference shear on depth and current strength. For example, drops 266 and 267 exhibit difference shear variances of $0.3 \pm 0.1 \times 10^{-6} \text{s}^{-2}$ each for east and north velocity components at all depths. This evidence suggests that the errors are not depth dependent.

The second error estimator, the deep water shears, yields values of $0.5 \times 10^{-6} \text{s}^{-2}$ at 4 km depth. Since we have no evidence that the errors are significantly larger in the thermocline than in the deep water, the level of mean square shear in the deep water would be at least an upper bound on the noise level.

Thus with deep shear variances of about $0.5 \times 10^{-6} \text{s}^{-2}$ and mean square shear differences of $0.6 \times 10^{-6} \text{s}^{-2}$ it seems reasonable to claim a noise level which does not exceed $0.6 \times 10^{-6} \text{s}^{-2}$. If this variance is spread equally over all wave numbers (i.e. white distribution) the shear spectral density is $1.20 \times 10^{-8} \text{s}^{-2}$. There is reason to believe that the error is not a white noise distribution. The spectrum of 4 km shear variances rises at approximately the first power of wave number, as shown in Fig. 3. For comparison, the spectral density is shown for the same drops but for the thermocline interval 300-1000 m. Taking the deep shear as the noise distribution, noise contributes very little to the measured thermocline shear levels.

3. SCIMP: INTERMEDIATE WAVENUMBER RANGE

SCIMP is a freely-sinking instrument platform with several sensor systems including a two-axis velocimeter. These sensors measure the relative velocity in two perpendicular nearly-horizontal directions using the acoustic time-of-flight principle (Middleton, 1955). In each of the two directions, simultaneous sound pulses are emitted from a pair of facing transducers and the difference in travel time on the two opposing paths is measured. This difference in travel time is assumed to be due to advection of the sound pulse by the average velocity along the acoustic path. The component of the velocity along the acoustic path is

$$\Delta u = \frac{c^2 \Delta t}{2d}$$

where c is the local average sound speed, Δt is the time difference, $d = 0.15 \text{ m}$ is the path length, and it is assumed that $\Delta u \ll c$. The sensor is inherently calibrated because of the simple geometric interpretation of the transducer characteristics, but sound speed variations are not accounted for in the system, and typical sound velocity variations of 5% can lead to an error of 10% in calculated velocity.

Velocity measurements in the intermediate wavenumber range are influenced by the interaction of the free vehicle with the horizontal flow field, and this interaction must be incorporated into the interpretation. In the highest wavenumber band where CAMEL measurements are applicable, the vehicle motion is assumed to be at much lower wavenumbers and ignored. The EMVP, on the other hand, seeks to measure low vertical wavenumber shear where the vehicle is assumed to be nearly in equilibrium with the local slowly varying component of the horizontal velocity. The velocity measurements from

SCIMP bridge these two extremes and include a vertical wavenumber range where the vehicle response to the horizontal velocity is critical to proper interpretation. The response of SCIMP to horizontal velocity has been investigated by Hendricks and Rodenbusch (1979). Three effects that describe the interaction between the platform and the horizontal velocity field have been identified and modelled. The influence of these measured velocity or shear spectra is described by the power transfer functions shown in Figure 4. The first effect is the tendency for the platform to be advected by the horizontal velocity it is attempting to measure thereby reducing the apparent velocity at the sensor. Analysis of the linearized equations of motion for a free platform shows that this is equivalent to a high-pass filter with an estimated 3dB point of 0.2 cpm for SCIMP. The power transfer function, which is the ratio of the sensed power to the power in the velocity profile, is indicated by the dashed line labeled $1-H_0^2$ in Figure 4. This function approaches unity at high wavenumber and drops off rapidly at low wavenumber (slope proportional to k^2). A second effect arises because the velocity transducers are located below the main body of the SCIMP platform as it sinks, which allows the sensors to measure the horizontal velocity before it has a chance to influence the horizontal motion of the platform. In effect, the sensors lead the center of mass in phase so that the sensed velocity is greater than if the sensors were located at the center of mass. The magnitude of this effect is surprisingly great for the 0.5 m offset between velocity sensors and center of mass for SCIMP as indicated by the solid line labeled H_{01}^2 in Figure 4. Apparent power is increased by nearly a factor of 3 at low wavenumber, there is an amplification near the point where the offset is $1/4$ wavelength, and there is oscillatory behavior in the transfer function at high wavenumber. The final effect considered by Hendricks and Rodenbusch tends to reduce the oscillations in the transfer function at high wavenumber introduced by the sensor offset. By taking into account the vertical distribution of drag force on the platform (as opposed to a point of force) the final power transfer function, indicated by H_{012}^2 in Figure 4 is calculated. In SCIMP spectra, the raw power spectra are divided by the function H_{012}^2 to correct for platform effects.

In a normal deployment, SCIMP is ballasted to sink at an average rate of 0.12 m/s. There are modulations of this rate on the order of 0.01 m/s with wavenumbers ~ 10 cycles/km that are presumably due to internal wave vertical velocities, but the velocity past the instrument must be monotonic if the drag force is to balance the monotonic, slowly changing net weight force. Two channels of horizontal velocity are sampled at 5 Hz and internally recorded on a digital cassette, corresponding to a vertical spacing of 24 mm between adjacent samples at the nominal sink rate. This places an apparent upper limit of 20 cpm on the resolvable wavenumber, but in practice the upper limit is considerably lower than this because of quantization noise. In the data processing for SCIMP shear measurements, the quantization noise is emphasized at high wavenumbers for two reasons. First, the data is recorded as velocity where the quantization noise has a flat spectrum with amplitude

$$\Delta S_q^2 = \frac{1}{12} \frac{(\delta u)^2}{B}$$

where $\delta u = 0.15$ mm/sec is the least significant bit of velocity, and $B \approx 20$ cpm is the bandwidth. Since shear, the derivative of velocity, is being calculated, the quantization noise spectrum becomes

$$k^2 S_q^2 = \frac{k^2 (\delta u)^2}{12 B}$$

which rises with a +2 power law. Furthermore, the data had been lowpass-filtered prior to digitization and the correction for this filter requires amplification of the data at high wavenumbers, including the quantization noise. The electronic filter had a half-power point at $0.21 \text{ Hz} \approx 1.7 \text{ cpm}$ with a power law slope of ω^{-2} (k^{-2}). Correction for the filter and the factor of k^2 introduced from the derivative results in a quantization noise spectrum that rises with a power law slope of k^4 at high wavenumbers. This noise dominates the measured shear spectra for SCIMP for wavenumbers above 5 cpm.

At the low wavenumber end of the measured spectrum there is a limitation imposed by the highpass filter function that is inherent to relative velocity measurements from a freely-sinking platform. Although no fundamental limitation is imposed at low wavenumber according to the analysis of Hendricks and Rodenbusch, corrections to the power spectrum by more than an order of magnitude are probably beyond the scope of the model. This places a low wavenumber limit in the vicinity of 0.03 cpm.

The major sources of uncertainty in the SCIMP velocity measurement system are the vehicle transfer function used to correct the measurements which are most significant at low wavenumber; the sound speed dependence, which may be significant for low wavenumber shear; and the quantization noise which limits the high wavenumber shear that can be sensed by the system. There is also the possibility of vehicle motion that can introduce spurious velocities at the sensors. These will be discussed below in conjunction with quantitative estimates of system noise.

Processing:

The data from SCIMP are first copied from a digital cassette to nine-track tape using a minicomputer and subsequent processing is performed on this secondary tape. Data from each velocity channel are broken into blocks of 2048 points, corresponding to approximately 50 dbar. Each block is then processed according to the following sequence:

- (a) First difference is calculated (the first difference is a good approximation to the derivative for low frequencies, but deviates significantly near the Nyquist frequency);
- (b) wild point removal; any point whose difference is more than four standard deviations from the block mean is removed;

- (c) formation of the raw single-sided power spectral density as:

$$\text{PSD} \left[\frac{\text{s}^{-2}}{\text{Hz}} \right] = \frac{2F \cdot F^*}{\Delta f}$$

where F = Fourier transform of the block

F^* = complex conjugate of F

$$\Delta f = 2.44 \times 10^{-3} \text{ Hz}$$

and the factor of 2 is necessary since the algorithm only calculates the power in the positive frequencies.

- (d) correct for first difference estimate of derivative, the ratio of power in the first difference to the first derivative is given by

$$R = \frac{2 \left[1 - \cos \left(\frac{\pi \omega}{\omega_N} \right) \right]}{\left(\frac{\pi \omega}{\omega_N} \right)^2}$$

where ω_N is the Nyquist frequency.

- (e) correct for electronic filter by multiplying the spectra by the function

$$S_e = 1 + \left(\frac{\omega}{\omega_1} \right)^2$$

where ω is the frequency of the spectral estimate and $\omega_1 = 0.21 \text{ Hz}$ is the characteristic frequency of the electronic filter. (Note that at the Nyquist frequency, this function is approximately 140.)

- (f) transform from frequency to wavenumber using the average sink rate (calculated from the pressure difference across the block);

- (g) correct for platform effects; divide the wavenumber spectrum by the function

$$H_{012}^2 = 1 + \frac{2 \frac{\sin \ell_2 k}{\ell_2 k} \left[\ell_0 k \sin \ell_1 k - \cos \ell_1 k \right] + \frac{\sin^2 \ell_2 k}{\ell_2^2 k^2}}{1 + \ell_0^2 k^2}$$

where $\ell_0 = 0.8$ m is the characteristic response length to horizontal velocity, $\ell_1 = 0.5$ m is the offset from the sensors to the center of mass, and $\ell_2 = 0.4$ m is a characteristic length for the vertical distribution of the drag force.

- (h) smooth the raw PSD by band-averaging; the number of bands in an average increases geometrically with wavenumber such that there is one average estimate per octave;
- (i) several 50 m blocks are normally averaged to form composite spectra.

Although we have calculated first-order corrections for platform interaction with the measured velocity field, there must certainly be some residual contamination that is unaccounted for. One indication of such contamination is apparent from examining the differences between the two nearly-horizontal channels of measured velocity. SCIMP is not a regularly shaped body, and one of its horizontal dimensions is much longer than the other. We find that velocity component aligned with the short axis, u , appears to have a higher background noise level than the component parallel to the long axis, v . This indicates that there is probably some residual variability in both channels or a more complicated dynamic model that takes into account asymmetries in the vehicle is required. To illustrate the difference between the two velocity channels, they have been plotted individually for two depth intervals in Figure 5. Each of the curves represents the average spectrum over 200 m and all are taken from the same SCIMP dive in the Sargasso Sea. The square symbols indicate data from the main thermocline in the depth interval 909 - 1094 dbar, while the other piece, indicated by the circular symbols, is somewhat below the thermocline at a depth of 1282 - 1465 dbar. Open symbols are used to indicate the component along the short axis of SCIMP and shaded symbols are used for the long axis component. As expected, the spectra from the main thermocline are more energetic than from the deeper water, but the figure also shows that shear in the longitudinal channel is generally less than in the transverse, except at the lowest wavenumber. The behavior at very low wavenumber should not be given much weight because of the large corrections that have been applied there and

because the low number of degrees of freedom in the estimates reduces the significance there.

Comparing the two channels of the deeper segment, the longitudinal component is lower by approximately a factor of two throughout the wavenumber range. The most plausible explanation for this difference is the difference in moments of inertia along the two axes and responses to random forcing, such as the horizontal velocity shear, and more regular forcing such as eddy shedding from the various components of SCIMP. In the more energetic region, the difference between the longitudinal and transverse components is approximately the same in magnitude except at the very low wavenumbers. Since it is expected that any noise component will add to the measured signal (although it is conceivable that the motion of the vehicle could be correlated in such a way that relative velocity would be attenuated), we have restricted subsequent analysis to the longitudinal or quieter channel, taking twice the value of shear from the v-channel as an estimate of the total shear. In addition to the obvious uncertainties introduced by this approximation, the number of degrees of freedom is effectively reduced by a factor of two.

Average Spectra:

The range of variability in the average shear spectra as measured by SCIMP during FAME is illustrated in Figure 6. The lowest curve is the same as the lowest curve in Figure 5, except that it has been doubled to account for the other component of shear. An active area in the upper layers of the Gulf Stream has been used to calculate the most energetic estimate shown. Between these extremes are three other shear spectra that appear to be typical of the upper waters of the Sargasso Sea, including the main thermocline.

There are basic characteristics that are common to all these spectra which may generally be found in shear spectra in this wavenumber band. The spectra seem to flatten above 1.0 cpm and below 0.1 cpm with a steeper slope that spans approximately a decade in power between these two levels. This break-in-slope at approximately 0.1 cpm appears to be a general feature of shear spectra from the upper ocean. The similarity in form means that regions that are energetic at low wavenumber are also energetic at the higher end of the wavenumber range considered.

At the highest wavenumber shown in Figure 6, the spectra are contaminated by quantization noise which is rising with a slope of k^{+4} at that point. The estimates do not appear to be contaminated for wavenumbers less than 5 cpm, with the possible exception of the quietest region.

4. CAMEL: HIGH WAVENUMBER RANGE

The highest wavenumber portion of the spectrum of vertical shear of horizontal velocity was sensed by an airfoil probe on CAMEL. Descriptions of the vehicle, the operating principle of the airfoil probe and the procedure used to calibrate it have appeared in the published literature Osborn (1974), Crawford and Osborn (1979): further detail is available in Osborn and Crawford (1977). Calibrations of the two probes used during FAME are present in Gargett and Osborn (1978). This report assumes that the reader is (or can become) familiar with the operation of this probe, and discusses only the treatment of the data leading to the averaged high-wavenumber spectra for use in the composite shear spectrum.

The data consist of two channels of digitized (at 200 Hz) voltages proportional to the time derivatives of mutually orthogonal horizontal velocity components: this time derivative can be converted to a vertical derivative by dividing by fall speed W , assuming the frozen field hypothesis. Sampled voltages V_i are related to shear $\partial u_i / \partial z$ by the formula:

$$\frac{\partial u_i}{\partial z} = \frac{C_i}{\rho S_i W^2} V_i = G_i V_i, \quad i = 1, 2 \quad (1)$$

where C_i is a dimensionless circuit constant, S_i is a channel calibration factor (volts/(g/cm s²)), ρ is water density (taken as 1.0 g/cm³) and W is fall speed (cm s⁻¹). One factor of W enters the above expression through conversion of the time derivative to a space derivative; the second factor of W is inherent to probe operation, see Crawford and Osborn (1979).

The wavenumber range of the shear measurement is limited at high wavenumbers by the physical size of the probe (diameter 4.7 mm), which causes averaging over smaller scales. High frequency response is presently unknown, but is not thought to be limiting compared to the spatial averaging. An attempt is presently underway to determine the high wavenumber response function by comparison with results from a hot-film anemometer in a high Reynolds number geophysical flow (Gargett, 1980). Low frequency (wavenumber) output is limited by a high-pass filter with 3 dbar point at 1 Hz, which is included in the shear circuitry to remove spurious low-frequency probe output due to finestructure temperature gradients (Osborn and Crawford 1977).

Contributions to absolute error in the shear measurements, as discussed by Gargett and Osborn (1979), arise due to uncertainty in C_i ($\pm 5\%$), error in S_i due to calibration error and/or probe non-linearity ($\pm 10\%$ maximum) and error in W due to bit size in digitization of the pressure record ($\pm 5\%$): since W appears squared in the gain factor of (1), this last source of error is as serious as the sensitivity error. With the worst case assumption of independent errors, absolute error in spectral level (proportional to

$\left(\frac{\partial u}{\partial z}\right)^2$) may thus be $\pm 50\%$.

Processing:

Data from a single channel are divided into 1024 point blocks, each representing approximately 2.5 dbar of vertical distance. Each individual block undergoes the following sequence:

- a) removal of block mean
- b) 10% cosine taper to eliminate any end-point discontinuity
- c) formation of the raw single-sided power spectral density as

$$\text{PSD} \left[\frac{\text{s}^{-2}}{\text{Hz}} \right] = (G_i)^2 \frac{2F \cdot F^*}{\Delta f} \quad (2)$$

where F = Fourier transform of the block

F^* = complex conjugate of F

$$\Delta f = \frac{200}{1024} = 0.195 \text{ Hz}$$

G_i = channel gain factor (eqn. (1)). The factor of 2 is included because calculations were performed on a Hewlett-Packard Fourier Analyser, which stores only one side of the (symmetric) transform. We have checked that integration of the PSD formed by (2) yields the mean square variance of the original signal (to 1% for our processing).

- d) the raw PSD estimates are smoothed by band-averaging over 4 points, yielding a frequency resolution of $4 \Delta f \approx 0.78 \text{ Hz}$.
- e) the PSD is multiplied by 1.052 to correct for loss of variance due to the 10% cosine window of stage (b) above.

Finally, spectra for all blocks within a desired depth interval are averaged, eliminating occasional blocks of bad data; for example, spikes due to CAMEL'S stretched-pin pressure release (Osborn and Crawford, 1977). The 200-dbar intervals chosen for the composite generally include 90-110 blocks, depending upon fall speed.

Variables are converted to wavenumber space by multiplying PSD (s^{-2}/Hz) and dividing frequency (Hz) by the mean fall speed \bar{W} over the entire 200-dbar interval, a procedure which assumes the frozen field hypothesis and a constant fall speed (for depths greater than $\sim 100 \text{ m}$, CAMEL falls at a speed in the range of $\bar{W} = 40 - 50 \text{ cm s}^{-1}$, with fall speed for a single drop constant to $\pm 4 \text{ cm s}^{-1}$). For comparison with EMVP and SCIMP, we should plot $\text{PSD}(S_1) + \text{PSD}(S_2)$ where S_1 and S_2 are the mutually orthogonal components of the vertical shear of horizontal velocity: instead, we plot $2 \cdot \text{PSD}(S_1)$, because the first shear channel is routinely available while the second channel is occasionally subject to data loss from some unidentified broad band noise. When both channels are operating, individual (2.5 dbar) shear estimates from the two channels are highly correlated, as seen in Figure 7. Thus substitution

of $2 \cdot \text{PSD}(S_1) = \text{PSD}(S_1) + \text{PSD}(S_2)$ seems justified, and greatly increases the data base available for comparisons.

Average Spectra:

Figure 8 illustrates the range of 200-dbar averaged spectra encountered during FAME, plotted against the fundamental frequency variable, a procedure which makes clear the relationship of the spectra to the "noise" spectra N_3 and N_8 , defined as the lowest spectral levels obtained during operation of the two probes (3 and 8) used during the experiment. The noise spectra differ, with N_3 lying consistently above N_8 at both low and high wavenumbers. For the purpose of the composite shear spectrum, we remove the appropriate noise spectrum from the 200-dbar average spectrum, a procedure justified by the fact that noise spectra measured for the same probe at different times are relatively constant, as can be seen in Figure 9.

As is obvious from Figure 8, the removal of a noise level affects the resulting spectra most at high wavenumbers where all the measured spectra eventually fall to meet the rising noise level. In the spectral mid-range which contributes the significant part of the shear variance (see following presentation of variance-preserving shear spectra), maximum corrections due to noise removal range from 30% to less than 1% respectively from the lowest (+) and the highest (o) averaged spectra shown in Figure 8. Noise corrected spectra are plotted in Figure 10 as a function of wavenumber, terminating with the largest wavenumber at which the measured spectral level exceeds the noise level by more than a factor of 2.

In assessing the reliability of the spectra shown in Figure 10 for purposes of the shear composite, we are most concerned with the lowest wavenumber estimates, since it is here that the CAMEL spectra must be matched to the intermediate wavenumber band. Unfortunately, it is in this range that the CAMEL results are most uncertain, due to possible contamination by low-frequency signals produced as the probe crosses large vertical temperature gradients of finestructure scale (Osborn and Crawford, 1977). These effects have been mostly eliminated from the recorded shear signal by a high-pass filter with 3 db point at 1 Hz, but the filter of course also rolls off the true shear signal in this range. Recovery of the true shear level at low frequency/wavenumber does not result from simply correcting for filter roll-off (plotted below the noise spectra in Figure 9), since such a correction builds back in the unknown temperature contamination. Removal of a noise spectrum does not leave true shear at low frequencies either, because regions with high levels of dissipation-scale shear are also regions of larger temperature finestructure levels (Gargett and Osborn, 1980). Since we do not know what fraction of the variance to restore, the shear spectra are not corrected for the high-pass filter response. Thus the lowest four spectral estimates in Figure 10 are connected by dashed lines, to indicate the range over which the degree of balance between spectra overestimation due to low-frequency temperature contamination and spectral underestimation due to high-pass filter roll-off is not known. For higher frequencies/wavenumbers, the filter correction is small (Figure 9), temperature contamination is not observed, and spectral values should be correct within the absolute accuracy of the measurement.

It should be noted that the uncertainty in the low wavenumber values of the CAMEL spectra, while unfortunate for the present purpose of a composite shear spectrum, is not significant for the primary purpose of the high wavenumber measurements, namely the direct measurement of two major components of the dissipation tensor and subsequent estimation of turbulent kinetic energy dissipation rate ϵ , assuming dissipation-scale isotropy. This is evident when the shear spectra of Figure 10 are re-plotted in the variance-preserving form shown in Figure 11. For the highest level spectrum (C13), the dashed line shows the maximum correction which would be necessary if all the variance removed by the high-pass filter had been due to shear alone: the associated change in the area under the dissipation curve is small.

5. THE COMPOSITE SPECTRUM

Although each profiler was deployed many times during FAME, the number of nearly simultaneous drops of all three profilers is very small. Instrument failures seldom occurred simultaneously, so there are more than the normal number of instrumental problems in the composite data set. In addition, the maximum depth of CAMEL measurements was 800 m, EMVP spectra were not always available averaged over the correct depth interval, SCIMP had three different fall speeds (of which only the intermediate speed provided data suitable for the dropped spectrum) and operated over a flexible depth interval which frequently did not include the upper 800 m. The records presented in Figures 12 and 13 are chosen from those available from at least two of the three instruments, with only Records 1 and 6 having all three profilers operating. Record 5, from an isolated SCIMP profile, is included to further demonstrate the constancy of slope in the intermediate wavenumber range. Profile numbers for the individual instruments and depth intervals over which spectra were calculated are shown in the table which forms part of each figure. The profilers were normally launched in a group at the same location, within 10-20 minutes of one another. An exception in the records presented here is Record 1, in which EMVP and CAMEL were launched simultaneously, while SCIMP was launched two hours before, approximately 2 km away. In view of the "universal" spectral levels which apparently are characteristic of the wavenumber ranges measured by SCIMP and EMVP (see discussion of composite spectrum below), these separations are probably inconsequential. The EMVP spectrum of Record 4 is an average of four profiles over a 24-hour period including SCIMP 16.

The data presented in Figures 12 and 13 range over the entire geographic area sampled during FAME. Record 1 ($32^{\circ}11'N$, $64^{\circ}42'W$) is from a location ~ 12 km south of Bermuda, just outside the 1000 fm (~ 1800 m) depth contour. Record 2 ($32^{\circ}58'N$, $64^{\circ}22'W$) is from a deep water site approximately 75 km to the northwest of Bermuda, while Records 3 and 4 were taken at $35^{\circ}00'N$, $66^{\circ}30'W$, a site in the Sargasso within the eddy active re-circulation region of the Gulf Stream. Record 5 ($32^{\circ}16'N$, $65^{\circ}06'W$) comes from a location inside the 1000 fm contour to the west of Bermuda. At the time of the FAME measurements, this area was one of strong eddy flow parallel to the depth contours about the island, while the area to the south of Bermuda (where Record 1 was taken) was characterized by much weaker large-scale flow (Hogg, Katz and Sanford, 1978). Record 6 ($38^{\circ}15'N$, $69^{\circ}07'W$) is from a site within the Gulf Stream system, probably slightly north of the transport maximum (Gargett and

Osborn, 1980). Record 7 is a WKB re-scaling of Record 4, which is significantly deeper than all the other records, hence characterized by a lower average Väisälä frequency. Shear spectral values and wavenumbers are adjusted by multiplying by $(N_0/N)^2$ and (N_0/N) respectively, where $N_0 \approx 2.3$ cph and $N \approx 1.4$ cph are averaged Väisälä periods for the shallow records ($200 \text{ m} < z < 1000 \text{ m}$) and deep record ($1300 \text{ m} < z < 1500 \text{ m}$) respectively. N_0 was determined as an average of 22 values (each calculated over 50 m vertical separation) from the appropriate depth intervals of SCIMP 11 and 13, while N is an average of 9 values (each calculated over 100 m vertical separation) from three CTD casts taken during the same 24-hour long period as the EMVP casts of Record 4. The depth interval covered by the profiles includes the 18° water of the Sargasso, the main thermocline, and the upper few hundred metres of the more weakly stratified water beneath the main thermocline.

To avoid excessive confusion, the spectra have been divided between two figures. Figure 12 contains spectra believed to be characteristic of deep-water sites far from boundaries: we feel that Record 1 is effectively a mid-ocean site, since the results of FAME work near Bermuda (Hogg, et al, 1978; Gregg and Sanford, 1979; Gargett and Osborn, 1980) all suggest that effects of the island occur very close to the island and then only in very localized regions where the island interacts with the eddy flow around it to produce higher levels of turbulent kinetic energy dissipation and associated microstructure. Figure 13 presents a record from one of these localized active regions, as well as a record from another boundary regime, the northern edge of the Gulf Stream.

Spectral values are plotted using a solid symbol for the highest wavenumber portion (CAMEL) and enclosing this symbol in respectively one and two larger open symbols for the intermediate (SCIMP) and low (EMVP) wavenumber portions. Error bars (shown only on Figure 12) are 95% confidence limits calculated from the number of raw spectral values averaged to produce the neighbouring spectral estimates: worst-case limits are shown, calculated for the data record with the smallest number of degrees of freedom. Confidence limits are uniform over EMVP spectral estimates, and decrease with increasing wavenumber over the SCIMP range due to the geometrical averaging employed. Confidence limits for CAMEL spectral values are less straightforward. As described in Section 4, spectral values for each 2.5 dbar block are averaged over four raw estimates, while subsequent averaging is over the number $N \approx 90$ -100 of blocks in a required 200 dbar interval. Confidence limits calculated as if each of these blocks were an additional degree of freedom are smaller than the plotted symbols. However, since a varying number of blocks are at the noise level of the system, it seems more appropriate to use M = number of blocks with signal above noise level as the number of additional degrees of freedom involved in block-averaging. The error bar shown on the CAMEL spectrum in Figure 12 is calculated with $M = 20$ for this particular record, and represents a worst-case error: since higher spectral levels are associated with a larger proportion of the interval above noise level (Gargett and Osborn, 1980), all other CAMEL spectra shown in Figures 12 and 13 have a larger number of degrees of freedom and smaller confidence limits.

Figures 12 and 13 show that spectra from EMVP and SCIMP match within their respective 95% confidence limits in the overlap range around $k = 0.04$ cpm, corresponding to vertical wavelengths of roughly 25 m. The degree of overlap between SCIMP and CAMEL spectra is more variable, but consistent with

our expectations of instrument performance. The high wavenumber range of SCIMP spectra show level changes which correspond to those of the CAMEL spectra; for example the difference between the 200-400 m range of Record 1 (Figure 12) and the Gulf Stream spectrum, Record 6 (Figure 13). However, at their highest wavenumbers the SCIMP spectra may lie considerably below the CAMEL spectra; for example, the 400-600 m range of Record 1 and the Gulf Stream, Record 6. This discrepancy is probably due to a combination of instrument limitations. First, the lowest two or three wavenumber estimates are the least reliable part of the CAMEL spectrum, due to an unknown contribution from temperature effects, as discussed in Section 4. Secondly, the SCIMP spectra cannot be simply interpreted as a vertical shear spectrum for those scales at which the velocity field becomes three-dimensional, i.e. produces velocity fluctuations along the transmission path of the acoustic current meter, which may partially cancel travel-time variations due to velocity fluctuations normal to the path. Thus the fact that a SCIMP spectrum falls significantly below an associated CAMEL spectrum at the scale $2L = 30$ cm (where L is the transmission path length of the acoustic current meters on SCIMP) may be taken as indirect evidence of the three-dimensional nature of the shear field at this and smaller scales. On this basis, the 400-600 m portion of Record 1 and the Gulf Stream Record 6 both show evidence of three-dimensional structure in the shear field on scales smaller than 30 cm. The much closer match in levels for the 200-400 m portion of Record 1 suggests that here the shear field was not three-dimensional at a vertical scale of 30 cm.

On the basis of these measurements (and the much larger base of non-simultaneous data from the three profilers) we suggest the form shown in Figure 14 for ϕ_s , the spectrum of vertical shear of horizontal velocity as a function of vertical wavenumber k , over a wavenumber range corresponding to vertical scales of 100 m to 1 cm. Over the range 10^{-2} cpm $< k < 10^{-1}$ cpm ($100 \text{ m} < \lambda < 10 \text{ m}$), there is no statistically significant wavenumber dependence; $\phi_s \approx (1-3) \times 10^{-4} \text{ s}^{-2}/\text{cpm}$ for $N \approx 2.3$ cph. Over the range 10^{-1} cpm $< k < 1$ cpm ($10 \text{ m} < \lambda < 1 \text{ m}$), ϕ_s falls roughly as k^{-1} to a value of $(1-3) \times 10^{-5} \text{ s}^{-2}/\text{cpm}$: the vertical wavelength at which the break-in-slope occurs between k^0 and k^{-1} regimes can range from ~ 20 m to ~ 5 m, depending upon whether the exponent of k in the latter regime is taken as respectively slightly less or greater than 1. Both these lower and intermediate wavenumber ranges appear to be "universal" in the sense of scaling with local Väisälä frequency N according to the linear theory of internal wave motions in a slowly varying medium. At a vertical scale between 1 m and 0.5 m, the observed spectra rise in a dissipation range, falling again at wavelengths between ~ 5 -10 cm. This highest wavenumber region does not follow internal wave scaling: for example, high wavenumber spectral levels of Records 1 and 5 differ by a factor of 10, while the low and intermediate wavenumber ranges remain effectively constant ($2.2 \text{ cph} < N < 2.6 \text{ cph}$ for these records). The level of the dissipation range of the velocity shear spectrum cannot be predicted from the shear level in the lowest wavenumber band, consistent with the notion of an internal wave spectrum which maintains its universal nature by rapidly passing energy to highly dissipative small scales whenever an energy excess occurs.

6. CONCLUSIONS:

Using nearly simultaneous profiles from three different instruments, we have produced a composite spectrum of the vertical shear of horizontal velocity from scales of 100 m to 1 cm. The agreement between spectra from different instruments in their overlap range is generally well within the statistical confidence limits: small systematic differences are readily understood in terms of responses of individual instruments and/or processing techniques. We feel that this constitutes a fairly stringent test of the three instruments involved.

7. REFERENCES

- Crawford, W.R. and T.R. Osborn, 1979: Microstructure measurements in the Atlantic Equatorial Undercurrent during GATE, Deep-Sea Res., GATE Suppl. to Vol. 26, 285-308.
- Gargett, A.E., 1980: Turbulence measurements through a train of breaking internal waves in Knight Inlet, B.C. Fjord Oceanography, ed. J.H. Freeland, D.M. Farmer and C.D. Levings. Plenum Publishing Corp., N.Y., 277-281.
- Gargett, A.E. and T.R. Osborn, 1978: Dissipation measurements from the Fine and Microstructure Experiment. University of British Columbia, Vancouver, B.C., Institute of Oceanography, Man. Report No. 33, 87 pp.
- Gargett, A.E. and T.R. Osborn, 1980: Small scale shear measurements during the Fine and Microstructure Experiment (FAME). J. Geophys. Res., in press.
- Garrett, C. and W. Munk, 1975: Space-time scales of internal waves: a progress report. J. Geophys. Res., 80, 291-297.
- Gregg, M.C. and T.B. Sanford, 1979: Signatures of mixing from the Bermuda Slope, the Sargasso Sea and the Gulf Stream. J. Phys. Oceanogr., 10, 105-127.
- Hendricks, P.J. and G. Rodenbusch, 1979: Interpretation of velocity measurements from a freely sinking platform. Submitted to Deep-Sea Res.
- Hogg, N.G., E.J. Katz and T.B. Sanford, 1978: Eddies, islands and mixing, J. Geophys. Res., 83, 2921-2938.
- Middleton, F., (1955) An ultrasonic current meter for estuarine research, J. Mar. Res., 14 (2), 176-186.
- Osborn, T.R., 1974: Vertical profiling of velocity microstructure. J. Phys. Oceanogr., 4, 109-115.
- Osborn, T.R. and W.R. Crawford, 1977: Turbulent velocity measurements with an airfoil probe. University of British Columbia, Vancouver, B.C., Institute of Oceanography, Man. Report No. 31, 39 pp.
- Sanford, Thomas B., 1971: Motionally induced electric and magnetic fields in the sea. J. Geophys. Res., 76 (15), 3476-3492.
- Sanford, Thomas B., Robert G. Drever and John H. Dunlap, 1974: The design and performance of a free-fall electro-magnetic velocity profiler. Woods Hole Oceanographic Institution, Ref. No. 74-76, 123 pp.

Sanford, Thomas B., Robert G. Drever and John H. Dunlap, 1978: A velocity profiler based on the principles of geomagnetic induction. Deep-Sea Res., 25, 183-210.

Sanford, T.B. and N. Hogg, 1977: The North Atlantic Fine and Micro-structure Cruise Knorr 52 and Eastward 75-12. Woods Hole Oceanographic Institution, Ref. 77-11 (unpublished manuscript), 88 pp.

Singleton, R.C., 1968: An algorithm for computing the mixed radix fast Fourier transform. Mathematical and Statistics Division, Stanford Research Institute, November 1978, 25 pp.

FIGURES

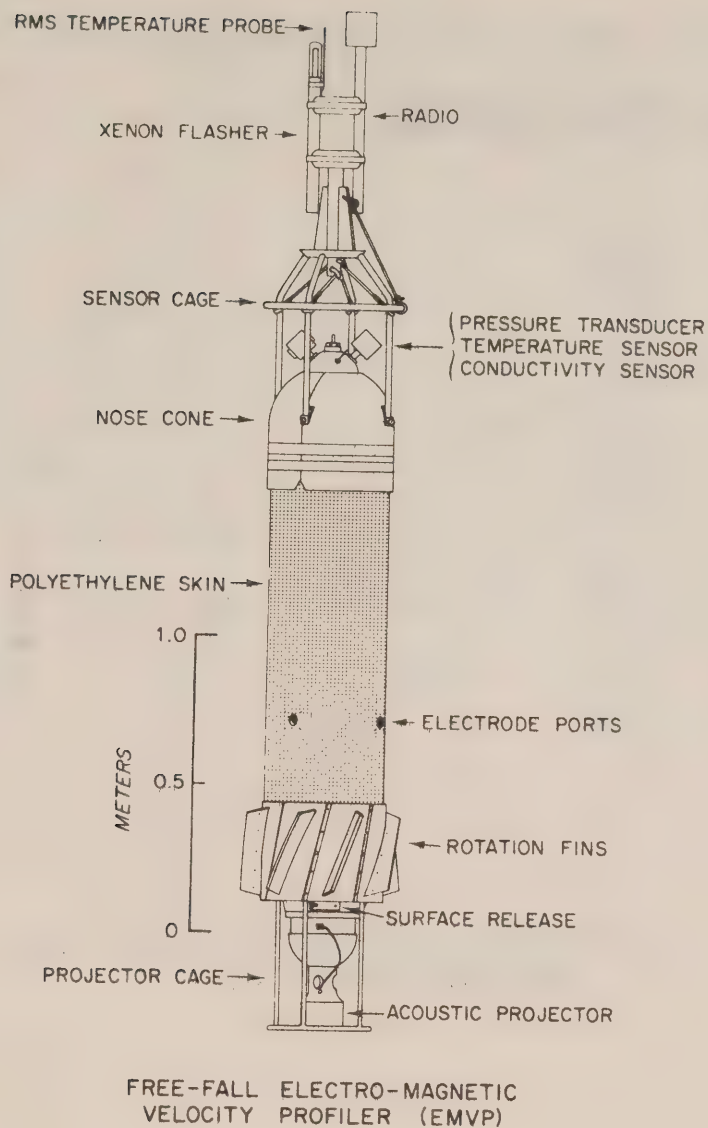


Figure 1: The free-fall Electro-Magnetic Velocity Profiler (EMVP) as configured for the FAME deployments.

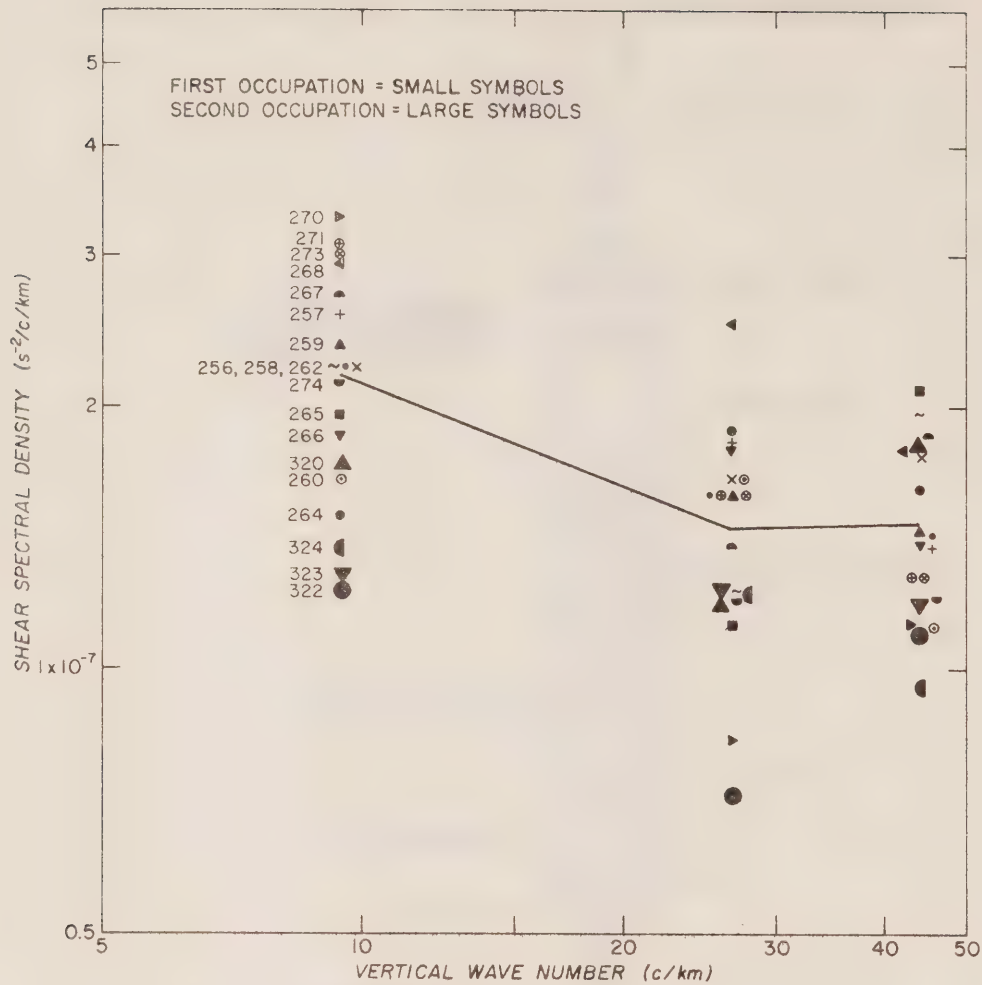


Figure 2: Spectra of vertical shear for 19 profiles collected during both occupations of the open-ocean site ($35^{\circ}N$, $66^{\circ}30'W$). Shear values were computed over the interval 225-975 dbar (80 values). The plotted points are spectral levels averaged over 13 wave number bands. The solid line is the average of the 19 spectra.

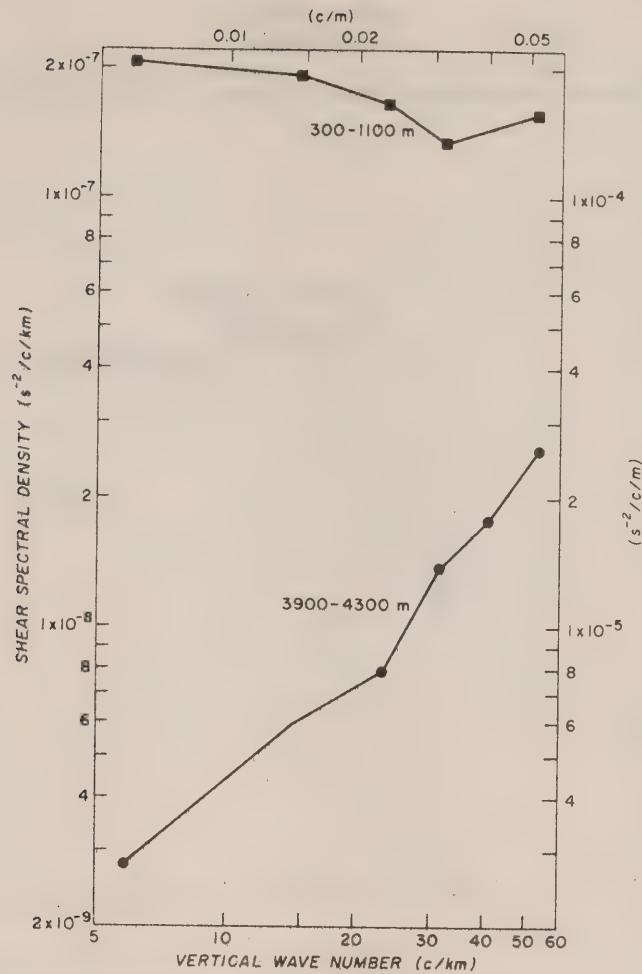


Figure 3: Average spectra for 13 profiles (256-271 excluding 261, 263 and 269 which are EMVP #2 drops paired with #1). The spectra are averaged over 3 adjacent wave number bands for two depth intervals: 300-1100 dbar and 3900-4300 dbar.

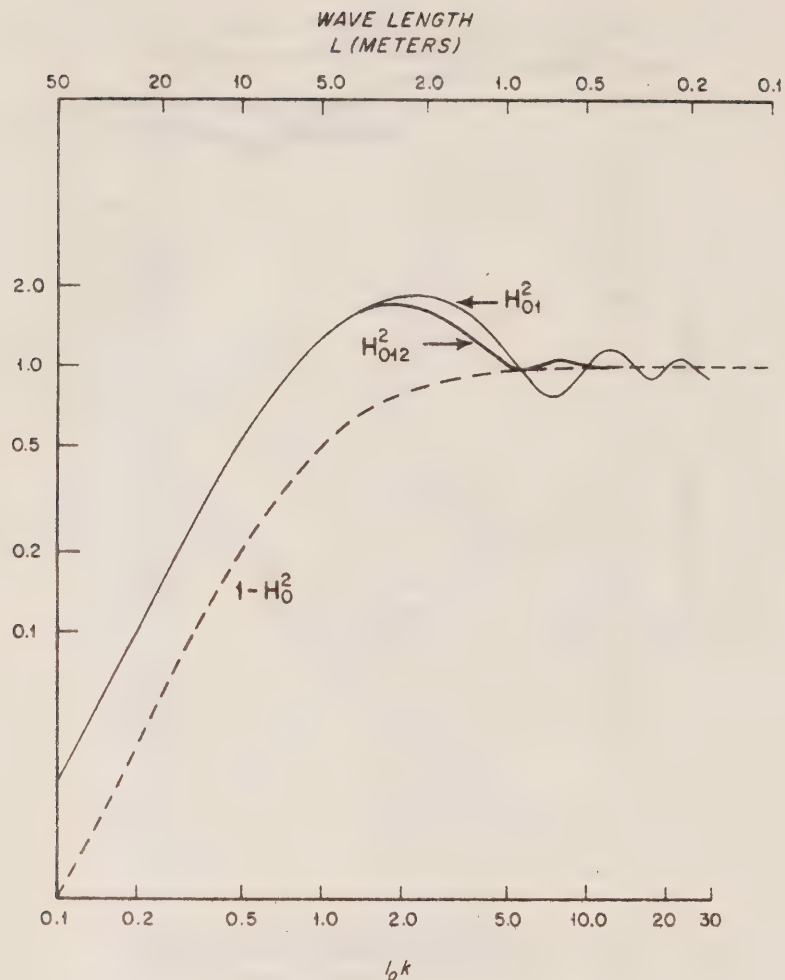


Figure 4: Transfer functions for SCIMP velocity measurements. The dashed curve labeled $1-H_0^2$ represents the reduction in measured power due to advection by horizontal velocity. The solid line labeled H_{01}^2 includes the effect of advection and the effect of sensor offset. The third curve, labeled H_{012}^2 , includes these two effects and the vertical distribution of drag. The independent variable indicated at the bottom is a dimensionless wavenumber scaled by the characteristic wave length for horizontal advection (Figure after Hendricks and Rodenbusch).

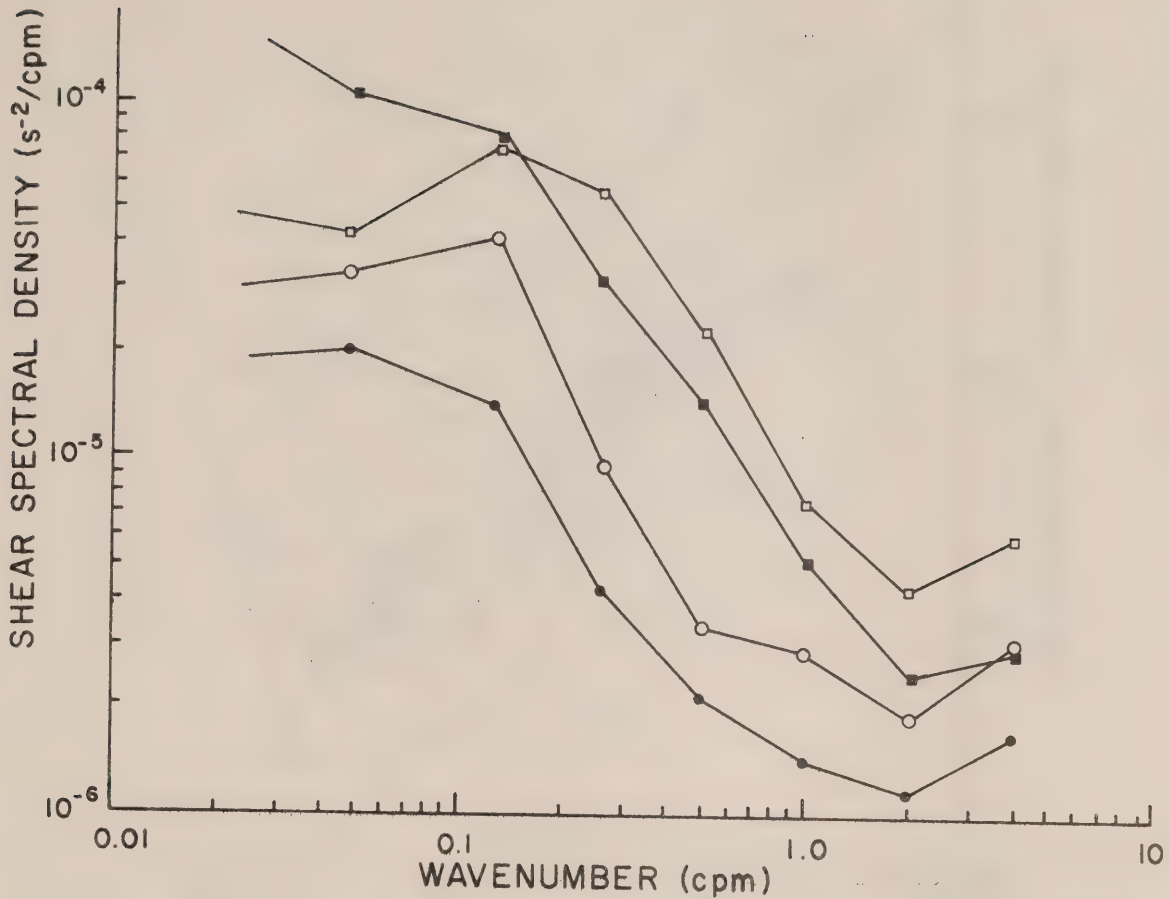


Figure 5: Shear spectra from two normal velocity channels. The shear along the long axis of the SCIMP vehicle is indicated by shaded symbols and that along the shorter horizontal axis by the open symbols. Square symbols indicate data from the main thermocline, 909-1094 dbar, while the circular symbols are for a deeper interval, 1282-1465 dbar. For the deeper piece, the power in shear measured along the short axis is approximately twice as large as along the longer vehicle axis. This difference is presumably due to greater vehicle motion along the shorter axis. In the thermocline, the shear is greater at all wavenumbers and for higher wavenumbers ($k > 0.1$ cpm) the difference between the two channels is nearly the same as in the deeper piece. At the low wavenumbers, the significance is relatively low; higher shear along the shorter axis is not generally found in the low wavenumber band.

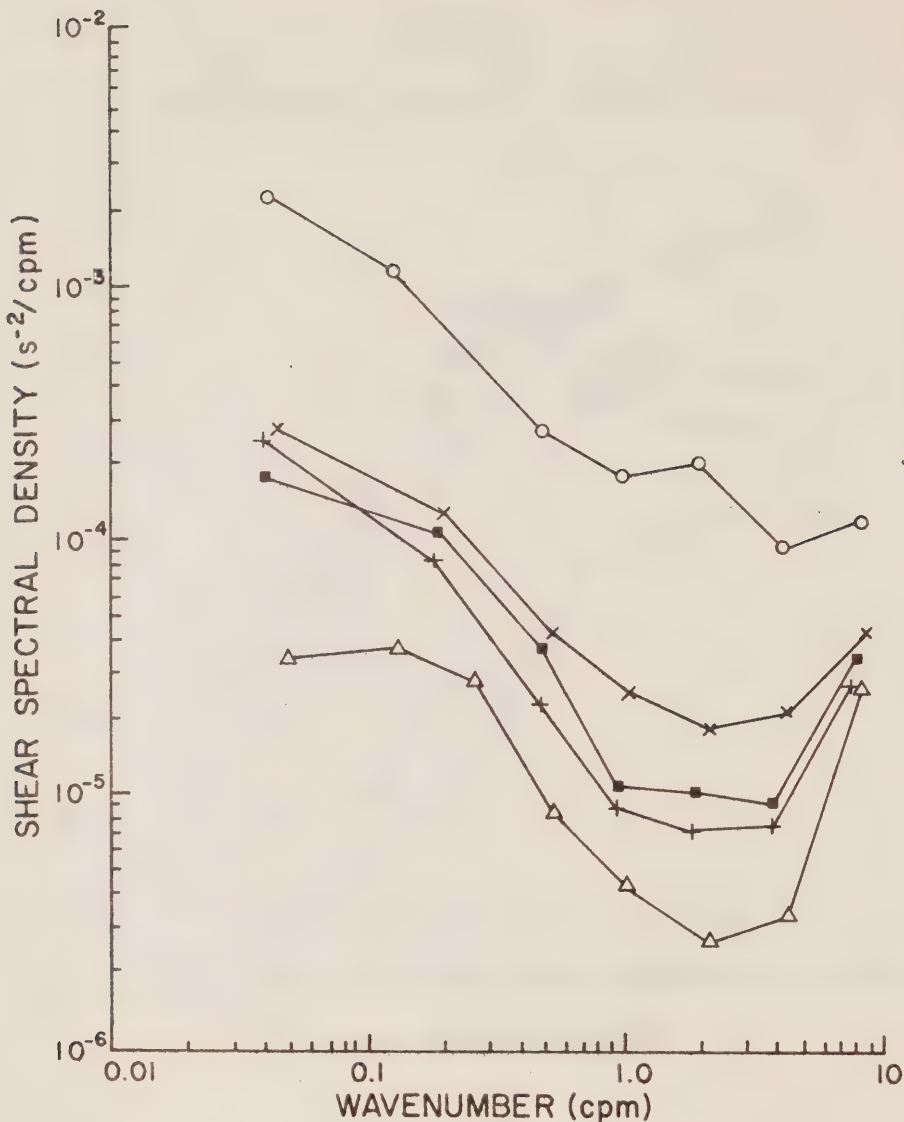


Figure 6: Average shear spectra from SCIMP illustrating the wide range of shear found during FAME (o S19 22-122 dbar; X S19 218-598 dbar; S13 412-624 dbar; + S13 213-412 dbar; Δ S16 1282-1465 dbar). S19 was taken in the Gulf Stream, S13 is near Bermuda, and S16 is at mid-ocean in the Sargasso Sea. In each case, twice the longitudinal component is used as an estimate of the total shear. All the spectra are falling between 0.1 cpm and 1.0 cpm and flatten out at higher wavenumber. The sharply rising portion of the spectra near 5 cpm is an artifact of the quantization noise.

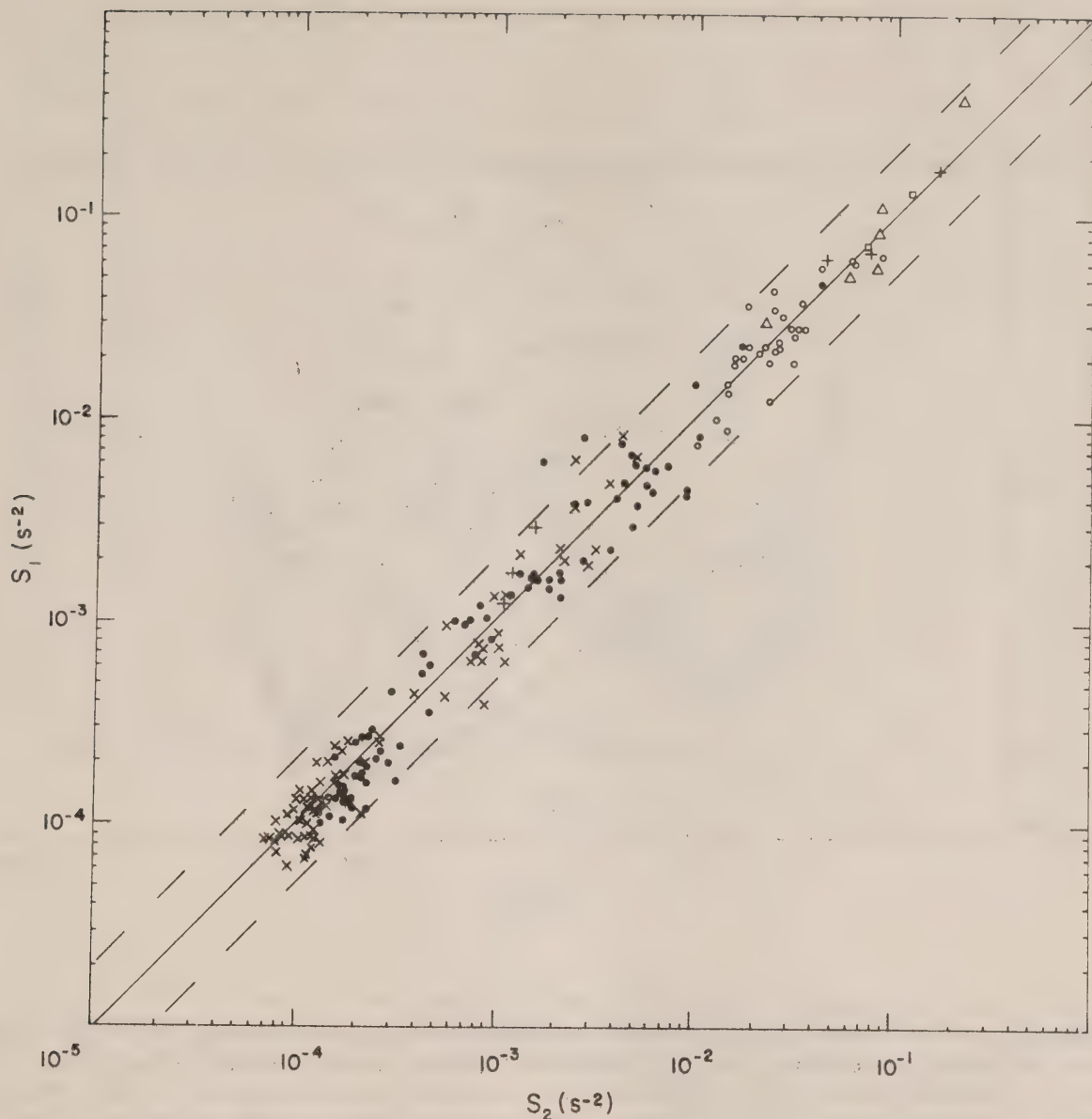


Figure 7: The airfoil probe on CAMEL measures two orthogonal components, S_1 and S_2 , of the vertical shear of horizontal velocity over the vertical wavelength range from about 50 cm down to a few centimeters. This figure presents (S_1, S_2) pairs of mean square shear obtained by integration of shear spectra over individual 2.5 dbar intervals. Data presented comes from a variety of FAME profiles, selected only to the extent of trying to cover the entire range of values observed during the experiment. A similar plot using all the FAME measurements would differ only by a much higher concentration of points in the range of 10^{-3} to 10^{-4} s^{-2} where most of the values lie. The solid line is $S_1 = S_2$; dashed lines above and below, marking $S_1 = 2S_2$ and $S_1 = S_2/2$ respectively, are seen to include all but a few points. The high degree of correlation between S_1 and S_2 allows us to replace $[PSD(S_1) + PSD(S_2)]$ by $2*PSD(S_1)$ for the purpose of the composite shear spectrum. (• C13; x C31; o C28; + C24 □ C8; Δ C5).

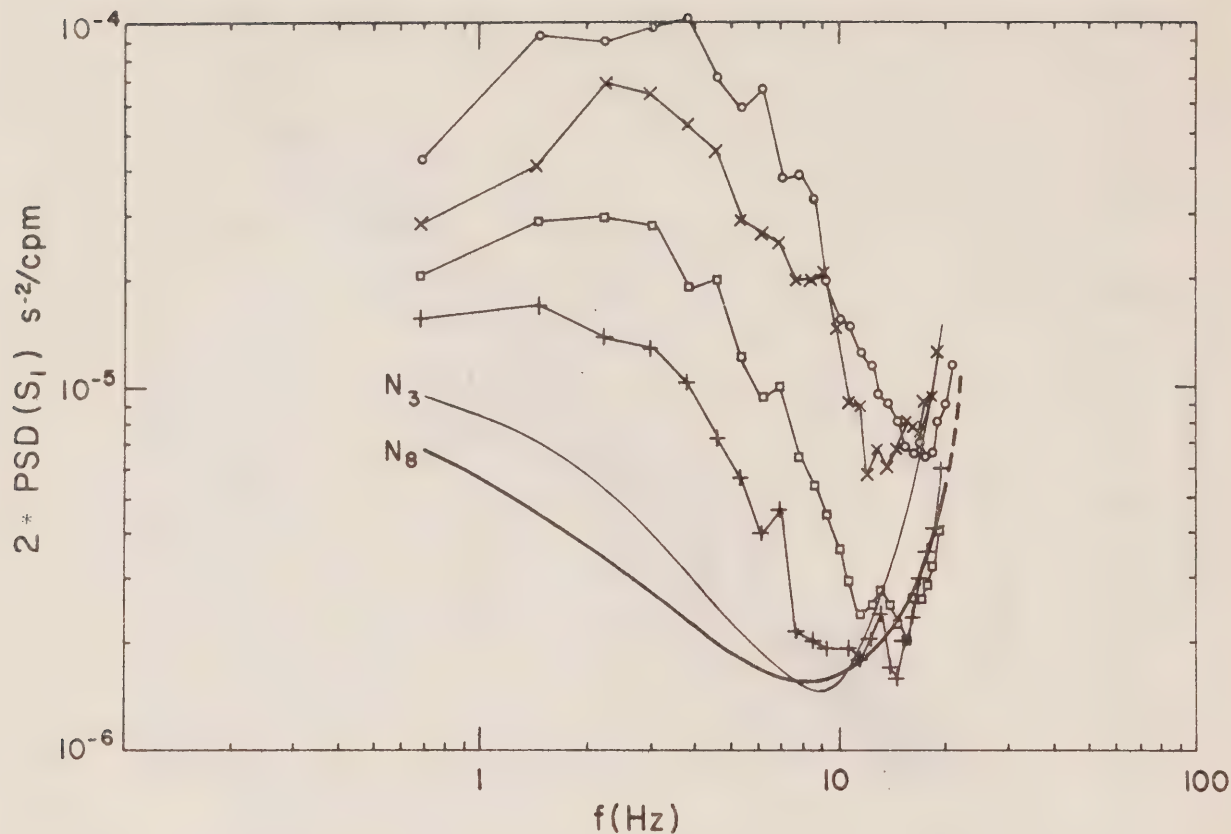


Figure 8: Power spectral densities averaged over approximately 200-dbar intervals, selected to demonstrate the range of levels encountered during FAME (o C13, 400-595 dbar; x C31, 200-552 dbar; \square C24, 395-595 dbar; + C24, 195-395 dbar). Spectra are plotted against frequency to demonstrate their relationship to noise level spectra at high frequency. Noise Spectra N_3 and N_8 differ between the two probes (3 and 8) used in the experiment: of the spectra shown, only C31 (x) uses probe 3. For the composite shear spectrum, the appropriate noise level spectrum is removed before conversion to wavenumber space.

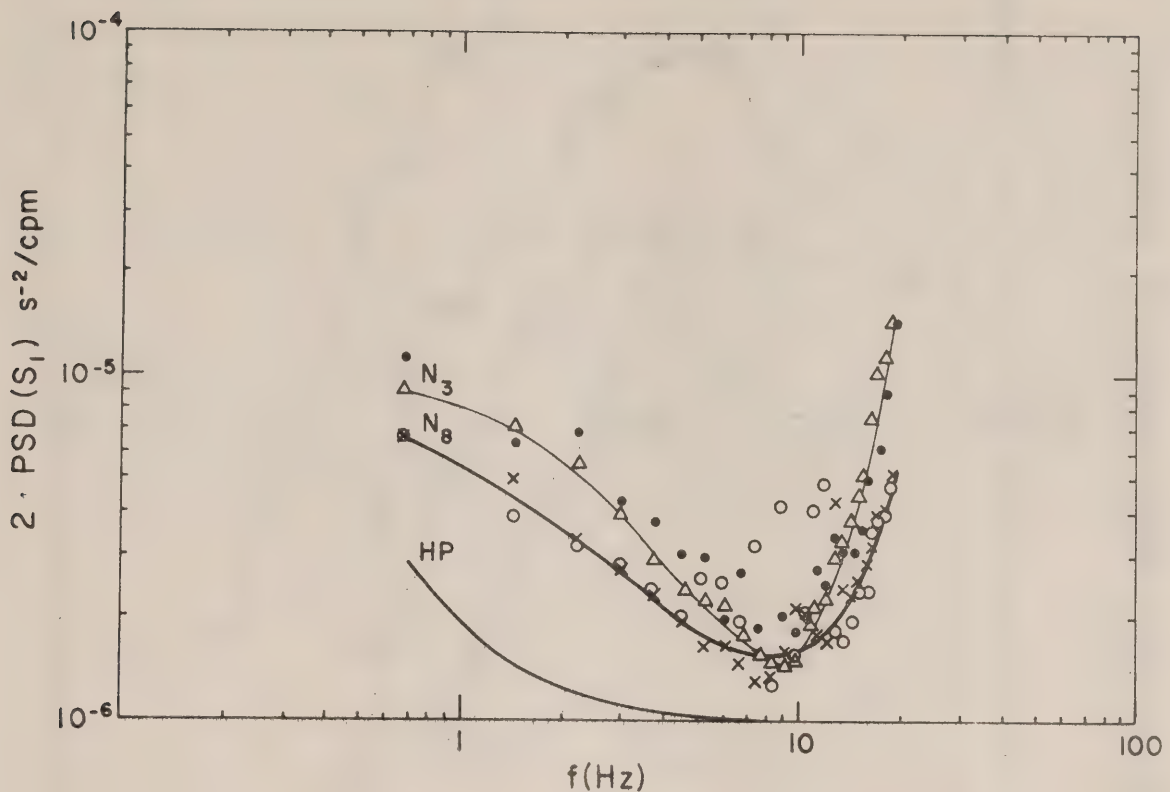


Figure 9: The degree of constancy of the noise level spectra N_3 and N_8 is shown by the relatively small differences between two sections of noise level signal from different profiles using the same probe: each section is an average of ~ 30 intervals, roughly 12 dbar in the vertical. Intermittent vibration peaks, such as the open circles between 6 - 10 Hz, will be left in the corrected spectra after the appropriate smoothed noise level spectrum is removed. Shown below (labelled HP) is the spectral correction due to a high-pass filter with 3 db point at 1 Hz (for discussion see text).

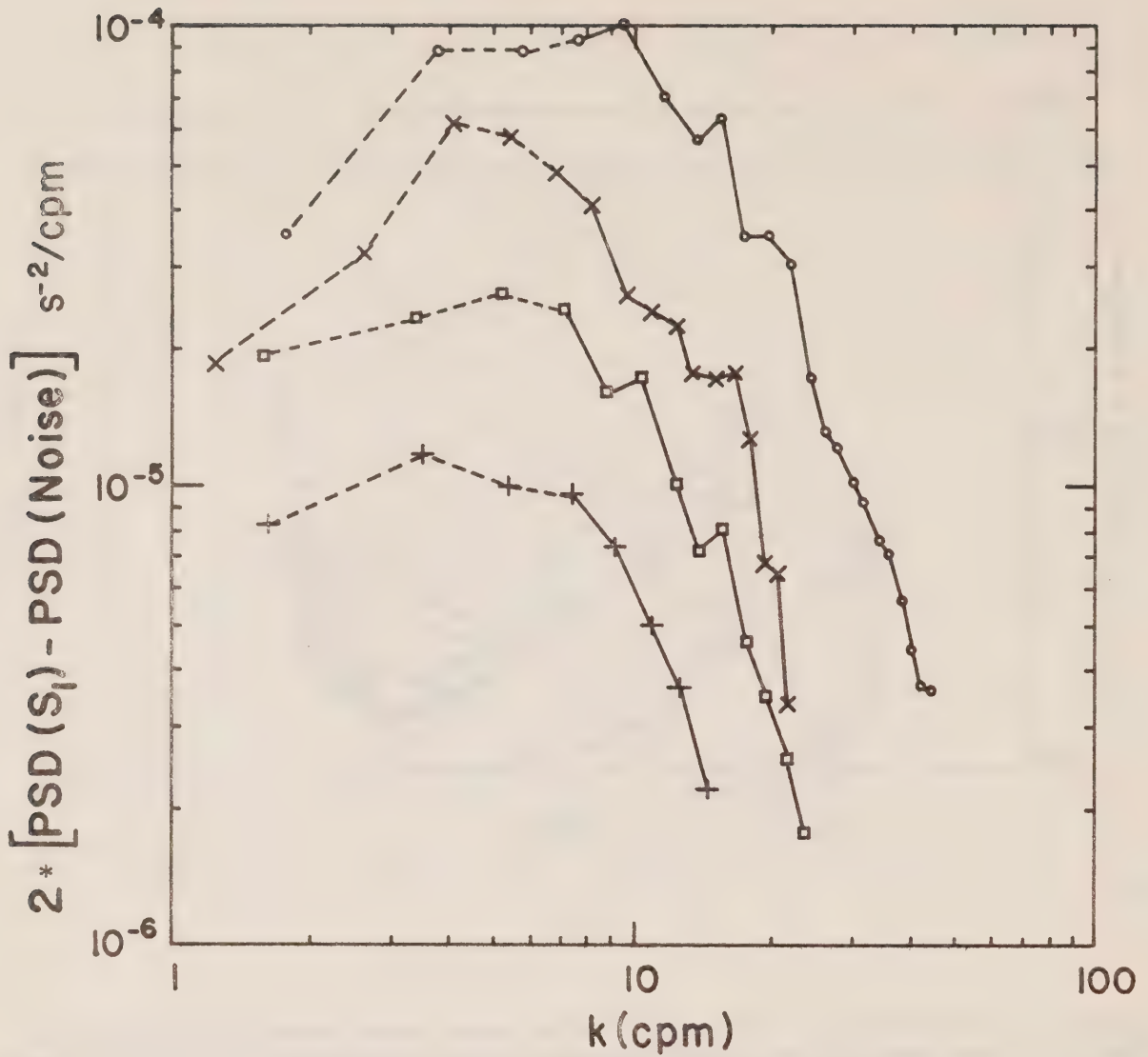


Figure 10: Noise-corrected versions of the averaged shear spectra presented in Figure 8, as a function of wavenumber. The reason for the dashed lines between the lowest four estimates is explained in the text.

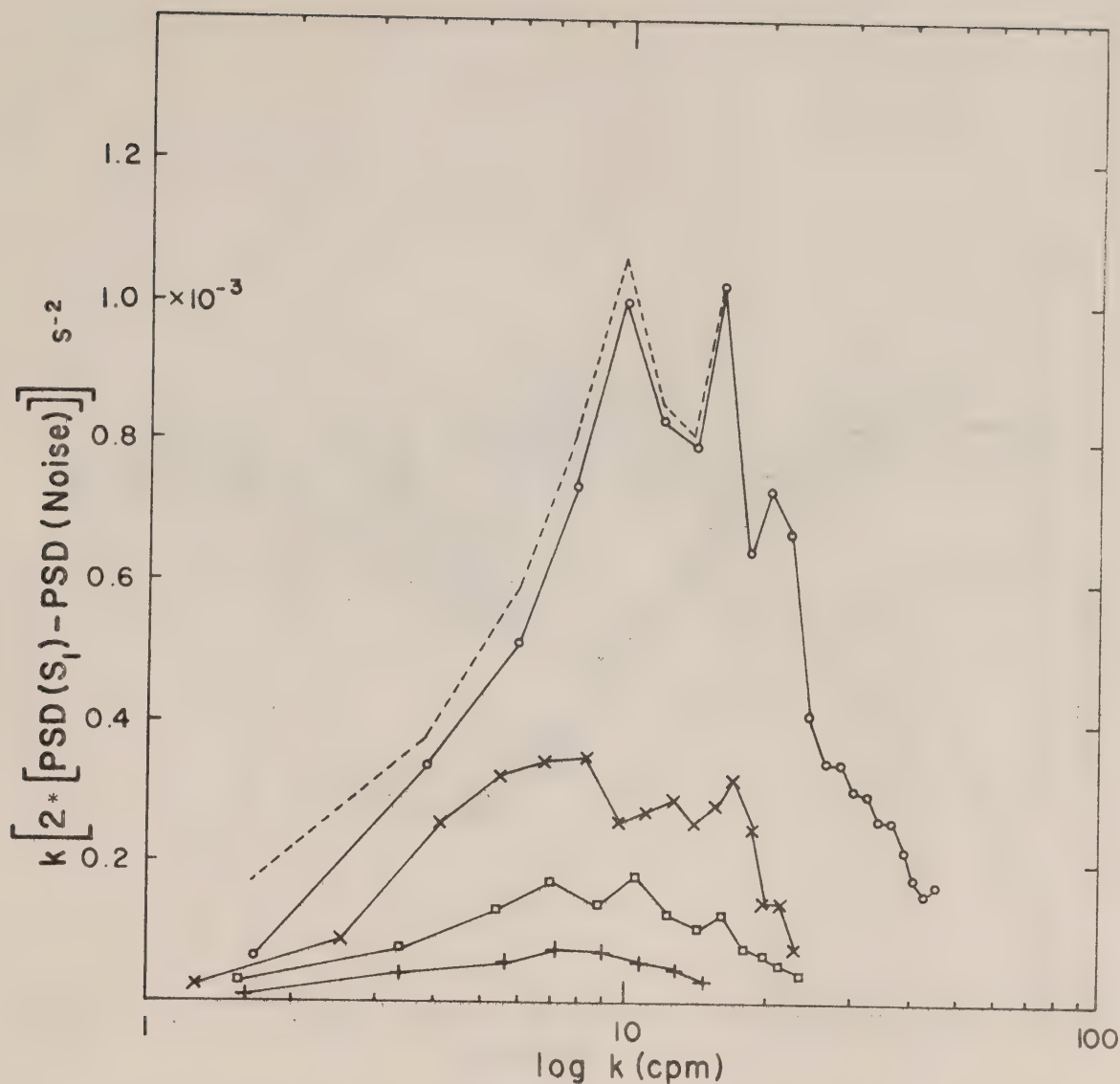


Figure 11 Variance-preserving plots of the noise-corrected shear spectra shown in Figure 10. The dashed line indicates the maximum low wavenumber correction which would be necessary if all of the variance removed by a high-pass filter in the circuit were due to shear and none to low-frequency contamination by temperature. The resulting change in the area under the dissipation curve ($\sim 5\%$) is not considered significant.

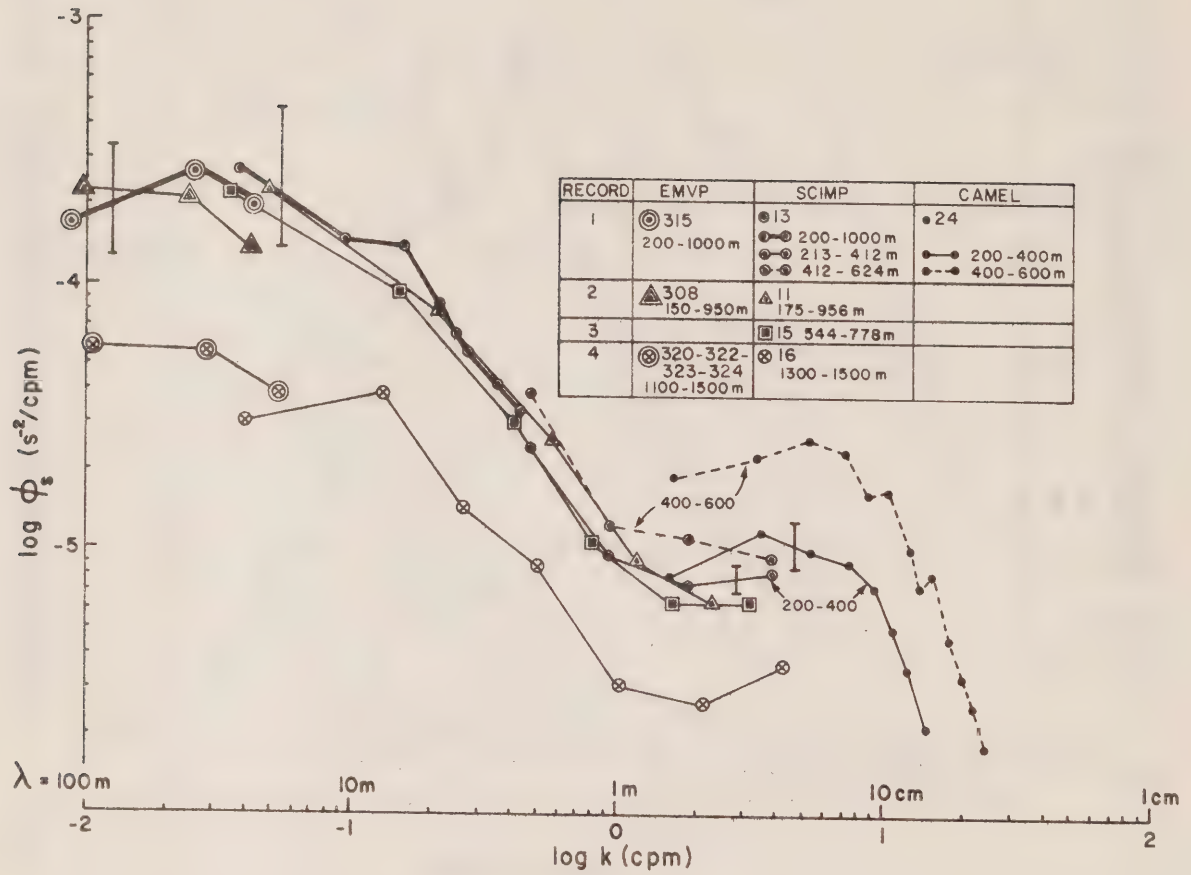


Figure 12: Shear spectral values measured by the three profilers at mid-ocean locations. Profiler drop numbers, depth ranges over which spectra are calculated and symbols used for each profiler are shown in the Table at upper right. For discussion, see text, Sections 5 and 6.

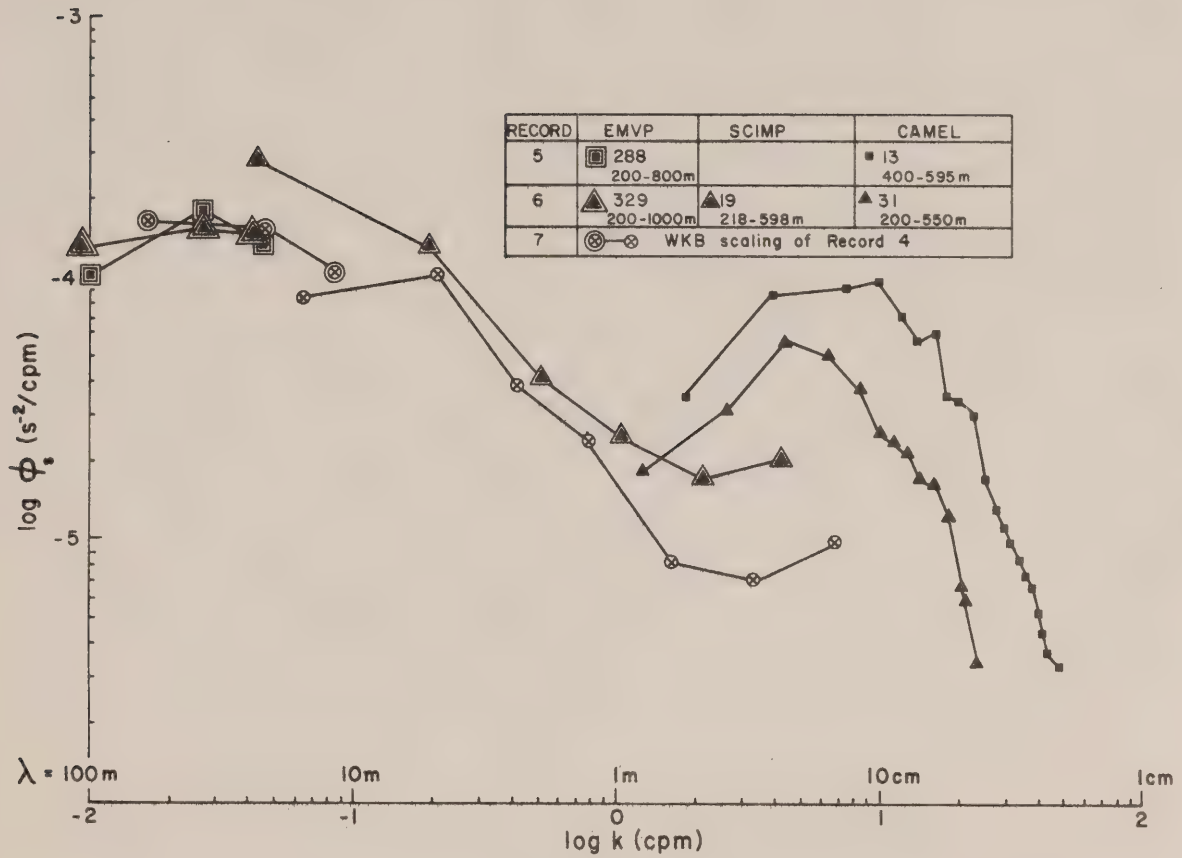


Figure 13: Shear spectral values measured by the three profilers at two "boundary" locations, a region of active interaction between the island of Bermuda and the large-scale eddy flows surrounding it (Record 5), and the northern edge of the Gulf Stream (Record 6). Record 7 is a WKB re-scaling of Record 4 (Figure 12) to allow for the smaller N characteristic of this single deeper record. For discussion, see text, Sections 5 and 6.

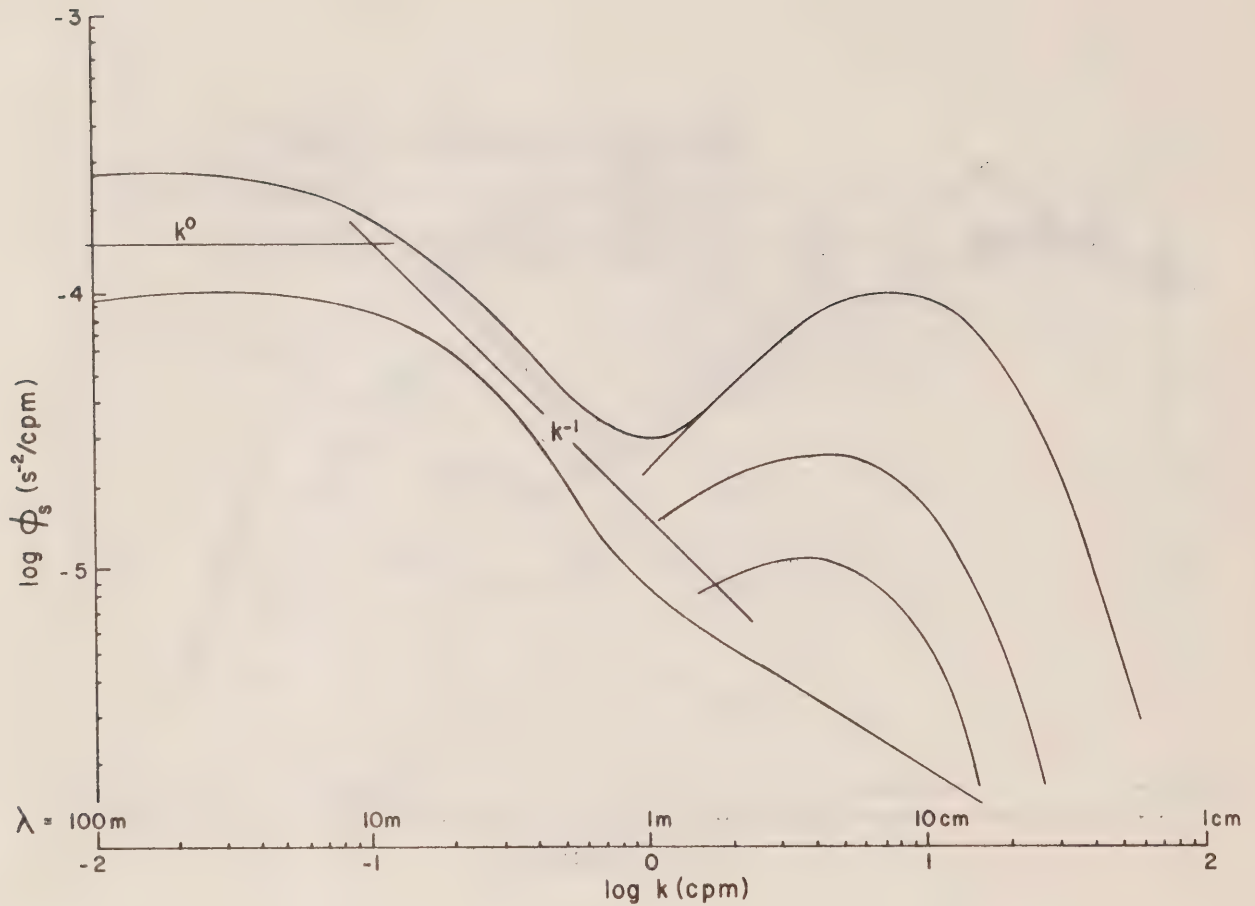
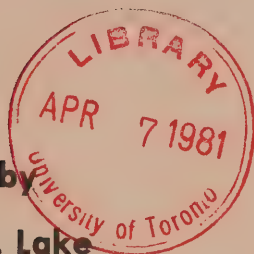


Figure 14: Proposed spectrum of vertical shear of horizontal velocity from vertical scales of 100 m to 1 cm, based on composite results from the three profilers EMVP, SCIMP and CAMEL. The low (k^0) and intermediate (k^{-1}) ranges are universal to within a factor of 2 when scaled by the local Väisälä frequency as suggested by linear internal wave theory (numerical values shown are for $N \approx 2.3$ cph). At the highest wavenumbers, spectral level in the dissipation range can vary by a factor of 10 at the same N . The non-universal nature of this sub-range compared to those at lower wavenumber implies that the magnitude of turbulent kinetic energy dissipation cannot be predicted from shear measurements on larger vertical scales i.e. 10-100 m.

CAI
EP 321
-80R12

**CALIBRATION TESTS ON THE
CONDUCTIVITY AND TEMPERATURE SENSORS
ON MODIFIED AANDERAA RCM-4
RECORDING CURRENT METERS**



by
R.A. Lake
and
R.A. Cooke

**INSTITUTE OF OCEAN SCIENCES
Sidney, B.C.**



For additional copies or further information please write to:

Department of Fisheries and Oceans

Institute of Ocean Sciences

P.O. Box 6000

Sidney, B.C. CANADA

V8L 4B2

LAI
EP 324
-10R/2

Pacific Marine Science Report 80-12

CALIBRATION TESTS ON THE
CONDUCTIVITY AND TEMPERATURE SENSORS ON
MODIFIED AANDERAA RCM-4 RECORDING CURRENT METERS

by

R.A. Lake and R.A. Cooke

Institute of Ocean Sciences

Sidney, B.C.

1980

<u>TABLE OF CONTENTS</u>	<u>PAGE</u>
TABLE OF CONTENTS	i
ABSTRACT	ii
LIST OF FIGURES	iii
LIST OF TABLES	iv
1. INTRODUCTION	1
2. FIELD CALIBRATION	6
a) Calibration method	6
b) Field calibration results	6
3. LABORATORY CALIBRATION	15
a) Calibration method	15
b) Laboratory calibration results	15
c) Comparison of field and laboratory calibration	16
d) The effect of the current meter rotor on conductivity readings	17
e) Performance of conductivity cells with and without quartz liners	18
4. TEMPERATURE SENSOR RESPONSE TIME	21
5. SUMMARY OF RESULTS	24
a) Temperature sensor	24
b) Conductivity sensor	24
REFERENCES	25

ABSTRACT

Nine Aanderaa RCM-4 recording current meters were modified to reduce the temperature and conductivity range of the respective sensors with a resulting increase in resolution. All sensors were calibrated in situ in the field at least twice over a period of up to 25 days. The sensors on two instruments were recalibrated in the laboratory for comparative purposes. The temperature sensors were found to have an accuracy of $\pm 0.015^{\circ}\text{C}$ or better when individually calibrated and on the average were stable up to within $\pm 0.006^{\circ}\text{C}$. The time constant of the temperature sensor on three meters agreed with the manufacturer's specification of 12 seconds. Individual conductivity sensors having quartz liners were on the average stable to 0.055 mmho/cm, while the newer quartz free cells were on the average stable to 0.019 mmho/cm. The corrections required when the conductivity range was modified varied widely between different sensors and between the field and laboratory for individual sensors. The mean conductivity error for all instruments was -0.360 mmho/cm with a standard deviation of 0.263 mmho/cm. The output of the conductivity channel appeared in some instances to vary with operating temperature. To ensure that optimum accuracy is obtained individual calibration of conductivity sensors in situ is required.

LIST OF FIGURES

	<u>PAGE</u>
1. Time series of salinity and temperature recorded by an Aanderaa RCM-4 meter with modified temperature and conductivity ranges.	4
2. Detail of salinity and temperature time series recorded by an Aanderaa RCM-4 meter with modified temperature and conductivity ranges.	5
3. Field temperature calibration errors as determined at intervals on 9 Aanderaa RCM-4 current meters.	8
4. Field conductivity calibration errors as determined at intervals on 9 Aanderaa RCM-4 current meters.	10
5. Temperature calibration error in the field and laboratory for two RCM-4 current meters.	19
6. Conductivity calibration error in the field and laboratory for two RCM-4 current meters.	20
7. Temperature response curves for temperature sensors on three Aanderaa RCM-4 current meters.	22
8. Temperature response curve as measured and as calculated from the time constant.	23

	<u>LIST OF TABLES</u>	<u>PAGE</u>
1a.	Aanderaa RCM-4 specification for temperature and conductivity sensors, (Aanderaa Data Sheet D147, October 1977).	1
1b.	Specification for temperature and conductivity sensors with ranges modified by user.	2
2.	Field calibration of temperature and conductivity sensors.	7
3.	Statistics of calibration errors.	13
4.	Stability of temperature and conductivity sensors.	14
5.	Binary output of conductivity cell circuitry with a 100 ohm calibration loop.	15
6.	Laboratory calibration of temperature and conductivity Sensors.	16
7.	Comparison of field and lab calibrations.	17

1. INTRODUCTION

The Frozen Sea Research Group of the Institute of Ocean Sciences is involved in physical oceanographic studies in the Canadian Arctic. During the spring of 1980 nine Aanderaa RCM-4 current meters equipped with modified temperature and conductivity sensors were deployed for a period of approximately 30 days. Because conductivity-temperature profiles (CTD's) were being taken throughout this period in situ evaluation of the accuracy and stability of the temperature and conductivity sensors on Aanderaa instruments could be conveniently undertaken. As a follow-up a selection of the current meters were recalibrated in the laboratory at which time the response time of the temperature sensor was also determined.

Our current meters are usually deployed through the sea ice and allowed to record during the spring period. Because values of temperature and salinity are within a narrow range at that time, e.g. changes less than 0.3°C and $0.3^{\circ}/\text{oo}$ or 0.25 mmho/cm in some cases, the normal ranges available on the Aanderaa meters are not optimum. Channel 4 of the Aanderaa meter was converted from pressure to measure high resolution narrow range temperature by introducing additional circuitry in accordance with Aanderaa Instrument's Technical Note No. 180, Dec. 1974. This modification switches in an additional bridge circuit utilizing the existing thermistor. In addition the bridge balancing circuit of the conductivity channel was modified to give the desired narrow range and high resolution required. The technique for this modification is described on page 2-08 of the "Operating Manual for Recording Current Meter, Model 4", supplied by the manufacturer. The specifications for the standard and modified temperature and conductivity sensors are given in Table 1. Without calibration the appropriate value for accuracy of sensors with modified range is uncertain. For temperature the manufacturer's specified accuracy of $\pm 0.15^{\circ}\text{C}$ should be valid, however, this value can be improved upon by calibrating meters individually thereby eliminating inaccuracies attributable to the variation in thermistor and bridge components occurring between any two meters. The source of inaccuracy left in the temperature is then the stability of the circuit components.

TABLE 1.

- a) Aanderaa RCM-4 specification for temperature and conductivity sensors, (Aanderaa Data Sheet, D147, October 1977).

<u>Temperature:</u>	
Sensor Type:	two series mounted type Fenwal GB32JM19 thermistors
Range:	Low: -2.46°C to 21.40°C (standard)
	High: 10.08°C to 36.00°C
	Wide: -0.34°C to 32.17°C
Accuracy:	$\pm 0.15^{\circ}\text{C}$
Resolution:	0.1 % of range selected, i.e. 0.02°C for standard range.
63% response time:	Slow response: 12 seconds (standard)
	Fast response: 6.5 seconds.

TABLE 1 (continued)Conductivity

Sensor Type:	Inductively coupled torodial coil
Range:	0 to 70 mmho/cm. (standard) 22 to 64 mmho/cm.
Resolution:	0.1% of range
Accuracy:	Not Stated.

b) Specification for temperature and conductivity sensors with ranges modified by user.

Temperature:

Range:	-2.0°C to +3.0°C.
Accuracy:	(see discussion)
Resolution:	0.005°C.
Response Time:	(see discussion)

Conductivity

Range:	23 to 30.7 mmho/cm (28.5 to 39 ‰ approximate equivalent salinity)
Accuracy:	(see discussion)
Resolution:	0.007 mmho/cm (approximately 0.01 ‰ equivalent salinity)

Finding the accuracy for the conductivity sensor is much less straightforward. For a particular meter this accuracy will depend on the stability of the circuit components, the most troublesome of which is the conductivity cell itself. The cell constant is critically dependent on the physical stability of the cell. Factors which could cause physical change to the cell during use are dimensional change resulting from the hydrostatic pressure of the water column, the absorption of water by the cell material, corrosion, coating by organisms, silt or chemical precipitates, or the varying proximity of electrically conducting material. The effect of pressure on Aanderaa conductivity cells was documented by Huyer (1975) and Smith et al (1978). The second paper states that the strongest effects of pressure appeared to occur between 0 and 50 psi (34 dbar). The conductivity cells of the type used by Huyer and Smith had air spaces between the quartz tube and the rubber lining outside the tube which was considered to be the source of the problem. Starting with conductivity cell number 2035 Aanderaa has provided cells without quartz tubing. Both the older and newer types of conductivity cells were used on the current meters being discussed in this paper and the performance of each is the subject of later discussion.

The practical problem that potential variation of the cell constant presents for the oceanographer trying to interpret recorded data is illustrated in Figure 1. Here data collected in the arctic by a modified Aanderaa RCM-4 current meter equipped with the newer conductivity cell lacking the quartz

tubing are reproduced. Most of the variations in salinity of periods longer than a day could equally well be attributed to nature or to variations in the cell constant. Conductivity channels frequently recorded a change in value of order 0.1 mmho/cm over a period of a few days commencing immediately on deployment. Invariably there was no corresponding change in recorded water temperature as would typically occur if water properties at the meter were changing. In Figure 1 a decrease in salinity (conductivity) was recorded at the beginning of the data record although no change or an initial increase in value has been recorded on other meters. The data do not permit one to determine if salinity changes are real or result from a shift in cell constant as the transducer adjusts to increased pressure on deployment. The meters under consideration were subjected to pressures up to 50 dbar over atmospheric. In Figure 1 recorded salinity slowly increases from Julian day 97 to 182 with no corresponding change in water temperature. While the salinity change may be real it could also be accounted for by silting, chemical deposit of material such as Calcium Sulfate, marine fouling, etc., although in fact in arctic waters during spring marine fouling has never been evident on meters deployed by our group. The relatively large excursions in salinity near the end of Figure 1 are accompanied by an increase in water temperature typical for the time of year and are "real" to the extent that they reflect the nearby run-off of freshwater from land. The absolute salinity value is in question however, because the run-off is accompanied by heavy siltation which can affect the conductivity reading.

While it may appear at this point that increasing the resolution of the Aanderaa conductivity channel is not a worthwhile exercise such is not the case. Figure 2 shows a segment of data record where the time scale is expanded compared to Figure 1. Much useful information is contained in such a record of temporal changes in water properties, for example, semi-diurnal variations of tidal origin in salinity and temperature of order 0.06‰ and 0.1°C respectively are evident.

Salinity rather than conductivity is of practical interest where conductivity is a function of both salinity and temperature. Salinities throughout this report were computed from conductivity and temperature values using the Practical Salinity Scale (1978) (Perkin and Lewis, 1980).

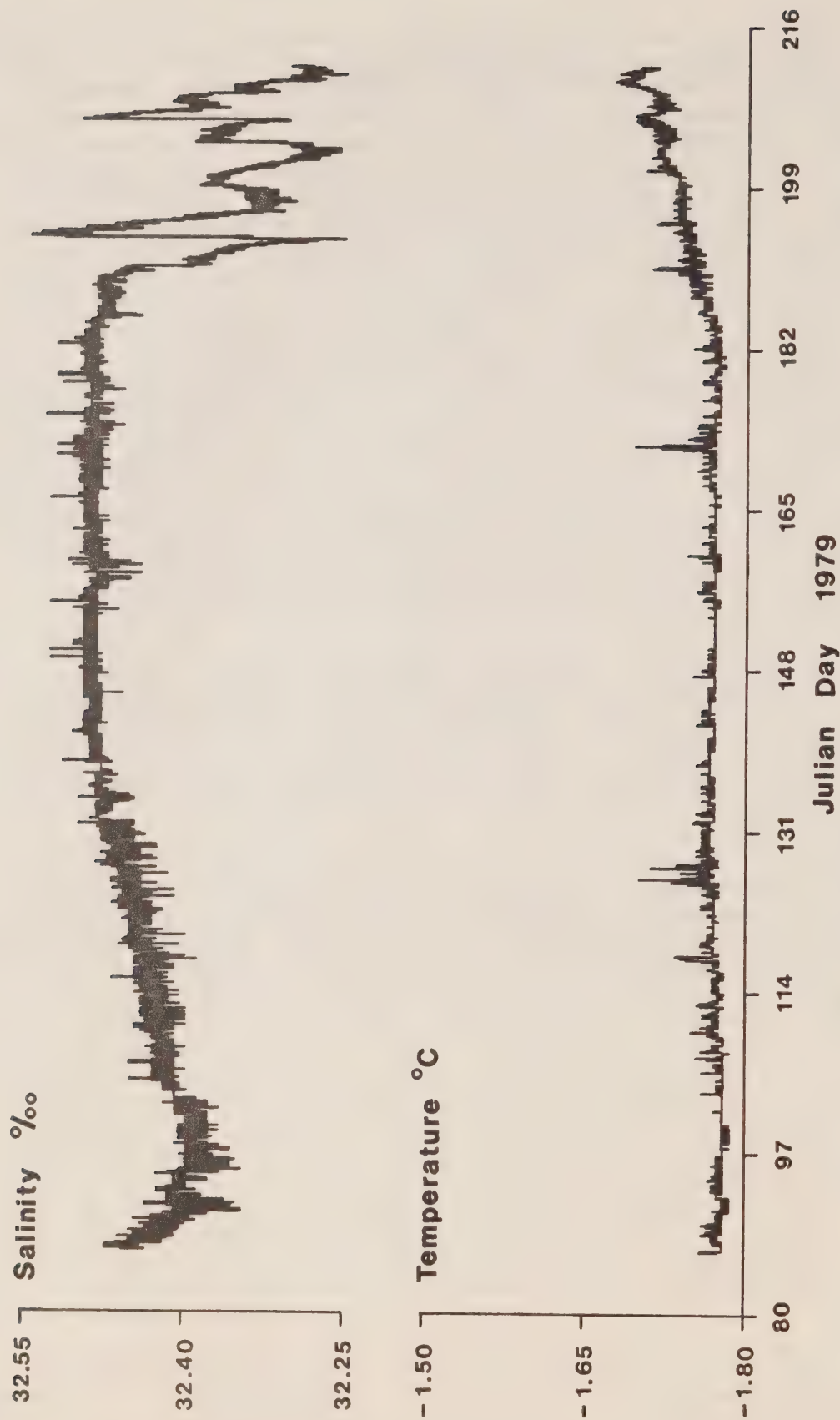


FIGURE 1. Time series of salinity and temperature recorded by an Aanderaa RCM-4 meter with modified temperature and conductivity ranges. Instrument serial No. 3388, conductivity cell serial No. 2231.

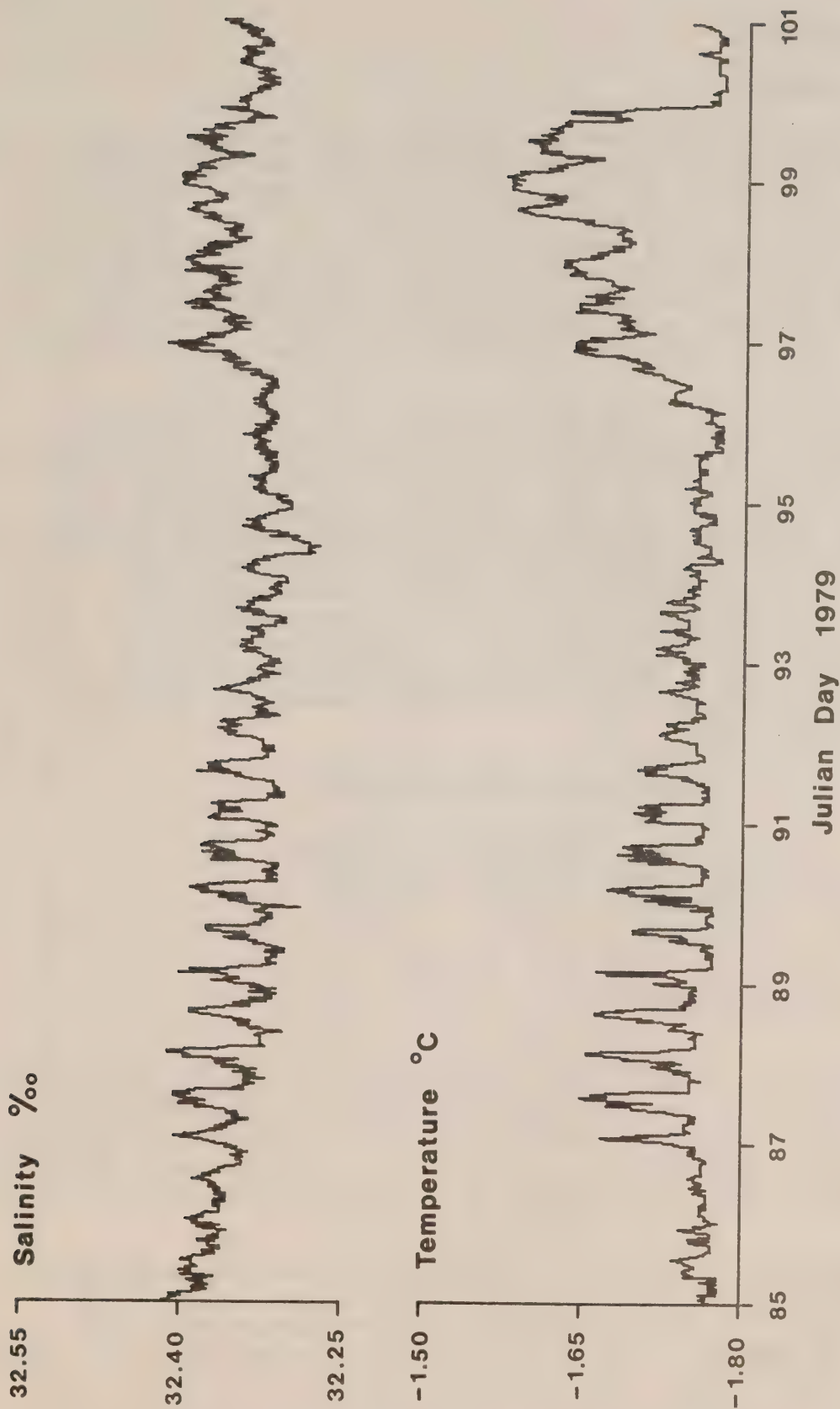


FIGURE 2. Detail of salinity and temperature time series recorded by an Aanderaa RCM-4 meter with modified temperature and conductivity ranges.

2. FIELD CALIBRATION

a) Calibration method

The nine Aanderaa RCM-4 recording current meters modified for arctic use were deployed for a nominal 30 day period off Melville Island in the Canadian arctic. While these meters were recording a detailed survey of water properties (temperature and conductivity) was conducted in the area using a Guildline 8101A CTD instrument. A number of CTD profiles were taken at the sites of the moored current meters coincident with recording of the same parameters by the Aanderaa meters themselves. This in situ calibration was done at least twice for each instrument, once near the beginning of the current meter deployment and again near the end of the recording period as detailed in Figures 3 and 4.

To monitor the accuracy of the CTD measurements, water samples were taken from time to time with oceanographic bottles. These water samples were run through a Hytech Model 6220 bench salinometer calibrated with Standard Sea Water. Thermistors used to check water temperatures were calibrated in a triple point cell. Values obtained from a bench salinometer and the thermistors were compared to the Guildline CTD values obtained coincidentally and temperature and salinity corrections were determined. A detailed discussion of our methods of in situ measurements of conductivity and temperature can be found in Lewis and Sudar (1972). The principal recording system for output of the Guildline instrument was a Vidar 5402 data logger with printed and punched paper tape output. The performance of the CTD instrument and recording system is specified below.

Guildline 8101A CTD Performance

	Resolution	Accuracy
Temperature	0.002 °C	±0.002 °C
Salinity	0.002 ‰	±0.005 ‰
Pressure	0.1 db	1.0% of reading.

b) Field calibration results

Temperature and conductivity values were determined from the RCM-4 data by using equations of the form given in the manufacturer's manual accompanying each instrument but with new coefficients appropriate to the modified sensor range and calculated from the values of new resistors installed in the bridge balancing circuit. Introduction of new circuitry by the user makes calibration of the two modified channels essential. Once determined the calibration error can be added to the zero offset term in the equation.

During each in situ calibration a number of separate CTD readings were made usually at 15 minute intervals, corresponding to the current meter sampling interval. A series of temperature and conductivity errors were then calculated by subtracting the RCM-4 value from the corresponding value reduced from the Guildline CTD data. An average error was calculated and the range of error values determined. Numerical values are given in tabular form in Table 2 while the average magnitude of the errors together with the lapsed

TABLE 2
Field Calibration of Temperature and Conductivity Sensors

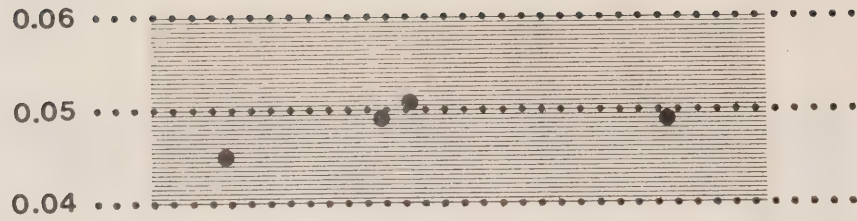
Serial No.	No. of T Readings	T. Calibr. (1)		No. of C Readings	C Calibr. (2)		Equiv. Salinity Error	
		Error °C	Range		Error mmho/cm	Range	°/∞	Range
1930	3	0.045	±.001	2	-0.296	±.005	-0.413	±.006
	10	0.049	±.004	10	-0.233	±.006	-0.324	±.009
	1	0.051		1	-0.231		-0.321	
	5	0.049	±.001	5	-0.279	±.002	-0.389	±.001
1931	3	0.014	±.010	3	-0.576	±.014	-0.80	±.020
	3	0.017	±.001					
1932	3	0.062	±.004	2	-0.702	±.002	-0.977	±.003
	10	0.066	±.016	10	-0.723	±.011	-1.003	±.023
	1	0.077		1	-0.735		-1.023	
	5	0.073	±.005	5	-0.731	±.006	-1.017	±.008
1936	3	0.044	±.003	3	-0.330	±.001	-0.460	±.001
	4	0.036	±.005	3	-0.299	±.002	-0.416	±.003
1939	3	-0.049	±.001	3	-0.230	±.006	-0.320	±.007
	3	-0.052	±.003	3	-0.117	±.005	-0.162	±.006
2466	3	-0.019	±.001	3	-0.317	±.010	-0.442	±.016
	3	-0.021	±.001	3	-0.324	±.004	-0.452	±.006
3223	3	0.014	±.009	3	-0.047	±.013	-0.065	±.018
	3	0.016	±.002	3	-0.038	±.002	-0.053	±.003
3228	3	0.035	±.003	3	-0.114	±.001	-0.159	±.001
	3	0.042	±.004					
3387	3	0.028	±.006	2	0.068	±.001	0.094	±.001
	3	0.038	±.004	3	0.050	±.010	0.067	±.013

(1) at -1.8°C

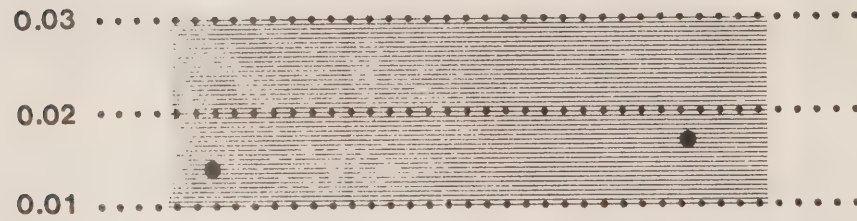
(2) at 26 mmho/cm.

Serial No.

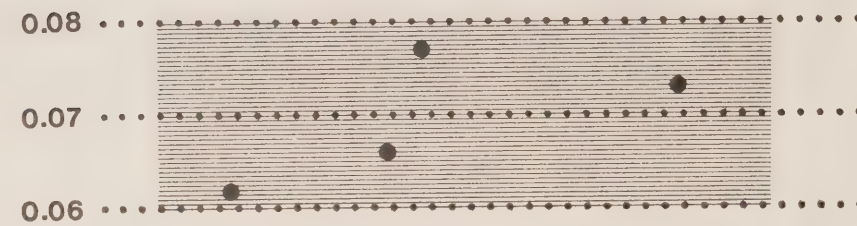
1930



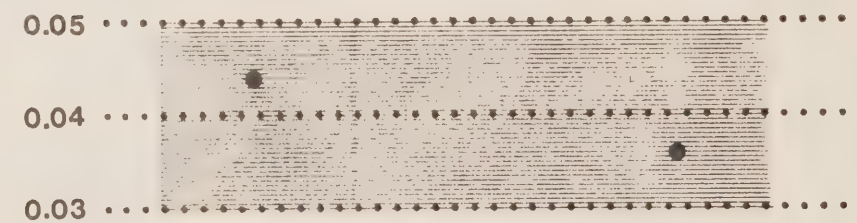
1931



1932



1936



1939

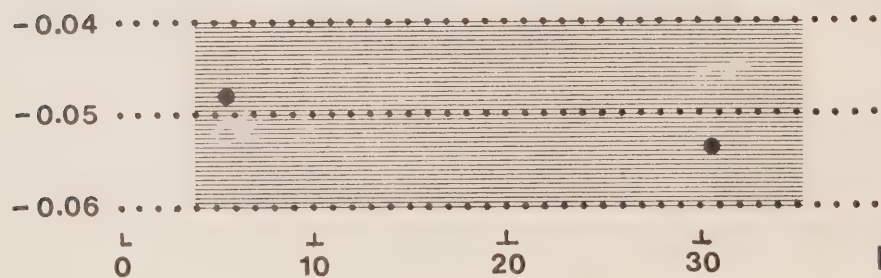
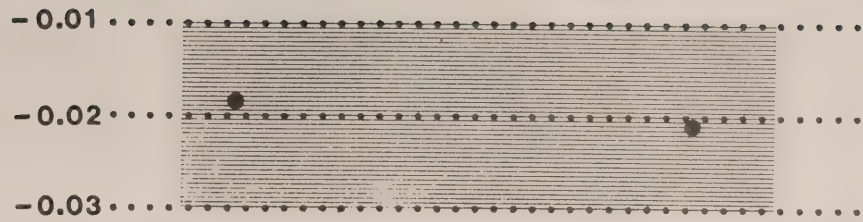


FIGURE 3. Field temperature calibration errors as determined at intervals on 9 Aanderaa RCM-4 current meters. Shaded areas indicate meter deployment period.

Serial No.

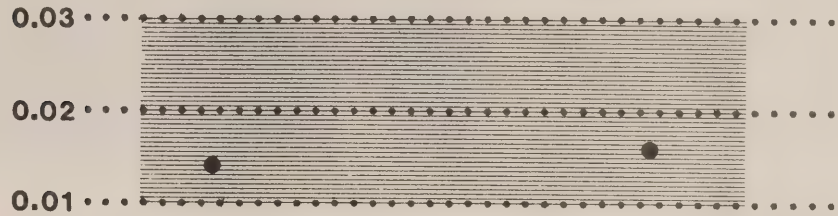
2466



3223

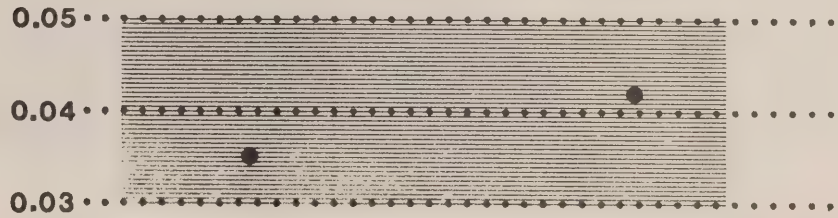
°C

Temperature Error

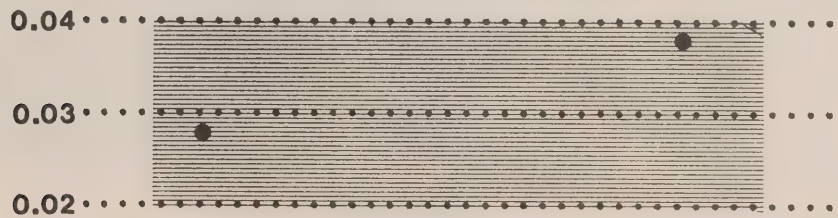


3228

Temperature Error



3387



L

0

⊥

10

⊥

20

⊥

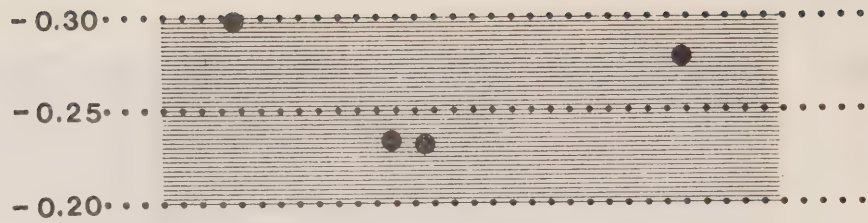
30

Days

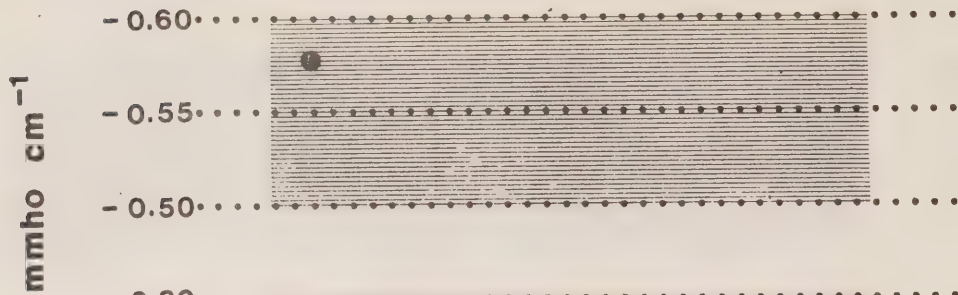
FIGURE 3. continued.

Serial No.

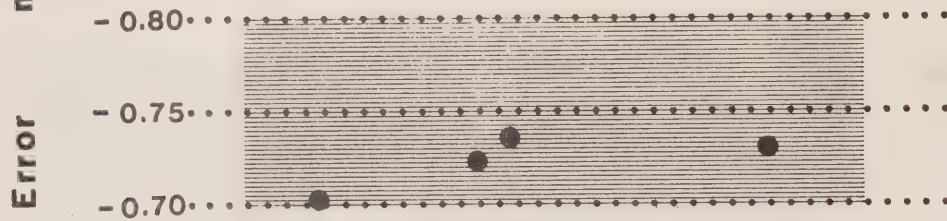
1930



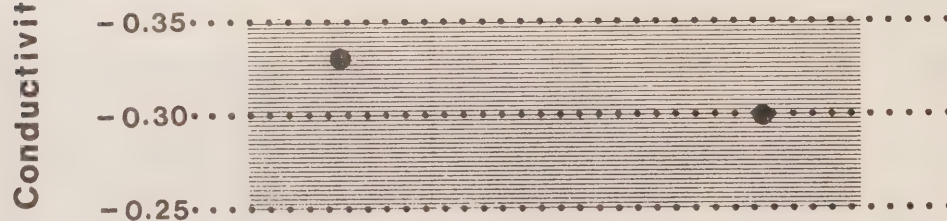
1931



1932



1936



1939

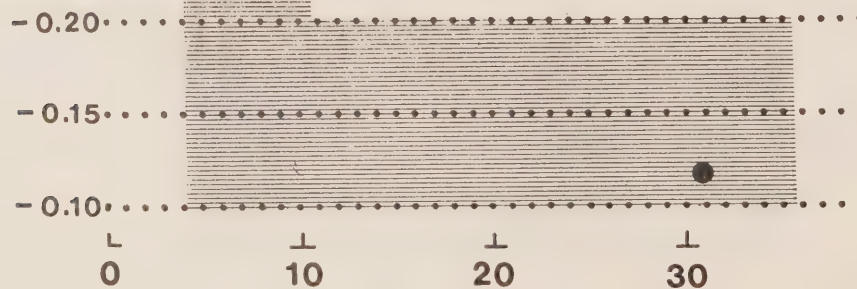
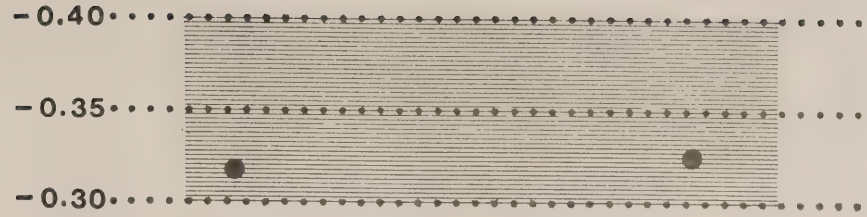


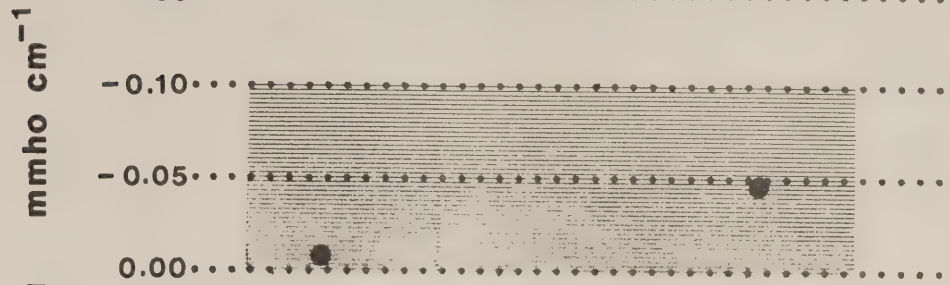
FIGURE 4. Field conductivity calibration errors as determined at intervals on 9 Aanderaa RCM-4 current meters. Shaded areas indicate meter deployment period.

Serial No.

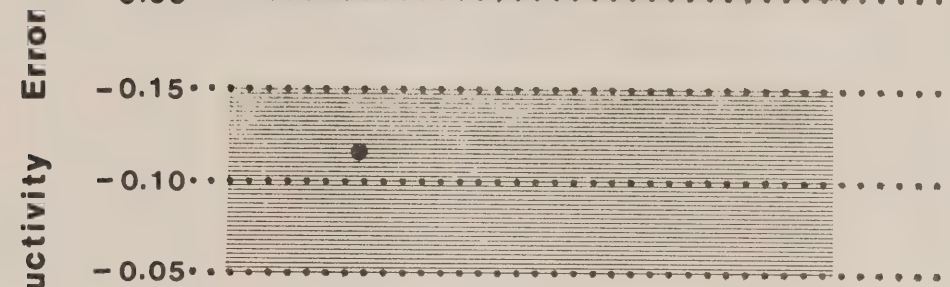
2466



3223



3228



3387

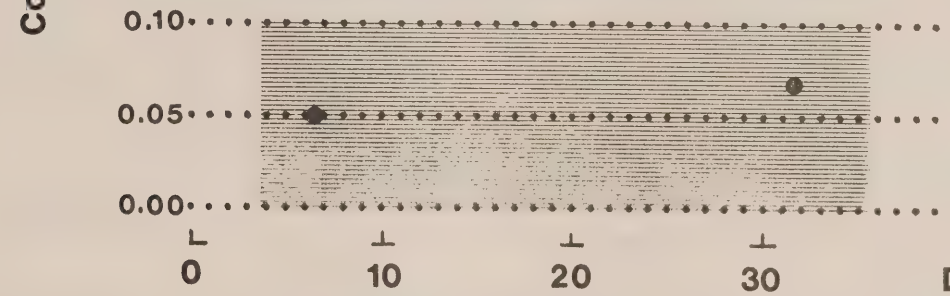


FIGURE 4. continued

time between calibration checks is shown graphically in Figures 3 and 4. In general, the range of error values within each calibration run is within the resolution of the Aanderaa instrument although a few exceptions will be noted in both temperature and conductivity. The equivalent salinity given in Tables 2 through 4 is computed from conductivity as read and corrected temperature.

It should be noted that the calculated errors apply strictly only to the values existing at the time of measurement, -1.8°C and 26 mmho/cm . Ideally one would want to check the error throughout the full temperature and conductivity range of the sensor, however, this was not possible under field conditions.

The statistics of calibration errors given in Table 3 are calculated from all individual readings on all instruments. The mean errors were found to be of order 0.04°C degrees for temperature and of order 0.36 mmho/cm for conductivity. The corresponding error in salinity is $0.50\text{ }^{\circ}/\text{oo}$. Standard deviations are rather large, particularly for conductivity and hence salinity. These values are applicable to the intercomparison of data between separate uncalibrated meters.

In practical terms the calibration error or accuracy of a sensor is much less important than stability. Provided an individual instrument is stable the inaccuracy can be determined for each sensor by calibration and can be taken into account during data reduction. As stability progressively improves it reaches a limit which is the resolution of the instrument. The stability of the temperature and conductivity sensors for the nine current meters tested is given in Table 4. On two current meters more than two calibration checks were made so there the period chosen corresponds to the interval over which maximum instability occurred. The mean stability of the temperature sensors is close to the resolution of the instrument and individual sensors are, with one exception, stable to 0.01°C . The stability of the conductivity sensors is marked by wide variations between individual sensors with values ranging from as much as 0.11 mmho/cm ($0.16\text{ }^{\circ}/\text{oo}$ at -1.8°C) to as little as 0.007 mmho/cm ($0.01\text{ }^{\circ}/\text{oo}$ at -1.8°C), the latter value corresponding to the resolution of the instruments.

Potentially false indications of sensor instability could occur if the recording current meter and the CTD were occasionally vertically displaced with respect to each other. This situation would arise if sufficiently strong currents displaced the mooring causing the instrument to vary its recording depth. During field calibrations current speeds measured by the meter were insufficient to cause any vertical displacement as calculated by Bell (Bell, 1979). Furthermore, vertical gradients of temperature and conductivity were sufficiently small to require vertical displacement of over a meter before a resolvable difference in water properties could be detected.

When considering stability of the conductivity channel it is interesting to look at the stability of the circuitry independent of conductivity cell. When a resistor is connected in a single loop passing through the center hole of the cell as described in the operating manual, the circuitry in the conductivity channel sees a constant conductance which is independent of the cell constant. By simply connecting the same precision resistor through the cell

the operation of the conductivity channel circuitry can be checked as the same binary value should be consistently recorded. A check of this nature was done just prior to current meter deployment and again soon after the meter was retrieved from the ocean although temperatures during the two checks were quite different. The binary values obtained from each meter are given in Table 5 together with the binary output of the standard channel. A subsequent check on the meters was taken in the laboratory in October. The difference in binary values before and after deploy was on the average 7 bits, equivalent to 0.05 mmho/cm or 0.07 ‰. The maximum change detected was 18 bits on meter 2466. The final check at 22°C gave values closer to the earlier values recorded at 15°C, the mean difference being 2 bits. The standard channel remained essentially constant so that it appears that some but not all meters had circuitry in the conductivity channel that was temperature dependent indicating the necessity of calibration under field conditions.

TABLE 3

Statistics of Calibration Errors

	Temperature <u>°C</u>	Conductivity <u>mmho/cm.</u>	Equivalent Salinity <u>‰</u>
Number of calibration checks	81	71	71
Mean error	0.040	-0.360	-0.501
Standard deviation	0.025	0.263	0.365

TABLE 4

Stability of Temperature and Conductivity Sensors

Serial No.	Period, Days	Magnitude of stability during period:		
		Temperature °C	Conductivity mmho/cm.	Equivalent Salinity ‰
1930 *	10	0.006	0.065	0.092
1931 *	25	0.003	-	-
1932 *	10	0.015	0.033	0.046
1936	22	0.008	0.031	0.044
1939 *	25	0.003	0.113	0.158
2466 *	24	0.002	0.007	0.010
3223	23	0.002	0.009	0.012
3228	20	0.008	-	-
3387	24	0.010	0.018	0.027
Mean		0.006	0.039	0.056
Standard deviation		0.004	0.038	0.052

* Conductivity cells with quartz liners.

TABLE 5

Binary Output of Conductivity Cell Circuitry with a 100 ohm Calibration Loop

Serial No.	Standard (ch.1.)			100 ohm loop (ch. 3.)		
	Mar. 15°C	Apr. 0°C	Oct. 22°C	Mar. 15°C	Apr. 0°C	Oct. 22°C
1930	564	564	-	872	873	-
1931	378	378	378	877	866	876
1932	178	178	176	879	885	879
1936	683	683	683	-	875	872
1939	257	257	257	910	927	914
2466	585	584	585	881	863	879
3223	929	929	929	870	871	868
3387	739	739	739	860	862	858

Note: A change of 1 in binary number is equivalent to a change in conductivity of 0.007 mmho/cm or approximately 0.01 ‰ equivalent salinity at -1.8°C.

3. LABORATORY CALIBRATION

a) Calibration method

Subsequent to the in situ calibration of the conductivity and temperature sensors on the RCM-4 meters the instruments were returned to the Institute of Ocean Sciences where laboratory calibration was carried out. Information is thus available on the applicability of laboratory calibration of these instruments.

To calibrate the sensors each meter complete with pressure case and rotor was submerged in a 58 litre (13.8 imperial gallons) tank of sea water. The insulated tank was chilled and the temperature maintained between -1.7 and -1.8°C by regulating with a Haake KR 30 temperature control device. The bath temperature was continuously monitored by three Fenwal thermistors which were recorded by the Vidar model 5402 data logger used for the field measurements and capable of resolving temperature to 0.002°C . The thermistors were previously calibrated in a triple point cell and are accurate to 0.002°C . To arrive at a value for the temperature calibration error two or three temperature values from the Aanderaa meter were averaged and subtracted from the average temperature determined by several readings from the standard thermistor. Salinity of the sea water bath was adjusted to an appropriate value by evaporating local surface sea water. Water samples were collected after each instrument calibration and the salinity determined by use of a Guildline Autosal model 8400 salinometer having a resolution of better than $0.0002^{\circ}/\text{oo}$ equivalent salinity at $35^{\circ}/\text{oo}$ and an accuracy better than $0.003^{\circ}/\text{oo}$ equivalent salinity. The value for the conductivity error was determined by subtracting the average of two or three Aanderaa readings from the conductivity value determined for the water samples.

b) Laboratory calibration results

The two current meters having the most extensive field calibration, serial numbers 1930 and 1939, were recalibrated in the laboratory and results are given in Table 6. Calibration was carried out at intervals spaced over several days with one to three values of error ("No. of Calibr." in Table 6) determined on each occasion. The mean value for each such occasion is given together with the scatter ("Calibr. Error" in Table 6). The temperature calibration error for both instruments remained essentially constant, scatter being less than the resolution of the instrument i.e. 0.005°C . Conductivity calibration errors determined for meter 1930 varied by up to 0.030 mmho/cm or four times the resolution of the meter (0.007 mmho/cm). For meter 1939 the corresponding variation was 0.018 mmho/cm . The difference in stability of the two meters may simply reflect the longer calibration period of meter 1930. This meter also shows a progressive decrease in the magnitude of the conductivity error which cannot be attributed to fouling of the cell during the twenty day test period as the conductivity sensor was brushed on each occasion when calibration was undertaken.

Subsequent to the laboratory calibration the conductivity cell on meter 1939 failed, however, the nature of the failure would cause us to believe the cell was operating properly during the field and laboratory work described in this report.

TABLE 6

Laboratory calibration of Temperature and Conductivity sensors

Serial No.	No. of T Calibr.	T Calibr. Error (1) $^{\circ}\text{C}$	No. of C Calibr.	C Calibr. Error (2) mmho/cm
1930	3	$0.048 \pm .003$	2	$-0.287 \pm .002$
	2	$0.049 \pm .002$	2	$-0.284 \pm .001$
	2	$0.046 \pm .001$	2	$-0.272 \pm .001$
	2	$0.047 \pm .001$	2	$-0.276 \pm .001$
	2	$0.050 \pm .001$	2	$-0.275 \pm .002$
	2	$0.048 \pm .001$	2	$-0.264 \pm .001$
	2	$0.047 \pm .001$	2	$-0.263 \pm .001$
	2	$0.050 \pm .001$	2	$-0.259 \pm .001$
	2	$0.049 \pm .001$	2	$-0.257 \pm .002$
mean		0.048		-0.271 $(-0.374^{\circ}/\text{oo})$
standard deviation		0.001		0.011
1939	1	-0.047	1	-0.028
	1	-0.051	1	-0.018
	1	-0.050	1	-0.030
	2	$-0.048 \pm .001$	2	$-0.026 \pm .008$
	1	-0.046	1	-0.036
mean		-0.048		-0.028 $(-0.039^{\circ}/\text{oo})$
standard deviation		0.002		0.005

(1) at a nominal temperature of -1.8°C .

(2) at a nominal conductivity of 26 mmho/cm for 1930 and 24 mmho/cm for 1939.

c) Comparison of field and laboratory calibration

Table 7 tabulates calibration errors for meters 1930 and 1939 as determined in the field and laboratory. For each parameter the mean calibration error and range of values is given. Figures 5 and 6 show the calibration error in the field and laboratory as a function of time.

The laboratory calibrations were carried out at single values of temperature and conductivity rather than at various values throughout the sensor range. The temperature values in the field and laboratory were very similar, about -1.8°C so that Table 7 is a comparison of errors at the same point. The conductivity in the field was nominally 26 mmho/cm which compares well with laboratory conditions for meter 1930, however meter 1939 was checked in water of approximately 24 mmho/cm conductivity. This may account for a portion of the greater conductivity discrepancy for meter 1939 but given the wide range of errors obtained in the field it is likely of secondary importance.

TABLE 7

Serial No.	Calib. Site	Comparison of Field and Lab Calibration			
		Mean T calibr. error	Range	Mean C calibr. error	Range
		$^{\circ}\text{C}$		mmho/cm	
1930	field	0.048	0.044 to 0.052	-0.260	-0.222 to -0.300
	lab	0.048	0.046 to 0.050	-0.271	-0.257 to -0.287
1939	field	-0.051	-0.049 to 0.053	-0.174	-0.112 to -0.233
	lab	-0.048	-0.046 to 0.051	-0.028	-0.018 to 0.036

Difference in mean field and lab calibration errors:

1930	0.000 $^{\circ}\text{C}$	-0.011 mmho/cm
1939	0.003	0.146

The temperature calibration error is consistent whether calibrated in the field or lab and the range of values is the best that could be expected given the resolution of the instrument. The conductivity measurements on the two meters give results which differ markedly. For meter 1930 the mean calibration errors differ by 0.011 mmho/cm. To some extent this degree of agreement may be fortuitous given the range of the limited number of field calibration points. The mean calibration errors for meter 1939 differ by 0.146 mmho/cm indicating that calibration of the conductivity cell in the laboratory may not provide a useful basis for the reduction of field data. The greater variation of field calibration values over values obtained in the laboratory reflects the vulnerability of the conductivity cell under field conditions as discussed earlier in this report.

d) The effect of the current meter rotor on conductivity readings

Tests were conducted on the effect of the current meter rotor on conductivity readings. The conductivity cell is mounted just over 1 cm from the rotor which contains either a bar or toroidal magnet. Any disturbance of the field of the inductive cell will affect the output of the cell, thus it was found that removing the rotor reduced the output of the cell by 0.022 mmho/cm. Clearly the rotor must be installed during any calibration check assuming the instrument is to be used with the rotor. Rotation of the rotor (and magnets) at speeds up to 2 rps (86 cm/sec equivalent velocity) had no effect on the conductivity reading.

e) Performance of conductivity cells with and without quartz liners.

The conductivity cells used on the nine current meters included both the quartz and newer quartz free models. The cells were installed as follows:

Meter Serial No.	C cell Serial No.	Cell Type
1930	1634	quartz
1931	1620	quartz
1932	1628	quartz
1936	2254	-
1939	1066	quartz
2466	1622	quartz
3223	2136	-
3228	2140	-
3387	2234	-

Table 4 provides information on the in situ stability of seven cells, four with quartz liners and three without. When grouped as to cell type the cells with quartz liners had a mean stability of 0.055 mmho/cm or greater than the overall mean of 0.039 mmho/cm, while the quartz free cells had a mean of 0.019 mmho/cm. Based on this small sample it appears that the newer cells are more stable by a factor of two or three; however, it should be noted that the most stable cell (2466) did contain a quartz liner. No meters containing quartz free cells were calibrated in the laboratory following the field deployment so we are unfortunately unable to check the applicability of laboratory calibration of this type of cell to field conditions.

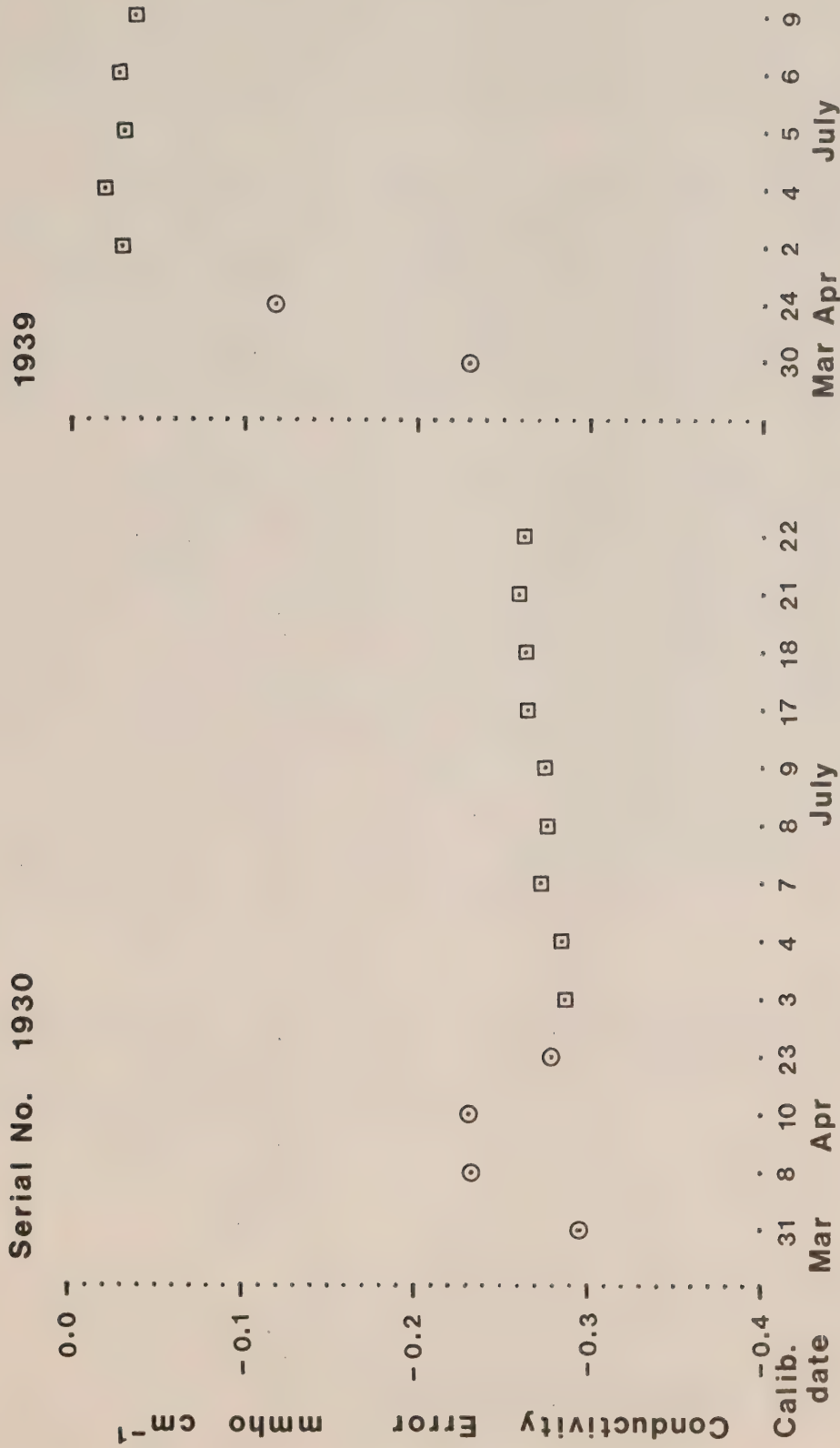


FIGURE 5. Conductivity calibration error in the field (\odot) and laboratory (\square) for two RCM-4 current meters.

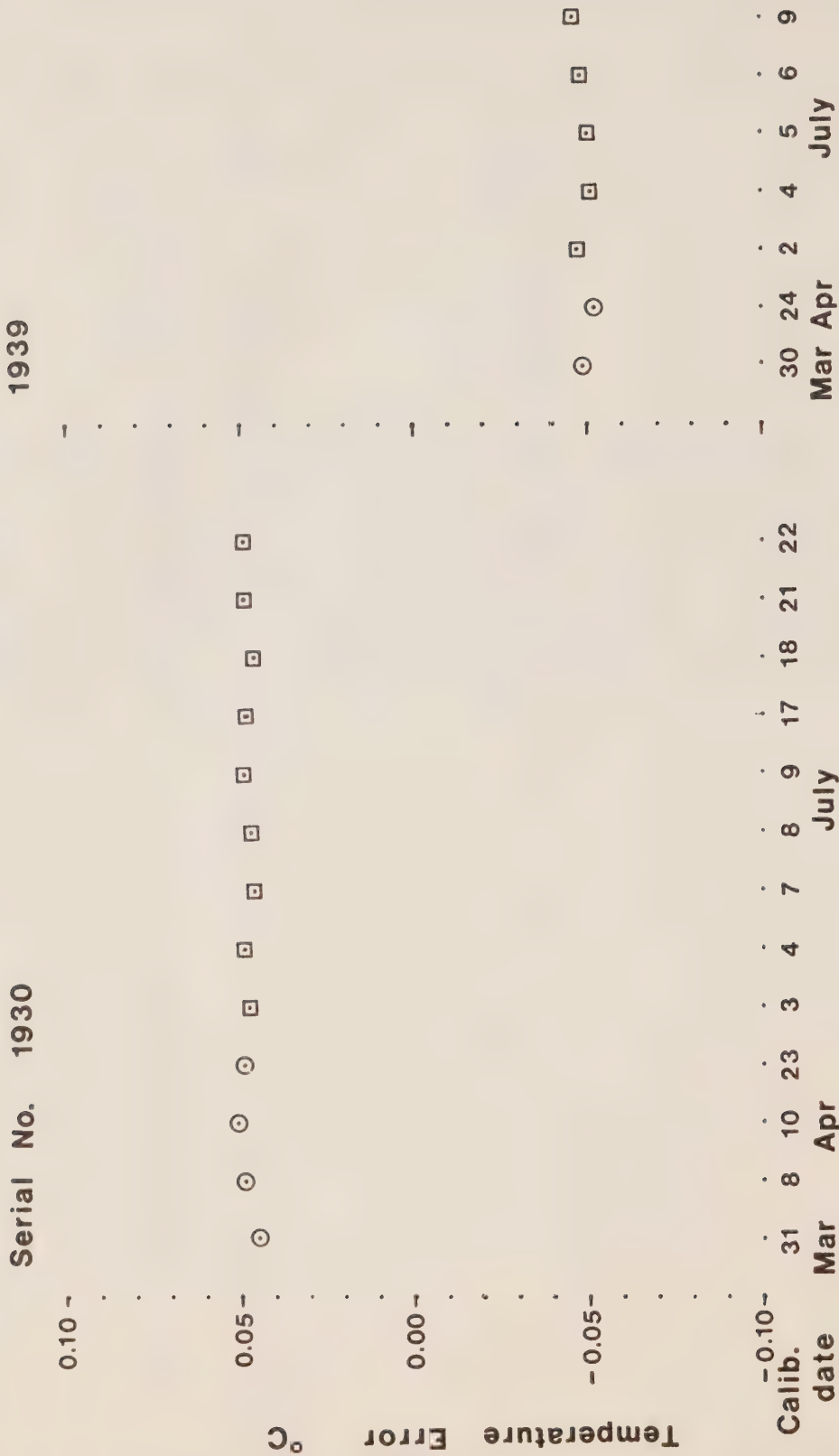


FIGURE 6. Temperature calibration error in the field (○) and laboratory (□) for two RCM-4 current meters.

4) TEMPERATURE SENSOR RESPONSE TIME

The response time of the temperature sensors on three Aanderaa meters was determined. All meters had the standard slow response sensors which according to the manufacturer's specification have a 63% response time of 12 seconds. The thermal capacity of the current meter itself, primarily the pressure case, precluded conducting meaningful temperature response measurements in the relatively small laboratory tank. As an alternative the meters were plunged from the air into the sea off the Institute's small boat wharf.

The meter was first connected to an Applied Microsystems Digi Print 701 readout unit through the standard waterproof bulkhead connector on the Aanderaa meter. On receipt of a start pulse from the Digi Print unit the meter scanned the temperature channel continuously with a nominal cycle time of 4 seconds. The actual cycle time was measured for each unit and was taken into account in the computation of the response time. After triggering the start pulse the meter was allowed to scan a few times and was then quickly plunged into the sea where recording continued until the Digi Print unit indicated the temperature sensor had reached equilibrium, usually a time span near 2 minutes.

The term response time is taken to be synonymous with the "time constant" or the time required for the sensor to read $1/e$ of the total temperature change assuming the change in temperature is an instantaneous step. In order to determine the size of the temperature step the initial and final temperatures had to be estimated. Figure 7 shows a plot of measured temperature versus time for the three meters tested. It is evident that the total temperature step seen by the sensor cannot be precisely determined. As the initial condition, i.e., the air temperature, was out of the range of the meter it was necessary to determine this temperature by extrapolation. Near the end of the temperature excursion the sensor sees a temperature anomaly due to the warming of water in contact with the instrument pressure case. This effect could have been minimized by holding the meter on its side and by keeping the meter in motion relative to the water. For purposes of calculating the time constant the final temperature was taken as the temperature existing after the anomalous temperature excursion occurred. The temperature, T at one time constant was calculated by the relationship:

$$T = T_0 - (1 - e^{-1})(T_0 - T_1)$$

where T_0 and T_1 are initial and final temperatures respectively as shown in Figure 8. The time at which the temperature T occurred was determined from the record of temperature versus time. The time constant or response time of the three meters was determined to be:

Serial No.	3395	T.C. = 12.5 ± 2 sec
	3388	12.1 ± 2
	1930	10.0 ± 2

The error limits are subjective based on our ability to determine the moment at which the temperature step occurred and possible errors in the initial and final temperatures. The values agree with Aanderaa's specification. Variations in response time between meters may result from inconsistency in the position of the thermistor element within its housing. Figure 8 also shows the temperature response curve of meter 3388 as measured and the theoretical response curve based on the calculated time constant.

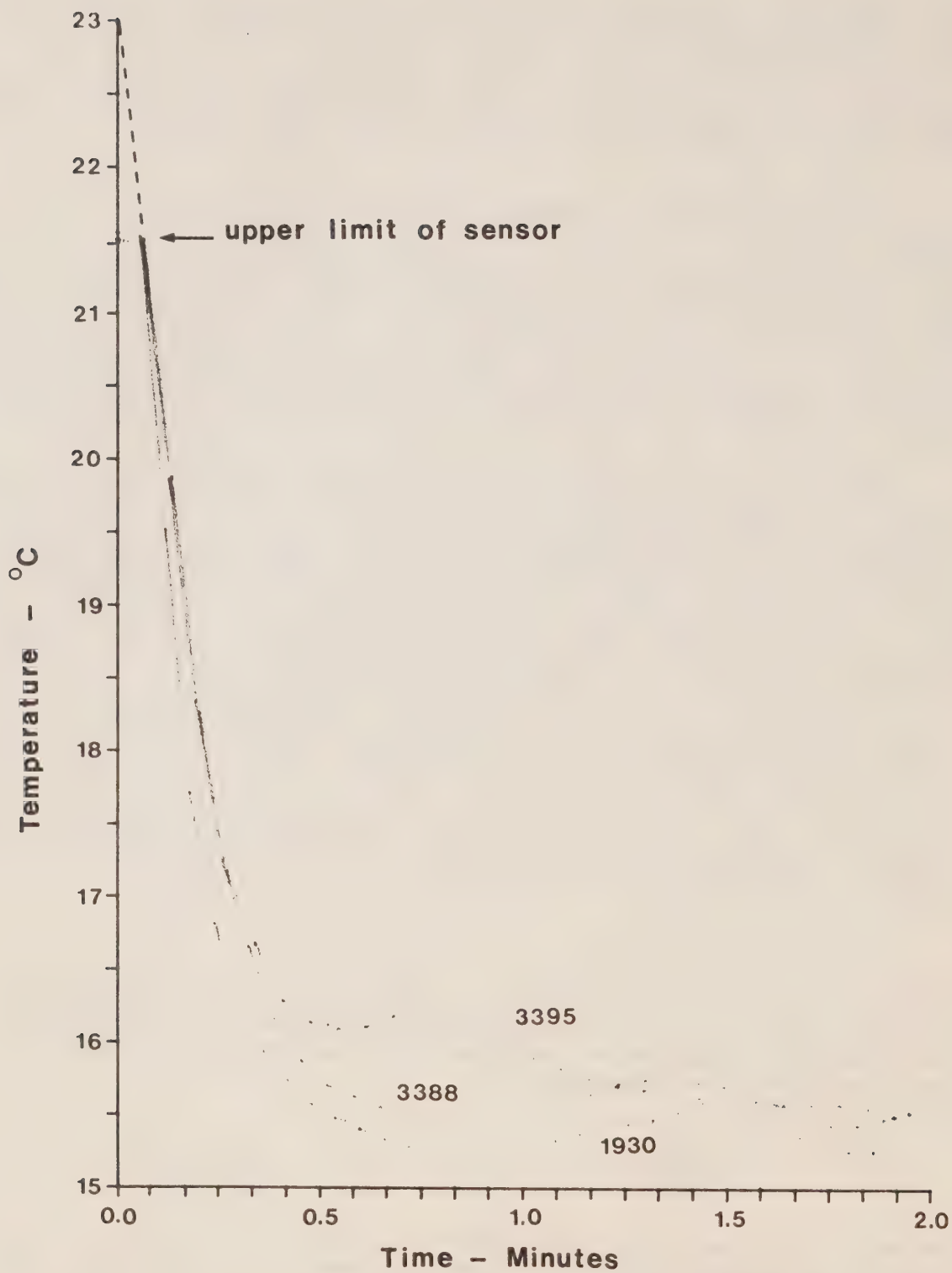


FIGURE 7. Temperature response curves for temperature sensors on three Aanderaa RCM-4 current meters.

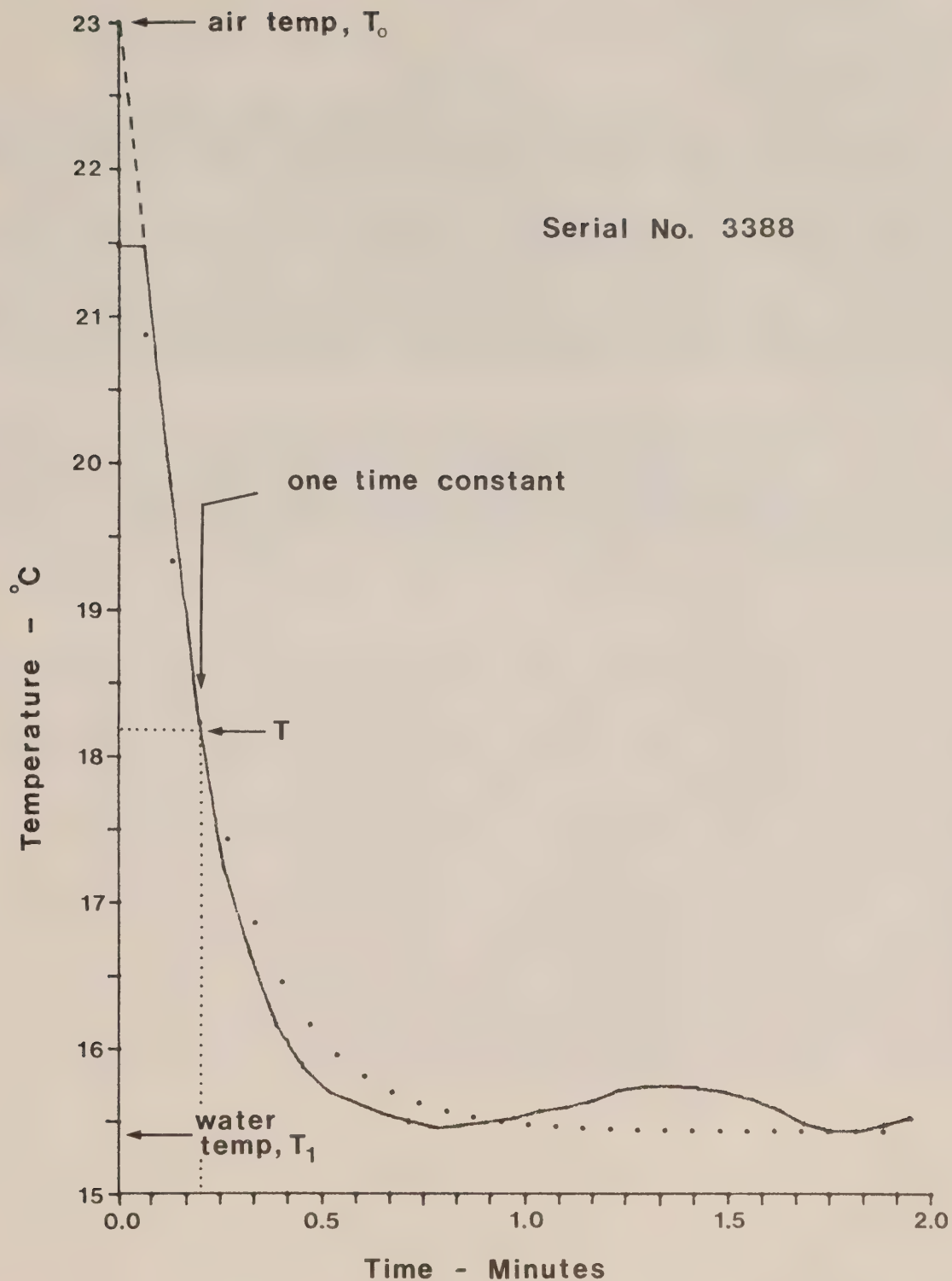


FIGURE 8. Temperature response curve as measured (—) and as calculated from the time constant (.....).

5. SUMMARY OF RESULTS

a) Temperature Sensor

With a modified temperature range of -2 to $+3^{\circ}\text{C}$ the uncalibrated temperature sensors on nine meters were accurate to better than 0.08°C . The mean error for all meters tested was 0.043°C with a standard deviation of 0.019°C . For periods up to 25 days the temperature sensor was stable to 0.015°C or less with a mean value of 0.006°C for all meters. The two meters recalibrated in the laboratory indicated no significant shift in temperature error indicating that laboratory calibration of the temperature sensor should permit correction of field data. The accuracy of temperature sensors when individually calibrated should be $\pm 0.015^{\circ}\text{C}$ or better for meters with a modified range. For the standard temperature range this corresponds to the resolution of the instrument of 0.02°C .

The slow response temperature sensor was found to have a 63% response time of 10 to 12 (± 2) seconds in agreement with the manufacturer's specification. If temperature changes are sufficiently abrupt the thermal capacity of the pressure case may thus affect the validity of the temperature measurements for a few minutes.

b) Conductivity Sensor

Nine Aanderaa RCM-4 meters with a nonstandard conductivity range of 23.0 to 30.7 mmho/cm recorded in the field for periods up to 25 days. In situ calibration indicated that conductivity cells with quartz liners were stable to 0.055 mmho/cm while those without liners were more stable at 0.019 mmho/cm. The sensors required conductivity corrections as great as 0.735 mmho/cm which is equivalent to a salinity correction of 1.3 ‰ at -1.80°C . The mean correction for all nine meters was -0.360 mmho/cm with a standard deviation of 0.263 mmho/cm. The two meters recalibrated in the laboratory gave inconsistent results with one meter differing from its conductivity error determined in situ by 0.011 mmho/cm while the second differed by 0.146 mmho/cm. Both meters had older cells with quartz liners. A series of checks of the conductivity circuitry using a resistive loop indicated that the output of some conductivity channels may be temperature dependent. The foregoing points indicate that in situ calibration of individual conductivity cells is essential in order to avoid errors in the order of 1 ‰ when comparing salinity differences determined from data collected by separate meters.

References

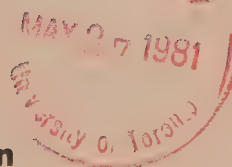
- Bell, W.H. 1979. A Three-dimensional Subsurface Mooring Model. Pac. Mar. Sci. Rept. 79-20, Institute of Ocean Sciences, Patricia Bay, Sidney, B.C.
- Huyer, A. 1975. Pressure effect on Aanderaa conductivity cells. Exposure, 3(5), pp 2-4.
- Lewis, E.L. and R.B. Sudar. 1972. Measurement of Conductivity and Temperature in the Sea for Salinity Determination, J. Geophys. Res. 77 (33): p. 6611.
- Perkin, R.G. and E.L. Lewis. 1980. The Practical Salinity Scale 1978: Fitting the Data. IEEE, J. Ocean Eng. 5(1): p. 9.
- Smith, P.C., T.R. Foote and R. Boyce. 1978. In Situ Calibrations of Temperature and Salinity for the Aanderaa RCM-5 Current Meter. Report Series, B1-R-78-7, September, 1978. Bedford Institute of Oceanography, Dartmouth, Nova Scotia.

CAI
EP321
-81R01

TURBULENCE IN THE EQUATORIAL PACIFIC OCEAN

By

W.R. Crawford and T.R. Osborn



**INSTITUTE OF OCEAN SCIENCES
Sidney, B.C.**



For additional copies or further information please write to:

Department of Ocean Science and Surveys

Institute of Ocean Sciences

P.O. Box 6000

Sidney, B.C. CANADA

V8L 4B2

TURBULENCE IN THE EQUATORIAL
PACIFIC OCEAN

By

W.R. Crawford and T.R. Osborn

Institute of Ocean Sciences

Sidney, B.C.

1981

Abstract

In January and February 1979 the CSS *Parizeau* served as a tropical wind observation platform during the First GARP Global Experiment. It was stationed at 150°W, within 3° of the Equator. Oceanographers from the Institute of Ocean Sciences used the occasion to survey the ocean currents, and results of the ocean microstructure measurements are given here.

We deployed a free-fall instrument called Camel to measure the vertical gradient of horizontal velocity at wavelengths between 1 and 50 cm. The dissipation range of ocean turbulence lies within these wavelengths, and the measurements permit an estimate of the rate of viscous dissipation of turbulent energy. The measurements show a maximum in the dissipation rate within 1/2° of the Equator, and uniformly lower rates beyond 1° of the Equator, as far as 3°S and 14°N. The vertical distribution of dissipation reveals a maximum between 40 and 120 metres depth, which coincides with the region of large average shear between the westward flowing South Equatorial Current at the surface and the Equatorial Undercurrent centred at 150m depth. Average dissipation rates at these depths are $10^{-3} \text{cm}^2 \text{sec}^{-3}$ ($= 10^{-4} \text{ Watts m}^{-3}$).

Table of Contents

	<u>Page</u>
Abstract	i
Table of Contents	ii
1. Introduction	1
2. Instrumentation and Data Analysis	2
2.1 General Description	2
2.2 Pressure Sensor and Fall Speed Computation	8
2.3 Shear Probes and Circuits	8
2.4 Temperature Measurement	12
2.5 Analysis of Shear Signals	14
2.6 Dissipation Profiles	18
3. Discussion	61
4. Acknowledgements	61
5. References	63

1. Introduction

During the cruise of the CSS *Parizeau* to the tropical Pacific in January and February, 1979, a free-fall ocean microstructure instrument "Camel" was deployed to observe small-scale velocity and temperature fluctuations. Most profiles were at 150°W, within 3° of the Equator, a position the *Parizeau* maintained for five weeks as a tropical wind observation platform during the first Special Observing Period of the First GARP Global Experiment (FGGE). The cruise track of the *Parizeau* is shown in Figure 1 along with positions of the Camel profiles, CTD, current meter, O₂ and nutrient samples taken on the cruise. The reader is referred to Curran (in preparation), for discussion of oceanographic measurements.

Camel, illustrated in Figure 2, is a 3m long free-fall vehicle described in several recent reports (Osborn and Crawford, 1977; Crawford, 1976; Osborn, 1978; Gargett and Osborn, 1978). It was built to house the airfoil shear probe, a special turbulence probe designed to examine microstructure scale (1 to 50 cm wavelength) velocity fluctuations in the ocean. Performance of this probe and its improvement in the past decade is described in several reports and papers (eg. Osborn and Crawford, 1980). Rather than repeat previous descriptions, this report will describe the instrument and its circuitry as it was during the *Parizeau* cruise, explain the analysis of data and present the results of the measurements.

The Equator is a unique region for ocean currents. The geostrophic balance which turns ocean currents at right angles to the pressure gradients is not possible. At the Equator in both Atlantic and Pacific Oceans, the Southeast Trade Winds force surface waters to the west. A sea surface slope is created with higher waters in the west. This water returns east through two "windows". One is in the convergence zone between the Southeast and Northeast trades at 4° to 10°N, and the other is at the Equator below the westward surface flow. Any eastward flow near the Equator is deflected toward the Equator, forming a strong undercurrent in the thermocline. This eastward flow is forced below the surface by a westward wind stress, and the turbulence which transmits this wind stress through the surface waters was observed in the Atlantic on a previous cruise in 1974 with Camel (Crawford, 1976).

It is possible with the microstructure velocity measurements to construct an energy balance for both the turbulent fluctuations and the large-scale zonal flow. From such an energy balance, coefficients of eddy viscosity and diffusivity can be computed (Crawford and Osborn, 1979b; Osborn, 1980).

2. Instrumentation and Data Analysis

2.1 General Description

The airfoil shear probe has evolved steadily in the ten years of its use for ocean turbulence measurements. It has been mounted on several free-fall vehicles and a submersible, and designs for expendable probes are in the works. We describe in this section the status of Camel during the FGGE cruise and document the probe and circuitry characteristics to enable later analysis of the data and possibly to guide future microstructure experimenters in the operation of free-fall vehicles and analysis of their data. The results of the 1979 FGGE cruise of CSS *Parizeau* are presented in Section 3.

Camel is just over 3m long, built around a 20.3 cm diameter aluminum tube, and when assembled weighs 700 Nt in air. Its slim profile when falling through the water forced us to mount six brushes around the main cylinder to slow its fall speed. With the brushes it falls at 40 cm/sec when 12 Nt negatively buoyant in seawater. At the Equator, in the Pacific, fall speeds of 50 and 75 cm/sec were used, with the lower fall speed giving lower noise levels.

Two airfoil shear probes and a microbead thermistor are mounted at the lower end of Camel, as illustrated in Figure 3. The shear probes are set perpendicularly to sense the two orthogonal components of velocity gradient: $\partial u_1 / \partial z$ and $\partial u_2 / \partial z$. A thermistor is mounted to the side on a separate support. In the upper end cap is a Vibrotron pressure sensor. The two shear signals, temperature, temperature gradient and pressure are converted to standard FM signals, multiplexed and transmitted up an expendable wire length (XWL) to the ship where they are recorded, and converted to analogue signals to be plotted in real time on strip charts.

A typical profile during the cruise took place at 1000 local time just prior to the noon launch of the Omegasonde balloon for the FGGE high altitude wind observation program. Whenever possible we repeated profiles as soon as weights and release pins could be reloaded. Our major problem at the Equator was to reach the desired depth before the salt block release dissolved, bringing Camel to the surface prematurely, or before the XWL reached the end of the spool and broke. The two spools which form the XWL have 450 and 1500 m of wire, and either one can be sent down on Camel. However the large shear between the South Equatorial Current and the under-current carries the ship far from the launch site while Camel free-falls. At a fall speed of 50 cm/sec the wire broke near 300 m depth. We increased the fall speed to 75 cm/sec and successfully reached 400+ metres, but at the cost of increased noise levels in the shear signals due to vibrations. For the later profiles the speed was reduced to 50 cm/sec, which gave satisfactory depths away from the Equator.

For daylight operations, two radios and a light in the upper endcap permitted easy recovery. The 27 MHz hand-held radio direction finder gave bearings accurate to 5° when held at the bow of the *Parizeau* (the only ship on which this device has worked). For the few night launches, one radio was replaced by a light to give two Xenon flashers which were visible for miles. Sighting Camel was easier at night but ship manoeuvring was more difficult as distances to the flashing lights were difficult to judge. For

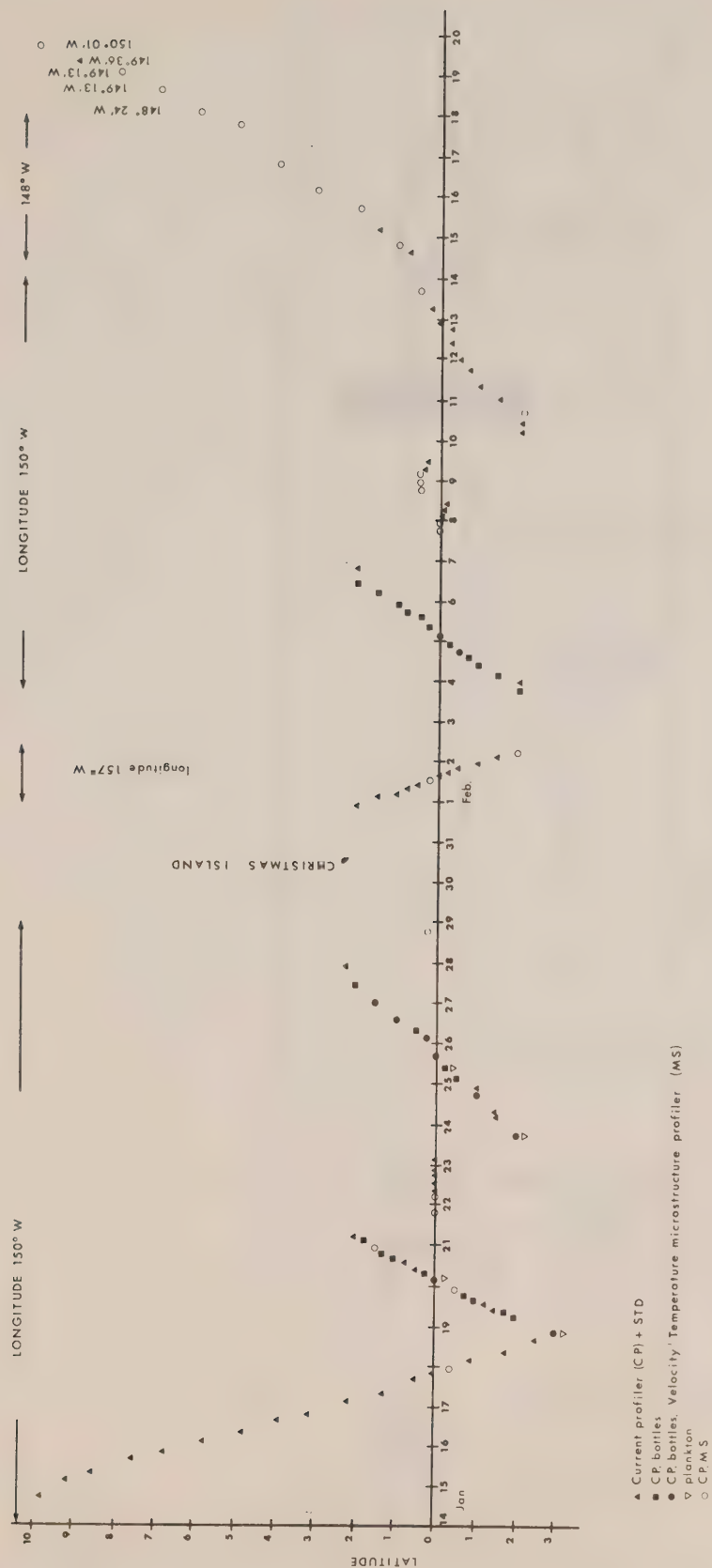


Figure 1. Cruise of the CSS *Pariseau*, January 14 to February 20, 1979.

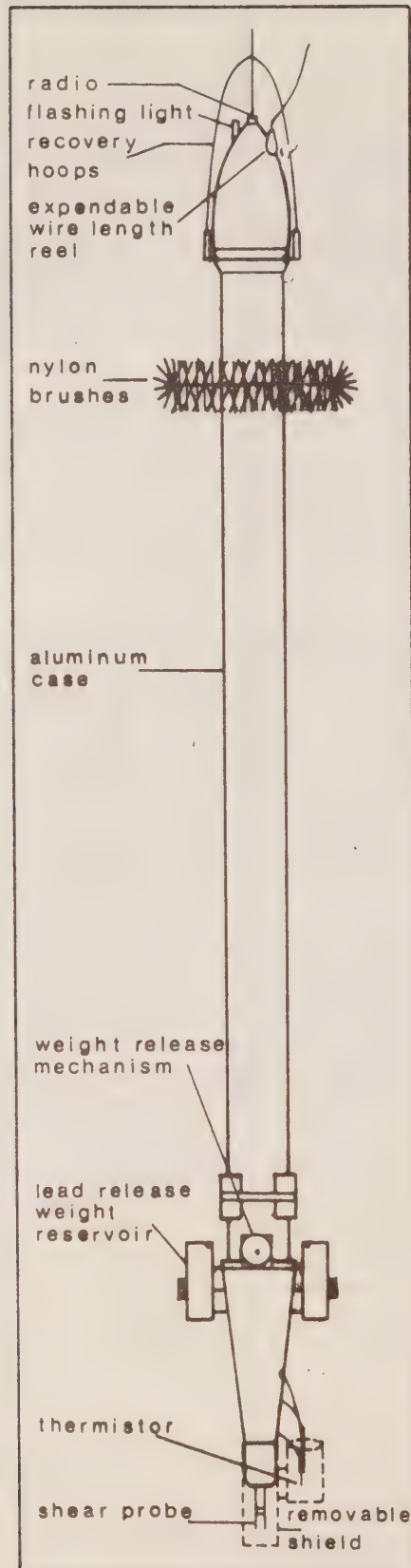


Figure 2. Camel.

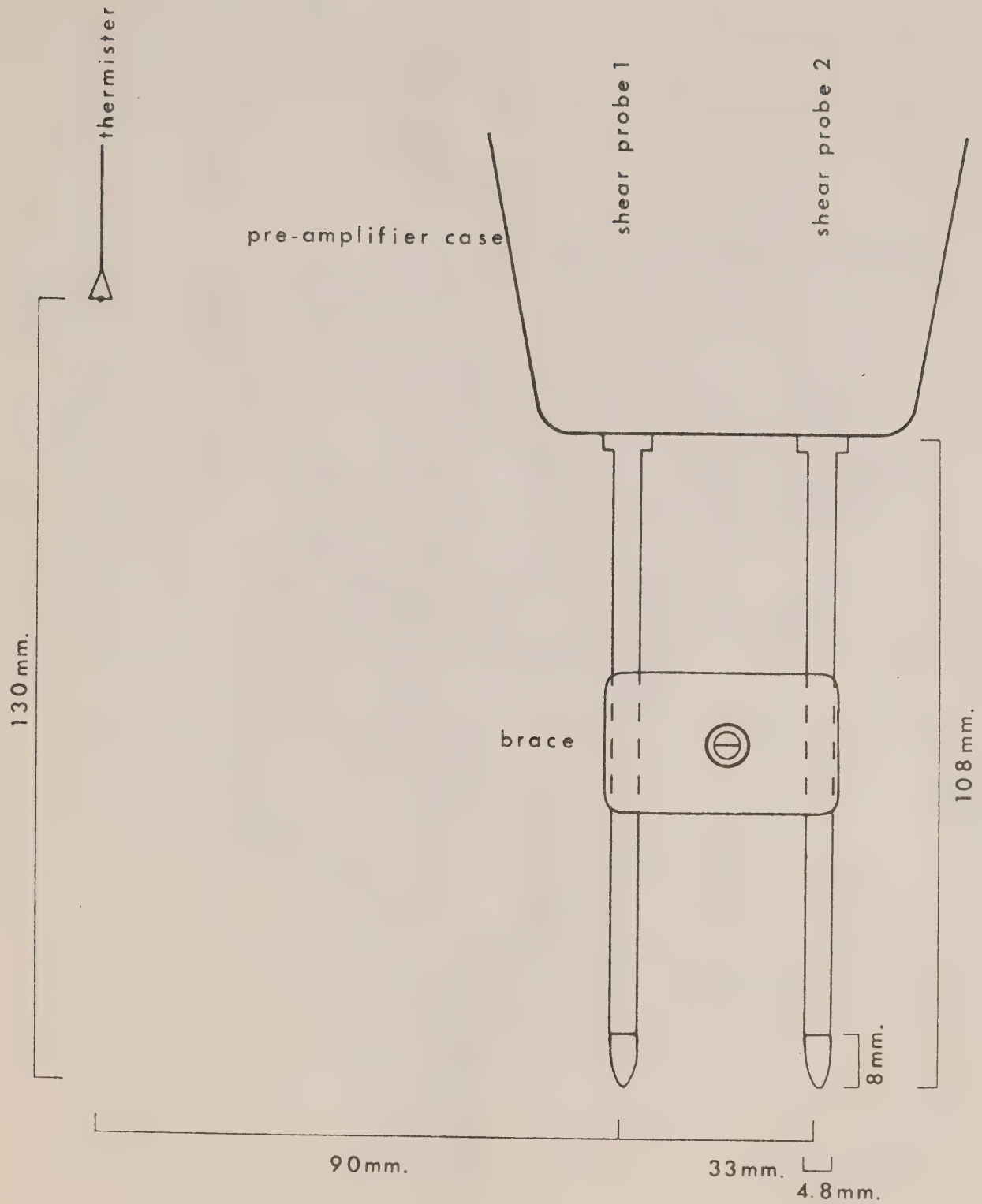


Figure 3. Sketch of probe assembly. The streamlined brace around the shear probes was added to reduce vibrations.

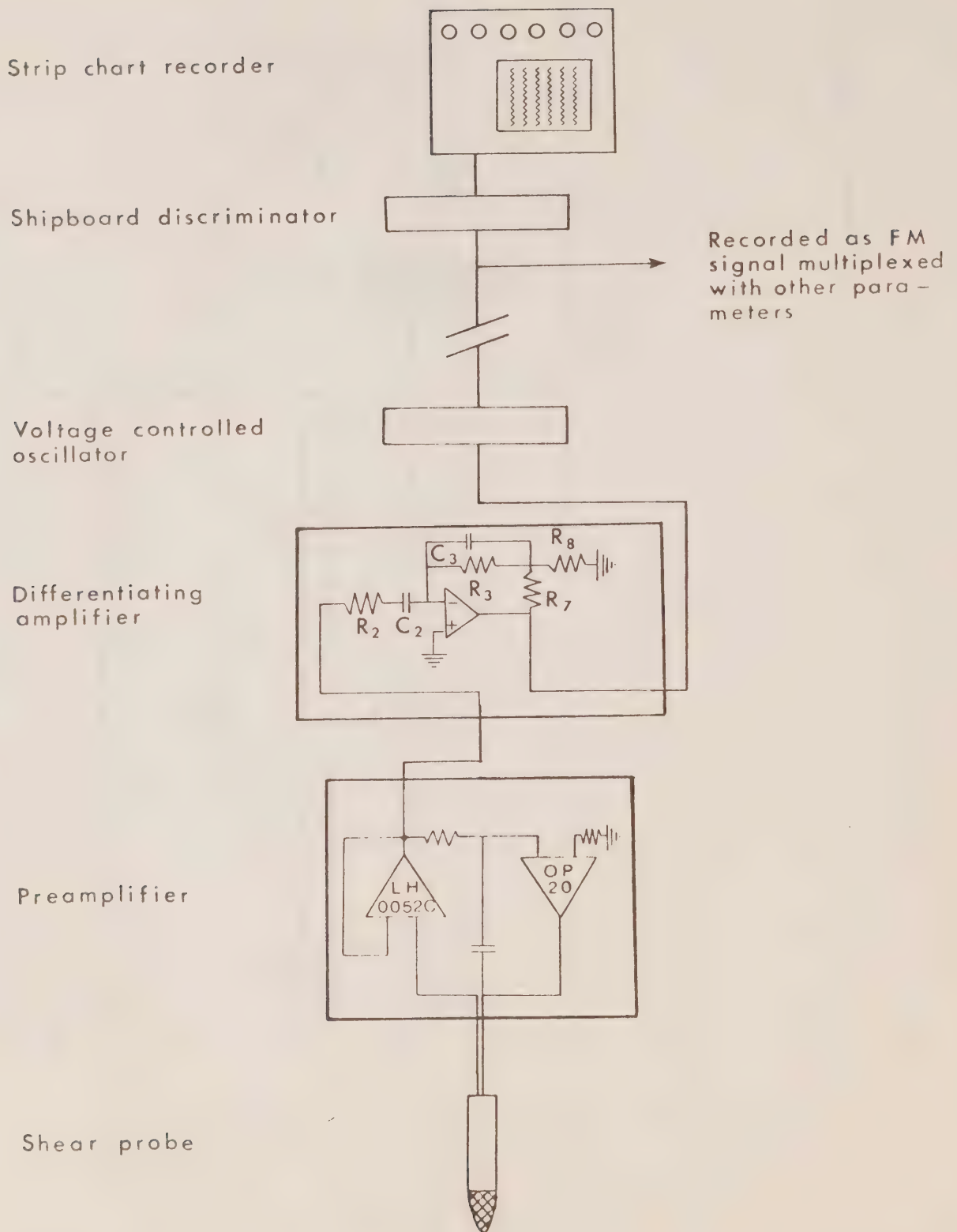
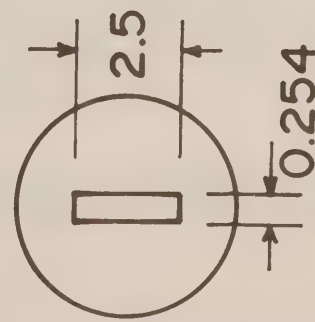
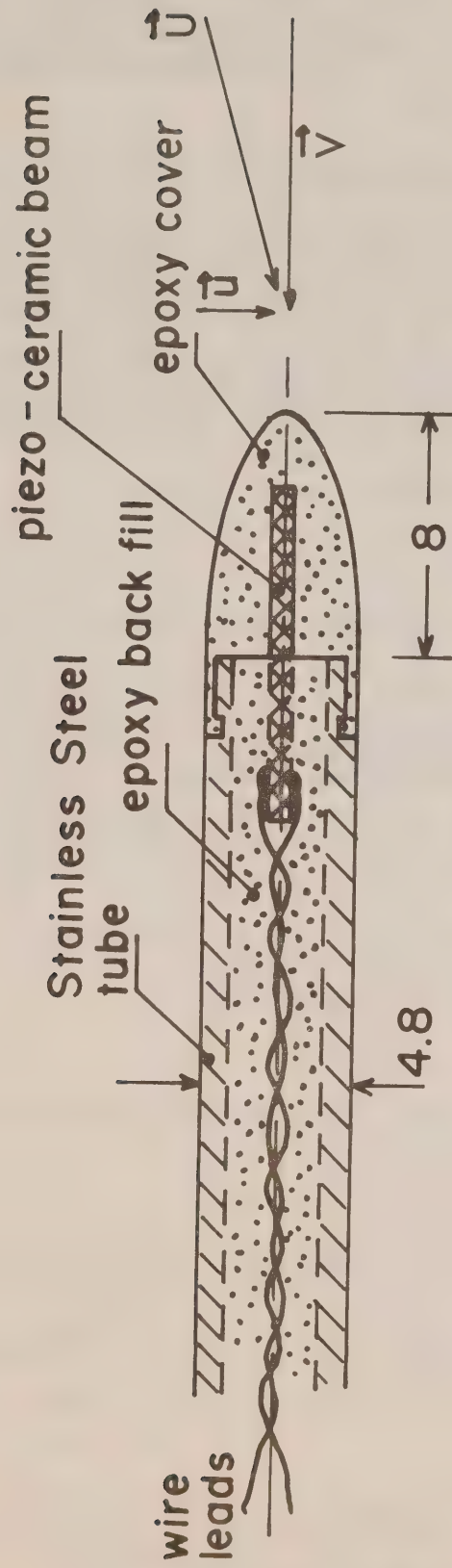


Figure 4. Signal processing for one shear probe.



V = Fall speed
 u = horizontal velocity
 U = Total speed relative to probe

Figure 5. Shear probe.

this reason most launches were made during daylight hours.

In all, 48 profiles were attempted with Camel, and 9 profiles were made using smaller temperature microstructure instruments called Pumpkins. Only the Camel data are discussed here.

2.2 Pressure Sensor and Fall Speed Computation

A Vibrotron 1000 psi (=680 dbar) pressure sensor in the upper end cap transmitted a pressure signal to the surface. Spikes were removed from the signal with a first differencing algorithm, and the cleaned record was smoothed with a spline function. For each record of 1024 or 768 (for fall speeds of 50 or 75 cm/sec respectively) the average pressure, average fall rate of Camel, and average temperature were computed, and stored on tape. These were used in the computation of dissipation described in Section 2.5. Uncertainties in the fall speed of 2 to 3 cm/sec due to internal waves can be expected (Desaubies and Gregg, 1978).

2.3 Shear Probes and Circuits

Piezo-ceramic crystals in the shear probes (shown in Figure 5) sense horizontal forces caused by motion of water relative to the probes. They are mounted at the forward end of Camel and fall vertically through the water to sense horizontal velocities. The probe and preamplifier are considered together as one unit, and are calibrated together. The preamplifier in use for this cruise and the calibrations are sketched in Figure 4. It has high input impedance to permit the probe to measure variations at frequencies as low as 0.1 Hz. On later cruises this preamplifier became unstable and was replaced.

Figure 5 shows the probe with a flow U directed at it, at angle α . The velocity can be considered as two components V and u . Potential flow theory gives the horizontal force on the probe as:

$$F = A\rho U^2 \sin 2\alpha \quad (1)$$

where A is a constant varying with the cross-sectional area of the probe. This formula can be rewritten as:

$$F = A\rho U^2 (2\sin\alpha\cos\alpha) = 2A\rho Vu \quad (2)$$

The piezo-ceramic crystal in the probe generates a voltage proportional to the bending moment. Calibration is accomplished by directing a submerged vertical jet of water at a spinning probe, which is inclined at 30° intervals. Output from the probe is measured on an rms voltmeter, and graphs of the quantity $\frac{E_{rms}}{\rho U^2}$ vs $\sin 2\alpha$ are plotted. The slope of this line is taken as the sensitivity S

$$E_{rms} = S\rho U^2 \sin 2\alpha \quad (3)$$

$$E = \sqrt{2}E_{rms} = 2\sqrt{2} S\rho Vu \quad (4)$$

A graph of the calibration of a probe is shown in Figure 6. Departure of actual flow from potential flow causes the upward curvature of the line. The slope of this line $d(E_{rms}/\rho U^2)/d(\sin 2\alpha)$ fitted to a cubic spline curve is also plotted, and from it one sees that sensitivity increases at larger angles of attack.

To determine expected angles at the Equator, we take a typical large scale shear there, which is 0.01 sec^{-1} . We expect (Osborn and Crawford, 1977) that a point on Camel 2m up from the tip will have no motion relative to the surrounding water. The probe tip will move at a horizontal speed of $(0.01)(200) = 2 \text{ cm/sec}$ and at a vertical fall speed of 50 cm/sec . The angle of attack is 2.3° , at which the sensitivity will be less than 2% greater.

Uncertainties in the calibration process due to flow speed uncertainties, angular adjustments, etc. introduce uncertainties of $\pm 10\%$ in the value of S .

Signals from the preamplifier when fitted onto Camel are passed to a differentiating amplifier which is drawn in Figure 4. Gain and rolloff were altered throughout the cruise to match the changes in fall speed. These are documented in Table 1. Gains are determined from the circuit calibration rather than the nominal circuit component values. The output of the amplifier is:

$$E_a = \frac{j\omega R_3 C_2}{(1+j\omega C_2 R_2)(1+j\omega C_3 R_3)} \frac{R_7 + R_8}{R_8} E \quad (5)$$

where E is the preamplifier output. The gain is stepped up by a factor $4.0/2.5$ in passing through the voltage controlled oscillator and the shipboard discriminator. Final output on ship is:

$$\begin{aligned} E_s &= \frac{4.0}{2.5} \frac{R_3 C_2}{(1+j\omega C_2 R_2)(1+j\omega C_3 R_3)} \frac{R_7 + R_8}{R_8} j\omega E \\ &= \frac{4.0}{2.5} \frac{R_3 C_2}{(1+j\omega C_2 R_2)(1+j\omega C_3 R_3)} \frac{R_7 + R_8}{R_8} 2\sqrt{2} S \rho V \frac{du}{dt} \end{aligned} \quad (6)$$

The time derivative du/dt is converted to a space derivative by division by V , the fall speed.

$$\frac{du}{dZ} = \frac{1}{V} \frac{du}{dt} \quad (7)$$

The shear is now

$$\frac{du}{dZ} = \frac{2.5}{4.0} \frac{(1+j\omega C_2 R_2)(1+j\omega C_3 R_3)}{2\sqrt{2} S \rho V^2 R_3 C_2} \frac{R_8}{R_7 + R_8} E_s = \frac{G(1+j\omega C_2 R_2)(1+j\omega C_3 R_3) E_s}{S \rho V^2} \quad (8)$$

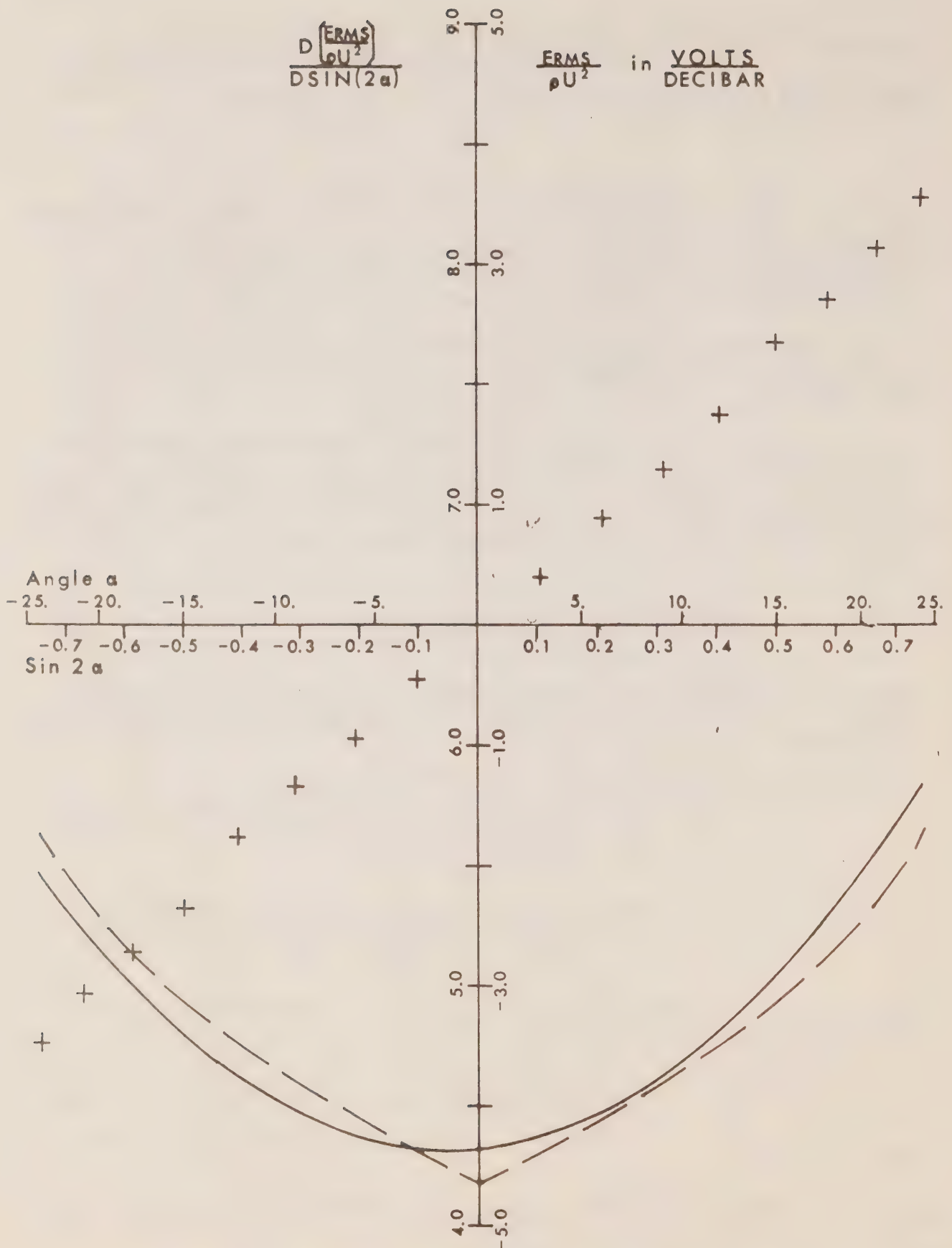


Figure 6. Shear probe calibration. Crosses are calibration points; solid line is a spline fit to the function $D \left(\frac{ERMS}{\rho U^2} \right) / D(\sin 2\alpha)$, dashed line is a least squares fit to this function.

Table 1a. Nominal values of circuit components in shear probe circuits.
S1 and S2 denote the circuits for $\partial u_1/\partial Z$ and $\partial u_2/\partial Z$ respectively.

Profile	R_2	C_2	R_3	C_3	R_7	R_8	G
4,5 S1,S2	2.74K	1.0 μ fd	162K	.015 μ fd	10K	499	0.065
6-18 S1,S2	2.74K	1.0 μ fd	162K	.015 μ fd	10K	1K	0.124
19-45 S1,S2	2K	1.0 μ fd	100K	.015 μ fd	10K	1K	0.201
46-57 S1	2.74K	1.0 μ fd	162K	.015 μ fd	10K	787	0.097
46-57 S2	2.74K	1.0 μ fd	162K	.015 μ fd	10K	499	0.065

Table 1b. Shear Probes and their sensitivities.

Profiles	Probe Channel 1	S_1	Probe Channel 2	S_2
4-6	9A	3.7×10^{-5}	3B	4.0×10^{-5}
7-18	3A	3.4×10^{-5}	3B	4.0×10^{-5}
19	14A	4.1×10^{-5}	4B	3.7×10^{-5}
20-27	3A	3.4×10^{-5}	3B	4.0×10^{-5}
28	3A	3.4×10^{-5}	14A	4.1×10^{-5}
33-38	5B	3.1×10^{-5}	4B	3.7×10^{-5}
46	5B	3.1×10^{-5}	6B	4.3×10^{-5}
47	7B	3.5×10^{-5}	6B	4.3×10^{-5}
48	3B	4.0×10^{-5}	10B	3.8×10^{-5}
51	3B	4.0×10^{-5}	6B	4.25×10^{-5}
52-57	6B	4.3×10^{-5}	3B	4.0×10^{-5}

Bracketed quantities in the numerator represent low pass filters required to prevent signal saturation by high frequency vibrations of Camel. The signal is proportional to du/dZ , the vertical gradient of the horizontal velocity.

High frequency short wavelength response of the airfoil shear probe is best given by comparison with a hot film probe. Preliminary results of recent comparisons of these two systems in a very strong turbulent flow in Knight Inlet by Gargett (personal communication) indicate that the shear probe can resolve the turbulent dissipation up to values of $0.01 \text{ cm}^2/\text{sec}^3$, and two-thirds of the dissipation when $\epsilon = 0.1 \text{ cm}^2/\text{sec}^3$. As the turbulence becomes more active and dissipates at a higher rate, the wavelengths at which large shears are found decrease. In isotropic turbulence the peak of the shear dissipation spectrum is at a wavenumber:

$$k = 0.15 k_s = 0.15 \epsilon^{1/4} \nu^{-3/4} \quad (9)$$

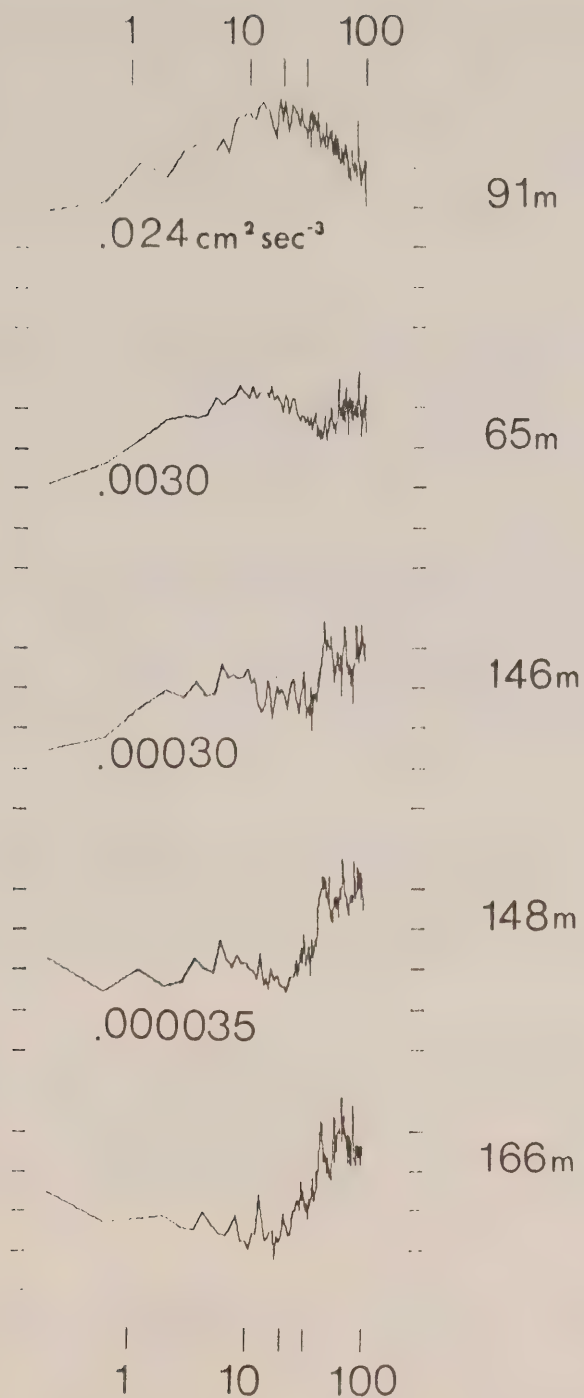
where ϵ is the dissipation rate and ν is the kinematic viscosity. With $\epsilon = 0.1 \text{ cm}^2/\text{sec}^3$ and $\nu = 0.014 \text{ cm}^2/\text{sec}$, $k = 2 \text{ cm}^{-1}$ and the corresponding wavelength is $\lambda = 2\pi/k = 3 \text{ cm}$. To resolve a $0.1 \text{ cm}^2/\text{sec}^3$ dissipation, a probe must sense fluctuations to wavelengths of one-third the peak, which is 1 cm.

The long wavelength limit of the shear probe is limited by thermal response of the probe. Except in regions of large temperature change and low dissipations this effect is not important at scales smaller than a metre. However, in such regions the voltage generated at low frequencies by temperature changes in the probe contaminates the signal, forces a 50 cm long wavelength limit to variance estimates, and is the limiting factor in low level dissipation resolutions.

2.4 Temperature Measurement

The temperature circuit consists of a simple bridge preamplifier with a 0.15 mm diameter microbead thermistor serving as one of the resistors. The bridge is designed for maximum linearity of output voltage versus temperature. The signal from the preamplifier passes through a differentiating amplifier, and both the input signal (temperature) and output (temperature gradient) are transmitted to the ship. We calibrate the temperature signal by comparing output from the Camel against the CTD temperatures. Output is linear to within 0.5°C . No extensive analysis was attempted on these signals. Both are plotted in the profiles of Figures 8 to 44.

Thermistors failed for a variety of reasons, or were replaced when output data was of poor quality. Five different thermistors were used, with one surviving for seventeen profiles.



Logarithm of the frequency in Hertz.

Figure 7. Shear spectra from Profile 17, Channel 2. Each spectrum represents a 2.3m vertical section.

2.5 Analysis of Shear Signals

The two shear signals, temperature and its gradient and pressure were stored as FM signals on one of four channels on 1/4" magnetic tape, using a Hewlett Packard 3960B recorder. A 14.5 KHz reference signal was recorded on a separate channel. Upon playback of these tapes, eight signals were passed through a 16 bit digitizer onto 1/2" - 9 track computer tape at 200 data points per second. These eight signals were the five noted above plus low passed shear signals and also a ground. The latter was introduced to examine the cross-talk between channels of the digitizer, which was later found to be negligible.

The unfiltered shear signals were removed from the combined digitizer records and Fast Fourier Transforms (FFT's) were computed on successive records of 1024 points when fall speeds were 50 cm/sec and on 768 points for 75 cm/sec fall speeds, giving vertical intervals of 2.6 and 2.9 metres respectively. These spectral values were corrected for the two filters in the differentiating amplifier which attenuate the high frequency signals.

The sum of squares of the sine and cosine terms of each FFT transform value gives the variance of the signal at that frequency. The sum over all frequencies gives total variance. To determine the variance within the band of frequencies at which the signal dominated over thermal and vibrational noise we plotted the spectra, printed out cumulative sums of variance and plotted long strip charts of the original time series of the data.

To plot the spectra, each squared transform value was multiplied by its frequency, and band averages of four transform values were computed for the first eight transform values, then averages of eight were computed for the remaining ones, and all were plotted on logarithmic scales versus the logarithm of frequency. Examples are shown in Figure 7, all taken from profile 17, channel 2.

Tickmarks across the top and bottom of Figure 7 represent frequencies of 1, 10, 20, 30 and 100 Hz. Units on the vertical scale are consistent from one plot to the next, but arbitrary. No attempt was made to calibrate the vertical scale as these plots served only to separate signal from noise. The value of ϵ , the rate of viscous dissipation, is computed from the variance of the $\frac{\partial u_1}{\partial z}$ and $\frac{\partial u_2}{\partial z}$ signals.

The upper spectrum, with a rate of viscous dissipation equal to $0.024 \text{ cm}^2/\text{sec}^3$, shows a strong signal dominating the noise up to a frequency near 90 Hz where a noise spike protrudes. In the second spectrum the dip in spectral values near 40 Hz is taken as the beginning of noise domination, while the next two show crossovers from signal to noise near 20 Hz and 10 Hz respectively. The bottom spectrum is assumed to be entirely dominated by noise; from it one can see that the shear signal falls spectrally into the gap between high frequency vibrational noise and low frequency thermal noise.

The upper four spectra show usable data. To compute the dissipations noted in the Figure, the two lowest band averages were discarded, and the cumulative variance of remaining successive band averages up to 50 Hz were printed out and the sum at the band closest to 20 Hz frequency was stored in a computer file. Then each plotted spectrum was examined to determine the upper limit of signal. For spectra such as the 91 m one in Figure 15 the sum of variance at 20 Hz was replaced by the 50 Hz sum. In the third and fourth spectra, the 10 Hz sum was substituted. Every spectrum of each of the two shear channels was examined to determine the upper limit of summation; in all, 10^4 spectra were examined.

The Nyquist frequency is 100 Hz, and to check that higher frequencies were not aliased back to frequencies below 100 Hz, we also computed spectra of the data which had been filtered through a 40 Hz Bessel filter before digitizing. At frequencies below 50 Hz they differed only by the filter rolloff and we assumed no aliasing problems up to 50 Hz.

The noise level was also determined for each channel from the printed sums and plots. Normally the low frequency thermally induced noise in the thermocline sets the noise limit for the profile, although high frequency vibrational noise in the 75 cm/sec profiles was often so high that entire profiles were unusable. The spectrum from 148 metres in Figure 7 illustrates the low dissipation spectrum in a high thermal noise region. The small spike at 14 Hz could be signal or noise, but examination of surrounding spectra with lower signal levels showed consistent 14 Hz spikes, such as found at 166 m in the fifth spectrum. For this reason summation stopped at 10 Hz.

In the same spectrum the large amplitude of the first transform value can be attributed to thermally induced noise, generated by large temperature changes in the thermocline. When this thermal shock effect is large it is difficult to distinguish signal from noise. At that point we ceased making dissipation estimates.

As a final check, the digitized data was run through a digital to analogue converter and plotted. A spike was introduced into the beginning of every 1024 or 768 point record, whichever one was appropriate, and the pressure, temperature gradient and the shears and filtered shears were all plotted on a high speed Brush recorder. Any noise spikes in the shear channels could be identified and the spectral estimate of variance from that record was discarded.

The observed peak of the universal dissipation spectrum G_2 is at a wavenumber $k_p = 0.15 k_s$ where k_s is the Kolmogoroff wavenumber given by $k_s = (\epsilon \nu^{-3})^{1/4}$. As dissipation ϵ increases, the peak moves to higher wavenumbers as the one-quarter power, of k , a slow rate which permits observations of widely differing values of ϵ with a narrow band of shear observations. With our band of 50 cm to 1 cm wavelength, losses at the long wavelength (small wavenumber) portion of the spectrum are 10% for dissipations of $10^{-5} \text{ cm}^2 \text{ sec}^{-3}$ at temperatures of 25°C (temperature controls viscosity which alters the value of k_s slightly). At 15°C the loss is 13%.

Computation of $\overline{\epsilon}$

The rate of viscous dissipation of turbulence varies with the spatial gradients of velocity:

$$\overline{\epsilon} = \frac{15\nu}{2} \overline{\left\{ \frac{\partial u_i}{\partial x_j} + \frac{\partial u_j}{\partial x_i} \right\}^2} \quad (10)$$

which may be written as:

$$\begin{aligned} \overline{\epsilon} = & \overline{\left(\frac{\partial u_1}{\partial x_1} \right)^2} + \overline{\left(\frac{\partial u_2}{\partial x_2} \right)^2} + \overline{\left(\frac{\partial u_3}{\partial x_3} \right)^2} \\ & + \overline{\left(\frac{\partial u_1}{\partial x_2} + \frac{\partial u_2}{\partial x_1} \right)^2} + \overline{\left(\frac{\partial u_2}{\partial x_3} + \frac{\partial u_3}{\partial x_2} \right)^2} + \overline{\left(\frac{\partial u_3}{\partial x_1} + \frac{\partial u_1}{\partial x_3} \right)^2} \end{aligned} \quad (11)$$

When turbulence is isotropic, which may be expected in uniformly mixed, actively turbulent waters above the Undercurrent (Crawford, 1976), then the above equation is simplified greatly:

$$\overline{\left(\frac{\partial u_1}{\partial x_1} \right)^2} = \overline{\left(\frac{\partial u_2}{\partial x_2} \right)^2} = \overline{\left(\frac{\partial u_3}{\partial x_3} \right)^2} \quad (12)$$

$$\overline{\left(\frac{\partial u_1}{\partial x_2} \right)^2} = 2 \overline{\left(\frac{\partial u_1}{\partial x_1} \right)^2}, \text{ etc.} \quad (13)$$

$$2 \overline{\left(\frac{\partial u_1}{\partial x_3} + \frac{\partial u_3}{\partial x_1} \right)^2} = - \overline{\left(\frac{\partial u_1}{\partial x_1} \right)^2}, \text{ etc.} \quad (14)$$

The formula for $\overline{\epsilon}$ can be written:

$$\overline{\epsilon} = \frac{15\nu}{2} \overline{\left(\frac{\partial u_1}{\partial x_3} \right)^2} = \frac{15\nu}{2} \overline{\left(\frac{\partial u_2}{\partial x_3} \right)^2} \quad (15)$$

If u_1 and u_2 represent horizontal velocities and x_3 the vertical direction, then equation 15 shows how to compute the viscous dissipation from the variance of the shear measured by the airfoil shear probes. In practice, both channels were input to the computation of $\overline{\epsilon}$:

$$\bar{\epsilon} = \frac{15\nu}{4} \left\{ \overline{\left(\frac{\partial u_1}{\partial x_3} \right)^2} + \overline{\left(\frac{\partial u_2}{\partial x_3} \right)^2} \right\} \quad (16)$$

If a channel displayed a noise spike, which often occurred following sharp temperature changes in the water column, then only one channel could be used and $\bar{\epsilon}$ was computed from equation 15. If both channels displayed spikes, no dissipation was computed.

To compute $\bar{\epsilon}$ from the digitized record, recall that the value of $\partial u_1 / \partial x_3$ (or $\partial u_1 / \partial Z$) in terms of the voltage E_s is:

$$\frac{\partial u_1}{\partial Z} = \frac{G}{S\rho V^2} (1+j\omega C_2 R_2)(1+j\omega C_3 R_3) E_s \quad (8)$$

The filters denoted by the two expressions in brackets have been compensated for in the Fourier Transform summations and can be removed from the equation. The remaining equation is rewritten:

$$\frac{\partial u_1}{\partial Z} = \frac{G}{\rho S V^2} E_s \quad (17)$$

where G is computed for each different circuit configuration. The voltage E_s is digitized at 1 volt = 8192 bits, and the variance of a signal can be computed from Fourier Transform values by the formula:

$$\sigma^2 = \frac{C_1^2}{N^2} + \frac{C^2 (N/2)+1}{N^2} + \frac{2}{N^2} \sum_{j=2}^{N/2} C_j C_j^* \quad (18)$$

where N is 768 or 1024.

We can neglect the first two terms on the right side as they were always discarded in the summation to compute variance. Hence, the dissipation was computed by the formula:

$$\bar{\epsilon} = \frac{15\nu}{4} \left(\frac{G}{8192 \rho S V^2} \right)^2 \frac{2}{N^2} \left(\sum_j \underbrace{C_j C_j^*}_{S1} + \sum_j \underbrace{C_j C_j^*}_{S2} \right) \quad (19)$$

Because both ν and V changed with depth, the computer file containing temperature and fall speed was read to a program which converted the raw transform sums into dissipations. The viscosity ν was computed from temperature using a formula of Miyake and Koisumi (1948). Estimates of $\bar{\epsilon}$ averaged over 2.5m (approx.) vertical intervals were computed, listed and plotted.

2.6 Dissipation Profiles

Figures 8 to 44 show profiles of dissipation, shear, temperature gradient and temperature. Only one of the two shear channels is displayed; the two are very similar, especially when plotted on the vertical scale of these figures. To plot this data, we ran the digitized data through the digital to analogue converter at twice the digitizing rate and into a Brush recorder advancing at 1 mm/sec. To reduce the noise levels in the temperature, temperature gradient and shear channels, all were filtered as shown in Table 2.

Table 2

Signal	High Pass	Low Pass
Temperature	none	1 Hz
Temperature gradient	none	20 Hz
Shears	1 Hz	20 Hz

Filtering allows low level signals to penetrate above background noise, but also attenuates strong signals. Accordingly, the shears and temperature gradients in regions of strong turbulence likely under-represent the strength of signals, but the plots are useful to examine qualitatively regions of strong and weak turbulence.

On the right side are plotted the estimates of dissipation for which the effects of any filters were removed. These should be accurate to $\pm 40\%$ for dissipations greater than $10^{-4} \text{cm}^2 \text{sec}^{-3}$. Deviations from isotropy will add to the uncertainty. Estimated values are plotted as horizontal bars on a logarithmic scale. The left side of each bar is at the noise level of the profile, and the right side gives the estimated value. Where no value is plotted, both shear channels were contaminated by noise. Where a spike appeared in one channel of the shear, the remaining channel only was used to compute $\bar{\epsilon}$. A dot indicates that dissipations were at or below the noise levels.

Profiles 4-10

Our Camel profiles began at 10°N but three profiles were required to debug the electronics. Profile 4, the first successful launch, was at 23°S and other profiles were at positions of the CTD survey to 3°S and back to 2°N . As close in time as possible we sampled the large scale currents with a three-axis Kaijo-Denki current meter, with a built in Guildline CTD (Curran, in preparation). However, for these Camel profiles no large scale currents are available.

Profiles 11-17

These profiles began at 0803 local time on January 21 and finished at 1522 local time on the same day. The Omegasonde balloon was launched at 1100 local time. While tracking the balloon, we deployed the current meter to sample the large scale currents. Results of these current measurements will be reported by Curran (in preparation). The winds were strong, as noted in Table 3, and stronger than found on most subsequent profiles. There were no sudden changes in temperature above 130m, and the thermocline did not begin until this depth, the deepest thermocline observed during the cruise. The bottom of this layer deepened during the day.

Dissipations observed at this position were the largest of the cruise. Profiles 13, 16 and 17 had larger dissipations than any others. The nearly uniform temperatures down to at least 130m suggests that heat had diffused downward.

Our only evidence of the duration of the high winds comes from observations of the sea (large wind waves made the launches of profiles 15 to 17 the most difficult of the cruise) and observations of the wind the previous day at the Equator, when 9.0m/sec winds were observed.

Dissipations were large above 150m depth, and small below this depth. There is no pattern to the distribution of average dissipation above 150 metres of all seven profiles taken together. Although the waters above 150m depth appear well mixed, there was a 0.5°C temperature difference between the surface and 120m depth.

Profiles 18-43

We increased the fall speed, beginning with profile 18 and maintained it near 75 cm/sec until profile 43. The noise levels increased, and the electronics also generated more noise. Some profiles gave data with noise levels too high and their data was discarded. Frequently dissipations could only be computed in the upper 100 to 150 metres, due to noise at greater depths. For five profiles we deployed Pumpkins to sense temperature microstructure.

These profiles were placed throughout the North-South sections, with profiles 22-24 close together in time and space. All were within 2° of the Equator, and give a clear picture of the difference in dissipation levels between waters near the equator and waters off the equator. On only two occasions did the winds exceed 7.5 cm/sec, and average dissipations near the equator (within 1/2°) were lower than observed previously.

Profiles 46-57

We brought the fall speed back to 50 cm/sec for these profiles. All profiles in this group were taken going north, with profile 46 at 30°N and profile 57 at 14°19'N. Winds were variable, with a minimum of 3m/sec found in the Convergence Zone at 7°N. Stronger winds were observed to the north and south of the Convergence Zone. Large scale current measurements ended after profile 53. The absence of large scale shear in the water column allowed these profiles to extend to greater depths.

Table 3. Details of Profiles

Profile	Lat.	Long.	Date	Time (GMT)	$\bar{\epsilon}$ 20-140 m ($\text{cm}^2 \text{sec}^{-3} \times 10^{-5}$)
4	0°23'S	150°W	1/17	2014	28.93
5	0°25'S	150°W	1/17	2255	155.45
6	3°02'S	150°W	1/18	2015	4.42
7	0°30'S	150°W	1/19	1946	87.21
8	0°00'	150°W	1/20	0222	69.62
9	1°30'N	150°W	1/20	1930	19.11
10	1°30'N	150°W	1/20	2010	6.11
11	0°00'	150°W	1/21	1803	94.80
12	0°02'S	150°W	1/21	1945	104.17
13	0°03'S	150°W	1/21	2020	177.58
14	0°04'S	150°W	1/21	2332	119.42
15	0°06'S	150°W	1/22	0010	124.38
16	0°06'S	150°W	1/22	0045	362.48
17	0°06'S	150°W	1/22	0122	613.21
18	2°00'S	150°W	1/23	2005	37.38
19	1°00'S	150°W	1/24	2003	4.10
21	0°01'N	150°W	1/25	2023	65.58
22	0°15'N	150°W	1/25	2332	35.33
23	0°15'N	150°W	1/26	0008	24.21
24	0°15'N	150°W	1/26	0047	155.59
25	1°00'N	150°W	1/26	1929	shallow
27	1°31'N	150°W	1/27	0009	39.71
28	0°00'	150°W	1/28	1929	shallow
33	0°23'S	150°W	2/4	1816	41.78
34	0°00'	150°W	2/5	0105	5.01
36	0°04'S	150°W	2/7	1844	57.84
38	0°07'S	150°W	2/7	1933	12.30
46	0°30'N	150°W	2/13	1745	shallow
47	1°01'N	148°W	2/14	2317	13.14
48	2°00'N	148°W	2/15	1902	9.33
51	5°10'N	148°W	2/17	1800	33.14
52	5°10'N	148°W	2/17	1936	11.58
53	6°00'N	148°W	2/18	0203	19.21
54	7°02'N	149°W	2/18	1716	6.93
55	8°01'N	149°W	2/19	0040	17.72
56	10°01'N	150°W	2/19	1851	16.91
57	14°19'N	153°W	2/20	2012	11.04

Table 4. Twenty metre averages of dissipation rates of profiles beyond 1 degree from the equator. A zero is listed where rates were at or below the noise level. A dash denotes the absence of data.

Profile	Latitude	20 40	40 60	60 80	80 100	100 120	120 140	140 160	160 180	180 200	200 220	220 240	240 260	260 280	280 300	300 320
6	3°S	7.40	11.5	5.59	.69	.38	.93	12.0	0	.37	0	0	0	0	0	12.6
9	1°30'N	66.3	9.44	19.1	2.46	5.40	12.1	1.83	5.70	0	0	0	0	.29	3.06	6.92
10	1°30'N	1.72	8.77	14.2	3.38	.27	8.31	3.48	1.46	0	0	.09	0	0	.19	-
18	2°S	48.4	127.	38.1	8.37	.32	1.46	.57	1.59	1.35	.21	.12	.22	.58	0	0
19	1°S	3.47	.38	13.1	2.14	2.79	2.66	13.1	3.50	.76	-	-	-	.27	0	0
25	1°N	145.	14.0	17.0	7.67	-	-	-	-	-	-	-	-	-	-	-
27	1°37'N	6.94	32.9	5.91	4.92	49.7	138	79.9	164.	173.	68.4	0	.74	0	0	0
47	1°1'N	26.0	24.2	24.8	2.07	1.31	.49	1.98	.73	.23	0	0	1.14	.38	0	0
48	2°N	28.0	12.6	4.53	7.69	1.55	1.63	0	-	-	-	-	-	-	-	-
51	5°10'N	40.6	65.1	12.8	70.4	3.66	6.38	8.05	.17	2.47	0	-	-	-	-	-
52	5°10'N	6.22	5.99	48.6	7.81	.54	.28	9.50	1.14	6.69	3.83	3.39	0	-	-	-
53	6°N	62.0	7.37	4.61	27.1	13.1	1.04	0	60.1	12.0	.74	.18	0	0	.19	.16
54	7°2'N	33.0	3.99	0	.82	.18	3.61	0	2.33	1.45	6.39	.09	0	0	0	.22
55	8°N	85.7	3.13	.63	11.1	2.31	3.45	1.58	0	0	0	0	.41	0	0	.77
56	10°N	40.4	65.8	29.6	3.97	.52	.38	1.13	0	0	0	0	0	0	.33	0
57	14°N	14.5	20.4	28.1	1.05	.90	1.29	1.18	.09	.40						

Units are $\text{cm}^2\text{sec}^{-3} \times 10^{-5}$

Table 5. Twenty metre averages of dissipation rates of profiles beyond 1 degree of the equator. A zero is listed where rates were at or below the noise level. A dash denotes the absence of data.

Profile	Latitude	20 40	40 60	60 80	80 100	100 120	120 140	140 160	160 180	180 200	200 220	220 240	240 260	260 280	280 300
4	23' S	5.97	42.2	64.0	28.0	33.0	.80	1.8	.53	2.3	.15	0	2.26	.90	0
5	25' S	1.82	31.6	15.6	53.9	825.	4.3	1.2	1.7	1.3	0	0	.12	.26	0
7	30' S	61.5	367.	87.0	6.13	.90	.34	1.05	.38	.67	1.89	.07	.85	.28	0
8	0'	69.2	144.	66.1	65.3	72.4	.91	2.43	.44	.29	.59	0	.75	6.81	0
11	0'	126.	155.	76.7	69.0	12.5	10.9	3.76	.26	.52	.44	.11	.06	1.07	-
13	0'	42.6	161.	175.	178.	11.1	57.5	.80	1.16	0	0	.68	.86	1.26	-
14	4' S	45.6	127.	85.5	222.	113.	123.	4.24	1.79	0	.43	1.18	16.8	.93	-
15	6' S	14.5	108.	72.4	218.	235.	97.9	41.4	.24	0	0	.50	0	0	-
16	6' S	3.69	75.9	533.	599.	947.	16.7	1.90	.66	0	.61	1.56	.84	.95	1.1
17	6' S	12.4	196.	450.	1260.	1530.	228.	49.4	.83	1.05	.34	.10	0	-	-
21	1' N	33.3	234.	83.7	22.7	6.06	1.32	.14	1.79	2.15	6.49	6.48	0	0	.75
22	15' N	4.57	7.70	117.	30.7	39.9	12.1	10.2	.96	.69	.82	0	0	.54	.14
23	15' N	3.96	17.7	56.3	12.8	42.3	12.3	33.3	0	.58	0	0	2.22	0	2.0
24	15' N	1.83	.96	364.	509.	8.87	51.1	15.6	.78	0	1.23	0	.60	.22	.38
28	0'	74.2	65.1	-	-	-	-	-	-	-	-	-	-	-	-
33	23' S	84.7	73.6	82.0	6.63	0	3.72	.30	3.62	-	-	-	-	-	-
34	0'	0	11.0	16.0	2.24	.89	0	57.4	1.03	.57	0	0	0	0	1.32
36	4' S	89.9	162.	80.9	12.7	1.03	0	4.54	1.53	1.26	.33	0	.33	.31	0
38	7' S	6.09	40.4	13.7	10.8	2.84	0	7.12	0	0	1.54	1.10	0	0	0

Units are $\text{cm}^2\text{sec}^{-3} \times 10^{-5}$

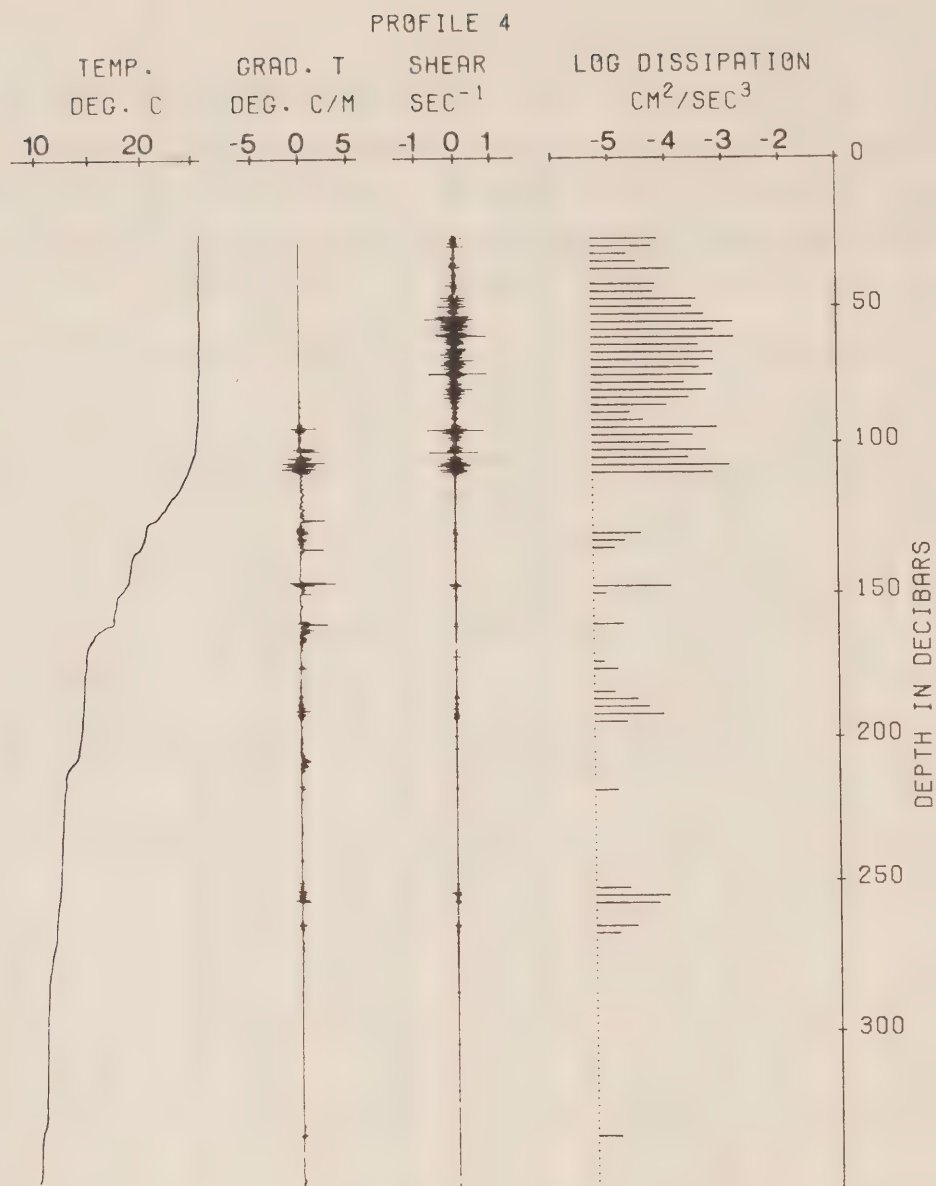


Figure 8. Profile at 0°23'S, 150°W on Jan.17 at 2014Z.

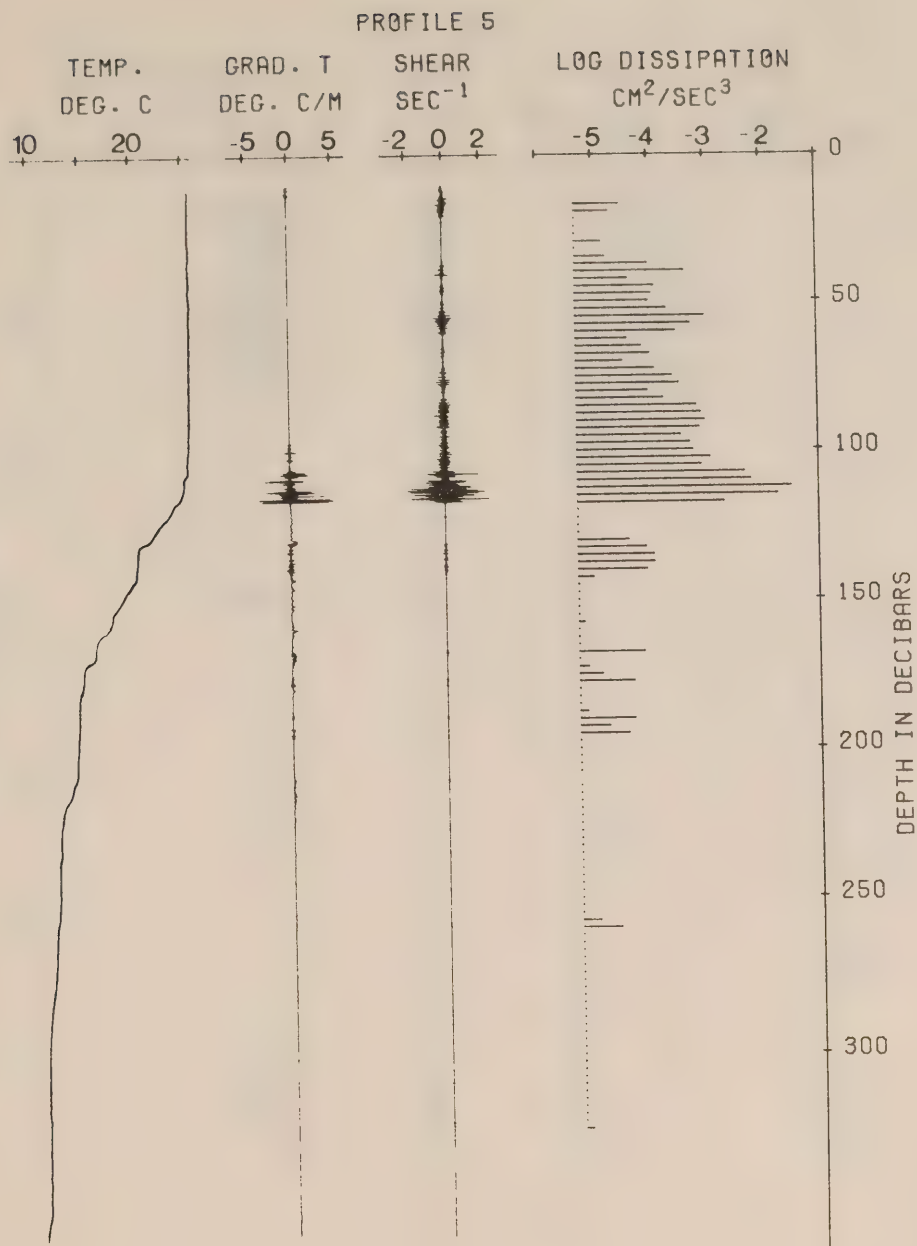


Figure 9. Profile at 0°25'S, 150°W on Jan.17 at 2255Z.

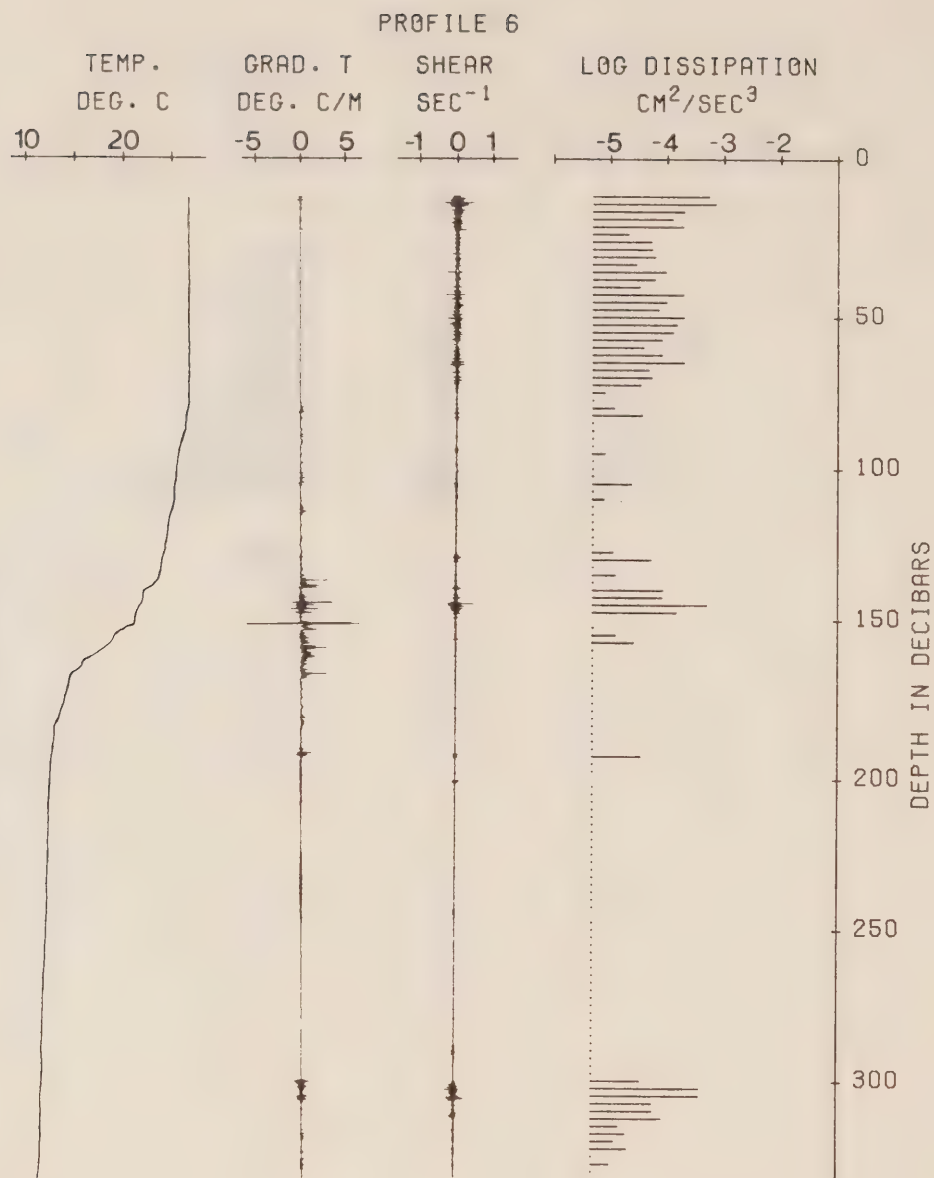


Figure 10. Profile at 3°02'S, 150°W on Jan.18 at 2015Z.

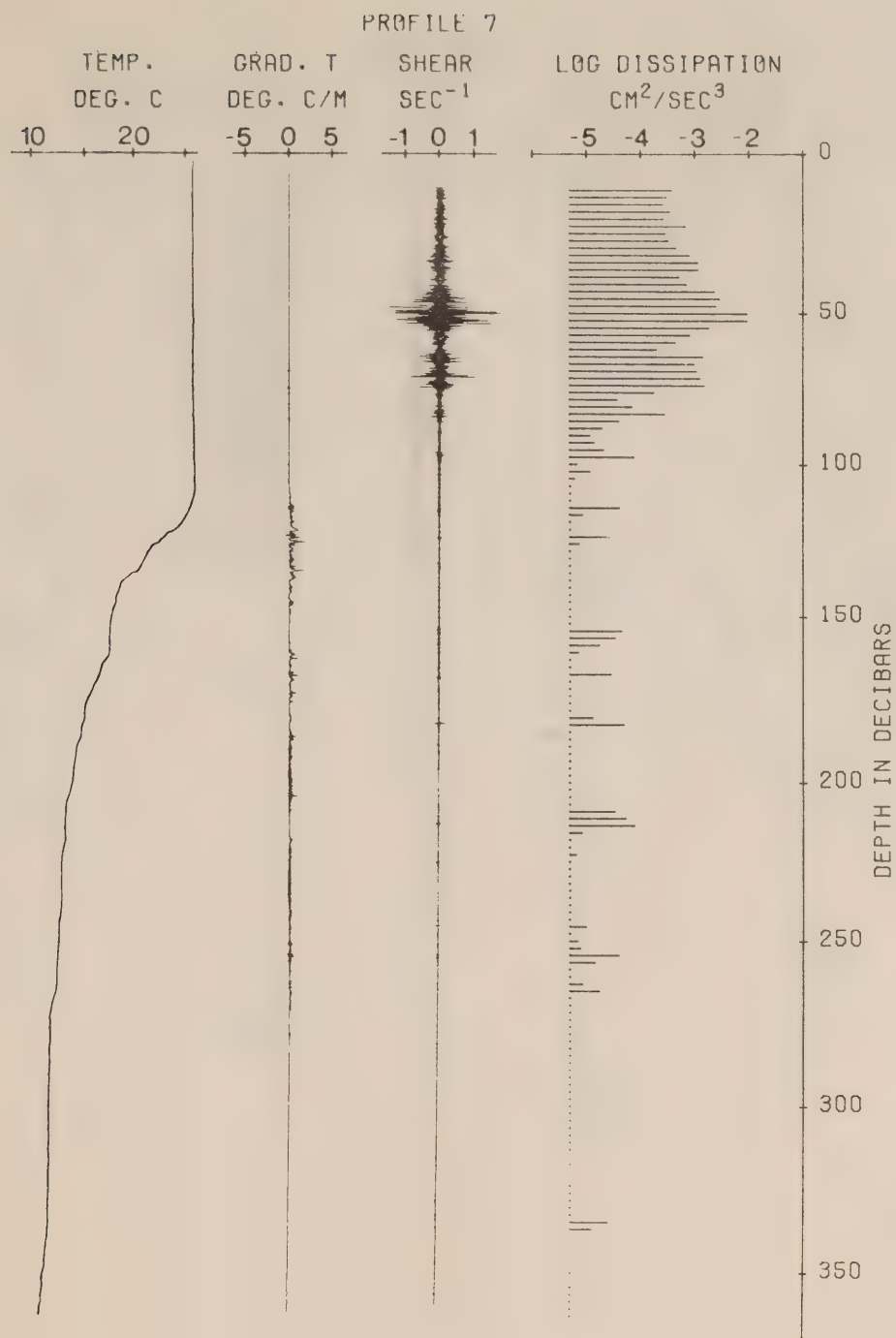


Figure 11. Profile at 0°30'S, 150°W on Jan.19 at 1946Z.

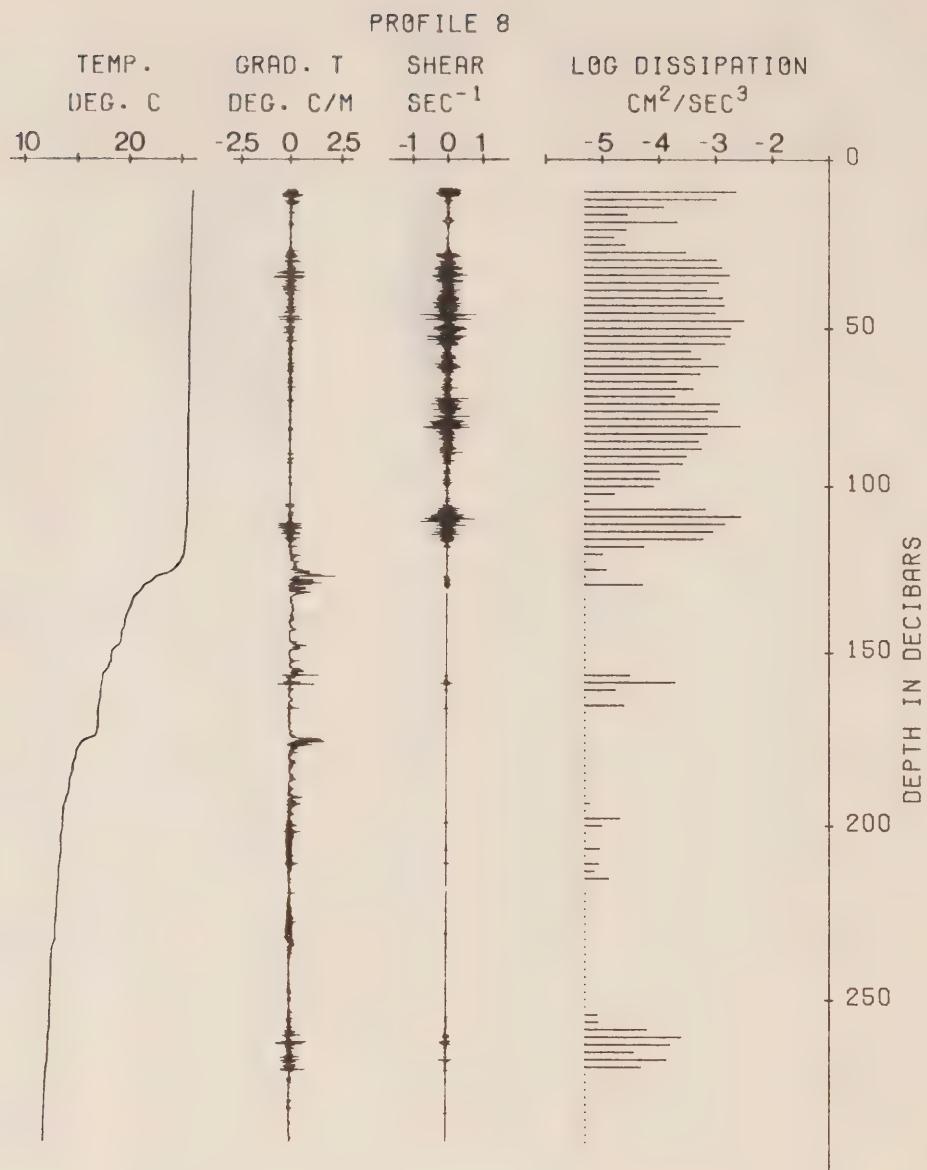


Figure 12. Profile at 0°, 150°W on Jan.20 at 0222Z.

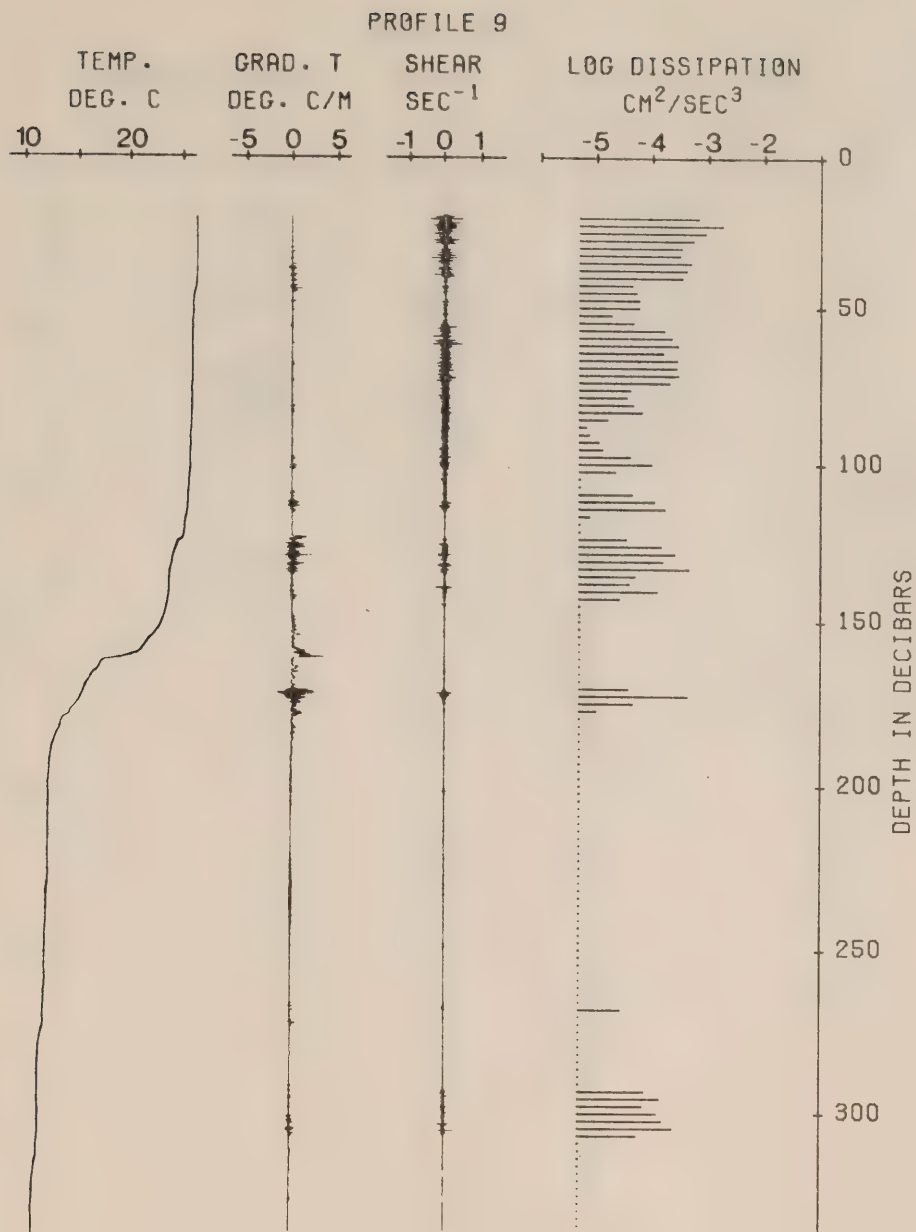


Figure 13. Profile at 1°30'N, 150°W on Jan.20 at 1930Z.

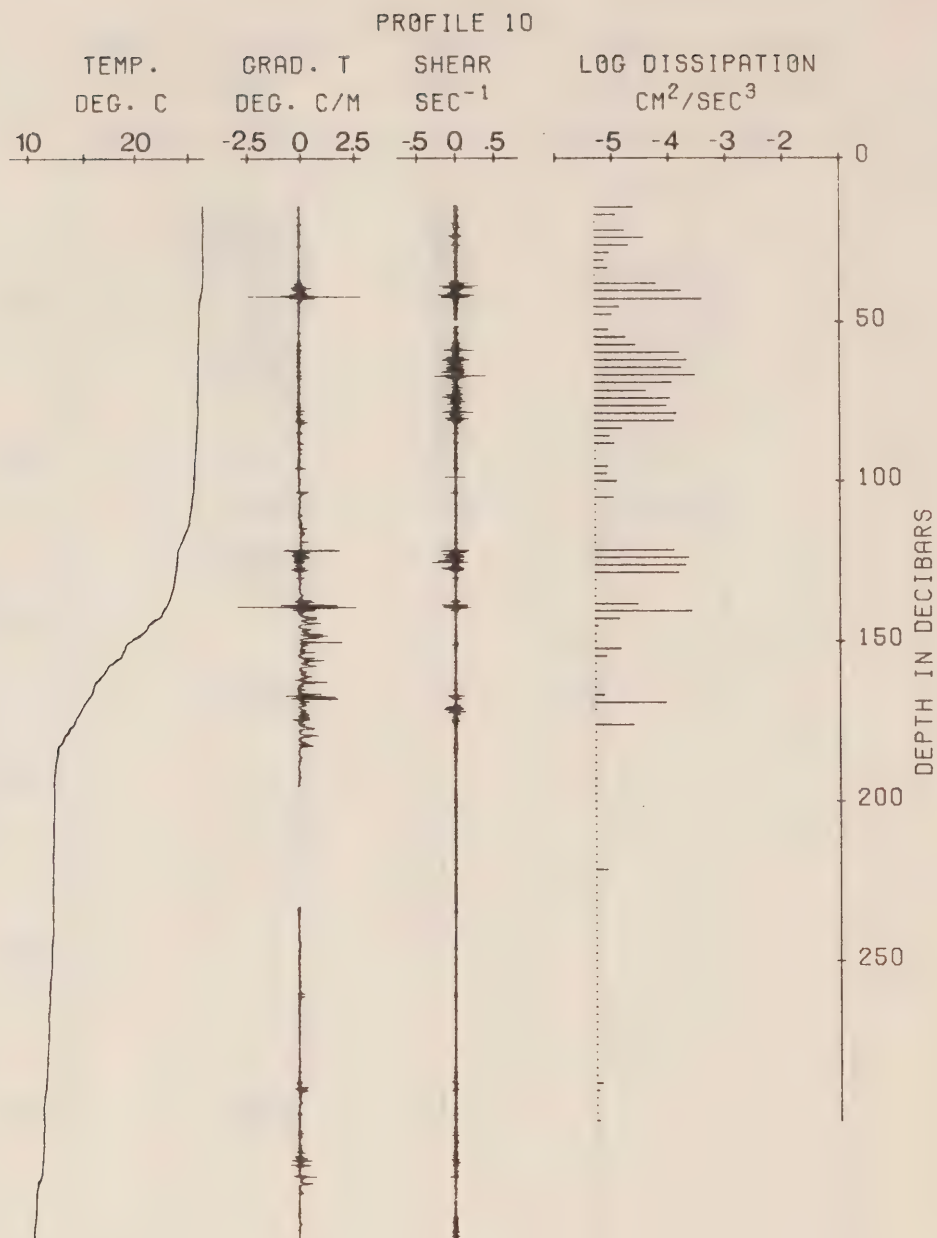


Figure 14. Profile at 1°30'N, 150°W on Jan.20 at 2010Z.

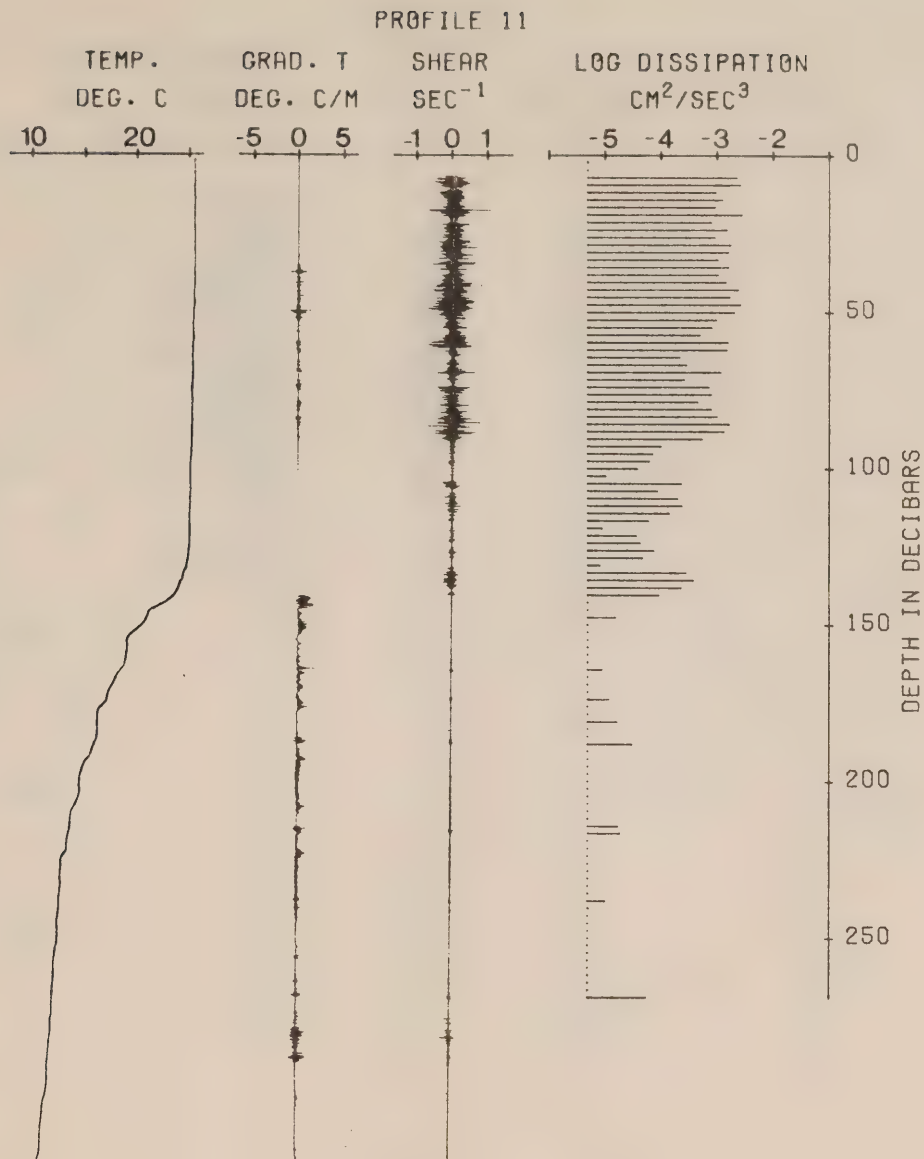


Figure 15. Profile at 0°, 150°W on Jan.21 at 1803Z.

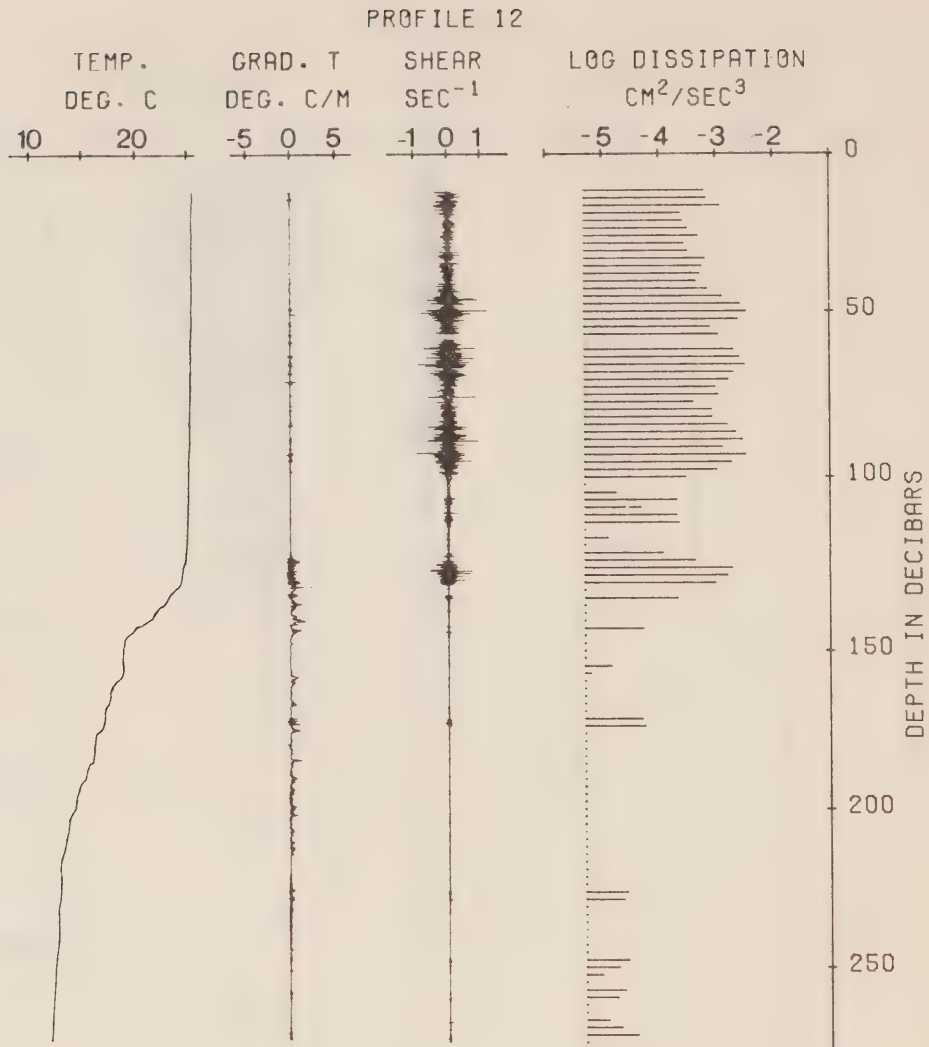


Figure 16. Profile at 0°02'S, 150°W on Jan.21 at 1945Z.

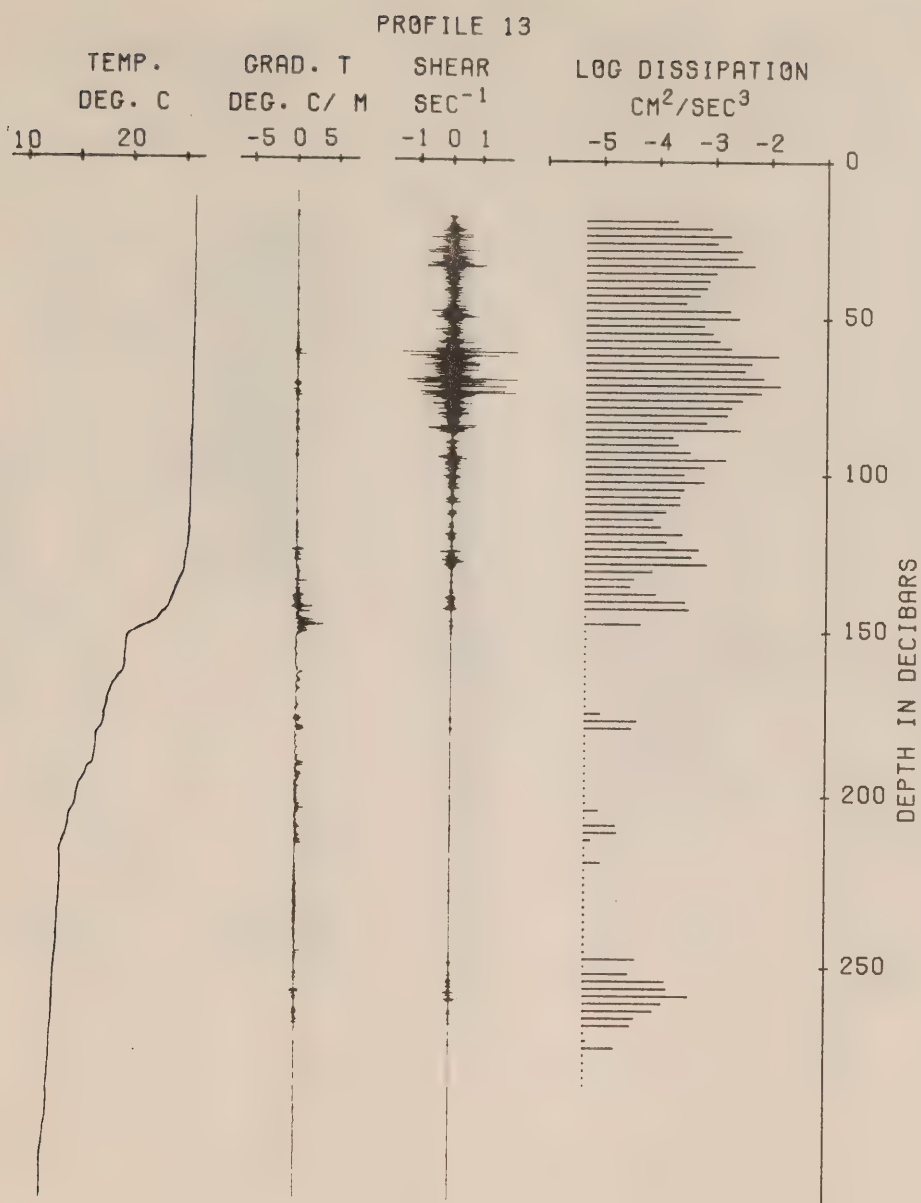


Figure 17. Profile at 0°03'S, 150°W on Jan.21 at 2020Z.

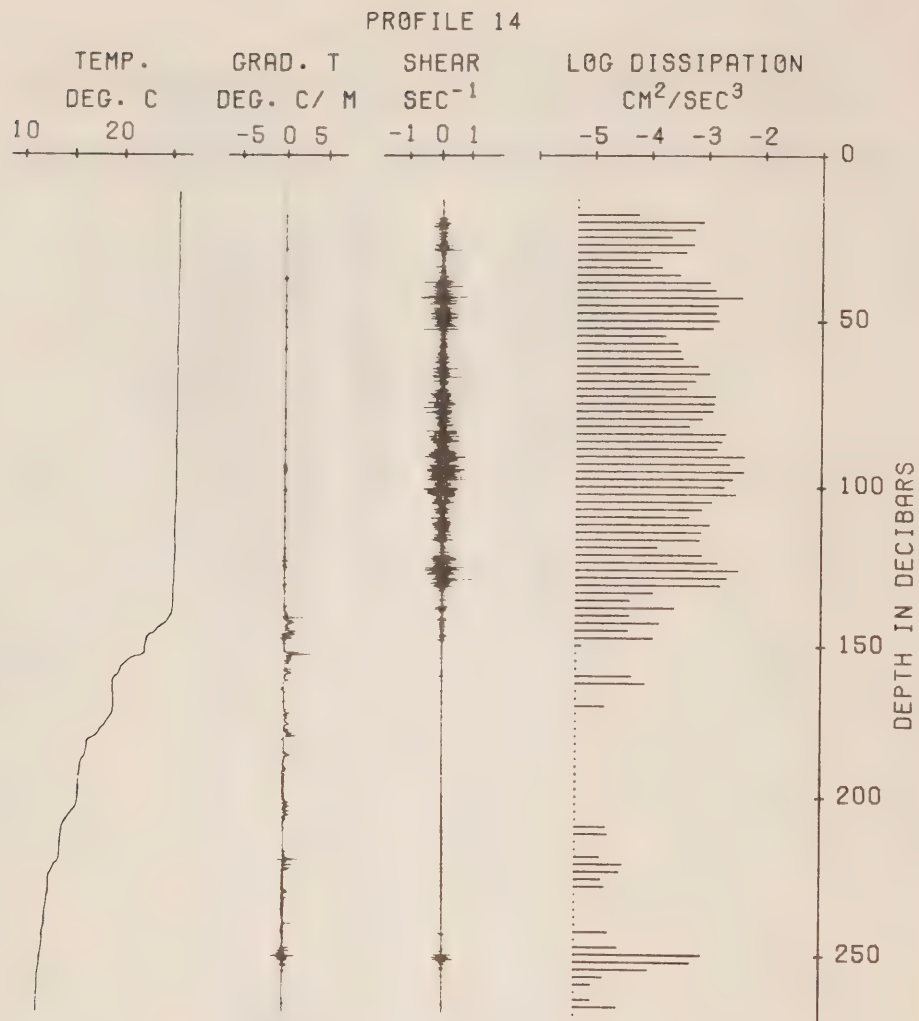


Figure 18. Profile at 0°04'S, 150°W on Jan.21 at 2332Z.

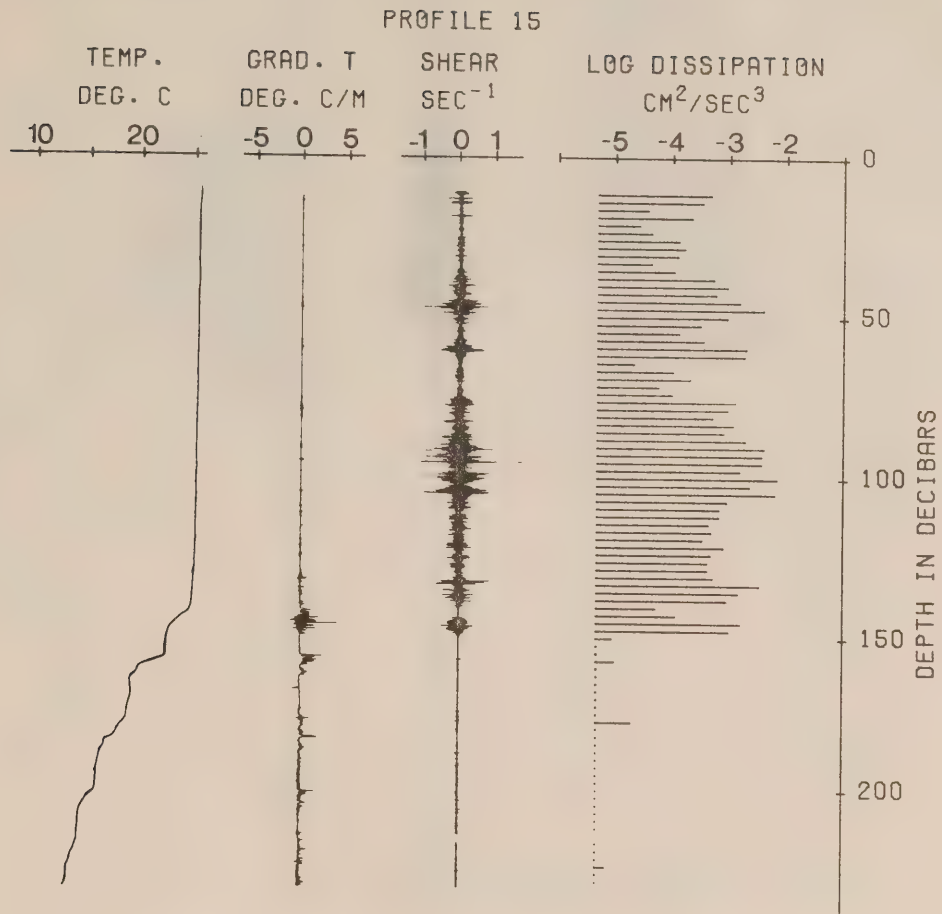


Figure 19. Profile at 0°06'S, 150°W on Jan.22 at 0010Z.

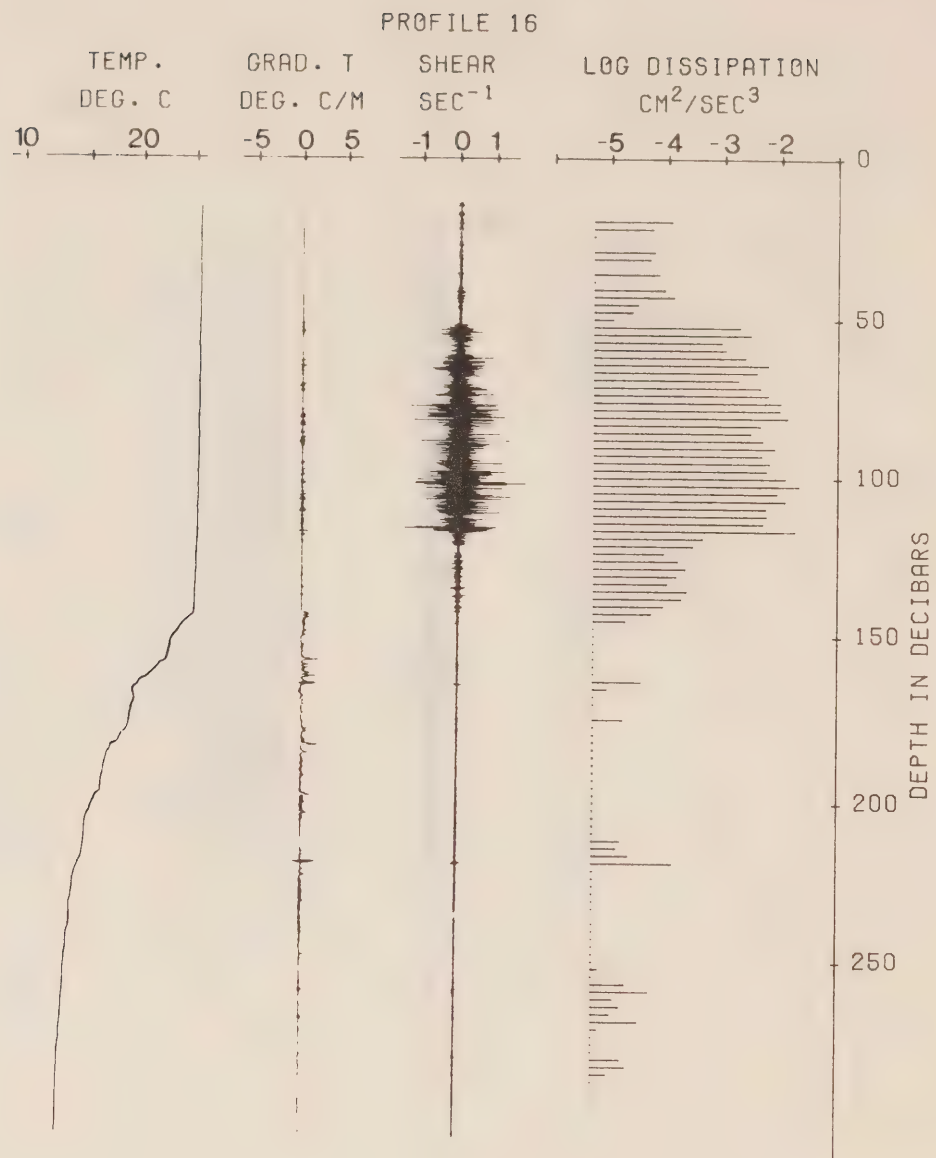
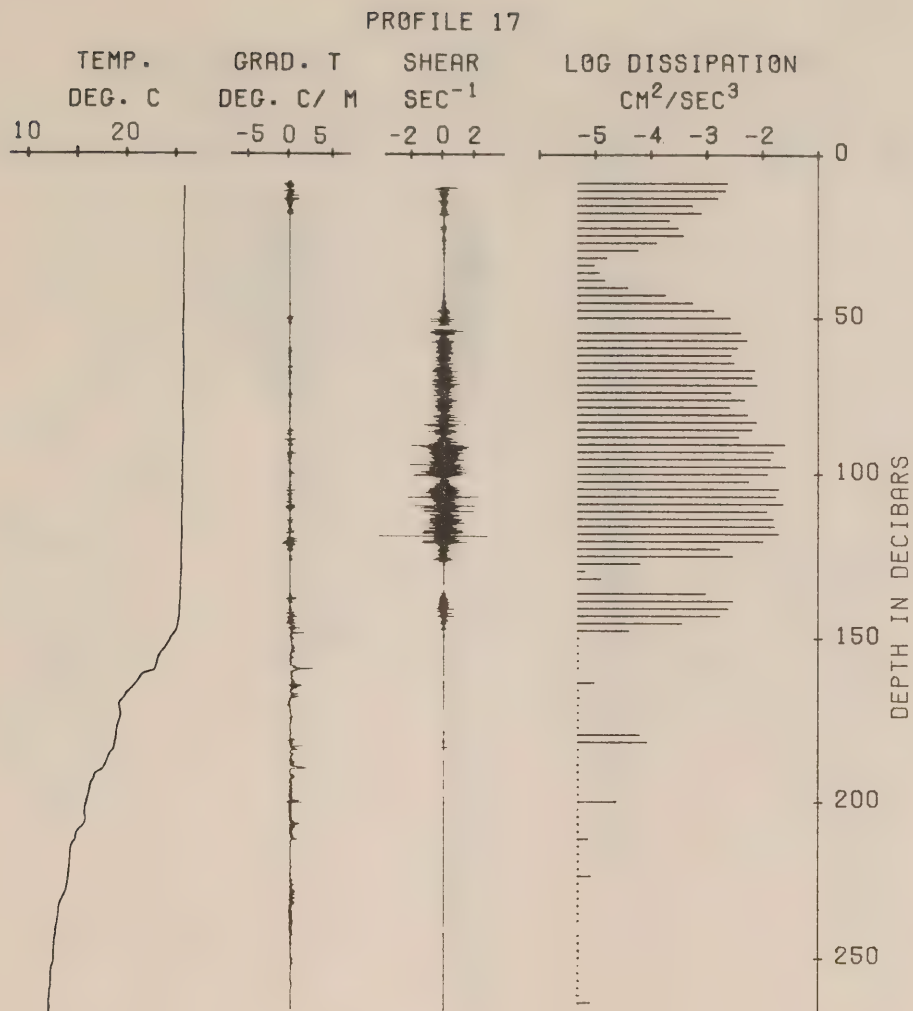


Figure 20. Profile at 0°06'S, 150°W on Jan.22 at 0045Z.



PROFILE AT 150°W, 0°4'S ON JAN 22, 1979 AT 0122Z

Figure 21. Profile at 0°06'S, 150°W on Jan.22 at 0122Z.

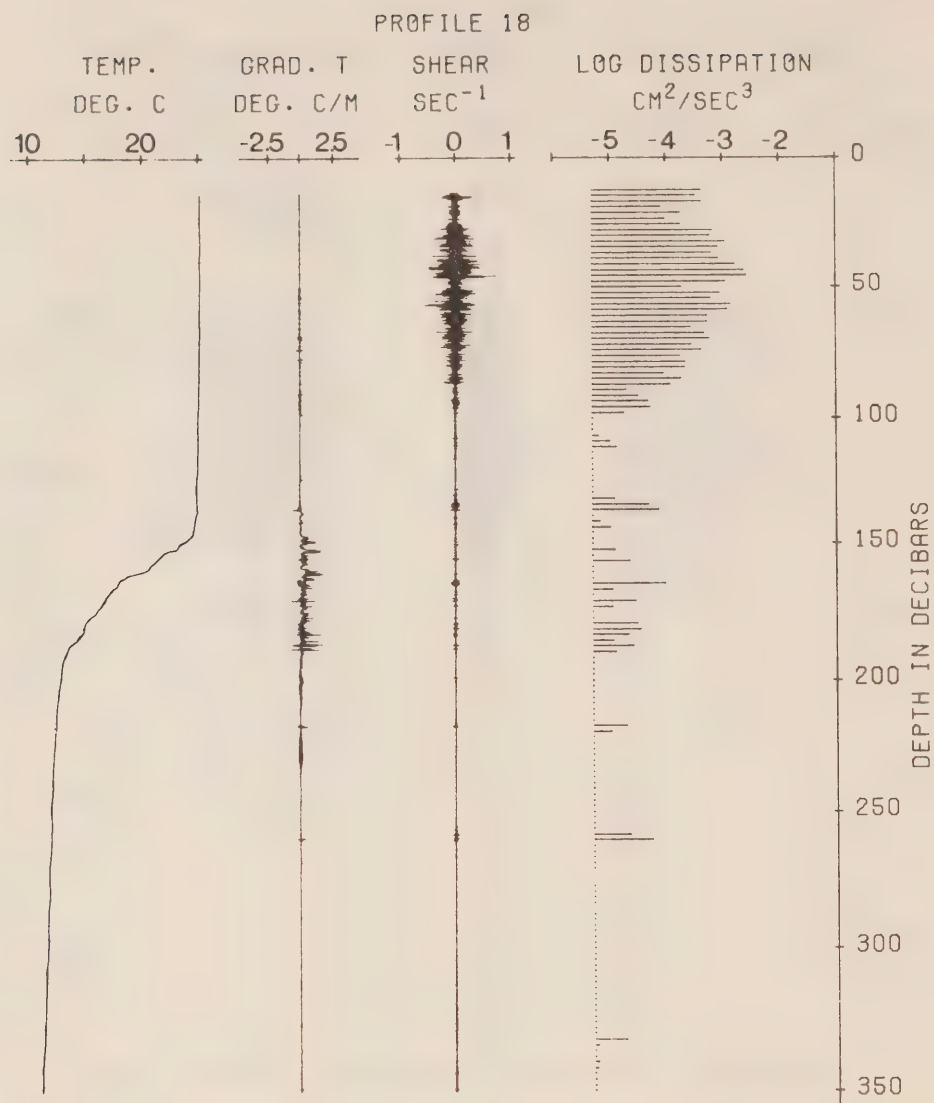


Figure 22. Profile at 2°00'S, 150°W on Jan.23 at 2005Z.

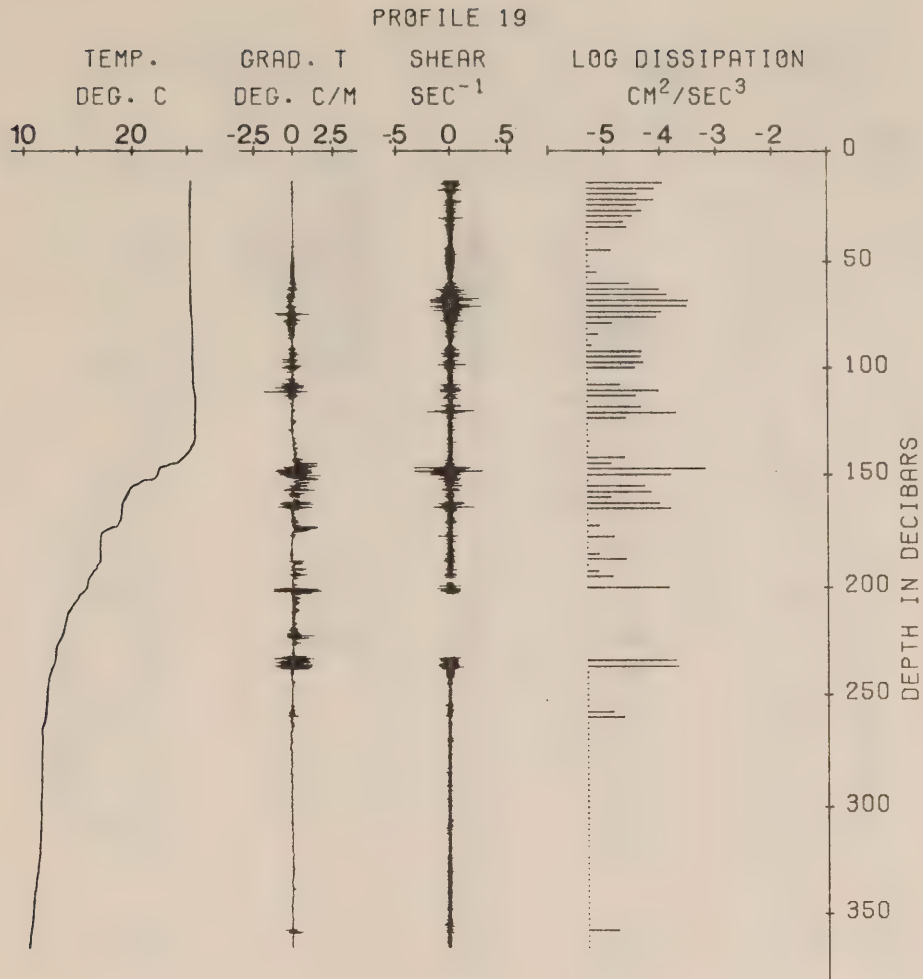


Figure 23. Profile at 1°00'S, 150°W on Jan.24 at 2003Z.

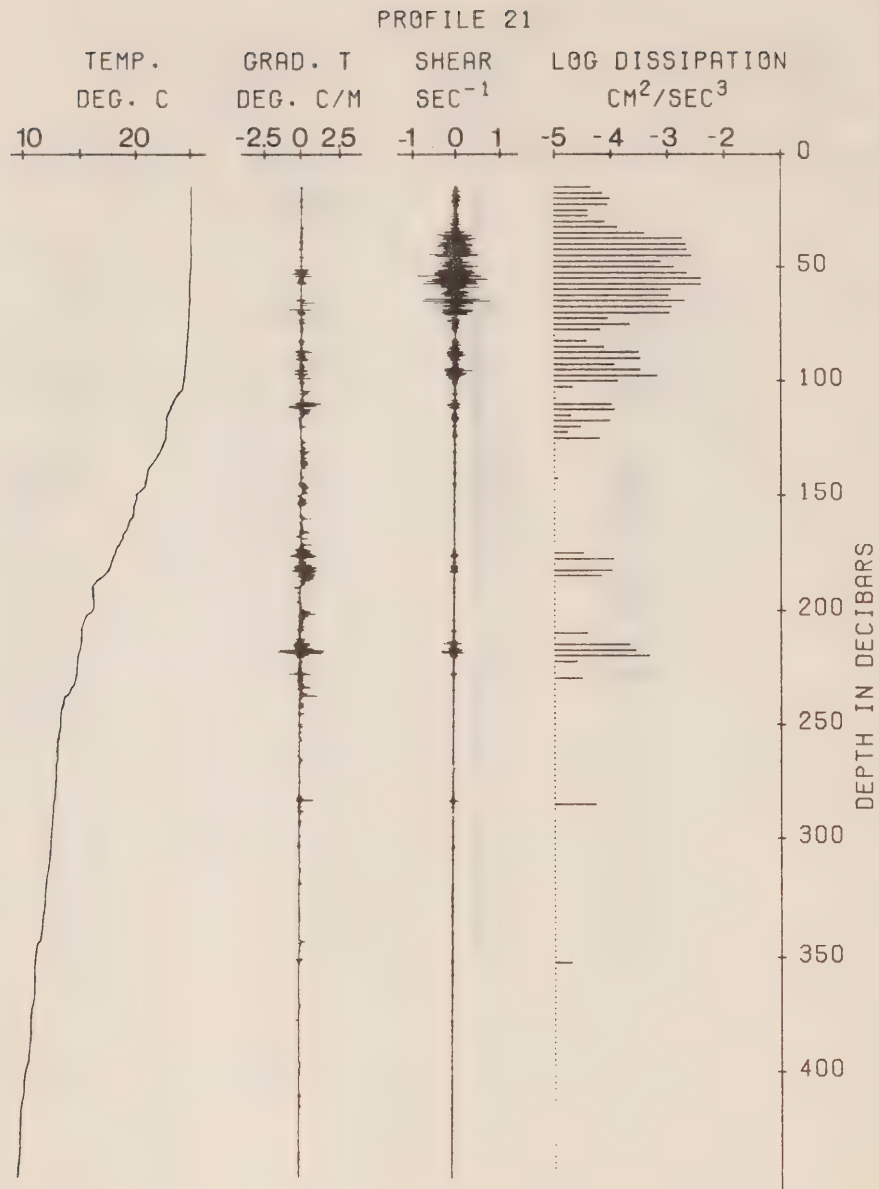


Figure 24. Profile at 0°01'N, 150°W on Jan.25 at 2023Z.

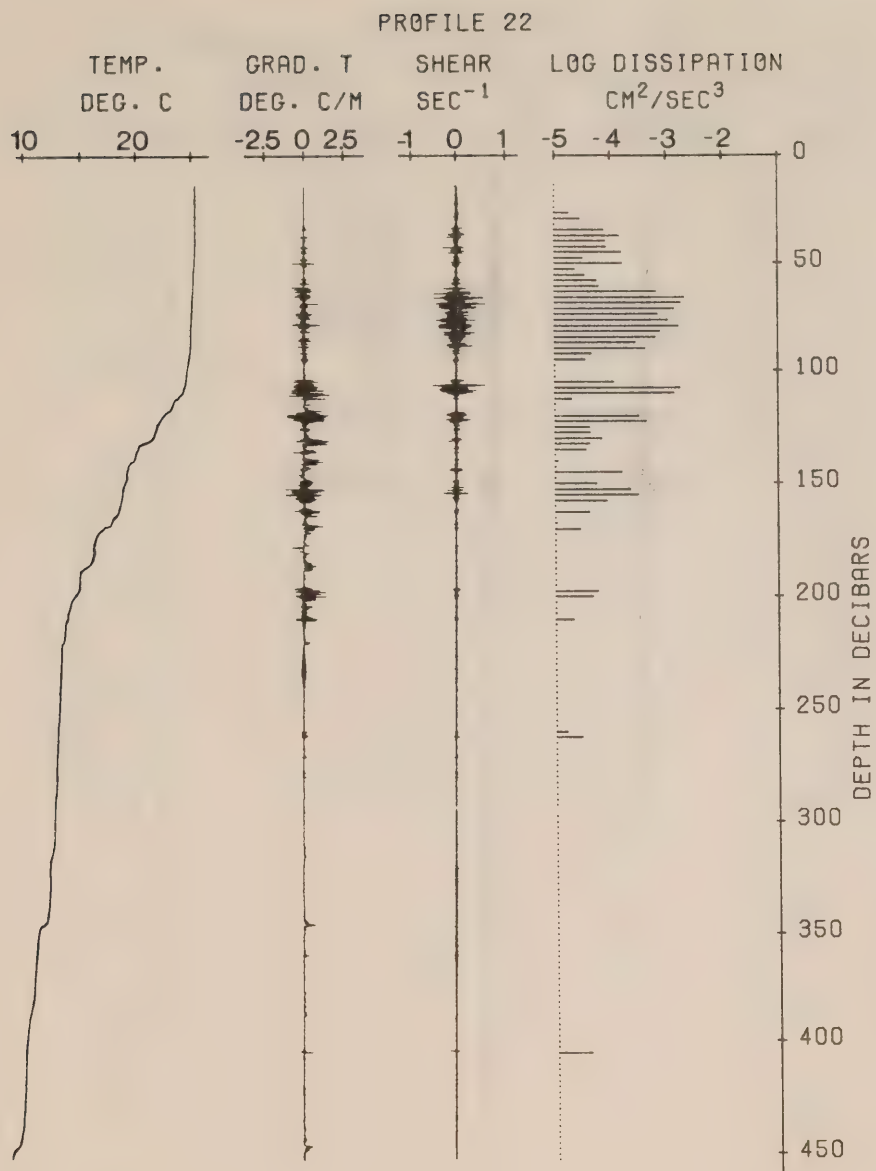


Figure 25. Profile at 0°15'N, 150°W on Jan.25 at 2332Z.

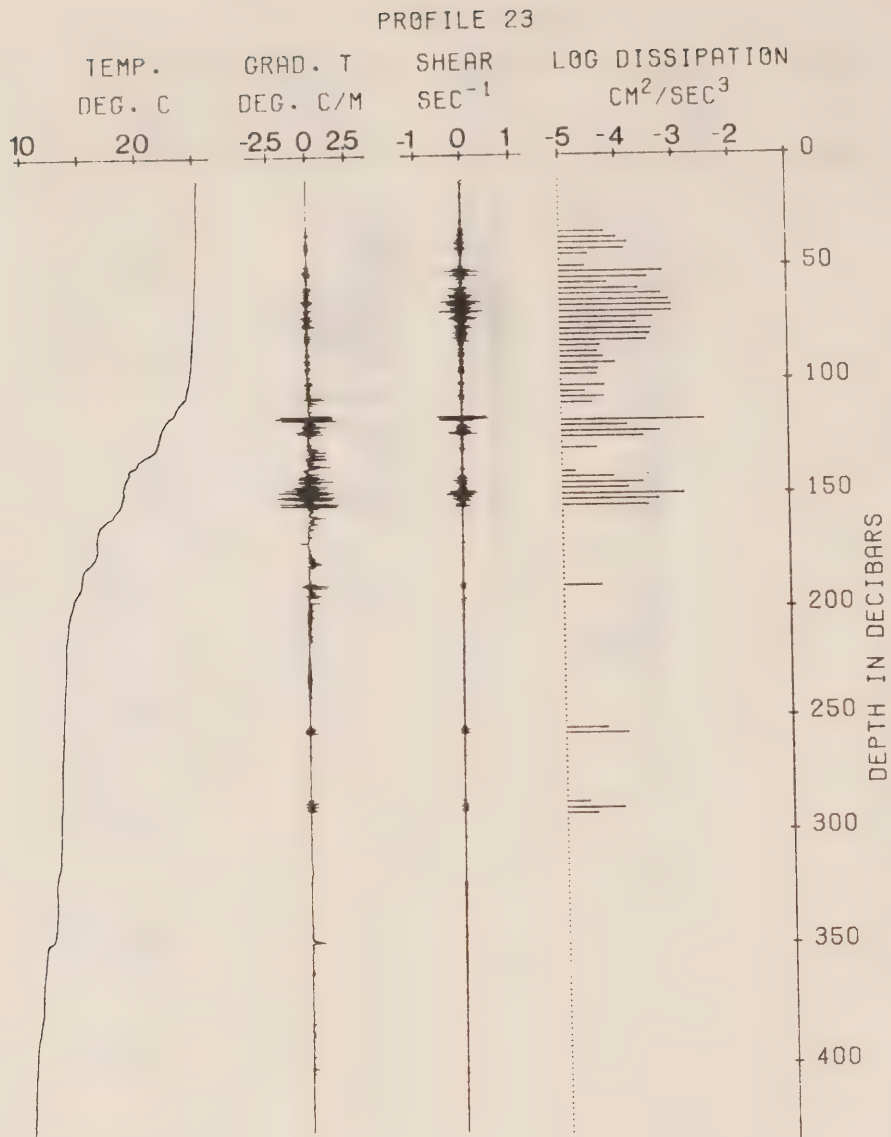


Figure 26. Profile at 0°15'N, 150°W on Jan.26 at 0008Z.

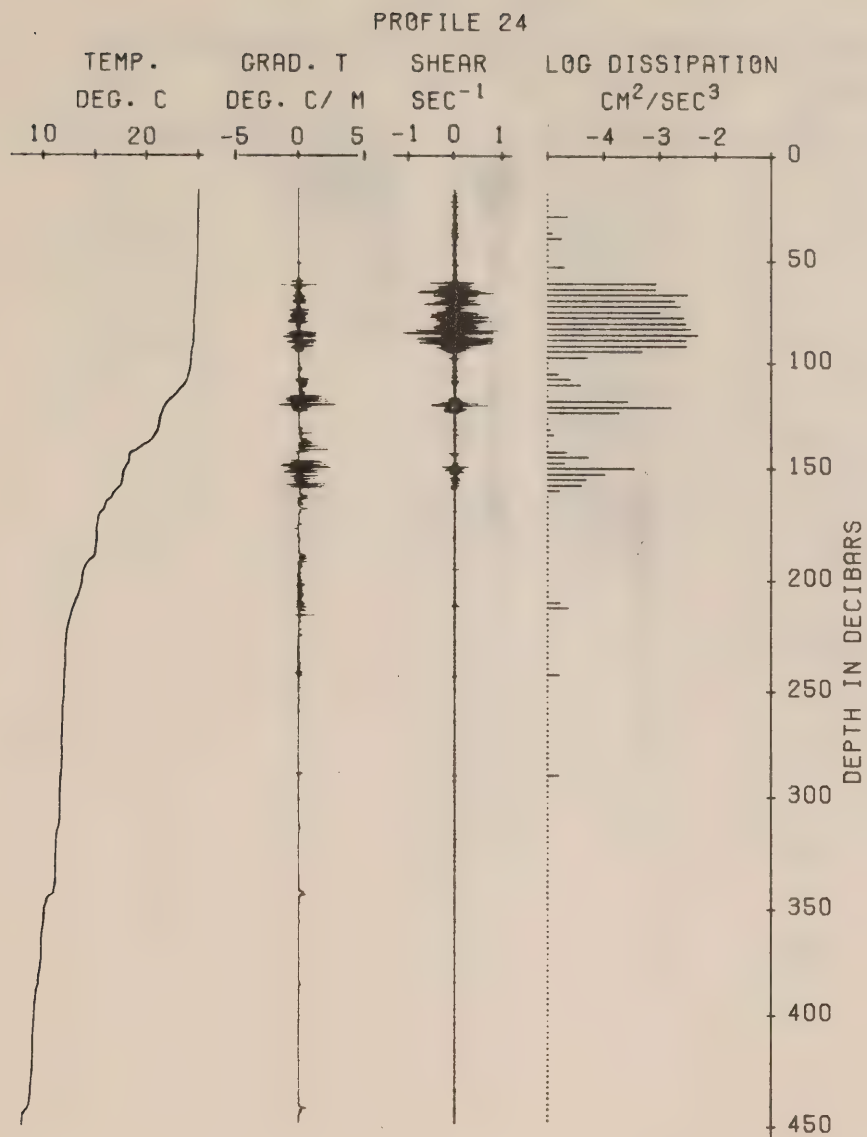


Figure 27. Profile at 0°15'N, 150°W on Jan.26 at 0047Z.

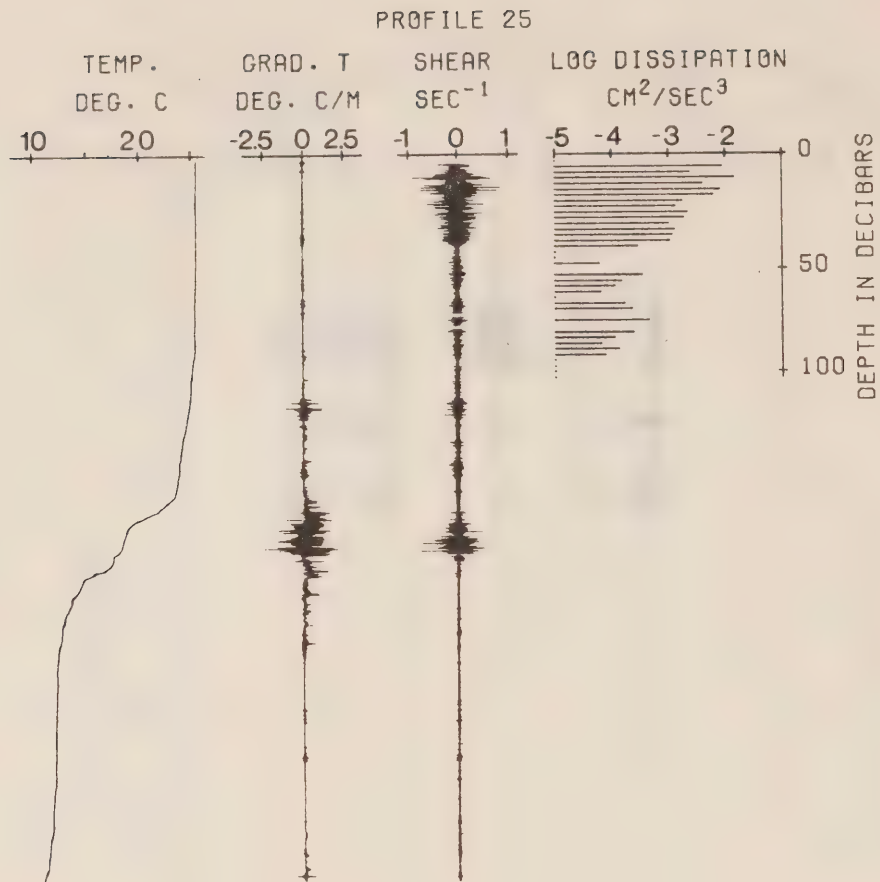


Figure 28. Profile at 1°00'N, 150°W on Jan. 26 at 1929Z.

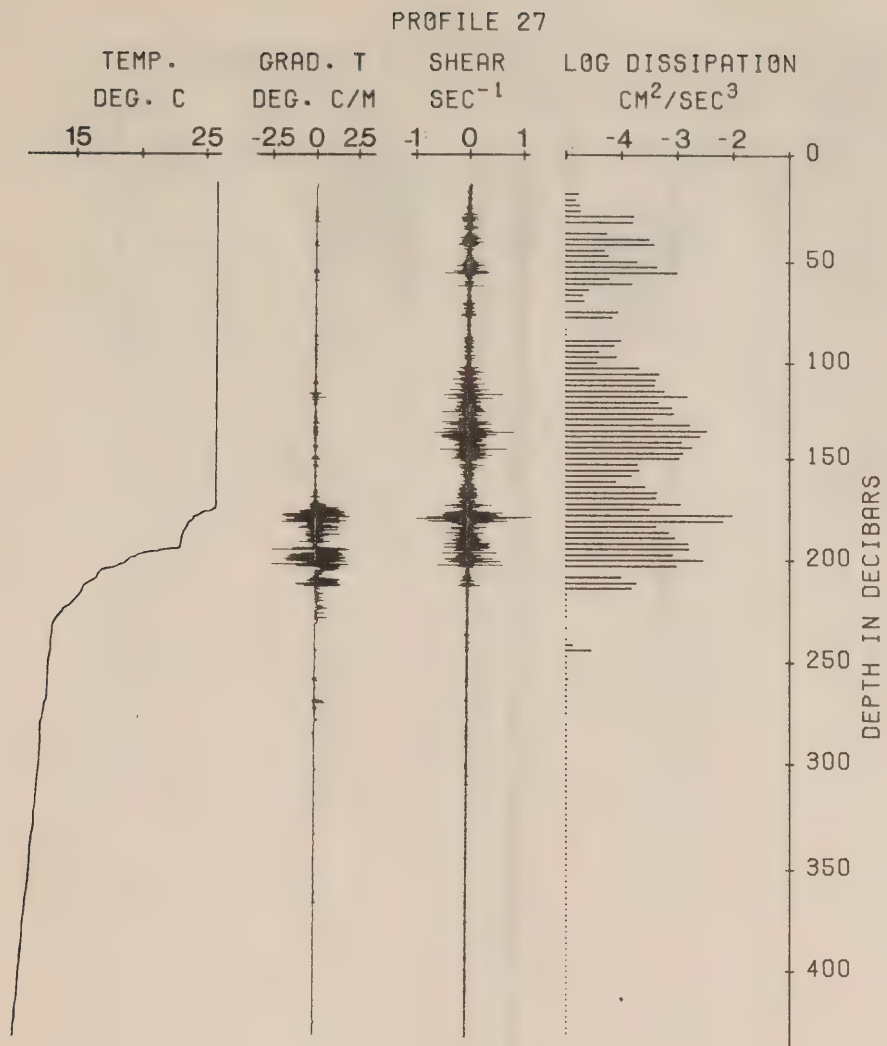


Figure 29. Profile at 1°31'N, 150°W on Jan.27 at 0009Z.

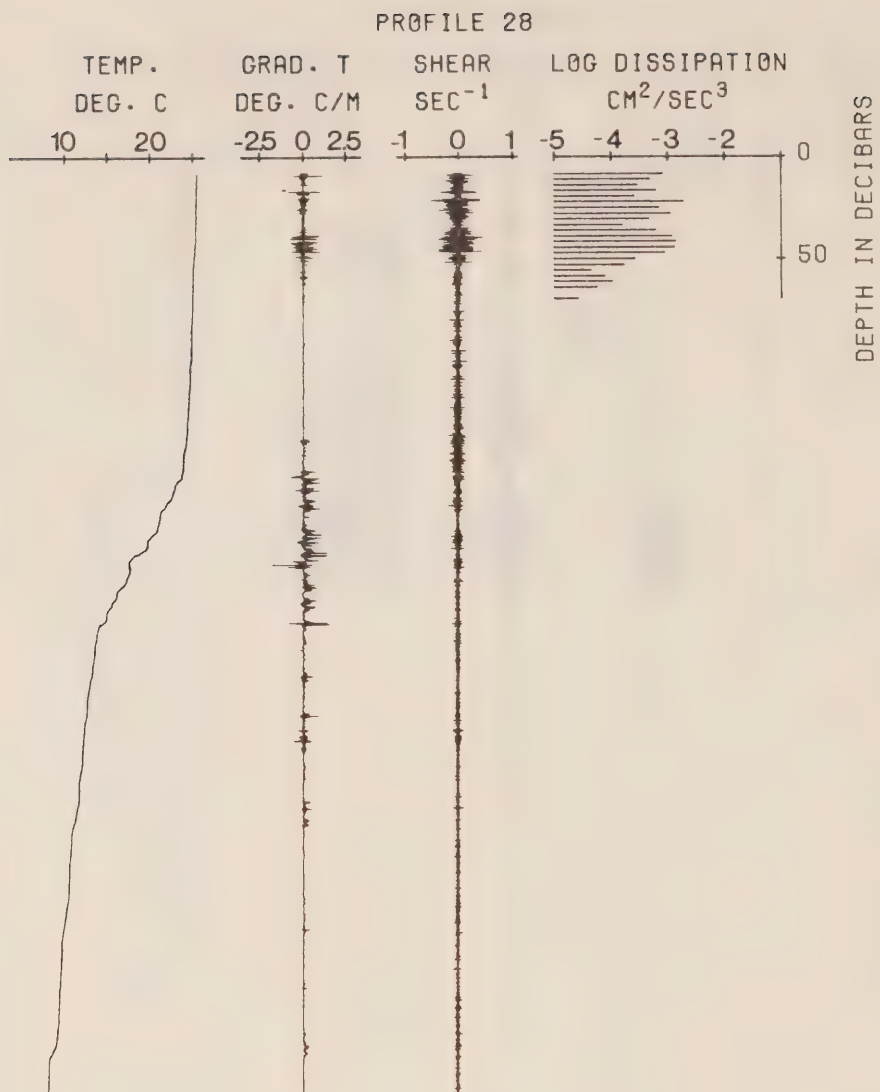


Figure 30. Profile at 0°, 150°W on Jan.28 at 1929Z.

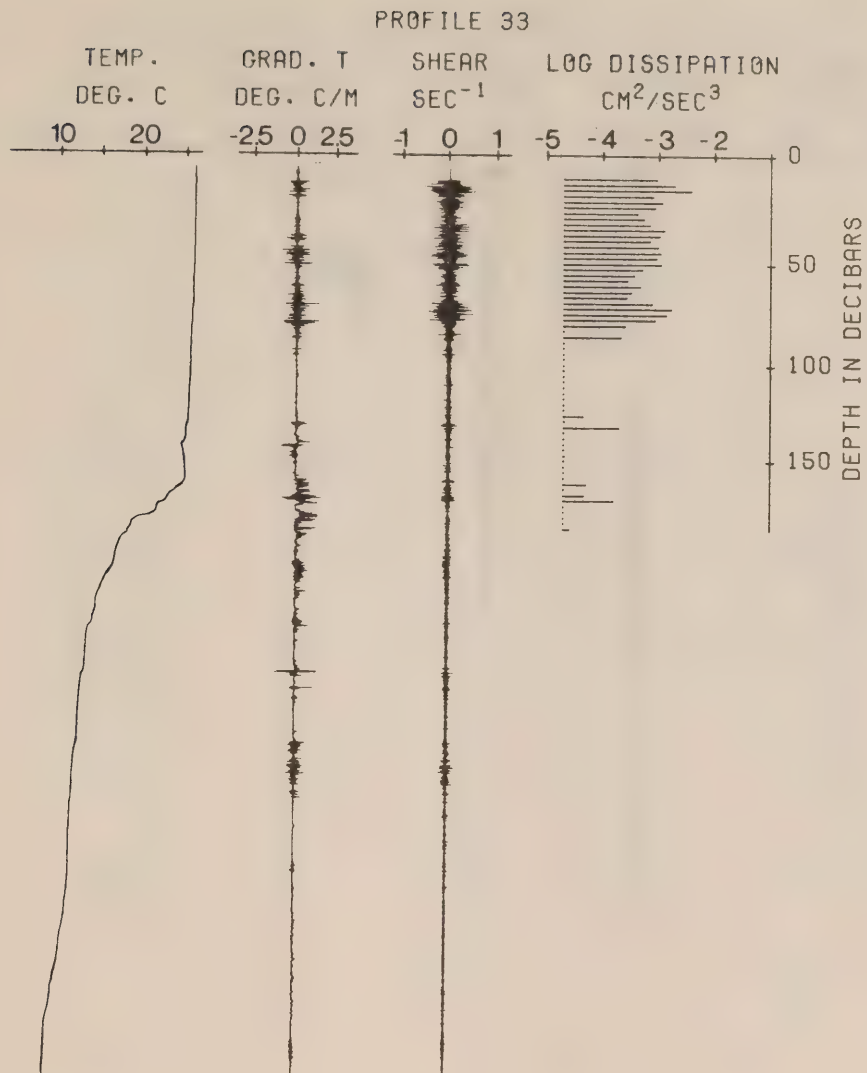


Figure 31. Profile at 0°23'S, 150°W on Feb.4 at 1816Z.

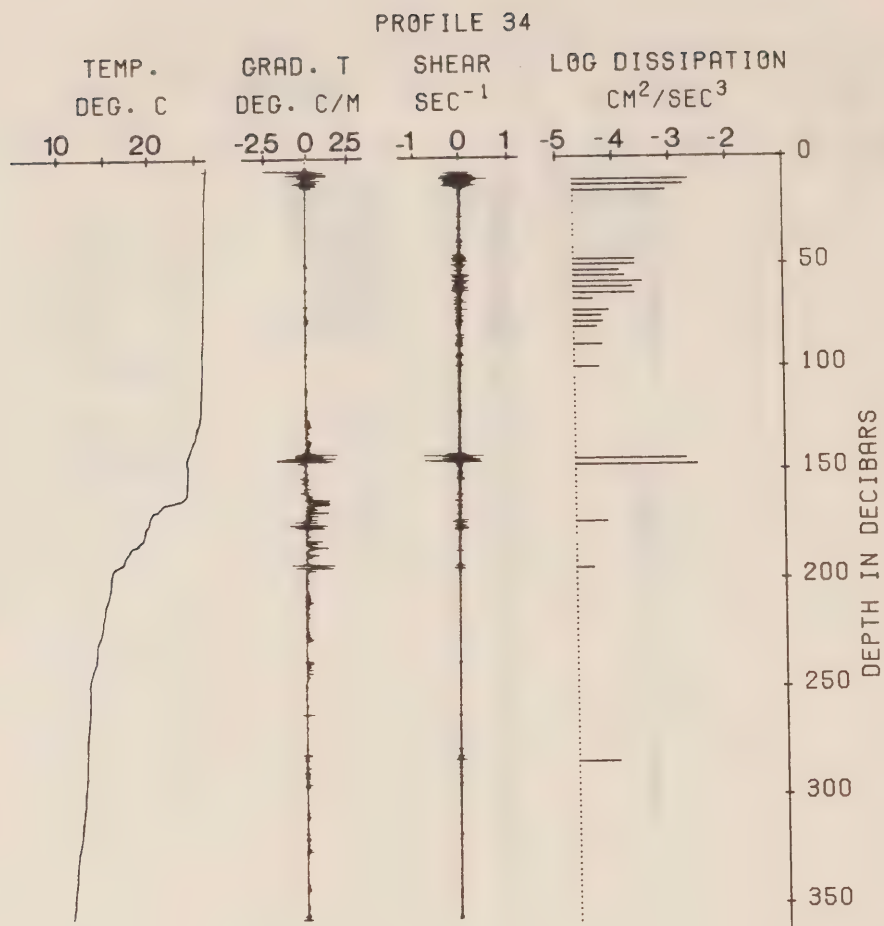


Figure 32. Profile at 0°, 150°W on Feb.5 at 0105Z.

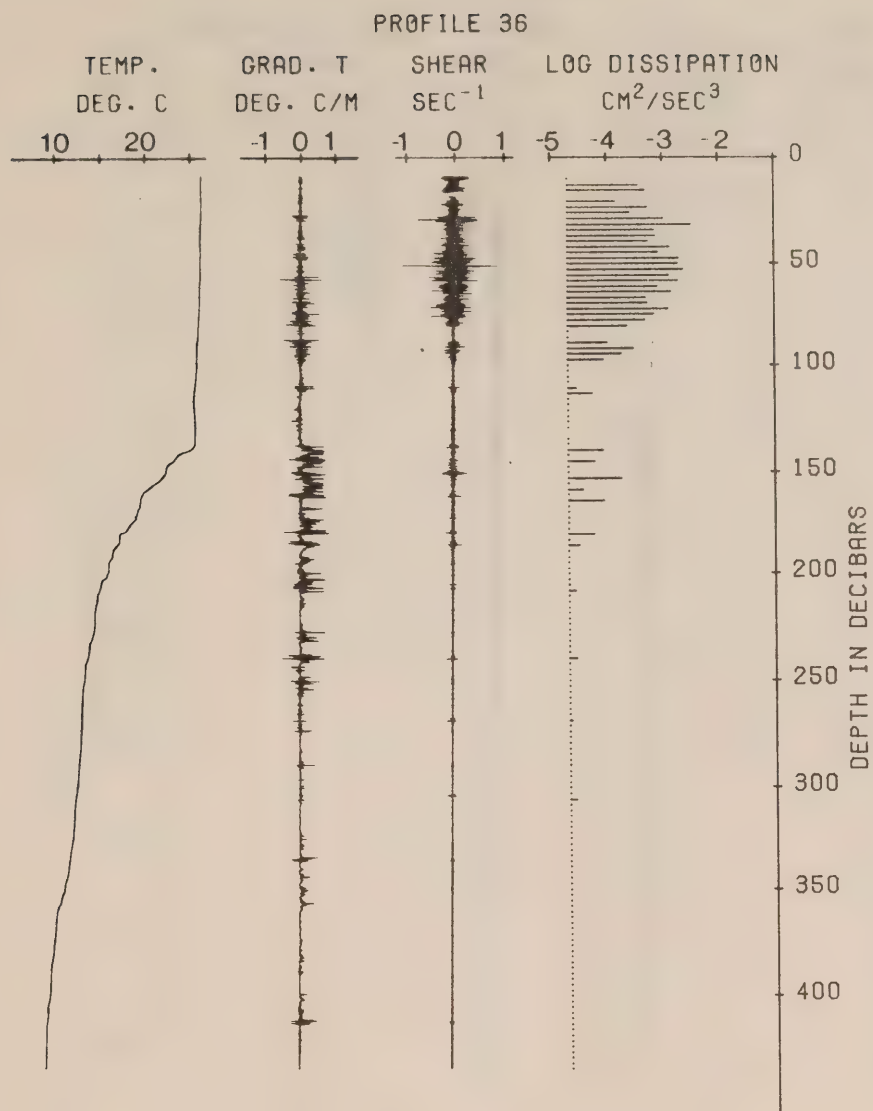


Figure 33. Profile at 0°04'S, 150°W on Feb.7 at 1844Z.

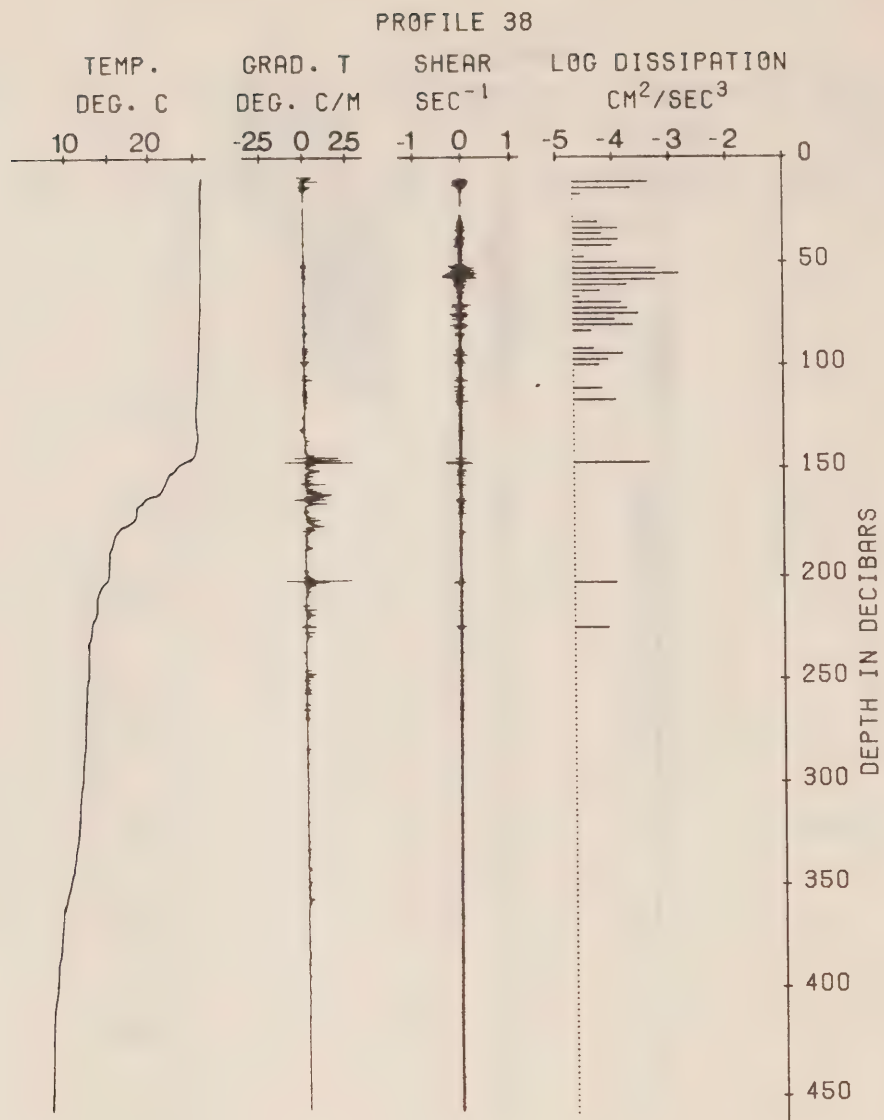


Figure 34. Profile at 0°07'S, 150°W on Feb.7 at 1933Z.

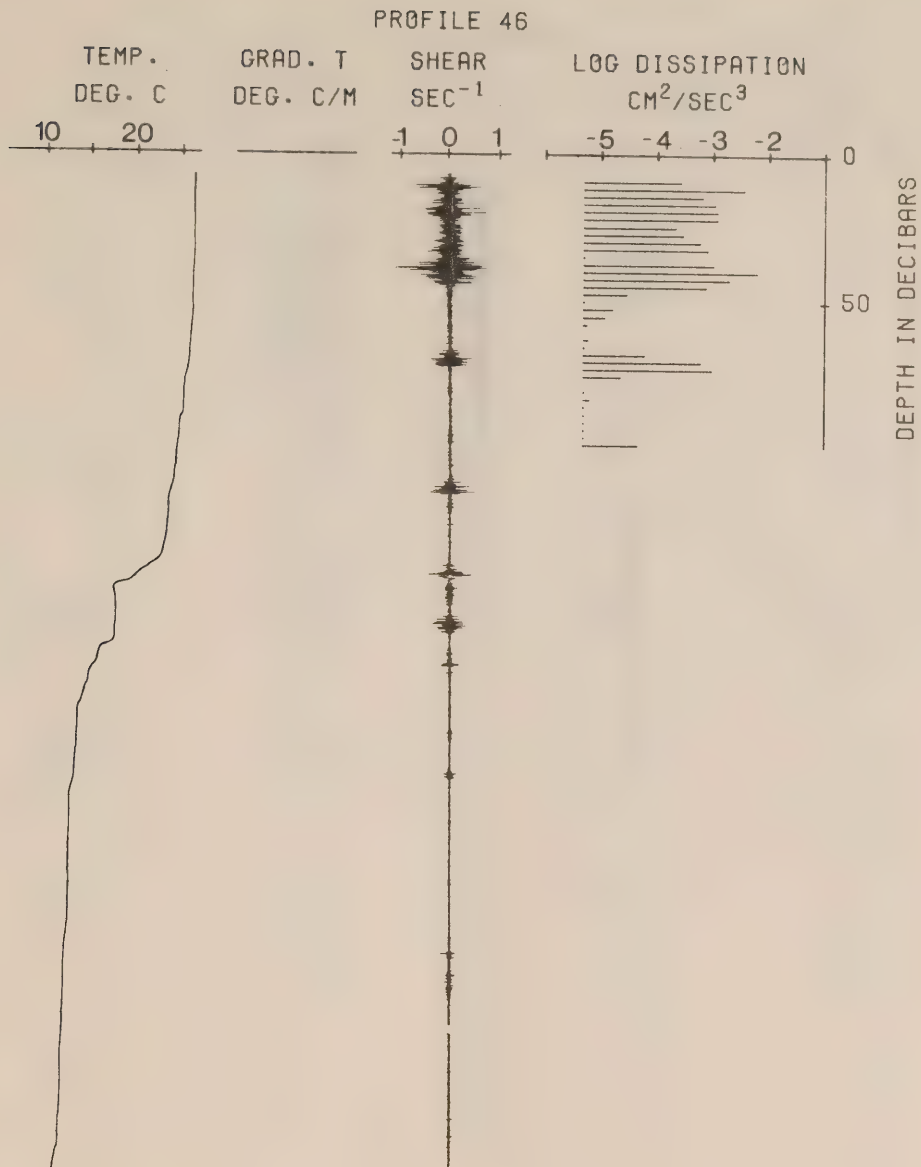


Figure 35. Profile at 0°30'N, 150°W on Feb.13 at 1745Z.

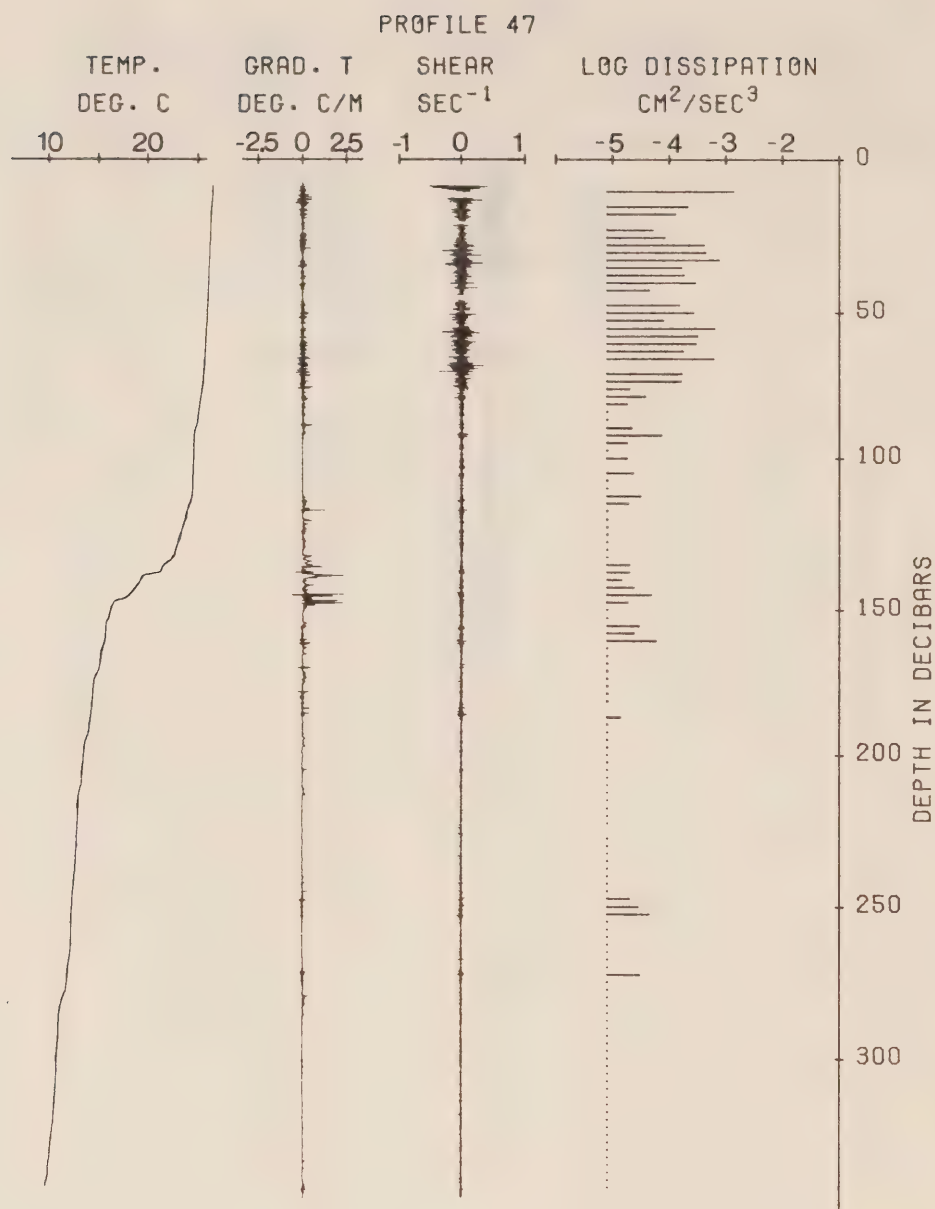


Figure 36. Profile at 1°01'N, 148°W on Feb. 14 at 2317Z.

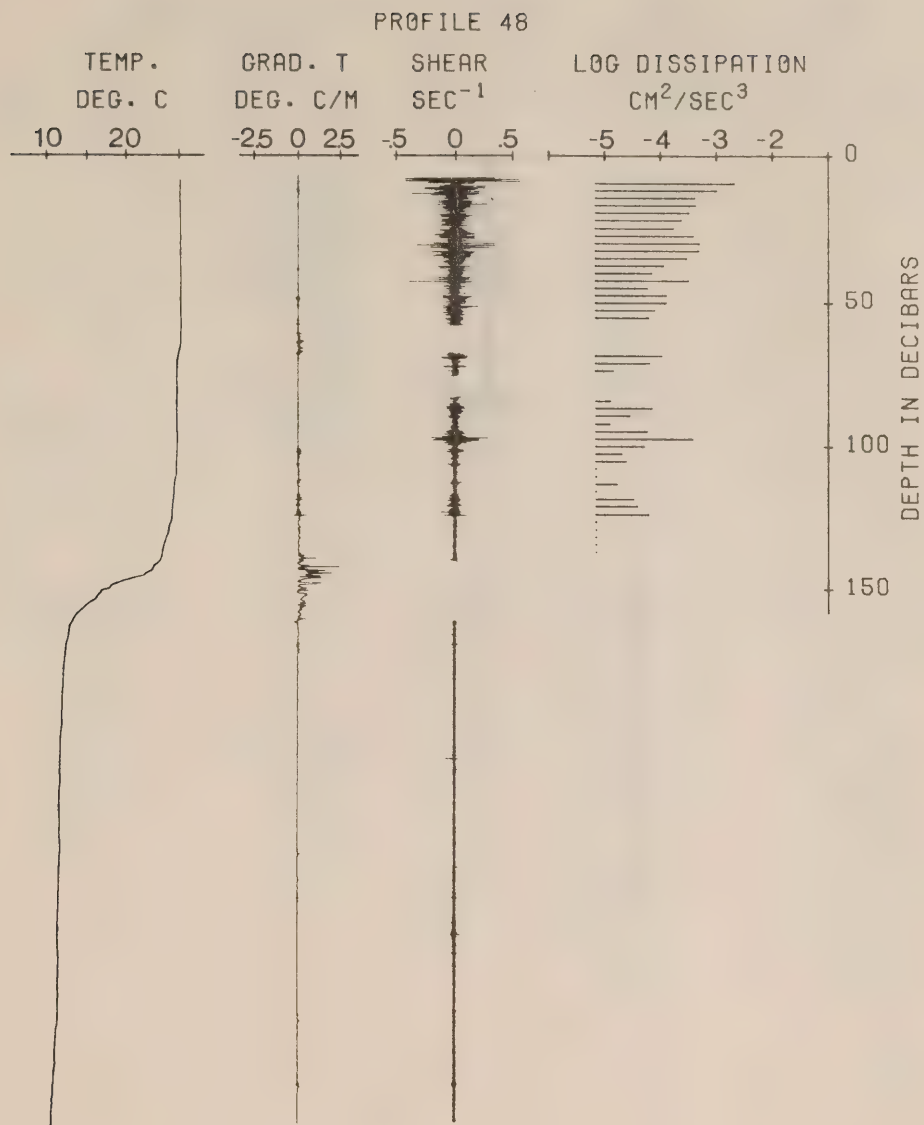


Figure 37. Profile at 2°00'N, 148°W on Feb.15 at 1902Z.

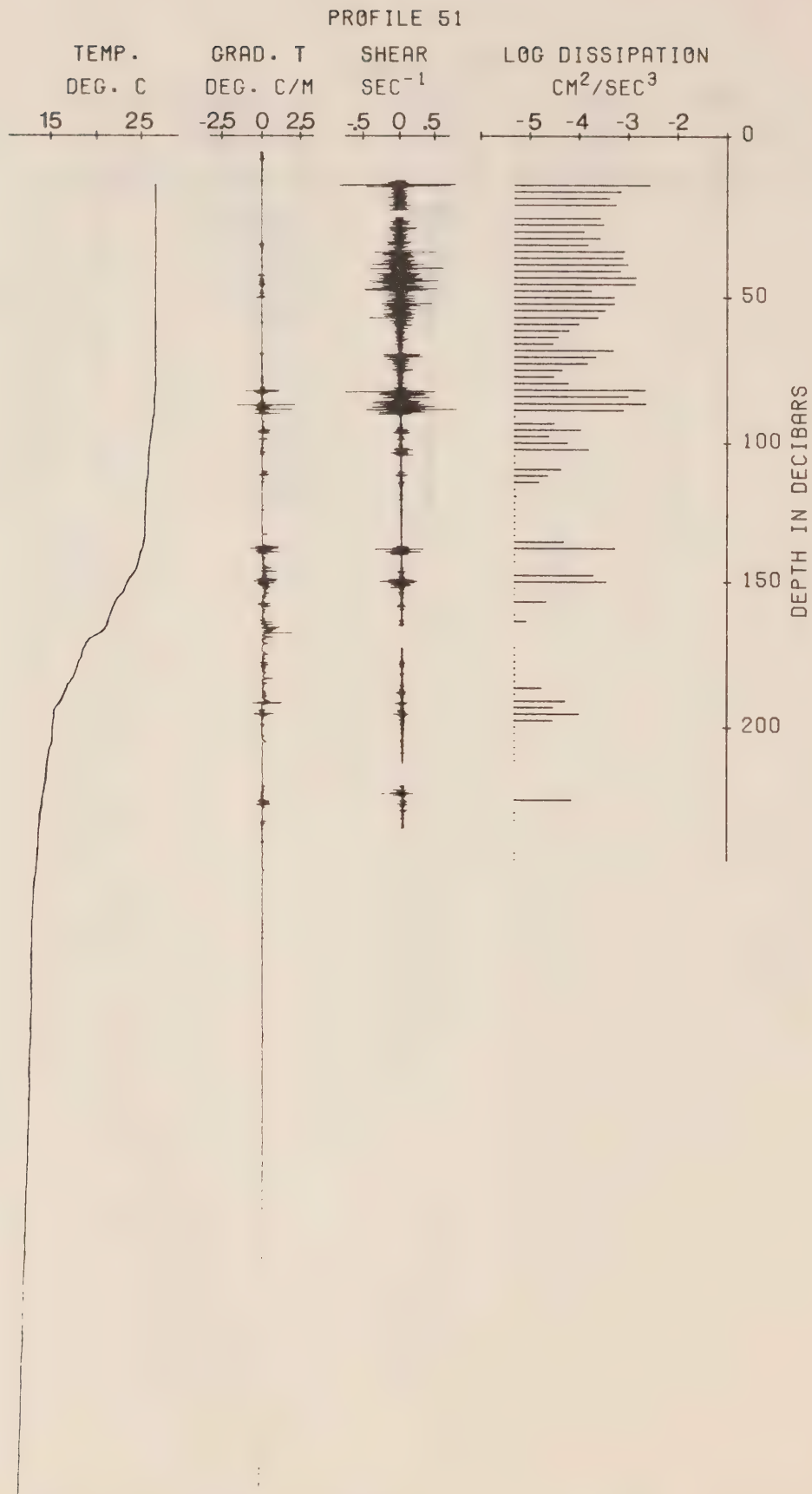


Figure 38. Profile at 5°10'N, 148°W on Feb.17 at 1800Z.

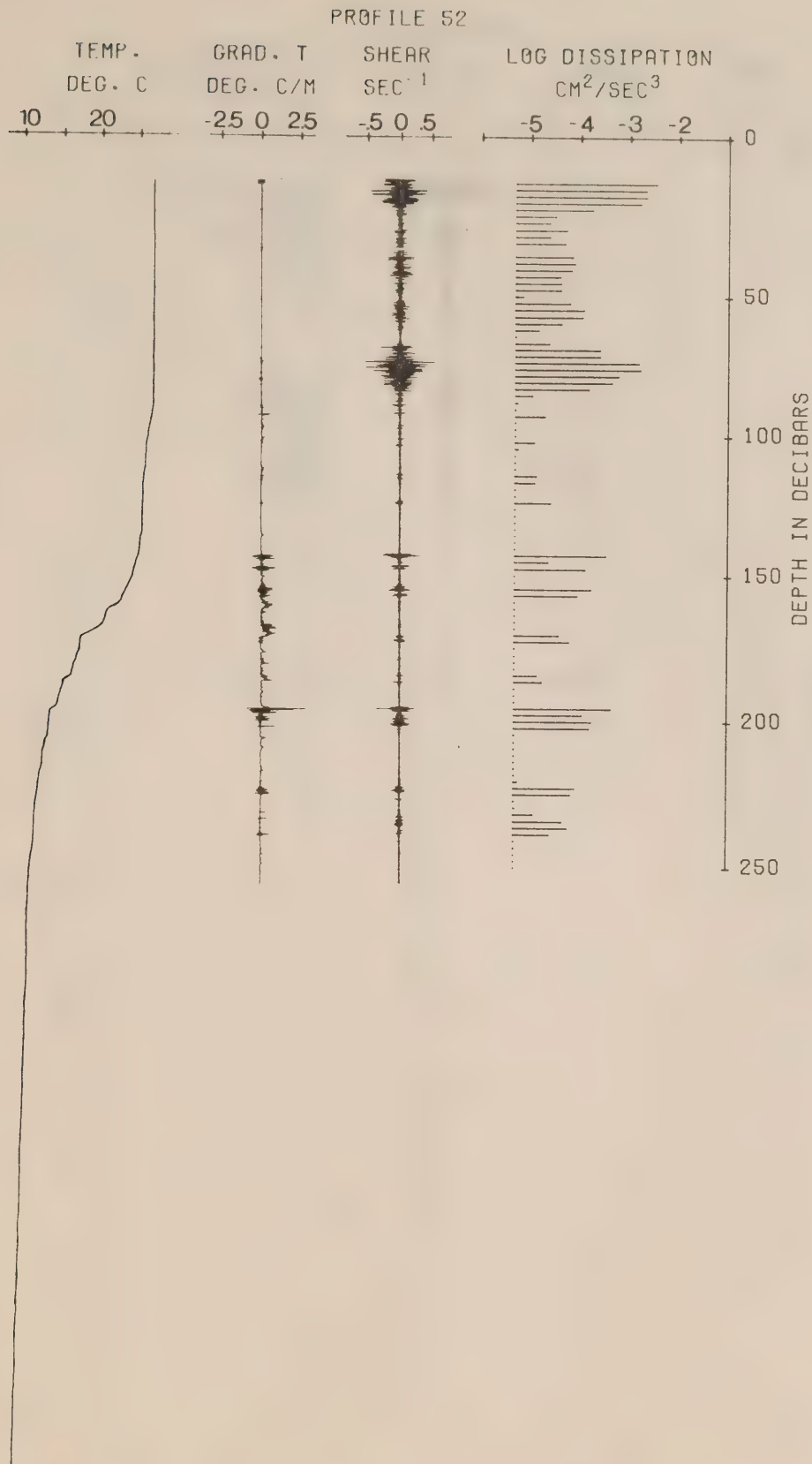


Figure 39. Profile at 5°10'N, 148°W on Feb.17 at 1936Z.

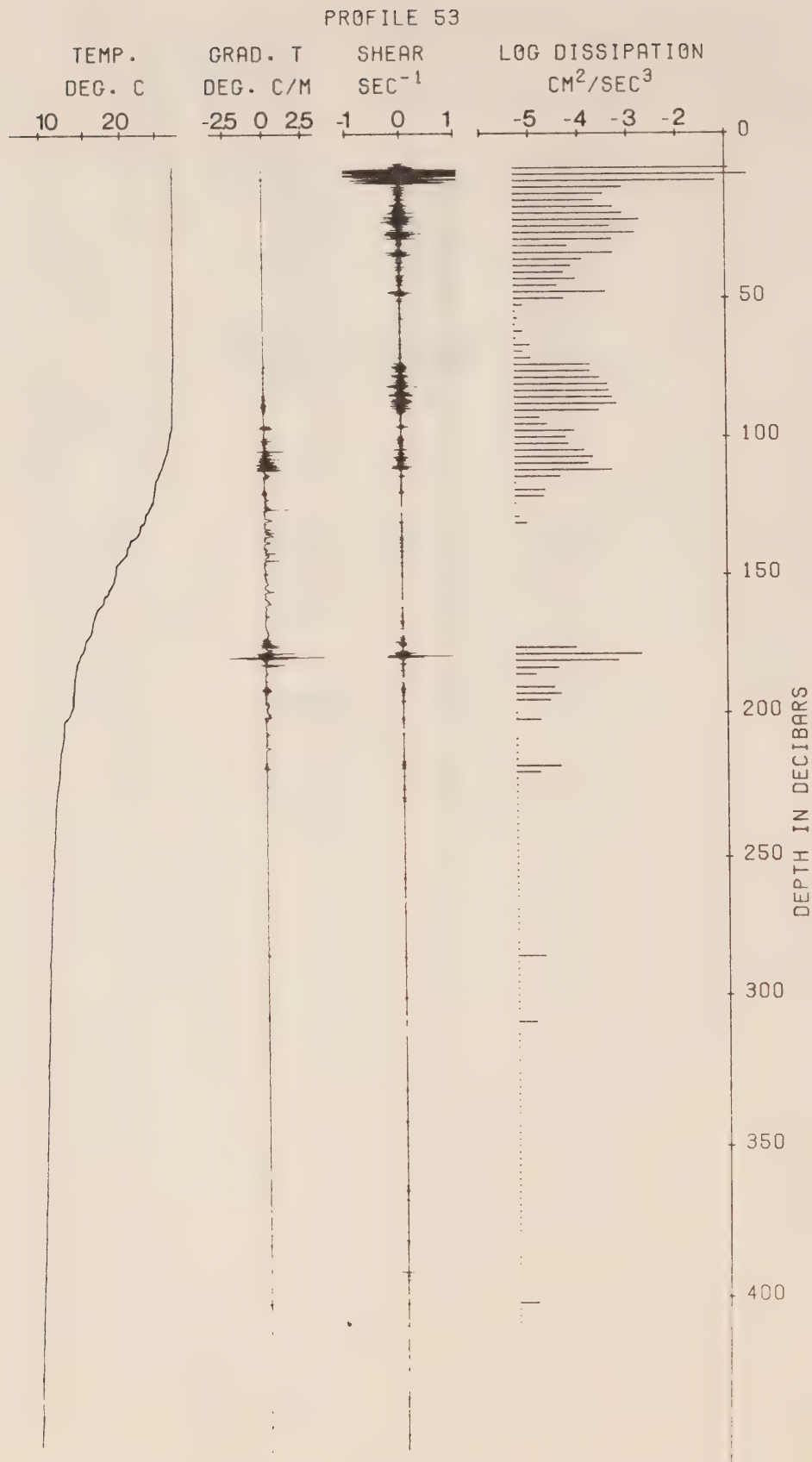


Figure 40. Profile at 6°00'N, 148°W on Feb.18 at 0203Z.

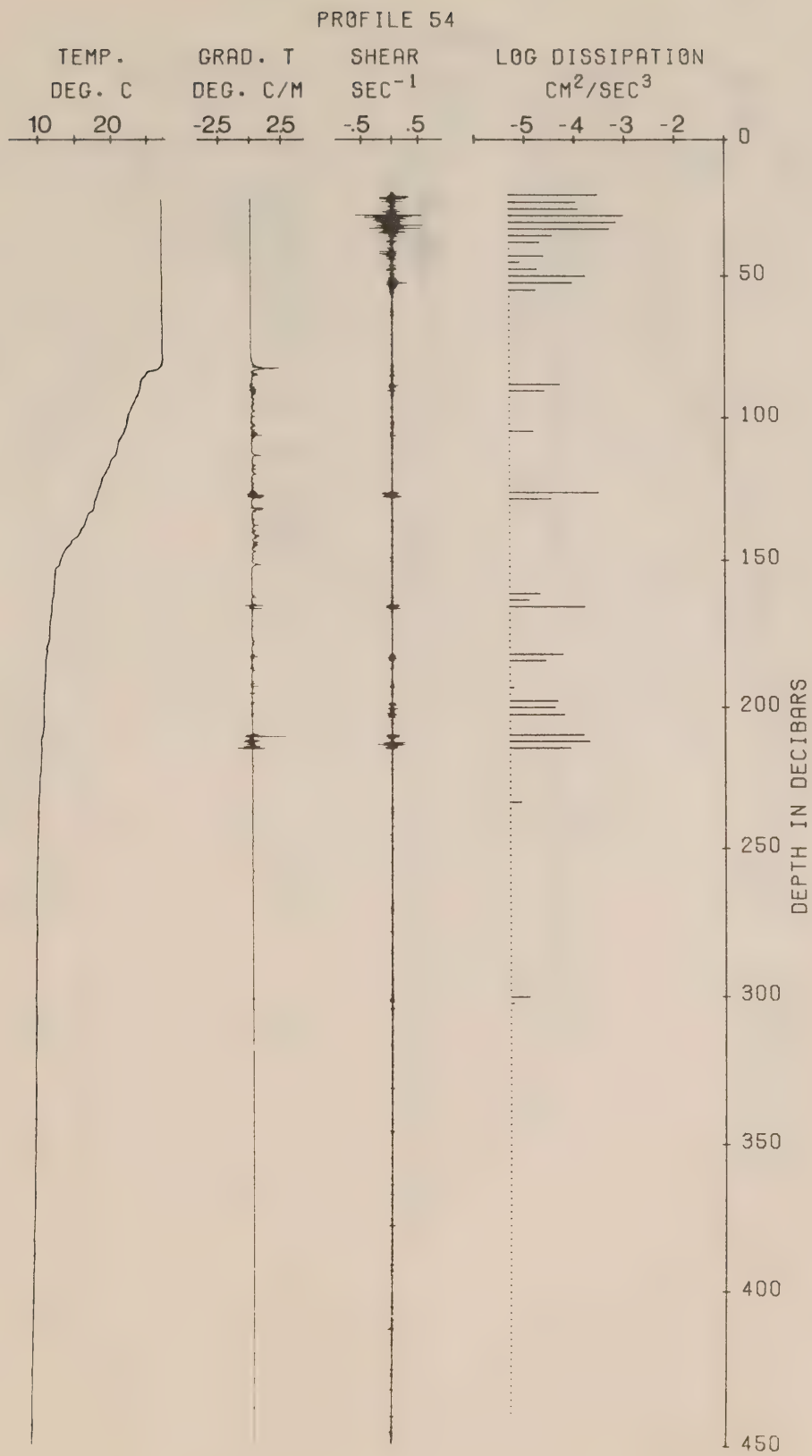


Figure 41. Profile at 7°02'N, 149°W on Feb.18 at 1716Z.

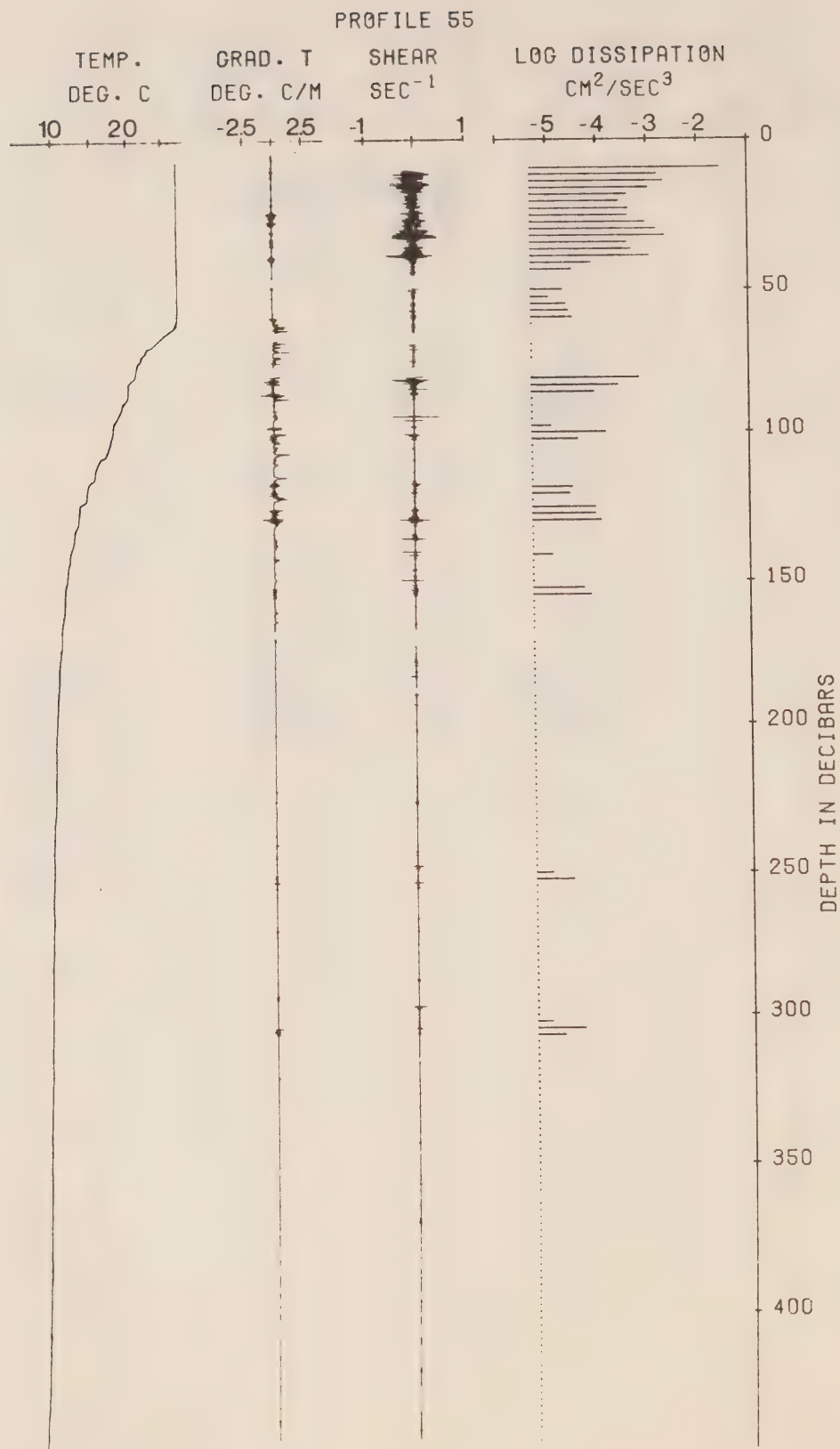


Figure 42. Profile at 8°01'N, 149°W on Feb.19 at 0040Z.

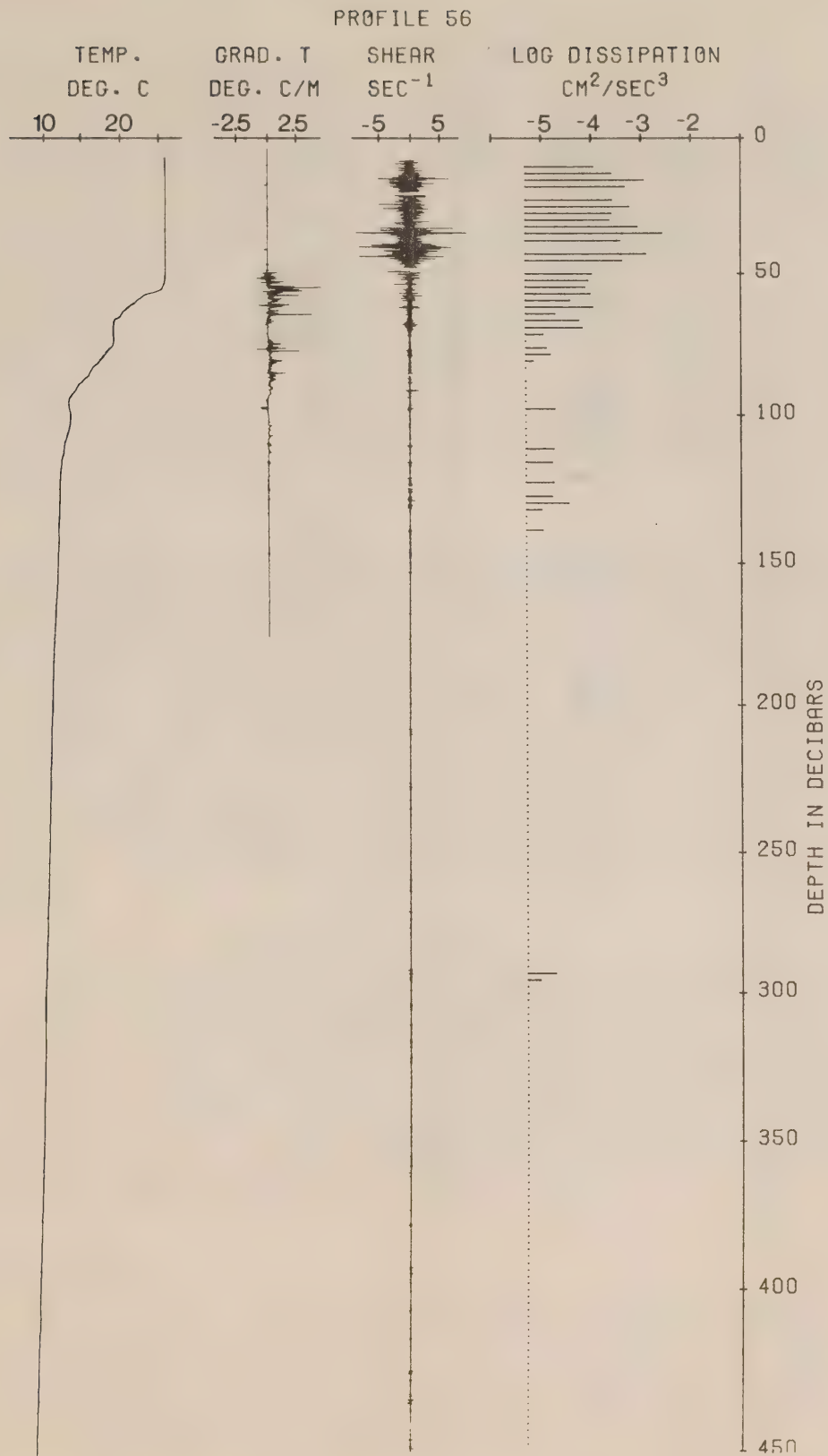


Figure 43. Profile at 10°01'N, 150°W on Feb.19 at 1851Z.

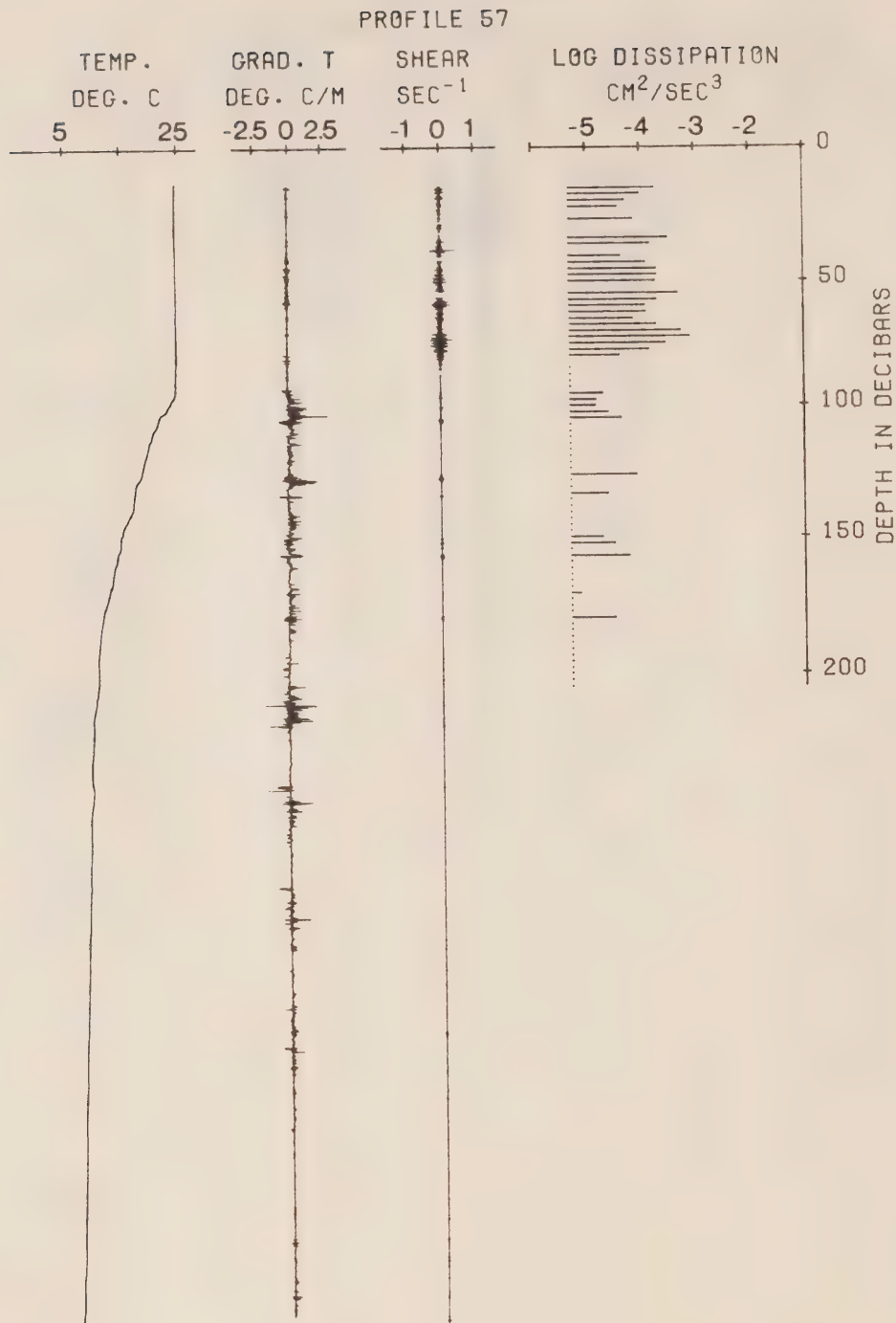


Figure 44. Profile at 14°19'N, 153°W on Feb.20 at 2012Z.

3. Discussion

The undercurrent core as determined from velocity profiles was near 150m throughout the cruise (Curran, in preparation) and the high dissipation rates did not extend down to the depth of the core. To show the difference between Equatorial and non-Equatorial turbulence we have plotted in Figure 45 the average dissipation observed between 20m and 140m depths for all profiles which span this interval. The increase near the Equator in $\bar{\epsilon}$ can be clearly seen. At 1° from the Equator dissipations were reduced to background levels. Also plotted are the coverage dissipations observed in the Atlantic in July 1974 with Camel (Crawford and Osborn, 1979a). Average rates are higher in the Atlantic, but the smaller number of profiles reduces the statistical significance of this comparison. Seven of the ten most energetic profiles in the Pacific were observed on January 21-22, a day of strong winds, and these seven significantly boosted the average of the values of $\bar{\epsilon}$ observed in the Pacific.

One significant difference between the two oceans is the low level of dissipations observed below the Pacific Equatorial Undercurrent. Over the 60 metre band between 160-220 metres depth within $1/2^\circ$ of the equator, the integrated dissipation rate is $0.05 \text{ cm}^3\text{sec}^{-3}$, while in the Atlantic below the velocity core of the undercurrent the integrated dissipation averages $2 \text{ cm}^3\text{sec}^{-3}$. Although only six profiles were taken in the Equatorial Atlantic, the integrated dissipation below the core in each was much higher than the average value of $0.05 \text{ cm}^3\text{sec}^{-3}$ observed in the Pacific. The differences may be related to lower shears below the Pacific Equatorial Undercurrent. Current measurements during the *Parizeau* cruise were not routinely made below 200m depth; hence it is difficult to attribute the lower dissipation rates to either a small shear or a small Richardson number below the core.

Average dissipation between 20 and 140m, between January 17 and February 7, 1979 was observed to be $6 \times 10^{-4} \text{ cm}^2\text{sec}^{-3}$. This value was computed by forming the mean of the daily average of $\bar{\epsilon}$ over the depth range. Because profiles concentrated closely in time tended to be at times of high dissipation rate, a simple average of each profile gives higher dissipations, but is less representative. Once data from sea level slopes, dynamic heights and currents are available for the Pacific in 1979, it may be possible to compare this dissipation rate to sources of energy in the Undercurrent, to determine an energy budget of this current.

4. Acknowledgements

Serge Milaire kept the instrumentation running despite the rolling ship. Richard Campbell helped examine 10,000 spectra and data records for spikes, and processed the signals. Keith Lee plotted the dissipation profiles and Brian Watt optically filtered, reduced and printed thirty-seven charts in total darkness. Barbara Smith drafted many of the figures and the manuscript was carefully typed by Susan McKenzie.

AVERAGE DISSIPATION

● Pacific, 1979 20 metres to
140 metres depth

○ Atlantic, 1974 20 metres to
undercurrent core

$\bar{\epsilon}$ (cm^2/sec^3)

NORTH

SOUTH

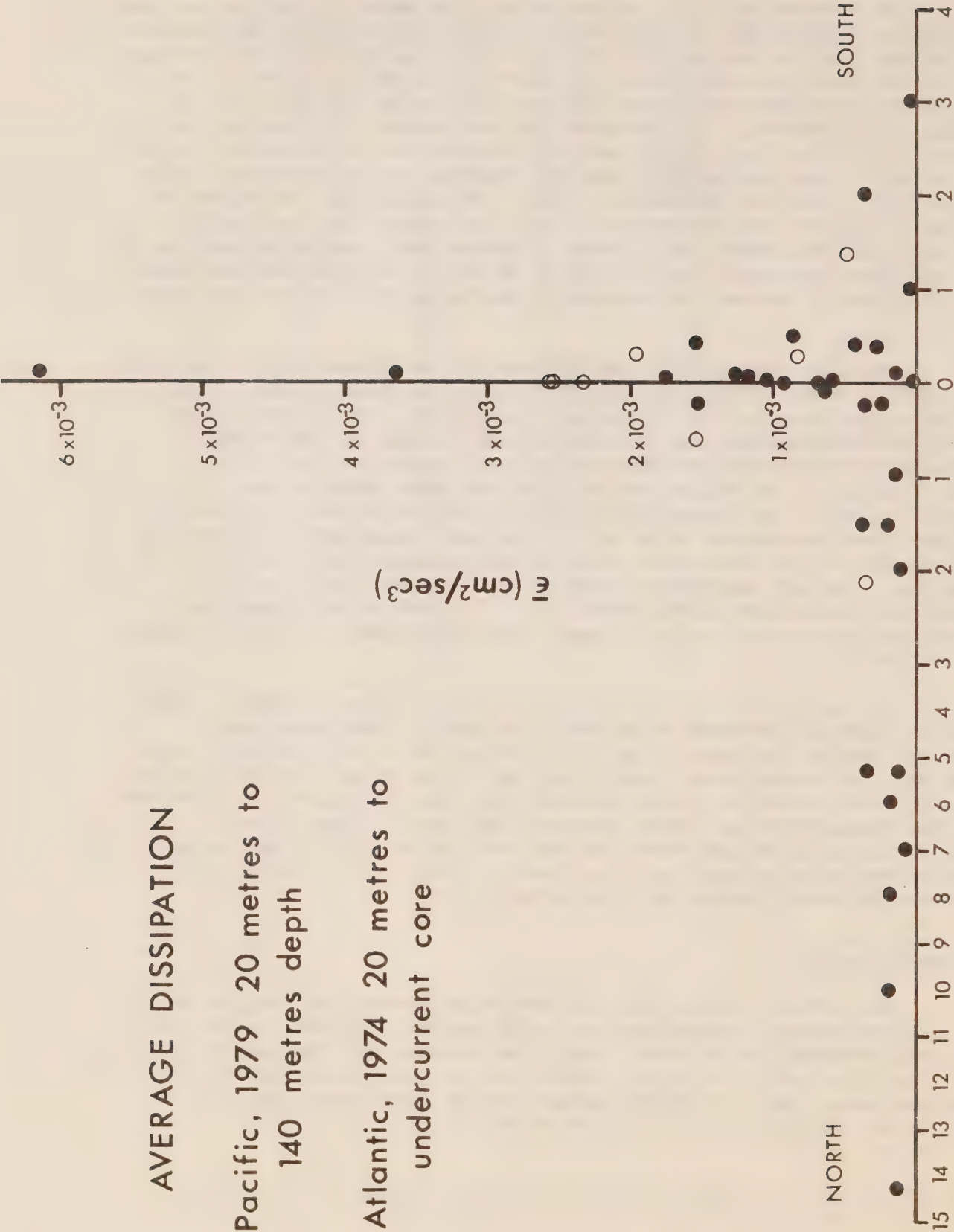


Figure 45. Average dissipations observed during *Parizeau* cruise in 1979 and *Atlantis II* cruise in 1974.

5. References

- Crawford, W.R. 1976. Turbulent Energy Dissipation in the Atlantic Equatorial Undercurrent, Ph.D. Thesis, University of British Columbia, Institute of Oceanography, Vancouver, B.C.
- Crawford, W.R. and T.R. Osborn. 1979a. Microstructure measurements in the Atlantic Equatorial Undercurrent during GATE. Deep-Sea Res., Suppl. II to V.26, 285-308.
- Crawford, W.R. and T.R. Osborn. 1979b. Energetics of the Atlantic Equatorial Undercurrent, Deep-Sea Res., GATE Supplement II to V.26, 309-324.
- Curran, T. (in preparation). Time Variations of the Pacific Equatorial Undercurrent, University of British Columbia, Dept. of Oceanography, M.Sc. thesis.
- Desaubies, Y.J.F. and M.C. Gregg. 1978. Observations of internal wave vertical velocities by a free-fall vehicle. Deep-Sea Res., 25, 933-946.
- Gargett, A.E. and T.R. Osborn. 1978. Dissipation Measurements from the Fine and Microstructure Experiment. Manuscript Report 33, University of British Columbia, Institute of Ocean Sciences.
- Miyake, Y. and M. Koizumi. 1948. The measurements of the viscosity coefficient of seawater. J. Mar. Res. 7, 63-66.
- Oakey, N.S. and J.A. Elliott. 1980. Dissipation in the mixed layer near Emerald Basin, Marine Turbulence, ed. by J.C.J. Nihoul, Elsevier Sc. Pub. Soc., Amsterdam.
- Osborn, T.R. and W.R. Crawford. 1977. Turbulent Velocity Measurements with an Airfoil Probe. Manuscript Report 31, University of British Columbia, Institute of Oceanography, Vancouver, B.C.
- Osborn, T.R. and W.R. Crawford. 1980. An airfoil probe for measuring turbulent velocity fluctuations in water, Chapter 19 of "Instruments and Methods in Air-Sea Interaction", ed. by F. Dobson, L. Hasse and R. Davis. Plenum, New York.

CAI
EP 321
-81R02



**REPORT ON OCEAN DUMPING
R AND D PACIFIC REGION
DEPARTMENT OF FISHERIES AND OCEANS
1979 - 1980**

Edited by

S. C. Byers

Dobrocky SEATECH Limited

For

Regional Ocean Dumping Advisory Committee (Pacific)

(R.O.D.A.C. (Pacific))

**INSTITUTE OF OCEAN SCIENCES
Sidney, B.C.**



For further information or additional copies please write to:

Department of Fisheries and Oceans

Institute of Ocean Sciences

P.O. Box 6000

Sidney, B.C. CANADA

V8L 4B2

REPORT ON OCEAN DUMPING R AND D PACIFIC REGION
DEPARTMENT OF FISHERIES AND OCEANS
1979 - 1980

Edited by
S.C. Byers
Dobrocky SEATECH Limited

For
Regional Ocean Dumping Advisory Committee (Pacific)
(R.O.D.A.C. (Pacific))

Institute of Ocean Sciences
Sidney, B.C.
1981

ACKNOWLEDGEMENTS

I would like to express my thanks to the speakers, contractors and workshop participants who contributed to the workshop and the contents of this report. A special mention goes to Hal Nelson of E.P.S., Vancouver who was chairman of the workshop and to Dick Herlinveaux of I.O.S., for his advice throughout the program. Thanks also to Pat Shaw of SEATECH for his drafting and assistance with the compilation of the report.

TABLE OF CONTENTS

	Page
I. SUMMARY AND CONCLUSIONS	1
II. ANALYSIS OF DATA RELATING TO DUMPSITE COLONIZATION AND TEMPORAL CHANGES IN BENTHIC COMMUNITIES, ALBERNI INLET. C.D. LEVINGS	4
III. REVIEW OF OCEANOGRAPHIC DATA RELATING TO OCEAN DUMPING IN THE PRINCE RUPERT AREA WITH COMMENTS ON PRESENT AND ALTERNATE DUMPSITES. E.R. McGREER, P.W. DELANEY AND G.A. VIGERS	5
IV. MIGRATION OF MERCURY AND CADMIUM FROM SEDIMENTS. R.W. MACDONALD AND R.D. MORSE	7
V. AVAILABILITY OF METALS FROM INORGANIC PARTICULATES (MINE TAILINGS) FOR UPTAKE BY MARINE INVERTEBRATES. E.R. McGREER, B.J. REID AND G.A. VIGERS	9
VI. CONTAMINANT MOBILIZATION AND BIOACCUMULATION FROM MARINE SEDIMENTS ADJACENT TO A SHIP REPAIR FACILITY. E.R. McGREER AND B.J. REID	11
VII. DETERMINATION OF BACKGROUND LEVELS OF CADMIUM IN CHURCHILL HARBOUR AND ITS APPROACHES IN HUDSON BAY. R.W. MACDONALD AND P. ERICKSON	12
VIII. TABLE	14
IX. FIGURES	16
X. APPENDICES	25
I. WORKSHOP ATTENDANCE LIST	26
II. 1979-80 CONTRACTS	27
III. 1980-81 CONTRACTS	28
IV. LOCATION OF PARTICIPANTS	30

TABLE

	Page
1. TWO-WAY ANALYSIS OF VARIANCE TO DETERMINE TEMPORAL CHANGES BETWEEN THE DUMPSITE AND CONTROL SITE COMMUNITIES, ALBERNI INLET	15

FIGURES

	Page
1. LOCATION OF EIGHT SITES PROPOSED FOR OCEAN DUMPING IN THE PRINCE RUPERT AREA (FROM E.V.S. CONSULTANTS LIMITED REPORT)	17
2. SCHEMATIC OF THE WATER COLUMN REACTION VESSEL: APPROXIMATE DIMENSIONS 75 CM x 14 CM (in part, FROM CHEMEX LAB LIMITED REPORT)	18
3. CONCENTRATION OF DISSOLVED AND PARTICULATE FORMS OF ^{203}Hg AND ^{109}Cd IN THE AQUEOUS PHASE	19
4a. TOTAL ^{203}Hg (DISSOLVED AND PARTICULATE) AS A FUNCTION OF TIME IN THE OXIC, NEAR ANOXIC AND ANOXIC VESSEL	20
4b. TOTAL ^{109}Cd (DISSOLVED AND PARTICULATE) AS A FUNCTION OF TIME IN THE OXIC, NEAR ANOXIC AND ANOXIC VESSEL	20
5. CONCENTRATION OF Hg AS A FUNCTION OF DEPTH IN THE SEDIMENTS	21
a) Oxidic vessel	
b) Near anoxic vessel	
c) Anoxic vessel	
6. ^{109}Cd AS A FUNCTION OF DEPTH IN THE SEDIMENTS FOR OXIC, NEAR ANOXIC AND ANOXIC WATER CONDITIONS	22
7. SAMPLING SITES FOR O.D.P.A. (4443-0234) IN CHURCHILL HARBOUR 1977-1978 (RENEWABLE RESOURCES CONSULTING SERVICES LIMITED) .	23
8. SAMPLING SITES IN CHURCHILL HARBOUR 1980 (FROM ARCTIC LABORATORIES LIMITED REPORT)	24

I. SUMMARY AND CONCLUSIONS

This report summarizes the progress and results of the 1979-1980 studies contracted in support of Ocean Dumping legislation and reviews a workshop on ocean dumping research held on December 4, 1980 at the Institute of Ocean Sciences, Sidney, B.C.

The focus of ocean dumping studies is gradually moving away from Alberni Inlet. The statistical analysis of the biological data from the Port Alberni dumpsite has been completed. Of the eight parameters considered, dissolved oxygen and biomass were the only features that were not significantly different when the dumpsite was compared to the "control" site. The dumpsite rapidly recolonized, even between dumping episodes, by opportunistic species. A physical oceanographic study which will provide velocity fields or flow patterns in the vicinity of the sill is the only contract currently underway in Alberni Inlet.

A study to review oceanographic data from the Prince Rupert area has been done, evaluating conditions present near the existing dumpsites. Recommendations were made regarding alternate dumpsites according to their suitability for disposal of contaminated and clean dredge spoils.

Laboratory studies monitoring, over a period of 180 days, the migration of mercury and cadmium from sediments in oxic, near anoxic and anoxic environments have been completed. The results show that Hg appears to travel with particulates, with concentrations decreasing at a slower rate under anoxic conditions than under more oxic conditions. Downward transport of Hg in sediments takes place under anoxic conditions possibly due to the formation of polysulphide complexes. The study suggests that an oxic environment is preferable for depositing Hg-containing sediments.

Cadmium is scavenged by particulates but some fraction remains to a certain degree in the dissolved phase. Although Cd is tied up more effectively in sulphide phases, the evidence shows that Cd releases are possible if the sulphidic sediments become oxic.

Bioavailability studies of heavy metals (Cu, Pb, Zn, Cd and Fe) from mine tailings have been completed, using the marine invertebrates *Mytilus edulis* and *Macoma balthica*. The highest concentrations of all metals were bioaccumulated by the organisms from the Greenland mine tailings. There was no direct relationship between the bioaccumulation of metals and salinity or temperature although the degree of bio-uptake was generally proportional to the concentration of metals in sea water. *M. balthica*, a deposit feeding clam, bioaccumulated higher levels of metals than *M. edulis*, a filter feeding mollusc. The release of metals from the mine tailings into sea water during leaching tests generally increased with increasing salinity and dissolved oxygen conditions.

Laboratory studies to determine the mobilization of contaminants (Cd, Cu, Pb, Zn, As, Hg and PCB's) from contaminated marine sediments have been done. The work was not funded by R.O.D.A.C. but came from E.P.S. funds for ocean dumping research. The tests showed there was bioaccumulation of lead and PCB Arochlor 1254 by *Macoma balthica* and *Mytilus edulis*. There was no direct relationship between salinity and contaminant uptake in tests conducted at 10 and 25 ‰. Bioaccumulation of the contaminants was not directly proportional to their concentration in sea water in the tests, or to their total concentration in sediments.

A study was conducted in Churchill Harbour, Hudson Bay to clarify and determine the background levels of Cd found in the sediments. Previous monitoring indicated Cd levels exceeding those permitted in the Ocean Dumping Act Regulations; however, further investigation showed that the high Cd levels were laboratory artifacts. Recommendations are made to alleviate similar problems from occurring in future ocean dumping studies.

Future ocean dumping research will focus on the logistics and rationale related to the disposal of materials at sea. Three approaches will be considered:

1. Short-term measures to handle disposal of material without violating the Ocean Dumping Act or other relevant acts;
2. Long-term research and investigations to develop suitable tests (e.g., bioavailability, bioaccumulation and mobilization experiments) to determine whether or not a material is a candidate for ocean dumping;
3. Research to determine the effects of "capping" the dumped material as a means of confinement.

Results from these investigations will provide the information necessary to amend the Ocean Dumping Regulations Act, if required.

The contents of this report are restricted to extended abstracts, since the majority of the presentations are for publication in other sources. A list of participants in the workshop is given in Appendix I. Contracts for 1979-1980 are summarized in Appendix II. A complete list of the contracted studies for 1980-1981 is found in Appendix III.

Some of the references cited here are manuscripts produced under contract, and are not available for distribution. For further information on any of the Institute of Ocean Sciences series of Contract Reports, contact the listed Scientific Authority. The locations of the Scientific Authorities and a key to the research institution abbreviations can be found in Appendix IV. Pacific Marine Science Reports (PMSR) are

available for limited distribution from the Institute of Ocean Sciences.

This report was prepared by Dobrocky SEATECH Limited under contract to the Institute of Ocean Sciences Ref. DSS File No. 05SB.FP833-0-1984.

II. ANALYSIS OF DATA RELATING TO DUMPSITE COLONIZATION AND TEMPORAL CHANGES IN BENTHIC COMMUNITIES IN ALBERNI INLET

C.D. Levings, W.V.L.

Contractor: E.V.S. Consultants Limited

Statistical analyses of the temporal changes in the major biotic and abiotic features at the Alberni dumpsite and a "control" site were performed using two-way analysis of variance. Plots of the temporal changes in eight parameters were constructed. A preliminary analysis using clustering techniques to examine the temporal change in community structure was also performed.

Table 1 shows the results of the two-way analyses. As shown, changes in all parameters were statistically significant over time. Dissolved oxygen (D.O.) and biomass were the only features that were not significantly different when the dumpsite was compared to the "control" site. Interaction between station and time were significant for all parameters. Because of the strong possibility that internal tides were operating in the Inlet, it would be difficult to interpret the D.O. data in terms of an effect of dumping, or, in this instance, the lack of an effect. The absence of a significant biomass difference was probably attributable to the rapid colonization of the dumpsite, even between dumping episodes, by opportunistic species such as the polychaete *Capitella* sp.

The C:N ratio was a particularly useful parameter which helped identify the suitability of the dumpsite sediments for colonization by fauna other than the opportunistic species. At the "control" site the C:N ratio ranged from 26:1 to 30:1. At the dumpsite, during the dumping season, the C:N ratio was 56:1, shifting to 26:1 after dumping ceased in March 1978.

III. REVIEW OF OCEANOGRAPHIC DATA RELATING TO OCEAN DUMPING IN THE PRINCE RUPERT AREA WITH COMMENTS ON PRESENT AND ALTERNATIVE DUMPSITES

E.R. McGreer, P.W. Delaney and G.A. Vigers

E.V.S. Consultants Limited

Subcontractors: J.W. McDonald, E.S.L. Consultants Limited
E.H. Owens, Woodward-Clyde Consultants Limited

Prepared for: C.D. Levings, W.V.L.

A review of oceanographic data in the Prince Rupert region of British Columbia was undertaken to evaluate suitable sites for ocean dumping. Eight sites were proposed after an initial review of the existing data and, from these, recommendations for the most suitable dumpsites were made.

The eight sites selected for review are listed below and their locations shown in Figure 1. The sites were selected on the basis that an adequate amount of scientific data existed upon which to make an evaluation of each location as a possible ocean dumping site. The sites selected were as follows:

<u>Site No.</u>	<u>Name</u>	<u>Depth Range</u>	<u>Approximate Location</u>
1	Chatham Sound - deep trench	90-120 m	54° 12'N, 130° 25'W
2	Porpoise Harbour - deep hole	17- 20 m	54° 14'N, 130° 18'W
3	Prince Rupert Harbour - deep hole	35- 50 m	54° 13'N, 130° 21'W
4	Tuck Inlet	55- 60 m	54° 25'N, 130° 17'W
5	North Prince Rupert Harbour	55 m	54° 22'N, 130° 16'W
6	Chatham Sound - Malacca Passage	90-140 m	54° 06'N, 130° 22'W
7	Brown Passage	90-100 m	54° 18'N, 130° 45'W
8	Ogden Channel	145-190 m	53° 53'N, 130° 18'W

Information was collected on historic dumpsites, physical oceanography, resource species (spawning grounds, locations of fishing areas), bottom sediment transport, disposal of contaminated material, and the economics and logistics of ocean dumping in the region. Interviews were also conducted with various government personnel, dredging proponents and local fishermen.

Potential sites were rated according to their suitability for disposal of contaminated and clean dredge spoils. The site most highly recommended for disposal of contaminated materials (i.e. containing toxic wastes but low oxygen demand) was Tuck Inlet. It was the most suitable site according to biological resource data and the second most suitable site in terms of physical oceanographic criteria. The site in North Prince Rupert Harbour was the second most favourable location for dumping of contaminated material in a combined rating of biological and physical oceanographic criteria.

Porpoise Harbour was third in the overall rating system, but concerns related to salmon enhancement projects scheduled in the area provide mitigating circumstances against its continued use for ocean dumping.

The site most suitable for dumping of clean materials was Ogden Channel. It rated third overall for biological criteria and fourth for physical oceanography. Brown Passage was the second most suitable site for dumping clean material. North Prince Rupert Harbour was also considered but a detailed study of the currents and bottom sediment transport in the area was recommended.

Specific data for many of the dumpsites were missing. Information which was available was most often the result of single samplings providing no data on seasonal variations or changes from one year to another. In particular, relevant data on bottom currents within 1 m of the sea bed, which are essential for assessing sediment bedload transport, were non-existent. It was recognized that collection of additional data might result in modifications or changes in the sites recommended for dumping in the present study.

IV. MIGRATION OF MERCURY AND CADMIUM FROM SEDIMENTS

R.W. Macdonald, I.O.S.
and R.D. Morse, Chemex Labs Limited

Contractor: Chemex Labs Limited

Experimental design to determine the migration of mercury and cadmium from sediments encompassed three sealed reaction vessels. Each vessel or plastic cylinder (~ 14 cm in diameter) was fitted with an aluminum cutter at the bottom, a gas tight plate with valves at the top, a sample withdrawal port and circulation ports (Figure 2). Each cylinder was pressed into an undisturbed sediment (box core) obtained at the Howe Sound ocean dumping site. Mercury contaminated sediments from near the F.M.C. (Food Machines Corporation) dock at Squamish were obtained with a Smith-McIntyre grab, labelled with ^{203}Hg and ^{109}Cd and homogenized. Sea water was collected in 30 L Niskin bottles from near bottom at the dumpsite. The experiment was initiated by dumping the labelled sediments into the reactor vessels after filling them with sea water. The vessels were allowed to remain oxic for the first 48 hours while sediments settled. After 48 hours, the remaining water was decanted and fresh sea water added. One vessel was maintained oxic ($6-8 \text{ mL L}^{-1} \text{ O}_2$), the second near anoxic ($1-2 \text{ mL L}^{-1} \text{ O}_2$) and the third anoxic (sulphide). Concentrations of Cd and Hg were monitored for a period of 180 days at which time the bottom sediments in each of the three vessels were cored and the distribution of Hg and Cd measured.

Results from the Initial Settling Phase (oxic environment) indicated that ^{203}Hg and ^{109}Cd behaved differently during this period. Initially, the radio-tracers associated with particulate matter dominated, with the dissolved fraction contributing only a small portion (Figure 3). Considering that both tracers were added in a dissolved form (chloride), it appears as if both were effectively scavenged by the solids. With time, the particulate concentration of radio-tracers decreased for both tracers. However, while the dissolved ^{203}Hg decreased in concentration, paralleling the particulates, the dissolved ^{109}Cd remained constant and within 6 hours, dominated the aqueous phase concentration of the radio-tracer.

The long-term Settling Phase included oxic, near anoxic and anoxic environments. During this 180-day period, the total Hg concentration decreased with time in all three vessels, although more slowly in the sulphidic conditions (Figure 4a). For Cd (Figure 4b), the water concentration increased with time, especially in the oxic containers. Due to leakage problems, the anoxic vessel became oxic after about 16 days, and the increased ^{109}Cd in water is apparent after that date.

Problems with particulates during this phase of the experiment made further interpretation at this point impossible.

Results of the Post Settlement Coring of the oxic, near anoxic and anoxic environments proved most informative. Mercury concentrations (total Hg and ^{203}Hg) are plotted as a function of depth in sediment for the oxic (Figure 5a), near anoxic (Figure 5b), and anoxic vessel (Figure 5c). The high surficial concentration was the result of the labelled F.M.C. sediments, and it was apparent that about 3 cm of this material overlay the undisturbed dumpsite material. Elevated mercury concentration deep in the core (12-16 cm) is real and has been previously observed in cores from this region. The sedimentation in the oxic vessel did not appear to have been subject to much Hg transport as evidenced by the sharp gradients at 3 cm and the near uniformity at the surface. The slight enrichment of ^{203}Hg at the surface may be due to scavenging by fine particulates and settling during the experiment as shown in Figures 3 and 4a. For the near anoxic and particularly the anoxic vessel, the cores showed evidence of Hg migration (Figures 5b, c). Gradients in the top 3 cm, and in the dumpsite sediments below showed movement of ^{203}Hg and total Hg downward. This transport may be the result of polysulphide complexes. Surface layer enrichment may be the result, as in the oxic case, of scavenging by fine particulates. Interestingly, no evidence was apparent of Hg migration out of the sediments and into the water.

Figure 6 shows the distribution of ^{109}Cd in sediments after the experiment. As was the case for ^{203}Cd , the ^{109}Cd seems to have migrated downward in the sediments of the anoxic vessel. Why this occurred is not presently clear and requires further investigation.

In view of ocean dumping, Hg appears to travel with particulates. This is in agreement with observed Hg concentrations in sediments of Howe Sound near F.M.C. Although increases in Hg concentration in the water were not observed under anoxic conditions, Hg concentrations did decrease at a slower rate than under oxic or near anoxic conditions. Furthermore, downward transport of Hg in sediments took place under anoxic conditions. This observed behaviour could be caused by formation of polysulphide complexes. The results suggest that an oxic environment is probably a safer place to deposit Hg containing sediments, although more research into this aspect is required.

Cadmium, although becoming scavenged by particulates, remains to a certain degree in the dissolved phase. While Cd is tied up more effectively in sulphide phases, the evidence here is that releases are possible if sulphidic sediments become oxic.

V. AVAILABILITY OF METALS FROM INORGANIC PARTICULATES
(MINE TAILINGS) FOR UPTAKE BY MARINE INVERTEBRATES

E.R. McGreer, B.J. Reid and G.A. Vigers
E.V.S. Consultants Limited

Prepared for: M. Waldichuk, W.V.L.

The availability of heavy metals (Cu, Pb, Zn, Cd and Fe) from three discrete mine tailings for uptake by two marine invertebrates was determined under different salinity and temperature conditions. Tailings incorporated for the experiments were from the Island Copper Mine, Rupert Inlet, B.C.; Nanisivik, Strathcona Sound, N.W.T., and the Greenex (Black Angel) Mine, Agfardlikavsa Fjord, Greenland. A filter feeding mussel, *Mytilus edulis*, and a deposit feeding clam, *Macoma balthica*, were used as test organisms.

All metals were bioaccumulated to their highest concentrations in the experiments which used tailings from the Greenex mine. Concentrations of Pb of 2302 and 865 $\mu\text{g g}^{-1}$ dry weight were recorded in *M. balthica* and *M. edulis*, respectively, in the test conditions of 5° C and 25 ‰ salinity. These values were 230 and 128 times the levels bioaccumulated by these animals when using the Nanisivik tailings, also a lead/zinc mine. Metals from the Island Copper mine were generally not available for uptake by these marine invertebrates.

No direct relationship between the bioaccumulation of metals and salinity or temperature was apparent, however, the degree of bio-uptake was generally proportional to the concentration of metals in sea water. Levels of metals in sea water were most strongly reflected in tissues of the deposit feeding clam, *M. balthica*. This result was surprising in that *M. balthica* feeds primarily on bottom deposits while *M. edulis* is a filter feeding mollusc. It appeared that the form of the dissolved metals from the tailings was one not readily available to *M. edulis*.

In the bioaccumulation tests, the concentrations of dissolved Cu, Zn and Fe were consistently higher for tests conducted at 5° C. This observation was most consistent for tailings from the two Arctic mines but no explanation was apparent. Release of metals from the mine tailings into sea water during leaching tests generally increased with increasing salinity and dissolved oxygen conditions, although considerable variation existed. It was concluded that the metal-binding associations within the mine tailings were responsible for controlling metal release. Results of the laboratory leaching and bioaccumulation studies were consistent with available data on the release and uptake of metals from the mine tailings when discharged into the sea.

Leaching and bioaccumulation tests were recommended for environmental assessment programs designed to assess the discharge of metal contaminated wastes into the sea. Development of a protocol for conducting bioaccumulation tests to predict availability of metals was also recommended. The importance of considering the chemical forms (speciation) of metals and their bio-availability to marine biota in such tests was stressed.

VI. CONTAMINANT MOBILIZATION AND BIOACCUMULATION FROM MARINE SEDIMENTS ADJACENT TO A SHIP REPAIR FACILITY

E.R. McGreer and B.J. Reid

Contractor: E.V.S. Consultants Limited

Prepared for: H. Nelson, E.P.S.

Laboratory studies were conducted to determine the mobilization of contaminants (Cd, Cu, Pb, Zn, As, Hg and PCB's) from contaminated marine sediments sampled near the Burrard Yarrows Ship Repair Facility in Vancouver Harbour, B.C. The deposit feeding clam *Macoma balthica* and the filter feeding mussel *Mytilus edulis* were used to assess bioaccumulation potential during thirty day up-take experiments. The concentration of contaminants in sea water and in invertebrate tissues were monitored.

Results showed that Cd, Hg and PCB's were below detectable limits in sea water in all tests. In tests with contaminated sediments maintained at 25 ‰, Cu, Pb, Zn, and As concentrations in sea water increased after 30 days. Lead and the PCB Arochlor 1254 were bioaccumulated to the greatest extent in the laboratory tests. Lead concentrations of $19.9 \mu\text{g g}^{-1}$ dry weight were detected in *Macoma balthica* when exposed to the contaminated sediments compared to concentrations of $7.85 \mu\text{g g}^{-1}$ in the controls. The PCB Arochlor 1254 accumulated in *Macoma balthica* ($0.59 \mu\text{g g}^{-1}$) and *Mytilus edulis* ($0.09 \mu\text{g g}^{-1}$) on exposure to contaminated sediment. The PCB Arochlor 1260 was detected in *M. balthica* but at lower levels ($0.12 \mu\text{g g}^{-1}$) than Arochlor 1254. No direct relationship between salinity and contaminant uptake was apparent in tests conducted at 10 and 25 ‰. Bioaccumulation of the contaminants was not directly proportional to their concentration in sea water in experimental containers, or to their total concentration in sediments.

Analysis of resident biota collected near the ship repair facility indicated noticeable accumulations of lead ($41.0 \mu\text{g g}^{-1}$), Arochlor 1254 ($0.35 \mu\text{g g}^{-1}$) and copper ($173 \mu\text{g g}^{-1}$) in invertebrate tissues, especially in the blue mussel *M. edulis*. Copper was not accumulated from sediments in the laboratory studies, suggesting that elevated levels in resident biota were due to a source other than sediments.

A comparison of the burrowing behaviour of the clam *M. balthica* in contaminated and control sediments was used as a measure of sublethal effects. The time required for 50% of the clam population to burrow (ET50) ranged from 1.2 h in the control to 5.2 h in the contaminated Burrard sediments.

Chemical analysis of contaminated marine sediments failed to detect some of the organic contaminants which were subsequently detected in laboratory test animals and resident biota. These data emphasized the need to carry out bioaccumulation studies for assessing the uptake of contaminants from marine sediments.

VII. DETERMINATION OF BACKGROUND LEVELS OF CADMIUM
IN CHURCHILL HARBOUR AND ITS APPROACHES
IN HUDSON'S BAY

R.W. Macdonald, I.O.S.
and P. Erickson, Arctic Laboratories Limited

Contractor: Arctic Laboratories Limited

In 1977 the Department of Public Works (D.P.W.) applied for an ocean dumping permit (4443-0234) to dredge Churchill Harbour. Both a suction dredge and a clam dipper were to be used to move a quantity not exceeding 1,300,000 cubic yards at a rate of 4000-7000 cubic yards/day. Figure 7 indicates the dredging and dumping locations. Monitoring was required as part of the permit application, and sediment samples were obtained in 1977-8. Total Cd as reported by the contractor (Renewable Resources Consulting Services Limited) generally exceeded the ocean dumping maximum of $0.6 \mu\text{g}^{-1}$ being in the range of $0.5 \mu\text{g}^{-1}$.

In order to clarify the problem and determine the source of the Cd, if possible, E.P.S. (Yellowknife) initiated the present work to investigate the background levels of Cd in Churchill Harbour and its approaches. Several results emerged: Cd concentrations measured in water from the Churchill River and Harbour were within limits reported for non-polluted oceans; Cd concentrations found in sediments were low relative to that reported for coastal regions ($0.2\text{-}3.0 \mu\text{g g}^{-1}$); and concentrations did not exceed the $0.6 \mu\text{g g}^{-1}$ cutoff of the Ocean Dumping Act. Sediments were found generally to be coarse and predominantly sand.

It is likely that the high Cd levels reported for the permit application were caused by inadequate laboratory technique. This is evidenced by the apparent lack of standards for Cd. Although the report supplied to us (October 30, 1978, File #5546-437, Renewable Resources Consulting Services Limited) does not supply sufficient detail it is also likely that FAA was used for the Cd determination. An unpublished report entitled "Laboratory Evaluation Program, First Quality Control Round Robin" by Samant, Loring and Ray shows very clearly the problem experienced by most laboratories when determining Cd in sediments. They used two standard sediments, a marine mud, MAG-1, and finely ground rock powder, SY-2. Both of these materials had a reported literature value of $0.2 \mu\text{g g}^{-1}$ Cd. The authors' comments are given below:

"Cadmium. MAG-1: Four laboratories reported values 1.4 - 4.0 ppm, mean 2.4 ppm Cd. Another group of five laboratories reported values 0.1-0.3, mean 0.2 ppm Cd.

SY-2: The same groups of laboratories reported mean values of 1.8 ppm and 0.2 Cd, respectively.

As the mean value 0.2 coincides with the literature value (0.2), it must be concluded that all the high group values are incorrect. The possible source of error is a failure to correct for background absorption in flame A.A. (atomic absorption). All the acceptable values were obtained by flameless A.A."

In view of the above results, the lack of an obvious source of the Cd to Churchill Harbour, the fact that other metals such as Pb, Zn, Cr and Cu were not found to be high, and the observation that sediments in general were coarse, we believe that the originally reported Cd values are in error.

Several recommendations can be made. When samples for ocean dumping are obtained, some material should be saved for checking or re-evaluation of results. In the case of proscribed elements (Hg, Cd) it is essential that adequate standards be run and perhaps this can only be done by supplying to the contractor a certified standard whose Cd and Hg content is known to the permit reviewer. For example, certified reference marine sediment material is now available from National Research Council in Ottawa. Future sampling of sediments in Churchill Harbour should be carried out in open water season to minimize expense and maximize sampling coverage. Due to time delays in funding, the present sampling was carried out at the worst period (Jan-Feb) with the result that water samples froze (as shown by salinity increases) and sediment samples could only be collected at a limited number of locations (Figure 8). Had representative sediment been saved from the original sampling period, checks of the Cd level could have been performed quickly and accurately. This would have been a far more cost effective approach.

VIII. TABLES

TABLE 1

TWO-WAY ANALYSIS OF VARIANCE TO DETERMINE TEMPORAL CHANGES BETWEEN
THE DUMPSITE AND CONTROL SITE COMMUNITIES, ALBERNI INLET.

<u>PARAMETER</u>	<u>TIME</u>	<u>STATION</u>	<u>INTERACTION</u>
Kjeldahl Nitrogen	p<0.05	p<0.05	p<0.05
Organic Carbon	p<0.05	p<0.05	p<0.05
Dissolved Oxygen	p<0.05	p>0.05	p<0.05
Silt Ratio	p<0.05	p<0.05	p<0.05
Loss-on-Ignition (LOI)	p<0.05	p<0.05	p<0.05
Number of Species	p<0.05	p<0.05	p<0.05
Number of Individuals	p<0.05	p<0.05	p<0.05
Biomass	p<0.05	p>0.05	p<0.05

IX. FIGURES

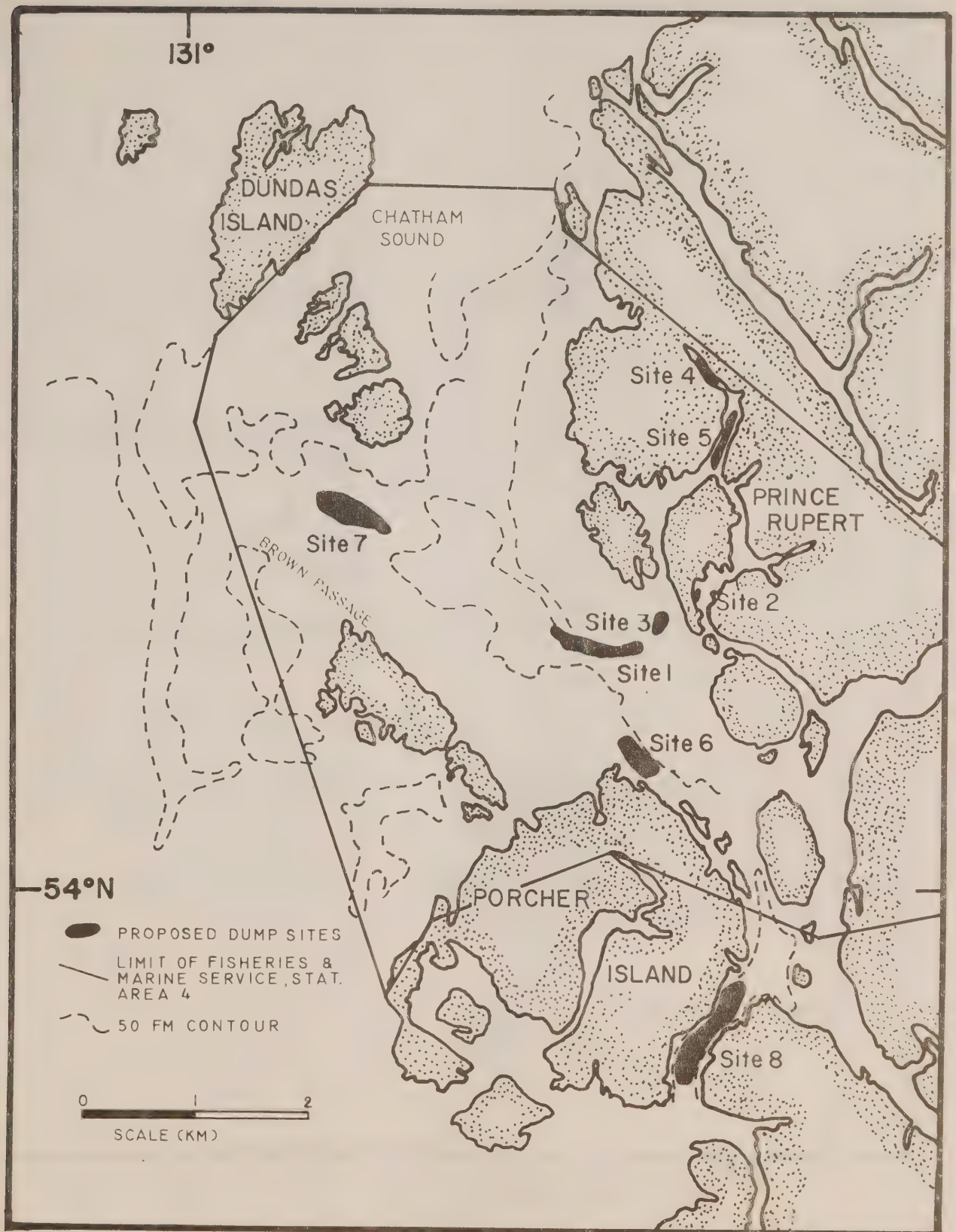


FIGURE 1. Location of eight sites proposed for ocean dumping in the Prince Rupert area (from E.V.S. Consultants Limited report).

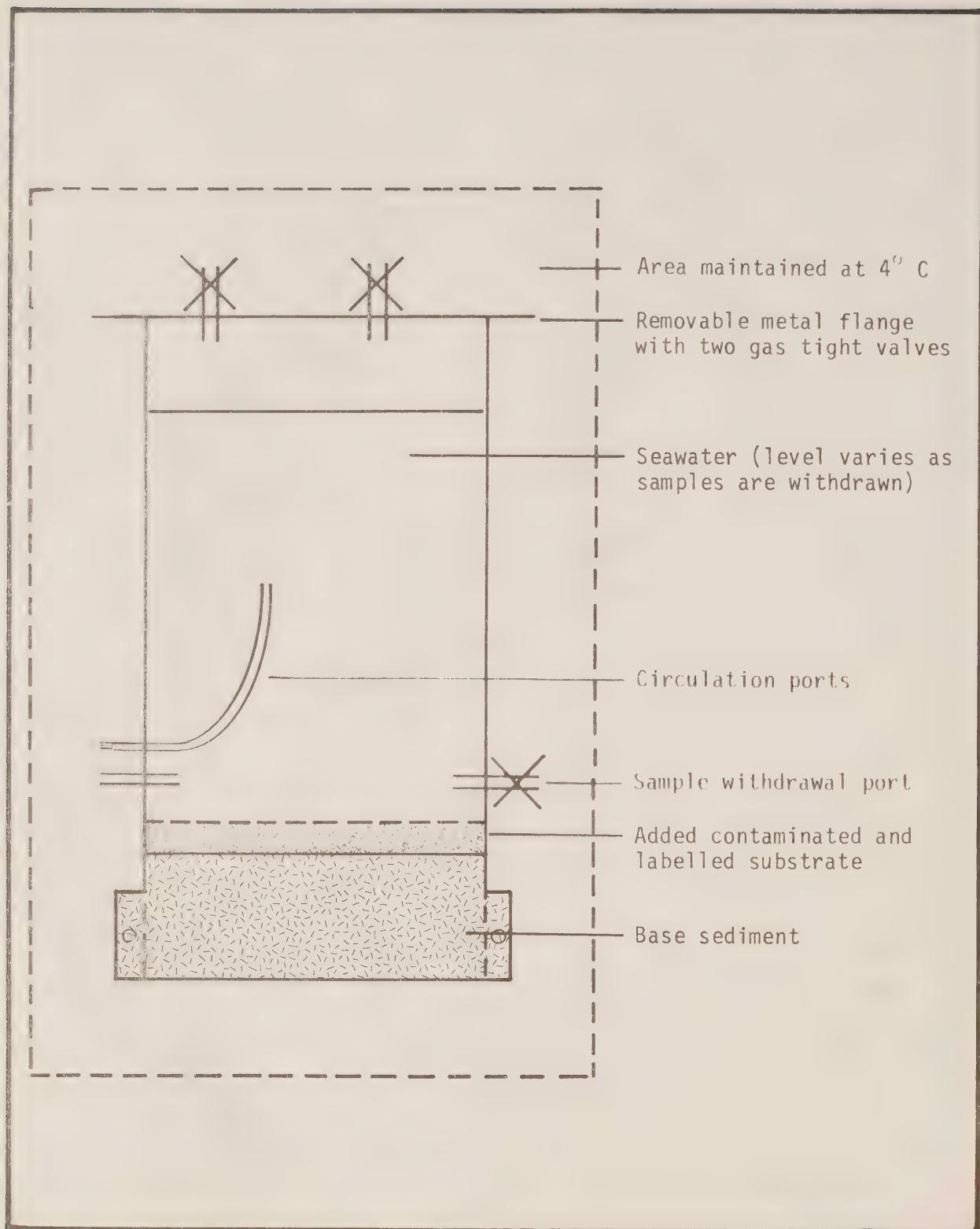


FIGURE 2. Schematic of the water column reaction vessel: approximate dimensions 75 cm x 14 cm (from Chemex Lab Limited report).

INITIAL SETTLING PHASE

COLUMN
 ■ 1
 ▲ 2
 • 3

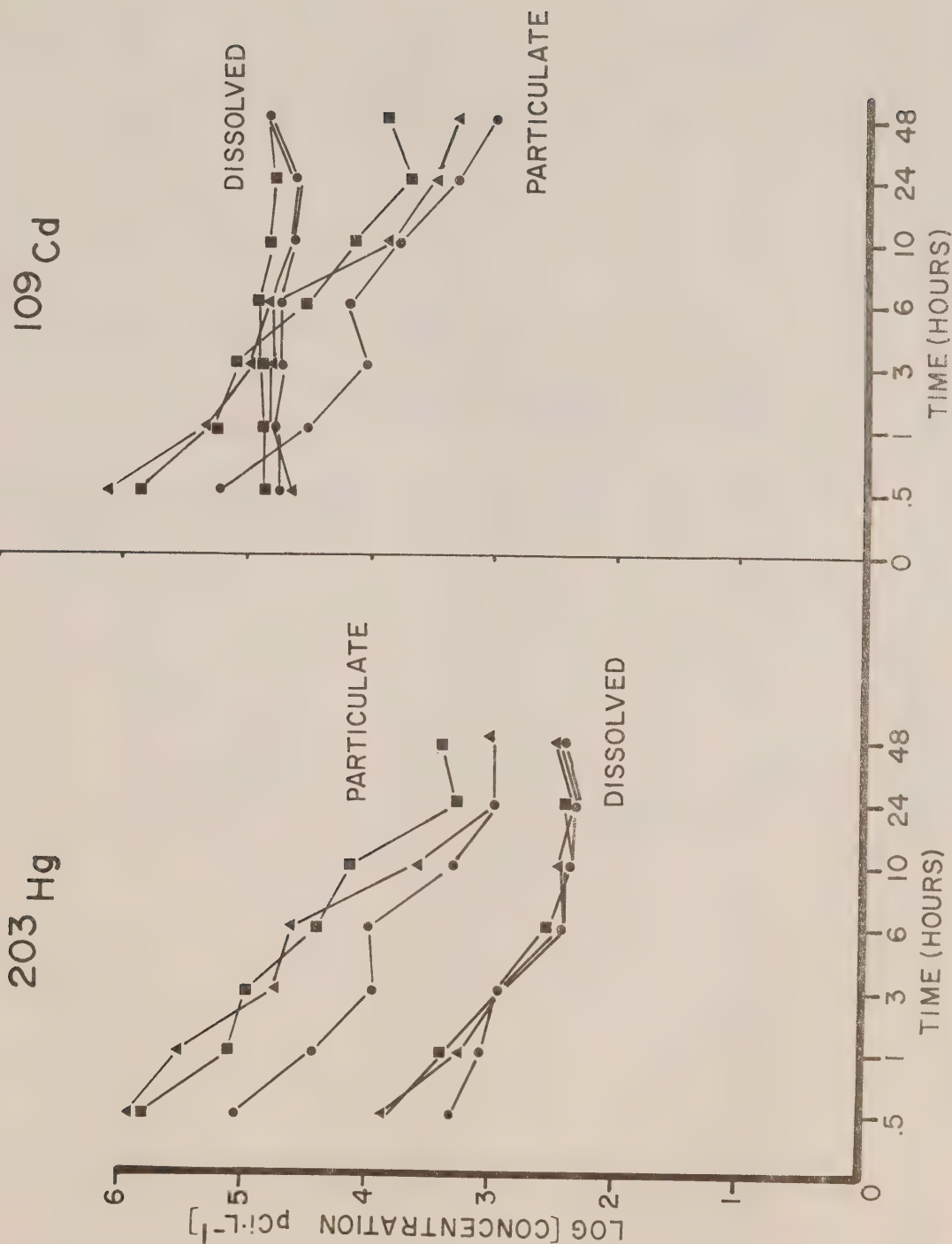


FIGURE 3. Concentration of dissolved and particulate forms of ²⁰³Hg and ¹⁰⁹Cd in the aqueous phase.

LONG TERM SETTLING PHASE

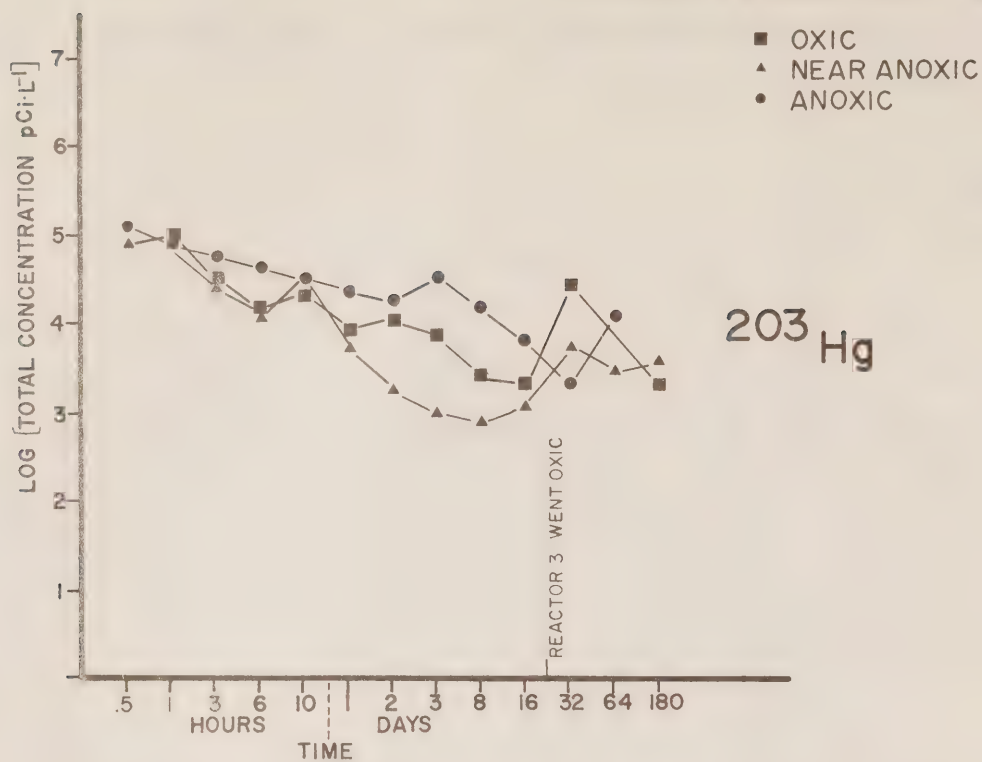


FIGURE 4a. Total ^{203}Hg (dissolved and particulate) as a function of time in the oxic, near anoxic and anoxic vessel.

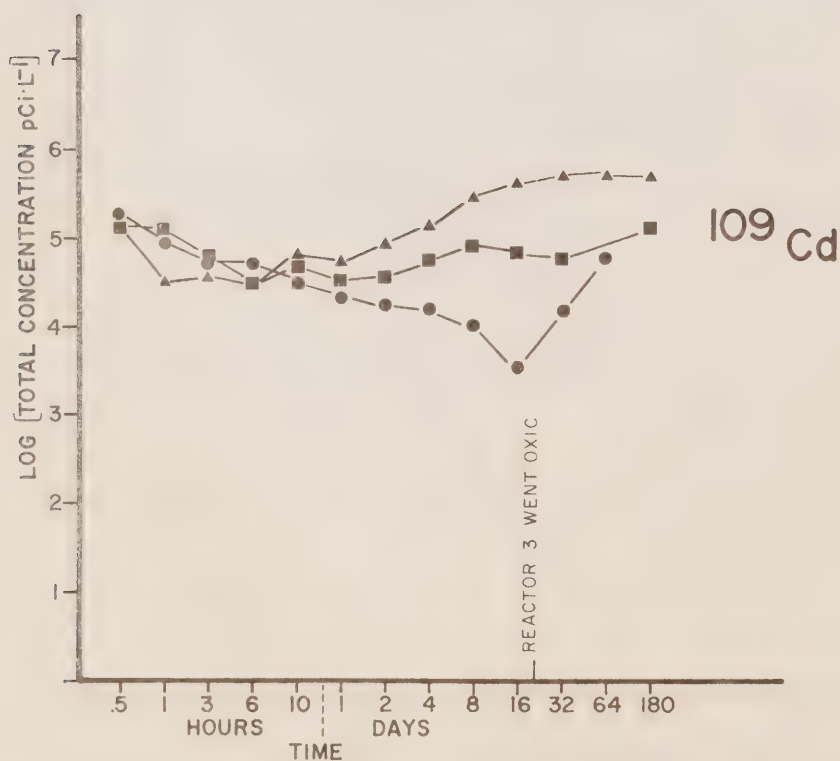


FIGURE 4b. Total ^{109}Cd (dissolved and particulate) as a function of time in the oxic, near anoxic and anoxic vessel.

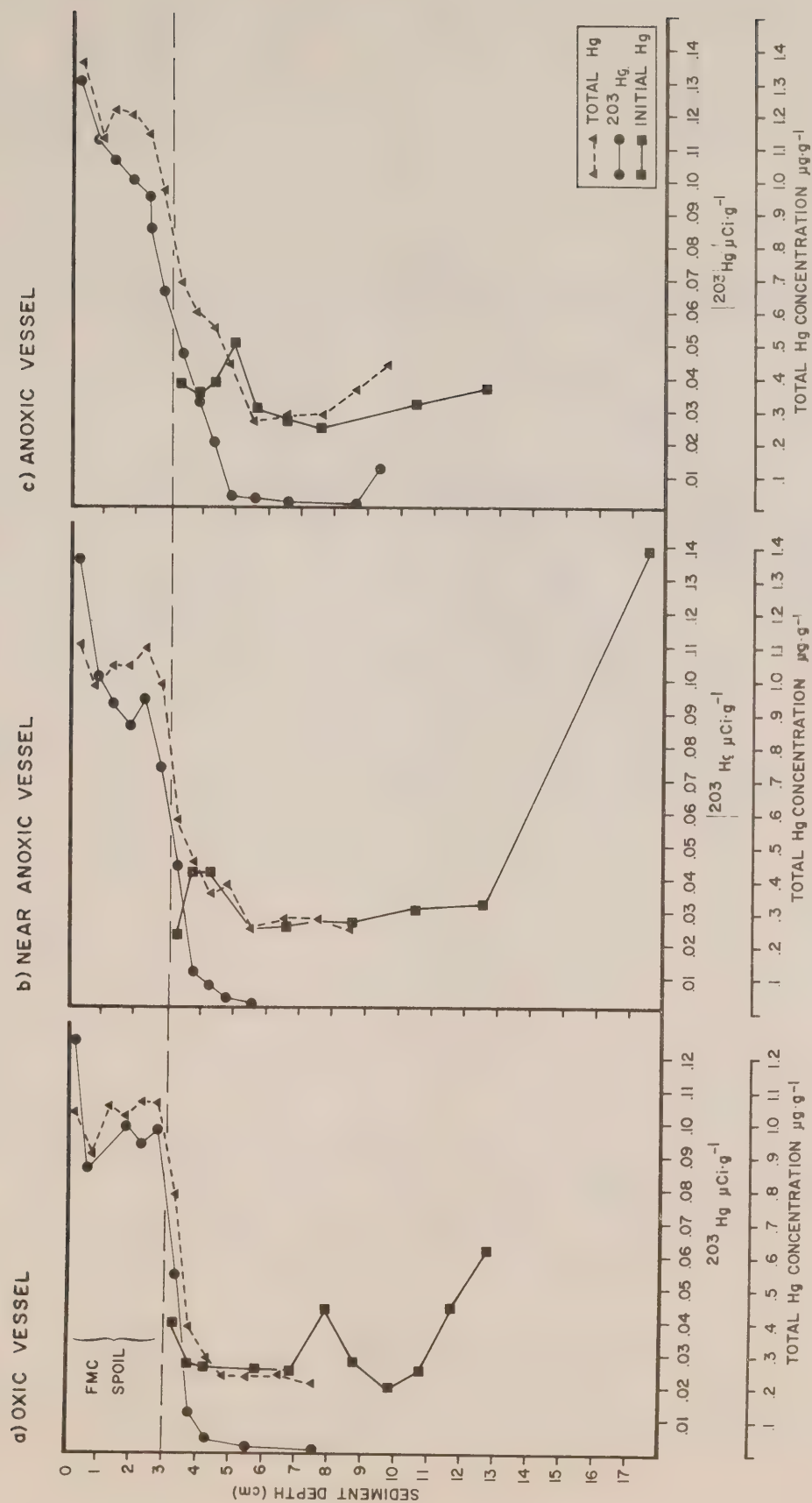


FIGURE 5. Concentration of Hg as a function of depth in sediments a) oxic vessel, b) near anoxic vessel, and c) anoxic vessel.

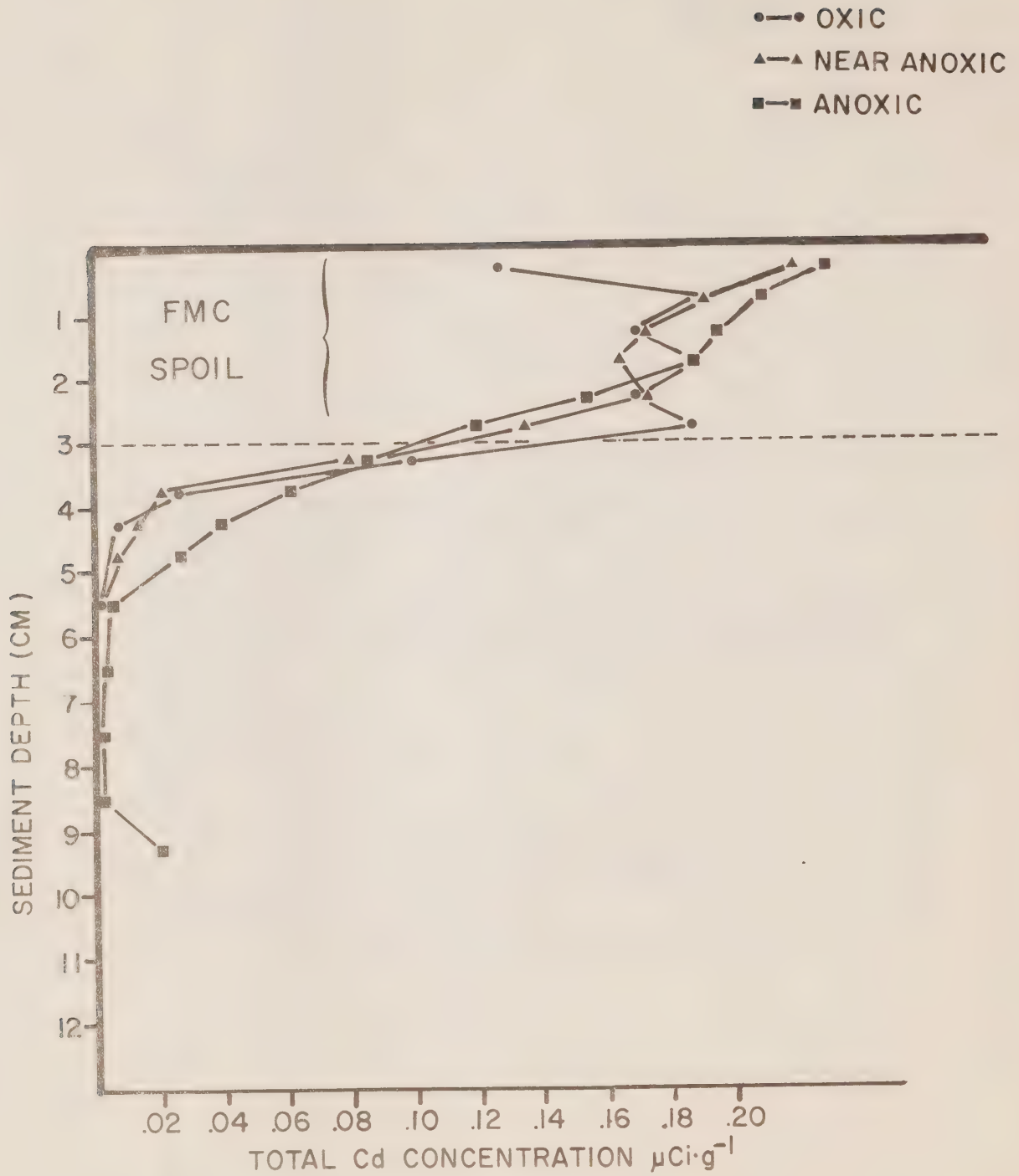


FIGURE 6. ^{109}Cd as a function of depth in the sediments for oxic, near anoxic and anoxic water conditions.

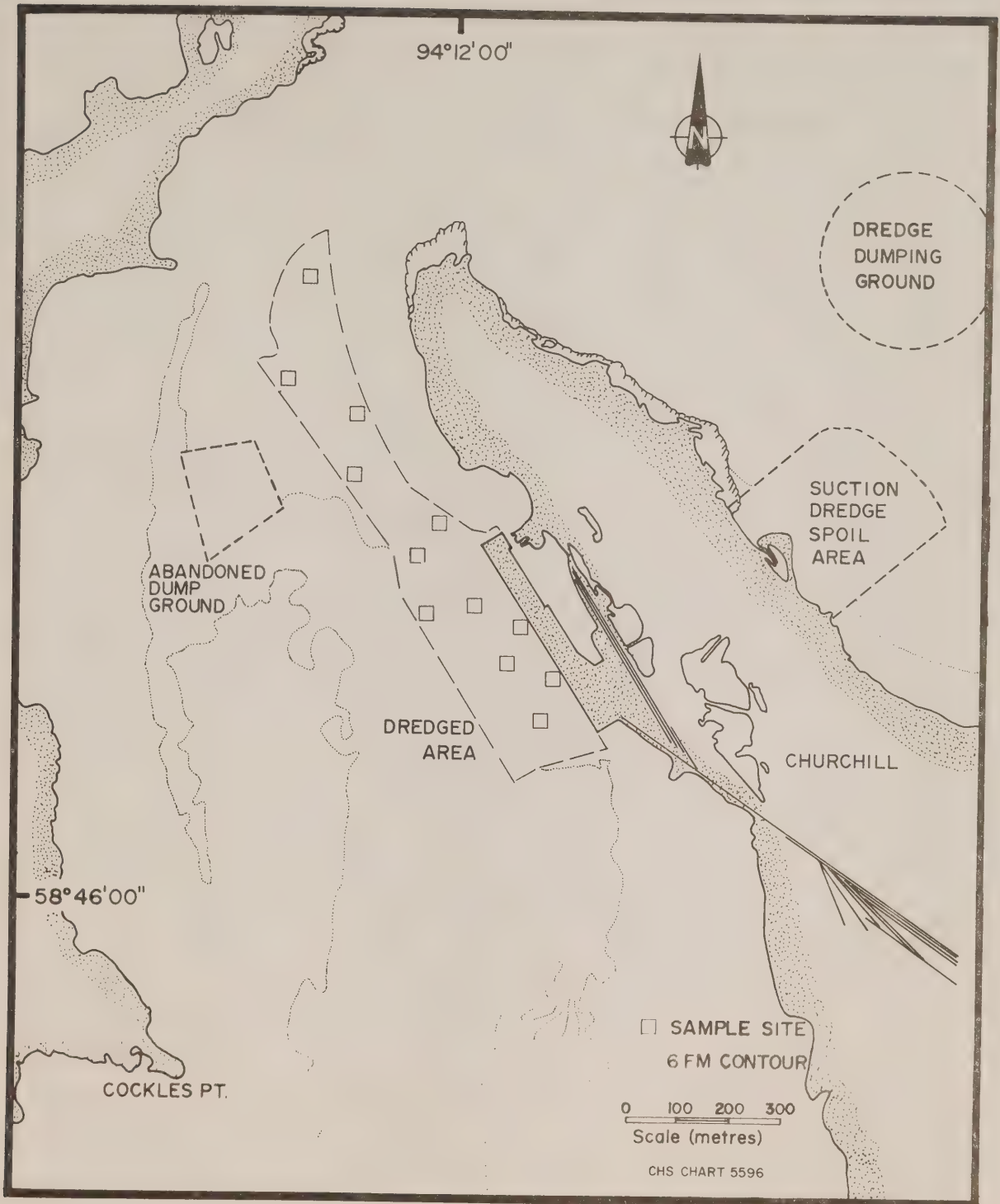


FIGURE 7. Sampling sites for O.D.P.A. (4443-0234) in Churchill Harbour 1977-1978 (Renewable Resources Consulting Services Limited).

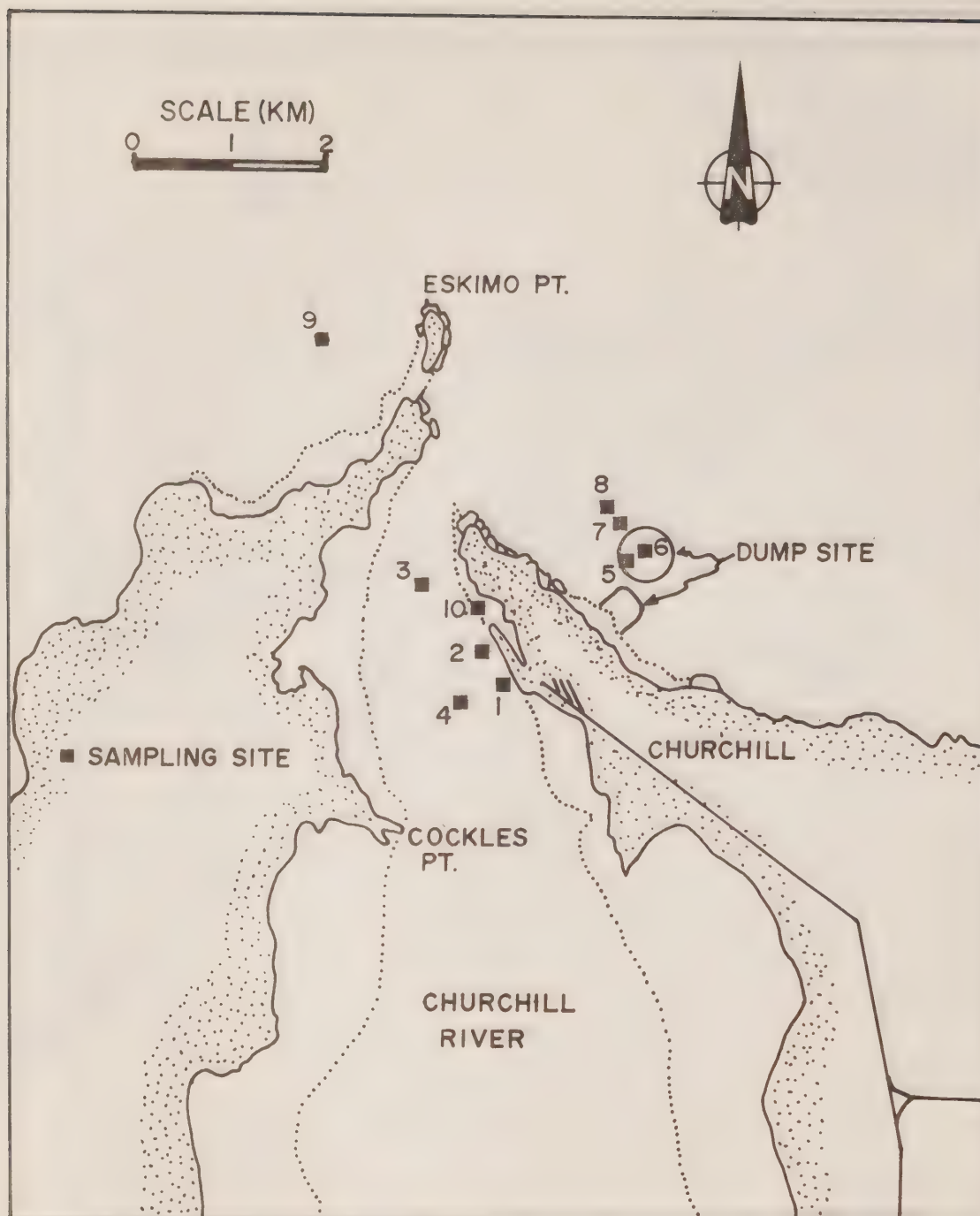


FIGURE 8. Sampling sites in Churchill Harbour 1980 (from Arctic Laboratories Limited report).

X. APPENDICES

APPENDIX I

OCEAN DUMPING WORKSHOP ATTENDANCE LIST

E.P. Anderson, University of Victoria
P. Berrang, Seakem Oceanography Limited, Sidney
D. Bradford, D.F.O./O.S.S., Ottawa
D. Brothers, D.O.E./E.P.S., Vancouver
S. Byers, Dobrocky SEATECH Limited, Sidney
R. Deverall, Can Test Limited, Vancouver
R.W. Drinnan, Dobrocky SEATECH Limited, Sidney
W. English, Plumper Ocean Projects, Victoria
P. Futer, D.F.O./Habitat Protection, Vancouver
M. Gordon, D.O.E./E.P.S., Yellowknife
K. Hutton, D.F.O./Habitat Protection, Vancouver
J. Karau, D.O.E./E.P.S., Ottawa
G. Kryzynski, L.G.L. Limited, Sidney
C.D. Levings, D.F.O./W.V.L., Vancouver
R.W. Macdonald, Ocean Chemistry, I.O.S., Sidney
E. McGreer, E.V.S. Consultants Limited, North Vancouver
J. Mitchell, Can Test Limited, Vancouver
D. Morse, Chemex Labs Limited, North Vancouver
H. Nelson, D.O.E./E.P.S., Vancouver
J. Nixon, D.O.E./E.P.S., Yellowknife
G. Packman, E.S.L. Environmental Sciences Limited
B. Reid, E.V.S. Consultants Limited, North Vancouver
D. Thomas, Seakem Oceanography Limited, Sidney
J. Thompson, Ocean Chemistry, I.O.S., Sidney
M. Waldichuk, D.F.O./W.V.L., Vancouver
M. Yunker, Dobrocky SEATECH Limited, Sidney

See Appendix IV for details of the research institution abbreviations.

APPENDIX II
1979-1980 CONTRACTS

A. BIOLOGY

REF. DSS FILE NO. 07SB.FP833-9-0576 \$ 6,974.75

Analysis of data relating to dumpsite colonization and temporal changes in benthic communities in Alberni Inlet.

Scientific Authority: C.D. Levings, W.V.L.

Contractor: E.V.S. Consultants Limited

B. CHEMISTRY

REF. DSS FILE NO. 07SB.FP833-9-0578 \$29,985.00

Study on migration of mercury from sediments.

Scientific Authority: R.W. Macdonald, I.O.S.

Contractor: Chemex Labs Limited

REF. DSS FILE NO. 07SB.FP833-9-1874 \$14,939.00

Study of the availability of metals from inorganic particulates for uptake by marine invertebrates.

Scientific Authority: M. Waldichuk, W.V.L.

Contractor: E.V.S. Consultants Limited

REF. DSS FILE NO. 07SB.FP833-9-1999 \$17,715.00

Study to determine the background levels of cadmium in Arctic marine sediments.

Scientific Authority: R.W. Macdonald, I.O.S.

Contractor: Arctic Laboratories Limited

C. ADMINISTRATION

REF. DSS FILE NO. 07SB.FP833-0-0554 \$14,212.00

Review of oceanographic data relating to ocean dumping in the Prince Rupert area.

Scientific Authority: C.D. Levings, W.V.L.

Contractor: E.V.S. Consultants Limited

REF. DSS FILE NO. 07SB.FP833-8-2465 \$ 9,100.00

Continuing support for the West Coast ocean dumping program.

Scientific Authority: R.O. Brinkhurst, I.O.S.

Contractor: Dobrocky SEATECH Limited

APPENDIX III
1980-1981 CONTRACTS

I. PACIFIC REGION

A. Biological/Chemical

REF. DSS FILE NO. 05SB.FP833-0-2306 \$17,368.00

Experimental investigation into the accumulation of Cd by the polychaete worm *Capitella capitata* and the bivalve *Macoma balthica*.

Scientific Authority: R.W. Macdonald, I.O.S.

Contractor: E.V.S. Consultants Limited

REF. DSS FILE NO. 05SB.FP501-0-0980 \$14,817.00

Effects of silt and organic debris on eggs and larvae of Pacific cod *Gadus macrocephalus*. Phase I.

Scientific Authority: M. Nassichuk, D.F.O.

Contractor: E.V.S. Consultants Limited

REF. DSS FILE NO. 04SB.FP833-0-0839 \$14,175.00

Organolead production in marine sediments.

Scientific Authority: J.A. Thompson, I.O.S.

Contractor: Dobrocky SEATECH Limited

B. Physical

REF. DSS FILE NO. 08SB.FP833-9-0702 Unsolicited Proposal: \$105,572.00

Examination of inner basin sill dynamics and internal tide generation in Alberni Inlet. Ocean Dumping Funds: \$ 15,000.00

Scientific Authority: W.H. Bell, I.O.S.

Contractor: Dobrocky SEATECH Limited

C. Administration

REF. DSS FILE NO. 05SB.FP833-0-1984 \$ 3,740.00

Organization and summary of ocean dumping workshops.

Scientific Authority: R.H. Herlinveaux, I.O.S.

Contractor: Dobrocky SEATECH Limited

REF. DSS FILE NO. 05SB.SP833-0-3110 \$ 9,684.00

R.O.D.A.C. national data base review.

Scientific Authority: R. Kussat, E.P.S.

Contractor: E.V.S. Consultants Limited

APPENDIX III - 1980-1981 CONTRACTS (cont'd)

II. NORTHWEST REGION

A. Biological

REF. DSS FILE NO. 04SB.KE108-0-0071 \$ 8,600.00

A statistical analysis of benthic invertebrate
sampling in Tuktoyaktuk Harbour, N.W.T.

Scientific Authority: W. Bryant, E.P.S., Yellowknife

Contractor: Arctic Laboratories Limited

REF. DSS FILE NO. Personal Service Contract \$ 17,400.00

Fish entrainment monitoring study

Scientific Authority: J. Stein, D.F.O., Winnipeg

Contractor: Personal Service Contract

APPENDIX IV
LOCATIONS OF PARTICIPANTS 1980

I. GOVERNMENT

D.O.E. - Department of the Environment

E.P.S. - Environmental Protection Service
Kapilano 100, Park Royal
WEST VANCOUVER, B.C. V7T 1A2

Environmental Protection Service
Fontaine Building
OTTAWA, Ontario K1A 0H3

Environmental Protection Service
Secretariat/Arctic Rodac
P.O. Box 370
YELLOWKNIFE, N.W.T. X1A 2N3

D.F.O. - Department of Fisheries and Oceans

Freshwater Institute
501 University Crescent
WINNIPEG, Manitoba R3T 2N6

Habitat Protection Division
1090 West Pender Street
VANCOUVER, B.C. V6E 2P1

I.O.S. - Institute of Ocean Sciences
P.O. Box 6000
SIDNEY, B.C. V8L 4B2

O.S.S. - Ocean Science and Surveys (formerly O.A.S. - Ocean and
Aquatic Sciences)
240 Sparks Street
OTTAWA, Ontario K1A 0E6

W.V.L. - West Vancouver Lab
4160 Marine Drive
WEST VANCOUVER, B.C. V7V 1N6

II. INDUSTRY

Arctic Laboratories Limited
P.O. Box 2630
INUVIK, N.W.T. X0E 0T0

Arctic Sciences Limited
P.O. Box 2639
1986 Mills Road
SIDNEY, B.C.

II. INDUSTRY (cont'd)

Can Test Limited

1650 Pandora Street
VANCOUVER, B.C.
V5L 1L6

Chemex Labs Limited

212 Brooksbank Avenue
NORTH VANCOUVER, B.C. V7F 2C1

Dobrocky SEATECH Limited

9865 West Saanich Road
P.O. Box 6500
SIDNEY, B.C. V8L 4M7

E.S.L. - Environmental Sciences Limited

34-1035 Richards Street
VANCOUVER, B.C. V6B 3E4

E.V.S. Consultants Limited

195 Pemberton Avenue
NORTH VANCOUVER, B.C.
V7P 2R4

L.G.L. Limited

Suite 333
2453 Beacon Avenue
SIDNEY, B.C. V8L 1X7

Plumper Ocean Projects

319 Stewart Street
VICTORIA, B.C. V9B 1R6

Seakem Oceanography Limited

2045 Mills Road
SIDNEY, B.C.

Woodward-Clyde Consultants

16 Bastion Square
VICTORIA, B.C. V8W 1H9

CAI
EP 321
-81R03

UCT 9 1981

**PENTACHLOROPHENOL IN A
PELAGIC MARINE ECOSYSTEM
Effects on the Ecosystem**

by F.A. Whitney, K. Perry, C. Philpott, A. Ramey
and *C.S. Wong

**INSTITUTE OF OCEAN SCIENCES
Sidney, B.C.**



For additional copies or further information please write to:

Department of Fisheries and Oceans

Institute of Ocean Sciences

P.O. Box 6000

Sidney, B.C. CANADA

V8L 4B2

* Address correspondence to C.S. Wong

CM
EPSC
- 21A03

Pacific Marine Science Report 81-3

PENTACHLOROPHENOL IN A PELAGIC MARINE ECOSYSTEM

Effects on the Ecosystem

by

F.A. Whitney, K. Perry, C. Philpott, A. Ramey
and *C.S. Wong

Institute of Ocean Sciences

Sidney, B.C.

1981

TABLE OF CONTENTS

	Page
ABSTRACT	2
INTRODUCTION	3
METHODS	4
EXPERIMENTAL OBSERVATIONS	6
CONCLUSIONS	7
REFERENCES	8
TABLES and FIGURES	9
1. Chlorophyll <u>a</u>	11
2. Primary productivity	13
3. Particulate organic carbon and nitrogen	15
4. Dissolved organic carbon	18
5. Oxygen	20
6. Nutrients; NO ₃ & NO ₂ , PO ₄ and SiO ₃	21
7. Saprophytic bacteria	25
8. Zooplankton	27
9. Light penetration	31
10. Sedimented material; POC/N, dry weight and chlorophyll	32

ABSTRACT

Pentachlorophenol (PCP) has recently created concern in many B.C. coastal areas because of its careless use as a wood preservative in the logging industry. Both environmental and health concerns have been voiced. The CEPEX enclosures therefore were employed to study the fate and effects of moderate levels (10 and 100 $\mu\text{g L}^{-1}$) of PCP in shallow coastal waters. The effects on the ecosystem were subtle, with bacteria being initially inhibited, and phytoplankton demonstrating reduced productivity and a species shift. Effects on zooplankton were complex, with carnivorous jellies apparently being most sensitive.

Sediment data reveal the magnitude of the inhibition of PCP on biological production. PCP treated enclosures produced between 30 and 38% less organic carbon than the control through the 25 day study.

INTRODUCTION

Enclosure experiments have been gaining broader use in the past decade as tools to study medium term (lmo to lyr) effects of pollutants on marine environments (Symposium on Marine Experimental Ecosystems, in prep.). In Saanich Inlet, CEPEX work in both 2.5 m and 10 m diameter enclosures has developed a well understood system. A broad range of stresses have been placed on pelagic organisms in experiments conducted between 1973 and the present, including nutrient limitation, Cu, Hg, Cd, fuel oil and crude oil extracts, naphthalenes, PCBs and glucose.

The most recent experiment studied the fate and effects of pentachlorophenol (PCP) in a pelagic ecosystem.

PCP has been newsworthy on several accounts recently, including industrial health problems, sludge disposal and accidental spills. To answer the questions of its longevity in surface waters, removal mechanisms and effects on organisms, a 4 week, 3 bag experiment was initiated. Preliminary studies (Interim Report, Dobrocky Seatech) indicated mild effects at $10 \mu\text{g L}^{-1}$ and more serious effects at $100 \mu\text{g L}^{-1}$ PCP on diatoms in incubation studies performed early in 1980.

On June 9, 1980, sampling began in bag B (control), bag C ($10 \mu\text{g L}^{-1}$ PCP, 0-10 m) and bag D ($100 \mu\text{g L}^{-1}$ PCP, 0-10 m). The experiment lasted 25 days, with two nutrient additions being made on Days 3 and 10 (N:P:Si, 10:1:10 μM , 0-10 m).

METHODS

The enclosures used in this study were the $\frac{1}{4}$ scale CEEs (Controlled Experimental Ecosystems) developed under the CEPEX funding from NSF. The CEEs are moored in 24 m of water at $123^{\circ}27.9'W$, $48^{\circ}39.6'N$ in Patricia Bay, B.C. The CEEs are 2.5 m in diameter and 16 m deep (14 m cylindrical and 2 m conical). The walls of the CEEs are constructed of a single layer of woven polyethylene (Fabrene).

Three CEEs were deployed on June 7, 1980, for the PCP study. The bags were lowered and raised to the surface by SCUBA diver teams within three minutes of each other. On the afternoon of June 7, the bags were pumped with an epoxy lined pump. It was discovered that the bags had been made 17 m long instead of 16 m, therefore extra dives and pumping were required on June 8. Estimated fills by SCUBA diver lift were; B - 60.5%, C - 49.7%, and D - 47.8%.

Water sampling was generally done with a peristaltic pump at a pumping rate of $7 \text{ L} \cdot \text{min}^{-1}$. Water was pumped from integrated depths of 0-5 m, 5-10 m, and 10-14 m through tygon tubing into 20 L polyethylene containers and then subsampled for various analyses. Niskin bottle casts were taken for O_2 and CO_2 (unanalyzed). A Kahlsico Underwater Irradiometer measured light penetration.

Chlorophyll a: 100 to 200 mL samples were filtered on GF/C filters with .5 mL $MgCO_3$. Filters were homogenized with 90% acetone, refiltered and the filtrate diluted to 12 mL. Fluorescence was measured on a Turner Designs Fluorometer.

Primary productivity: 4h *in situ* incubations of 2 light and 1 dark bottle were carried out between 1000 and 1400 h each day. The bottles were inoculated with $2.5 \text{ uCi NaH}^{14}CO_3$. After incubation, the bottles were transported to the lab in the dark, filtered on .45 μm filters (Millipore HA), the filters placed in vials and 10 mL Aquasol (NEN) added. ^{14}C activity was measured on a Beckman LS 3133 liquid scintillation counter. See Strickland and Parsons (1972) for details of chlorophyll and primary productivity procedures.

POC/N: 1 to 3 L samples were filtered on 47 mm GF/C filters (Whatman) and the filters rinsed with 3% NaCl. After drying, the filters were combusted at $750^{\circ}C$ in a CHN analyzer (Perkin Elmer, model 240).

DOC: analyses were done by the wet oxidation method of Menzel and Vaccaro (1964) using the Oceanography International system.

Oxygen: analyzed by micro-Winkler titration.

Nutrients: Technicon auto analyzer methods with minor modifications.

Saprophytic bacteria; as described by Carlucci and Pramer (1957) with some changes. Incubations all done in triplicate at $4^{\circ}C$. Dilutions (1:10) were done with distilled water.

Zooplankton: 30 cm, 202 μ m net tows were taken twice weekly from 14 to 0 m. Species were identified from the "Laboratory Zooplankton Atlas for the Strait of Georgia", (Fulton, 1968).

Sediment: Settled material was collected each sampling day by pumping 46 L of water from the bottom of each CEE. A subsample was taken for chlorophyll a, POC/N and dry weight measurements.

EXPERIMENTAL OBSERVATIONS

It was anticipated that a rapid diatom growth would occur in the first few days of the experiment. Therefore extensive sampling was conducted between Days 1 and 5. Chlorophyll a and primary productivity (figures 1 and 2) show a distinct initial effect on the phytoplankton in bag D. Phytoplankton counts (report in prep.) explain this as a species shift, with complete inhibition of *Skelatonema costatum* occurring. Throughout the experiment, decreased primary production is observed in C and D (figure 2).

Nutrient additions were made twice to stimulate autotrophic and heterotrophic activity. Saprophytic bacteria (those grown on agar) showed a distinct response to nutrient additions and inhibition from PCP (figure 7). It is predictably apparent that PCP has a major effect on bacteria, as that is its function as a wood preservative. Other CEPEX experiments have noted that after an initial inhibition, bacteria populations adapt to a pollutant and subsequently respond to conditions much as controls do (Azam *et al*, 1977). This is observed with PCP, as all populations respond to the second nutrient addition in a similar way.

Zooplankton interactions are complex, rendering interpretation somewhat speculative. The sensitivity of ctenophores to pollutant stress has been previously noted (Reeve *et al*, 1977). Under PCP stress, ctenophore numbers remain less than in the control. Reduced grazing pressure could then explain the higher numbers of adult calanoid copepods in C and D in the latter part of the experiment. Larvaceans (figure 8a) may be responding to differences in food supply (ie. bacteria; King *et al*, 1980) and to predatory pressure.

Perhaps the striking feature in this study is the distinct difference in the amount of sedimented material between the control and the PCP treated enclosures. The summed dry weights from all samples between Days 1 and 25, yields 206 g in B, 146 g in C and 141 g in D. This is reflected in particulate organic carbon data, 42.8 g, 30.0 g, and 26.5 g settling out of B, C and D respectively. Whereas chlorophyll, POC and primary productivity measurements do not accurately integrate total production with time, sediment data do.

CONCLUSIONS

The observable effects of 10 and 100 $\mu\text{g L}^{-1}$ PCP on a pelagic ecosystem were not catastrophic in this study. Bacterial activity, phytoplankton productivity and zooplankton community structure were all impacted. Similar responses have been observed with Cu and Hg in previous CEPEX work (Menzel, 1977; Grice and Menzel, 1978). From this work, it becomes obvious that ecosystems have great adaptive capabilities. Species shifts are the rule under moderate stresses. When nutrients are available, whether organic or inorganic, some opportunistic organism invariably utilizes them. Therefore, the assessment of pollutant impact is not simple.

One method of assessing impact severity is to estimate the reduction in total production of a system. Efficient carbon fixation and energy transfer between trophic levels is a measure of the success of an ecosystem. In considering the possible uses of nutrients, two extremes exist. When conditions are favourable, autotrophic uptake will rapidly deplete nutrient stocks, with active CO_2 fixation resulting. The opposite extreme is a system in which primary productivity is suppressed and nutrients are used to recycle organics. The net effect of this system is respirative production of CO_2 . When pollutants suppress primary production, the organic-inorganic carbon balance is affected, and the magnitude of this shift becomes an assessment of impact.

The PCP study provides data for estimating total productivity. The simple comparison of sedimented material indicates a 30-38% decrease in carbon in the PCP treated enclosures. Including changes in total organic carbon in the water column would not alter the magnitude of the impact, as initial and final concentrations in all three enclosures were similar.

REFERENCES

- Azam, F., R.F. Vaccaro, P.A. Gillespie, E.I. Moussalli and R.E. Hodson. 1977. Controlled ecosystem pollution experiment: Effect of mercury on enclosed water columns. II. Marine bacteria. Mar. Sci. Comm., 3(4), 313-329.
- Carlucci, A.F. and D. Pramer. 1957. Factors influencing the plate method for determining abundance of bacteria in sea water. Proc. Soc. Exp. Biol. Med., 96, 392-394.
- Grice, G.D. and D.W. Menzel. 1978. Controlled ecosystem pollution experiment: Effect of mercury on enclosed water columns. VII. Summary of results. Mar. Sci. Comm., 4(1), 23-31.
- King, K.R., J.T. Hollibaugh and F. Azam. 1980. Predator-prey interactions between the larvacean *Oikopleura dioica* and bacterioplankton in enclosed water columns. Mar. Biol. 56, 49-57.
- Fulton, J.D. 1968. Laboratory zooplankton atlas for the Strait of Georgia. F.R.B. of Canada, Tech. Rep. No. 55.
- Menzel, D.W. 1977. Summary of results: controlled ecosystem pollution experiment. Bull. Mar. Sci. 27(1), 142-145.
- Reeve, M.R., J.C. Gamble and M.A. Walter. 1977. Experimental observations on the effects of copper on copepods and other zooplankton: controlled ecosystem pollution experiment. Bull. Mar. Sci. 27(1), 92-104.
- Strickland, J.D.H. and T.R. Parsons. 1972. A practical handbook of seawater analysis. F.R.B. of Canada. Bulletin 167.
- Grice, G.D. and M.R. Reeve. Symposium on marine experimental ecosystems. In prep.

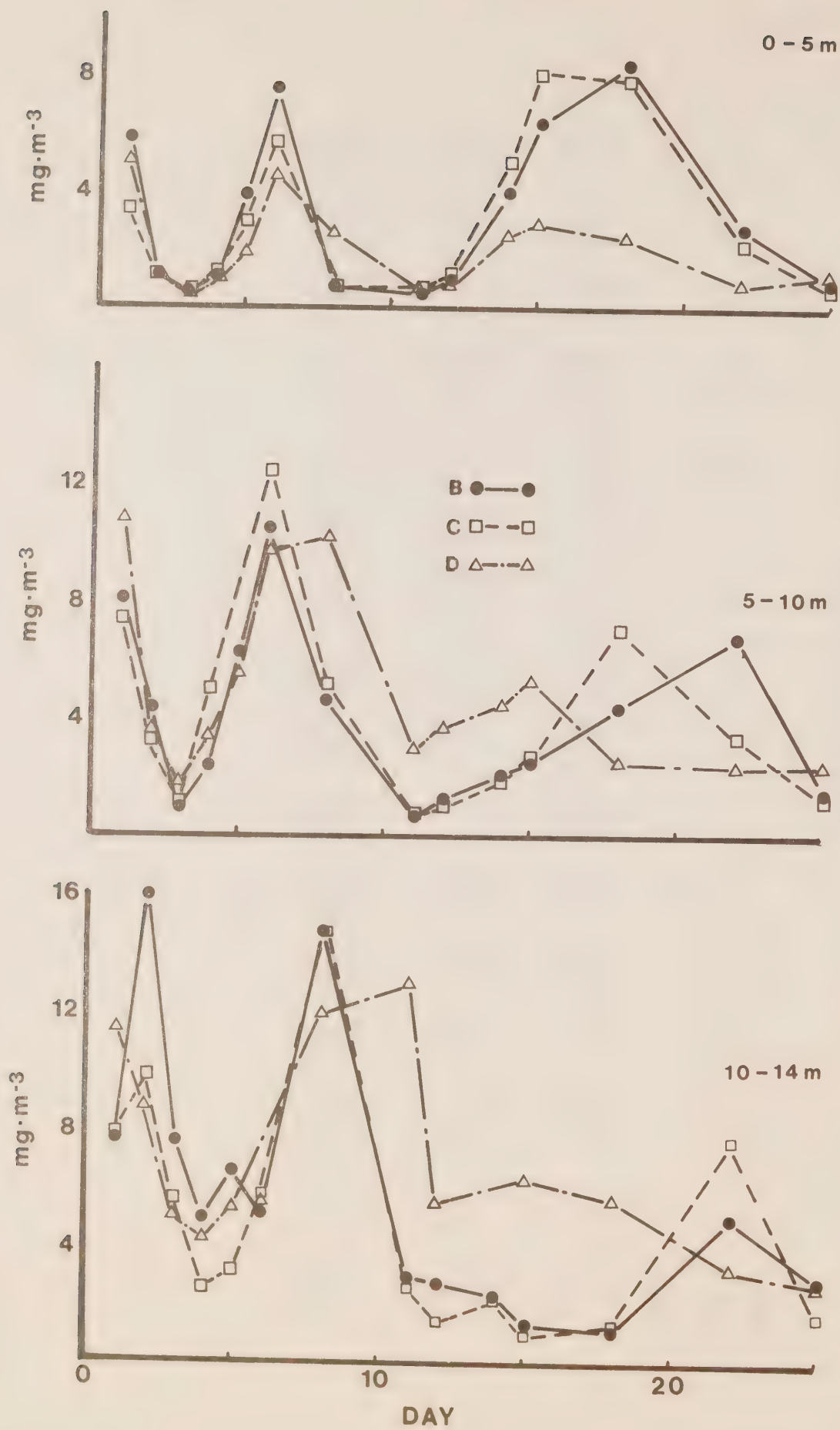
TABLES AND FIGURES

PENTACHLOROPHENOL STUDY

TABLE 1 Chlorophyll a (mg.m⁻³)

DAY	1	2	3	4	5	6	8	11	12	14	15	18	22	25
SAMPLE														
B 0-5 m	5.76	1.11	0.46	1.11	3.83	7.48	0.71	0.52	0.95	4.08	6.29	8.33	2.67	0.05
5-10	8.08	4.37	0.99	2.39	6.21	10.5	4.68	--	1.28	2.19	2.62	4.25	6.89	1.56
10-14	7.65	17.0	7.57	4.93	6.60	5.12	14.8	3.06	2.78	2.44	1.36	1.16	5.10	2.89
C 0-5 m	3.40	1.02	0.42	1.16	2.89	5.70	0.71	0.58	1.11	5.02	7.99	7.82	2.19	0.71
5-10	7.40	3.15	1.22	5.02	5.53	12.5	5.19	0.91	1.07	1.93	2.81	7.14	3.49	1.39
10-14	7.91	9.94	5.70	2.64	3.15	5.83	14.8	2.67	1.45	2.33	0.99	1.39	7.65	1.70
D 0-5 m	5.02	1.05	0.50	1.02	1.93	4.46	2.50	0.57	0.67	2.41	2.78	2.33	0.75	0.94
5-10	10.8	3.57	1.79	3.40	5.53	9.67	10.2	2.98	3.78	4.51	5.36	2.61	2.39	2.47
10-14	11.4	8.76	5.02	4.34	5.36	5.55	12.0	12.9	5.61	13.1	6.38	5.70	3.32	2.81

CHLOROPHYLL a

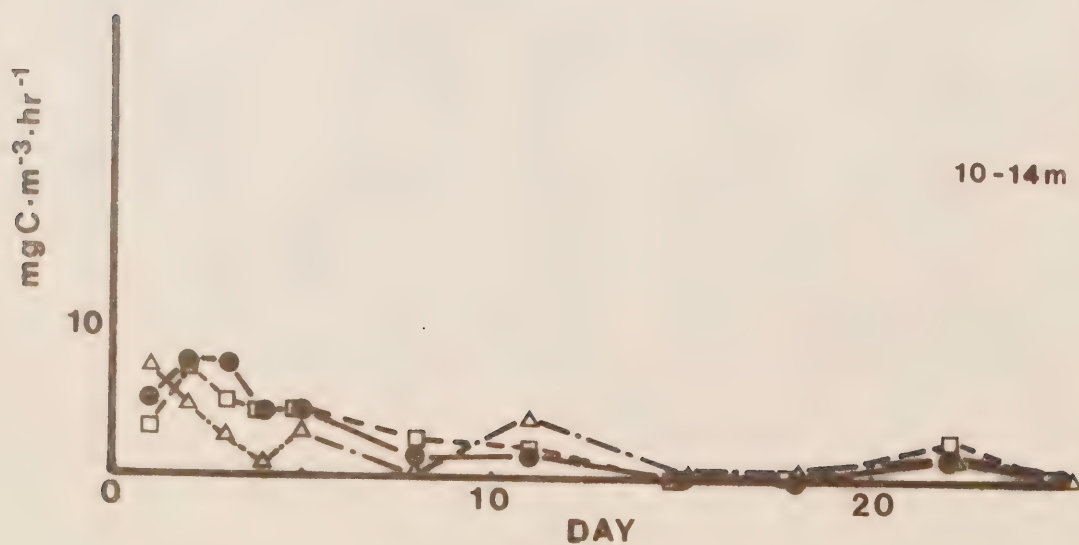
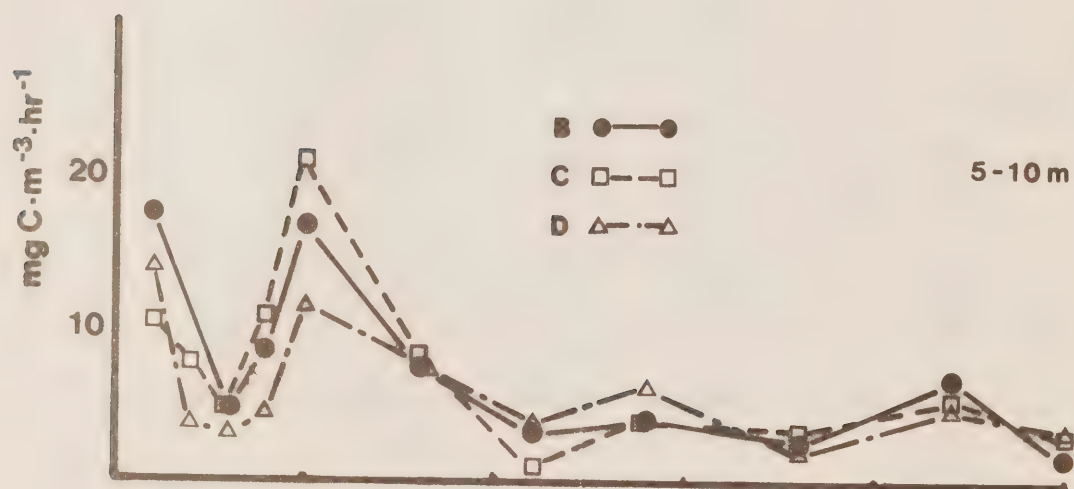
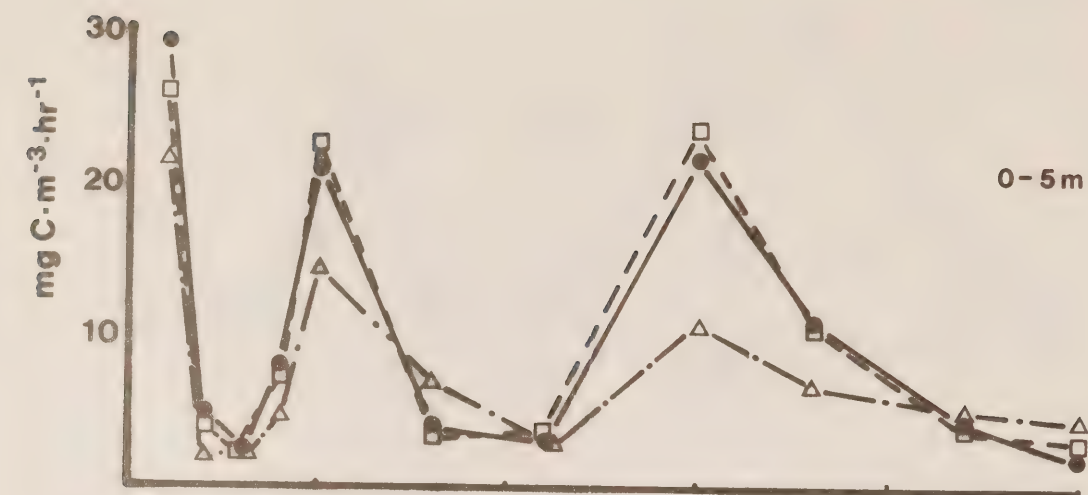


PENTACHLOROPHENOL STUDY

TABLE 2 ^{14}C Primary Productivity ($\text{mgC}\cdot\text{m}^{-3}\cdot\text{hr}$)

DAY	1	2	3	4	5	8	11	15	18	22	25
SAMPLE											
B 0-5 m	29.00	4.89	2.37	7.87	21.21	3.97	2.98	21.56	10.70	4.44	1.90
5-10	17.56	10.26	4.56	8.85	17.00	7.78	3.19	4.23	2.73	7.08	1.72
10-14	5.10	7.88	7.60	4.26	4.55	1.38	1.70	0	0.26	1.65	0.57
C 0-5 m	25.96	4.01	2.47	7.69	22.47	3.32	3.69	23.41	10.30	3.96	2.94
5-10	10.45	7.85	4.57	10.78	21.14	8.33	0.79	4.09	3.21	5.47	3.35
10-14	3.31	7.07	5.04	4.27	4.53	2.57	2.24	0.17	0.17	2.65	0.71
D 0-5 m	21.56	2.14	2.26	4.72	14.35	6.70	3.04	10.54	6.75	4.35	5.23
5-10	14.01	3.74	3.37	4.45	11.48	8.00	3.86	6.14	2.03	4.86	3.38
10-14	7.07	4.79	2.63	0.97	2.97	0.14	4.13	0.65	0.82	1.50	0.61

PRIMARY PRODUCTIVITY



PENTACHLOROPHENOL STUDY

TABLE 3 POC/N ($\mu\text{g}\cdot\text{L}^{-1}$)

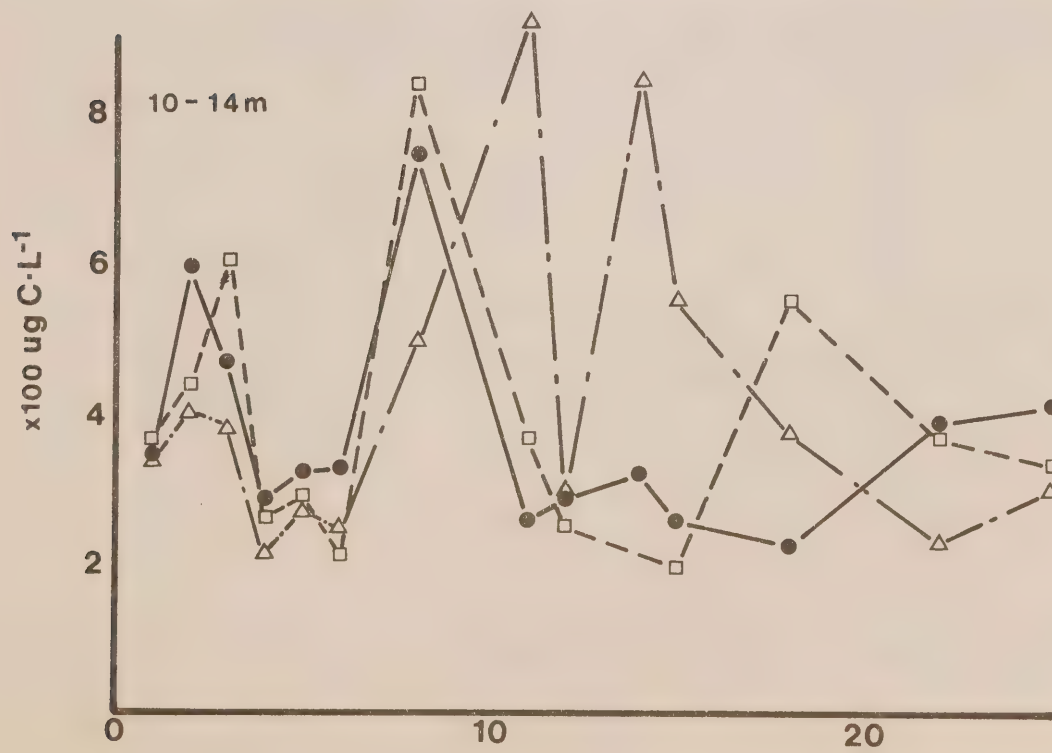
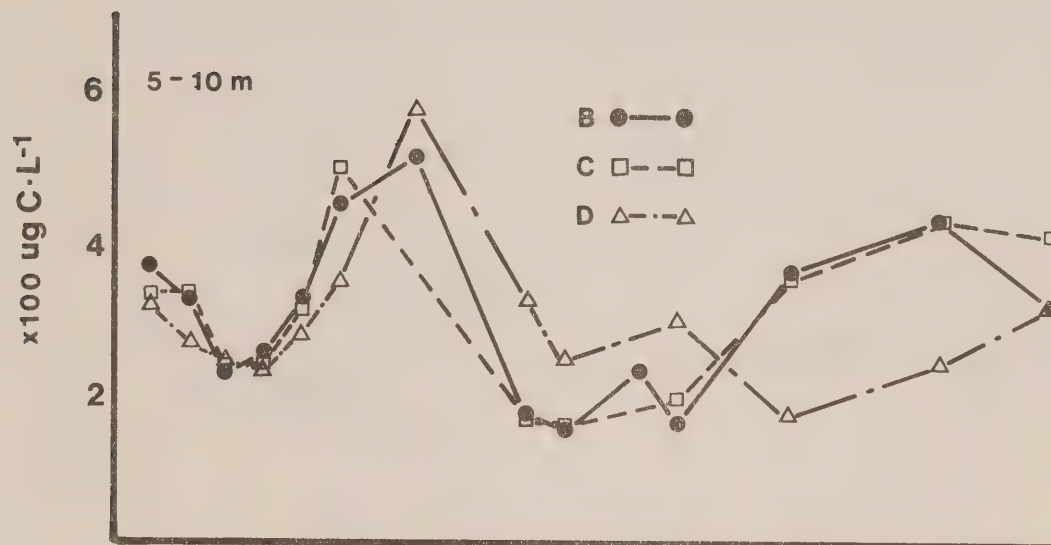
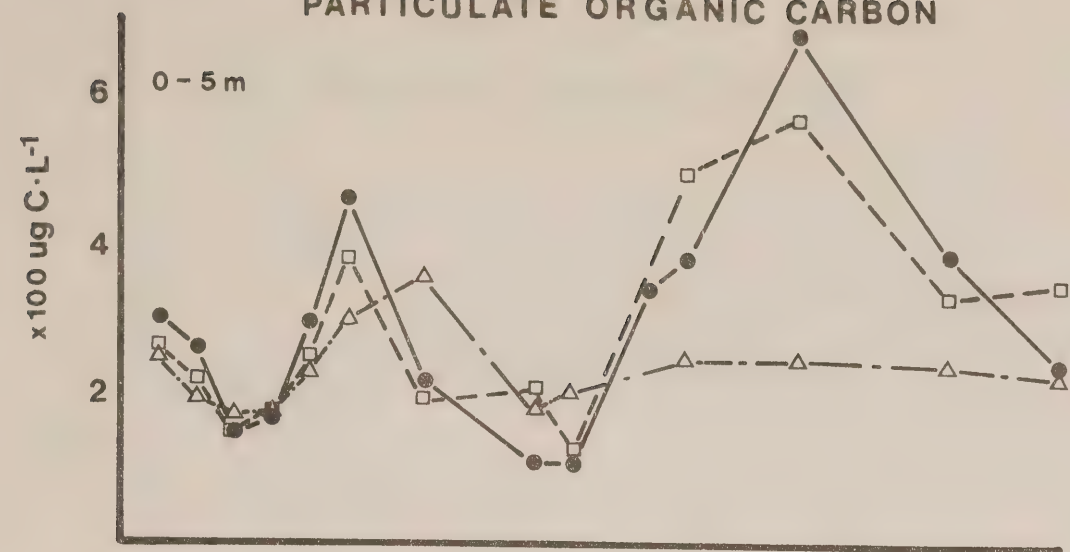
DAY	1		2		3		4		5		6		8	
	C	N	C	N	C	N	C	N	C	N	C	N	C	N
SAMPLE														
B 0-5 m	305	57.7	263	47.0	149	26.8	167	--	298	57.2	464	87.4	225	38.1
5-10	372	73.1	327	51.6	230	36.6	258	51.7	329	63.0	451	83.3	519	75.8
10-14	342	68.1	595	101.5	468	78.5	285	55.7	325	61.1	324	53.6	746	135.
C 0-5 m	269	54.1	222	35.3	145	25.8	172	35.8	252	50.0	384	76.8	194	30.8
5-10	331	66.8	334	55.6	-	--	245	50.1	316	62.3	499	103.	-	75.6
10-14	365	72.8	439	77.9	607	115.	262	50.1	288	56.3	210	42.1	837	141.
D 0-5 m	302	--	200	34.2	175	34.8	179	35.9	232	47.8	301	64.0	360	69.3
5-10	316	66.6	267	50.2	247	45.4	233	46.2	283	56.2	350	66.9	577	100.
10-14	335	67.7	399	80.3	383	71.7	212	42.0	269	56.9	249	49.5	494	93.5

PENTACHLOROPHENOL STUDY

TABLE 3 POC/N ($\mu\text{g}\cdot\text{L}^{-1}$)

SAMPLE	11		12		14		15		18		22		25	
	C	N	C	N	C	N	C	N	C	N	C	N	C	N
B 0-5 m	112	20.4	113	20.3	343	60.8	383	70.3	682	117.	391	61.7	246	39.7
5-10	177	31.8	153	27.1	239	46.8	164	32.5	367	66.5	437	75.2	325	58.0
10-14	258	47.4	288	47.7	322	63.3	255	51.8	224	44.2	390	73.2	415	77.9
C 0-5 m	212	43.7	130	23.1	-	--	496	87.9	572	92.8	333	51.8	350	60.7
5-10	170	28.8	157	--	-	--	194	35.6	355	61.9	432	74.7	416	77.7
10-14	366	65.4	247	46.2	-	--	195	40.5	554	10.5	368	64.1	333	60.8
D 0-5 m	185	36.1	206	39.5	-	--	249	49.3	249	48.3	241	44.5	227	40.7
5-10	325	63.9	247	45.4	-	--	297	57.7	176	35.4	243	48.5	323	59.1
10-14	923	159.	296	54.8	-	--	553	107.	373	70.8	234	45.7	302	54.3

PARTICULATE ORGANIC CARBON

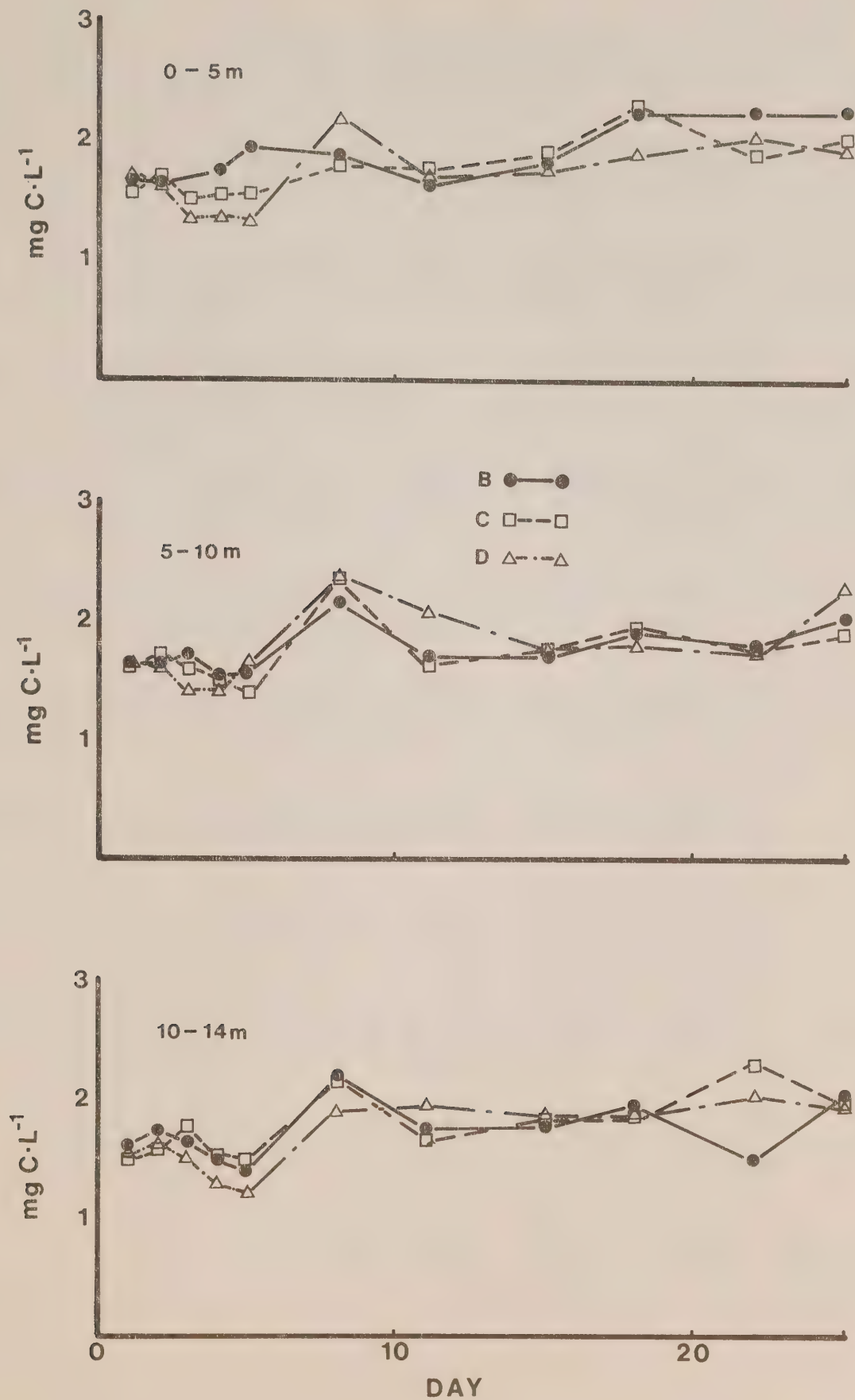


PENTACHLOROPHENOL STUDY

TABLE 4 Dissolved Organic Carbon (mg·L⁻¹)

DAY	1	2	3	4	5	8	11	15	18	22	25
SAMPLE											
B 0-5 m	1.66	--	2.48?	1.75	1.95	1.88	1.64	1.82	2.26	2.25	2.25
5-10	1.63	1.64	1.71	1.53	1.56	2.16	1.70	1.68	1.92	1.80	2.06
10-14	1.60	1.77	1.64	1.49	1.83	2.22	1.74	1.77	1.97	1.49	2.06
C 0-5 m	1.56	1.63	1.50	1.54	1.57	1.78	1.77	1.93	2.32	1.88	2.03
5-10	1.61	1.71	1.60	1.51	1.39	2.35	1.63	1.77	1.94	1.76	1.89
10-14	1.48	1.59	1.78	1.55	1.49	2.16	1.64	1.85	1.87	2.28	1.97
D 0-5 m	1.69	1.67	1.34	1.37	1.32	2.19	1.72	2.40?	1.89	2.04	1.93
5-10	1.64	1.63	1.41	1.42	1.66	2.38	2.07	1.78	1.80	1.71	2.26
10-14	1.56	1.67	1.50	1.29	1.22	1.89	1.94	1.89	1.89	2.03	1.90

DISSOLVED ORGANIC CARBON



PENTACHLOROPHENOL STUDY

TABLE 5 Oxygen ($\text{mL} \cdot \text{L}^{-1}$)

DAY	1	22	3	4	5	8	11	15	18	22	25
<u>SAMPLE</u>											
B 0m	8.697	8.699	8.610	8.576	8.687	10.79	9.343	10.16	10.34	9.643	8.814
2.5	8.638	8.916	8.910	8.657	8.748	11.21	9.914	10.17	11.46	9.794	9.255
5	8.277	8.851	8.901	8.858	8.940	11.20	10.70	10.29	11.19	10.81	9.871
7.5	8.270	8.715	8.788	8.762	8.977	10.73	10.50	10.03	10.45	10.46	9.726
10	7.931	8.173	8.502	8.352	8.636	8.715	9.881	9.241	9.592	9.283	9.062
12	8.012	7.069	7.310	7.348	7.202	6.691	6.780	5.736	5.545	5.030	5.233
14	6.759	6.688	6.704	6.662	6.397	5.981	5.761	5.187	5.146	4.810	4.785
C 0m	8.496	8.522	8.521	8.400	8.573	10.53	9.413	10.57	11.06	9.914	8.826
2.5	8.601	8.668	8.642	8.494	8.597	10.94	9.960	10.61	11.80	10.04	9.328
5	8.215	8.668	8.747	8.687	8.893	10.98	10.61	10.49	11.44	10.85	10.03
7.5	8.256	8.491	-	8.467	8.988	10.70	10.52	10.08	10.63	10.58	9.897
10	-	8.213	8.503	8.420	8.704	9.714	8.827	9.074	9.493	9.074	9.328
12	7.316	7.314	7.403	7.334	7.507	6.938	6.952	6.602	5.841	5.168	5.765
14	6.914	6.848	6.826	6.702	6.652	6.222	6.088	5.359	5.160	5.457	4.805
D 0m	8.491	8.224	8.226	7.998	8.158	10.39	9.482	10.02	9.666	9.210	8.793
2.5	8.552	8.533	8.436	8.214	8.097	10.91	10.00	10.03	10.72	9.271	8.868
5	8.230	8.485	8.473	8.203	8.283	10.67	10.53	10.10	10.46	10.02	9.625
7.5	8.169	8.263	8.361	8.277	8.386	9.687	10.14	9.931	10.07	9.774	9.147
10	8.112	8.125	8.126	8.092	8.276	8.926	9.478	9.001	9.389	8.212	8.537
12	7.711	7.700	7.448	7.430	7.659	7.190	7.854	6.697	5.992	6.131	6.409
14	7.119	7.088	7.140	6.952	6.620	6.057	5.632	5.048	4.790	4.813	5.205

PENTACHLOROPHENOL STUDY

21

TABLE 6a Nitrate & Nitrite (uM)

DAY	1	2	3	4	5	8	11	15	18	22	25
SAMPLE											
B 0-5 m	0.5	0.1	0.0	12.1	8.4	0.2	10.0	2.8	0.2	0.0	0.0
5-10	1.4	0.0	0.0	6.1	4.7	0.1	9.6	7.0	2.8	0.2	0.3
10-14	7.2	6.2	4.5	5.6	5.7	4.4	6.9	6.4	5.9	4.9	3.8
C 0-5 m	0.4	0.0	0.0	10.2	6.5	0.2	10.6	1.7	0.2	0.0	0.1
5-10	1.6	0.1	0.0	8.2	5.6	0.1	9.6	6.7	2.3	0.2	0.2
10-14	6.4	5.6	4.7	6.9	6.5	4.5	6.3	6.7	6.3	4.5	3.9
D 0-5 m	0.4	0.1	0.1	12.8	12.0	0.1	9.0	2.5	0.4	0.1	0.1
5-10	2.0	0.2	0.1	4.5	4.5	0.4	8.6	5.1	2.5	1.4	0.7
10-14	5.1	4.2	3.5	5.1	5.2	4.9	6.6	5.8	5.9	4.4	3.9

PENTACHLOROPHENOL STUDY

TABLE 6b Phosphate (μM)

DAY	1	2	3	4	5	8	11	15	18	22	25
SAMPLE											
B 0-5 m	0.56	0.40	0.35	1.52	1.34	0.57	1.59	1.1	0.76	0.67	0.68
5-10	0.65	0.48	0.39	1.00	0.97	0.69	1.50	1.4	1.11	0.93	0.97
10-14	1.18	1.17	0.98	1.08	1.17	1.29	1.54	1.8	1.92	2.08	2.02
C 0-5 m	0.51	0.42	0.35	1.20	1.15	0.57	1.52	1.0	0.66	0.62	0.67
5-10	0.64	0.48	0.39	1.19	1.10	0.70	1.50	1.4	1.04	0.88	0.86
10-14	1.10	1.02	0.96	1.07	1.11	1.20	1.23	1.7	1.76	1.78	1.77
D 0-5 m	0.54	0.45	0.42	1.76	1.67	0.68	1.55	1.1	0.81	0.76	0.75
5-10	0.68	0.56	0.45	0.94	0.99	0.84	1.51	1.3	1.06	1.03	0.98
10-14	0.96	0.91	0.78	0.95	1.02	1.17	1.54	1.9	1.90	2.16	2.24

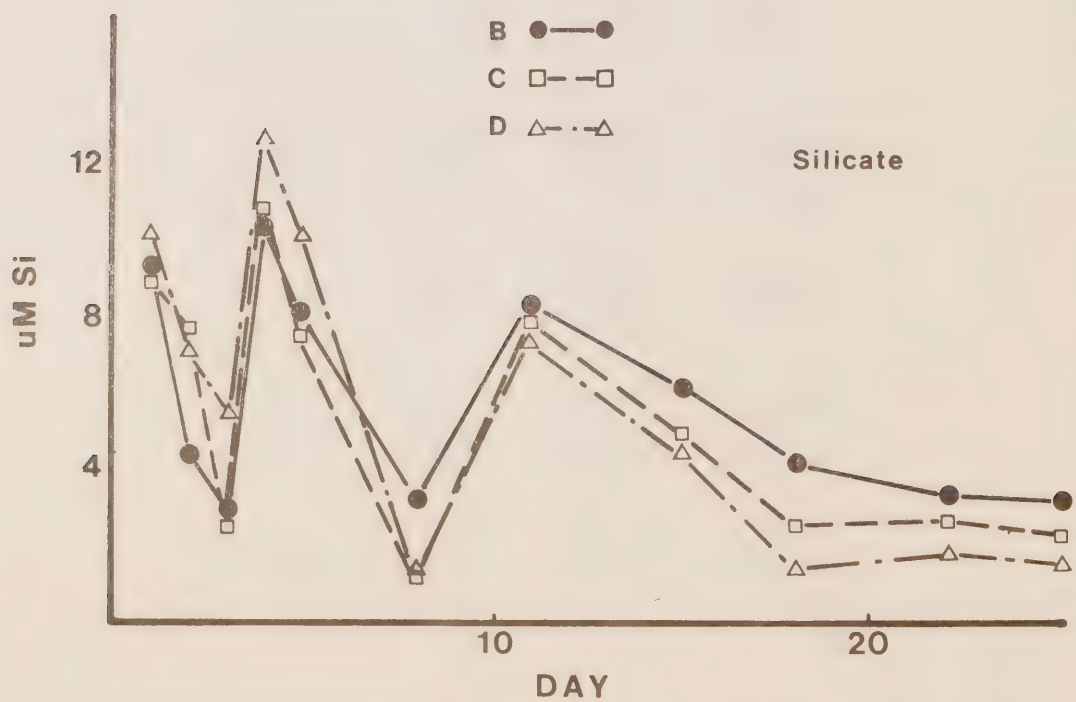
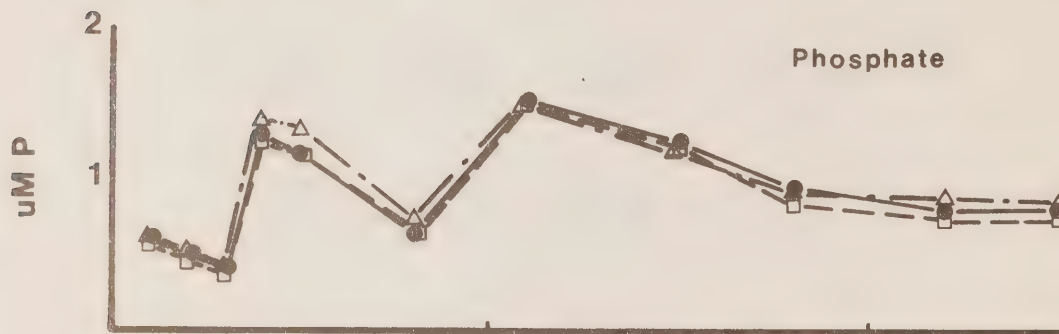
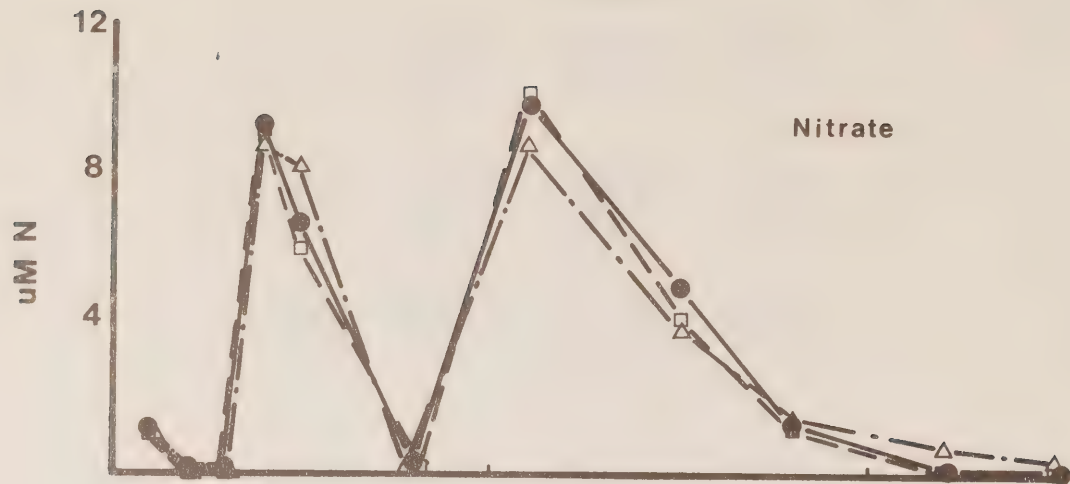
PENTACHLOROPHENOL STUDY

TABLE 6c Silicate (uM)

DAY	1	2	3	4	5	8	11	15	18	22	25
SAMPLE											
B 0-5 m	8.6	4.0	3.5	11.5	8.0	5.7	8.0	5.2	2.8	2.9	2.4
5-10	10.4	5.1	2.8	10.8	8.4	0.9	8.9	7.4	5.7	4.1	4.4
10-14	17.8	16.4	13.5	13.7	13.8	8.7	2.9	5.9	5.8	12.4	12.4
C 0-5 m	8.0	5.0	2.8	13.9	9.4	0.9	8.4	4.2	1.7	2.7	1.7
5-10	10.1	10.6	2.4	8.1	6.0	1.7	7.6	6.1	3.6	2.9	3.1
10-14	16.8	14.8	11.9	11.7	10.1	7.6	3.7	4.4	5.5	10.2	11.6
D 0-5 m	9.2	6.7	5.6	12.3	11.4	0.9	8.1	6.6	1.2	1.5	0.8
5-10	11.5	7.8	5.6	13.3	9.2	2.0	6.9	2.6	1.7	2.2	2.4
10-14	15.1	13.0	12.2	12.5	13.1	11.6	6.5	6.3	7.3	12.4	13.6

NUTRIENTS

(0 - 10m)



PENTACHLOROPHENOL

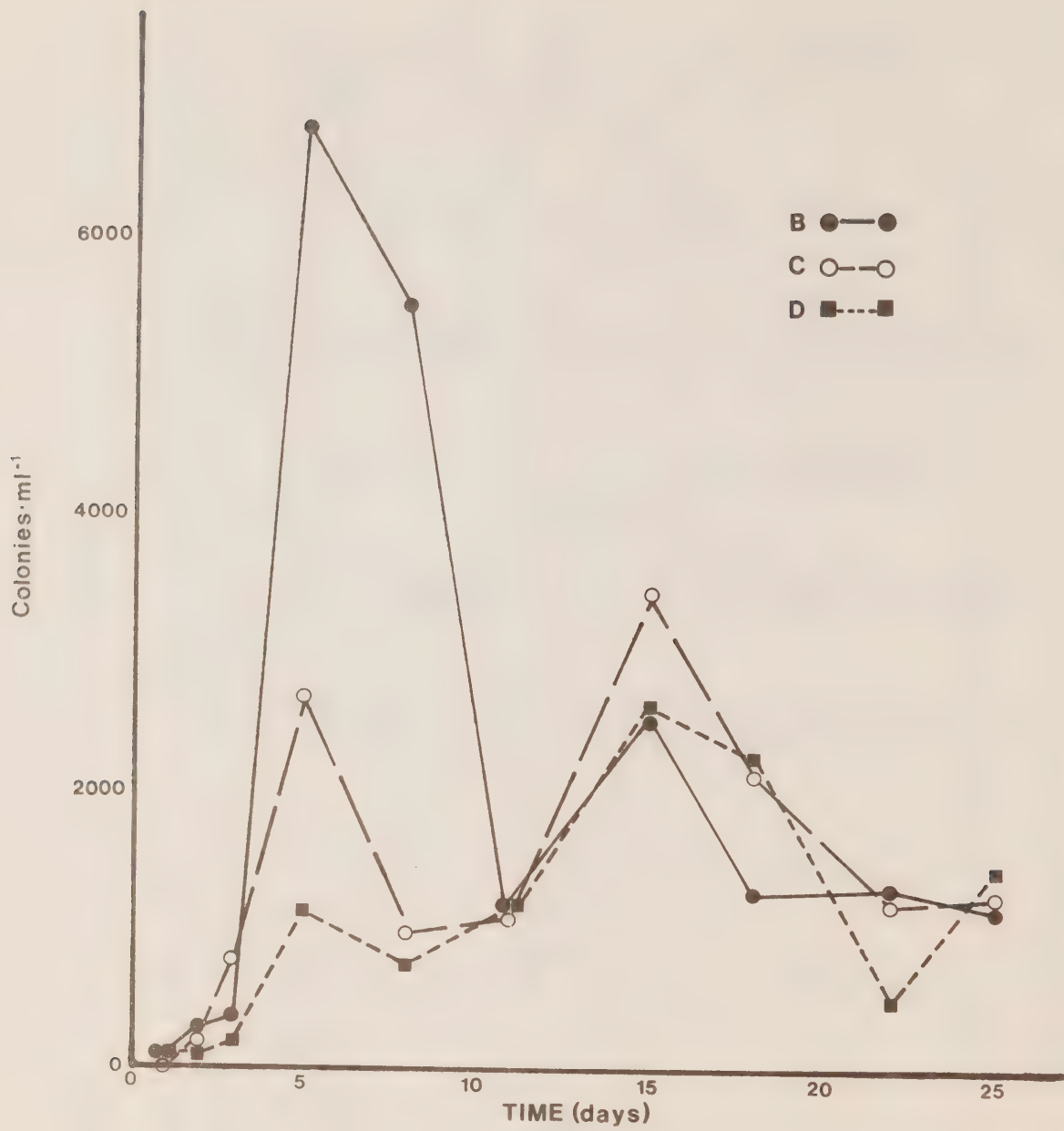
STUDY

Table 7 Saprophytic bacteria (colonies/plate), 0-14m									
DAY	1	2	3	5	8	11	15	18	22
SAMPLE: 1:10 dilution of sample, before adding 0.1mL to plate. (x100 for colonies·mL ⁻¹)									
B 1	1	3	3	63	57	17	15	12	8
2	2	3	7	55	55	11	27	7	24
3	0	3	1	85	54	13	30	14	15
av.	1	3	4	68	55	14	24	11	16
C 1	0	2	8	23	5	10	22	20	14
2	0	2	8	27	12	9	38	21	13
3	0	1	8	30	13	21	38	19	15
av.	0	2	8	27	10	13	33	20	14
D 1	1	0	0	6	7	19	*	22	7
2	1	0	2	8	2	15	*	24	6
3	0	0	1	7	7	10	*	19	13
av.	1	0	1	7	5	15	-	22	9
undiluted seawater, 0.1mL added to each plate. (x10 for colonies·mL ⁻¹)									
B av								138	202
C av								208	179
D 1	-	15	18	96	77	129	241	282	99
2	-	18	27	122	89	154	239	222	104
3	-	14	17	137	62	145	303	193	108
av	-	16	21	118	76	143	261	232	104

*"uncountable" Colonies grown on agar at 4°C from 11 to 16 days.

"av." refers to the average count from three plates inoculated from the same sample.

SAPROPHYTIC BACTERIA (0-14 m)



PENTACHLOROPHENOL

STUDY

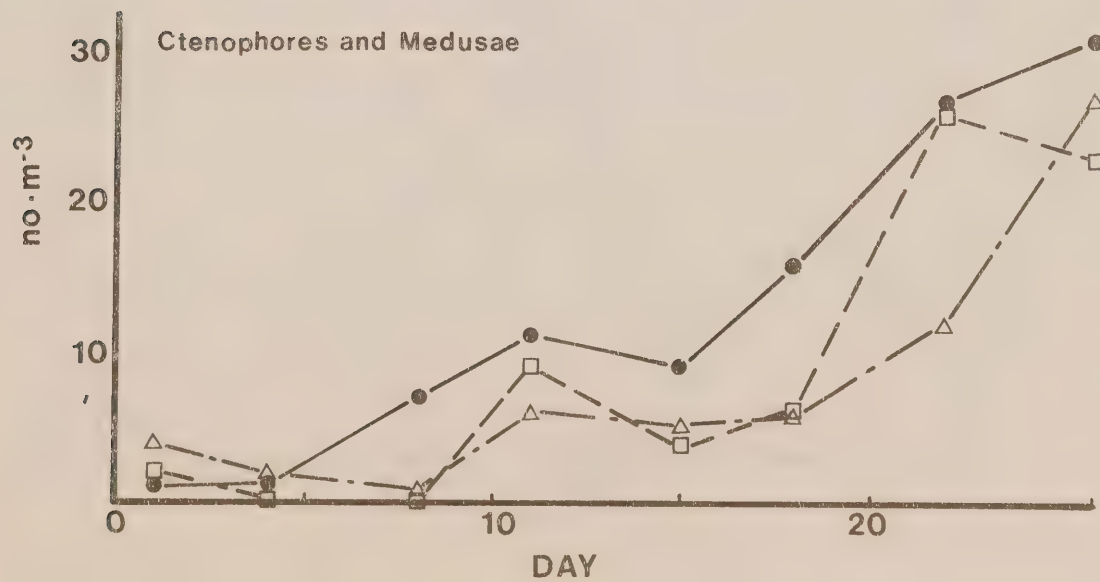
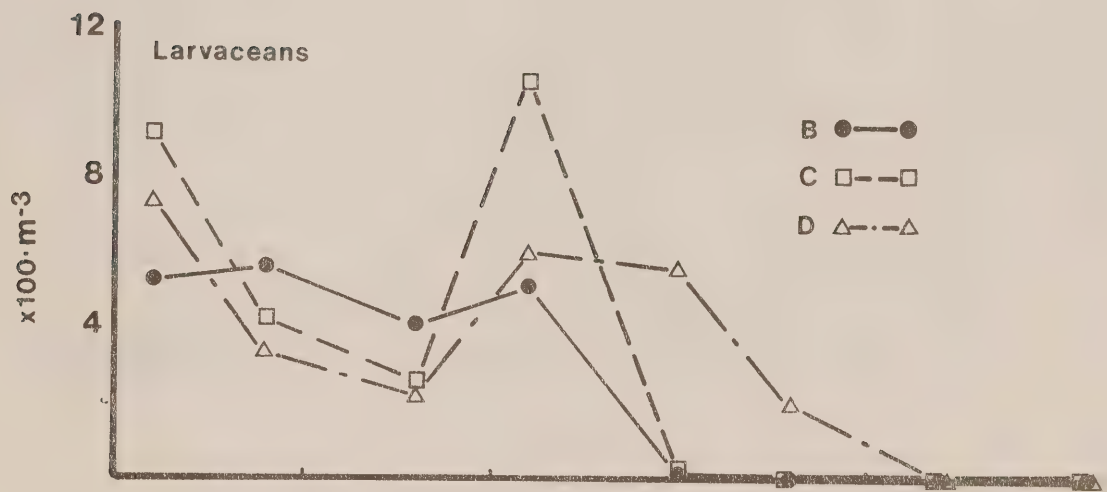
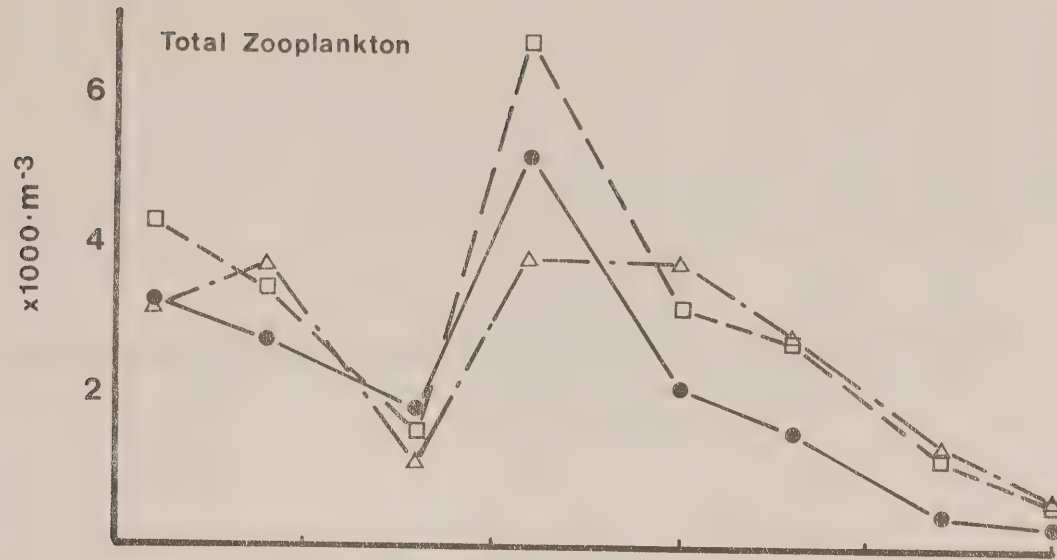
TABLE 8 Zooplankton (numbers/m³, >202u)

	DAY <u>1</u>			DAY <u>4</u>			DAY <u>8</u>			DAY <u>11</u>		
	B	C	D	B	C	D	B	C	D	B	C	D
Calanus	8	16	8	88	40	0	40	0	12	144	160	72
Pseudocalanus	160	96	56	656	240	272	216	272	100	1120	1568	904
Paracalanus	544	688	400	616	616	1040	384	288	296	1360	1232	752
Acartia	64	112	72	16	32	144	8	8	12	128	112	48
Centropages	64	64	32	64	40	0	24	0	16	64	16	56
Tortanus	152	64	40	64	16	176	56	0	0	80	48	24
calanoid copepodites	752	1184	80	536	632	1056	312	504	348	1584	2080	1144
nauplii (>202u)	432	368	480	0	392	448	16	16	8	0	32	0
Total calanoids	2176	2592	1888	2040	2624	3136	1176	1088	792	4480	5248	3000
Oithona	248	352	208	24	88	16	32	8	16	64	64	8
Corycaeus	56	48	104	56	56	64	56	56	36	48	224	88
Total copepods	2480	2992	2200	2120	2789	3216	1264	1152	844	4592	5536	3096
Larvaceans	520	912	736	560	424	336	408	256	220	512	1056	608
Ctenophores	0	0	1	0	0	1	0	0	0	0	3	2
Medusae	1	2	3	1	0	2	7	0	1	11	6	4
Polychaetes	24	48	40	0	64	0	72	0	4	16	0	16
Chaetognaths	56	80	24	0	8	16	0	16	4	0	32	8
Barnacle nauplii & cyprids	72	240	144	24	112	144	40	96	36	16	0	16
Other zooplankton	16	32	40	16	16	32	1	0	12	32	96	88
TOTAL ZOOPLANKTON	3169	4306	3188	2721	3392	3747	1792	1520	1121	5179	6729	3838

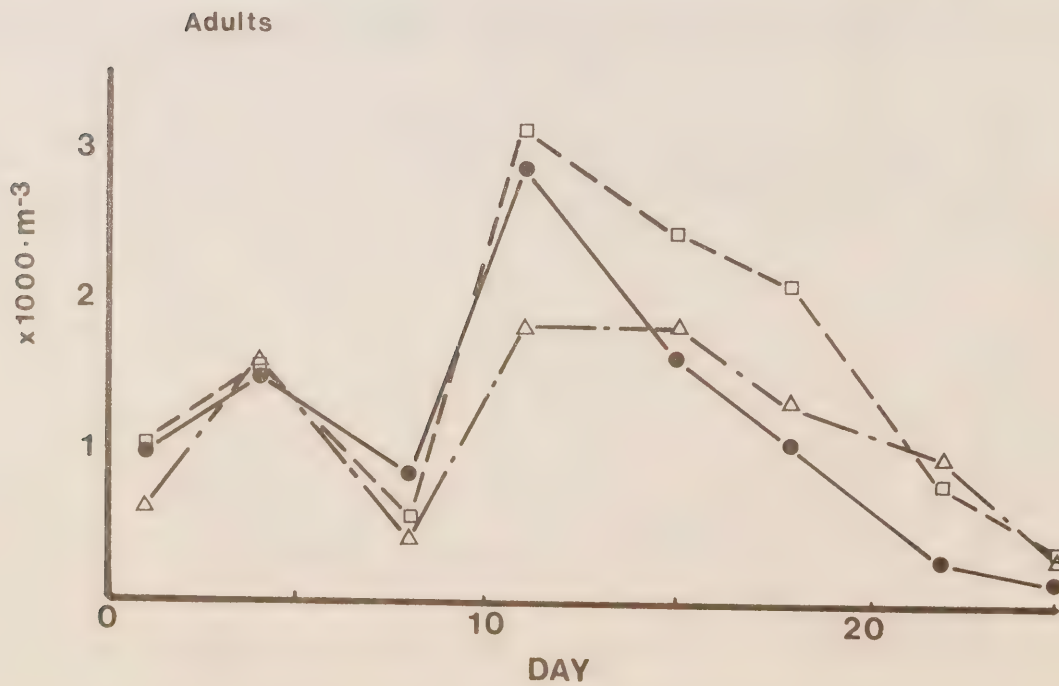
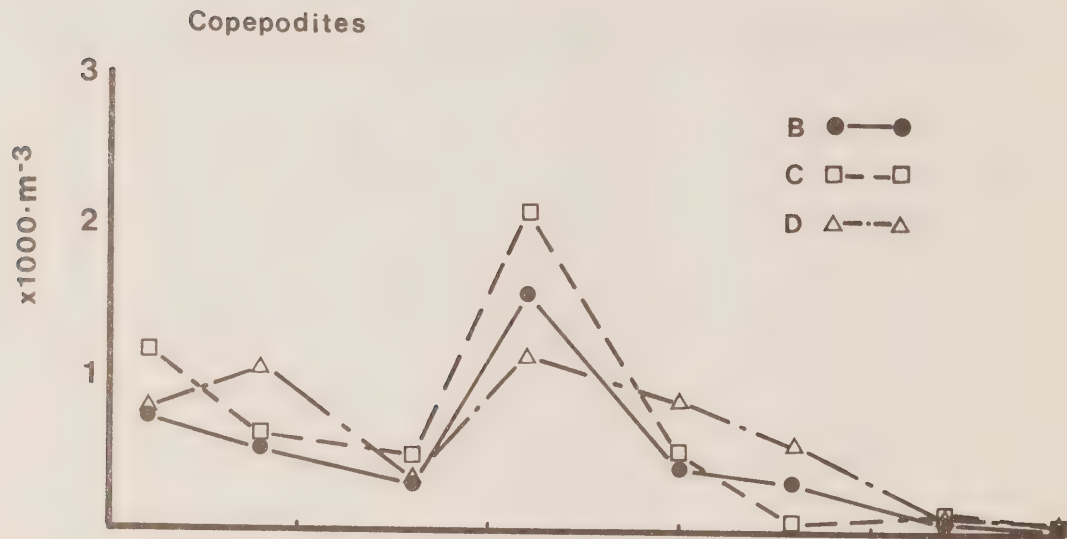
TABLE 8 Zooplankton (numbers/m³, >202u)

	DAY 15			DAY 18			DAY 22			DAY 25		
	B	C	D	B	C	D	B	C	D	B	C	D
Calanus	144	192	144	160	288	168	24	108	64	19	64	40
Pseudocalanus	680	1104	696	332	952	520	80	388	376	42	132	118
Paracalanus	680	1040	720	416	608	520	140	236	352	47	92	98
Acartia	72	40	128	60	104	80	14	12	64	6	14	28
Centropages	8	24	8	0	16	16	14	40	24	28	10	18
Tortanus	48	56	160	116	48	48	30	24	104	16	44	18
calanoid copepodites	400	528	848	340	536	576	56	152	112	16	68	68
nauplii (>202u)	0	0	72	0	0	24	2	4	0	0	4	4
Total calanoids	2032	2984	2776	1424	2552	1952	360	964	1096	174	428	392
Oithona	0	0	8	0	16	24	0	0	0	0	2	2
Corycaeus	72	48	176	52	136	152	36	84	136	57	78	90
Total copepods	2104	3032	2960	1476	2704	2128	396	1048	1232	231	508	484
Larvaceans	0	16	560	0	0	200	0	0	8	0	0	4
Ctenophores	2	2	1	16	2	2	22	23	7	21	20	13
Medusae	7	1	5	0	4	4	5	3	5	10	3	9
Polychaetes	8	8	56	8	8	128	2	8	56	0	2	50
Chaetognaths	0	8	8	4	8	1	2	0	2	0	0	0
Barnacle nauplii & cyprids	8	0	0	0	0	0	0	0	0	0	0	4
Other zooplankton	0	104	224	48	64	352	38	84	56	32	78	96
TOTAL ZOOPLANKTON	2129	3171	3814	1552	2790	2815	465	1166	1366	294	611	660

ZOOPLANKTON



CALANOID COPEPODS



PENTACHLOROPHENOL STUDY

TABLE 9 Light Penetration (% of incident solar radiation)

DAY	1	4	8	11	15	18	25
DEPTH							
B 0	46%	59%	64%	63%	57%	50%	49%
2.5	13	13	14	5.7	5.0	10	14
5	7.9	7.2	7.5	5.3	5.0	6.6	7.3
7.5	3.9	4.4	3.7	3.4	2.8	3.9	3.7
10	1.8	2.5	1.1	1.9	1.0	2.1	1.6
12	1.1	1.5	0.3	1.2	0.4	1.4	1.0
14	0.6	0.8	0.1	0.7	0.06	0.2	0.5
C 0	45	59	68	64	58	62	55
2.5	18	14	17	10-39	4.9	13	15
5	8.8	9.3	9.4	7.7-31	3.8	5.6	8.3
7.5	4.3	4.7	3.8	5.6	2.2	3.2	3.8
10	1.7	2.7	1.9	2.2	0.9	2.1	1.8
12	0.9	1.6	0.3	1.3	0.4	1.2	1.1
14	0.5	0.7	0.1	0.6	0.2	0.7	0.5
D 0	58	55	66	61	58	49	49
2.5	18	13	16	4.7	6.4	16	14
5	8.2	8.9	8.0	4.3	4.9	7.4	7.4
7.5	3.6	4.9	2.3	2.9	2.6	4.1	3.2
10	1.8	2.3	0.5	1.4	0.8	2.1	1.5
12	1.0	1.3	0.2	0.8	0.3	1.0	0.8
14	0.5	0.8	0.1	0.4	0.1	0.5	0.4
surface ₂ ($\mu\text{W}\cdot\text{cm}^{-2}$)	31,000	46, - 58,000	41, - 75,000	93, - 98,000	54, - 88,000	47, - 81,000	74, - 88,000

Note: bag wall shading results in highly variable results near the sunlight-shade boundary (2.5-5m).

PENTACHLOROPHENOL

STUDY

TABLE 10 Sedimented material ($\text{g}\cdot\text{d}^{-1}$)

DAY	1-2	2-3	3-4	4-5	5-8	8-11	11-15	15-18	18-22	22-25
SAMPLE										
B Carbon	2.28	1.01	3.21	2.77	1.67	1.34	.857	1.75	1.83	2.86
Nitrogen	.382	.161	.528	.469	.266	.202	.126	.256	.275	.483
Dry Wt.	11.1	13.3	16.7	13.5	9.22	6.27	3.76	7.6	8.34	11.4
C Carbon	3.40	.927	2.81	1.03	.987	.777	.488	1.14	1.66	1.84
Nitrogen	.570	.153	.454	.179	.160	.127	.077	.177	.206	.293
Dry Wt.	17.3	12.8	13.4	4.56	5.99	3.39	2.15	4.8	5.65	7.96
D Carbon	2.80	.863	2.57	1.36	1.12	.903	.625	.803	1.26	1.37
Nitrogen	.470	.150	.442	.221	.187	.127	.091	.138	.153	.240
Dry Wt.	14.5	10.1	14.2	7.50	6.74	4.94	2.56	3.7	4.27	6.68
Chlorophyll a ($\text{mg}\cdot\text{d}^{-1}$)										
B	59.1	54.3	72.4	54.1	32.1	1.20	6.85	6.54	16.4	24.7
C	81.8	54.4	49.9	14.4	19.4	5.46	4.58	15.3	11.2	18.2
D	83.0	57.8	69.6	26.46	17.9	7.41	4.91	-	9.45	13.7

